



Investigating the impact of α -synuclein and PD-L1 deletion on platelet function

By

Christopher James Sennett

Doctor of Philosophy in Medical Science

June 2024

Hull York Medical School

Investigating the impact of α -synuclein and PD-L1 deletion on platelet function

being a thesis submitted for the Degree of Doctor of Philosophy in Medical Science

at Hull York Medical School

by

Christopher James Sennett MSc BSc

June 2024

Abstract

Platelet proteomic studies suggest that platelets express over 1,000 proteins, most of which have no known function in platelets. This thesis investigates two such proteins, α -synuclein and Programmed Death Ligand 1 (PD-L1), and their roles in essential platelet functions and associated pathological processes.

Granular secretion is critical for platelet function, contributing not only to haemostasis, but also wound healing and inflammation. The release of granule contents requires the assembly of the Soluble N-ethyl maleimide-sensitive factor (NSF) Attachment Protein Receptor (SNARE) complex. In neurons, α -synuclein is known to regulate granule secretion by facilitating the SNARE complex assembly. Platelet proteomic studies suggest that α -synuclein is highly expressed in platelets, but its function(s) remain unknown. In human platelets, we demonstrate that α -synuclein co-localises with VAMP8, SNAP23, and STX11. Immunoprecipitation shows a significant increase in interaction between α -synuclein and VAMP8/STX11 and STX4 following thrombin stimulation. In α -synuclein knockout mice, we show that α -synuclein facilitates haemostasis, granule secretion, and the immune response to endotoxemia. These mice exhibit a bleeding tendency and prolonged activated partial thromboplastin time (APTT), mirroring *in vitro* aggregation defects. α -synuclein deletion resulted in poorer outcomes following acute endotoxemia. These findings suggest that α -synuclein regulates platelet secretion by facilitating SNARE complex formation.

In this thesis, we present evidence that PD-L1 is abundantly expressed in platelets. Whilst PD-L1 is recognised as an immunomodulator, recent studies revealed that PD-L1 deletion inhibits platelet function. We generated the first platelet-specific PD-L1 knockout mouse, which exhibited reduced platelet aggregation *in vitro*. This reduction was accompanied by a significant decrease in platelet activation and secretion. In humans, PD-L1 inhibitors significantly reduced platelet aggregation. Flow cytometric analysis showed that patients with myeloproliferative neoplasms (MPN) have a significantly higher percentage of PD-L1 positive platelets compared to healthy donors. Additionally, incubation of healthy donor platelets with interferon-gamma (IFN- γ) significantly increased PD-L1 expression, a result confirmed by plasma swap experiments where healthy donor platelets upregulated PD-L1 expression after incubation with plasma from MPN patients. These findings suggest that PD-L1 plays a role in platelet activation and can be induced by plasma factors such as IFN- γ .

Acknowledgements

Firstly, I would like to sincerely thank my supervisors Dr. Ahmed Aburima and Dr. Francisco Rivero Crespo for their advice and support throughout my PhD. I would also like to thank everyone in the Hardy013 Lab/Platelet group for their advice and support throughout my PhD. Alongside this, thanks to the technical staff, in particular Andrew Gordon and Ellie Beeby, without whom the lab would have ground to a halt.

I would like to thank my parents and grandparents, for all the support and patience you have shown me throughout my education, and the inspiration to pursue science further. Thank you to my friend Stephen, although studying for his PhD at the same time, he always found the time and energy for support and encouragement. I would also like to thank my friends in IP-Org for keeping me sane, particularly Julian, who's advice was indispensable. To Danielle, thank you for always being there, listening to me complain when nothing worked, or going on about it for hours when it did. Thank you for providing me with support, encouragement and love, I couldn't have done this without you.

Publications to date

PEER REVIEWED PUBLICATIONS:

- **Investigating the effects of arginine methylation inhibitors on micro-dissected brain tumour biopsies maintained in miniaturised perfusion system.**
Antonia Barry ¹, Sabrina F Samuel ¹, Ines Hosni ¹, Amr Moursi ², Lauric Feugere ³, **Christopher J Sennett** ¹, Srihari Deepak ², Shailendra Achawal ², Chittoor Rajaraman ², Alexander Iles ⁴, Katharina C Wollenberg Valero ³, Ian S Scott ⁵, Vicky Green ¹, Lucy F Stead ⁶, John Greenman ¹, Mark A Wade ¹, Pedro Beltran-Alvarez ¹
- **α -synuclein deletion impairs platelet function: a role for SNARE complex assembly**
Christopher James Sennett, Wanzhu Jia, Jawad S Khalil, Matthew S Hindle, Charlie Coupland, Simon Calaminus, Julian D Langer, Sean Frost, Khalid M Naseem, Francisco Rivero, Natalia Ninkina, Vladimir Buchman, Ahmed Aburima
- **Trapped in the NETs: Multiple Roles of Platelets in the Vascular Complications Associated with Neutrophil Extracellular Traps**
Christopher sennett, Giordano Pula

CONFERENCE PRESENTATIONS:

- SNAREs and Platelets: An Old Script and New Players – CAM Seminar series 2021
- α -synuclein promotes platelet activation by facilitating SNARE complex formation and secretion – The Platelet Society UK 2022
- Investigating α -synuclein interactions with the SNARE complex in platelets – HYMS PGR day 2023
- α -synuclein promotes platelet activation by facilitating SNARE complex formation and secretion – The Platelet Society UK 2023

Contents

Abstract	ii
Acknowledgements	iii
Publications to date	iv
Contents	v
List of figures	xi
List of Tables	xv
Abbreviations	xvii
Chapter 1. Introduction	20
1.1. Platelet overview	20
1.2. The role of platelets	21
1.2.1. Haemostasis and Thrombosis	22
1.2.2. Immune function	22
1.3. Platelet production	23
1.3.1. Platelet haemostatic response	24
1.3.2. Platelet activation by collagen	29
1.3.3. Platelet activation by thrombin	32
1.3.4. Platelet activation by thromboxane A ₂	34
1.3.5. Platelet activation by ADP	36
1.4. Shape change	38
1.5. Platelet aggregation	39
1.6. Granular secretion	40
1.6.1. α -granules	41
1.6.2. Dense Granules	42
1.6.3. Lysosomes	43
1.6.4. T-granules	44

1.6.5.	The Soluble NSF (N-ethylmaleimide-sensitive factor) Attachment Protein Receptor (SNARE) complex.....	45
1.6.6.	Vesicle-associated membrane proteins (VAMP).....	49
1.6.7.	Syntaxins	51
1.6.8.	Synaptosomal-Associated Protein (SNAP).....	52
1.6.9.	The functional SNARE complex in platelets.....	52
1.6.10.	Associated proteins and regulation.....	53
1.7.	The synuclein family	56
1.7.1.	α - synuclein.....	57
1.7.2.	α -synuclein in disease	60
1.7.3.	The Role of α - synuclein in the SNARE complex.....	62
1.7.4.	Post translational modifications of α -synuclein.	65
1.7.5.	The current roles of α -synuclein in platelets	67
1.8.	Thesis Aims	68
Chapter 2.	Materials and Methods.....	69
2.1.	Animal handling and breeding of α -synuclein knockout mice.....	69
2.2.	Preparation of Platelet-Rich Plasma	70
2.2.1.	Human	70
2.2.2.	Murine blood.....	71
2.3.	Preparation of Washed platelets	71
2.3.1.	Human	71
2.3.2.	Murine blood.....	71
2.3.3.	Platelet count and adjustment.....	72
2.4.	Light Transmission aggregometry (washed platelets).....	72
2.5.	Inhibition of α -synuclein with pharmacological agents	73
2.6.	DNA extraction.....	74
2.6.1.	Guanidinium thiocyanate method	74

2.6.2.	TRIZOL® method.....	74
2.6.3.	Kapa	75
2.7.	Genotyping.....	76
2.7.1.	PCR Methodology for α -synuclein Knockout mice	76
2.8.	Protein concentration assay.....	77
2.9.	Western blotting	79
2.10.	Sample Preparation	80
2.10.1.	Subcellular fractionation analysis.....	80
2.10.2.	Preparation of Western Blot Gel	80
2.10.3.	Chemiluminescent imaging.....	81
2.10.4.	Fluorescent western blot Imaging	82
2.11.	Immunoprecipitation.....	82
2.11.1.	Coomassie Staining	84
2.12.	Microscopy	85
2.12.1.	Static platelet adhesion assay	85
2.12.2.	Immunofluorescence.....	86
2.12.3.	Platelets adhesion under flow	87
2.13.	Flow Cytometry	87
2.13.1.	Flow cytometric analysis	89
2.13.2.	Compensation.....	90
2.13.3.	t-SNE analysis	90
2.14.	Statistical analysis.....	93
Chapter 3.	Characterisation of α -synuclein movement and interactions in human platelets	94
3.1.	Introduction	94
3.2.	Aims for Chapter 3	95
3.3.	Results.....	95

3.4.	The role of α -synuclein in human platelets.....	95
3.4.1.	Effect of incubation time in ELN484228 on aggregation	99
3.4.2.	Western blotting optimization.....	101
3.4.3.	Immunofluorescence optimisation – antibody and blocking.....	102
3.4.4.	Immunofluorescence optimisation - antibody concentration	103
3.5.	A-syn reaction to agonists.....	105
3.5.1.	Movement of α -synuclein upon stimulation.....	105
3.5.2.	Co-localisation of α -synuclein with vesical-associated membrane proteins.	112
3.6.	Examining platelet function using the α -synuclein inhibitor, ELN484228.	114
3.7.	Interaction of α -synuclein with SNARE complex proteins following stimulation.....	117
3.8.	The effects of platelet stimulation on α -synuclein serine129 phosphorylation.....	119
3.9.	Effects of platelet inhibitors on α -synuclein phosphorylation.....	123
3.10.	Discussion.....	126
3.10.1.	Limitations.....	129
Chapter 4.	The analysis of α -synuclein, using a knockout mouse model	131
4.1.	Introduction	131
4.2.	Generation of α -synuclein knockout mice on a C57BL/6J background	132
4.2.1.	Optimisation of PCR	134
4.2.2.	Confirmation of an α -synuclein knockout mouse model.....	136
4.2.3.	Assessment of knockout impact on platelet phenotypes	137
4.3.	α - synuclein deletion results in a bleeding phenotype.....	140
4.4.	α - synuclein knockout platelets have an aggregation defect.....	142
4.5.	Platelet adhesion to extracellular molecules	144
4.5.1.	α -synuclein deletion has no impact on platelet adhesion to fibrinogen. ...	144

4.5.2.	α-synuclein deletion has no impact on platelet adhesion to collagen.....	148
4.5.1.	α-synuclein deletion impairs thrombus formation <i>in vitro</i>	150
4.6.	Immunofluorescence analysis of α-synuclein with SNARE components..	151
4.7.	Flow cytometric analysis of platelet activation.....	167
4.7.1.	Optimisation of flow cytometry conditions.	167
4.7.2.	Whole population flow cytometric analysis of platelet activation and secretion.	171
4.7.3.	Flow cytometry single-cell analysis of platelet activation	178
4.7.4.	Classification of activated platelets for t-SNE analysis.....	182
4.7.5.	Flow cytometric single-cell analysis of platelet activation and secretion markers	184
4.7.6.	Single cell flow cytometric analysis of Thrombin stimulated platelets	196
4.8.	Effects of endotoxemia on α-synuclein knockout platelets.....	198
4.9.	Discussion.....	202
4.9.1.	Limitations.....	207
Chapter 5.	Assessment of PD-L1 function in platelets using a knockout model and MPN patient blood.....	210
5.1.	Introduction	210
5.2.	Results.....	214
5.2.1.	Investigation platelet PD-L1 expression in MPN Patients	227
5.3.	Discussion.....	234
5.3.1.	Limitations.....	237
5.4.	Future work.....	238
Chapter 6.	Discussion	240
6.1.	Summary of Results.....	240
6.1.1.	Interpretation of the overall findings.....	242
6.1.2.	Smith 2023 paper	244

6.2. PD-L1.....	246
6.2.1. Future work.....	250
References.....	251
Supplementary.....	i
6.3. Reagents.....	i
6.4. Buffers and solutions	v
6.4.1. Modified Tyrode's	v
6.4.2. Acid-citrate dextrose buffer (ACD)	v
6.4.3. Sodium citrate	v
6.4.4. Wash buffer	vi
6.4.5. Laemmli buffer pH 6.8.....	vi
6.4.6. SDS sample buffer.....	vi
6.4.7. TAE.....	vii
6.4.8. 4% paraformaldehyde.....	vii
6.4.9. 0.2% Formyl Saline.....	vii
6.4.10. Subcellular fractionation buffer	vii
6.4.11. Gel buffer I	viii
6.4.12. Gel buffer II	viii
6.4.13. Running buffer	viii
6.4.14. Citric Acid.....	ix
6.4.15. ECL Reagents	ix
6.5. α -Synuclein Deletion Impairs Platelet Function: A Role for SNARE Complex Assembly	x

List of figures

Figure 1-1. Platelet adhesion and shape change.	25
Figure 1-2. Structure of the thrombus in-vivo.	28
Figure 1-3. Collagen signalling mechanism.	31
Figure 1-4. Signalling cascade when Thrombin cleaves PAR1 and PAR4 in platelets.....	33
Figure 1-5. Signalling pathway induced via Thromboxane prostanoid (TP) receptor.	35
Figure 1-6. P2Y ₁ and P2Y ₁₂ signalling pathways.	37
Figure 1-7. parameters delineating Q- R-SNARE quantification.	46
Figure 1-8. Structure and function of the SNARE complex.	48
Figure 1-9. Ribbon Diagram of the Structure of a monomer of a-synuclein.	58
Figure 1-10. Biomedical assessment of patients with Parkinson's disease.....	61
Figure 1-11. String analysis of α -synuclein protein interactions in homo sapiens.	63
Figure 1-12. proposed a-synuclein interaction within the SNARE complex in neurons.	64
Figure 2-1. Diagram of whole blood components after centrifuging.	70
Figure 2-2. Explanatory diagram of aggregation curve generated by LTA.	73
Figure 2-3. α -synuclein knockout generation (Ninkina et al., 2015).....	77
Figure 2-4. Layout of a 96-well-plate for a typical Protein concentration assay.....	78
Figure 2-5. Diagram of Chemiluminescent Western blot mechanism.....	83
Figure 2-6. Schematic diagram of Immunoprecipitation.	84
Figure 2-7. Manual gating of platelet populations.	88
Figure 2-8. Rainbow bead calibration for Flow cytometry.....	89
Figure 2-9. t-SNE settings window in FlowJo.	92
Figure 3-1. α -synuclein is present within human platelets.....	95
Figure 3-2. Platelet aggregation optimisation in response to different agonists.....	97
Figure 3-3. Pharmacological α -synuclein inhibitor optimisation.....	99
Figure 3-4. Effects of incubation period with ELN484228 on platelet aggregation to thrombin.	100
Figure 3-5. Western blotting optimisation and membrane fixing.	102
Figure 3-6. Antibody selection with Human serum vs BSA for blocking in immunofluorescence.....	103
Figure 3-7. Titration of α -synuclein antibodies for immunofluorescence.....	104

Figure 3-8. α -synuclein migrates to the periphery of platelets when stimulated with an agonist.	106
Figure 3-9. Co-localisation of p- α -synuclein and α -synuclein in basal and stimulated platelets.	107
Figure 3-10. α -synuclein is not secreted by platelets but expressed on the platelet surface when stimulated.....	109
Figure 3-11. α -synuclein is not secreted by platelets following stimulation.	111
Figure 3-12 Representative images of the movement and co-localisation of α -synuclein with VAMP8 in stimulated human platelets.	113
Figure 3-13. movement and. Movement and localisation of α -synuclein with VAMP2 in stimulated human platelets.....	114
Figure 3-14. Effects of Pharmacological α -synuclein Inhibitors on Human platelet aggregation to platelet agonists.....	116
Figure 3-15. Interaction of α -synuclein with SNARE complex proteins in basal and thrombin stimulated conditions.	118
Figure 3-16. Thrombin stimulation of platelets induces the phosphorylation of α -synuclein.	120
Figure 3-17. Collagen stimulation of platelets effects on phosphorylation of α -synuclein. ...	121
Figure 3-18. U46619 stimulation of platelets effects on phosphorylation of α -synuclein.....	122
Figure 3-19. Effect of PGI2 on a-synuclein phosphorylation.....	124
Figure 3-20. Effect of intracellular calcium on a-synuclein phosphorylation.....	125
Figure 4-1. Breeding strategy of α -synuclein knockout mice.	133
Figure 4-2. DNA extraction methods.....	134
Figure 4-3. Effects of annealing temperature on PCR output.	135
Figure 4-4. Effects of magnesium concentration on PCR output.	135
Figure 4-5. Effects of primer concentration on PCR output.....	136
Figure 4-6. Quantification of α -synuclein knockout mice.	137
Figure 4-7. Quantification receptor expression in α -synuclein knockout, heterozygous and wild-type platelets.....	138
Figure 4-8. Western blot analysis of SNARE complex proteins from platelet samples isolated wild-type or knockout mice.	139
Figure 4-9. Bleeding time assay of wild-type and knockout mice with Prothrombin time and activated partial thromboplastin time.....	141
Figure 4-10. Platelet aggregation is reduced in α -synuclein deficient mouse platelets.	143

Figure 4-11. Effects on the static spreading of murine platelets to fibrinogen matrices in untreated and pre-stimulated conditions.	146
Figure 4-12. Static spreading of unstimulated murine platelets on a matrix.	147
Figure 4-13. Static spreading of unstimulated murine platelets on a collagen matrix.	149
Figure 4-14. Platelet adhesion to collagen matrices under flowing conditions.	151
Figure 4-15. Confirmation of specificity of secondary antibodies.	153
Figure 4-16. Effects of α -synuclein knockout on Syntaxin 11 in platelets.	155
Figure 4-17 Effects of α -synuclein knockout on SNAP23 in platelets.	157
Figure 4-18. Effects of α -synuclein knockout on VAMP8 in platelets.	159
Figure 4-19. Effects of α -synuclein knockout on Syntaxin 4 in platelets.	161
Figure 4-20. Effects of α -synuclein knockout on VAMP2 in platelets.	162
Figure 4-21. Effects of α -synuclein knockout on VAMP7 in platelets.	164
Figure 4-22. Movement of α -synuclein and in α -synuclein pser129 platelets.	166
Figure 4-23. Antibody titration of flow cytometry antibodies.	169
Figure 4-24. Effect of bleed quality on flow cytometry data.	170
Figure 4-25. Whole population analysis of thrombin-stimulated platelets.	173
Figure 4-26. Whole population analysis of CRP-XL stimulated platelets.	175
Figure 4-27 Whole population analysis of U46619 stimulated platelets.	176
Figure 4-28. Whole population analysis of ADP stimulated platelets.	177
Figure 4-29. t- SNE analysis condition selection.	179
Figure 4-30. t-SNE analysis optimisation, - perplexity tuning.	181
Figure 4-31. t-SNE analysis optimisation - learning rate optimisation.	182
Figure 4-32. Gating strategy for activated platelets plotted on a tSNE map.	183
Figure 4-33. t-SNE analysis of platelets with no agonist simulation.	187
Figure 4-34. t-SNE analysis of thrombin stimulated platelets comparing Wild-type and knockout platelets.	190
Figure 4-35. t-SNE analysis of CRP-XL stimulation comparing Wild-type and knockout platelets.	192
Figure 4-36. t-SNE analysis of U46619 stimulation comparing Wild-type and knockout platelets.	195
Figure 4-37. Flowsom analysis of t-SNE maps generated from thrombin stimulated Wild-type and knockout murine platelets.	197
Figure 4-38. Effects of endotoxemia on α -synuclein knockout mice.	200
Figure 4-39. Effects of Clinical score on basal expression of platelet activation and secretion markers.	201

Figure 5-1. Breeding strategy, and quantification of whole-body PD-L1 knockout mice.	215
Figure 5-2. Targeting strategy to generate the platelet-specific PD-L1 Knockout Mouse. ...	216
Figure 5-3. Breeding strategy to generate the platelet-specific knockout mice with genetic and proteomic confirmation.	218
Figure 5-4. Effects of PD-L1 knockout on platelet aggregation to Thrombin and collagen. .	220
Figure 5-5. PDL-1 knockout significantly reduces granule secretion markers in response to thrombin stimulation.....	221
Figure 5-6. Overall structure of PD-L1/Atezolizumab complex.....	222
Figure 5-7. Platelet aggregation to agonists is differentially affected by PD-L1 blocking agents.	224
Figure 5-8. Commercial PD-L1 inhibitors Effect platelet aggregation to U41669 and thrombin but not collagen.	226
Figure 5-9. Platelets from MPN patients are significantly inhibited following incubation with PD-L1 inhibitors.....	229
Figure 5-10. Patients with MPNs express similar levels of PD-L1 to healthy donors but by significantly fewer platelets.....	231
Figure 5-11. Incubation of platelets with IFN- γ increases PD-L1 expression in a time-dependent manner.....	232
Figure 5-12. Incubation of healthy donor platelets in MPN plasma increases PD-L1 expression.....	233
Figure 6-1. Proposed mechanism of action for α -synuclein in platelet granule secretion. ...	245

List of Tables

Table 1. Platelet receptors involved in adhesion, and aggregation.....	26
Table 2. Platelet receptors involved in the amplification phase of thrombus formation.	27
Table 3. Platelet receptors with known ligands in the stabilisation phase and negative platelet activators.	29
Table 4. Key components of α -granules and their functions.	42
Table 5. Key components of dense granules and their functions.....	43
Table 6. Key components of Lysosomes, and their functions.....	44
Table 7. VAMP family and their roles within the body.	50
Table 8. Known SNARE complex regulatory proteins in platelets.....	55
Table 9. Elucidated roles of α -syn within the body.	60
Table 10. PCR component volumes for genotyping	76
Table 11. Antibodies used for Western blot analysis.....	80
Table 12. Components of different percentage acrylamide resolving gels Gel buffer1 components as in Table 36.	81
Table 13. Components of Stacking Gel, Gel buffer2 components as in Table 37.	81
Table 14. Flow cytometry compensation values.	90
Table 15. Antibody panel used for multicolour platelet viability and secretion flow cytometry.	93
Table 16. Example of reagent volumes in secretion analysis flow cytometry.	93
Table 17. Compensation matrix of 5 colour flow cytometric analysis	171
Table 18. Proteins secreted from platelets affecting the immune response.	211
Table 19. General reagents.....	i
Table 20. Primary Antibodies for western blotting	ii
Table 21. Secondary antibodies for Western blot	ii
Table 22. Antibodies used in Flow cytometry.	iii
Table 23. Primary antibodies used in Immunofluorescence.....	iii
Table 24. secondary antibodies used in Immunofluorescence.....	iii
Table 25. Platelet inhibitors used in inhibition experiments.....	iv
Table 26. Platelet agonists used in experiments.....	iv
Table 27. Modified tyrodes buffer components	v
Table 28. Acid Citrate Dextrose components	v
Table 29. Sodium citrate components	vi

Table 30. Platelet wash buffer components	vi
Table 31. Laemmli buffer components.....	vi
Table 32. SDS sample buffer components	vi
Table 33. Tris-Acetate-EDTA buffer components	vii
Table 34. 4% Paraformaldehyde components	vii
Table 35. 0.2% formyl saline components	vii
Table 36. Subcellular fractionation components	viii
Table 37. Resolving gel buffer components.....	viii
Table 38. Stacking gel buffer components.....	viii
Table 39. SDS page run buffer components.....	viii
Table 40. Citric acid components	ix
Table 41. ECL reagent components	ix

Abbreviations

AA	arachidonic acid
ADP	Adenosine diphosphate
AMP	Adenosine monophosphate
APL	aminophospholipids
ARC syndrome	arthrogryposis, renal dysfunction, and cholestasis
ARP2	actin-related protein 2
ATP	adenosine triphosphate
Ca ⁺²	Calcium ion
cAMP	cyclic adenosine 3',5'monophosphate
CD110	mpl receptor
CD31	Platelet endothelial cell adhesion molecule 1
cGMP	Cyclic guanosine monophosphate
CLEC-2	C-type lectin-like 2
CORVET	class C Core Vacuole/endosome tethering
COX-1	Cyclooxygenase 1
CRP-XL	cross-linked collagen-related peptide
CTGF	connective tissue growth factor
CVD	Cardiovascular disease
CXCL-1	chemokine ligand 1
DAG	1,2-diacylglycerol
DTS	dense tubular system
eNOS	endothelial nitric oxide synthase
Ephr	Ephrin receptor
FcR γ	Fc receptor γ -chain
FHL	familial hemophagocytic lymphohistiocytosis
FSC	Forward Scatter
GPCR	G Protein-coupled Receptors
GPIb-IX-V	glycoprotein Ib-IX-V
GPVI	Glycoprotein VI
HOPS	homotypic fusion and protein sorting
IGF-1	insulin-like growth factor-1
IgG	Immunoglobulin G
IL	interleukin
IP	prostacyclin receptor
IP3	inositol 1,4,5-trisphosphate
IPSDs	Inherited Platelet Secretion Disorders
ITAM	immunoreceptor tyrosine-based activation motif
JNK	c-Jun N-terminal kinases
LAMP	lysosomal-associated membrane protein
LatA	Latruncullin A
LRO	lysosome-related organelles
MAPK	mitogen activated protein kinase
MKs	megakaryocytes
MLC	myosin light chain

MLCK	Myosin light chain kinase
MLCP	myosin light chain phosphatase
MPN	Myeloproliferative Neoplasm
munc13-4	unc-13 homolog D
Munc18b	syntaxin binding protein 2
NAC	non-amyloid- β component
NFAT	nuclear factor of activated T cells
NK	Natural killer cell
NO	Nitric oxide
OCS	open canalicular system
O- α -syn	oligomeric α -Synuclein
P38	mitogen-activated protein kinase 14
PARs	Protease-activated receptors
PD	Parkinsons disease
PDGF	Platelet-derived growth factor
PDI	Protein disulphide-isomerase
PE	phosphatidylethanolamine
PF4	platelet factor IV
PGD ₂	Prostaglandin D2
PGE ₂	Prostaglandin E2
PGH2	prostaglandin H2
PGI ₂	Prostaglandin I2
PIP2	phosphatidylinositol 4,5 trisphosphate
PKA	protein kinase A
PKC	Protein kinase C
PKG	cGMP-dependent protein kinase
PLC β	Phospholipase C Beta
PMNs	Polymorphonuclear neutrophils
PS	phosphatidylserine
PTMs	post-translational modifications
RBCs	Red blood cells
ROCK	Rho-associated coiled-coil containing protein kinase
sGC	soluble guanylate cyclase
SH2	Src Homology 2
SM	splicosomal protein
SNAP	Synaptosomal-Associated Protein Soluble NSF (N-ethylmaleimide-sensitive factor)
SNARE	Attachment Protein Receptor
Src	Proto-oncogene tyrosine-protein kinase
STX	Syntaxin
STX-BP5	Tomosyn
SYK	spleen tyrosine kinase
TLR-1	Toll-like receptor 1
TLT-1	TREM-like transcript 1
TMD	trans-membrane domain
TPO	Thrombopoietin

TREM1	Triggering Receptor Expressed On Myeloid Cells 1
TRPC6	transient receptor potential cation channel subfamily C member 6
TSP-1	Thrombospondin-1
TxA2	Thromboxane A2
ULvWF	Ultra-long variants of vWF
VASP	vasodilator-stimulated protein
VEGF	Vascular endothelial growth factor
VTI1b	Vesicle transport through interaction with t-SNAREs homolog 1B
vWF	von Willebrand factor
WASF1	WASP family member 1
$\alpha 2\beta 1$	GPIa/IIa

Chapter 1. Introduction

1.1. Platelet overview

Platelets (thrombocytes) were first discovered by Giulio Bizzozero in 1882. Platelets are unique in that they are anucleate with an average diameter of 2-3 μ m (Ribatti and Crivellato, 2007). A normal platelet count ranges from 150,000-to 350,000 platelets per millilitre of blood in healthy humans, with approximately 2/3 of platelets in circulation and the remaining stored in the spleen (Frojmovic and Milton, 1982). The platelet plasma membrane is composed of a phospholipid bilayer expressing multiple surface markers interspersed with lipid rafts, aiding in signalling and intracellular trafficking (Blair and Flaumenhaft, 2009).

Platelets play a key role in haemostasis and thrombosis but are also increasingly recognised to play important roles in inflammation and immune response. Platelet activation is a key step in the process of haemostasis and thrombosis. Platelets adhere rapidly to sites of injury, forming aggregates necessary for forming a platelet plug causing the cessation of blood loss. This process relies on strictly controlled signalling and secretion of molecules from the platelets themselves, which have been observed to both recruit, and stimulate, platelets by autocrine and paracrine mechanisms. Platelets' high sensitivity to disease states, have made them one of the most accessible markers for multiple pathologies, due to the amount of platelet interactions with leukocytes and endothelial cells. They are also known as an important inflammatory marker (Cerletti et al., 2012).

Secretion is the most far-reaching product of platelet activation. As such, it accounts for many of the functions of the platelets involvement in immune regulation, platelet recruitment and wound healing. Although much research has been undertaken on the platelet secretion machinery, the full mechanism is yet to be elucidated. Aberrations in secretion can cause a spectrum of pathologies ranging from bleeding to excessive clotting. Inherited Platelet Secretion Disorders (IPSDs) encompass a group of coagulopathies that can be classified into various categories based on their underlying mechanisms (Mumford et al., 2015). Due to coagulopathies playing a pivotal role in cardiovascular disease (CVD), understanding the underlying platelet secretion mechanisms is of utmost importance (Jennings, 2009a, Fisch et al., 2013).

1.2. The role of platelets

Although primarily recognised for their role in haemostasis and thrombosis, platelets contribute to immune function, wound healing, and inflammation. Platelets have been shown to be involved in several disease states such as atherosclerosis and tumour progression (Holinstat, 2017, Menter et al., 2014). Platelets also drive various physiological processes, due to a variety of chemokines stored in their granules (Blair and Flaumenhaft, 2009). The granular contents give platelets a unique role in communicating and modulating the function of the surrounding cells, including endothelial and immune cells (Semple et al., 2011). Platelets are known to play a role in immune surveillance due to their capability to engulf both bacteria and viruses, release anti-microbial and anti-fungal proteins, produce reactive oxygen species (ROS), and modulate the production of inflammatory cytokines (Yeaman, 2010, Ali et al., 2015, Portier and Campbell, 2021).

Platelets are also heavily involved in wound healing and the resolution of inflammation. This is due to the vast number of cytokines and chemokines released from their granules (Cognasse et al., 2019). Examples of these include platelet-derived growth factor (PDGF), insulin-like growth factor-1 (IGF-1), vascular endothelial growth factor (VEGF), and connective tissue growth factor (CTGF) (Karina et al., 2019). Angiogenesis is key for embryonic development and wound healing however, when dysregulated, can be a factor in many pathogenesises. The secretion of epithelial growth factors and CD40 ligand (CD40L) can stimulate the growth of new epithelial cells and the migration of these cells for the healing of sites of injury. The storage and release of inhibitors of vessel growth are also an important function of the platelet, to effectively modulate response (Italiano et al., 2008a, Nurden, 2011).

1.2.1. Haemostasis and Thrombosis

Haemostasis is the body's normal response to blood vessel injury and bleeding, to prevent exsanguination while maintaining blood fluidity within the vascular system (Rasche, 2001). Thrombosis, on the other hand, is the formation of thrombi within a blood vessel preventing normal blood flow and is associated with the excessive activation of haemostasis in the absence of bleeding. Due to the importance of haemostasis, and the potential for deleterious effects of thrombosis, platelets must be stringently regulated with multiple controlling mechanisms. Activation is a key step in the regulation and function of platelets, which is achieved in 3 sequential events: adhesion, secretion, and aggregation. First, platelets adhere to the newly exposed extracellular matrix proteins, namely, collagen fibres, von Willebrand factor (vWF), and fibronectin. Once activated, platelets secrete a plethora of molecules, which amplify and regulate the growth of the platelet plug. Additionally this stimulates the recruitment of platelets to the platelet plug, the exposure of binding sites, and the release of fibrinogen, allowing the capture of red blood cells, leukocytes and the recruitment of more platelets; creating a mesh like structure that stabilises a thrombus over the injury site to maintain vessel integrity (Golebiewska and Poole, 2015).

1.2.2. Immune function

Alongside the haemostatic function at the site of injury, platelets play a critical role in recruiting and activating the immune system (Sonmez and Sonmez, 2017). This recruitment relies, at least in part, on platelet secretion via the release of bioactive amines from dense granules, such as histamine and serotonin which mediate inflammation and recruitment of leukocytes. The release of many chemokines and cytokines from α -granules, such as chemokine ligand 1 (CXCL-1) and chemokine ligand 2 (CCL-2), recruit lymphocytes. Platelets also release microbicidal proteins such as kinocidins and defensins to aid in innate immunity (Ali et al., 2015, Yeaman, 2010). In addition to these granular cargo, platelets are able to detect pathogens through Toll-like receptor 1 (TLR1) to 7 and Triggering Receptor Expressed On Myeloid Cells 1 (TREM1) present on their plasma membrane, and enhance antigen presentation of B cells through the CD40L (Ghasemzadeh and Hosseini, 2013). Upon platelet activation, P-selectin is expressed on their surface, the presence of P-selectin is an important modulator of platelet-leukocyte interactions such as adhesion,

immobilisation, and cell recruitment, due to its interaction with P-selectin glycoprotein ligand-1 (PSGL1) on monocytes (Freedman and Loscalzo, 2002, Han et al., 2020a). Platelets also express other immune checkpoint receptors on their membrane, which they upregulate after activation such as programmed death-ligand 1 (PD-L1) (Guo et al., 2022).

1.3. Platelet production

The formation and release of platelets into the bloodstream is a cumulative process driven by an intricate series of remodelling events and orchestrated by transcription factors and cytokine signalling called thrombopoiesis. This process takes place in the bone marrow, particularly in the bones of ilium and sternum (Kaushansky, 2005). Platelets are formed in the bone marrow by the precursor cells, megakaryocytes (MKs), with each MK producing between 5000 and 10000 platelets in its lifetime (Wang and Zheng, 2016). In an average day, a healthy adult can produce one-hundred billion platelets, with the old cells being phagocytosed in the spleen and liver (Ghoshal and Bhattacharyya, 2014). Once the MKs mature, they move to sinusoids and extend proplatelets, which then shed platelets into the bloodstream and can circulate for up to 9 days (Pluthero and Kahr, 2016). Thrombopoietin (TPO) is a glycoprotein hormone primarily produced in the liver and kidneys and is responsible for the regulation of platelet production (Kaushansky, 2006). TPO regulates the differentiation of MKs via binding to the mpl receptor (CD 110). Thrombopoiesis is a constant process in healthy humans starting in the foetus, until death. Studies have identified platelets in circulation in the embryonic bloodstream as early as day 10 in murine embryos, and MKs as early as day 7, similar to erythrocyte progenitors (Margraf et al., 2019). In the human foetus, megakaryopoiesis is observed as early as 5 weeks gestation in the yolk sac, and 10 weeks in the liver and spleen. In the second half of foetal life, the transition to bone marrow becomes the main site for megakaryopoiesis, which is the process of developing haemopoietic stem cells, this process continues here for the remainder of life (Margraf et al., 2019).

Additionally, the lungs have been identified as a site of platelet biogenesis, and storage for many hematopoietic stem cells as early as 1937. In 2017, this was arguably quantified as a main site for thrombopoiesis; however, this is still debated (Lefrançois et al., 2017, Asquith et al., 2024). With all biological processes, the opportunity for aberrations in platelet development is present. There are several inherited platelet

function disorders that result in a broad spectrum of pathologies. One of these groups is the inherited platelet disorders (IPDs), which includes disorders such as δ -storage pool disease and Grey Platelet Syndrome, which occur when the biogenesis of the platelet is disrupted, both of which have been shown to exhibit a bleeding phenotype, highlighting the importance of platelet secretion (Nurden and Nurden, 2007).

Platelets are removed at the end of their lifespan in the liver through the interaction of desialyated surface proteins on aged platelets with Ashwell-morrell receptors (Grewal, 2010). This interaction in turn induces the transcription and translation of hepatic TPO to regulate platelet production (Grozovsky et al., 2015). Platelets then undergo programmed cell death, which is primarily characterised by mitochondrial membrane depolarisation, alongside the release of cytochrome C. Following this, phosphatidylserine is exposed on the platelet surface causing cellular blebbing and fragmentation of the cell (Gyulkhandanyan et al., 2013).

1.3.1. Platelet haemostatic response

Blood platelets circulate the blood stream in a quiescent state monitoring the integrity of the vessel walls, until a blood vessel experiences an insult and the subendothelial matrix is exposed. The subendothelial matrix of blood vessels is comprised of multiple proteins, which interact with receptors on the platelet surface resulting in platelet adhesion and activation as shown in (Table 1). When collagen comes into contact with glycoprotein VI (GPVI), and the newly exposed vWF comes into contact with glycoprotein Ib-IX-V (GPIb-IX-V), this causes rolling, adhesion, tethering and activation, followed by aggregation of platelets ending in thrombus formation (Jennings, 2009b, Surin et al., 2008). The shear stress within the vessel affects whether collagen or vWF drives platelet adhesion (McGrath et al., 2010). For high shear stress such as in the small arteries and arterioles, platelets interact with the collagen-bound vWF through the GPIb-IX-V complex and activate platelets by binding to GPVI. Under lower shear stress conditions found in the veins, platelets bind to the collagen via GPIa/IIa ($\alpha 2\beta 1$) if primarily activated through GPIb-IX-V, which allows for activation by GPVI interacting with collagen (Shida et al., 2014, Shida et al., 2019, Ruggeri et al., 2006, Rana et al., 2019). While GPVI and GPIb-IX-V can bind to collagen and vWF without activation, forming the initial platelet monolayer, activation

is required to expose the binding sites of $\alpha 2\beta 1$ for further thrombus formation (Konstantinides et al., 2006). Platelet activation is primarily associated with the initiation of outside-inside signalling pathways and is characterised by rapid changes in platelet morphology relying primarily on a large number of surface receptors (Table 1) (Yun et al., 2016).

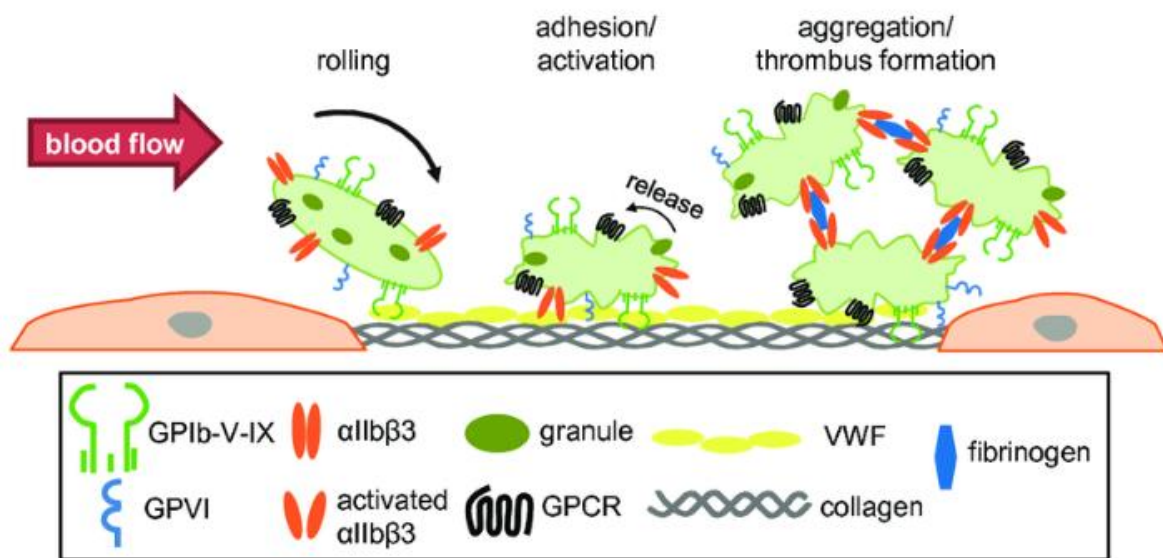


Figure 1-1. Platelet adhesion and shape change. Platelets circulate at the periphery of the lumen, once a site of insult is created, the underlying tissue is exposed. Platelet activation begins by rolling across the surface of the collagen and vWF, the GPVI and GPIb-IX-V are then in close enough proximity to bind more firmly to the tissue causing adhesion and activation of the platelets. The platelets can then secrete multiple molecules to recruit more platelets and to bind with each other forming a platelet plug, and thrombus. From (Gitz, 2013).

Table 1. Platelet receptors involved in adhesion, and aggregation.

Receptor	Location	Ligand	Reference
GPIb-IX-V complex	Platelet surface	vWF, Thrombin P-selectin, TSP1	(Nurden and Caen, 1975)
GPVI	Plasma membrane	Collagen, laminin	(Jung and Moroi, 2008)
$\alpha 2\beta 1$	Plasma membrane	Collagen	(Nieswandt et al., 2001)
$\alpha 5\beta 1$	Plasma membrane	Fibronectin	(McCarty et al., 2004)
$\alpha 6\beta 1$	Plasma membrane	Laminin	(Schaff et al., 2013)
$\alpha 5\beta 3$	Plasma membrane	Vitronectin, fibrin, vWF, osteopontin	(Gawaz et al., 1997)
$\alpha 2b \beta 3$	Plasma membrane	Fibrinogen, fibrin, vWF, TSP1	(Du et al., 1991)
CD148	Platelet surface	Thrombospondin-1	(Senis et al., 2009) (Takahashi et al., 2012)
CLEC-2	Plasma membrane	Podoplanin, Hemin	(May et al., 2009)

Following platelet adhesion and activation, the subendothelial matrix will no longer be exposed to the circulating platelets due to the obscuration of bound platelets, therefore an amplification phase is required for further cell recruitment. This amplification phase is highly regulated and is reliant on multiple receptors that bind to soluble mediators from neighbouring cells as well as platelets themselves which form the platelet plug and thrombus (Table 2). During this amplification phase, the majority of platelet receptors are utilised to assist in platelet activation and platelet recruitment, which in turn increases the thrombus size.

Table 2. Platelet receptors involved in the amplification phase of thrombus formation.

Receptor	Ligand	Reference
P2Y ₁	Adenosine diphosphate (ADP)	(Abbracchio et al., 2006)
P2Y ₁₂	ADP	(Kunapuli et al., 2003b)
PAR1	Thrombin	(Covic et al., 2000)
PAR4	Thrombin	(Covic et al., 2000)
Thromboxane A ₂ receptor (TP)	Thromboxane A ₂	(Paul et al., 1999)
PGE ₂ Receptor (EP3)	Prostaglandin E ₂ (PGE ₂)	(An et al., 1994)
PAF receptor	Platelet activating factor	(Doebber et al., 1985)
Lysophosphatidic acid receptor	Lysophosphatidic acid	(Gueguen et al., 1999)
Chemokine receptor	Chemokines	(Clemetson et al., 2000)
V1a Vasopressin receptor	vasopressin	(Launay et al., 1987)
A _{2a} adenosine receptor	Adenosine	(Varani et al., 1999)
B ₂ adrenergic receptor	Epinephrine	(Kobilka et al., 1987)
Serotonin receptor	Serotonin	(Mercado and Kilic, 2010)
Dopamine receptor	Dopamine	(Ricci et al., 2001)
P2X ₁	Adenosine triphosphate (ATP)	(Mahaut-Smith et al., 2004)
c-mpl	TPO	(Gurney et al., 1994)
Leptin receptor	Leptin	(Nakata et al., 1999)
Insulin receptor	Insulin	(Falcon et al., 1988)
PDGF receptor	PDGF	(Hart et al., 1990)

The final phase of haemostasis is the stabilisation of the thrombus, where platelets form direct and indirect bridges (Cossemans et al., 2013). This tight formation of cells allows for a much more powerful paracrine signalling between the platelets, facilitated by the formation of a fibrin mesh that restricts the diffusion of plasma factors and prevents the premature fibrinolysis. (Rivera et al., 2009). This tightly packed area of the thrombus is termed the core region, and it can be characterised by a high concentration of thrombin, and low solute transport (Figure 1-2). The core region is surrounded by the shell region, which is comprised of loosely adherent platelets with high solute transport and lower concentrations of thrombin (Welsh et al., 2014). The shell region is key for the downregulation of platelet activation, requiring the use of

different receptors (Table 3) (Swieringa et al., 2016, Ahmed et al., 2020). Failure in the downregulation of platelet agonists and recruitment in the shell region may result in total occlusion of the vessel.

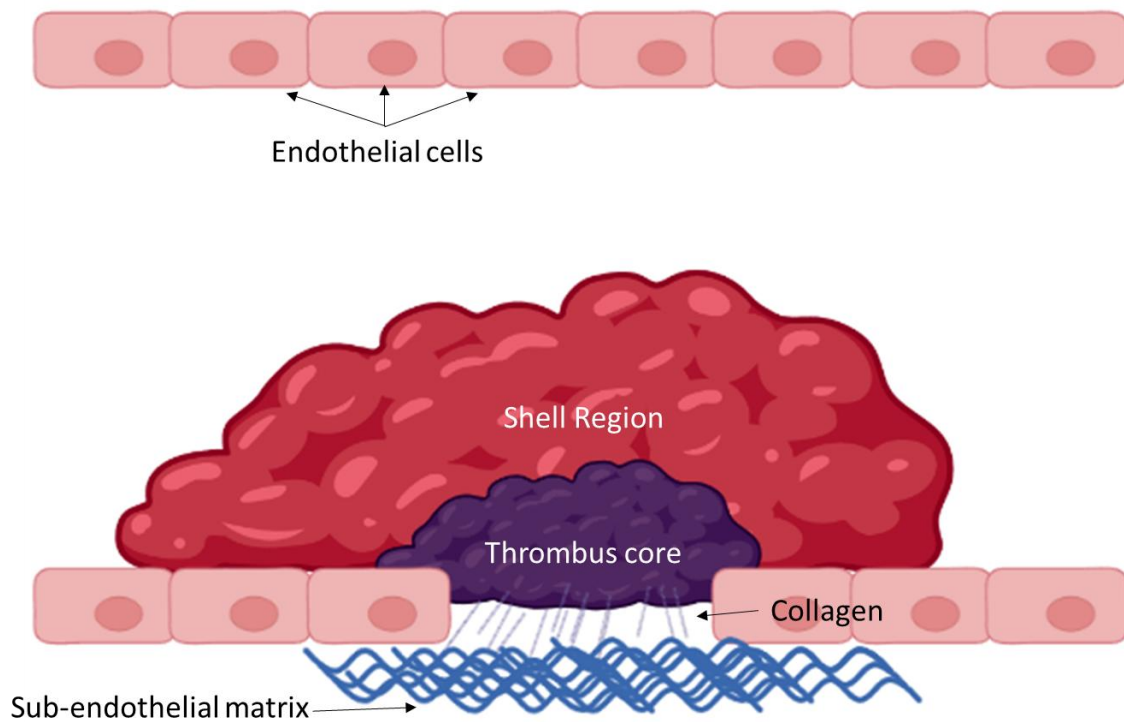


Figure 1-2. Structure of the thrombus in-vivo. The outer shell of the thrombus (red) exhibits platelets with lower concentration of soluble agonists, and smaller amount of fibrin. The thrombus core (purple) has significantly higher platelet activation markers and thrombin generation, it is also more tightly packed together with a fibrin mesh. (Biorender)

Table 3. Platelet receptors with known ligands in the stabilisation phase and negative platelet activators.

Receptor	Ligands	Role	Reference
Ephrin receptor (Ephr)	Ephrin	Stabilisation	(Rivera et al., 2009)
P-selectin	PSGL-1, GPIb, TF	Stabilisation	(Merten and Thiagarajan, 2000)
CD36	TSP1, oxLDL, VLDL	Stabilisation	(Golebiewska and Poole, 2015)
TREM-like transcript 1 (TLT-1)	Fibrinogen	Stabilisation	(Jessica et al., 2018, Noé et al., 2010)
VPAC1	PACAP	Negative regulation	(Noé et al., 2010)
CD31	PECAM-1, Collagen	Negative regulation	(Savchenko et al., 2014)
PGI ₂ receptor	Prostaglandin I ₂ (PGI ₂)	Negative regulation	(Yui et al., 1988)
PGD ₂ receptor	Prostaglandin D ₂ (PGD ₂)	Negative regulation	(Nishizawa et al., 1975)
PGE ₂ receptor	PGE ₂	Negative regulation	(Yamashita and Asada, 2008)

1.3.2. Platelet activation by collagen

Collagen is a key component of the extracellular matrix, present ubiquitously in the connective tissues. There are 28 variants of collagen, with type I collagen being the most abundant, comprising 90% of the total collagen (Ricard-Blum, 2011, Myllyharju and Kivirikko, 2001). Within the blood vessel, type I and III collagen are the major constituents, the ratios of these vary with growth and different diseases, such as ischemic heart disease (Xu and Shi, 2014). Both Type I and III are fibrillar collagens, which means they usually exist in bundles with more than one type and bind to multiple other matrix components. However, these can be broken down into their monomeric forms by peptidases. Collagen is comprised of a triple helix of three fibrils, the different fibrils present define the type of collagen that is observed. In the case of type I, it is comprised of 1 α_1 fibril and 2 α_2 fibrils, while type III collagen is comprised of 3 α_1 fibrils (Shoulders and Raines, 2009).

Collagen has been found to bind to several receptors on the platelet surface, however, the $\alpha_2\beta_1$ integrin and immunoglobulin superfamily member GPVI are the most notable (Nieswandt et al., 2001). Collagen interacts with $\alpha_2\beta_1$ in suspension but requires cross-linking or immobilisation to a surface at sufficient densities to stimulate platelet activation. GPVI binds to the GPO motif on collagen, however, due to the low affinity of the binding motif and its relatively low frequency on monomeric collagen, it is not able to adhere to platelets. The binding strength increases proportionally with the GPO motif count (Smethurst et al., 2007). Interestingly, it has been shown that when platelets bind with a singular GPO triplet, no activation occurs. However, when platelets bind with two or more GPO triplet's, platelet activation is observed (Smethurst et al., 2007). Additionally, confirmation of GPVI activation and binding was observed with the use of collagen-related peptide cross-linked (CRP-XL), which was able to induce platelet activation in the presence of $\alpha_2\beta_1$ blocking antibodies (Morton et al., 1995). The synthesis of a CRP-XL was created by inserting the GFOGER sequence into a $\alpha_2\beta_1$ and GPVI inactive backbone of GPP; importantly showing the peptide was able to mediate adhesion through $\alpha_2\beta_1$ (Knight et al., 1999, Knight et al., 2000).

GPVI is the major signalling receptor for collagen on platelets; it is in complex with Fc receptor γ -chain (FcR γ) on the platelet membrane and is responsible for collagen-induced platelet activation through the tyrosine phosphorylation cascade by Src-family kinases (Figure 1-3). GPVI contains 4 distinct regions, an Ig region, the mucin-like region, the transmembrane region, and the cytosolic region. GPVI is composed of two Ig domains, which are linked to a mucin-rich region, leading into the transmembrane region and the cytosolic tail. This transmembrane region has an arginine group which allows the association with FcR γ through the formation of a salt bridge. When collagen binds to GPVI alone, there is no observed signalling activity, however when interacting with FcR γ containing the immunoreceptor tyrosine-based activation motif (ITAMs), further signalling observed as confirmed by FcR γ deficient platelets (Boulaftali et al., 2014, Poole et al., 1997). The cytosolic tail of GPVI contains a proline-rich motif that binds to Src homology 3 (SH3) domains of Fyn and Lyn (Suzuki-Inoue et al., 2002, Nieswandt and Watson, 2003). This linking of GPVI to the SH3 domain and FcR γ brings these together spatially, allowing for the phosphorylation of the ITAM to take place and initialising the Src/SYK signalling cascade (Figure 1-3) (Turner et al., 2000). The activation of spleen tyrosine kinase (Syk) triggers a signalling cascade which in

turn activates phosphoinositide 3-kinase (PI3-K), nuclear factor of activated T cells (NFAT) and mitogen activated protein kinase (MAPK) pathways inducing the release of ADP from dense granules, by PLC γ 2, it also causes the release of TxA $_2$ by increasing intracellular calcium (Ca $^{2+}$) levels (Makhoul et al., 2020).

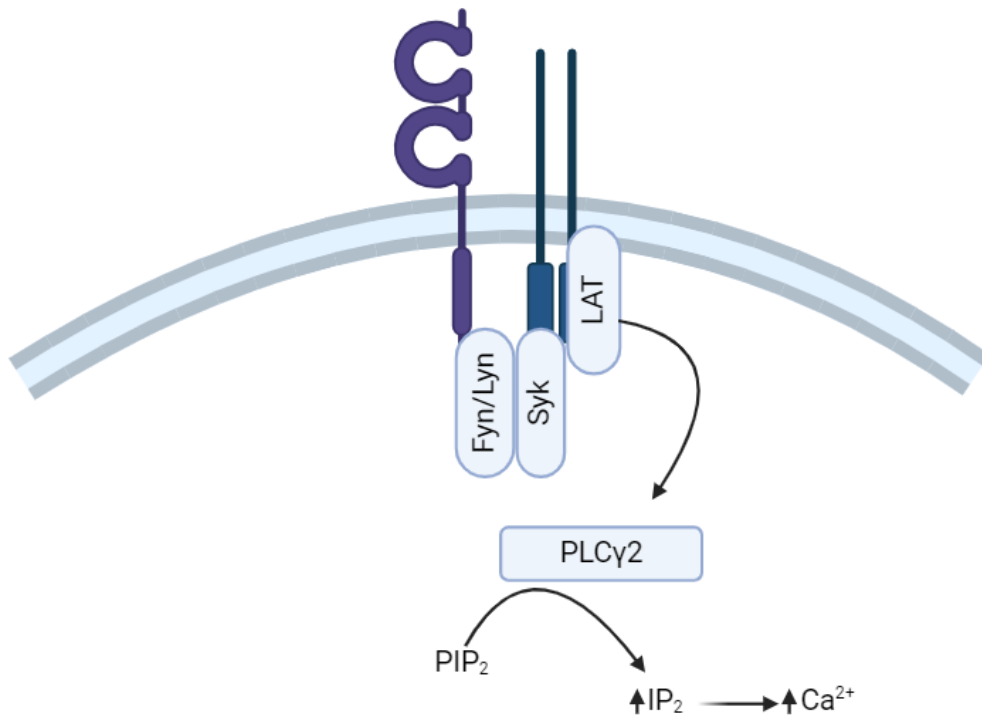


Figure 1-3. Collagen signalling mechanism. Collagen binds to GPVI and its homo-dimeric receptor FcR γ , triggering a signalling cascade initiated by tyrosine phosphorylation of the immunoreceptor tyrosine-based activation motif (ITAM) which is located on the tail of FcR γ . This phosphorylation causes recruitment and activation of the tyrosine kinase Syk, which phosphorylates and activates additional proteins such as LAT and PI3K which activates PLC γ 2, increasing cytosolic IP $_3$ levels, causing Ca $^{2+}$ release from the storage pool. Figure created using biorender.com.

1.3.3. Platelet activation by thrombin

Thrombin is a multifunctional serine protease generated in the liver and secreted into the circulation in an inactive zymogen form (prothrombin). This can then be converted to thrombin by prothrombinase in response to injury. Thrombin is the final enzyme in the coagulation cascade with a primary function of cleaving fibrinogen into fibrin, it also is a potent platelet activator through binding to GPIIb-IX-V and the cleaving of G protein-coupled Protease-activated receptors (PARs) at the N-terminal. Thrombin also enhances platelet adhesion by inactivating von Willebrand factor-cleaving protease (ADAMTS13) (a disintegrin and metalloprotease with thrombospondin type1 motif). Alongside its procoagulant role, thrombin also activates protein C, which degrades factor VIIIa and FVa. Thrombin also binds to endothelial protein C receptor (EPCR) which cleaves PAR1, resulting in downstream signalling (Schuepbach et al., 2012). PAR1 is also cleaved by the interaction of thrombin with the highly negatively charged C-terminal tail of GPIIb α , causing the reorientation of the protease exosite 1 resulting in the cleavage of the PAR1 exodomain (De Candia et al., 2001, Acquasaliente et al., 2022).

There are 4 members of the mammalian PAR family, PAR-1 and 4 in humans, and PAR-3 and 4 in mice (Estevez et al., 2014). PARs are irreversibly activated through proteolytic cleavage by thrombin; PAR1 is cleaved by thrombin only at R41 and PAR4 only cleaved at R47. When cleaved, the PAR becomes irreversibly activated, this cleavage results in a conformational change in the protein and alters affinity to intracellular G proteins (Macfarlane et al., 2001). Cleavage at specific sites results in different cellular responses, termed "biased signalling"; this is how PARs are able to induce protease-specific responses (Russo et al., 2009). PAR1 and 2 bind to multiple heteromeric G-protein subtypes, such as G_i, G_q and G_{12/13}, whereas PAR4 only binds to the latter three, and PAR3 is not believed to signal autonomously in platelets (Nakanishi-Matsui et al., 2000, Russo et al., 2009). The activation of the G-protein subtypes triggers a large signalling cascade, which can cause multiple cellular effects on the platelet including shape change, adhesion, secretion and activation. The interaction of G_q with Phospholipase C Beta (PLC β) causes downstream phosphorylation of both DAG and IP₃, which can both induce the release of Ca²⁺ into the cytosol or phosphorylate Protein kinase C (PKC), which can induce dense granule secretion (Konopatskaya et al., 2011, Steinhoff et al., 2005).

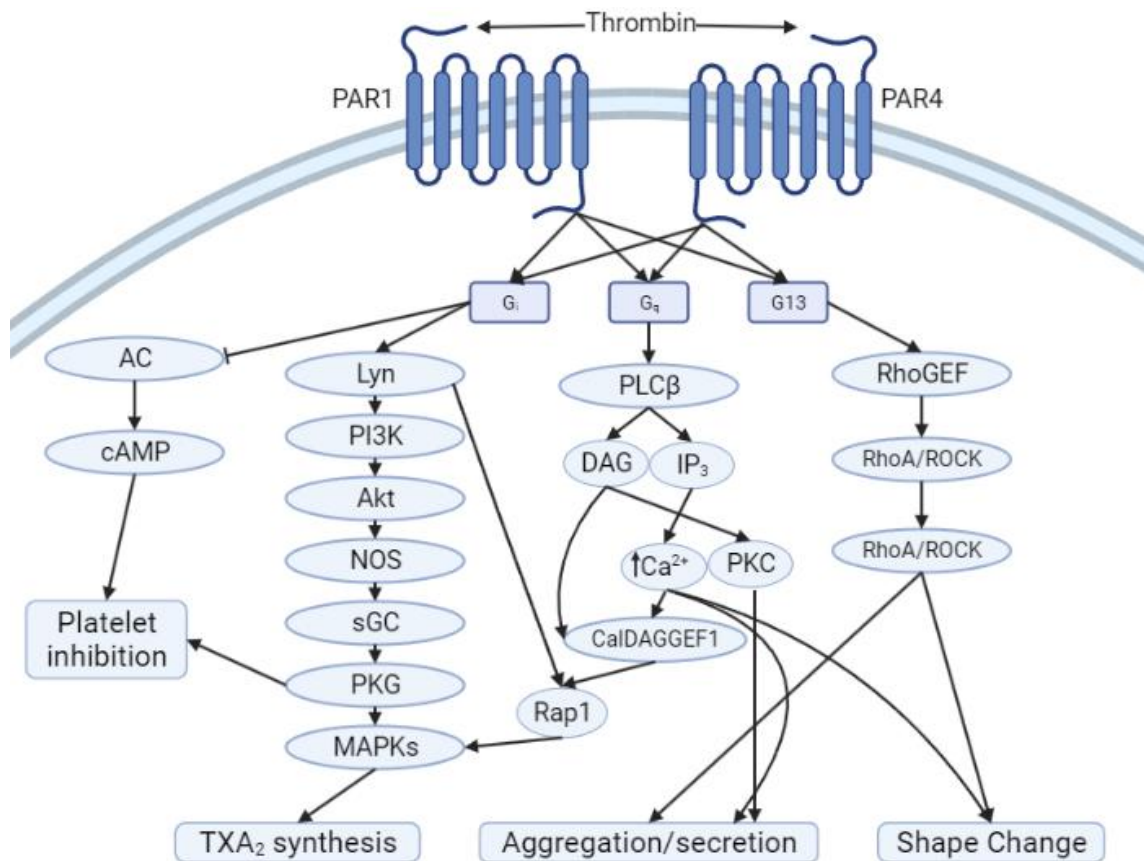


Figure 1-4. Signalling cascade when Thrombin cleaves PAR1 and PAR4 in platelets. Thrombin activates Gq G13 and Gi via the PAR receptors, Gq activate PLCβ which hydrolyses Phosphatidylinositol phosphate to diacylglycerol (DAG) and inositol trisphosphate (IP3) leading to PKC activation and the increased intracellular Ca²⁺ this pathway is also able to activate MAPKs to induce TxA₂ synthesis. Activation of G13 has been shown to activate RhoGTPase and exchange factors, activating the Rho/ROCK pathway to initiate shape change and secretion. When activated Gi results in PKG activation and inhibition of Adenyl cyclase (AC) which inhibits platelet inhibition, it also induces TxA₂ synthesis. Figure created using biorender.com.

Thrombin also activates factors V, VIII, and XI, which have a multitude of roles including further formation of thrombin on the cell surface, and the prevention of fibrinolysis. Thrombin also cleaves fibrinogen to fibrin, whilst activating factor XIII, enabling cross-linking of fibrin monomers creating a mesh like structure which stabilises the clot. Alongside this pro-coagulant role, thrombin is also able to mediate coagulation through its interaction with thrombomodulin on the endothelial cells of the blood vessel, which leads to fibrinolysis (De Candia, 2012).

A model of thrombus structure separates the structure into two parts, the core and the shell, in this model platelets are observed to have a non-uniform activation pattern dependant on their location within a thrombus (Hechler et al., 2010). They showed 2 distinct populations within the thrombi, the “core” of stable p-selectin expressing

platelets exhibiting higher thrombin dependency, and a more porous “shell” containing a much lower p-selectin expression, and to be dependent on ADP signalling with P2Y₁₂ which was a smaller region with more efflux of granules observed (Stalker et al., 2013).

1.3.4. Platelet activation by thromboxane A₂

Thromboxane A₂ (TxA₂) serves as a positive feedback mediator following platelet activation. TxA₂ is known as an eicosanoid, a family of lipids which are metabolised from arachidonic acid (AA). Due to the short half-life of around 30 seconds, it acts in an autocrine or paracrine manner to activate platelets directly adjacent (Nakahata, 2008). Initially, TxA₂ was characterised as being released from platelets, however, it has since been elucidated to be released from other cell types such as macrophages, neutrophils and endothelial cells (Touchberry et al., 2014). TxA₂ is also known to be a vasoconstrictor when activated during tissue injury and inflammation; working agonistically to prostacyclin (PGI₂) (Cheng et al., 2002). In platelets, the production of TxA₂ starts by the cleavage of AA from the phospholipid membrane, by phospholipase A₂. This then is processed by Cyclooxygenase 1 (COX -1) into prostaglandin H₂ (PGH₂), and then converted to TxA₂, by TxA₂ synthase. This process is slightly different in endothelial cells during cases of inflammation due to the presence of COX-2, which processes AA into prostacyclin (PGI₂), a major vasoactive prostanoid, mediating vasodilation and platelet inhibition (Smyth, 2010).

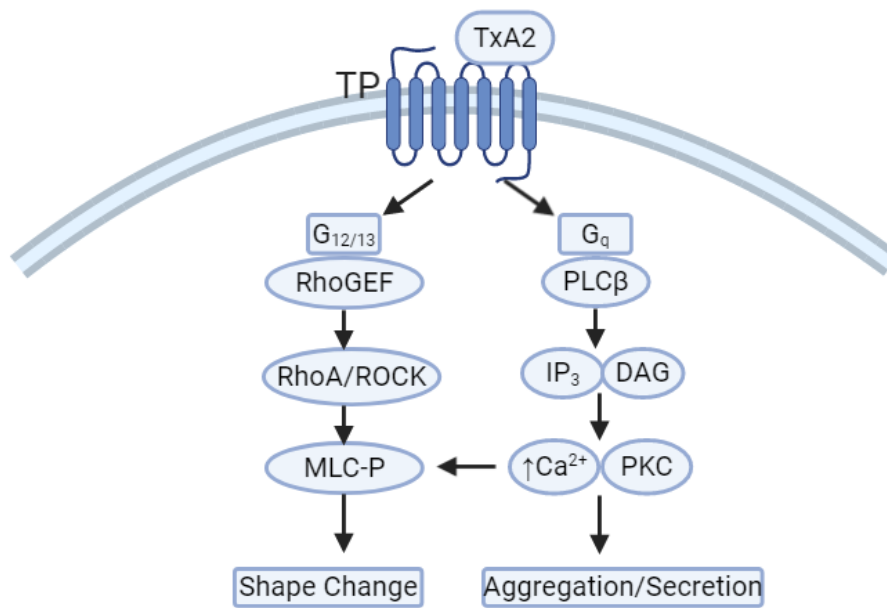


Figure 1-5. Signalling pathway induced via Thromboxane prostanoid (TP) receptor. When TxA2 binds to TP two pathways are activated, the activation of Gq stimulates the upregulation of CA2+ within the cytosol of the platelet, increasing aggregation, it also acts upon G12/13 inducing the activation of the Rho/ROCK signalling pathway which results in the movement of actin throughout the platelet causing shape change. Figure created using biorender.com.

While key for the function of platelets, TxA2 has been linked with multiple disease states such as acute myocardial ischemia, where TxA2 synthesis is increased. Most pathologies are related to vessel occlusion such as myocardial Infarction and atherosclerosis, however, TxA2 has also been observed to contribute to the pathogenesis of other inflammatory illnesses such as asthma, rhinitis, and atopic dermatitis. In multiple cases, the use of a COX-1 inhibitor such as aspirin is often used as a prophylaxis against vascular thrombotic events (Khan et al., 2019).

1.3.5. Platelet activation by ADP

ADP is a small molecule that is actively released from platelet dense granules; it is also passively released from damaged erythrocytes and endothelial cells. ADP is involved in further amplification of platelet activation, commonly known as secondary aggregation. Through the use of different agonists and antagonists, it was shown that there are two receptors for ADP on platelets, one that inhibits cyclic adenosine 3',5'-monophosphate (cAMP) synthesis, and another that activates Phospholipase C and induces shape change (Daniel et al., 1998). The release of ADP forms a positive feedback loop through its binding to the two G Protein-coupled Receptors (GPCRs), P2Y₁ and P2Y₁₂ (Remijn et al., 2002). When binding with the latter receptor, it has been found that TxA₂ generation is increased (van der Meijden et al., 2005, Shankar et al., 2006). The activation of the G_q-coupled P2Y₁ receptor by ADP causes PLC β activation, which hydrolyses phosphatidylinositol 4,5 trisphosphate (PIP₂) to generate the second messengers; inositol 1,4,5-trisphosphate (IP3) and 1,2-diacylglycerol (DAG). The latter in turn releases intracellular calcium stores and activates classical and novel isoforms of protein kinase C (PKC). There are no P2Y₁ inhibitors used in clinical practice, due to the receptor being expressed by many different tissues, meaning that these drugs could have multiple off-target effects (Kunapuli et al., 2003a).

P2Y₁₂ is the predominant receptor in ADP stimulated activation of GP IIb/IIIa, which results in TxA₂ production and prolongs platelet aggregation. The action of ADP P2Y₁₂ receptor also inhibits adenylyl cyclase, thus decreasing the formation of cAMP in platelets, an important regulator of platelet activity which inhibits platelet aggregation (Noé et al., 2010). ADP can be inhibited by the release of endothelium derived PGI₂ and nitric oxide (NO), these both raise platelet cAMP and guanosine 3',5'-cyclic monophosphate (cGMP) levels, which hydrolyse ADP into inactive Adenosine monophosphate (AMP).

Clinically, the P2Y₁₂ inhibitors - clopidogrel and ticagrelor, have been used as antiplatelet therapies in patients with cardiovascular and cerebrovascular disease. However, their mechanism involves the generation of a reactive metabolite which has an irreversible effect on P2Y₁₂. The metabolite generation itself also comes with the downside of a slow onset. Due to these factors, research into new P2Y₁₂ inhibitors is currently ongoing (Bennett, 2001). One new inhibitor, prasugrel, has been shown to have a greater and more rapid inhibition on platelet function, but still has a slower than desired onset (Golino, 2013).

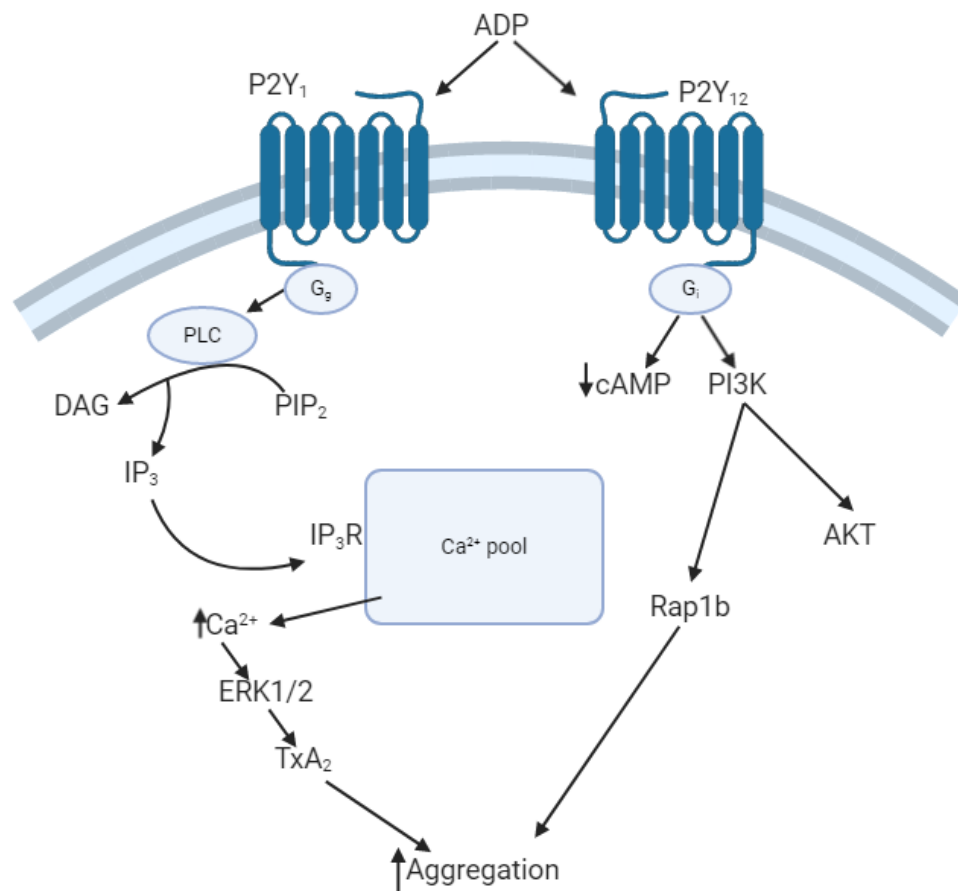


Figure 1-6. P2Y₁ and P2Y₁₂ signalling pathways. ADP binds with both P2Y₁ and P2Y₁₂. The former pathway P2Y₁ interacts with G_s stimulating the activation of PLC, which converts PIP₂ into DAG and IP₃. IP₃ then binds to IP₃R on the Ca²⁺ pool, causing a pore to open inducing calcium efflux into the cytosol. This interacts with ERK1/2 causing interactions with TxA₂ which stimulates aggregation. P2Y₁₂ interacts with G_s activating PI3K and reducing levels of cAMP by inhibiting adenylyl cyclase. The activation of the PI3K pathways leads to fibrinogen receptor activation, increasing platelet aggregation. Created with biorender.com.

1.4. Shape change

Inactivated platelets circulate in a small discoid conformation, protecting the cells from getting sheared in the bloodstream (Ghoshal and Bhattacharyya, 2014). When activated, platelets undergo a rapid reorganisation of the cytoskeleton, forming a spheroidal shape with pseudopodial protrusions, this conformation assists the platelet in its role in haemostasis (Warren, 1971, Aslan et al., 2012). The cytoskeleton of platelets comprises three main components: spectrin-based membrane skeleton, actin cytoskeleton, and the marginal microtubule coil. Each component of the cytoskeleton has a specific and specialised role within the platelet morphology. The membrane skeleton is formed primarily of spectrin and filamin, this is linked to the plasma membrane by GPIb-IX-V, giving structural integrity and flexibility (Hartwig and DeSisto, 1991). In a resting state, the microtubule coil forms a marginal band on the inner periphery to give the platelet its discoid shape. However, studies show that the marginal band is not required for the shape change process, only the maintenance of the resting shape (Patel-Hett et al., 2008).

Actin is the most abundant protein in platelets, making up over 10% of the protein content of the cell (Bearer et al., 2002). In resting platelets, cross linked F-actin associates with the spectrin based membrane skeleton, aiding its function. For platelet shape change to occur, the actin filaments must fragment. Following this fragmentation of actin filaments, they are reassembled creating lamellipodia and filopodia emanating out from the cells resulting in a much larger surface area (Shin et al., 2017). The shape change is largely mediated by gelsolin, adducin, and myosin light chain (MLC) phosphorylation, controlled through Ca^{2+} and Rho/Rho-kinase-mediated regulation of myosin phosphatase (Bauer et al., 1999). When activated through GPCR, ITAM receptor, or other ligands, Myosin light chain kinase (MLCK) is activated through PLC signalling pathways. Thromboxane receptor and PAR activation result in activation of myosin light chain phosphatase (MLCP) through the G_{13} cascade including Rho-ROCK signalling. Both result in MLC phosphorylation which then interacts with the actin filaments to generate the contractile forces required to remodel the platelet membrane.

1.5. Platelet aggregation

Platelet aggregation is the process by which platelets adhere to each other at the site of vascular injury. This process has 3 distinct mechanisms by which it occurs, depending on shear conditions (Frojmovic, 1998). Fibrinogen interacts with $\alpha\text{IIb}\beta\text{3}$, vWF, and fibronectin, all of which have been found to mediate platelet-platelet interactions, with the former most ubiquitous mechanism. This process involves the binding of the surface bound integrin $\alpha\text{IIb}\beta\text{3}$ to fibrinogen between multiple platelets forming a bridge between them. Integrin $\alpha\text{IIb}\beta\text{3}$ is the most abundant heterodimeric receptor on the platelet surface that plays a critical role in haemostasis due to its role of bidirectional communication. Bidirectional signalling allows platelets to regulate and respond to external conditions, these complexes are comprised of two noncovalently bound subunits α and β (Bennett et al., 2009). $\alpha\text{IIb}\beta\text{3}$ is maintained in a low energy state where the external domain is in a closed conformation, for this to open, inside-out signalling must occur; through the binding of c-Src to the cytoplasmic tail of the β3 integrin via the RGT motif on the SH3 domain (Durrant et al., 2017). Once this binding occurs, the integrin forms a conformation which allows it to bind to other ligands (such as fibrinogen) with a high affinity. Integrin clustering is required for the full activation of c-Src: this process involves the movement of integrins into proximity, which allows trans-autophosphorylation. Syk is a tyrosine kinase which binds to ITAMs; there are three ITAM receptors in human platelets: Fc γ R γ , which associates with GPVI, C-type lectin-like 2 (CLEC-2, for the glycoprotein podoplanin, and Fc γ RIIa which interacts with and allows for crosstalk with immune cells (Arman and Krauel, 2015). Syk can interact directly with the SH2 domain on the cytoplasmic tail of β3 , unlike ITAM binding, this is independent on the phosphorylation of the β3 domain. Syk can also associate with Fc γ RIIa through ITAM which has been hypothesised to be the typical mechanism for Syk activation of $\alpha\text{IIb}\beta\text{3}$ (Boylan et al., 2008).

1.6. Granular secretion

Once activated, platelets secrete over 300 active substances from their intracellular granules, with the 3 categories having specific contents and functions; these include adhesive proteins, growth factors, chemokines, and cytokines (Golebiewska and Poole, 2015, Manne et al., 2017). Platelet secretion affects multiple target cells including themselves, via autocrine signalling, this allows for the controlled orchestration of haemostasis and thrombosis alongside other functions. Platelets have a large amount of invaginated membrane structures throughout the membrane system called the open canalicular system (OCS); it is believed that these structures have three functions: to aid in granule secretion, give entry of external elements into the platelet, and for increasing membrane volume aiding in platelet spreading facilitation the formation of filopodia (Selvadurai and Hamilton, 2018, Chung et al., 2021).

The exact mechanism for the cargo release from granules is still poorly understood, there are currently three models with evidence supporting each. Jack-in-the-box mechanism, actin-driven granule constriction and channel-mediated granule swelling. Both jack—in-the-box and actin-driven granule constriction were initially identified in epithelial cells; however, channel-mediated granule swelling was initially seen in procoagulant platelets (Han et al., 2017, Erent et al., 2007, Agbani et al., 2018). The lattermost mechanism relies on the granule swelling prior to fusion due to water influx from the cytosol mediated by aquaporin-1 channels (Agbani et al., 2018). Actin-driven granule constriction has been well defined in other cell types; however, it is debated whether this mechanism is utilised in platelets. The actin cytoskeleton has been shown to interact with Soluble NSF (N-ethylmaleimide-sensitive factor) Attachment Protein Receptor (SNARE) proteins to assist in α -granule secretion (Rosado et al., 2000, Woronowicz et al., 2010). Interestingly a motif throughout all three mechanisms is the involvement of the SNARE complex for the binding of granules to the platelet membrane.

1.6.1. α -granules

α -granules are the most abundant granule within platelets, composing approximately 10% of the total platelet volume. In mature human platelets, α -granules are between 200-500 nm in diameter (Flaumenhaft, 2011). These granules differ from dense granules by their size, granularity and constituents; however, it is believed that there are multiple subtypes of α -granules which are differentially regulated and released (Italiano et al., 2008a). The overall data suggests that the α -granule is structured as a condensed and dehydrated matrix which must be decondensed during the exocytosis event (Wencel-Drake et al., 1985, van Nispen tot Pannerden et al., 2010). α -granules contain over 200 different polypeptides and cytokines such as vWF, platelet factor IV (PF4) and fibrinogen, which propagate activation and assist in thrombus formation (Table 4). Thrombospondin-1 (TSP-1) is highly concentrated in α -granules; when released this acts upon the thrombus binding to CD36 on the surface, stabilising by forming crosslinking platelets, (Kuijpers et al., 2014). With this CD36 binding, the cAMP PKA signalling cascade is inhibited through a tyrosine kinase signalling pathway via the phosphorylation of the Src kinases, mitogen-activated protein kinase 14 (P38) and c-Jun N-terminal kinases (JNK) (Roberts et al., 2010). P-selectin is a transmembrane protein that is specific to the α -granule, upon platelet activation it is translocated to the plasma membrane of the platelet, where it functions as a receptor for monocytes and neutrophils (Koedam et al., 1992). Platelet granule exocytosis is a regulated secretion event, the release rate and amount of granules involved is dependent on the strength of stimulation observed (Jonnalagadda et al., 2012). This has been confirmed by the observation of granules stimulated with varying concentrations of agonist, where lower concentrations initiated the release of individual granules, and higher concentrations resulted in the formation of multi-granular compartments (Eckly et al., 2016). It has also been found that with higher concentrations of agonists, the granules are more likely to fuse with the open canalicular system (OCS), however, this was not observed in other literature (Pokrovskaya et al., 2020). The speed of content release is believed to be affected by the length of the “neck” of the granule which was found to vary greatly (Pokrovskaya et al., 2018). There has been debate regarding receptor-dependent cargo release; however, a study by van Holten et al. (2014) observed that the stimulation of platelets using different receptors released statistically similar components and concentrations.

Table 4. Key components of α -granules and their functions.

Component	Function	Reference
Albumin	Transport	(Mikhailidis and Ganotakis, 1996)
Fibrinogen	Processed to form fibrin, platelet adhesion	(Alshehri et al., 2015)
Fibronectin	Platelet adhesion	(McCarty et al., 2004)
Vitronectin	Enhances platelet adhesion	(Gawaz et al., 1997)
Osteonectin	Enhances collagen binding	(Kelm et al., 1994)
Calcitonin	Calcium regulation	(Austin and Heath III, 1981)
Von Willebrand Factor	Platelet binding and activation	(Bennett et al., 2009)
Thrombospondin-1	Mediates Cell-cell interaction binds platelets	(Chen et al., 2000)
P-selectin	Mediates the interaction of activated platelets with leukocytes	(André, P. 2004)

1.6.2. Dense Granules

Dense granules are smaller in both number and size than α - granules, with 3-8 per platelet with an approximate diameter of 150 nm. They also appear much more granular than their counterparts (White, 1998). These granules are unique to platelets, and are a subtype of lysosome-related organelle (LROs), which are usually observed in cytotoxic T-cells (Ambrosio and Di Pietro, 2017). Dense granules contain a range of small molecules that are required for effective haemostasis (Table 5); defects in dense granules in platelets cause haemorrhagic disorders (Chen et al., 2018, Wei and Li, 2013). A study by Jonnalagadda and colleagues indicates that the release of dense granules is significantly faster than α - granules and is more sensitive to agonists (Jonnalagadda et al., 2012). Small molecules released act on circulating platelets, contributing to positive feedback sustaining aggregation (Golebiewska and Poole, 2015).

Table 5. Key components of dense granules and their functions.

Component	Function	Reference
Serotonin (5-HT)	Vasoconstrictor	(Duerschmied and Bode, 2009)
Histamine	Vasodilation	(Kilbourne and Winneker, 2001)
ATP	Provides energy	(Heemskerk et al., 2002)
ADP	Stimulates Secondary aggregation	(Makhoul et al., 2020)
Calcium	Thrombus formation	(Furie and Furie, 2008)
Magnesium	Platelet inhibition	(Ravn et al., 1996)
Glutamate	Increase platelet membrane fluidity	(Karolczak et al., 2017)

1.6.3. Lysosomes

Lysosomes are the third form of granule within the platelet, and they contain predominantly acid hydrolases (cathepsins, hexosaminidase, β -galactosidase, arylsulfatase, β -glucuronidase and acid phosphatase), alongside CD63 and lysosomal-associated membrane protein (LAMP)-1/2 (Israels and McMillan-Ward, 2005). The function of platelet lysosomes *in vivo* is poorly characterised, however, it has been speculated to have extracellular functions in receptor cleavage, fibrinolysis and degradation of extracellular matrix components (Heijnen and Van Der Sluijs, 2015). Platelets also can engulf bacteria and has been shown that the lysosomes have a role in the digestion of the phagocytic components they produce. The exocytosis of lysosome contents is slow and requires a higher stimulation threshold than that of both α - and dense- granules (Jonnalagadda et al., 2012).

Table 6. Key components of Lysosomes, and their functions

Component	Function	Reference
Cathepsin D	Protein degradation	(Tsukuba et al., 2000)
Cathepsin E	Protein degradation	(Tsukuba et al., 2000)
Carboxypeptidase A	Cleaves peptide bonds	(Van Oost, 1986)
Carboxypeptidase B	Cleaves single amino acids off proteins	(Van Oost, 1986)
Proline carboxypeptidase	Cleaves C-Terminals off proteins	(Van Oost, 1986)
β -N-axetyl-d-hexosaminidase	Breakdown of glycoproteins	(Van Oost, 1986)
β -D-Glucuronidase	Catalyses breakdown of β -D-glucuronic acid residues from glycosaminoglycans	(Van Oost, 1986)
β -D-galactosidase	Hydrolyses β -galactosides	(Van Oost, 1986)
CD63	Mediate Signal transduction	(Heijnen and Van Der Sluijs, 2015)
LAMP 1/2	Provide selectins with carbohydrate ligands	(Erbe et al., 1993)

1.6.4. T-granules

T-granules were identified recently in 2012 and were characterised by an electron-dense tubular morphology (Thon et al., 2012, van Nispen tot Pannerden et al., 2010). They were observed to contain large amounts of toll-like receptor 9 (TLR9), VAMP-7, and VAMP-8. Interestingly T-granules are also characterised to contain protein disulphide-isomerase (PDI), which is localised to the dense tubular system (DTS); this (alongside other studies) shows that T-granules belong to a reticular membrane network as opposed to being a granule (van Nispen tot Pannerden et al., 2009). Multiple studies have shown the release of PDI from activated platelets, but the direct fusion of the DTS to the cell surface has not been observed (Essex et al., 1995, Cho et al., 2008).

1.6.5. The Soluble NSF (N-ethylmaleimide-sensitive factor) Attachment Protein Receptor (SNARE) complex

The lipid bilayer structure of the cell membrane is stabilised by hydrophobic acyl chains separated by hydrophilic head groups, due to this repulsion the process of membrane fusion has a large energy barrier. This makes spontaneous membrane fusion either very slow or not possible, necessitating the use of fusion machinery proteins known as the SNARE proteins. The SNARE proteins are a super family comprising of more than 60 members, all of which contain a conserved coiled-coil stretch of amino acids termed the SNARE motif (Fasshauer et al., 1998). Advances in proteomic analysis, along with the use of knockout models, led to the delineation of this superfamily into v- and t- SNAREs in relation to their interaction with the vesicle or target membrane (Hong, 2005, Rothman, 1994). Further elucidation of these proteins and their mechanism of action resulted in the additional classification of R, Qa, Qb and Qc, the SNAREs are delineated by the presentation of amino acids at the ionic “central” 0 Layer with R presenting arginine and Q presenting glutamine (Yoon and Munson, 2018). A layer is defined as a full α -helical turn where the centre “0” layer is where 1 arginine and 3 glutamine residues form a polar centre, at contrast the otherwise hydrophobic SNARE bundle, the layers are then numbered in a positive direction towards the C-terminus and a negative towards the N- Domain (Fasshauer et al., 1998). The further classification of Q-a, -b, -c is dependent on the location of the SNARE within the four-helix bundle. Although not mutually exclusive, R-SNAREs are v-SNAREs and Q-SNAREs are usually t-SNAREs.

A

		-7	-6	-5	-4	-3	-2	-1	0	1	2	3	4	5	6	7	8																																					
Q-SNARES	Sx1a	RN	E	I	K	E	N	S	R	E	L	H	D	M	D	A	M	L	E	S	G	E	M	D	R	E	Y	N	V	E	H	A	V	D	Y	V	E	R	A	V	S	D	K	K	V									
	unc-64b	CE	D	M	K	E	S	S	R	E	L	H	D	M	D	A	M	L	E	S	G	E	M	D	R	E	Y	N	V	E	H	A	V	D	Y	V	E	R	A	V	S	D	K	K	V									
	Sx3	RN	D	V	R	E	S	S	K	E	L	H	D	M	D	A	M	L	E	N	G	E	M	D	N	E	L	N	V	M	H	T	V	D	H	V	E	K	A	R	D	E	K	R	M									
	Sx4	RN	E	I	Q	Q	L	E	R	T	R	E	L	H	E	I	T	F	A	T	E	E	M	G	E	M	N	R	E	K	N	L	S	A	D	Y	V	E	R	G	E	H	K	I	L									
	Sso1	SC	E	L	K	L	E	K	S	A	E	L	T	Q	L	N	D	E	E	L	V	E	Q	E	N	D	V	D	K	N	V	E	D	A	Q	L	D	V	E	Q	V	G	H	D	K	V								
	Sed5	SC	A	V	E	T	E	S	T	I	Q	E	V	G	N	L	Q	Q	A	S	M	Q	E	G	E	V	Q	R	D	A	N	V	D	D	I	D	L	N	I	S	G	A	Q	R	E	L	K	F						
	Sx5	RN	T	M	Q	N	E	S	T	I	V	E	L	G	S	I	F	Q	A	H	M	K	E	G	E	T	Q	R	D	E	N	V	L	G	A	Q	L	D	V	E	A	A	H	S	E	L	K	F						
	Vam3	SC	Q	L	G	R	I	H	T	A	V	Q	E	V	N	A	I	H	Q	G	S	L	K	E	G	E	Q	T	T	D	E	N	I	S	H	L	H	D	N	M	Q	N	A	N	K	Q	T	R	D					
	SNAP-25B	RN	S	T	R	R	L	Q	L	V	E	S	K	D	A	G	I	R	T	L	V	M	D	E	G	E	Q	D	R	V	E	E	G	M	N	H	I	N	Q	D	M	K	E	A	E	K	N	K	D	G				
	Syndet	MM	S	T	R	R	L	G	L	A	I	E	S	Q	D	A	G	I	K	I	T	M	D	E	G	E	Q	N	R	E	E	G	M	D	Q	I	N	K	D	M	R	E	A	E	K	T	T	E	N					
	SNAP-25	DM	S	T	R	R	L	A	L	C	E	E	S	K	E	A	G	I	R	L	V	A	D	D	E	G	E	Q	D	R	E	E	G	M	D	Q	I	N	A	D	M	R	E	A	E	K	N	S	G	E				
	Y22F5A.5	CE	S	T	R	R	L	A	L	C	E	E	S	K	E	A	G	I	K	I	L	V	M	D	E	G	E	Q	E	R	E	G	A	D	T	I	N	Q	D	M	K	E	A	E	D	H	K	G	E					
	Sec9	SC	S	T	R	N	L	K	M	A	Q	D	A	E	R	A	C	M	N	L	G	M	G	H	S	E	Q	N	N	V	E	G	N	D	L	M	K	V	Q	K	V	A	D	E	K	V	A	E	K					
	Spo20	SC	T	S	R	T	L	E	K	A	I	E	A	R	C	T	K	R	V	L	Q	Q	S	C	S	N	Q	T	K	I	E	S	N	C	D	M	L	K	I	Q	S	N	V	A	D	R	K	D	E	A				
	SNAP-25B	RN	N	I	E	Q	V	S	G	I	G	N	L	R	H	M	A	L	D	M	G	N	E	D	T	N	R	Q	D	R	M	E	K	A	D	S	N	K	T	R	I	D	E	A	N	Q	R	A	T	K	L			
	Syndet	MM	N	I	T	Q	V	G	S	I	G	N	L	K	N	M	A	L	D	M	G	N	E	D	A	N	Q	Q	Q	K	T	E	K	A	D	T	N	K	N	R	I	D	I	A	N	T	R	A	K	K	I			
	SNAP-25	DM	N	M	G	Q	V	N	T	M	I	G	N	L	R	N	M	A	L	D	M	G	S	E	N	O	N	R	Q	D	R	I	N	R	K	G	E	S	N	E	A	R	I	A	V	A	N	Q	R	A	H	Q	L	
	Y22F5A.5	CE	N	V	Q	V	S	T	M	V	G	N	L	R	N	M	A	I	D	M	S	T	E	V	S	N	O	N	R	Q	D	R	I	H	D	K	A	Q	S	N	E	V	R	V	E	S	A	N	K	R	A	K	N	I
	Sec9	SC	N	I	D	Q	I	Q	V	S	N	R	L	K	K	M	A	L	T	G	K	E	D	S	Q	Q	K	R	I	N	N	E	E	S	D	D	I	D	I	N	L	H	M	T	N	R	A	G	R					
Spo20	SC	N	I	E	Q	I	K	A	V	S	G	D	L	K	I	M	A	H	A	G	R	E	E	A	N	T	R	F	D	I	E	N	N	V	Q	A	D	N	A	I	Q	A	K	R	Y	R	E	K	I					
Bet1	SC	Q	G	A	G	Q	R	K	A	K	S	L	S	L	K	M	G	D	E	R	G	S	N	Q	T	D	Q	G	D	T	F	H	N	S	V	K	L	K	R	T	F	G	N	M	E	A								
mbet1	MM	L	E	S	R	S	K	V	T	A	I	K	S	L	S	I	E	L	G	H	E	K	N	O	N	K	L	A	E	D	S	Q	D	S	T	G	F	L	G	K	T	M	G	R	K	I	S							
Vti1	HS	S	E	R	S	H	R	I	A	T	E	D	Q	I	G	S	E	I	E	E	G	E	O	R	D	Q	E	R	K	S	R	V	N	T	S	E	N	L	S	K	S	R	K	I	R	S	S							
Vti1	SC	R	K	D	A	S	R	I	A	N	E	F	E	G	I	C	S	Q	M	M	D	R	S	O	R	E	T	E	N	R	Q	T	L	F	Q	A	D	S	Y	V	D	K	S	I	K	T	T							
Membrin	RN	S	Q	N	I	H	H	G	M	D	L	I	G	G	H	S	T	L	E	G	R	A	O	R	L	T	K	G	Q	K	K	L	D	T	A	N	M	I	G	L	S	N	T	V	A	R	L	E						
Bos1	SC	V	E	R	G	N	A	Q	I	D	Y	I	L	E	M	S	Q	S	F	E	N	V	E	O	N	K	I	T	S	K	Q	D	R	S	N	S	L	R	T	I	G	V	S	E	Q	T	S	N						
Vam7	SC	E	V	A	F	H	R	I	I	Q	A	Q	R	G	L	A	L	E	M	N	E	E	Q	T	N	E	L	T	A	E	D	D	V	D	M	T	G	R	R	L	Q	I	A	N	K	K	R	H	N					
R-SNARES	Sb2	RN	R	Q	Q	Q	A	Q	V	D	E	V	V	D	I	M	R	V	N	V	D	K	L	E	S	D	Q	K	S	E	D	D	R	A	D	A	L	Q	A	G	A	S	Q	P	E	T	S	A	K	K				
	cb	RN	R	Q	Q	Q	A	Q	V	D	E	V	V	D	I	M	R	V	N	V	D	K	L	E	S	D	Q	K	S	E	D	D	R	A	D	A	L	Q	A	G	A	S	Q	P	E	T	S	A	K	K				
	Sb	HM	R	Q	Q	Q	A	Q	V	D	E	V	D	M	R	V	N	V	D	K	L	E	S	D	Q	K	A	E	D	G	R	A	D	A	L	Q	A	G	A	S	Q	P	E	A	S	G	K	K						
	Sb1	CE	R	Q	Q	Q	A	Q	V	D	E	V	V	G	I	M	K	V	V	E	K	L	E	S	D	Q	K	S	Q	D	D	R	A	D	A	L	Q	E	G	A	S	Q	P	E	K	S	A	T	K					
	Snc1	SC	R	A	E	Q	A	E	T	D	D	T	V	G	I	M	R	D	N	I	N	K	A	E	G	E	R	T	S	E	D	K	A	D	N	L	A	V	S	A	Q	G	Y	K	R	G	A	N	R					
	Sb7	MM	K	V	M	E	Q	A	Q	V	D	E	K	G	I	M	V	R	N	I	D	L	V	A	Q	G	E	R	E	L	I	D	K	E	N	L	V	D	S	V	T	K	T	R	N	A								
	Sb5/6	MM	E	K	Q	Q	Q	A	D	E	V	T	E	I	M	L	N	F	D	K	L	E	S	H	G	K	A	E	E	Q	R	S	D	Q	L	D	M	S	S	A	S	K	T	K	T	A								
	Nyv1	SC	I	G	D	A	E	D	Q	I	K	D	Y	I	Q	I	M	N	D	I	D	K	L	E	S	Q	E	R	S	L	V	D	K	T	S	Q	I	N	S	S	N	K	F	R	R	K	V	N	K					
	Sec22	SC	N	D	Q	N	Q	E	V	G	V	K	Q	I	M	S	K	N	I	E	D	L	Y	A	G	D	S	D	K	S	D	M	S	S	L	K	E	T	S	K	R	V	R	K	S	Q	E	N						
	Sec22b	MM	N	G	S	I	N	T	E	L	Q	D	V	Q	R	I	M	V	A	I	E	E	L	Q	G	E	A	S	A	D	S	K	A	N	N	L	S	S	L	S	K	K	V	R	Q	D	K	Y	N					
	Tomosyn	RN	G	E	G	V	K	G	A	S	G	V	V	G	E	L	A	R	L	A	D	E	S	G	Q	K	S	D	E	E	R	T	A	A	M	S	S	A	D	S	S	K	H	A	H	E	M							

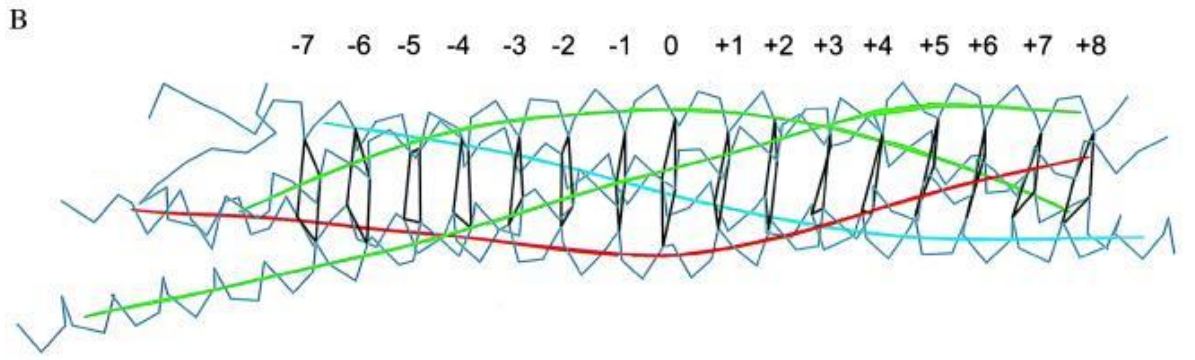


Figure 1-7. parameters delineating Q- R-SNARE quantification.(a) known SNARE complex proteins and their amino-acids presented at each layer of the complex. (b) structural diagram of the SNARE complex (Fasshauer et al., 1998).

The interaction of the SNARE motifs on both R and Q SNARE families form a highly stable four-helix bundle called the trans-SNARE complex; this complex drives the vesicle and target membranes together. The process of membrane fusion can be delineated into 4 steps: tethering, docking, priming and fusion with target and

membrane mixing (Bonifacino and Glick, 2004, Ramakrishnan et al., 2012, Jahn et al., 2003) (Figure 1-8). To achieve this, the assembly of the complex starts at the N-terminus and proceeds through 16 layers past the 0 layer to the C-terminus in a zippering mechanism (Weber et al., 1998). This “zippering” begins with the unzipping of the linker regions, followed by the carboxyl-terminal and finally the SNARE portion. The zippering of the SNARE complex is energetically favourable, with an estimated release of 65 $k_B T$, this additional energy generated by the assembly of the trans-SNARE complex is then used to drive the lipid bilayer fusion (Gao et al., 2012). Following the completion of the SNARE complex zippering it becomes a cis-complex within the target membrane; the Synaptosomal-Associated Protein (SNAP) proteins with ATPase NSF (*N*-ethylmaleimide-sensitive factor) can then dissociate the cis-SNARE complex to be reused within the cell.

This mechanism is similar in multiple cell types; however, it has been observed to be differentially controlled depending on the spatiotemporal activity of the cell, and the cell type itself. Initially, it was thought that N-terminal domains of the SNARE proteins did not affect the specificity of fusion between membranes, however, in later research this was contested (Paumet et al., 2004, Koike and Jahn, 2019). Research also shows that the N-terminal is instrumental in the selective recruitment of tethering factors, which is required to maintain specificity of membrane fusion. Additionally, initial tethering selection SNARE proteins have been observed to bind in specific combinations, further aiding accurate delivery and trafficking (Jahn and Scheller, 2006, Fasshauer et al., 1998, Koike and Jahn, 2019, Reales et al., 2011).

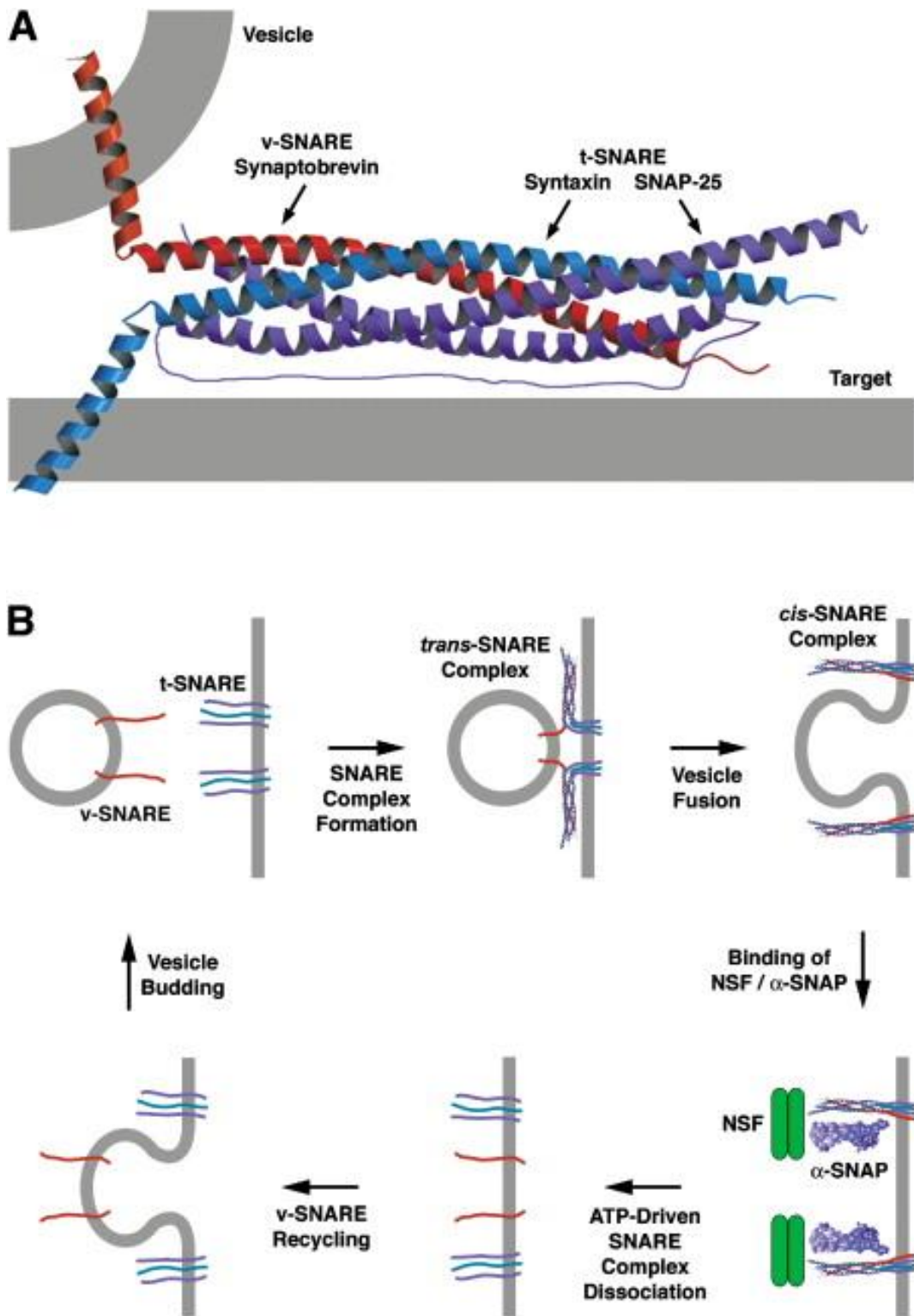


Figure 1-8. Structure and function of the SNARE complex. The current model of the SNARE complex is comprised of 4 alpha-helices, comprising the v-SNARE synaptobrevin, t-SNARE Syntaxin, and a soluble component in the form of SNAP-25. (A) The stepwise process of vesicle binding with the membrane during secretion followed by the recycling of SNARE components back into the cytosol, vesicles travel towards the target membrane, once in close proximity, if phosphorylation occurs the trans-SNARE complex is formed between the v-SNARE, t-SNARE and SNAP proteins. This pulls the membranes closer together, and causes vesicle fusion to the membrane, NSF and α -SNAP then binds to this complex, which leads to the ATP-driven SNARE complex dissociation, causing v-SNARE recycling (B).

1.6.6. Vesicle-associated membrane proteins (VAMP)

The V-SNAREs (vesicle-associated membrane proteins (VAMPs)) are a family of 7 members, VAMP1-5, 7, and -8. Each VAMP has been characterised to have a specific role, however, the true extent of their localisation and full role remains unknown (Table 7). A recurring theme between all 7 VAMPs is that they reside in post-Golgi vesicular compartments and mediate vesicle fusing. The members of the VAMP family which have been observed in platelets are VAMP 2, 3, 7, and 8, with the lattermost two having shown to be the most important in the context of granule release. This was due to the observation that the deletion of VAMP2 and 3 combined with VAMP 8 deletion is cumulatively worse than each deletion on its own, but VAMP 2,3 deletion had little effect when VAMP7 and 8 were present. These data suggest that VAMP 8 is the dominant (but not exclusive) VAMP responsible for the control of platelet secretion (Ren et al., 2007, Joshi et al., 2018, Feng et al., 2002).

VAMP3 was first identified in human platelets in 1999, and has been shown to interact with SNAP-23 and Syntaxin (STX) 2 within platelets; it is highly homologous to VAMP-1 and -2 making it a member of the “brevin” family (Feng et al., 2002, Bernstein and Whiteheart, 1999). However, it was later observed that the platelets of VAMP2/3 knockout mice had unimpaired secretion; suggesting they were either not absolutely required or were part of a redundant mechanism. VAMP7 was first identified to be involved with exocytosis within epithelial cells, unlike VAMP-2, -3 and -8, it contains an N-terminal extension called the longin domain (Martinez-Arca et al., 2000). The longin domains have been shown to be involved with membrane trafficking and regulation of the SNARE complex formation, they achieve this regulation by folding back onto the fusion inducing SNARE coiled-coil domain, inhibiting membrane fusion (Vivona et al., 2010). VAMP8 was originally identified to be involved with the fusion between early and late endosomes, resulting it being named “endobrevin” (Antonin et al., 2000a). Initially, VAMP8 was thought to only interact with STX-7, -8, and vesicle transport through interaction with t-SNAREs homolog 1B (VTI1b) to form endosomal fusion complex, but has since been observed to also bind to SNAP-23 and STX-11 in platelet exocytosis of dense- and α -granules alongside lysosomes (Ye et al., 2012, Antonin et al., 2000b, Diao et al., 2015). There is a ranked redundancy observed with VAMPs within platelets, with VAMP-8 being the most important for secretion, followed by VAMP-7 with VAMP-2 and -3 providing only a minor role. Interestingly, in VAMP-7

knockout mice, platelets displayed a defective spreading phenotype. VAMP7 also localises differentially to VAMP8, suggesting it has a separate unelucidated role (Sharda and Flaumenhaft, 2018). Similarly to VAMP7, VAMP3 has been associated with a separate role within the platelets, linked with endocytosis of viral particles and resultant activation (Banerjee et al., 2020).

Table 7. VAMP family and their roles within the body.

VAMP/ additional name	Role	Location	Reference
1 / synaptobrevins	Regulate neurotransmitter release	Neurons within the brain skeletal muscle,	(Liu et al., 2011b)
2 / synaptobrevins	Regulate neurotransmitter release	Neurons within the brain	(Yan et al., 2022)
3 / cellubrevin	Exocytosis of secretory granules, integrin trafficking	Ubiquitous platelet α -granule	(Ligeon et al., 2014)
4	Transport from the Golgi, within the cell	Trans-golgi network Ubiquitous	(Tran et al., 2007, Zeng et al., 2003)
5	Constitutive exocytosis	Muscle cells	(Zeng et al., 2003)
7/ synaptobrevin-like -protein 1 (SYBL-1)	Constitutive exocytosis	Ubiquitous secretory granules and endosomes	(Vivona et al., 2010)
8 / endobrevin	Both endocytosis and exocytosis fusion of autophagosomes with endosomes and lysosomes	Early endosomes, pancreatic acinar cells, platelets. Ubiquitous	(Ren et al., 2007)

1.6.7. Syntaxins

The t-SNARE (Q-SNARE) component of the SNARE complex resides on the target membrane and mediates fusion, the t-SNAREs present in human platelets are syntaxin-2, -3, -4, -7, -8 and -11 (STX). Different STX bind with certain SNAPs and v-SNAREs, due to the association of different VAMPS with alternate structures, which dictates what cargo is released (Yu et al., 2013). Syntaxins are comprised of 3 main domains, the N-terminal regulatory Domain, the SNARE domain and the C-terminal transmembrane domain. STX-11, unlike most STX members, lacks a trans-membrane domain (TMD), which makes STX-11 functionally reliant on a lipidic membrane anchor associated with the platelet membrane cholesterol-dependent lipid rafts through palmitoylation of C-terminal cysteine (Zhang et al., 2018, Dieckmann et al., 2015b). The Habc domain is the N-terminal regulatory domain present on syntaxin, it forms a three-helix bundle that has the ability to fold back on itself, resulting in the closed conformation of the protein (Margittai et al., 2003). Syntaxins bind with synaptogamin in a calcium-dependent manner, through interaction with voltage dependent calcium and potassium channels within the SNARE domain (Chapman, 2002). Between the C terminal transmembrane domain and the SNARE domain lies a linker region; the linker region of the STX protein is required for force transmission from the zippering action of the SNARE complex to the membrane, triggering membrane fusion (Jahn and Fasshauer, 2012).

Several reports show that VAMP-8 is a key regulator for dense granule secretion and can form a complex with STX-11 in platelets ((Golebiewska et al., 2015). Knockout studies have shown that STX-8 deficient mice lack only dense granule secretion, whereas STX-11 knockout significantly reduces secretion of all α - and dense granules, with a moderate reduction of lysosomal secretion. Knockout studies of STX -2 and -4 yielded no difference from wild-type (Ye et al., 2012, Sepulveda et al., 2013). The SNARE complex and secretion pathway in platelets was initially assumed to use the same mechanism as that observed in other cell types such as neurons and parotid cells, however, recent research found the secretion mechanism in platelets is similar to Natural Killer (NK) cells. Unlike many other cell types such as pancreatic and parotid cells which rely heavily on STX-2 and -4, platelet secretion mechanisms rely heavily on STX-11 which is unique to blood cell lineage exocytosis mechanisms. Unlike NK

cells, platelets secretion regulation has been linked to rely more on Rab27b, similarly to some neural cells. Although the proteins may differ from those in other cell types the stepwise mechanism remains the consistent (Tang, 2015).

1.6.8. Synaptosomal-Associated Protein (SNAP)

Synaptosomal-associated proteins (SNAPs) are anchored to the cytosolic face of membranes, they do not have a transmembrane domain (Chapman et al., 1994). The SNAP family consists of 4 members, SNAP-25, -23, -29 and -47, however, only SNAP -25 and -23 are involved in regulation of exocytosis. The most highly characterised member is SNAP-25, which is key for the release of neurotransmitters from the synapse. SNAP-23 is found more ubiquitously and is studied particularly in platelet biology (Kádková et al., 2019). The SNAP proteins provide two of the four α -helices present in the SNARE complex and are required for the docking and fusion phase of granule secretion. Studies have shown that SNAP-23 and -25 can partially compensate if the other is not present, however other members of the family lack this compensatory mechanism (Delgado-Martínez et al., 2007). Once granule exocytosis has completed, SNAP proteins have been shown to have the capability to disassemble the SNARE complex for further exocytotic events (Söllner et al., 1993). It has also been shown that nitric oxide inhibition of granule secretion is in a part due to the reversible inhibition of these SNAP proteins (Morrell et al., 2005). SNAP-23 has also been shown to be essential for platelet development (Cardenas et al., 2021).

1.6.9. The functional SNARE complex in platelets

Using loss-of-function studies, it has been identified that the predominant SNARE complex triad utilised in platelets is highly likely to be the STX-11, VAMP8 and SNAP23 mechanism regulated by RAB27b, Syntaxin binding protein 2 (munc18b) and unc-13 homolog D (munc13-4). However, this is contested due to the incomplete ablation of secretion with the removal of one of any of its members; this is highlighted by the interaction of STX-11 with vesicle transport through interaction with t-SNAREs 1B (VTI1b) (Offenhäuser et al., 2011). VTI1b is also expressed in platelets and is known to regulate endosome and lysosome fusion in macrophages. Studies also show that the interaction of STX11 with VTI1b and STX8 contribute to the secretion of dense granules and reduced embolization rates (Golebiewska et al., 2015, Ren et al., 2007).

It is known that multiple members of the SNARE complex bind promiscuously to other members of the SNARE complex, which may explain the redundant binding observed in platelets which are present due to their aforementioned differential roles within the cell (Banerjee et al., 2020, Ren et al., 2007). The SNARE proteins are closely associated with the actin cytoskeleton, and it can modulate the response (Morales et al., 2000). Latrunculin A (LatA) is a toxin which has been shown to depolymerise actin filaments, which, when added to platelets inhibits α -granule release; highlighting the importance of actin reorganisation. Filamin A has been observed to interact with STX11 and SNAP23 to propagate granule release (Flaumenhaft et al., 2005, Golla et al., 2022, Fujiwara et al., 2018, Woronowicz et al., 2010). The SNARE complex has also been observed to interact with multiple other proteins within the platelet such as gelsolin, actin-related protein 2 (ARP2)/3 and WASP family member 1 (WASF1) (Hong et al., 2015, Poulter et al., 2015).

1.6.10. Associated proteins and regulation

The regulation of secretion is key for cellular function. To achieve this, multiple mechanisms are in place to regulate secretion; the first of which is the resting inactive state of the SNARE proteins. Alongside this, there are multiple mechanisms involved in the regulation of secretion, such as the localisation of SNARE proteins to district membranes, requiring movement along the cytoskeleton, inhibitory domains present on the proteins (Habc domain), and regulatory molecules. These associated proteins are involved with the modulation of SNARE function, affecting the biological specificity and activity (Table 8).

In Munc13-4 knockout mice, platelets exhibited highly impaired capacity for exocytosis of all granule types. This is analogous to familial hemophagocytic lymphohistiocytosis type 3 (FHL3) in humans that is caused by a mutation in the UNC13D gene which encodes the Munc13-4 protein (Croizat et al., 2007, Meeths et al., 2011). Munc13-4 is an effector of Rab27b, Rab27 is a Ras-like small GTPase known to regulate intracellular membrane traffic (Hutagalung and Novick, 2011). Rab27A and Rab27B are widely expressed in various tissues, and both interact with the same effectors, however, they have been shown to perform different roles, even within the same cell type (Ostrowski et al., 2010). Rab27b has been found on the membrane of dense

granules and is thought to promote motility or enhance tethering and fusion with the platelet membrane (Tolmachova et al., 2007, Seabra and Coudrier, 2004, Fukuda, 2006). In knockout studies of Rab27b mice, secretion of dense granules was significantly decreased and the amount of granules moderately declined (Feng et al., 2014). Munc13-4 also contains the MUN domain that is involved in vesicle priming, the C2 domain in the N-terminal binds to the plasma membrane in a Ca²⁺ manner facilitating tethering of granules (Boswell et al., 2012).

Platelets express all homologs of Munc18, (-1, -2 and -3) the Munc18 protein binds to syntaxins to form a tight complex basally, termed the “closed” form; this makes it unavailable for other SNARES (Dulubova et al., 1999). To transition to an “open” conformation, interactions between Munc18 and -13 are required, which makes the SNARE domain of STX favour VAMP and SNAP proteins instead (Ma et al., 2011, Zhang and Hughson, 2021, Yu et al., 2013). Munc18-2 knockout mice saw a significant reduction in granule release, and a resultant haemostatic defect that was not observed in munc18-1 or -3 knockouts. Munc18-3 has also been observed to interact with STX4 to keep it in a closed state (Houng et al., 2003, Reed et al., 1999).

Tomosyn (STX-BP5) was first discovered as an STX1 binding protein from rat cerebral tissue, and was found to co-localise with STX1 in synapse-forming regions (Zhu et al., 2014b). STX-BP5 has since been observed to be expressed in many other tissues, and mutations cause thrombotic risk factors (Smith et al., 2011). Furthermore, STX-BP5 knockout models exhibited a significant bleeding phenotype coupled with a significant decrease in α -granule and lysosome release, coupled with mispackaging of granules due to changes in protein content amounts. Whilst platelets exhibited reduced secretion capabilities of vWF and histamine, secretion of these factors from endothelial cells was increased (Zhu et al., 2014a).

Vacuolar protein sorting-associated protein 33 (VPS33) is a spliceosomal (SM) protein, and is a subunit of the HOPS (homotypic fusion and protein sorting) and CORVET (class C Core Vacuole/endosome tethering) structures, which are key in regulating endocytic traffic (Lo et al., 2005, López-Berges et al., 2017). Like the Munc proteins, VPS33 is involved in intracellular vesicle trafficking, bringing them close together facilitating zippering from the amino-terminal ends. When mutated in patients with ARC syndrome (arthrogryposis, renal dysfunction, and cholestasis), platelets

have reduced aggregation, and have an absence of α -granules (Weyand et al., 2016). Interestingly, VPS33 is not present in platelets, only their progenitor MK cells further highlighting the heterogeneity of the SNARE complex in different cell types, even as closely related as platelets and MK (Lo et al., 2005). The HOPS complex in conjunction with RAB proteins have been proposed to target membranes from long distances to assist in quality control and aid in granule movement, these have also been referred to as SNARE Chaperones (Zhang and Hughson, 2021). Another protein which has been associated in SNARE chaperoning is α -synuclein through interactions with SNAP-25 and Munc13/18 (Sharma et al., 2011, Yoo et al., 2023).

Table 8. Known SNARE complex regulatory proteins in platelets.

Protein	Function	Reference
Munc18-1	Regulating syntaxin availability	(Gerber et al., 2008)
Munc13-4	Ca ²⁺ sensor at rate-limiting priming steps in granule exocytosis	(Boswell et al., 2012)
RAB-27 a + b	tethering secretory lysosomes at the plasma membrane	(Elstak et al., 2011)
STXBP5 (tomosyn-1)	Regulate binding with STX4 an 1	(Zhu et al., 2014a)
Complexin	controls the transfer of the force generated by SNARE complex assembly to the fusing membranes	(Trimbuch and Rosenmund, 2016)
synaptotagmin (SYTs)	mediates vesicle docking and displacing complexin	(Malsam et al., 2012)
Multisubunit tethering complexes (MTC)s	Regulation of tethering	(Baker and Hughson, 2016)
VTI1b	Late endosome homotypic fusion	(Offenhäuser et al., 2011)
Munc18-2 (STX-BP2)	directs SNARE fusion activity in a spatial and temporal manner	(Misura et al., 2000)
VPS33	Intracellular vesicle trafficking and α -granule development	(Lo et al., 2005)

1.7. The synuclein family

The synuclein family is a group of proteins originally isolated from neural cells in 1988 by Maroteaux et al. (1988), due to its localisation to the nuclear envelope of neurons they were named synuclein. Simultaneously, α -synuclein was identified as the non-amyloid- β component (NAC) found in amyloid plaques (Siddiqui et al., 2016). There are three distinct protein groups within the synuclein family: α -, β -, and γ -, all of which have been identified in human, murine and bovine models (George et al., 1995). The synuclein family was later recategorised as phosphoneuroproteins, and they are encoded for by SNCA, SNCB, and SNCG respectively in the location chromosome 4q21.3–q22 (Shibasaki et al., 1995). All 3 genes are composed of 5 coding exons and three 5' exons, the former of which are all well conserved SCNA contains alternative splice sites at exons 1 and 2, and 4 and 6, this, however, is not observed in SNCB, and SNCG. Rat coding DNA for the synucleins: SYN1 (α), SYN2 (β), and SYN3(γ) also have been observed to have similar splice variants as SNCA. Both human and rodent sequences are very similar, only differing in a few amino acids throughout the length of the protein resulting in an 86.7%, 98.5%, and 87.7% homology (Touchman et al., 2001).

Synucleins are small with a calculated molecular mass of around 14KDa, although testing shows that α -synuclein in particular can aggregate together tetramERICALLY causing it to appear as 56KDa (Lashuel et al., 2013). All human synuclein proteins have a highly conserved amino-terminal with variable number of 11-residue repeats and a less-conserved carboxyl terminal, β -synucleins have a deletion of 11 amino acids within their repeat domain in comparison to α - and γ - variants. The residue repeats forms the “KTKEGV” repeat motif, a d apolipoprotein-like class-A2 helix; this motif mediates binding to phospholipid vesicles and normal tetramerization of the proteins. (Perrin et al., 2000, Dettmer et al., 2015). Through proteomic analysis it was revealed that α -synuclein is the only member of the synuclein family present in platelets (Burkhart et al., 2012, Stefaniuk et al., 2018).

1.7.1. α -synuclein

α -synuclein is the most highly characterised of the synuclein family, and is found in several tissues throughout the body, however, is primarily found in neural tissue, making up 1% of all proteins in the cytosol of brain cells. Many other cell types in the periphery express α -synuclein, such as polymorphonuclear neutrophils (PMNs), red blood cells (RBCs) and platelets, with platelets having the highest concentration per mg of cellular protein at 264 ± 36 ng (Barbour et al., 2008, Hashimoto et al., 1997). α -synuclein is encoded by the SNCA gene, which consists of 6 exons ranging in size from 42 to 1110 base pairs. The predominant form is the full length protein, however, other shorter isoforms have also been observed (Venda et al., 2010). Most notably, in neurons it has been shown that α -synuclein regulated neurotransmitter release and the transport of synaptic vesicles (Cabin et al., 2002).

α -synuclein is comprised of three domains: N-terminal lipid-binding α -helix, amyloid-binding central domain (NAC) and C-terminal acidic tail (Figure 1-9). It can present as an α -helix when in association with phospholipids, or unfolded when in the cytosol similarly to its presentation in neural cells (Ahn et al., 2002, Stefaniuk et al., 2022). The N-terminal domain is positively charged with seven 11-AA repeats, each with a highly conserved KTKEGV hexameric motif (Sode, 2007). The NAC domain is composed of non-polar side-chains and is found in the centre of α -synuclein, which is involved with fibril formation and the aggregation of α -synuclein (Rajagopalan and Andersen, 2001). The C-terminal domain is a highly acidic tail of 43-AA presented in a random coil structure which is easily manipulated by changes in the pH. Further investigation into the structure of α -synuclein shows that it is a natively unfolded protein in the IDPs family; it is characterised by low hydrophobicity, low complexity and high net charge (Lee et al., 2007).

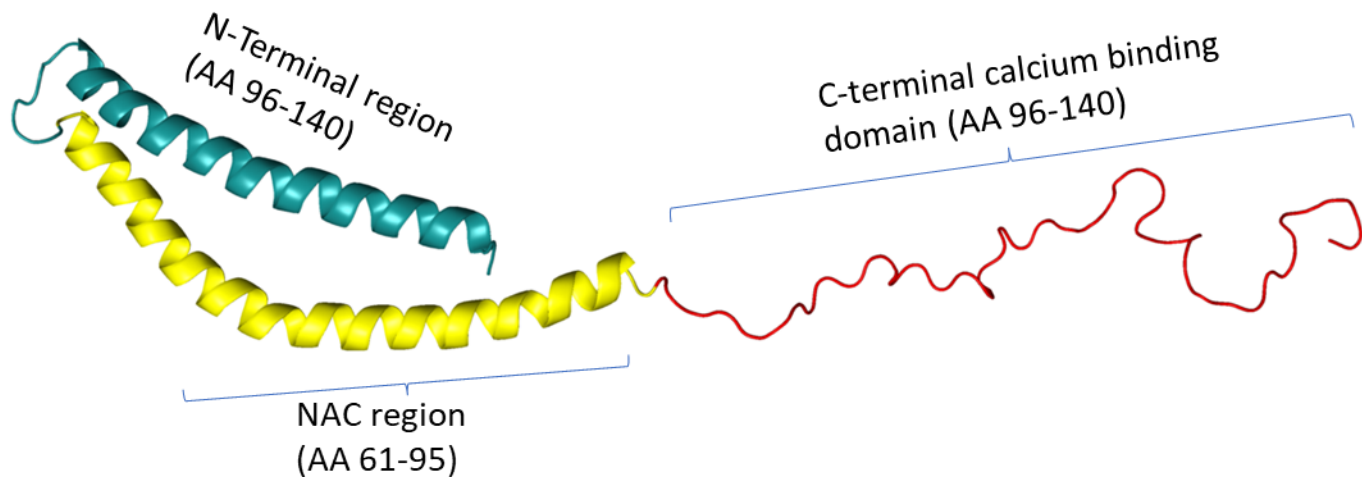


Figure 1-9. Ribbon Diagram of the Structure of a monomer of α -synuclein. The N terminal is an amphipathic α -helix separated into 2 regions, AA 1-60 involved with membrane binding, and AA 61-95, which is involved in regulation of α -synuclein function. The C terminal AA 96-140 is involved with Ca^{2+} binding and chaperoning roles. Pink regions highlighted are common point mutations, which have been heavily associated with Parkinsons disease (RCSB PDB).

In vitro studies have shown that α -synuclein preferably binds to small unilamellar- or large unilamellar- vesicles, with a diameter ranging from 10nm to $1\mu\text{m}$, but will bind with larger membranes (Pfefferkorn et al., 2012, Wang et al., 2010a). This is mediated by the aforementioned N-terminal due to its lysine rich structure containing multiple class A2 lipid-binding helices, it is suggested to bind to anionic lipids electrostatically (Perrin et al., 2000). This is concordant with findings that α -synuclein preferably binds to specific acidic head groups; phosphatidylethanolamine, phosphatidic acid (PA), phosphatidylinositol, and ganglioside opposed to phosphatidylserine or phosphatidylglycerol (Pfefferkorn et al., 2012). Binding of α -synuclein to membranes was shown to coincide with a significant increase in α -helix content; the transition occurs when α -synuclein inserts into hydrophobic acyl chains; taken with previous data, this indicates that α -synuclein has a preference for interacting with membranes containing unsaturated fatty acids with small anionic head groups and high curvature (Wang et al., 2010a). Interestingly, when binding with different membranes the formation of α -helices was different; when binding to sodium dodecyl sulfate (SDS) micelles, two anti-parallel helices (Val3- Val37 and Lys45-Thr92) were observed, whereas when binding to a lipid bilayer a single curved α -helix containing residues 1-90 was formed (Jao et al., 2008, Ulmer et al., 2005). There are two known mechanisms by which α -synuclein binds to membranes, termed binding mode SL1

and SL2, these are dependent on the lipid to protein stoichiometry. When high enough, SL1 is preferential, binding with the first 22AA residues, otherwise, SL2 is used which involves binding with the first 97 residues (Bodner et al., 2009a).

α -synuclein was found to be loosely associated with the plasma membrane, organelles and α -granules within platelets (Figure 1-8), as well as extracellular platelet-derived macrovesicles (Xiao et al., 2014, Tashkandi et al., 2016, Abeliovich and Gitler, 2016). While α -synuclein's role in neurotransmission has been extensively studied, its role(s) in platelets remains largely unknown; a study by Park et al., (2002) indicates a negative regulation on calcium dependent α -granule release preventing degranulation. Due to the increased blood plasma levels of α -synuclein following storage and some disease states multiple studies have focused on the effects of exogenous α -synuclein. These studies show that exogenous α -synuclein prevents the release of von-Willebrand factor from weibel-palade cells, and that α -synuclein inhibits the PAR1 induced expression of P-selectin (Kim et al., 2010, Acquasaliente et al., 2022). Interestingly, studies have also shown that patients with Parkinson's disease (PD) exhibit platelets with an abnormal morphology; being larger with a more pronounced OCS, and that are less sensitive to stimulation with both thrombin and ADP, resulting in a decreased risk of ischemic stroke and blood clots (Sharma et al., 1991, Pei and Maitta, 2019, Chang et al., 2020).

Further Investigations of PD patients show an inflammation and immune dysfunction; it has been shown that microglial cells may become activated by α -synuclein aggregate secretion, as well as activation of the innate immune response (Roodveldt et al., 2008, Koçer et al., 2013, Factor et al., 1994). Interestingly, studies have suggested that α -synuclein may regulate both B and T cell related responses. A study by Xiao et al. (2014) showed that α -synuclein^{-/-} mice significantly inhibit B cell lymphopoiesis and IgG production (Kim et al., 2004, Shin et al., 2000). Alongside aberrations in platelet function observed in PD patients, using α -synuclein overexpression or α -synuclein knockout mouse models, it was observed that the protein plays an important role in maturation and function of multiple haemopoietic lineages (Xiao et al., 2014, Shameli et al., 2016, Tashkandi et al., 2018, Tashkandi et al., 2016).

Table 9. Elucidated roles of α -syn within the body.

Function	Target	Mechanism	Result	Reference
Suppression of apoptosis	Protein kinase C	Deactivation of NF κ B	Protection of cell	(Sugeno et al., 2008)
Regulation of glucose level	GPCR in the pancreas	Increase glucose uptake, inhibit insulin secretion	Diabetes resistance	(Rodriguez-Araujo et al., 2015)
Chaperone SNARE/Vesicle	Presynaptic membrane	Maintenance of SNARE complex during assemble	Correct SNARE complex assembly	(Burré et al., 2010, Smith et al., 2020)
Membrane remodelling	phospholipids	Acidic head group binds to the α -synuclein	Remodeling of the vesicle membrane	(Bodner et al., 2009b)

1.7.2. α -synuclein in disease

The structure of α -synuclein has been shown to be present in different conformations, in patients with synucleinopathies. They can arrange into oligomers, protofibrils and fibrils which are mostly detected in Lewy bodies. In PD it has been observed that these conformations can result in lipid dysregulation resulting in oxidative stress, interestingly it was also observed that platelet activating factor-acetylhydrolase (PAH-AH) activity was significantly decreased in PD patients (Seet et al., 2010). Although platelet count is normal in most cases, small subsets of patients do exhibit platelet abnormalities. When interrogated, it was observed that 32% of patients with a platelet abnormality, 9.4% of patients also presented with thrombocytopenia, 11% with prolonged Bleeding time, 18% with prolonged closure time of Platelet function analyser-100 (Chou et al., 2022)(Figure 1-10).

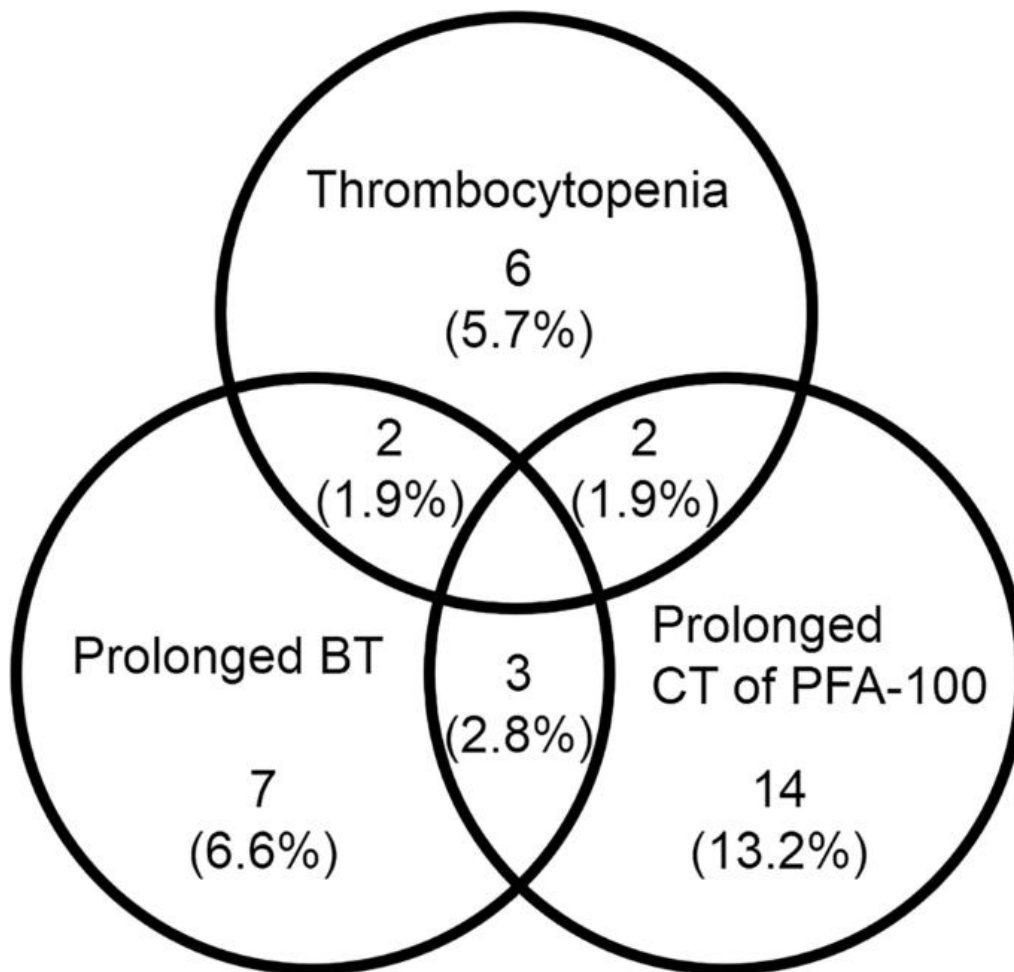


Figure 1-10. Biomedical assessment of patients with Parkinson's disease. The number and percentage of patients with thrombocytopenia, prolonged closure time of platelet function analyzer 100 (CT of PFA-100), and/or prolonged bleeding time (BT) in 106 patients with Parkinson's disease.

There are characterised point mutations within the SNCA gene at A30P, E46K and A53T encoding for α -synuclein that are heavily associated with familial autosomal-dominant forms of PD (Hardy et al., 2009, Nalls et al., 2011, Polymeropoulos et al., 1997). In families with the A53T mutation, 85% of affected individuals show clinical features that are more progressive with earlier onset than sporadic PD. The global structure of α -synuclein was not observed to be affected by these mutations, however, NMR spectroscopy revealed the mutation of A30P strongly reduced the propensity for N-terminal helical structure formation (Bussell and Eliezer, 2001, Li et al., 2002b, Greenbaum et al., 2005). The A53T mutation reportedly results in a lightly increased propensity for extended conformations, although this was limited to a small region around the mutation itself (Bussell and Eliezer, 2001). While the E46K mutation resulted in slight changes in monomeric conformation, it enhanced the contacts in the

N- and C- termini, reportedly modifying the long-range transient structure of the protein, however this is contested (Bertoncini et al., 2005, Sung and Eliezer, 2007). All three mutations resulted in accelerated α -synuclein aggregation, with the A30P mutation promoting oligomer formation and the A53T and E46K mutations promoting fibrilization; showing that the modest changes to the primary structure have much larger effects on the secondary structure to promote its aggregation.

Utilising both transgenic mice and flies for the α -synuclein mutants A30P and A53T motor deficits, neuronal inclusions and extracellular α -synuclein deposits similar to PD have been observed (Feany and Bender, 2000, Masliah et al., 2000). Furthermore, *in vitro* studies of co-cultured over- and under-expressing α -synuclein dopaminergic cells show direct neuron-to-neuron transmission of α -synuclein aggregates forming Lewy-like inclusions (Desplats et al., 2009).

1.7.3. The Role of α -synuclein in the SNARE complex

A number of studies have indicated the interaction between α -synuclein and the SNARE complex in neurons such as with VAMP8 and -2, however, this has not been assessed within the context of platelet secretion (Burré, 2015, Burré et al., 2010). Throughout human tissue studies, α -synuclein has been linked to multiple interaction partners, notably with multiple SNARE protein members, although this does not discriminate upon cell-type (Figure 1-11). The standard conformation of α -synuclein in the cytosol is the full-length disordered strands, however, other conformations have been observed such as oligomeric α -synuclein (O- α -syn) which have been observed to affect its functionality. In red blood cells, O- α -syn is often upregulated; these different conformations may have an effect on its function, PD patients with particularly upregulated O- α -syn induced an inflammatory phenotype (Daniele et al., 2018, Liu et al., 2022).

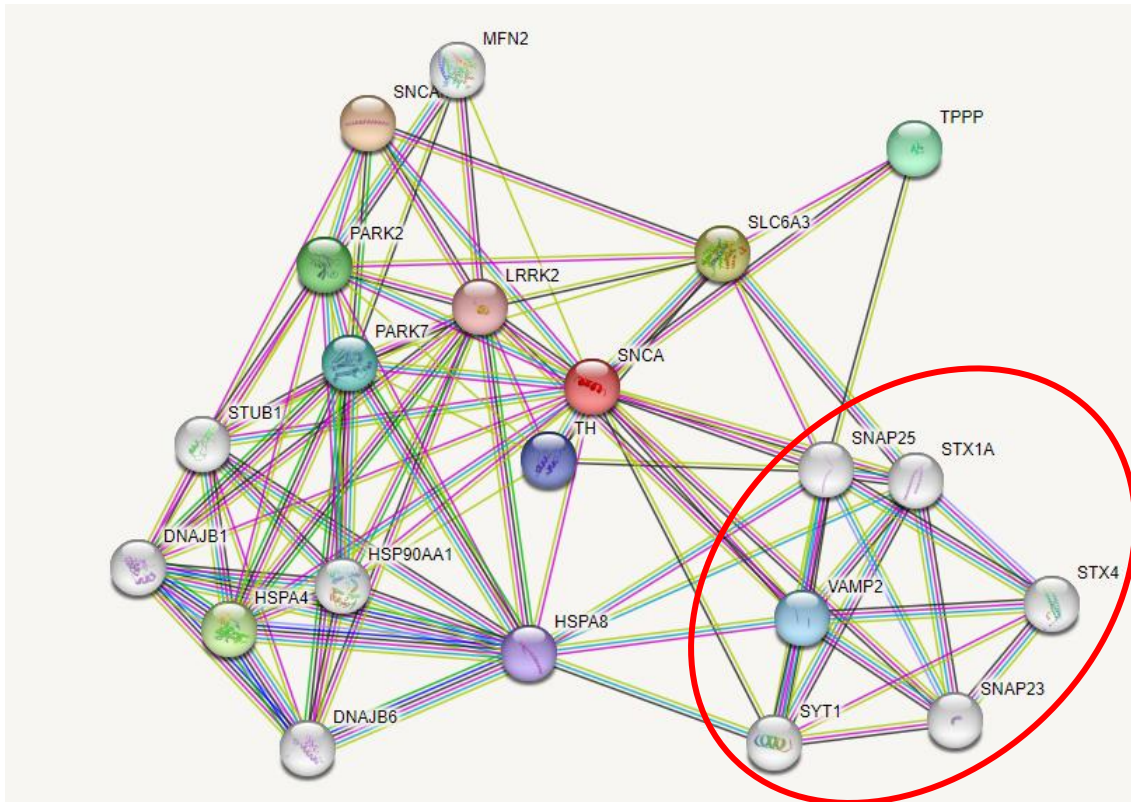


Figure 1-11. String analysis of α -synuclein protein interactions in homo sapiens. Limited to 20 interactions, SNARE proteins circled in red (String-db).

The SNARE regulatory protein Munc18-1 and α -synuclein have been shown to interact with each other in neurons, with Munc18-1 performing a chaperoning role (Chai et al., 2016). Studies have shown that a complex chaperoning system is present for SNARE complex formation, and the interactions of α -synuclein with VAMP2, and ,8, alongside membrane bound proteins which also perform a regulatory effect on Syntaxin proteins (Deshpande and Rodal, 2016, Hawk et al., 2019). Further studies utilising overexpression models demonstrate an inhibition to neurotransmission, with *in vitro* studies corroborating this (Lai et al., 2014, Nemani et al., 2010). However, this was refuted in later research, showing that inhibition of neurotransmission only occurs with α -synuclein aggregation after binding with VAMP2, and unaggregated α -synuclein binding can have up to a 10-fold increase in binding activity (Choi et al., 2013). In concordance with this, using a single-vesicle-to-supported bilayer assay, it was shown that the vesicle docking was significantly higher with increased concentrations of α -synuclein (Hawk et al., 2019). It was proposed that α -synuclein binds to the VAMP protein on the vesicle and binds to the target membrane or Munc protein to facilitate

chaperoning, this can then be inhibited by the oligomerisation of α -synuclein in significantly increased concentrations or mutations (Figure 1-12) (Hawk et al., 2019, Lou et al., 2017).

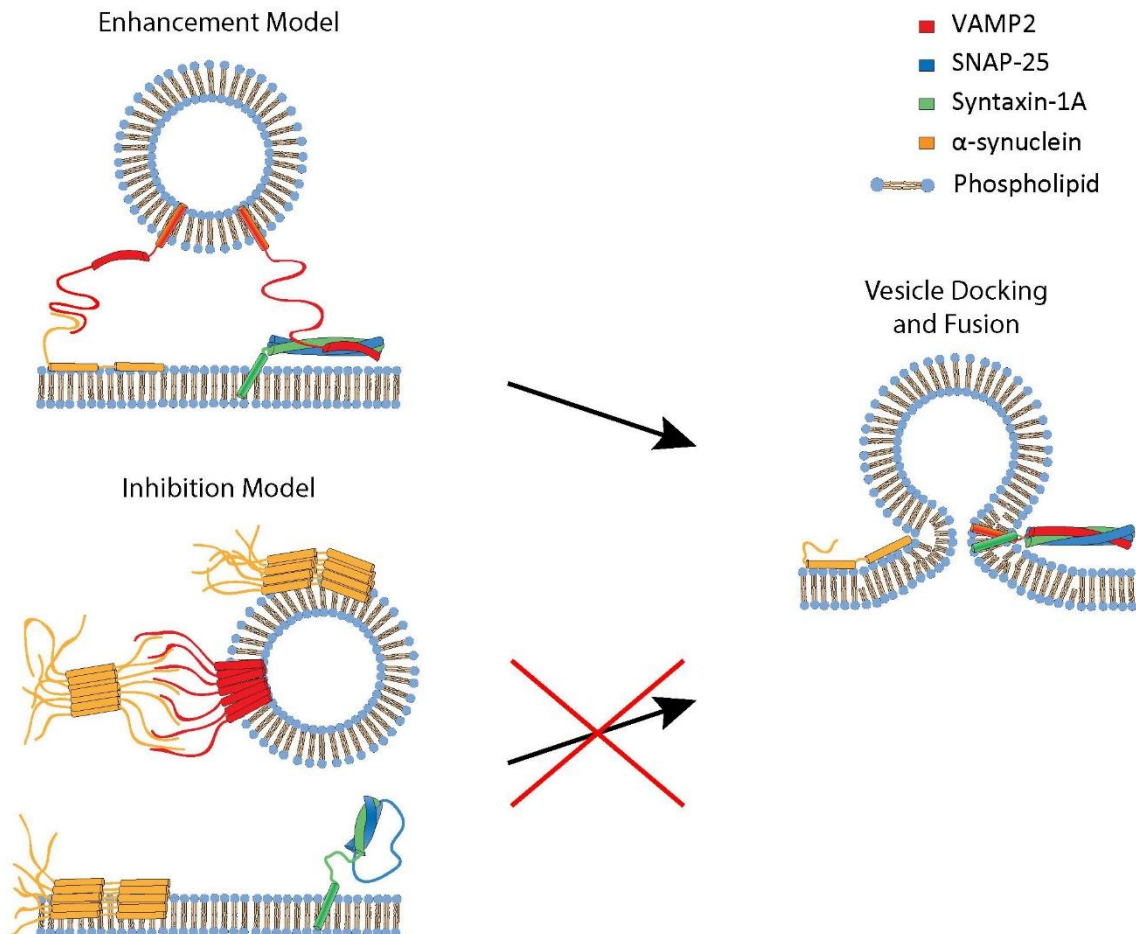


Figure 1-12. proposed α -synuclein interaction within the SNARE complex in neurons. The interaction of the C-terminus with VAMP2 facilitates chaperoning of vesicles and draws it to a proximity where the SNARE complex can dock and fuse the vesicle to the membrane. If α -synuclein oligomerises it binds as normal with VAMP2, and to the membrane but due to competitive inhibition is unable to chaperone the vesicle towards the target membrane.

1.7.4. Post translational modifications of α -synuclein.

α -synuclein undergoes multiple post-translational modifications (PTMs) all of which have an effect on the structure and role of the protein; from increased membrane binding to pathological processes, such as aggregations, Lewy body formation and neurotoxicity (Okochi et al., 2000). PTMs observed on α -synuclein include phosphorylation, ubiquitination, nitration, truncation, and O-GlcNAcylation, however, many of their functions have not been characterized (Zhang et al., 2019).

Phosphorylation is the best studied α -synuclein PTM, and the addition of a phosphate group to serine129 and -87 are a key indicator of synucleinopathies within the brain. These modifications have been shown to promote the formation of cytoplasmic inclusions in some cells. Interestingly, in dementia with Lewy body brains, 90% of the insoluble α -synuclein is phosphorylated at S129, compared to only 4% of soluble cytosolic α -synuclein (Anderson et al., 2006). Furthermore, it has been reported that α -synuclein can be phosphorylated at tyrosine -125, -133 and -135, with no apparent impact on its function (Burai et al., 2015).

The second most common PTM in α -synuclein is ubiquitination, mainly at the lysine residues K6 -10 and -12, The ubiquitination at these sites has shown to influence α -synuclein localisation and its degradation. Ubiquitination at K46 and -6 is a common modification, which targets them for proteasomal degradation within the cell by ubiquitin-specific proteases such as USP30,-33 -8 and -15 (Wang et al., 2022). Alongside this, α -synuclein can be ubiquitinated at sites K6 and -23; this has been shown to inhibit fibre formation, whereas ubiquitination at K96 both inhibits fibre formation and the structure of fibres created, causing them to not lie parallel to one another (Nonaka et al., 2005, Lee et al., 2008, Moon et al., 2020). Interestingly, recent studies have shown that, in PD patients, the polyubiquitination of α -synuclein at K6 -27 -29 and -33 is highly prevalent in the Lewy bodies, and as such have been termed atypical ubiquitination and have been shown to be crucial for the development of PD (Buneeva and Medvedev, 2022).

Nitration of α -synuclein at tyrosine residue 39 (Y39) is linked to accelerating the oligomerisation of α -synuclein, alongside increased rates of apoptosis due to mitochondrial impairment (Jones, 2012, Danielson et al., 2009). Interestingly, when Y39 is not available for nitration the formation of dimers is highly favoured. Common

mutants of α -synuclein have mutations at Y125F, Y133f and Y136F which can crosslink easily with Y39 nitration forming a highly helical structure forming oligomers (Burai et al., 2015, Kaylor et al., 2005). Concentration of nitrated α -synuclein at residues Y39, -125, -133, and 136 found in Lewy bodies, which has been associated with the elevated levels of oxidative stress present in these diseases (Giasson et al., 2000, Liu et al., 2011a). Alongside this, truncation of the C-terminals from residues 109-140 are frequently observed in Lewy bodies, and have been shown to affect the organisation of α -synuclein into fibrils (Iyer et al., 2017). There are two commonly observed C-terminal truncations, 109-140 truncation and 103-140, both increasing the pH threshold value for autocatalytic activity, making them more susceptible to aggregate. Both C- truncated variants were seen to be more likely to form protofibrils, in the presence of vesicles, but the 103-140 truncated variants alone had the capacity to convert into mature fibrils and aggregate further (van der Wateren et al., 2018). The truncation of the C terminal at both lengths, causes the release of the long- range interactions between the N and C terminal, (Zhang et al., 2022, Sorrentino and Giasson, 2020).

The final PTM that is often seen in α -synuclein is O-GlcNAcylation; the role of this modification is debated, with studies showing both inhibition and propagation of α -synuclein oligomerization depending on the site (Wu et al., 2020, Balana et al., 2023, Levine et al., 2019). O-GlcNAcylation is the addition of monosaccharide N-acetylglucosamine to the side chain of the serine or threonine residues; currently there have been 9 identified sites of O-GlcNAcylation in α -synuclein, five of which are located in the NAC region (Alfaro et al., 2012, Wang et al., 2010b). Studies have shown that O-GlcNAcylation may have an effect on the interaction of α -synuclein with many proteins, however it has not been observed to have an effect on its ability to bind to phospholipid membranes (Balana et al., 2023). Interestingly, the current Pan O-GlcNAc antibodies RL2 and CTD110.6 do not recognise the modification on α -synuclein, which inhibits further interrogation of O-GlcNAcylation on the protein (Levine et al., 2019). Due to the role of PTMS and their prevalence in disease states, particularly Lewy bodies, most PTMs have not been characterized in normal α -synuclein function.

1.7.5. The current roles of α -synuclein in platelets

Little is known of the function of α -synuclein in platelets, since the first observation in 2002. Initial studies have shown that extracellular recombinant α -synuclein can have an inhibitory effect on platelets, reducing the PF4 release from α -granules, but not affecting Ca^{2+} levels, which is ameliorated by removal of either the C- or N-terminals of the protein (Ling et al., 2022, Park et al., 2002). The inhibitory effect was linked to the blocking of thrombin cleaving GPIIb/IIIa Exosite 2, and therefore inhibiting the cleavage of PAR1 (Acquasaliente et al., 2022). Interestingly, although some studies have linked extracellular α -synuclein to the downregulation of platelet secretion, other studies contest this and observe a bleeding phenotype in α -syn^{-/-} mice; it has also been observed that α -synuclein may interact with Cysteine string protein in its role (Smith et al., 2020, Acquasaliente et al., 2022). This has been further contested with a study showing that, although α -synuclein is present in platelets with high abundance, knockout models did not present a bleeding phenotype (Smith et al., 2023). Interestingly this study also showed that there was a significant decrease in platelet activation when stimulated with convulxin, with modest decreases at high dosages of CRP and U46619. Overall, there is little known regarding the role of α -synuclein in platelets, currently, there is a single published study which shows no bleeding defect, but a potential defect in platelet activation and α -granule secretion (Smith et al., 2023). Due to previous studies in different cell types, it is assumed that α -synuclein interacts with the SNARE complex (Smith et al., 2020, Hawk et al., 2019, Burré, 2015).

1.8. Thesis Aims

The aims of this thesis are to Investigate the role of α -synuclein in human platelets *in vitro*, initially using a pharmacological inhibitor on platelet function, and its effect on platelet activation and secretion. Next will be to assess the effects of α -synuclein knockout on platelet form and function in mouse models, using LTA, Flow cytometry and immunofluorescent techniques. Additionally, we sought to elucidate the interactions of α -synuclein in platelets through Immunofluorescence and Immunoprecipitation.

We hypothesise that α -synuclein interacts with SNARE complex proteins to facilitate the formation of the functional complex. Inhibiting the function of α -synuclein will decrease platelet functionality through the reduction of granule release. In α -synuclein knockout mice there will be a significant bleeding phenotype.

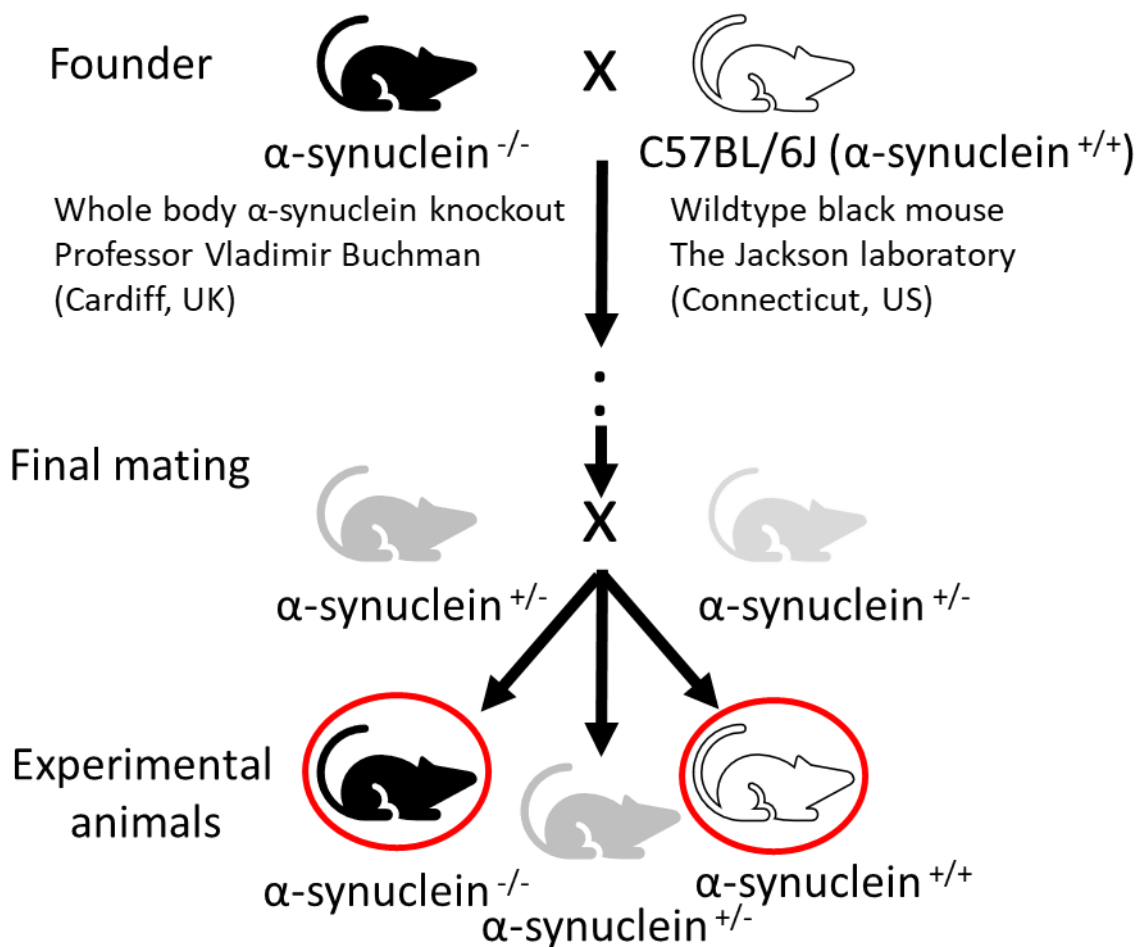
Finally, to distinguish the role of PD-L1 on platelet function, through the use of pharmacological inhibitors, knockout mice and MPN patients over-expressing PD-L1. The creation of a PD-L1 mouse will be a key goal to assess the effect of platelet derived PD-L1 in disease states such as endotoxemia. And here!

We hypothesise that the reduction of PD-L1 will result in a mouse colony that exhibits a hypersensitive immune response. We also expect to see a reduced aggregation capability in the knockout and inhibited population, conversely to the increased expression profile observed in the over-expressing population.

Chapter 2. Materials and Methods

2.1. Animal handling and breeding of α -synuclein knockout mice.

The initial breeding of α -synuclein included a knockout mouse kindly supplied by Professor Vladimir Buchman (Cardiff University) and crossed with C57BL/6J mice from the Jackson laboratory. Heterozygous mice were then bred resulting in knockout, WT and heterozygous offspring. Mice were only weaned from their mothers within 30 days and biopsies of the ear were taken for the dual purpose of identification and genotyping. The mice were allowed to age until large enough for experiments, usually around the age of 3 months. All procedures were approved by the UK Home Office under the Animals (Scientific Procedures) Act 1986. Mice were sacrificed using a CO₂ chamber (Clinipath, UK) to reduce the chance of platelet activation which cervical dislocation or anaesthesia can cause.



2.2. Preparation of Platelet-Rich Plasma

2.2.1. Human

Platelets were isolated from whole blood, obtained from healthy volunteers in accordance with the University of Hull regulations (HYMS Ethics 1501 for healthy controls). Before donation, it was confirmed that no anti-coagulants or anti-platelet drugs had been administered for 14 days prior, due to the COVID-19 pandemic, a 28-day period after all vaccinations were also implemented. For the study of platelets, whole blood was drawn using a 21-gauge butterfly needle into vacutainers, either 1:5 (v/v) Anti-coagulant Citrate Dextrose solution (ACD) (29.9mM sodium citrate, 72mM sodium chloride 2.9mM citric acid 114mM glucose, pH6.4) or 1:10 (v/v) sodium citrate (109 mM tri-sodium citrate, pH 7.4). The whole blood/anti-coagulant mixture was then transferred into 15ml polystyrene tubes, with no more than 10mL per tube and centrifuged (Eppendorf 5810R) at 190g for 15 minutes with no brake separating plasma from red blood cells (Figure 2-1). Plasma was then transferred into another 15mL polystyrene tube.

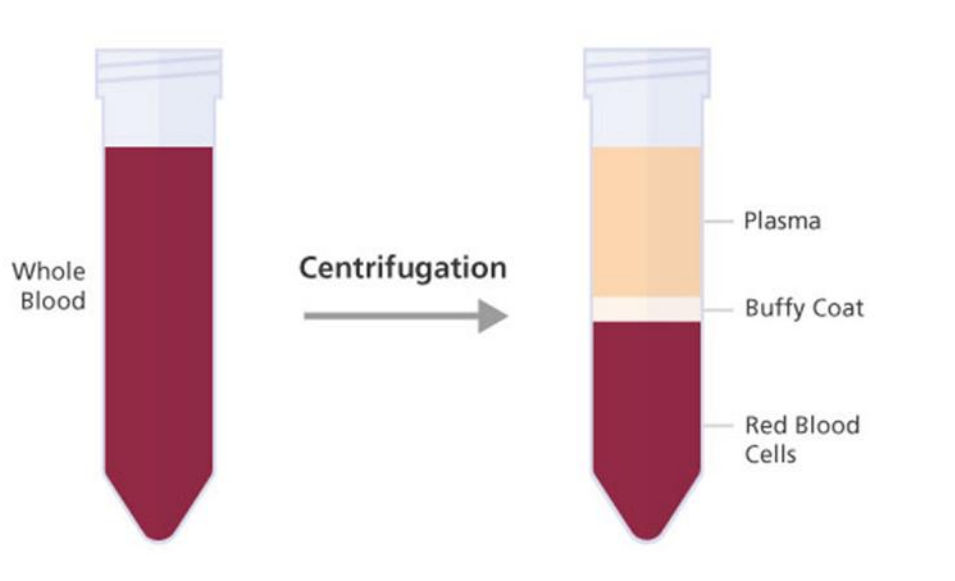


Figure 2-1. Diagram of whole blood components after centrifuging.

2.2.2. Murine blood

Murine blood was collected from CO₂ narcosis sacrificed mice by direct cardiac puncture into a syringe with 1:20 (v/v) Tri-Sodium Citrate (109mM) or a heparin and D-Phenylalanyl-L-prolyl-L-arginine chloromethyl ketone (PPACK) dihydrochloride mixture (4U/mL 150 μM/L). The blood was gently mixed and 150μL Modified Tyrodes buffer was added before centrifugation at 90g for 5 minutes at 37°C. The plasma was removed into a 1.5mL polystyrene tube, 150μL was added back to the whole blood, mixed and centrifuged again with the plasma fraction added to the polystyrene tube.

2.3. Preparation of Washed platelets

2.3.1. Human

Preparation of washed platelets continues from section 2.2.1 adding 1:50 (v/v) 0.3M citric acid, to PRP in the polystyrene tube to lower the pH to 6.4 before centrifugation at 800g for 12 minutes with brake. For some experiments, 0.2μM indomethacin, tirofiban (0.5μg/mL) and/or apyrase (2U/mL) were also added. Indomethacin is a COX (1/2) inhibitor, and apyrase attenuates platelet activation through the degradation of ADP to AMP, whereas tirofiban inhibits GP IIb/IIIa receptors by mincing the RGD sequence and blocking the binding pocket. The platelet-poor plasma was discarded, and the platelet pellet was resuspended in wash buffer (Table 30). The platelet solution was then centrifuged a second time at 800g for 12 minutes with brakes, and the supernatant wash buffer was removed. The newly washed platelet pellet was then resuspended in Modified Tyrode's buffer (20mM HEPES 134mM NaCl 2mM KCl 0.34mM Na₂HPO₄·12H₂O 12mM NaHCO₃ 1mM MgCl₂ 5mM glucose, pH 7.4) for counting.

2.3.2. Murine blood

Preparation of washed murine platelets continues from section 2.2.2 by adding 1:100 0.3 M citric acid to the PRP and centrifuging at 800g for 5 minutes at 37°C. The supernatant was discarded, and the pellet resuspended in 250μL Modified Tyrode's buffer, for counting.

Sodium citrate was used for washed platelet experiments, as it suppresses unwanted platelet activation by binding the free calcium which is a necessary co-factor for

multiple steps in the clotting cascade. The addition of citric acid and dextrose in this anticoagulant is for pH regulation and maintaining isotonicity. The addition of 0.3M citric acid was used to lower the pH of PRP which also inhibited platelet activation.

2.3.3. Platelet count and adjustment

Platelet count must be kept consistent between donors for comparable results, for this 2.5µL of platelet mix was added to 10mL of ISOTON™ (Beckman coulter) and inverted to ensure a homogeneous mixture. This solution was then analysed by a Z1 coulter counter (Beckman coulter) set to count events between the sizes of 1.79µm and 3.85µm. The counter provides a count of platelets per mL with a simple calculation:

$$Dilution\ volume = \frac{Platelet\ count}{Desired\ count} - 1$$

Platelet concentration was adjusted using modified Tyrode's buffer and left to rest for 30 minutes at 37°C. to examine platelet aggregation, Platelets were adjusted to a concentration of 3.0x10⁸/ml, and for immune-blotting platelets were adjusted to 1.0x10⁹ platelets per mL. This procedure was also conducted on PRP using the same methodology, for aggregation platelets were adjusted to the same 3.0x10⁸, for flow cytometric analysis platelets were adjusted to 3.0x10⁷.

2.4. Light Transmission aggregometry (washed platelets)

Light Transmission aggregometry (LTA) was developed in 1962 by Gustav born, it relies on the changes of light scattering through the platelet suspension to analyse platelet function (Born, 1962). When unstimulated in stirring conditions, platelets form a uniformly opaque solution, (0% aggregation) when agonist is added, platelets clump together causing the solution to become more transparent. As more platelets are activated more platelet clusters are made which increases the amount of light that can pass through the sample tube. A tube containing modified Tyrodes buffer only was used as the 100% aggregation control (Figure 2-2).

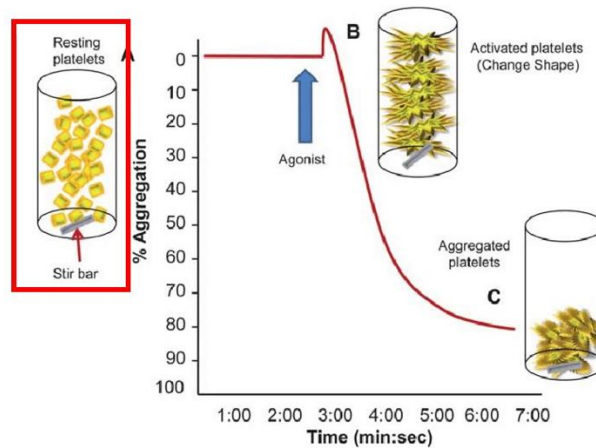


Figure 2-2. Explanatory diagram of aggregation curve generated by LTA. a) resting platelets in glass cuvette b) soon after the addition of agonist, platelets rapidly change shape, this results in the LTA trace. c) platelets aggregate together causing them to become less turbid in the buffer, this increased transmissibility so then converted into an aggregation.

LTA was conducted on both murine and human-washed platelets, diluted to a concentration of 3.0×10^8 /mL stirred at 1000rpm at 37°C. Platelets were then stimulated with varying concentrations of different agonists; thrombin, U41669 and collagen in washed platelets. When stimulating PRP, CRP-XL, TRAP-6 and ADP were used, this was to circumvent the interaction of collagen and thrombin with other constituent parts of the PRP.

2.5. Inhibition of α -synuclein with pharmacological agents

The inhibition of α -synuclein has been investigated in neuronal cells, due to its hallmark involvement with multiple neurodegenerative disorders. This has led to the identification of the drug-like phenyl-sulfonamide compound ELN484228, through computational and experimental techniques, by Toth et al. (2014). There were 8 binding pockets (BP) identified, ELN484228 binds to BP 1, the Toth et al. (2014) study demonstrates that ELN484228 has a protective role in cellular models of α -synuclein mediated vesicular dysfunction (E46k cells). It was also shown that different conformations of α -synuclein express differential open BPs, to which differential small molecules could be used.

2.6. DNA extraction

2.6.1. Guanidinium thiocyanate method

Tissue samples were acquired and homogenized with 1mL guanidinium thiocyanate in a Dounce homogenizer, this was then transferred to a 1.5mL polystyrene tube left at room temperature for 5 minutes. 200 μ L of chloroform was added and the solution vortexed before being left to rest for 15 minutes at room temperature. This solution was then centrifuged at 12000g at 4°C for 15 minutes, and placed on ice, the aqueous phase was removed and stored in a new 1.5 mL tube. It was key that all aqueous phase was removed from the interphase, this was due to the prior phase containing RNA and the latter DNA. 0.3mL of 100% ethanol was added to this mixture, which was then inverted to mix, this was then rested at room temperature for 2-3 minutes. After the rest, the sample was centrifuged at 2000g for 5 minutes at 4°C to pellet the DNA. The Phenol-ethanol supernatant was removed and stored at -80°C.

The DNA pellet needed to be washed to remove all protein and RNA contaminants, 1mL of citrate/ethanol solution (0.1M sodium citrate in 10% ethanol, pH=8.5) was added to the DNA pellet and incubated at room temperature for half an hour, being inverted gently every 5 minutes. This mixture was then centrifuged for 5 minutes at 4°C, and the supernatant was removed and discarded. This was then repeated to ensure the DNA sample was clean, after this second repeat 1.5mL of 75% Ethanol was added to the pellet and incubated for 20 minutes, gently inverting every 5 minutes. The solution was then centrifuged at 2000g for 5 minutes at 4°C and the supernatant removed and discarded.

To resuspend the DNA, 0.3-0.6mL of 8mM NaOH per 50-70mg of initial tissue was added, this was then ensured that all DNA was dissolved then centrifuged at 12000g for 10 minutes at 4°C to remove any insoluble material. The supernatant containing the DNA was then transferred into a new tube, and pH adjusted to 7.4 by addition of HEPES and 1mM EDTA, which allowed the long-term storage of DNA at 4°C.

2.6.2. TRIzol® method

Tissue samples were homogenised in a Dounce homogenizer in the presence of TRIzol® reagent and left for 5 minutes at room temperature. After incubating, 200 μ L

chloroform was added, vortexed and left to incubate at room temperature. The mixture was then centrifuged at 12,000g for 15 minutes at 4°C and placed on ice, the aqueous phase containing RNA was then aliquoted into a new tube, the removal of all aqueous phase is critical for the quality of the DNA. Ethanol was added (0.3mL per 1mL TRI reagent) the sample was then inverted repeatedly to mix; the samples were then incubated for 2-3 minutes at room temperature before centrifugation at 2000g for 5 minutes at 4°C to pellet the DNA. The phenol-ethanol supernatant was removed and stored in another tube at -70°C.

To wash the DNA, 1mL of sodium citrate/ethanol (0.1M sodium citrate 10% ethanol, pH8.5) was added to the pellet and incubated for 30 minutes at room temperature, inverted every 5 minutes. After incubation, the mixture was centrifuged at 2000g for 5 minutes at 4°C, the incubation with sodium citrate and centrifuged was repeated twice. Ethanol was then added (75% in water) (v/v) for 15 minutes with gentle inversion every 5 minutes, before centrifuging at 2000g for 5 minutes at 4°C the supernatant was then removed and discarded, and DNA pellet was left to air dry for 5-10 minutes.

The pellet then was resuspended in 0.5mL of 8mM NaOH per 60mg of tissue, this was then centrifuged at 12000g for 10 minutes at 4°C and supernatant transferred to a new tube to remove any insoluble material. For long-term storage the pH was adjusted to pH7.4 using HEPES and 1mM EDTA added.

2.6.3. Kapa

For DNA extraction KAPA EXPRESS EXTRACT (KK7103 Merck, Germany) was used throughout using a modified version of the manufacturer's instructions. The Biopsies from each mouse were added to the extraction mix (44µL Nuclease-Free Water (fisher), 5µL Extraction buffer, 1µL extraction enzyme). This mixture was then vortexed and added into the thermocycler, the lid was set at a constant 105°C to prevent condensation on the top of the tube, the reaction mixture was then heated to 75°C for 15 minutes, followed by a step of 95°C for 5 minutes, before holding at 4°C. The DNA extraction solution was then spun in a bench top microfuge for 20 seconds to ensure all debris was at the bottom of the tube.

While the Phenol and TRIzol® methods yielded larger volumes of pure DNA, they were too time consuming to repeat on the volume of samples that would be required

to genotype the colony on a weekly basis, therefore the KAPA system was chosen, this also came with the benefit of the reaction being contained to a single tube and no need for hazardous chemicals.

2.7. Genotyping

2.7.1. PCR Methodology for α -synuclein Knockout mice

For all Genotyping experiments, KAPA2G fast genotyping mix (Merck, Germany) was used, alongside Nuclease-Free Water (fisher) in a 5prime (Techne, UK) thermocycler. A modified version of the manufacturer's instructions was used. The program used started with an initial denaturing step at 94°C for 2 minutes followed by 30 cycles of a 30-second denaturation step at 94°C, a 30-second annealing step at 61°C a 30 second and 45-second extension step at 72°C, this was followed by a 5-minute final extension at 72°C. Two reactions were required to ascertain the genotype of the mice, the Wild-type used the following primers: aS-ups (common upstream primer) CAGCTCAAGTTCAGCCACGA and AKoC2 (WT downstream primer) AAGGAAAGCCGAGTGATGTAC, and the knockout reaction: aS-ups (common upstream primer) CAGCTCAAGTTCAGCCACGA NeoA (knock-out downstream primer) ATGGAAGGATTGGAGCTACG. Wild-type reactions form a product of 520 bp, and the knockout reaction of 470 bp (Ninkina et al., 2015). All primers were purchased from Eurofins (Grimsby UK).

Table 10. PCR component volumes for genotyping

Component	Volume per sample (μ L)
dH ₂ O	7
KAPA reagent	10
Forward primer	1 (10pM)
Reverse primer	1 (10pM)
DNA	1

The PCR product was loaded into a 1.2% Agarose Gel prepared by adding 1.8g of agarose to 150mL tris-acetate-ethylenediamine tetra acetic acid (TAE) and heating while mixing gently. Once the agarose was fully dissolved into the mixture 1:20000 (v/v) Ethidium Bromide was added, and the mixture transferred into the cell cast. Once

cooled the gel was submerged in TAE buffer and 15µL of sample was added per well, alongside 3µl 100 bp DNA Ladder (New England Biolabs) and run at 100V for 30 minutes to separate the bands. The gel was then imaged in a Versadoc (Biorad California, USA), the optimise exposure setting was used to generate 15 images between 5- and 20-seconds exposure, and the optimal exposure was chosen.

Gel electrophoresis is the movement of the charged DNA fragments through the gel media, with increased agarose the resistance for larger DNA fragments is increased which yields greater separation for smaller DNA fragments. Ethidium bromide (EtBr) is a non-radioactive marker for visualising nucleic acid bands in electrophoresis, it fluoresces with a wavelength of 605nm when exposed to ultraviolet light with its intensity increasing 20-fold after binding to DNA. It is believed that the movement of the hydrophobic environment between the base pairs of DNA and EtBr is the cause of the increased fluorescence (Sharp et al., 1973, Olmsted and Kearns, 1977). Ethidium bromide intercalates into the DNA between the base pairs of the DNA, while this changes the weight of the DNA it can be ignored as it binds to all DNA fragments equally.

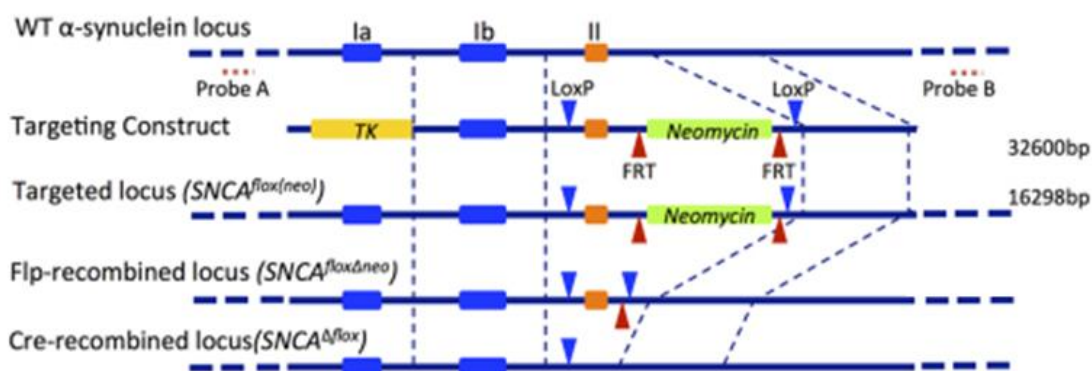


Figure 2-3. α -synuclein knockout generation (Ninkina et al., 2015).

2.8. Protein concentration assay

Aliquots of samples that were prepared for blotting were subjected to the Bio-Rad DC Protein Assay was used for quantification of solubilized protein; this kit is based on the lowry assay (Lowry et al., 1951). This assay relies on the interaction between protein

and copper tartrate within an alkaline medium including folin reagent. The protein first reacts with the copper and subsequently results in the reduction of the folin reagent, this reduction causes a characteristic blue colour with a maximum absorbance at 750nm, this change can then be measured by a photo spectrometer. The working reagent was made by mixing 20 μ L of reagent S to 1mL of reagent A, this working reagent was used within 7 days of mixing. A protein standard was then prepared in PBS with doubling dilution from 2.0mg/mL to 0.0625mg/mL BSA, 160 μ L of Standards were added in triplicate to the plate and 40 μ L dye reagent added. Once all samples were added 200 μ L of reagent B was added into each plate and agitated for 10 seconds; If bubbles formed at any point, they were popped using a clean dry pipette tip and left to incubate at room temperature for 20 minutes. After incubation the plate was read using a TEKAN plate reader set to 750nm.

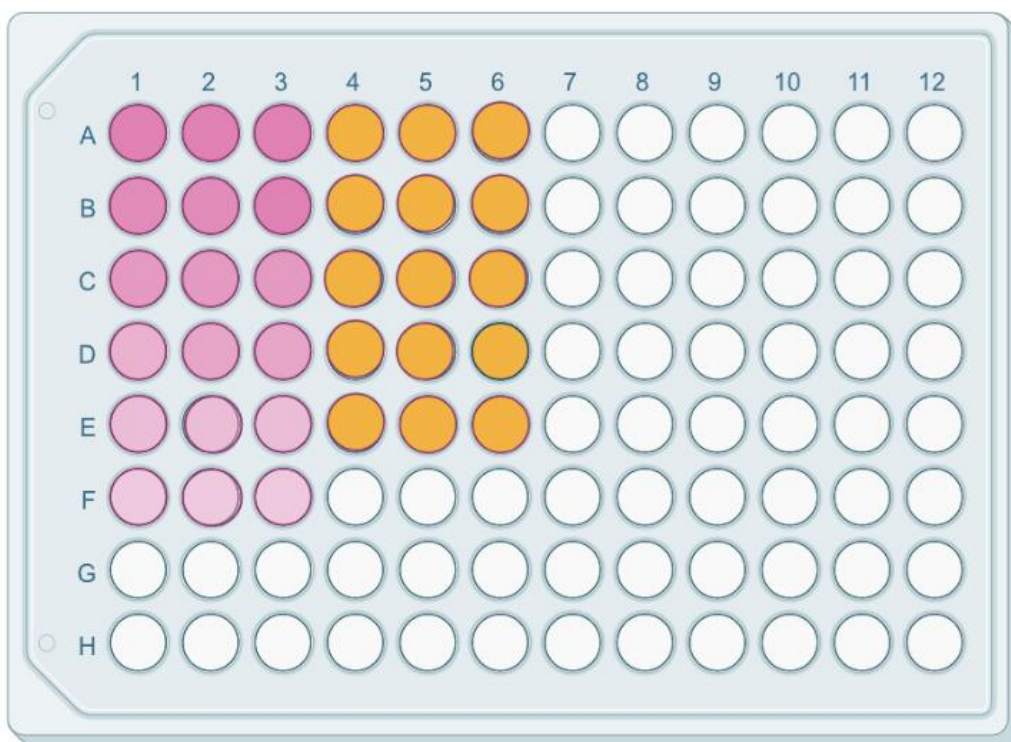


Figure 2-4. Layout of a 96-well-plate for a typical Protein concentration assay. Protein standards (pink) samples in triplicate (orange).

A standard curve was generated from the standards, giving a line equation to which the sample absorbances could be input yielding an accurate protein concentration. If the standard curve R value was less than 0.95 the experiment was repeated.

2.9. Western blotting

Washed platelets (1×10^9 plt/mL) were treated with agonists at 37°C with stirring. Reactions were stopped by the addition of an equal volume of ice cold Laemmli buffer. Lysates were separated by SDS-PAGE (sodium dodecyl sulphate–polyacrylamide gel electrophoresis). SDS-Page is a discontinuous electrophoretic system developed by Ulrich K. Laemmli, used for separating proteins (Laemmli, 1970). SDS-PAGE separates out proteins based on their size and charge; the Stacking gel is used to aid in protein sorting with larger molecules at the top and smaller at the bottom. The Resolving gel has a higher pH and smaller pores (due to the higher acrylamide concentration) This higher pH places a greater negative charge on glycine anions. The SDS in the gel creates a charge to mass ratio that is equal for all proteins which allows for the sorting of proteins by size alone (Shapiro et al., 1967). Upon application of an electrical current the negatively charged proteins move through the polyacrylamide towards the anode. In gels with a higher acrylamide percentage the pores are smaller, allowing for greater separation of smaller proteins, initially a 10% gel was used however a 12% gel was found to give better separation and used henceforth.

The proteins were then transferred to a Polyvinylidene fluoride or polyvinylidene difluoride (PVDF) membrane with a pore size of 0.45µm using the trans-blot turbo transfer system (Bio-Rad) 10-minute transfer. Semi-dry transfer was used over traditional due to its improved speed; this is achieved by passing current directly through the gel, instead of around it, allowing for a higher overall current. Membranes were then blocked with 5% BSA in TBS for 60 minutes at room temperature on a plate rocker. Blocked membranes were then incubated with primary antibody at 4°C on a plate rocker overnight. Probed membranes were incubated with HRP conjugated secondary antibody for 60 minutes at room temperature with rocking. The membranes were then washed 4 times with 0.1%TBST for 5 minutes each to ensure all unbound secondary is removed before imaging.

2.10. Sample Preparation

Table 11. Antibodies used for Western blot analysis

Antibody	Dilution	Brand
Alpha synuclein ^{ser129}	1:1000	Santacruz Sc-135638
Alpha synuclein total (D-10)	1:1000	Santacruz Sc-515879
Alpha synuclein total	1:1000	Cell signalling 51510T
VAMP8	1:1000	Cell signalling 13060
VAMP7	1:1000	Cell signalling 14811
VAMP2	1:1000	Santacruz Sc-569706
Syntaxin 11 (A-4)	1:1000	Santacruz Sc-377121
Syntaxin 4	1:1000	Santacruz Sc-101301
SNAP23 (F-1)	1:1000	Santacruz Sc-373743

2.10.1. Subcellular fractionation analysis

To elucidate whether α -synuclein differentially associates from the cytosol to the membrane following platelet activation, samples were stimulated with 0.1U Thrombin for varying timepoints before the addition of 1:1 Ice cold subcellular fractionation buffer. These samples were then subject to 5 cycles of snap freezing in Liquid nitrogen and thawing to lyse all cells. Samples were then centrifuged at 5000g for 10 minutes at 4° to remove non lysed cells. Following this platelet lysates were decanted into polycarbonate ultracentrifuge tubes and spun at 100,000g for 60 minutes at 4°C. After ultracentrifugation the supernatant was aspirated and placed in a separate tube, the remaining pellet was then resuspended in 100 μ L fractionation buffer. Protein concentrations were then matched to the supernatant and run on SDS-PAGE for Western blotting, following which, STX4 was used as a pellet positive control and PLC γ as a positive control for supernatant.

2.10.2. Preparation of Western Blot Gel

For all gels used the Mini-PROTEAN® Tetra Hand-cast System (BIO-RAD, USA) was used, the reagents for the resolving gel (Table 12) in a 50mL tube and mixed, 8mL was added to the cast and 1mL of Methanol added gently on top to ensure resolving gel was flat and remove all bubbles. This was then left to set for 1 hour before the removal of the methanol. The stacking gel (Table 13) was then mixed in a separate tube before addition to the cast, and the comb inserted, and left to set for a further 30 minutes.

Table 12. Components of different percentage acrylamide resolving gels Gel buffer1 components as in Table 37.

Component	10% Resolving Gel	12% Resolving Gel	15% Resolving Gel
dH ₂ O	6.48 mL	5.38 mL	3.25 mL
30% Acrylamide/BIS	5.3 mL	6.4 mL	8 mL
Gel Buffer 1	4 mL	4 mL	4 mL
TEMED	100 µL	100 µL	100 µL
10% Ammonium Persulphate (APS)	5.3 µL	5.3 µL	5.3 µL

Table 13. Components of Stacking Gel, Gel buffer2 components as in Table 38.

Component	Stacking gel
dH ₂ O	4.87 mL
30% Acrylamide/BIS	750 mL
Gel Buffer 2	1.87 mL
TEMED	100 µL
10% APS	10 µL

2.10.3. Chemiluminescent imaging

Probed membranes with HRP conjugated secondary antibody were incubated in Enhanced Chemiluminescence Reagent (ECL 1+2) (Table 41) for 5 minutes and imaged in a Chemi doc (Bio-Rad) for up to 150 seconds. The oxidation of luminol by peroxide within the ECL reagent results in creation of an excited state product called 3-aminophthalate. This product decays to a lower energy state by releasing photons of light. A colorimetric image of the membrane was taken and merged with the chemiluminescent image on image lab (Bio-Rad). The Chemi-doc was used due to its utilisation of a Charge-coupled device (CCD) sensor allowing for imaging of both HRP and colorimetric methods.

2.10.3.1. X-ray film

X-ray film utilises the same mechanism for chemiluminescence as the Chemi doc, however, instead of utilising a CCD for digital image production, X-ray photo film was used. X-ray film visualisation was conducted in a dark room at all times. The film was placed directly on top of the membrane and sealed inside a cassette for 5 minutes.

Due to the close proximity and length of exposure, this method is able to resolve much fainter bands than the CCD method. The film was then placed in a developer (KODAK) and agitated constantly until bands became visible. At this point the film was immediately removed and placed into the fixative (KODAK) for 15 seconds, before rinsing in dH₂O and hanging to dry. Once dry the films could then be imported to the computer using a scanner at 600dpi.

2.10.4. Fluorescent western blot Imaging

Western blot membranes were stained with fluorescent secondary antibodies with either 680 or 800nm conjugated fluorophores in the dark for 1 hour while being agitated. Membranes were visualized using an odyssey CLx (LiCOR Cambridge, UK), Using this imaging system allowed for the imaging and delineation of 2 separate bands simultaneously due to the different fluorophores. Images were stored and analysed in image studio (LICOR).

2.11. Immunoprecipitation

Immunoprecipitation was used for assessing protein complexes. Washed platelets (1.0×10^9 plt/mL) were treated with agonists at 37°C with stirring in the presence of tirofiban to inhibit aggregation. Reactions were stopped by the addition of an equal volume of ice-cold sample buffer supplemented with phosphatase inhibitors (Roche) and put on ice. The samples were then precleared using protein A Sepharose beads (LIFE, UK) 1:20 and rotated at 4°C for 1 hour, pipette tips were cut to ensure beads were able to be pipetted. Preclearing was used to reduce the non-specific binding and background, therefore, increasing the efficiency of the IP. The mixture was then centrifuged at 9000g for 30 seconds at 4°C and the supernatant removed to a new tube. Antibody was then added to the sample 1:50 and left to rotate overnight at 4°C, Sepharose beads were then added to the sample/antibody mixture and left to rotate for a further 3 hours at 4°C. addition of the antibody only at the beginning, and later addition of the beads was chosen due to its ability to yield higher volumes of pure protein and ensure binding of antibody to the protein and no other antibody/ bead constructs (Bonifacino et al., 2016).

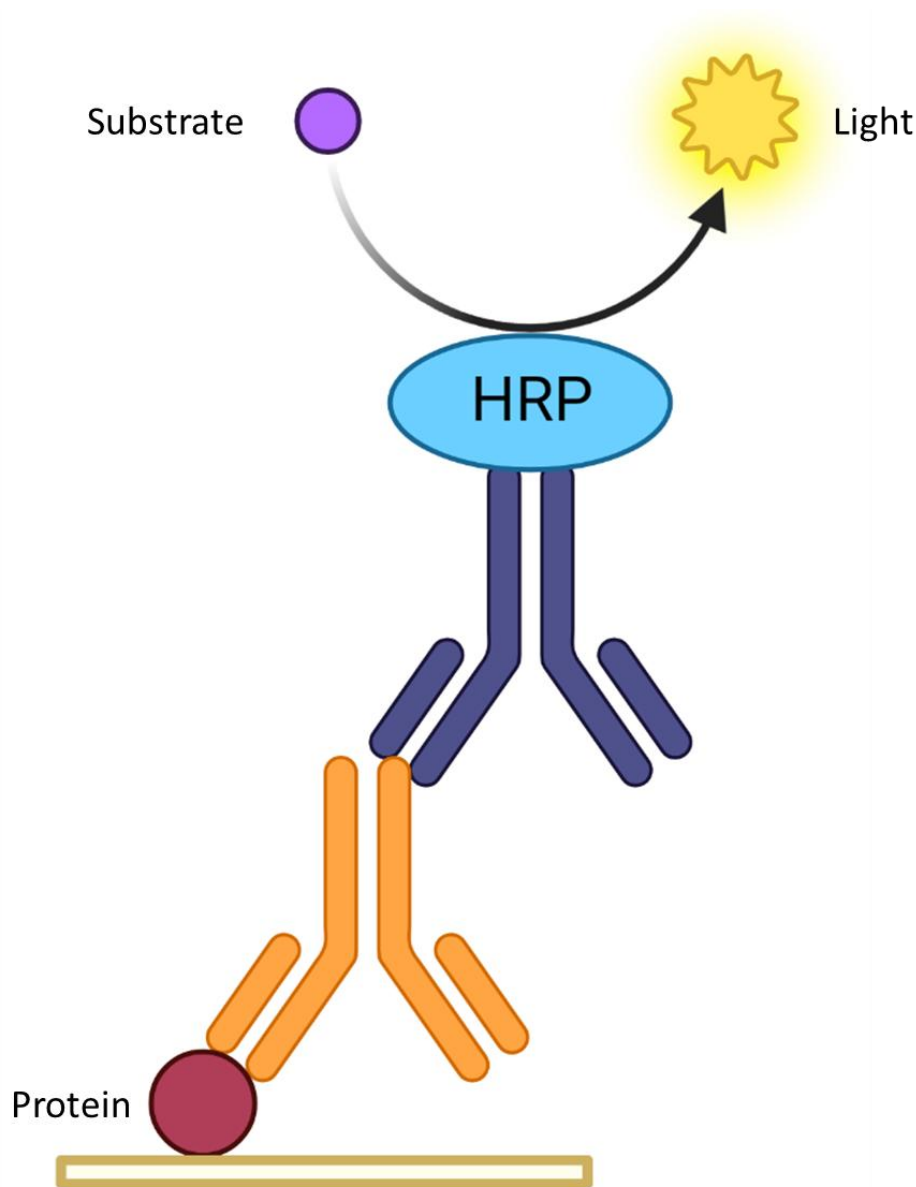


Figure 2-5. Diagram of Chemiluminescent Western blot mechanism. Proteins attach to the PVDF membrane, the Primary antibody (orange) binds specifically to these proteins, a secondary antibody is then added which binds specifically to the primary. These secondary antibodies are conjugated to HRP, when ECL is added the HRP catalyses the reaction emitting light as a by-product which is then observed.

After incubation with beads, the mixture was centrifuged at 9000g for 3 minutes at 4°C and supernatant removed, this was stored and tested for depletion of the target protein. The pellet was then washed in lysis buffer 3 times before resuspension in 30µL 3x Laemmli buffer to elute the bound protein from the beads. This mixture was then heated for 5 minutes at 70°C to assist in elution and then frozen at -20°C before thawing in a heat block at 80°C for 5 minutes. With the protein eluted from the beads

the mixture was spun in a benchtop microfuge and the supernatant was added to the SDS-PAGE gel as in (Section 1.9).

Alongside the samples with antibody, a lysate was incubated with the corresponding IgG, which was used as a control to estimate that the proteins stained in the experiment result are due to the specific interaction with the antibody.

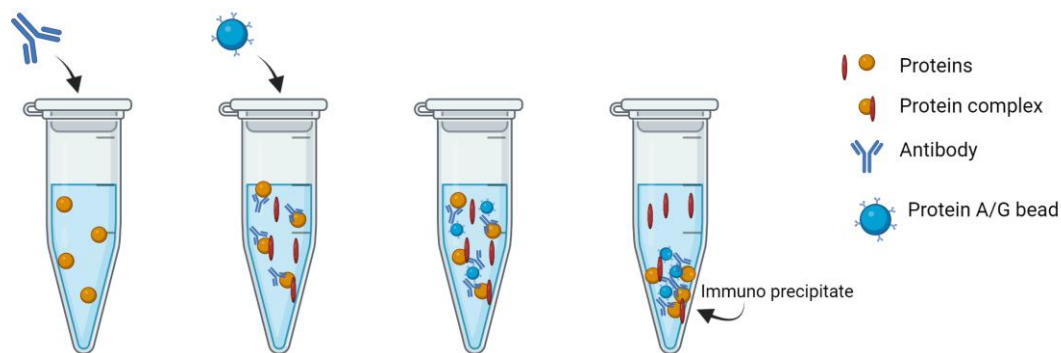


Figure 2-6. Schematic diagram of Immunoprecipitation. Antibody for the protein of interest is added and incubated overnight at 4°C while being rotated, Protein A/G beads are added these beads bind to the primary antibody aggregating them together forming a protein/bead complex the sample is then centrifuged causing the bound proteins to pellet at the bottom of the tube, allowing for the purification of protein after the removal of supernatant.

2.11.1. Coomassie Staining

To prepare samples for mass spectroscopy IP purified samples were run through SDS-PAGE and the gels were stained using Coomassie g250 staining solution for 45 minutes. Coomassie forms a strong noncovalent complex with the carboxyl group of the protein and the amino group through electrostatic interactions. Due to the strong bond, the unbound reagent can be washed off leaving the bound complex remaining allowing for clear colorimetric visualisation of the proteins present on the gel. After incubation, the gel was rinsed in distilled water before adding the de-staining solution on a rocker at room temperature. This solution was drained and fresh solution added twice in the first 2 hours before leaving to de-stain overnight in fresh de-staining solution. After cleaning, the gels could then be stored in acetic acid or bands of interest cut out and proteins digested then snap frozen and stored at -80°C.

2.12. Microscopy

Microscopy was completed on a Zeiss Axio Observer fluorescence microscope. For imaging through samples requiring multiple focal planes the apotome 2.0 module was used. The apotome functions by projecting a grid structure into the focal plane of the specimen and moves to different positions and acquiring an image at each position. These images are then processed together allowing for emitted light emanating from outside the focal plane to be removed which increases the resolution of the image and allows for 3D structural imaging in Z stacks.

2.12.1. Static platelet adhesion assay

Coverslips were incubated with either 100 μ L: 100 μ g/mL collagen diluted in dH₂O, 200 μ L 100 μ g/mL fibrinogen, 200 μ L 3 μ g/mL CRP-XL, or 5 mg/mL fatty acid-free denatured BSA. All cover slips were incubated overnight at 4°C to allow sufficient time for matrix binding, BSA was used as a negative control. After the slides were functionalized, they were washed with PBS to remove excess protein.

Washed platelets as prepared in (Section 2.3.2) with concentration adjusted to 2.0×10^7 through addition of modified Tyrode's buffer, were used; for initial experiments, platelets spread on fibrinogen were pre-stimulated using 0.1U thrombin due to reports of poor adhesion to human fibrinogen, but was not continued after the first experiments (Pierre et al., 2018). Platelets were added to the slides and left to incubate for indicated time points. After incubation, unbound platelets were carefully aspirated and rinsed with PBS. Adhered platelets were fixed by adding 100 μ L 4% PFA for 10 minutes, this was then aspirated before permeabilization with 0.3% Triton x-100. The actin cytoskeleton of the platelet was then stained using FITC-phalloidin (100 μ g/mL) for 1 hour at 37°C in the dark and washed three times with PBS, and then once with dH₂O before mounting on a cover slide using Gelvitol. Slides were left to dry in the dark overnight and imaged on a Zeiss Axio Observer fluorescence microscope at 630x magnification with oil immersion (Pierre et al., 2018).

To quantify adhered platelets all conditions were completed in duplicate and 5 images taken at random locations for each cover slide. Images were then imported to ImageJ (NIH USA) and thresholding using the LI preset then converted to black and white, the number of white pixels was then divided by the count of black pixels to calculate the

overall platelet coverage the platelet count of each field of view was also used to calculate the platelets per mm². To quantify stress fibres and actin nodules each field of view was manually counted, for a platelet to be classed as having actin nodules 3 or more must be present within the cell, stress fibres were classified in cells where they were clearly visible.

2.12.2. Immunofluorescence

To analyse the location and movement of α -synuclein within platelets, they had to be imaged at both a basal and stimulated state. To achieve this, slides treated with 0.05mg/mL Poly L lysine which creates a positively charged surface for the platelets to adhere to without fully activating them. Upon interaction, Poly-L-lysine induces a leak of Adenine and Lactic dehydrogenase (LDH) from the platelet, however does not cause the release of granular contents (Jenkins et al., 1971). These slides were incubated for 15-30 minutes, at room temperature, the Poly-L-Lysine was then aspirated, and slides rinsed gently with PBS, the slides were then left to dry in a sterile laminar flow hood. The dried cover slips were placed in a light proof box on a platform covered in parafilm before platelets were added. 200 μ L of washed platelets were then seeded at a concentration of 2.0×10^7 plt/ml and incubated at room temperature for an hour, for stimulated samples, platelets were stimulated in tubes and added to cover slips immediately. Platelets were then carefully aspirated and washed with PBS once and aspirated. Following washing 200 μ L of heat inactivated lipid free BSA for 1 hour at room temperature. The BSA was then aspirated and washed with PBS once before fixation of the platelets by adding 150 μ L 4% PFA for 10 minutes. PFA causes covalent cross-links between molecules that binds them together in an insoluble meshwork, leaving them in a “fixed” state.

After fixation, 0.3% Triton X-100 in PBS was for added for 5 minutes to permeabilize the membranes of the platelets. Triton is a non-ionic surfactant, it permeabilizes the membrane by disrupting the lipid bilayer, therefore it was important to use as little triton as possible due to its toxicity and the potential for over-permeabilization of the membrane. Primary antibody was diluted in PBS then 150 μ L added to the platelets as in (Table 16) and incubated at 37°C for 1 hour and then aspirated and washed with PBS. Following washing fluorescent antibodies were diluted as in (Table 11) and

incubated in the dark at 37°C for 1 hour. After incubation antibodies were aspirated and slides were washed 3 times with PBS with 5 minutes of incubation for each wash step. Finally, slides were dipped in dH₂O and dried before being placed face down on gelvitol mounting media. Slides were then incubated overnight ensuring they were kept flat.

2.12.3. Platelets adhesion under flow

Murine blood was acquired through direct cardiac puncture into Heparin and PPACK dihydrochloride (100µM). Cells were then stained with 3,3'-Dihexyloxacarbocyanine iodides (DIOC6) in the dark, Whole blood was constantly agitated on a plate rocker to reduce the possibility of spontaneous platelet aggregation.

Cellix Vena8 fluoro+ chips were coated by adding either 15µL 100µg/mL fibrinogen or 15µL 100µg/mL fibrillar collagen and kept in a humidified box at 4°C overnight. After coating 10µL of heat inactivated BSA was added to each channel and incubated for 30 minutes to reduce nonspecific binding of proteins. To wash the chip 40µL of Modified Tyrodes was added to the chip and flowed at a shear stress of 40 dynes.cm² to wash the chip of excess collagen and BSA. The stained whole blood was added to the reservoir of the chip and flowed at a shear stress of 1000s⁻¹ for 2 minutes. Once completed 100µL of PBS was flowed through the chip to remove excess red blood cells. 4% PFA was then added to the chip and incubated at 4°C in the dark to fix the platelets before imaging at 400x magnification on a Zeiss Axio Observer fluorescence microscope.

2.13. Flow Cytometry

Initial Flow cytometric analysis utilized fluorescent flow cytometry, measuring cells under flow in suspension. Cells must be in a suitable concentration, have a suitable viscosity to be pushed through the sheath into a sample core of single cells, to allow lasers to excite each individual cell as it passes to enable the detection of scattered light (Cossarizza et al., 2019). Not only does this allow for fluorescence analysis but also counting, analysis of granularity and size of cells passing through. Size and granularity of the sample is traditionally used for gating populations of cells, which initially was used for experimentation. Gating refers to the process of selecting a

subpopulation of the total collected events for further analysis, in this case giving the ability to characterise platelets alone (Figure 2-7). It was essential to use a low enough concentration of platelets in non-aggregating conditions, to ensure no aggregates were formed, which would cause erroneous data due to being counted as a single event. Platelets were diluted to 2.5×10^8 and 1:40 (v/v) Tirofiban was added to negate these issues.

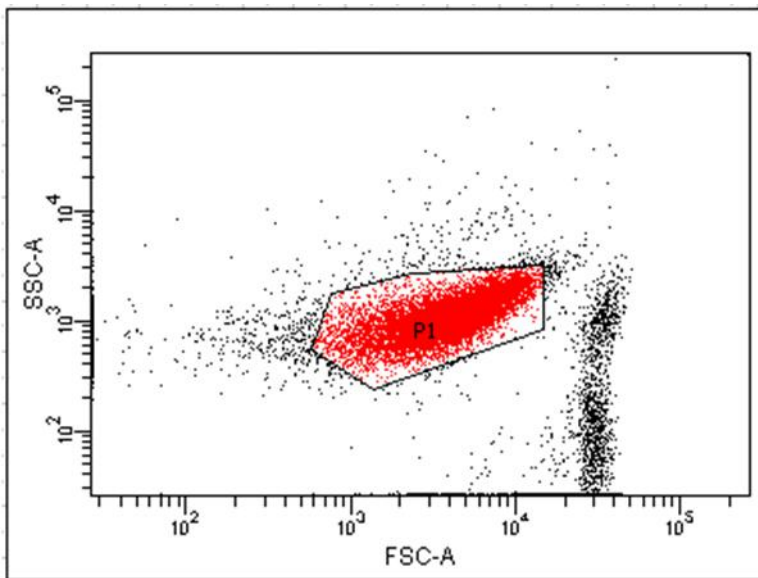


Figure 2-7. Manual gating of platelet populations. Platelets are gated using FSC-A vs. SSC-A, a gate (P1) this gating allows the delineation of singular platelets from cellular debris, and duplet events.

A LSRFortessa™ Cell Analyzer (Oxford, UK) was used for all flow cytometry, a mixture of 5 antibodies were used simultaneously for all experiments (Table 15) PRP was added to the antibody mixture followed by, Gly-Pro-Arg-Pro amide before the addition of thrombin, this was to suppress fibrin polymerization. The reagents were mixed gently, then incubated at 37°C for 20 minutes in the dark, before the addition of 250µL 0.2% paraformaldehyde in Saline. This mixture was then stored in the dark at 4°C until use on the flow cytometer, all samples were vortexed then run. Between each sample, FACS rinse (BD, USA) was run through for 20 seconds to ensure the machine was fully cleared of all old sample.

The use of Rainbow beads was used as a calibration step before samples were run, to ensure that laser powers were giving the same Median fluorescent intensity (MFI) (Figure 2-8). If the MFI is different the laser power can be altered before any experimentation begins, this allowed for the accurate comparison of multiple datasets.

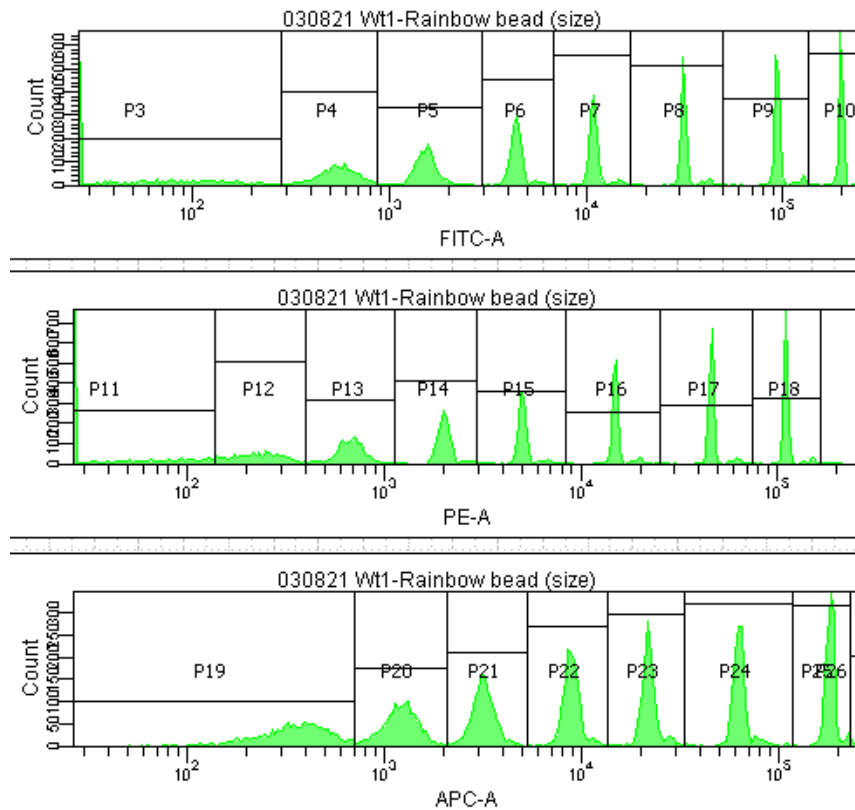


Figure 2-8. Rainbow bead calibration for Flow cytometry. Gates were created with the peak approximately in the middle where possible, if peaks shift left or right this will be evident and Laser power can be adjusted accordingly.

2.13.1. Flow cytometric analysis

Population analytics

All flow cytometric data was first collected and initially gated in BD FACSDiva software using FSC and SSC; This data was then exported in the FCS3.0 format and analysed in FlowJo (v10.8). The FCS3.0 format was chosen due to the higher resolution and inclusion of more parameters in comparison to FCS2.0. Both the Median Fluorescent intensity (MFI) and percentage population were calculated automatically on gated samples. The Median fluorescent intensity was used over the mean due to it representing the 50th percentile and are less impacted by outliers, making it a more robust estimator of the central tendency of the population than the mean. Alongside

this analysis of the (%) frequency of positive cells was recorded, by gating above 1.5% of basal positive cells and using the “Freq. of total” functionality to output the percentage of positive cells.

2.13.2. Compensation

When multiple fluorophores are used, there is the potential for overlap of emission. To remove this error, the fluorescence which is not from that specific fluorophore must be subtracted. To determine the amount of correction, samples were made up containing only a single fluorophore; by analysing these it is possible to see the effects each has on its neighbouring channels, which can then be adjusted in the BD FACSDiva software (Table 14). Single fluorophores only needed to be compensated once, whereas tandem fluorophores e.g., PE-Cyanine7 required compensation with each new vial used, due to the variability even within single batches.

Table 14. Flow cytometry compensation values. Compensation values were adjusted by using single fluorophore-stained samples and changing compensation values until no aberrations in other channels were observed.

	FITC	PE	PE/Cyanine7	APC	Alexa Fluor 700
FITC	100	3.0	0	0	0
PE	3.1	100	1.6	0	0
PE/Cyanine7	0	0	100	0	0
APC	0	0	0	100	9
Alexa Fluor 700	0	0	3.2	0	100

2.13.3. t-SNE analysis

T-distributed stochastic neighbour embedding (t-SNE) is a method for dimensionality reduction, for highly dimensional datasets, in this case used for visualising multiple flow colours in a 2D map; This is accomplished by converting the data into a matrix of pair-wise similarities and plotting this data on a dot plot. The parameters are optimised to have data points that are close to each other in the raw high dimensional data are close in the t-SNE data. T-SNE was first reported in 2008 as an improvement on the SNE (stochastic neighbour embedding) algorithm (Van der Maaten and Hinton, 2008). We used t-SNE analysis for its flexibility, it allowed for the visualisation of data for exploratory analysis of differential clustering.

All t-SNE analysis was completed on FlowJo version 10.8 (Figure 2-9). The data which was compensated and gated for whole population analysis was concatenated allowing for multiple datasets to be analysed together. This sample was then selected and t-SNE analysis opened at this point all used, compensated fluorophores were selected for analysis alongside SSC and FSC. The Opt-SNE algorithm was used, this setting can terminate iterations once the algorithm stops improving. Iterations are the number of times the algorithm is run on the data, initially the data starts out as a single point and then is separated out, however, the data reaches a maximally separated state, and further iterations result in the convergence of the dataset again.

The perplexity is related to the number of nearest neighbours that are used in the learning algorithms. The most appropriate value to use is highly dependent on the density of the data, with larger datasets requiring a larger perplexity, this value is most commonly between 2 and 100, and the perplexity for the datasets were set to 30. Finally, the use of the gradient algorithm (KNN) must be selected, this is the final step which maps the high-dimension data into the two-dimensional graph, the Fast Fourier Transform (FFT) interpolation was used as a recent optimisation of the original Barnes-Hut algorithm.

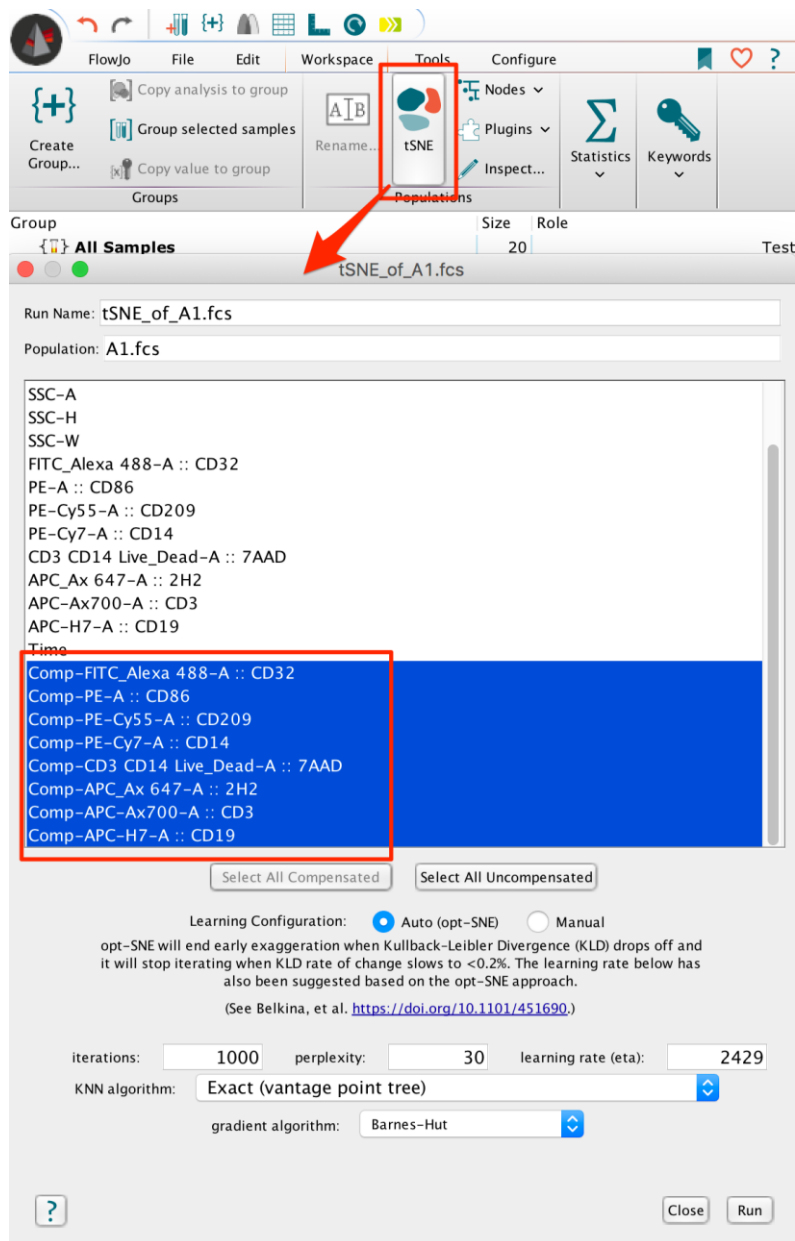


Figure 2-9. t-SNE settings window in FlowJo. The t-SNE settings used in FlowJo, selected all compensated fluorophores, and opt-SNE was selected to generate maps with the greatest separation profile. The learning rate is 7% of the total population with the exact point KMN algorithm used.

After t-SNE analysis, the t-SNE parameters, TSNE_X and TSNE_Y are available on the graph window in FlowJo, after selecting these a pseudo-colour graph is then displayed. From here the colouring was then able to be changed to display the expression of a single fluorophore, this allows for the visualisation of different fluorophore expression on a group-by-group basis.

Table 15. Antibody panel used for multicolour platelet viability and secretion flow cytometry.

Antibody	Manufacturer	Fluorophore	Volume used (µL)
Jon/A	Emfret	FITC	5
Wug.E9	Emfret	PE	5
CD107a	Biolegend	Alexa Fluor 700	1.25
CD63	Biolegend	PE/Cyanine7	5
α-synuclein			
PD-L1	Biolegend	APC	2.5

Table 16. Example of reagent volumes in secretion analysis flow cytometry.

Samples Type	Modified Tyrode's (mL)	Platelets (mL)	Antibodies (mL)	Agonist (mL)	Peptide (mL)
Knockout basal	21.25	5	18.75	0	5
Knockout stimulated	16.25	5	18.75	5	5
Wild-type basal	21.25	5	18.75	0	5
Wild-type stimulated	16.25	5	18.75	5	5
Control (no stain)	35	5	0	5	5

2.14. Statistical analysis

All statistical analysis was completed in GraphPad Prism™ 8 software (GraphPad, USA). All data was initially tested for distribution by use of the Shapiro Wilk normality test. Data with a normal distribution was subjected to either a one- or two- way ANOVA, unless otherwise specified. If the data was observed to not have a gaussian distribution it was subject to either an ANCOVA or Kruskal Wallis one-way analysis of variance unless otherwise specified. To investigate significance in datasets with multiple conditions, Tukey's post hoc analysis was implemented. Data to be quantified as significantly different a P value of less than 0.05 must be achieved.

Chapter 3. Characterisation of α -synuclein movement and interactions in human platelets

3.1. Introduction

The activation of platelets occurs upon adhesion to constituent parts of the subendothelial matrix of blood vessels, such as von Willebrand factor (vWF) and collagen. Platelet activation results in the secretion of granular contents facilitating their role in haemostasis, coagulation, inflammation, and immune response. Dense granules contain small molecules such as ATP, ADP, and serotonin, which are required for platelet recruitment and activation. α -granules contain a plethora of molecules, notably, vWF, P-selectin, and prothrombin which promote platelet aggregation and clot stabilization (Blair and Flaumenhaft, 2009, Italiano et al., 2008b). Lysosomes contain hydrolases, which have been associated with thrombus formation (Rendu and Brohard-Bohn, 2001). Disorders of granule formation or secretion result in excessive bleeding and platelet dysfunction.

Granule release must be tightly regulated while remaining efficient and rapid, to ensure an appropriate response. Alongside this, the fusion of vesicles requires a large amount of energy to overcome the repulsive ionic forces between the lipid bilayers (Aunis and Bader, 1988). Platelets utilize the SNARE complex, primarily to transport the vesicle to the target membrane and “prime” it for the release of its contents. These proteins can be grouped into three broad subfamilies: VAMPs, Syntaxins, and SNAPs (Golebiewska and Poole, 2013). In presynaptic nerve terminals, α -synuclein has been found to interact with and potentiate the assembly of the SNARE complex, however, this has not been fully investigated in platelets (Burré et al., 2010, Hawk et al., 2019, Yoo et al., 2023).

Fluorescence imaging combined with Immunoprecipitation and western blotting allowed for the assessment of α -synuclein movement and interactions within the platelet at basal and stimulated conditions. Interrogation of α -synuclein phosphorylation by Western blot allowed for the elucidation of α -synuclein function and regulation within platelets.

3.2. Aims for Chapter 3

- Assess the effects of pharmacological α -synuclein inhibitors on platelet function.
- Determine protein interactions with α -synuclein in platelets.
- Elucidate the mechanisms underlying α -synuclein phosphorylation.

3.3. Results

3.4. The role of α -synuclein in human platelets

In the first instance, we confirmed the presence of α -synuclein by western blotting in washed platelet lysates (Figure 3-1). Upon confirmation of α -synuclein in platelets, immunofluorescence analysis was used for the visualization of the spatial distribution of α -synuclein throughout the platelet. FITC phalloidin was used to stain the actin cytoskeleton, and the α -synuclein primary antibody was conjugated to a PE secondary allowing for the delineation of both proteins simultaneously. The red signal shows that α -synuclein was present in small clusters located throughout the platelet in unstimulated conditions.

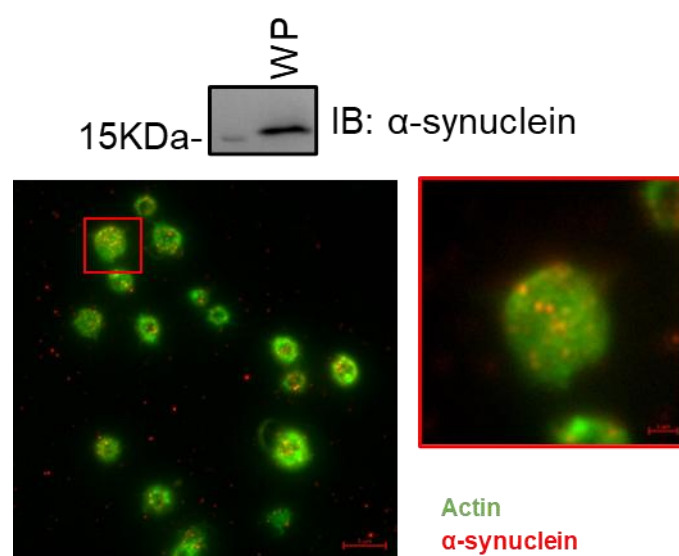


Figure 3-1. α -synuclein is present within human platelets. Western blot analysis of human washed platelets, blotting against α -synuclein. Washed human platelets were left to adhere to cover slides coated in 1x Poly-L-Lysine for 15 minutes before fixing with 4% PFA; mouse-anti-human α -synuclein primary was then incubated on the cover slides for 1 hour before incubation with FITC phalloidin (1:200) and anti-mouse PE antibody in the dark for 1 hour.

Next, we assessed the response of washed platelets to various concentrations of thrombin, collagen and the TxA2 analogue, U46619 to establish a baseline

aggregation profile (Figure 3-2). Initially, we tested three doses of thrombin, 0.05U/mL, 0.025U/mL, and 0.0125U/mL. Stimulation of platelets with these concentrations resulted in maximal aggregations of $77.5\% \pm 2.5$, $61.2\% \pm 3.8$, and $6.25\% \pm 2.1$, respectively at 5 minutes (Figure 3-2). Following the stimulation of platelets with collagen, there was a dose-dependent increase in platelet aggregation. Here we saw that the maximal aggregation plateaued between 1.0 μ g/mL and 3.0 μ g/mL showing that 1.0 μ g/mL was reaching the maximal aggregation. Similarly, when platelets were stimulated with U46619, this resulted in increased platelet aggregation in a dose-dependent manner. Importantly, platelet aggregation in response to the lowest doses of both collagen and U46619 resulted in a high variability, highlighting donor-specific sensitivity to certain agonists. Furthermore, we noted that the maximal aggregation measured through LTA is equivalent to approximately 80%. This enabled us to choose appropriate dosages of agonists going forward.

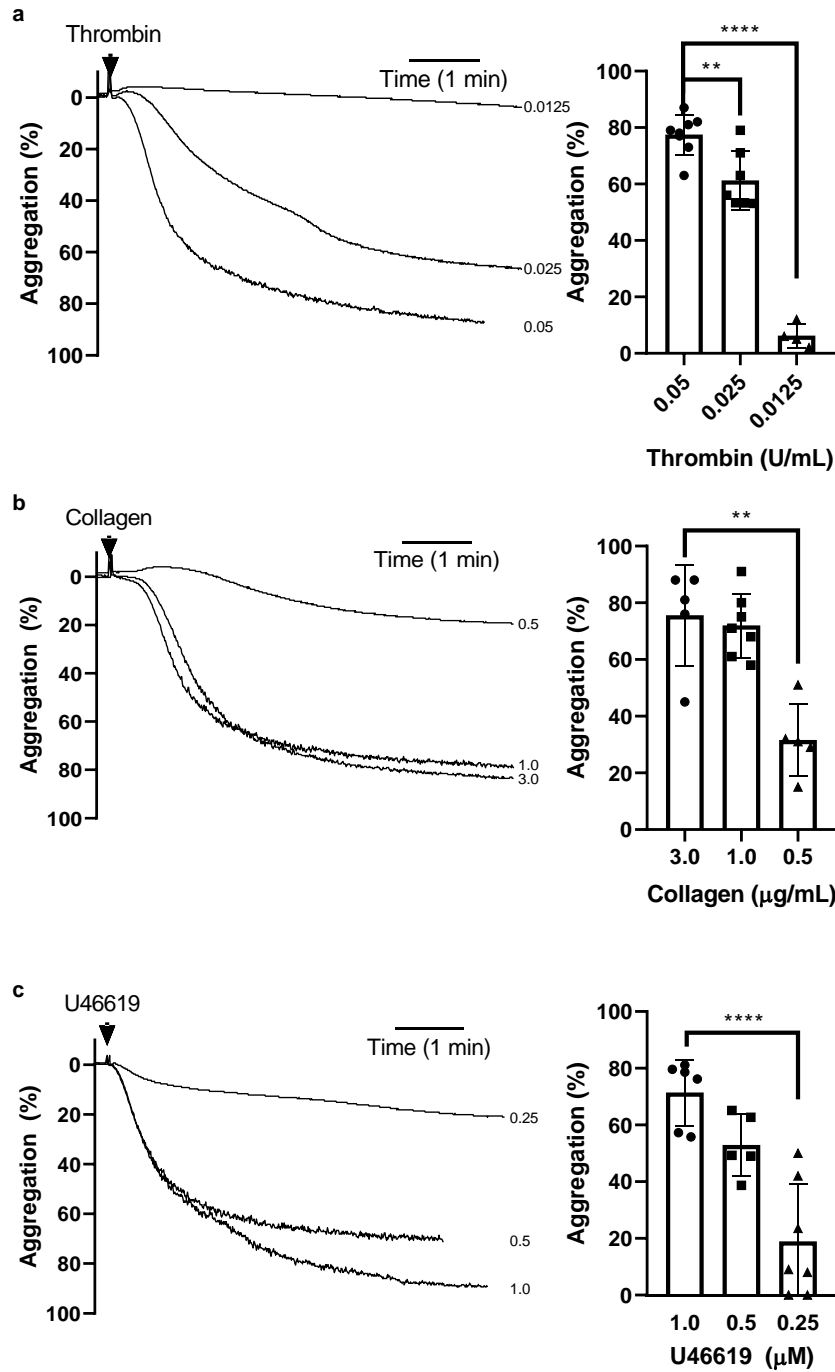


Figure 3-2. Platelet aggregation optimisation in response to different agonists. Washed human platelets at a concentration of 3.0×10^8 were added to cuvettes for light transmission aggregometry, platelets were stirred at 1000 RPM and different concentrations of thrombin (a) Collagen (b) or U46619 (c) were added. All aggregations were measured on a chrono-log 4+4 aggregometer for 5 minutes with Representative traces for dosages (left) and overall data presented as a bar chart. Thrombin N=7 Collagen N=5 U46619 N=5 Percentage aggregation is presented by mean \pm standard error of mean (SEM) * $P < 0.05$, ** $P < 0.01$

Having established the platelet aggregation response to agonists, we next assessed the impact of the α -synuclein inhibitor, ELN484228, on platelet aggregation at different doses. ELN484228 is a benzene sulphonamide-containing compound (N-(4-fluorophenyl)benzenesulfonamide) that has been shown to block α -synuclein-dependent vesicular dysfunction in neurons (Toth et al., 2014). In the first instance, we examined a wide range of ELN484228 concentrations to determine the optimum concentration (Figure 3-3). To do this, platelets were incubated with indicated concentrations of ELN484228 at 37°C for 15 minutes prior to stimulation with either thrombin or collagen.

Following stimulation with 0.05U/mL of thrombin, platelet aggregation was significantly reduced with incubation with both the 20- and 40 μ M dose of ELN484228 (20 μ M, $P=0.0208$ 40 μ M; $P=0.0105$). However, there was no significant difference in the inhibitory effect in the lowest dose tested ($P=0.96$).

Interestingly, platelets stimulated with collagen exhibited a more linear dose-dependent response when incubated with ELN484228. When challenged with low doses of inhibitor, there was a smaller defect in platelet aggregation, in comparison to that of thrombin but exhibited greater inhibition at 40 μ M. The middle dose of 20 μ M still resulted in a significant decrease in platelet aggregation, compared to the control ($P=0.037$) which decreased further with 40 μ M ELN484228 reducing aggregation to 23.667% \pm 13.19 ($P=0.0051$).

In all data sets, we observed a high degree of variability between donors highlighting inter-donor variability, The 20 μ M dose of ELN484228 was the lowest dose of inhibitor to significantly inhibit platelet aggregation to both thrombin and collagen, therefore we continued to use this dose for future experiments.

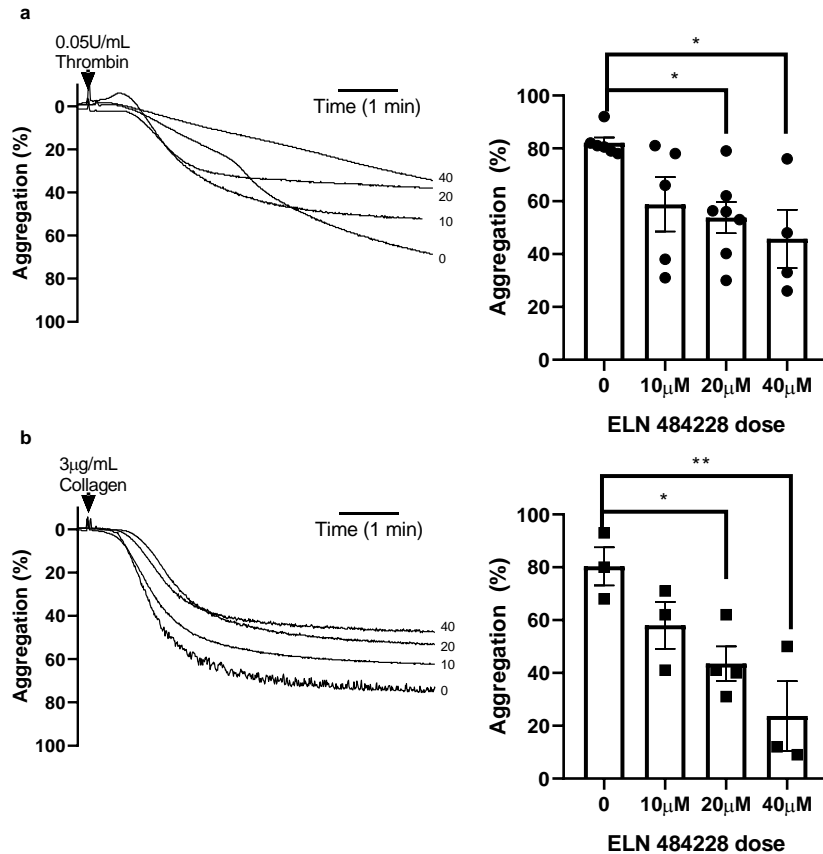


Figure 3-3. Pharmacological α -synuclein inhibitor optimisation. Platelets were incubated with ELN484228 for 15 minutes at 37°C and stirring conditions (1000RPM) before the addition of 0.05U/mL Thrombin (a) or 1µg/mL Collagen (b). All aggregations were measured on a chrono-log 4+4 aggregometer 5 minutes with Representative traces for dosages (left) and overall data presented as a bar chart (right). Thrombin N=6, Collagen N=3 Percentage aggregation is presented by mean \pm standard error of mean (SEM) *P<0.05, **P<0.01.

3.4.1. Effect of incubation time in ELN484228 on aggregation

The addition of inhibitors can result in almost instantaneous inhibition of target proteins however this is not true for all inhibitors, some of which require multiple hours to take effect. Previous studies using ELN484228 have incubated cell lines, for up to 48 hours, however this incubation period is not appropriate for use in platelet samples. Therefore, we sought to assess the effects of ELN484228 for shorter timeframes in platelets, to ensure the shortest incubation period while allowing sufficient time for the inhibitor to act upon α -synuclein (Figure 3-4).

The shortest period examined was 15 minutes, following stimulation with 0.05U/mL thrombin, the maximal aggregation at 5 minutes was 77.9% \pm 2.61 following incubation with ELN484228, this was significantly reduced to 59.82 \pm 1.916 (P=0.0016, n=10). At a 1-hour time point, we observed a significant decrease in the aggregation of the

platelets not incubated with ELN484228 falling to a maximal aggregation of 49.02% \pm 3.04. Platelets incubated with ELN484228 also saw a significant decrease between time points falling to 50.5% \pm 8.06, however there was no significant difference in platelet aggregation between ELN484228-treated samples and control (P=0.994, n=6). The final timepoint observed was 4 hours. Between the 1- and 4-hour time points there was a slight decrease in the aggregation of untreated platelets decreasing to 46.70% \pm 3.2. In contrast, platelets incubated with ELN484228, the maximal aggregation at 4 hours decreased to 21.69% \pm 6.59 yielding a significant difference to the untreated samples (P=0.014, n=4).

These data suggest that the ELN484228 is effective at inhibiting platelet aggregation at 20 μ M in time periods as short as 15 minutes. It shows the most efficacy at the 4-hour time point, however, at the longer timepoints there was a reduction of the maximal aggregation of untreated samples and a much larger spread of data. Therefore, going forward, we incubated platelets for 15 minutes with 20 μ M ELN484228.

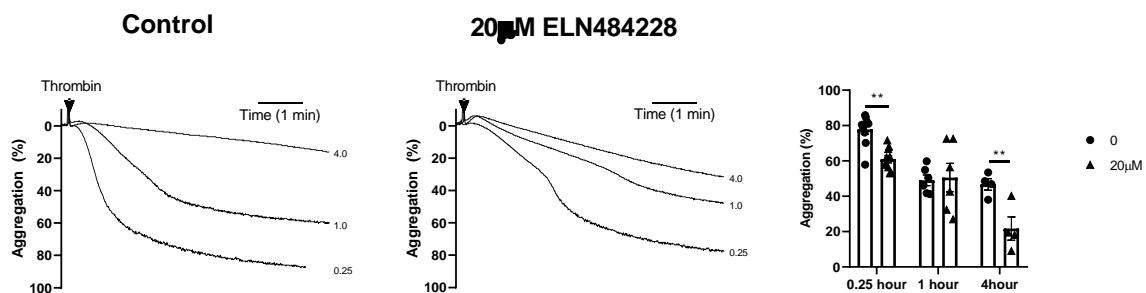


Figure 3-4. Effects of incubation period with ELN484228 on platelet aggregation to thrombin. Platelets were incubated with ELN484228 for indicated timepoints at 37°C. Following incubation 0.05U/mL Thrombin was added to platelets in stirring conditions (1000RPM). All aggregations were measured on a chrono-log 4+4 aggregometer 5 minutes with Representative traces for dosages (left) and overall data presented as a bar chart (right). Percentage aggregation is presented by mean \pm standard error of mean (SEM) *P<0.05, **P<0.01. N=7

3.4.2. Western blotting optimization

Western blot analysis is the most widely used method for detection of specific proteins. When α -synuclein was examined by Western blotting, it did not bind strongly to the PVDF membrane resulting in very low to no signal following wash steps. Therefore, fixation of PFA was required to attain sufficient signal upon imaging (Figure 3-5).

Initially, membranes were incubated for 20 minutes in 4% PFA. Although the amount of α -synuclein observed was increased, there was a significant amount of non-specific binding observed. Following this, membranes were incubated with 0.4% PFA in TBS for 20 minutes, which yielded a significantly higher signal than the non-fixed sample but had a much lower background with no visible non-specific binding. Going forward, all blots were incubated in 0.4% PFA before blocking and addition of primary antibody.

The preparation of cell lysates is also key for effective Western blotting, especially when investigating phosphorylated protein targets (Figure 3-5). Initially the pH inhibition of platelets was used for all samples, with additional tirofiban before addition of agonists to inhibit platelet aggregation. However, this resulted in a high basal phosphorylation of α -synuclein, therefore indomethacin was also added to PRP during the platelet preparation. Indomethacin inhibits cyclo-oxygenase 1 (COX1) which produces TxA_2 , which is required for amplifying platelet activation. At a $10\mu\text{M}$ dosage of indomethacin added to PRP, there was a significant decrease in the basal phosphorylation of α -synuclein ($P=0.015$), which had no impact on α -synuclein phosphorylation levels when stimulated with thrombin ($P=>0.999$). There was also a significant decrease in basal phosphorylation when dosages of indomethacin were increased to $20\mu\text{M}$ ($p=0.48$), however there was no difference between the 10 and $20\mu\text{M}$ dosages ($P=0.959$). The $20\mu\text{M}$ dose of indomethacin had no effect on the phosphorylation of α -synuclein after stimulation with thrombin. Due to the decreased phosphorylation of α -synuclein at $10\mu\text{M}$ that gave highly comparable data to the higher dosage that was used for all lysates going forward.

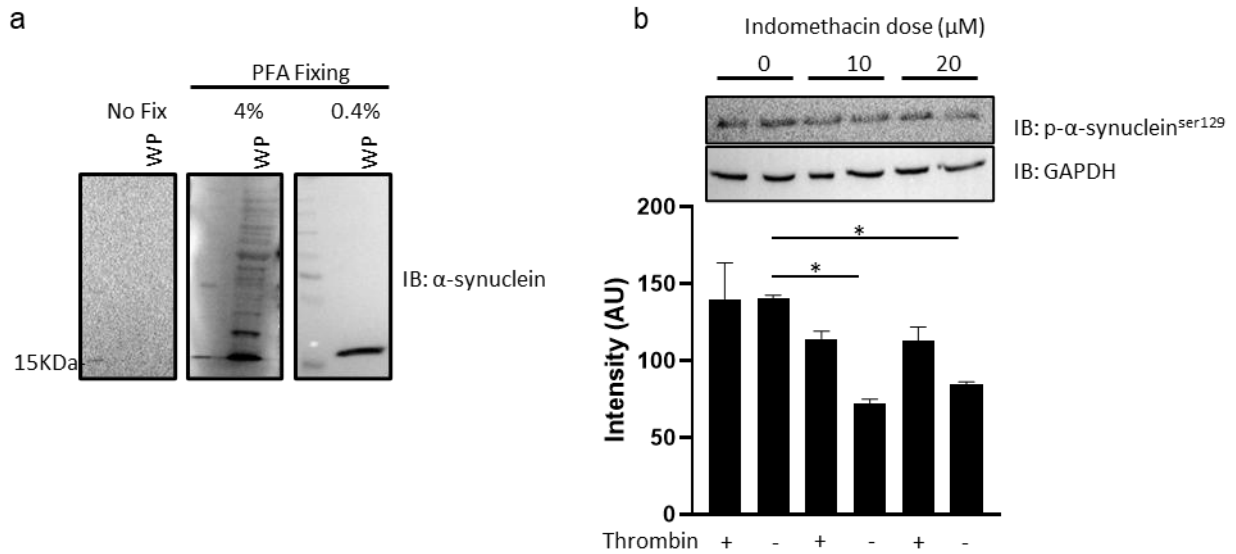


Figure 3-5. Western blotting optimisation and membrane fixing. (a) Representative western blot of membranes fixed with no, 4% and 0.4% PFA. Human platelet lysates were separated through SDS-PAGE and transferred to 0.45 μ M PVDF membranes through semidry transfer. Membranes were then fixed in 4% (middle) 0.4% PFA (Right) or not (Left) for 20 minutes at room temperature with agitation, before blocking with 5% BSA for 1 hour. Membranes were incubated overnight at 4°C with agitation with CST51510 antibody (1:1000). (b) Representative western blot analysis of indomethacin dosage in platelet preparation (top). Densitometry analysis of western blot, comparing the p- α -synuclein^{ser129} to the loading control represented as Mean \pm SEM N=3.

3.4.3. Immunofluorescence optimisation – antibody and blocking

To generate viable immunofluorescence images, effective blocking and correct antibody selection and concentration is required. Initially, we tested two blocking methods were examined: heat denatured lipid-free BSA, and human serum in both unstimulated and stimulated conditions (Figure 3-6). Slides were blocked with the corresponding serum for 1 hour before washing and adding primary antibody. With the use of either α -synuclein total antibody (CST4179 or SC-515879) the boiled BSA had a lower background fluorescence. Interestingly, the SC515879 antibody had a higher background in the 580nm channel with human serum blocking, whereas, with the use of CST4179, there was less interaction, which highlighted the higher background for the WGA antibody. Therefore, heat denatured lipid-free BSA was used for all subsequent immunofluorescences (Figure 3-6). Both CST4179 or SC-515879 antibodies were used going forward, in conjunction with other primary antibodies for multicolour immunofluorescence.

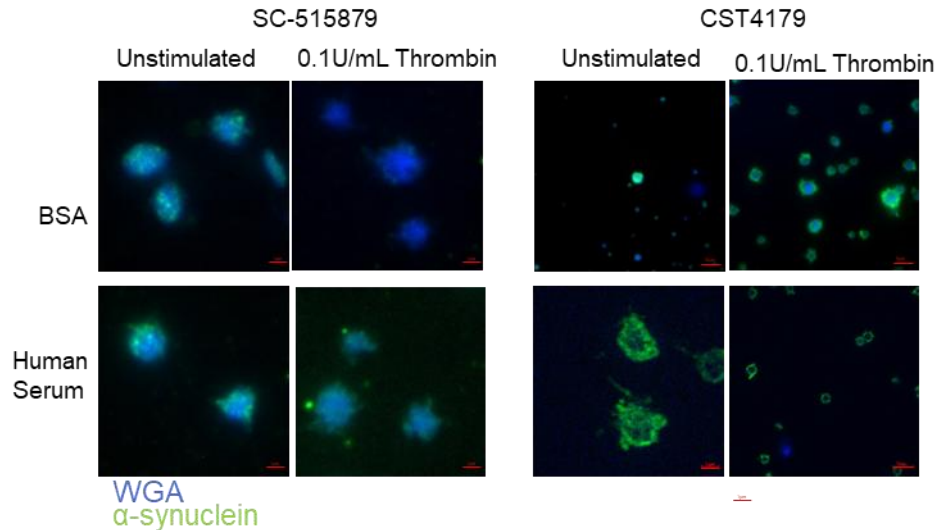


Figure 3-6. Antibody selection with Human serum vs BSA for blocking in immunofluorescence. Platelets were added to Poly-L-Lysine coated coverslips for 1 hour at a concentration of 2.0×10^7 at room temperature, Thrombin was added to platelets immediately before adding to the coverslips for stimulated samples. The slides were then washed with PBS before the addition of either BSA (top) or Human serum (bottom) for 1 hour then fixed with PFA for 10 minutes and permeabilized with 0.3% triton for 5 minutes. α -synuclein antibody was added for 1 hour at room temperature SC-515879 (1:200) CST 4179(1:200), before the addition of Anti-mouse 488 (left) or anti-rabbit 488 (right) and WGA 350 and further 1 hour incubation at room temperature away from light. All images were captured on a 100x objective with a field of view (FoV) 1000x1000 Px.

3.4.4. Immunofluorescence optimisation - antibody concentration

Antibody concentration can have a significant effect on the quality of the image produced; insufficient antibody concentration will result in unclear/ faint images, and with excessive concentrations of antibody the background staining may increase. Therefore, a titration experiment of antibodies was conducted. A 1:100 dilution of antibody resulted in a clear bright image with little background. When the antibody concentration was doubled to 1:200, both the wide field and close-up image yielded bright and clear images, however when the antibody was titrated further to 1:400, the FoV photobleached very quickly resulting in indistinguishable close field images (Figure 3-7). Therefore, a dilution of 1:200 CST4179 was used going forward, previous antibodies were optimized previously.

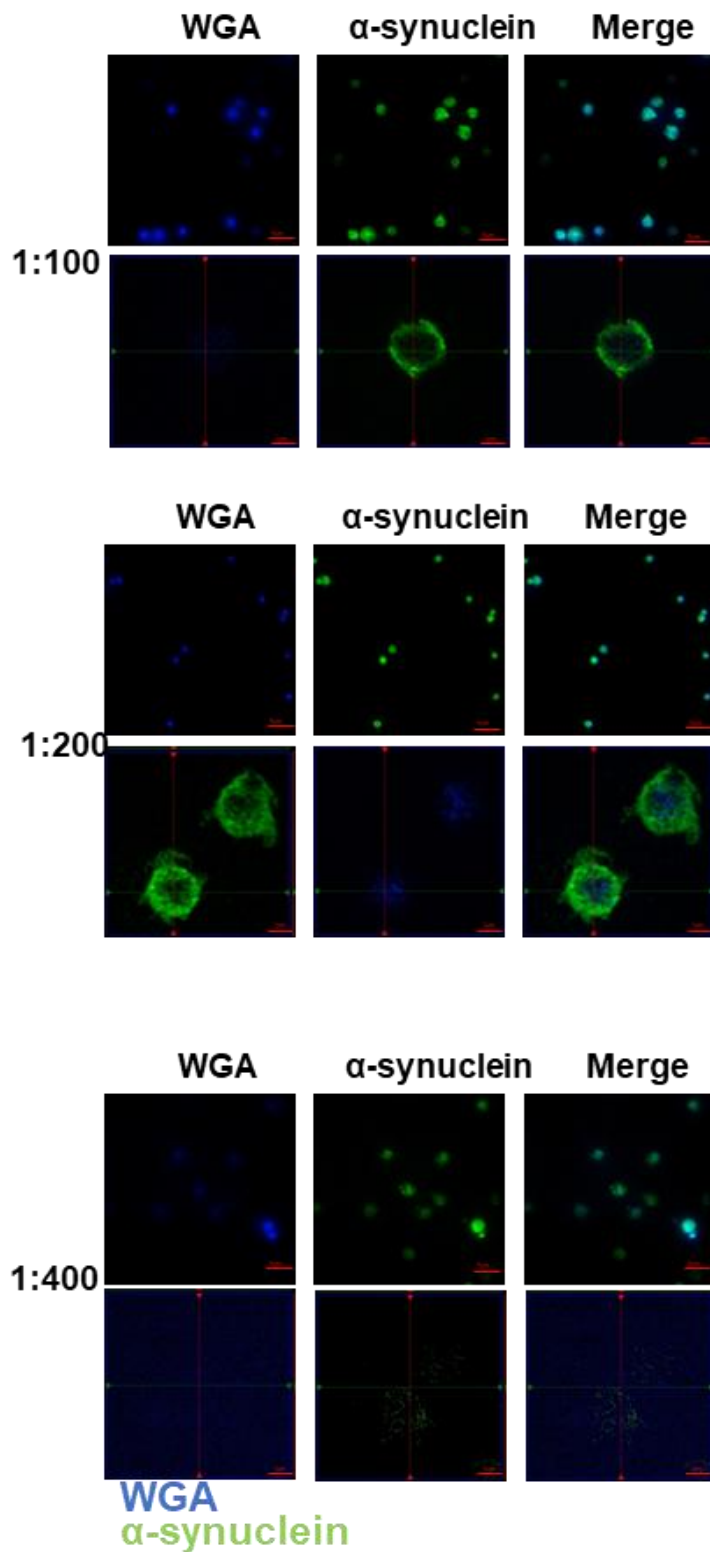


Figure 3-7. Titration of α -synuclein antibodies for immunofluorescence. Platelets were added to Poly-L-Lysine coated coverslips for 1 hour at a concentration of 2.0×10^7 at room temperature, Thrombin was added to platelets immediately before adding to the coverslips. The slides were then washed with PBS before blocking with boiled BSA for 1 hour then fixed with PFA for 10 minutes and permeabilised with 0.3% triton for 5 minutes. α -synuclein antibody at indicated dilutions was added for 1 hour at room temperature (CST4179) before the addition of anti-rabbit 488 and WGA 350 and a further 1-hour incubation at room temperature away from light. All images were captured on a 100x objective with a field of view 1000x1000px, bottom images were a selected FoV on a single platelet.

3.5. A-syn reaction to agonists

3.5.1. Movement of α -synuclein upon stimulation

The movement of proteins following the activation of the platelet can provide an insight into their potential function. Proteins that move towards the peripheries of the cells following stimulation may be involved with either a secretory mechanism or part of the granular contents. Therefore, the subcellular localisation of α -synuclein was assessed in unstimulated and thrombin-stimulated platelets by immunofluorescence microscopy. In unstimulated platelets, α -synuclein was found to spread in clusters throughout the cell (Figure 3-8). When stimulated with 0.1U/mL thrombin, α -synuclein was seen to have translocated towards the periphery of the cell. When phosphorylated- α -synuclein serine 19 (p- α -synuclein^{ser29}) was interrogated, it was observed that in unstimulated platelets, like its unphosphorylated counterpart, α -synuclein was clustered throughout the cell. When platelets were stimulated by thrombin, p- α -synuclein^{ser129} was also observed to have moved towards the periphery of the cell.

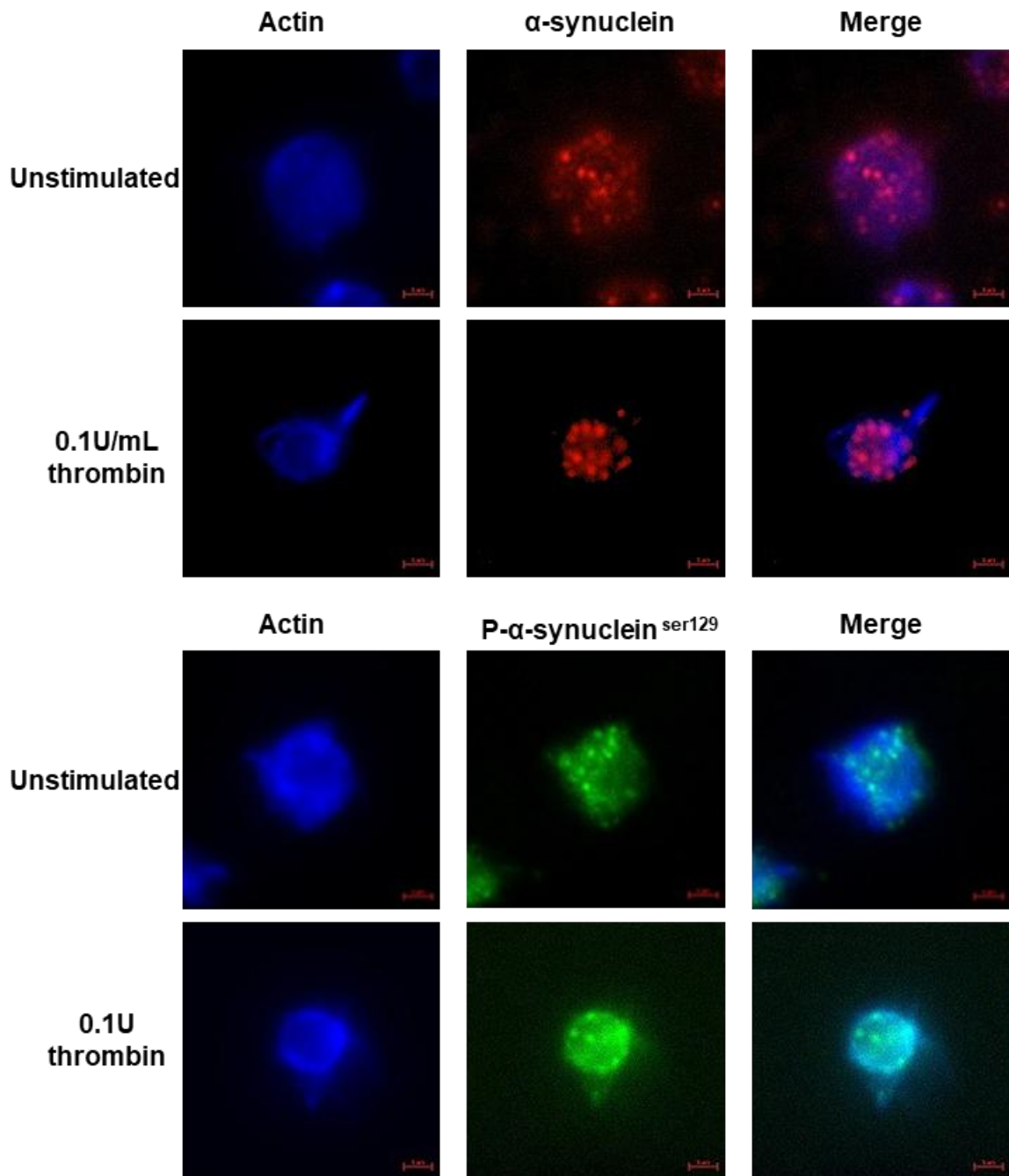


Figure 3-8. α -synuclein migrates to the periphery of platelets when stimulated with an agonist. Platelets were added to Poly-L-Lysine coated coverslips for 1 hour at a concentration of 2.0×10^7 at room temperature, for stimulated samples thrombin was added to platelets immediately before adding to the coverslips. The slides were then washed with PBS before blocking with heat denatured BSA for 1 hour then fixed with PFA for 10 minutes and permeabilised with 0.3% triton for 5 minutes. α -synuclein antibody (CST4179) was added for 1 hour at room temperature before the addition of anti-rabbit 575 and WGA 350 and a further 1-hour incubation at room temperature away from light. All images were captured on a Zeiss AXIO observer 100x objective with a field of view 128x128.

After observing both α -synuclein and the serine129 phosphorylated variant exhibit highly analogous movements within the platelet, we implemented the use of three colour immunofluorescence to assess whether the phosphorylation state affects protein movement (Figure 3-9). As previously seen, the α -synuclein and α -synuclein^{ser129} are present clustered throughout the platelet, and upon stimulation translocate to the peripheries. Interestingly, although there are some clusters of co-localised α -synuclein and p- α -synuclein^{ser129} in basal platelets, towards the middle of the cell most clusters observed are towards the periphery. After stimulation with thrombin, the α -synuclein translocated to the periphery, where the amount of phosphorylation is increased, as shown by a much higher propensity of co-localisation events.

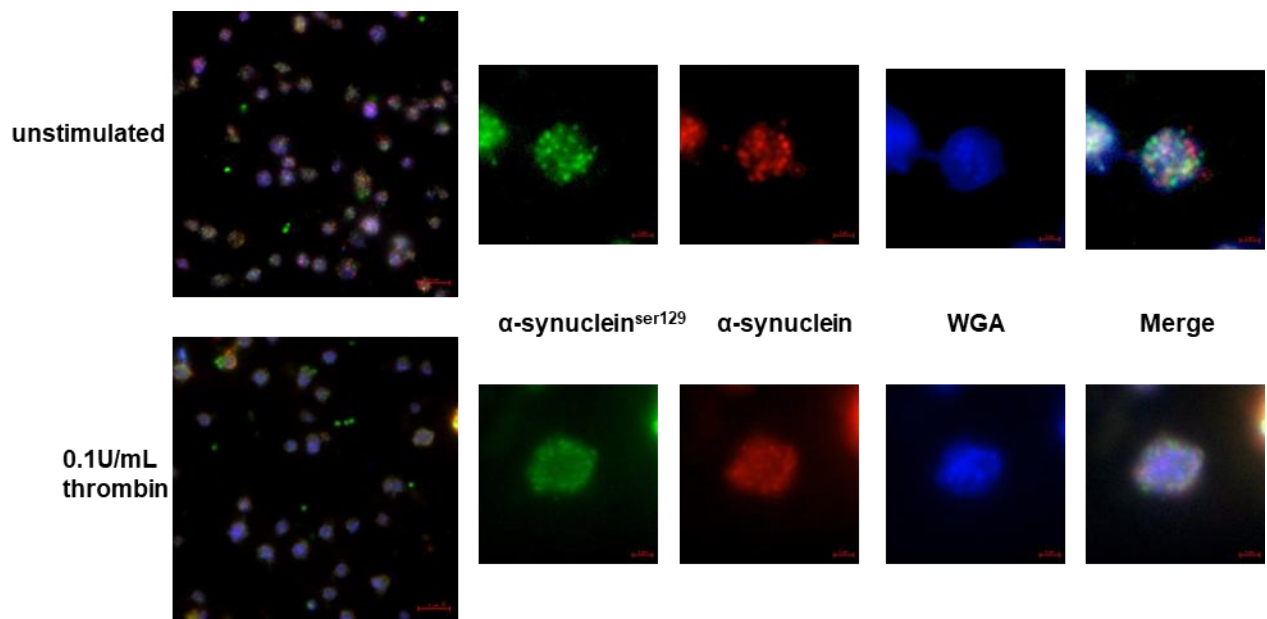


Figure 3-9. Co-localisation of p- α -synuclein and α -synuclein in basal and stimulated platelets. Platelets were added to Poly-L-Lysine coated coverslips for 1 hour at a concentration of 2.0×10^7 at room temperature, Thrombin was added to platelets immediately before adding to the coverslips for stimulated samples. The slides were then washed with PBS before the addition BSA for 1 hour then fixed with PFA for 10 minutes and permeabilized with 0.3% triton for 5 minutes. Both α -synuclein and p- α -synuclein antibodies were simultaneously added for 1 hour at room temperature SC-515879 (1:200) SC-135638 (1:200), before the addition of Anti-mouse 488 (left) or anti-rabbit 575 (right) and WGA 350 and further 1-hour incubation at room temperature away from light. All images were captured on a 100x objective with a field of view 128x128.

Having established that α -synuclein translocates to the cell membrane following platelet activation, we assessed whether α -synuclein is secreted by platelets, is expressed on the platelet surface, or remains within the cell (Figure 3-10). In the first instance, we visualised the expression of α -synuclein and p- α -synuclein^{ser129} on the platelet surface, using immunofluorescence on non-permeabilised platelets. Under unstimulated conditions, there was a signal for p- α -synuclein^{ser129} spread across the platelet surface, which contrasted with the non-phosphorylated form of α -synuclein where no signal was observed. Upon stimulation, there was much more signal for p- α -synuclein^{ser129} around the periphery of the cell, but no α -synuclein fluorescence was detected. There were “nodes” of significant clustering and high signal for both phosphorylated and non-phosphorylated α -synuclein, but these clusters were not observed to be co-localised together.

Following this observation, we sought to quantify the changes in expression of α -synuclein on the cell surface through flow cytometry. Platelets that were stimulated with thrombin were seen to have a 1.65-fold increase over unstimulated samples, suggesting that α -synuclein is translocated to the outer leaflet of the membrane following membrane mixing of the granule. Taken together these data suggest that the α -synuclein is expressed in low levels on the platelet surface, and this significantly increases upon platelet stimulation, due to its involvement in the release of granules.

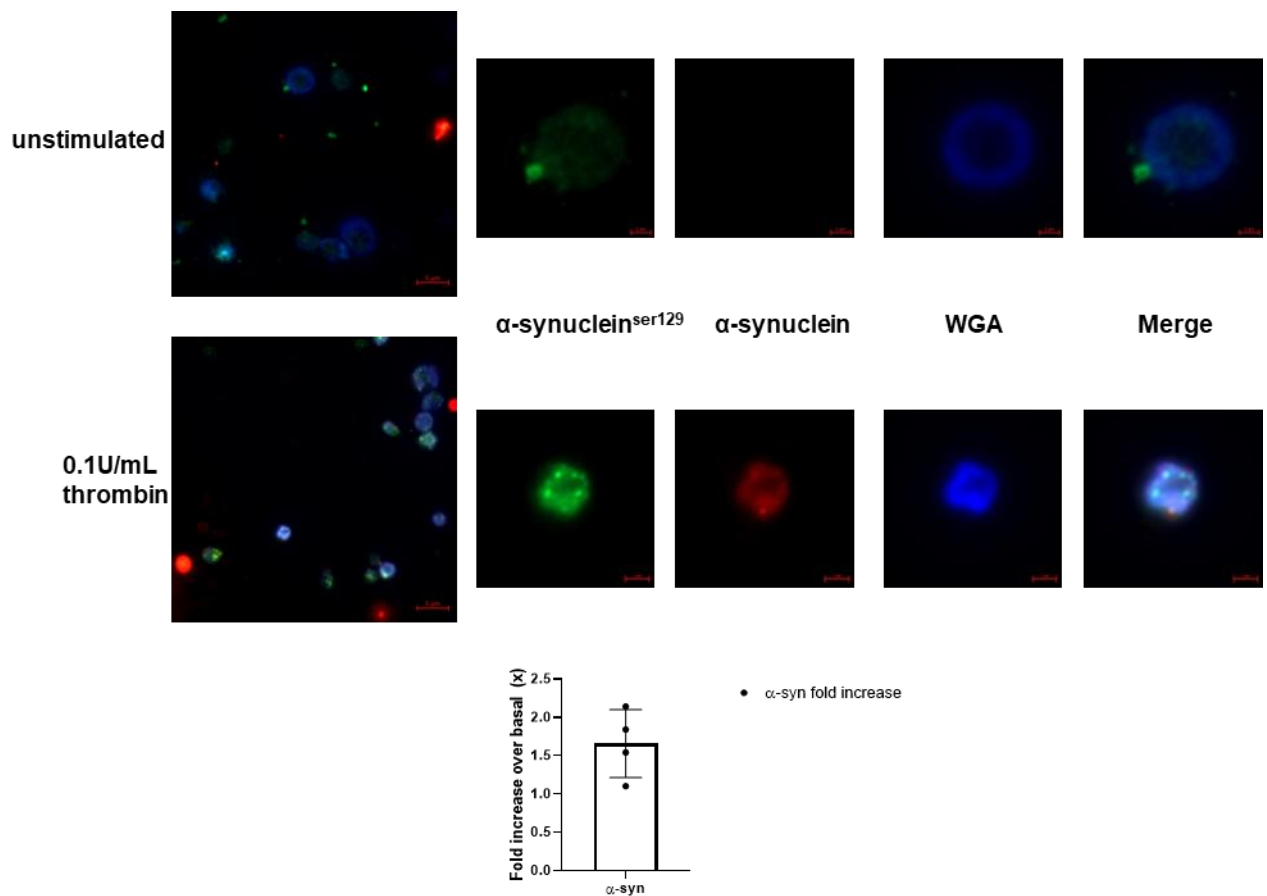


Figure 3-10. α -synuclein is not secreted by platelets but expressed on the platelet surface when stimulated. (A) Representative immunofluorescent images of platelets stained for α -synuclein (red) p- α -synuclein^{ser129} (Green) and actin (blue). Platelets were added to Poly-L-Lysine coated coverslips for 1 hour at a concentration of 2.0×10^7 at room temperature, Thrombin was added to platelets immediately before adding to the coverslips for stimulated samples. The slides were then washed with PBS before the addition BSA for 1 hour then fixed with PFA for 10 minutes and permeabilized with 0.3% triton for 5 minutes. both α -synuclein (red) and p- α -synuclein (green) antibodies were simultaneously added for 1 hour at room temperature SC-515879 (1:200) SC-135638 (1:200), before the addition of Anti-mouse 488, anti-rabbit 575 and TRITC phalloidin (Blue) and further 1-hour incubation at room temperature away from light. All images were captured on a 100x objective wide field of view 1000x1000 close field of view 128x128px (A) platelets were incubated with α -synuclein antibody (SC-515879) 1:10 at 37°C for 20 minutes, before the addition of anti-mouse FITC for 30 minutes and incubated away from light. These samples were then run through a BD- Fortessa LSR II. Data displayed as Fold increase over basal \pm SEM N=4.

Next, we assessed whether α -synuclein was within the granules, present in the cytosol or secreted. To achieve this, we used centrifugation to separate the platelet releaseate and the platelets, followed by western blotting (Figure 3-11). Immunoblotting for α -synuclein shows the maintenance of the protein within the platelet pellet with no observed release. To confirm this, we probed for thrombospondin-1 (TSP1) which is a known α -granule component. Under unstimulated conditions, TSP1 was observed only within the platelet pellet, following stimulation with 0.1U/mL thrombin the TSP1

was secreted from the platelets resulting in a decrease in the pellet and an increase in the releaseate in a time-dependent manner.

Next, we assessed the presence of α -synuclein in the pellet and releaseate, membranes were re-probed with anti- α -synuclein antibody, and it was found that α -synuclein was only present in the pellet fractions, both in unstimulated and thrombin-stimulated samples, demonstrating that α -synuclein is not within the granular contents and is not secreted upon platelet activation.

Having observed the movement of α -synuclein from the centre of the cell towards the periphery, and that it is not secreted when platelets are stimulated with agonist, we sought to determine whether α -synuclein is bound to the membrane or remains as a cytosolic protein. To achieve this, basal and stimulated thrombin-platelets were snap-frozen repeatedly to lyse the cells, these were centrifuged to remove intact cells, and the supernatant of lysed cells was then ultracentrifuged to separate the cytosol and membrane portions. Western blot analysis revealed that p- α -synuclein^{ser129} was seen to be in both the cytoplasm and interacting with the membrane in stimulated conditions. We did not observe any p- α -synuclein^{ser129} in the cytoplasm or on the membrane in unstimulated conditions, however, we did observe non-phosphorylated α -synuclein. This suggests that the activation of platelets phosphorylates α -synuclein, which may facilitate its interaction with the platelet membrane.

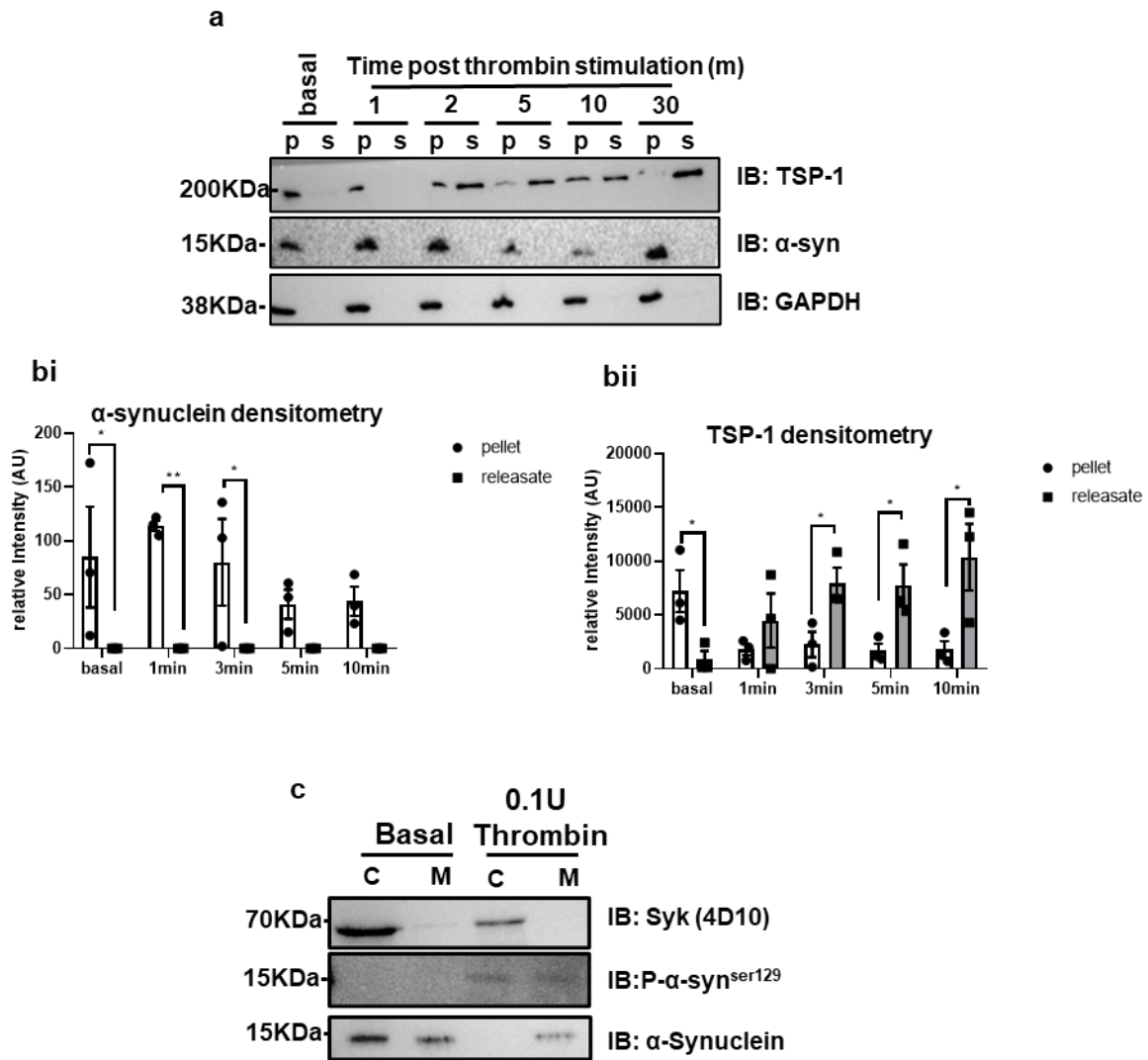


Figure 3-11. α -synuclein is not secreted by platelets following stimulation. (A) Representative blot of α -synuclein expression in pellet or supernatant from activated platelets. Washed human platelets, either stimulated or basal, were snap-frozen 4-5 times in liquid nitrogen, centrifuged in a Beckman-coulter TL-01 Ultra-centrifuge at 100,000g for 75 minutes at 4°C. Pellets were washed with Lysis buffer before the addition of 2x Laemmli buffer to be separated using SDS PAGE. (B) Quantification of western blot analysis by calculating the relative intensity of the target protein to GAPDH, Data represented as a bar graph with Datapoints Mean \pm SEM (N=3) (c) western blot analysis of platelet membrane and cytoplasm fractions separated through ultra-centrifugation staining for Syk and p- α -synuclein^{ser129}.

3.5.2. Co-localisation of α -synuclein with vesical-associated membrane proteins.

Co-localisation of proteins within cells can be indicative of protein-protein interactions or proteins with a similar function. Here, we sought to examine the movement of α -synuclein in relation to other SNARE complex members present within the platelet known to be involved with granule secretion (Dunn et al., 2011a). Due to the chaperoning interaction of α -synuclein and VAMP2 in neurons; In the first instance, we started by elucidating the movement of VAMP8 in comparison to α -synuclein (Figure 3-12). This allowed us to elucidate where the platelet granules were located within the platelet and compare their movement in relation to α -synuclein.

Under unstimulated conditions, VAMP8 was observed to be spread throughout the platelet, which was expected due to its association with the platelet granules. Interestingly, α -synuclein was also observed to be throughout the platelets with some occasional co-localisation throughout the platelet. When platelets were stimulated with 0.1U/mL thrombin, VAMP8 and α -synuclein were found to translocate towards the periphery of the cell. Importantly, the intensity of co-localisation between VAMP8 and α -synuclein also increased, suggesting that the two proteins may act synergistically to facilitate platelet secretion. These data also suggest that α -synuclein has a basal level of interaction with VAMP8 in unstimulated conditions.

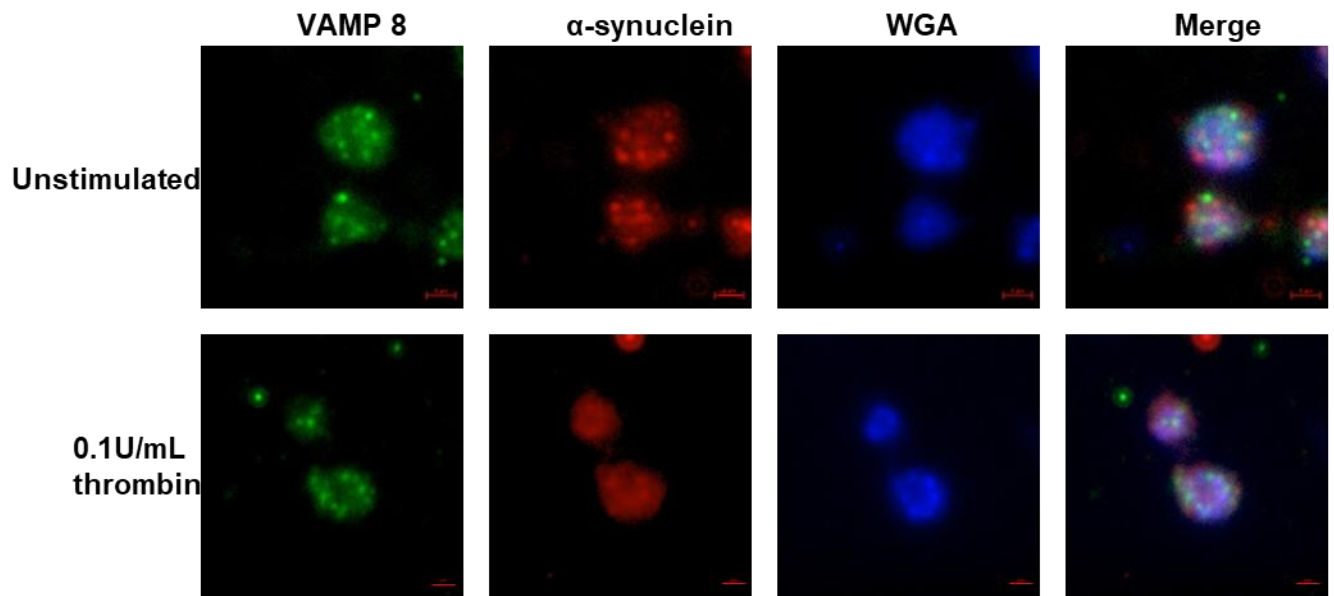


Figure 3-12 Representative images of the movement and co-localisation of α -synuclein with VAMP8 in stimulated human platelets. Platelets were isolated from whole blood through centrifugation collected by venipuncture from healthy donors. Stimulated samples were activated with 0.1U thrombin directly before addition to Poly-L-Lysine coverslips followed by incubation for 1 hour at 37°C. Cover slides were then washed and blocked with 0.5% BSA for 1 hour, before fixing and permeabilisation at room temperature with 4% PFA and 0.3% Triton-x100 respectively. Platelets were then incubated with 1:200 α -synuclein (CST 4179) and 1:100 VAMP8 (cst -13060s) for 1 hour at 37°C. Following washing with PBS the slides were incubated 1:1000 Anti-mouse (568), Anti-rabbit (667) and 5.0 μ g/mL WGA, Alexa Fluor® 350 for 1 hour at 37°C, protected from light. Samples were mounted with gelvitol and imaged. Representative image of N=3. Images were then false-coloured α -synuclein (red) VAMP8 (green) membrane (blue).

Subsequently, we sought to assess the movement of VAMP2 and α -synuclein co-localisation. VAMP2 also associates with platelet α -granules and is involved in their secretion, albeit to a lesser extent than that of VAMP8 (Ren et al., 2007, Golebiewska and Poole, 2013). VAMP2 has been observed to interact with α -synuclein in neural cells, therefore, we assessed whether indications of this interaction were present in platelets (Sun et al., 2019) (Figure 3-13).

Under unstimulated conditions, VAMP2 and α -synuclein were homogeneously spread throughout the platelet with a small amount of co-localisation events. Upon stimulation with 0.1U/mL thrombin, the VAMP2 translocated towards the periphery of the platelet, forming a ring around the outer edges. Interestingly, α -synuclein was observed to recapitulate this movement and many sites of co-localisation were observed between the two populations

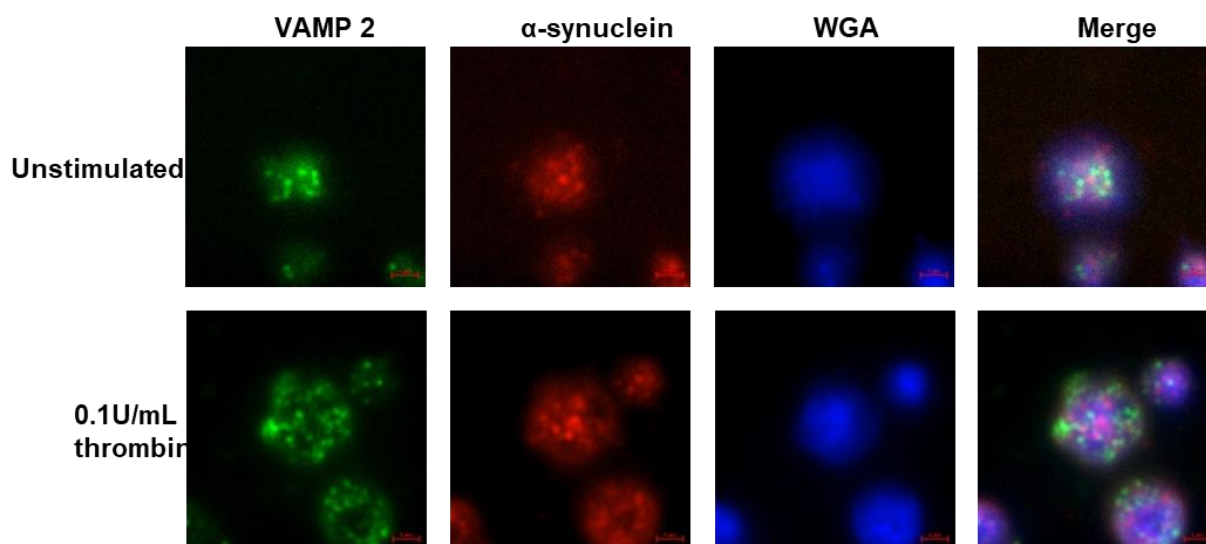


Figure 3-13. movement and. Movement and localisation of α -synuclein with VAMP2 in stimulated human platelets. Platelets were isolated from whole blood through centrifugation collected by venipuncture from healthy donors. Stimulated samples were activated with 0.1U thrombin directly before addition to Poly-L-Lysine coverslips followed by incubation for 1 hour at 37°C. Cover slides were then washed and blocked with 0.5% BSA for 1 hour, before fixing and permeabilization at room temperature with 4% PFA and 0.3% Triton-x100 respectively. Platelets were then incubated with 1:200 α -synuclein (CST 4179) and 1:100 VAMP2 (SC-69706)) for 1 hour at 37°C. Following washing with PBS the slides were incubated 1:1000 Anti-mouse (568), Anti-rabbit (667) and 5.0 μ g/mL WGA, Alexa Fluor® 350 for 1 hour at 37°C, protected from light. Samples were mounted with gelvitol and imaged. Representative image of N=3. Images were then false-coloured α -synuclein (red) VAMP2 (green) membrane (blue).

3.6. Examining platelet function using the α -synuclein inhibitor, ELN484228.

Next, we examined the inhibitory effect of ELN484228 using a range of agonist concentrations to assess whether inhibition changed with different levels of platelet activation. Stimulation of platelets with 0.05U/mL of thrombin induced 77.5% \pm 2.5 aggregation, the addition of 20 μ M ELN484228 no change in platelet aggregation (P=0.998 n=6). When incubated in 20 μ M ELN484228 stimulation with 0.025U/mL of thrombin resulted in a modest but insignificant decrease (66.95% \pm 4.13 vs 51.04% \pm 7.202; P=0.231 n=6). Interestingly when the dose of thrombin was decreased to 0.025U/mL the variance in the ELN-treated population was much greater than both the 0.5U/mL stimulated and control samples.

To examine whether the inhibitory effect is shared with other agonists, we assessed the effect of ELN484228 on collagen-induced platelet aggregation (Figure 3-14). Stimulation of platelets with collagen (3.0 μ g/mL), resulted in an aggregation of 60.8% \pm 3.24, which was reduced to 56.67% \pm 9.14 (P=0.120 n=5) in the presence of

ELN484228. Interestingly, ELN484228 seemed to increase platelet aggregation when stimulated with a lower collagen concentration. Increasing from $44.3\% \pm 6.90$ to $56.67\% \pm 9.1$, however, this change was also not significant ($P=0.73$ $n=5$). These large variances could indicate off-target effects of the inhibitor increasing propensity for platelet activation through GPVI signalling, or an interpatient variation, whereby platelets with higher α -synuclein expression are more greatly affected.

Next, we interrogated the impact of ELN484228 on TxA₂-induced platelet aggregation using the thromboxane analogue U46619. ELN484228 had no impact on U46619-induced aggregation at any of the concentrations tested ($0.025\mu\text{M}$ $P=0.0994$ $N=6$, $0.05\mu\text{M}$ $P=>0.999$ $N=8$, $0.1\mu\text{M}$ $P=>0.999$ $N=6$). Interestingly we saw that at lower doses of agonist, a larger variance in the dataset was present, this was ameliorated at the top dose, however, this may have been due to the dosage being so high it was overcoming any inhibitory effect induced by ELN484228.

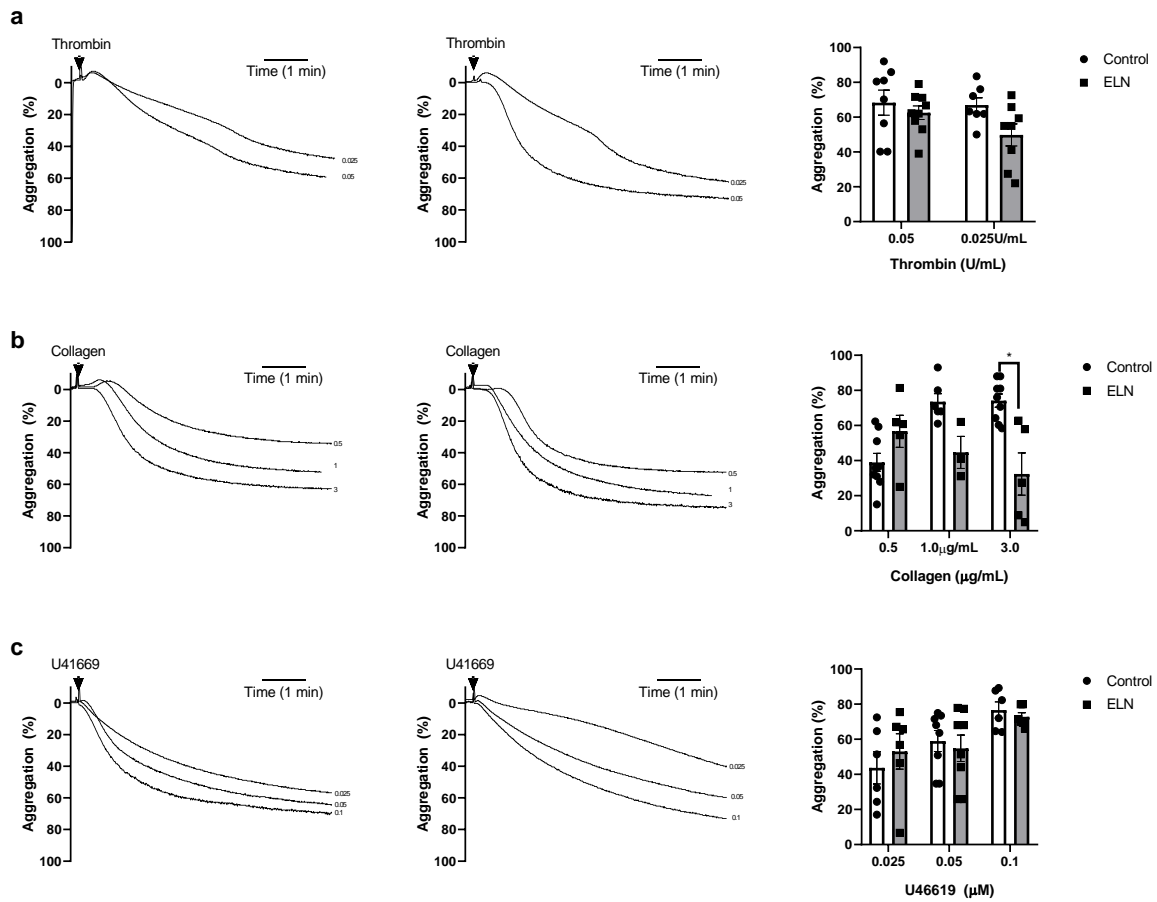


Figure 3-14. Effects of Pharmacological α -synuclein Inhibitors on Human platelet aggregation to platelet agonists. Washed platelets at 3.0×10^8 were either incubated with or without ELN484228 for 15 minutes at 37°C and stirring conditions (1000RPM) before the addition of Thrombin (a), Collagen (b) or U41669 (c), Aggregation was then measured using a chrono-log 4+4 aggregometer 5 minutes with Representative traces for dosages (left) and overall data presented as a bar chart (right). Percentage aggregation is presented by mean \pm standard error of mean (SEM) * $P < 0.05$, ** $P < 0.01$. Thrombin N=8, Collagen N=6 U46619 N=6.

3.7. Interaction of α -synuclein with SNARE complex proteins following stimulation.

Given that α -synuclein is known to interact with SNARE protein in neurons (Ramakrishnan et al., 2012, Hawk et al., 2019), we sought to assess whether this mechanism is conserved in platelets. To achieve this, we used the immunoprecipitation approach, allowing us to precipitate α -synuclein and its interaction partners, before processing the samples by Western blotting (Figure 3-15). Here we show that in unstimulated conditions, α -synuclein interacts with STX11, STX4, VAMP7, VAMP2 and SNAP23, while there is very little interaction with VAMP8. However, following stimulation with 0.1U/mL thrombin, interaction with VAMP8, STX4, -11 was increased, with no change in SNAP23, VAMP2 or -7 interaction. In a study published in 2010, Burre and colleagues showed that VAMP2 interacts with α -synuclein in presynaptic terminals of neurons, which may indicate a similar interaction in platelets. However, in contrast, there was a much more pronounced increase in α -synuclein association with the Syntaxin proteins, having a 2.3 x increase with Stx11 and a 1.74x fold increase with Stx4. We also saw an increase in interaction with VAMP8 upon stimulation, which indicates further integration of α -synuclein with the SNARE complex machinery.

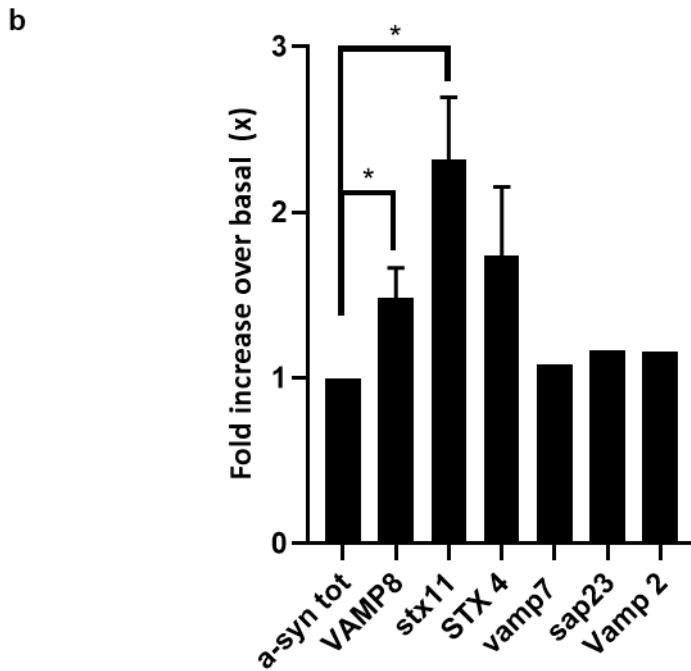
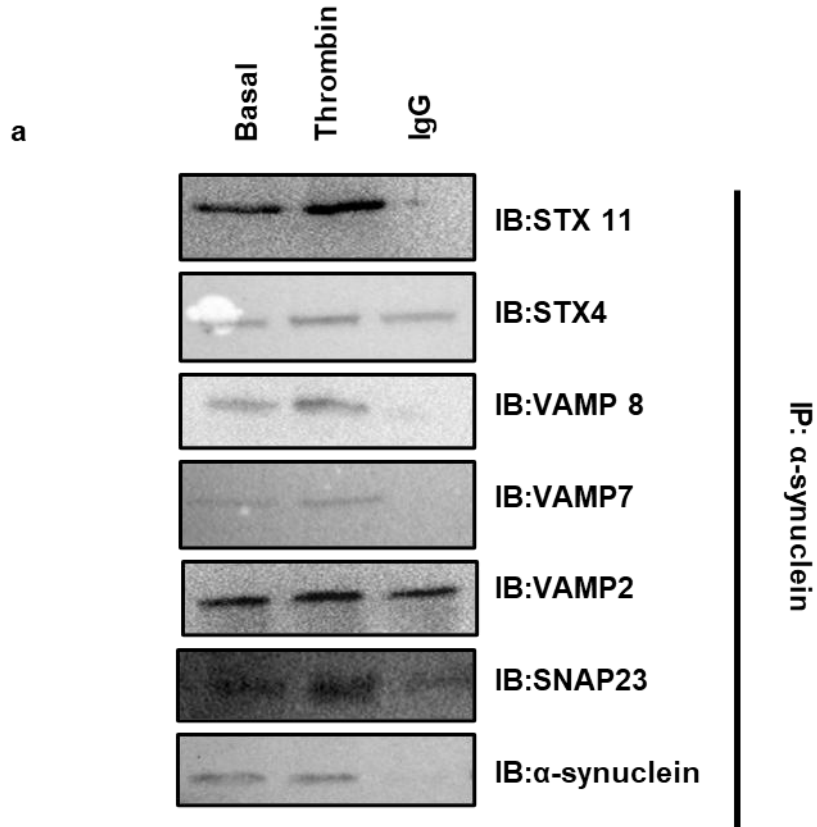


Figure 3-15. Interaction of α -synuclein with SNARE complex proteins in basal and thrombin stimulated conditions. (a) Representative immunoblots from immunoblots of α -synuclein immunoprecipitations (CST4179) collected from basal, and 0.5U/mL thrombin-stimulated Platelets samples. Samples were precleared with 20 μ L Sepharose Beads for 1 hour before incubation with 4 μ L (24 μ g/ml) CST4179 rotating overnight at 4°C. Sepharose A/G beads were then added for 2 hours and rotated at 4°C before centrifugation at 10,000g for 1 minute, and supernatant placed in a separate tube and the beads washed twice more before the addition of 3x Laemmli, and heating and placed on ice. (b) Densitometric analysis of immunoblots, displayed as fold increase of thrombin stimulated samples over basal., Data presented as fold change Mean \pm SEM N=3 *P<0.05, **P<0.01 N=3.

3.8. The effects of platelet stimulation on α -synuclein serine129 phosphorylation.

The phosphorylation of α -synuclein at serine129 has been associated with aggregation and neurotoxicity in neural cells, additionally, it has been shown to increase the propensity for membrane binding (Kawahata et al., 2022, Samuel et al., 2016). In this work, we assessed the impact of thrombin stimulation on the phosphorylation of serine129 on α -synuclein, to establish whether a similar mechanism is present in platelets (Figure 3-16).

There was a basal expression of phosphorylated α -synuclein in unstimulated platelets ($25.68\text{AU} \pm 7.42$), which increased in response to thrombin in a dose- and time-dependent manner. Stimulation of platelets with thrombin (0.05U/mL) increased serine 129 phosphorylation, reaching statistical significance at the 5-minute timepoint, increasing further to 15 minutes $101.9\text{AU} \pm 16.8$ ($P=0.0059$, $n=4$). Stimulation of platelets with 0.025U/mL and 0.0125U/mL for 5 minutes increased serine129 phosphorylation to an average intensity of $61.6\text{AU} \pm 24.5$ and $23.33\text{AU} \pm 4.37$, respectively, indicating that phosphorylation was both time and dose dependent. We noted that the phosphorylation of α -synuclein did not decrease at any time point prior for those tested, this implies that the phosphorylation of α -synuclein is not reversible following platelet activation.

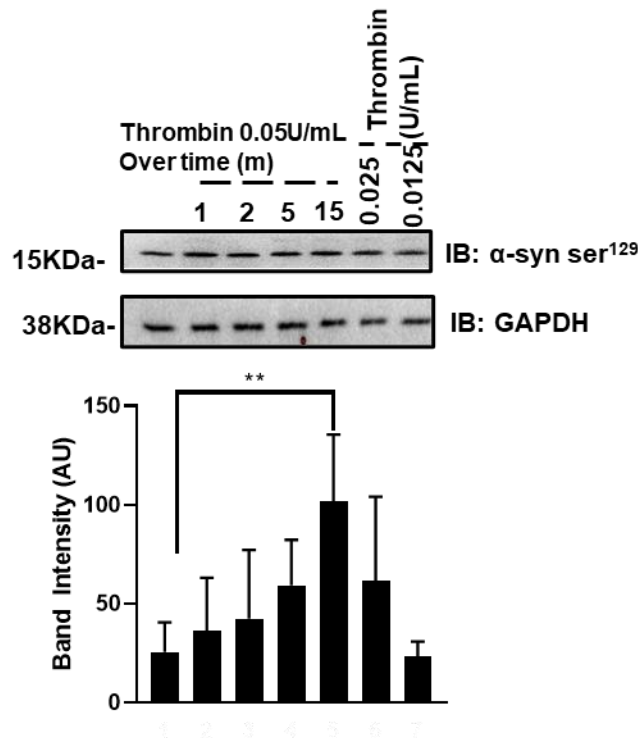


Figure 3-16. Thrombin stimulation of platelets induces the phosphorylation of α -synuclein. Representative immunoblot of thrombin-stimulated samples interrogated for p- α -synuclein^{ser129}. Densitometry was conducted on all blots and relative intensity against the loading controls, which are presented as Mean \pm SEM. * P <0.05, ** P <0.01 * p >0.05 ** P >0.01 N =4.

We sought to assess whether the phosphorylation of α -synuclein was induced through the downstream signalling cascade of GPIb/IX/V, PAR1, or PAR4, or a systemic change within the platelet. The effect of collagen and CRP-XL stimulation on the phosphorylation of α -synuclein (Figure 3-17). As with thrombin there was an observable basal expression of α -synuclein^{ser129}, (99.0AU \pm 5,292), When stimulated with 2.5 μ g/mL collagen the level of phosphorylation increased in a time dependent manner, however, this increase was only significant at the 5-minute time point with a relative intensity of 190.0AU \pm 15.95 (P =0.0058 N =3). Interestingly, unlike thrombin, the amount of α -synuclein phosphorylation decreased between the 5- and 15-minute timepoint to 105AU \pm 7.6. When the dose of collagen was reduced the phosphorylation levels at 5 minutes were also reduced, with insignificant increases over basal levels (1.25 μ g/mL P =0.999, 0.725g/mL P =0.351).

Next, we examined the effects of CRP-XL stimulation on α -synuclein phosphorylation allowing us to elucidate the effects of GPVI activation in isolation. Here, we observed

basal phosphorylation, in unstimulated conditions similarly to other samples $47.9\text{AU}\pm 8.5$. Following stimulation with $10\mu\text{g/mL}$ CRP-XL phosphorylation of serine 129 increased insignificantly until 2 minutes then decreased back down to basal levels by the 15-minute time point. There was no significant change in serine129 phosphorylation in relation to dosages of CRP-XL, however, this is to be expected as the phosphorylation on the time course had decreased by this time point also ($5\mu\text{g/mL}$ $43.8\text{AU}\pm 8.45$, $2.5\mu\text{g/mL}$ $60.5\text{AU}\pm 18.9$). To assess whether the CRP-XL was influencing the platelets we assessed tyrosine phosphorylation using the 4G10 pan-phosphorylation antibody, this showed a significant increase in phosphorylation in all time points and dosages over basal.

Taken together, this shows that when platelets are activated through the GPVI receptor, the phosphorylation of α -synuclein at serine129 is not induced; however, when stimulated through $\alpha 2\text{b}1$ and GPVI, there is an observed phosphorylation at early time points.

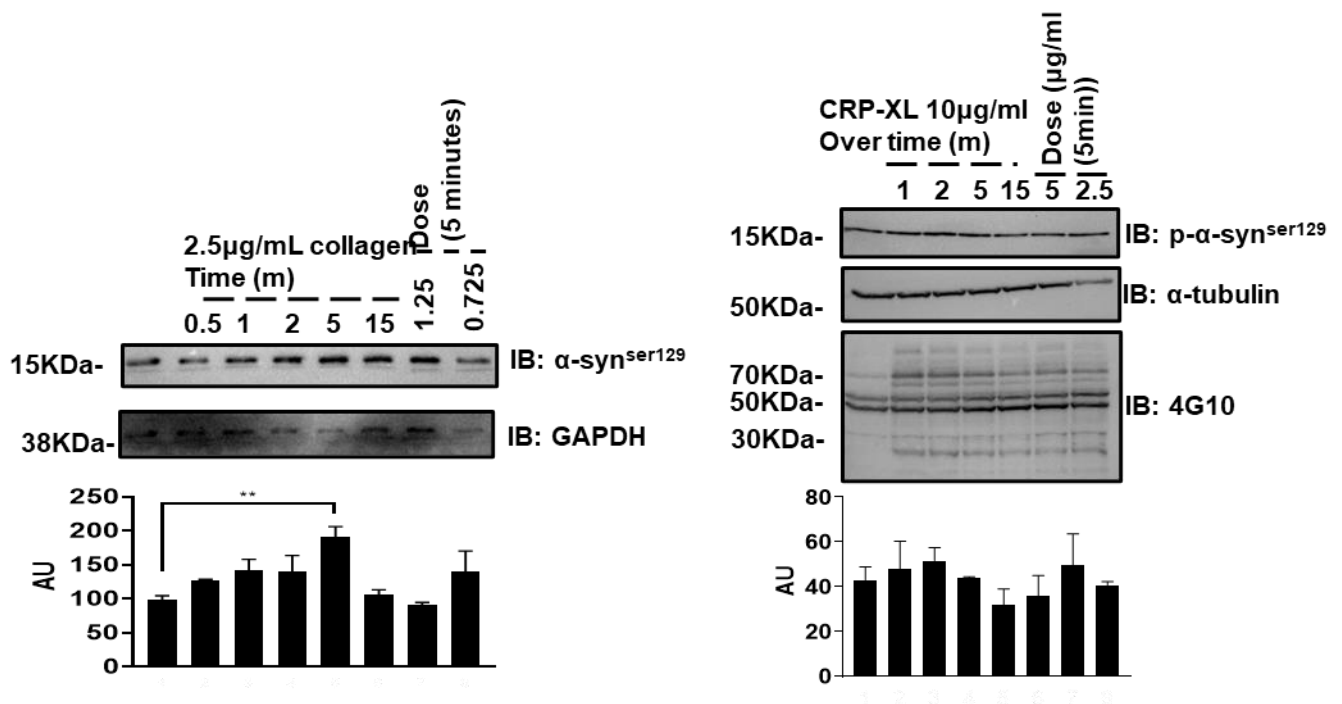


Figure 3-17. Collagen stimulation of platelets effects on phosphorylation of α -synuclein. Representative immunoblot of Collagen stimulated samples interrogated for $p\text{-}\alpha\text{-syn}^{\text{ser}129}$. Densitometry was conducted on all blots and relative intensity against the loading controls, which are presented as Mean \pm SEM. * $P<0.05$, ** $P<0.01$ * $p>0.05$ ** $P>0.01$. N=3.

Additionally, we assessed whether phosphorylation of α -synuclein was induced downstream of thromboxane A₂ receptor (TP). To achieve this, we used U46619 (Figure 3-18).

In the highest dose of U46619 (0.1 μ M) which yielded maximal aggregation, there was no significant change in the phosphorylation of α -synuclein until the 5-minute time points, where we saw a significant increase, which increases further at 15 minutes. Basal unstimulated expression measured at 102AU \pm 6.0- which increases to 191AU \pm 67.5 at 15 minutes (N=4). When the dose of U46619 was decreased to 0.05- and 0.025 μ M, the level of phosphorylation was highly analogous to the basal sample 0.05 μ M P=0.999, 0.025 μ M P=0.999, N=3.

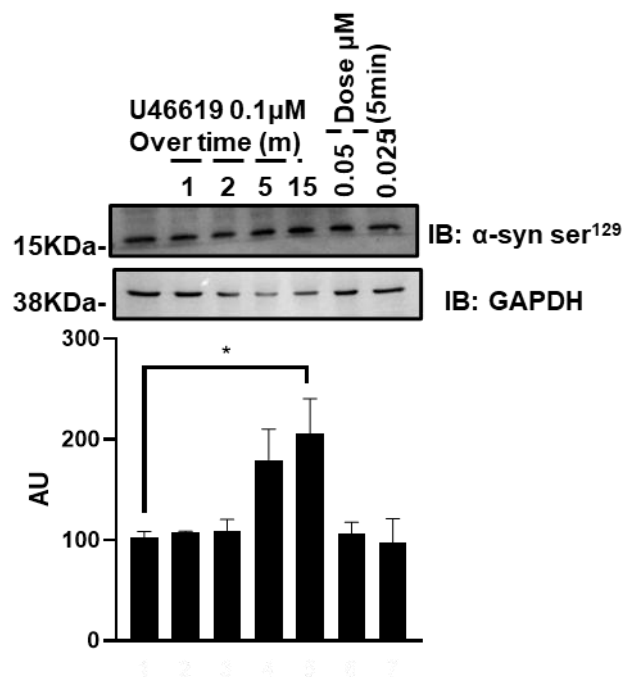


Figure 3-18. U46619 stimulation of platelets effects on phosphorylation of α -synuclein. Representative immunoblot of U4166 stimulated samples interrogated for p- α -synuclein^{ser129}. Densitometry was conducted on all blots and relative intensity against the loading controls, which are presented as Mean \pm SEM. *P<0.05, **P<0.01 *p>0.05 **P>0.01. N=3.

The phosphorylation of α -synuclein was observed to be significantly increased by thrombin and to a lesser extent activation through collagen and U46619 at longer time points. Interestingly, Collagen and CRP-XL samples exhibited different phosphorylation profiles, with CRP-XL exhibiting no changes at any dose or timepoint, which suggests that the phosphorylation may occur downstream of $\alpha_2\beta_1$ as opposed to GPVI. We also note that a downstream pathway of PAR1 must be involved in the phosphorylation of α -synuclein, but not downstream of the TP receptor.

3.9. Effects of platelet inhibitors on α -synuclein phosphorylation

Prostaglandin I₂ (PGI₂) is an agonist of the IP receptor, which acts via adenylyl cyclase (AC) to upregulate cAMP in turn inhibiting multiple factors of platelet activation, including secretion. We sought to assess whether the addition of PGI₂ would reduce the phosphorylation even after stimulation with thrombin (Figure 3-19).

We examined the effects of three doses of PGI₂ on α -synuclein^{ser129} phosphorylation. As expected, unstimulated platelets exhibited a small amount of phosphorylation (35.8AU). With stimulation of thrombin alone, the amount of phosphorylated α -synuclein greatly increased (80.2AU). Following preincubation with PGI₂ (25nM), the levels of phosphorylation were much lower (44.5 AU), this same result was observed at the 50nM dose (51.9AU). When the dosage of PGI₂ was increased to 100nM, this reduced the phosphorylation back to basal levels (31.2AU). This shows that the phosphorylation of α -synuclein can be reduced to basal levels with sufficient concentrations of PGI₂ present.

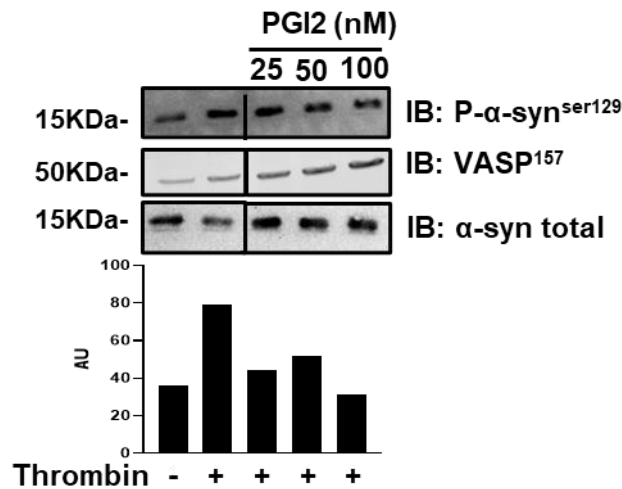


Figure 3-19. Effect of PGI₂ on α -synuclein phosphorylation. Human washed platelet lysate unstimulated or stimulated in the presence of indicated concentrations of PGI₂ and samples collected 5 minutes post activation. proteins were separated through SDS-Page and probed with anti- α -synuclein^{ser129} (top blot). Membranes were also probed for Phospho-VASP157 to assess the function of Pgi₂ (middle) GAPDH was used as a loading control (bottom). Densitometric analysis was then conducted and plotted as Median \pm SEM (bottom graph) N=2.

Calcium is a major second messenger for platelet activation; increased intracellular calcium is required for full platelet activation following thrombin stimulation, therefore we next sought to assess its effect on α -synuclein^{ser129} phosphorylation (Figure 3-20). This was achieved through the incubation with BAPTA2-AM which chelates the calcium within the platelet. When platelets were incubated with 30 μ M BAPTA2-AM for 20 minutes prior to stimulation, the thrombin stimulation was completely ameliorated, with the amount of α -synuclein phosphorylation remaining at basal levels.

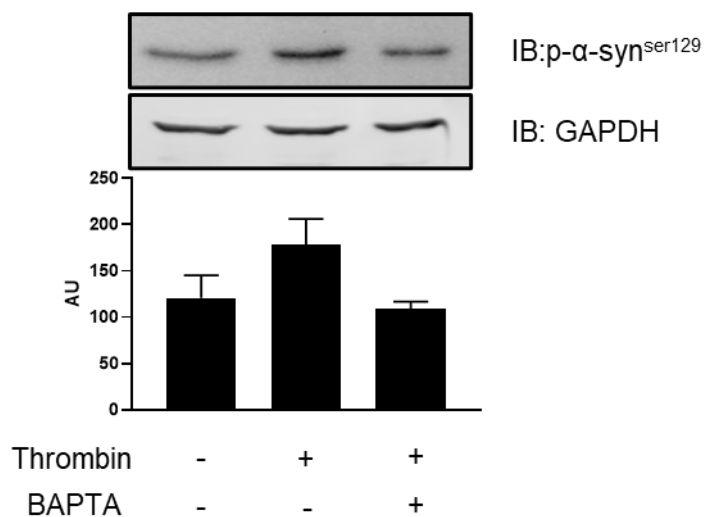


Figure 3-20. Effect of intracellular calcium on α -synuclein phosphorylation. Human-washed platelets were incubated or not with 30 μ M BAPTA AM for 20 minutes. Unstimulated or stimulated lysates as indicated were separated through SDS-Page and probed with anti- α -synuclein^{ser129} (top blot). Membranes were also probed for α -synuclein total to be used as a loading control (second blot). Densitometric analysis was then conducted and plotted as Median \pm SEM (bottom graph) N=3.

3.10. Discussion

In this chapter, we demonstrated the presence and distribution of α -synuclein within human platelets. We show a significant expression of α -synuclein using western blot, congruent with previous proteomic studies, with reported copy numbers of 42000 , however there are few studies, reporting the exact copy number (Pienimaeki-Roemer et al., 2015, van Holten et al., 2014, Zeiler et al., 2014). We also noted issues with western blot reliability for the α -synuclein; this was also observed in multiple papers studying α -synuclein in neuronal cells, we were able to circumvent these issues by modifying the protocol (Sasaki et al., 2015, Stojkovska and Mazzulli, 2021). Next, we showed a heterogeneous distribution of α -synuclein throughout the platelet, which moved towards the periphery of the cell upon stimulation with thrombin; other studies have shown the movement of α -synuclein towards the presynaptic bulb in neural cells depending on activity, which shows that α -synuclein can perform this function in other cell types (Fortin et al., 2010). A study by Smith et al. (2023) demonstrates that α -synuclein is present on both the α -granules and lysosomes within the platelet. Interestingly, they did not observe a change in membrane interaction between unstimulated, and stimulated platelets, albeit utilising a different form of elucidation to that used in this thesis.

Alongside this movement, we also observed an increase in α -synuclein^{ser129} phosphorylation upon stimulation with thrombin, which was replicated when platelets were stimulated with collagen and U46619, but not CRP-XL, showing that this phosphorylation is not tied to GPVI activation. A study by Samuel et al. (2016) has also linked the activity of α -synuclein with its phosphorylation at serine129. Although previously thought to just have pathogenic function, a recent study by Parra-Rivas et al. (2023) has elucidated physiologic roles within synaptic function.

We also observed the co-localisation of α -synuclein with SNARE complex proteins upon stimulation using immunofluorescence, which we confirmed using immunoprecipitation; this confirmed that α -synuclein is interacting with various SNARE complex proteins within the platelet. The use of immunoprecipitation yielded more sensitive results allowing for the visualisation of additional interactions which were not observed in immunofluorescent analysis. Alongside the co-localisation with the

SNARE complex proteins, we saw the same pattern of movement between the VAMP proteins and α -synuclein. The interactions we observed also increased upon platelet stimulation with thrombin. When combined with the observation of similar movement patterns it further implicates α -synuclein to be a functional component of the SNARE machinery.

In addition to the movement and co-localisation of α -synuclein with SNARE complex proteins, we also saw that α -synuclein was not secreted from the platelet upon activation, strongly suggesting that it is not a granular component. It was however translocated to the surface of the platelet, this could be due to its interaction with the granule membrane and subsequent membrane mixing resulting in the expression on the outer leaflet of the platelet.

We also assessed the effects of different activation pathways within the platelet on α -synuclein. Interestingly, we did see that the addition of PGI₂ post-stimulation with thrombin did reduce the phosphorylation of α -synuclein to basal levels, this effect was also observed when calcium was chelated using BAPTA2-AM. This indicates that the phosphorylation of α -synuclein is not only dependent on platelet activation, but it is reliant on intracellular calcium.

We also demonstrated a mild inhibitory effect following incubation with ELN484228 on platelet aggregation in response to collagen and thrombin. However, we observed a wide variance of inhibition of aggregation in response to incubation with ELN484228 which was also influenced by incubation times. These data suggest that ELN484228 may have off-target effects on platelets, which are not consistent between donors, highlighting the need to move away from chemical inhibitors and utilise a knockout mouse model to elucidate the effects of α -synuclein. Interestingly multiple small molecule inhibitors which are being assessed for α -synuclein inhibition are targeted to inhibit the aggregation of α -synuclein opposed to their physiological binding (Horne et al., 2024). Due to this focus, the effect of these agents is yet to be reported in the context of platelets.

We Show the localisation of p- α -synuclein^{ser129} towards the periphery of the cell, with increased phosphorylation after stimulation. This has not been examined in platelets before, and the localisation in neurons is contentious with studies showing localisation with the nucleus, while others show the movement towards the bulb with a subsequent

study showing that localisation is dependent on the different neuronal subtypes (Vivacqua et al., 2011). However, studies suggest that phosphorylation at serine 129 increases the propensity to aggregate and bind to membranes (Li et al., 2002a, Yu et al., 2007, Samuel et al., 2016).

We demonstrate that α -synuclein interacts with multiple SNARE complex proteins, namely STX11, STX4, VAMP-8, -7 and -2, and SNAP23 in platelets through immunoprecipitation and immunofluorescence. At the time of experimentation, there were no studies investigating the interaction of α -synuclein with different SNARE complex proteins in the context of platelets. However, some studies focused on α -synuclein interactions with select members in neurons. Research by Burré et al. (2010) elucidated the interaction between α -synuclein and VAMP2, which was later shown to be responsible for vesicle clustering and docking in neural cells (Jo et al., 2000, Diao et al., 2013). To date, there has been only one study on the interaction between α -synuclein and other SNARE complex proteins in platelets (Smith et al., 2023).

In this study we observed the phosphorylation of α -synuclein at serine129 in response to multiple agonists; however, when calcium was chelated or signalling through the Rho/ROCK pathway was blocked, phosphorylation at serine 129 was reduced. This was also seen upon the addition of PGI₂, which suggests that this PTM is dependent on platelet activation. Specifically, phosphorylation of α -synuclein is dependent on complete Rho/ROCK signalling, therefore, it is likely that one of these downstream proteins is required.

The culmination of this chapter shows that α -synuclein moves with the granules from heterogeneous expression to the periphery and is phosphorylated downstream of the Rho/ROCK pathway, which enhances its ability to bind to the plasma membrane. This function is utilised in the SNARE complex, perhaps in a chaperoning capacity similar to neural cells, but with its main VAMP binding partner being VAMP8, as opposed to VAMP2. Reduction of α -synuclein capacity using ELN484228 resulted in lesser aggregation of washed platelets, however, this had widely varying effects between both donors and incubation times, making it unsuitable to pursue further.

3.10.1. Limitations

The use of a pharmacological inhibitor (ELN484228) that was not specifically designed for use in platelets caused variable effects within the platelets resulting in unreliable data. This inhibitor also proved to be unreliable in this context, which can be attributed to its off-target effects within the cell. There has since been the development of other small molecule inhibitors of α -synuclein. However, these have not been tested in the context of platelets, and are not widely commercially available, therefore we were unable to test these compounds (Wang et al., 2023).

To assess co-localisation in the platelets we use multi-colour immunofluorescence; this allowed for the visualisation of proteins of interest throughout the cell. However, this technique can be subjective and lacks the resolution required to be completely accurate. To remedy this, the use of a Protein Ligation assay could be implemented, which will only yield a signal when proteins are within 40nm of each other, removing the limitations of bias or resolution (Dunn et al., 2011a). Another improvement on this would be the use of super-resolution microscopy which is capable of higher resolving power and visual acuity.

Additionally, we were unable to assess the ultrastructure of the platelets following the addition of ELN484228, in unstimulated and stimulated conditions. Further research may assess the effects of the ELN484228 incubation on the structure and exocytosis of granules from the platelet utilising Transmission Electron Microscopy (TEM), this may also highlight additional physical effects that could be present.

We established the interaction of α -synuclein with multiple SNARE complex components, however, due to limitations on both time and resources this was not an exhaustive panel of proteins. We also did not interrogate the interaction of α -synuclein with other proteins within the platelet for the same reason. This could be overcome by further immunoprecipitation experiments, or through immunoprecipitation and subsequent proteomic analysis to observe increased enrichment in the IP sample.

Although adding much to the subject area, this study leaves some questions unanswered. Going forward, elucidating how α -synuclein interacts with members of the SNARE complex in platelets would be valuable. Alongside further interrogation of SNARE complex proteins, top-down proteomics on immunoprecipitated samples

could be utilised to provide a much broader scope of α -synuclein interactions. This could be further expanded to compare the difference between unstimulated, and stimulated conditions, alongside different agonists to assess changes in interaction partners.

Further experimentation may also be possible by utilising new α -synuclein inhibitors which may not induce off-target effects within the platelet this would allow for the direct observation of α -synuclein function and requirement in human platelets. We showed the amelioration of α -synuclein phosphorylation upon rho/ROCK signalling inhibition; however, we did not observe the exact protein on this pathway which leads to phosphorylation, or whether multiple pathways are required. There have been multiple PTMs reported of α -synuclein, however, their functions remain mostly unexplored in any cellular context. Studies into the function of these modifications in different milieu would deepen the understanding of the scope of α -synuclein functions. This could be achieved by using phospho-proteomics which can elucidate more phosphorylation sites, which can also be assessed in both unstimulated and stimulated conditions.

Chapter 4. The analysis of α -synuclein, using a knockout mouse model

4.1. Introduction

There are many benefits to using knockout mouse models in comparison to pharmacological inhibitors, although there are also some drawbacks that come with these models. Mouse models have played an integral role in the understanding of platelet biology and are responsible for most of the mechanistic knowledge within the haemostatic system; they are key in overcoming the inability to perform molecular biology on human platelets, due to their lack of nucleus. For the study of α -synuclein, the use of a knockout mouse model is needed due to the current pharmacological inhibitors demonstrating large variation in human platelets, which we attributed to off-target effects within the platelet. Additionally, the utilization of mice for assessing haemostasis has well-established and robust literature to which we can compare our findings. While human and mouse platelets exhibit subtle differences, these do not prohibit the use of mouse models in the study of haemostasis and thrombosis (Stalker, 2020, Sachs and Nieswandt, 2007). However, off-target effects are not unique to pharmacological inhibitors, knockout models can cause multiple phenotypic changes within cells and differential regulation of related proteins (El-Brolosy and Stainier, 2017).

In this study we utilised a previously generated knockout model known to have no interactions with neighbouring genes, essential to create reliable data. In the first instance we needed to elucidate whether there were any further interactions in platelets resulting in up or down-regulation of associated proteins. The specific α -synuclein knockout was developed in the laboratory of Prof. V. Buchman (Cardiff University). This was achieved by utilising a targeting vector containing an FRT site-flanked NEO cassette with a LoxP site inserted downstream of the first coding exon2 of the SNCA gene, with a second LoxP site inserted upstream of exon2. This construct was then electroporated into 57BL/6N-Atm1Brd-derived JM8A3.N1 embryonic stem cells and resultant mice bred for 2 generations with C57BL/6J mice. These resultant mice were then crossbred with a C57BL/6 mouse expressing FLP recombinase. The FLP-mediated recombination removed the FRT-flanked neo cassette leaving exon 2 floxed. The floxed allele mice were then bred with further wild-type C57BL/6J mice for

2 generations to remove the FLP recombinase which was then crossed to generate homozygotes (Ninkina et al., 2015).

We first sought to assess haemostatic and platelet function defects in knockout platelets through bleeding time assays and LTA. Alongside this, we assessed for deficiencies in the expression of secretory VAMP and STX proteins using Western blot. We then utilised traditional LTA techniques alongside Western blotting and platelet adhesion assays to assess the effect of the knockout on platelet function *in vitro*. Following the phenotypic assessment, we aimed to examine the mechanism(s) by which α -synuclein regulates platelet function. Flow cytometric analysis provides a powerful tool for the expression of markers on single cells. We sought to understand how the knockout of α -synuclein affected granule secretion using multi-colour flow cytometry, to assess the overall population effect. We then implemented multidimensional reduction analysis allowing for the identification of subsets of platelets that were more significantly affected by the knockout in response to different platelet agonists.

4.2. Generation of α -synuclein knockout mice on a C57BL/6J background

To accurately assess the effects of α -synuclein on platelet structure and function, the confirmation of α -synuclein knockout at both a DNA and protein level must be attained. To reduce heterogeneity between mice, heterozygous breeding pairs were generated by breeding the α -synuclein knockout mice with C57BL/6J wild-type mice and henceforth used as the progenitors to the experimental animals (Figure 4-1). The breeding of these heterozygous mice yields 25% wild-type, 25% knockout, and a 50% chance of heterozygous progeny, this enabled us to exclude the litter variations alongside gender and age variables.

In addition to this breeding strategy, we also implemented backcrossing of inbred knockout mice to fresh wild-type mice from Charles River every 5-10 generations to reduce the chances of genetic drift, resulting in a phenotypic change. To ensure that the colony was sufficiently backcrossed, a homozygous female was crossed with a fresh male to produce a heterozygous population (N1), A male from this population was then mated with a fresh WT female, to generate the N2 population. A N2 heterozygous male was then taken from this population and mated with an original inbred female, to generate the N3 population. Finally, the N3 male and female heterozygous mice were mated to resume the colony.

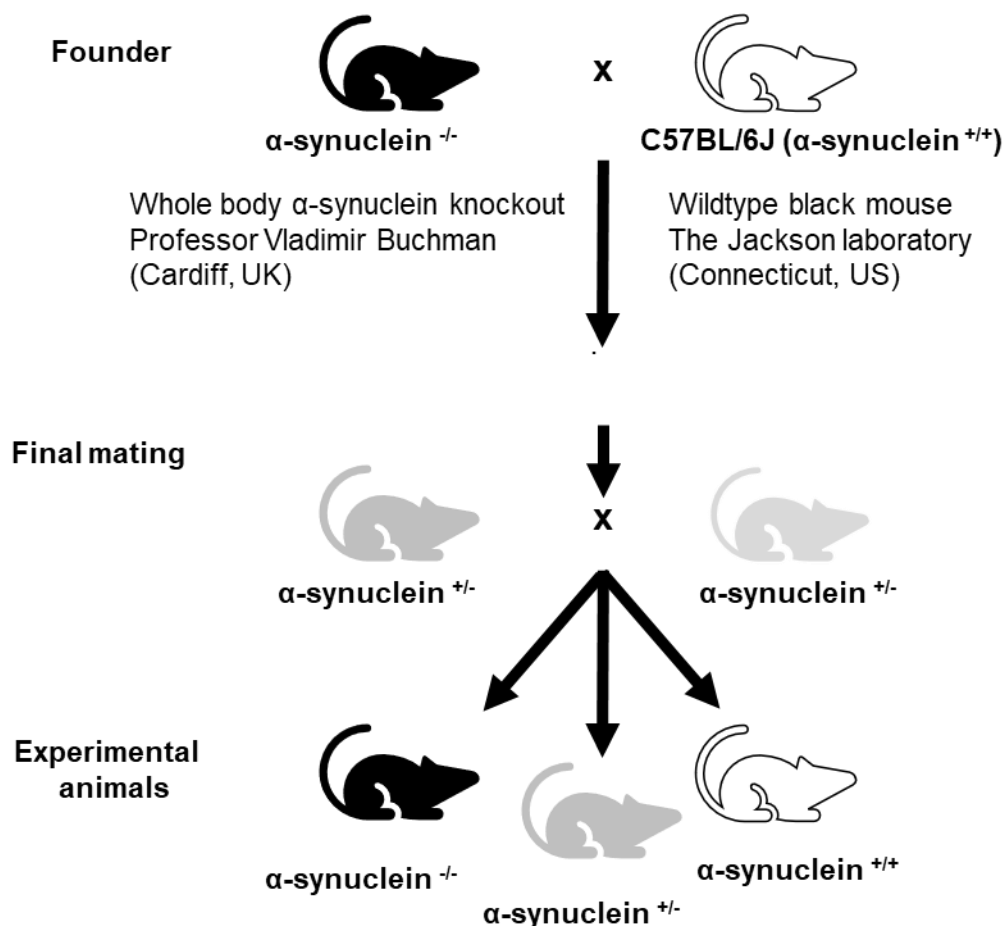


Figure 4-1. Breeding strategy of α -synuclein knockout mice. Homozygous knockout mice (Cardiff, UK) were bred with C57bl/6J mice from Charles River (Harlow, UK). Heterozygous offspring were then mated to generate experimental animals.

4.2.1. Optimisation of PCR

To quantify the genotype of the mice generated an endpoint PCR was used, due to the knockout being a whole-body knockout ear biopsies were used. The first stage that required optimisation was the extraction of DNA from these samples and maintaining a high purity. Three methods were tested, Proteinase K, Trizol, and the KAPA extract kit (Figure 4-2). The extracted DNA was then subject to PCR with the α -synuclein primers, after PCR the Proteinase K, yielded no observable bands, whereas the Trizol extraction had a clear band. The KAPA extraction kit yielded the strongest and clearest band of all extraction methods tested, however, there was some slight smearing due to the suboptimal reaction and potential slight contamination, for all PCRs going forward the KAPA Kit was used.

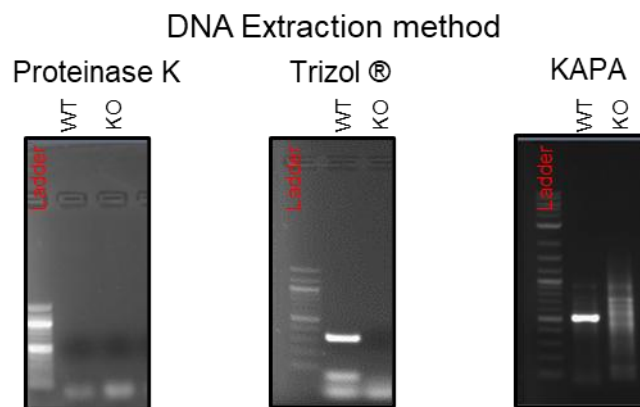


Figure 4-2. DNA extraction methods. DNA samples were obtained from mouse ear biopsies using either Proteinase K (i), Trizol (ii) or KAPA (iii) extraction methods. 1 μ L of extracted DNA was then subject to wild-type and knockout PCR reactions to assess the purity, and presence of DNA. The PCR product for proteinase K and trizol methods were then mixed with a gel loading buffer, where the KAPA is premixed. This was added into a 1% agarose gel containing EtBr and run until sufficient separation was observed and imaged on a versa doc (Bio-Rad).

Following this, the temperatures of the PCR reaction were probed (Figure 4-3). To achieve this, a temperature gradient was applied to the thermocycler, and identical samples were used, 2 $^{\circ}$ C increments were observed in the annealing ranging from 52-62 $^{\circ}$ C (Figure 4-3). In the lowest tested annealing temperature of 52 $^{\circ}$ C the expected band was present however it was faint and there was a large amount of smearing. As the temperature of the annealing phase is increased, the bands observed were more pronounced up to 62 $^{\circ}$ C. The most intense band was observed at the 62 $^{\circ}$ C temperature, however, it exhibited a larger amount of smearing to 60 $^{\circ}$ C, therefore going forward the 60 $^{\circ}$ C annealing temperature was used.

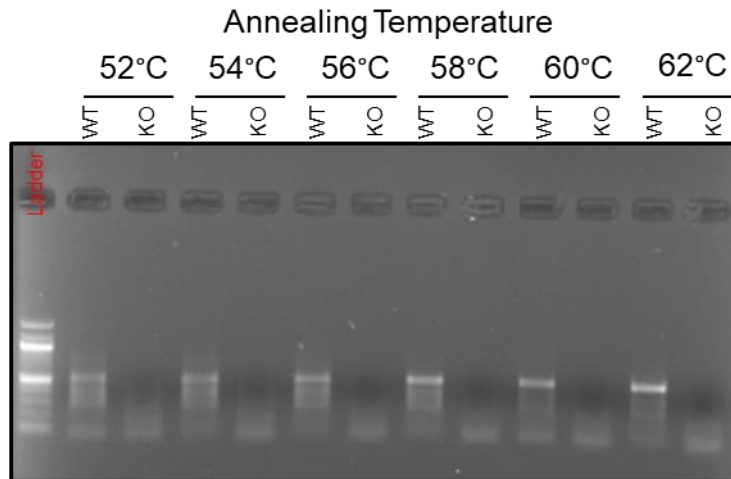


Figure 4-3. Effects of annealing temperature on PCR output. DNA extracted using the KAPA extraction method was subject to PCR, utilising an identical 30-cycle program except for the annealing temperature, which was increased in 2°C increments. Samples were then loaded into a 1% Agarose gel with EtBr and run until bands were separated. This gel was then imaged utilising a versa doc (Bio-Rad).

In the experiments it was noted that the bands were weak, in PCR magnesium chloride acts as a cofactor, enhancing the enzymatic activity of DNA polymerase, however too much MgCl₂ results in non-specific binding of primers. The KAPA kit has a base magnesium concentration of 1.5mM. We tested this concentration and increased it to 2.0mM (Figure 4-4). While the band appeared slightly clearer with the higher magnesium concentration, the increased smearing prevented any improvement in band visibility.

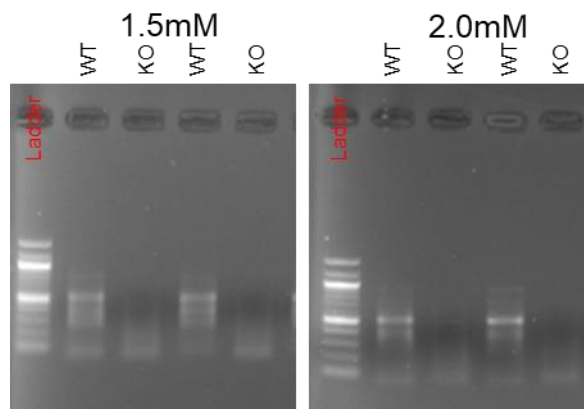


Figure 4-4. Effects of magnesium concentration on PCR output. DNA extracted using the KAPA extraction method was subject to PCR with two different concentrations of magnesium 1.5mM (left) and 2.0mM (right), samples were subject to 30 cycles. Samples were then loaded into a 1% Agarose gel with EtBr and run until bands were separated. This gel was then imaged utilising a versa doc (Bio-Rad). The primer concentration was then

titrated to minimise the primer dimer formation, resulting in a clearer output (Figure 4-5). In the initial experiments, 10pM was used, which yielded a primer dimer in the bottom of the wild-type lanes indicative of an excess of primer in the reaction. To remedy this, the primer concentration was halved to 5pM which had no observable primer dimer, and yielded bands of comparable intensity.

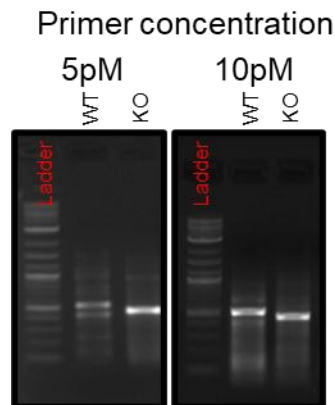


Figure 4-5. Effects of primer concentration on PCR output. DNA extracted using the KAPA extraction method was subject to PCR with two different primer concentrations 5pM (left) and 10pM (right). Samples were subject to 30 cycles. Samples were then loaded into a 1% Agarose gel with EtBr and run until bands were separated. This gel was then imaged utilising a versa doc (Bio-Rad).

4.2.2. Confirmation of an α -synuclein knockout mouse model

To confirm the successful deletion of α -synuclein, we assessed the genotype of the mice through end-point PCR, and the protein expression through Western blot analysis (Figure 4-6). The WT sample was devoid of the NEO cassette target present in the knockout samples, which yielded the most intense bands through western blot analysis. Where the heterozygous sample showed both a wild-type and knockout allele present, when subject to western blot analysis it was observed that there was significantly less α -synuclein protein present than in the wild-type samples ($p=0.048$), however, it did not result in a complete knockout of the protein. The knockout sample showed no wild-type allele through PCR analysis, this caused the complete elimination of all α -synuclein expression on a protein level.

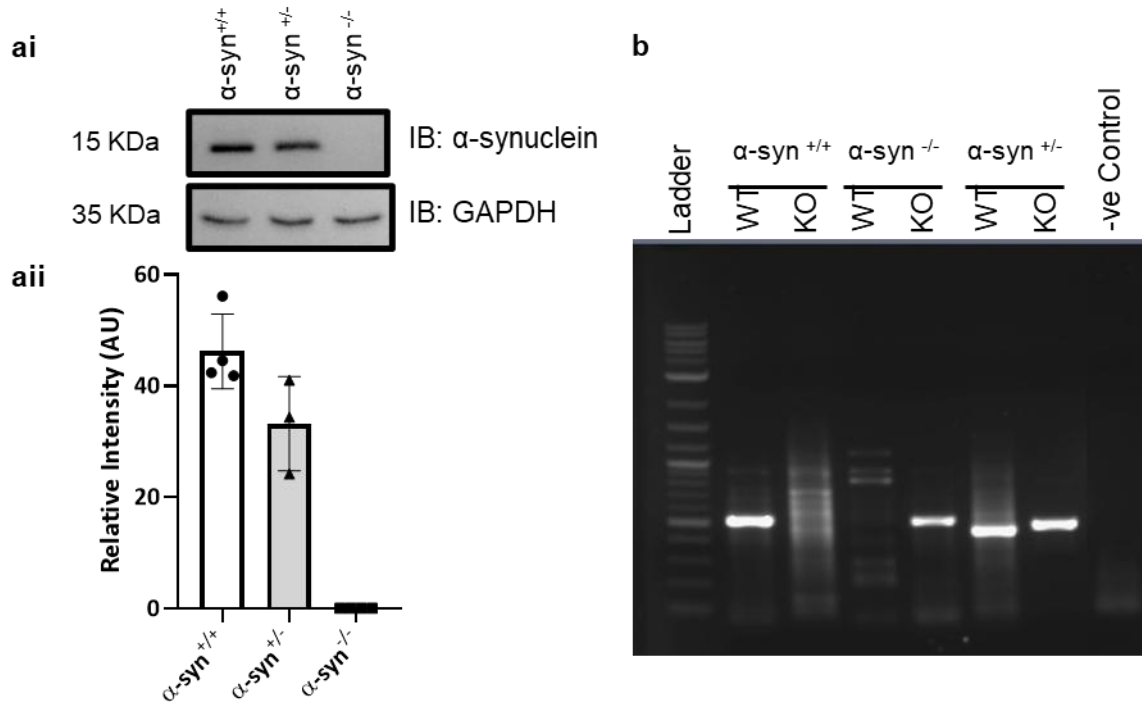


Figure 4-6. Quantification of α -synuclein knockout mice. *ai* representative western blot of α -synuclein from lysates of wild-type or α -synuclein knockout mouse platelets. *aii* Relative intensity was calculated by comparing the α -synuclein signal to the loading control, and presented as a scatter plot with a bar, with each point representing a data point. *b* A representative PCR gel showing wild-type, knockout, and heterozygous samples. Data are presented as mean \pm standard deviation. $N \geq 3$

4.2.3. Assessment of knockout impact on platelet phenotypes

The whole-body knockout of proteins may have an off-target effect on the production of platelets, and their ability to respond to stimuli (Figure 4-7). To ensure that receptor expressions of the major platelet-activating receptors remained congruent, CD49b($\alpha 2\beta 1$), CD42b (GPIb alpha), GPVI, and CD41 (GPIIb) expression levels were investigated by flow cytometry (Figure 4-7). Platelet samples from wild-type, knockout, and heterozygous mice were assessed for receptor expression levels. This knockout of α -synuclein did not affect the expression of CD49b, CD42b, GPVI or CD41, this is recapitulated in the heterozygous mice. As a result, any difference in platelet function between the knockout and wild-type mice is not attributable to the expression of CD49b, CD42b, GPVI, or CD41 on the platelet.

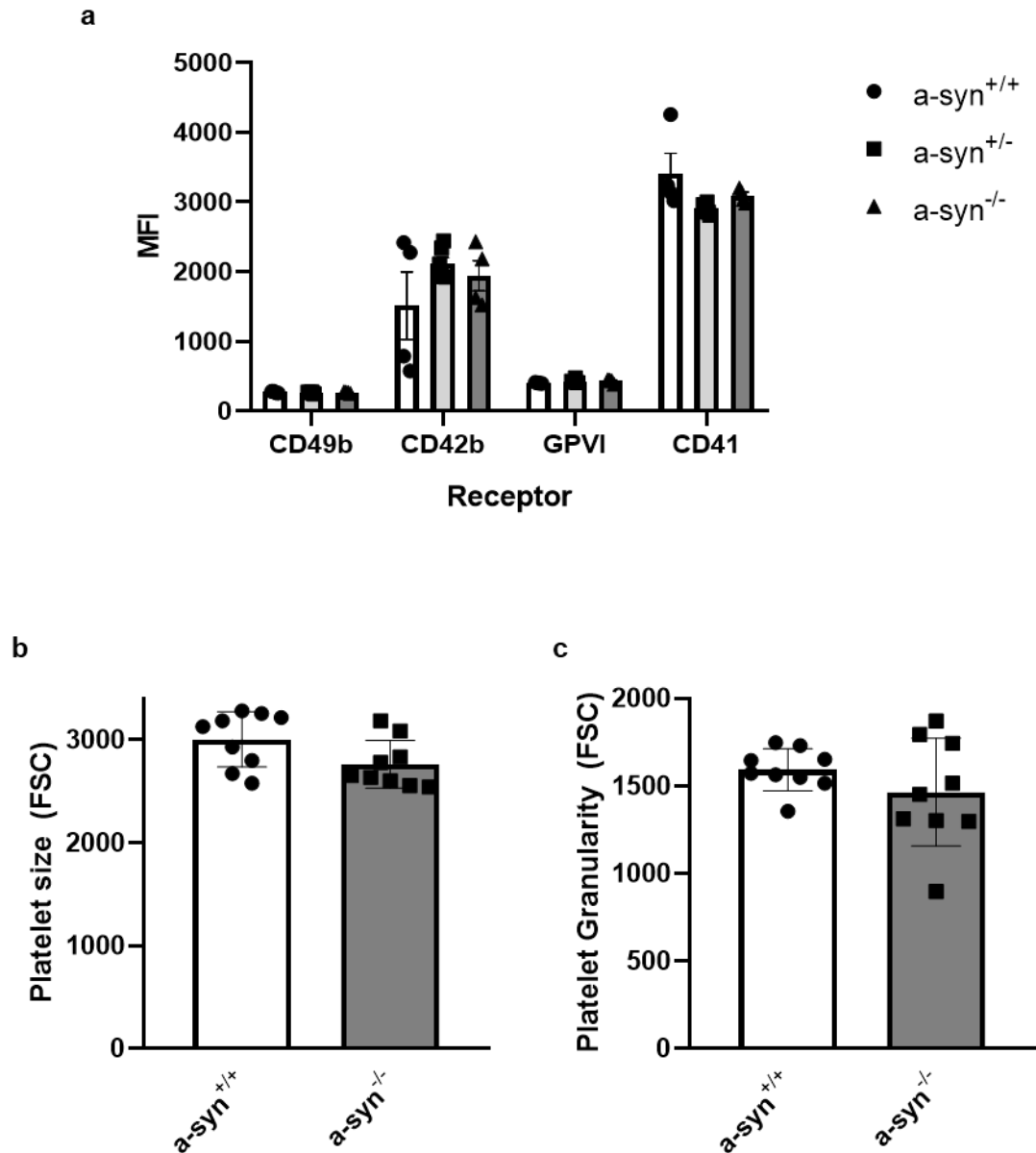


Figure 4-7. Quantification receptor expression in α -synuclein knockout, heterozygous and wild-type platelets. a. quantitative analysis of four major platelet surface receptors, CD49b, CD42b GPVI and CD41 was assessed on wild-type (Clear), α -synuclein knockout (light grey) and heterozygous (dark grey) platelet samples through Flow cytometry. The Median fluorescent intensity (MFI) is presented as Mean \pm SEM N=5. b. Platelet size was examined through the forward scatter (FSC) in flow cytometry, Data are presented as the mean \pm SEM N=9. c. The granularity of platelets was assessed through the side scatter (SSC) in flow cytometry. Data are presented as the mean \pm SEM N=9.

Changes in platelet size and/or granularity may indicate an abnormality in platelet generation and granule packaging during thrombopoiesis (Gresele et al., 2015). The platelet size was assessed through the Forward Scatter (FSC) characteristics using flow cytometry and we found that α -synuclein knockout platelets appeared slightly smaller, however, this was not significant. When granularity was assessed through the

Side Scatter (SSC) characteristics, we found that knockout platelets were similar in granularity in comparison to wild-type platelets, but this was not significant. These results show that the deletion of α -synuclein does not affect the receptor expression of major surface receptors, nor the size and granule packaging of platelets, suggesting that any differences in platelet function are highly likely to be due to mechanistic changes post-activation.

Following the quantification of four of the major platelets activating surface receptors, we next interrogated the effects of α -synuclein deletion on SNARE complex protein expression (Figure 4-8). As stated previously (1.4.6) the reduction in VAMP8, STX11 or SNAP23 can have a significant reduction in granule secretion from the platelet. Changes in expression levels of the SNARE proteins upon the deletion of α -synuclein is indicative of a compensatory mechanism within the cell. In lieu of a change, it enables the assumption that a change in granule release is not dependent on changes in SNARE protein concentration but in the abolition of α -synuclein expression.

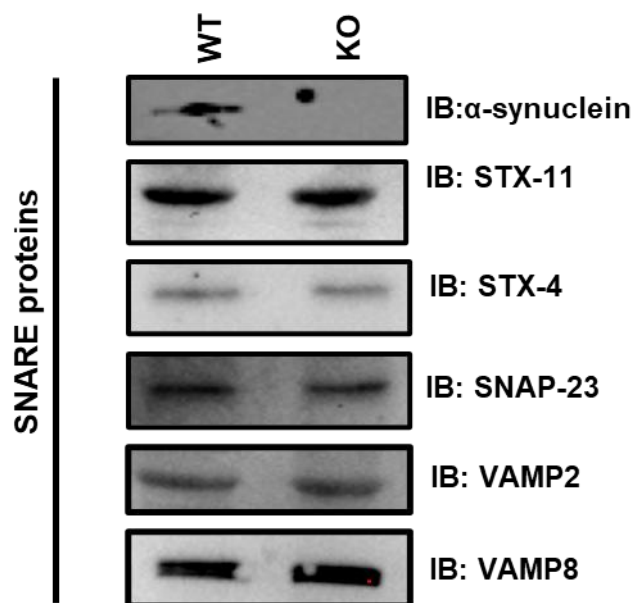


Figure 4-8. Western blot analysis of SNARE complex proteins from platelet samples isolated wild-type or knockout mice. Western blots of the SNARE complex members in Wild-type and knockout platelet samples N=1.

4.3. α -synuclein deletion results in a bleeding phenotype.

In the first instance, we assessed the haemostatic capacity of both the wild-type and α -synuclein knockout mice, through the implementation of a bleeding time assay (Figure 4-9). The knockout mice displayed a significantly increased bleeding time of 618 ± 97.7 seconds in comparison to their wild-type littermates at just 216 ± 51.4 seconds; $P=0.0051$). In addition to the increased bleeding time, there was an increased propensity for rebleeding events in α -synuclein knockout mice, which is indicative of reduced clot stability.

Following this a prothrombin time (PT) assay was conducted, the PT measures the time taken for the blood to clot following the addition of thromboplastin. If there is an increased PT it indicates that there is a deficiency in a clotting factor. The PT was consistent between the wild-type and knockout mice models, meaning that there are no deficiencies in the extrinsic pathway of the clotting cascade. Furthermore, we conducted an Activated Partial Thromboplastin Time (aPTT) in the presence of platelets. The aPTT assesses the intrinsic and common pathways of the coagulation cascade, which involve clotting factors both within the plasma and platelets. Dysfunction in platelet granule secretion, which releases Factor VIII and Factor V, could potentially lead to a prolonged aPTT. Importantly, the prothrombin time remained unchanged, suggesting that the reduction of Factor V on the platelet surface does not affect this aspect. (Yarovoi et al., 2003).

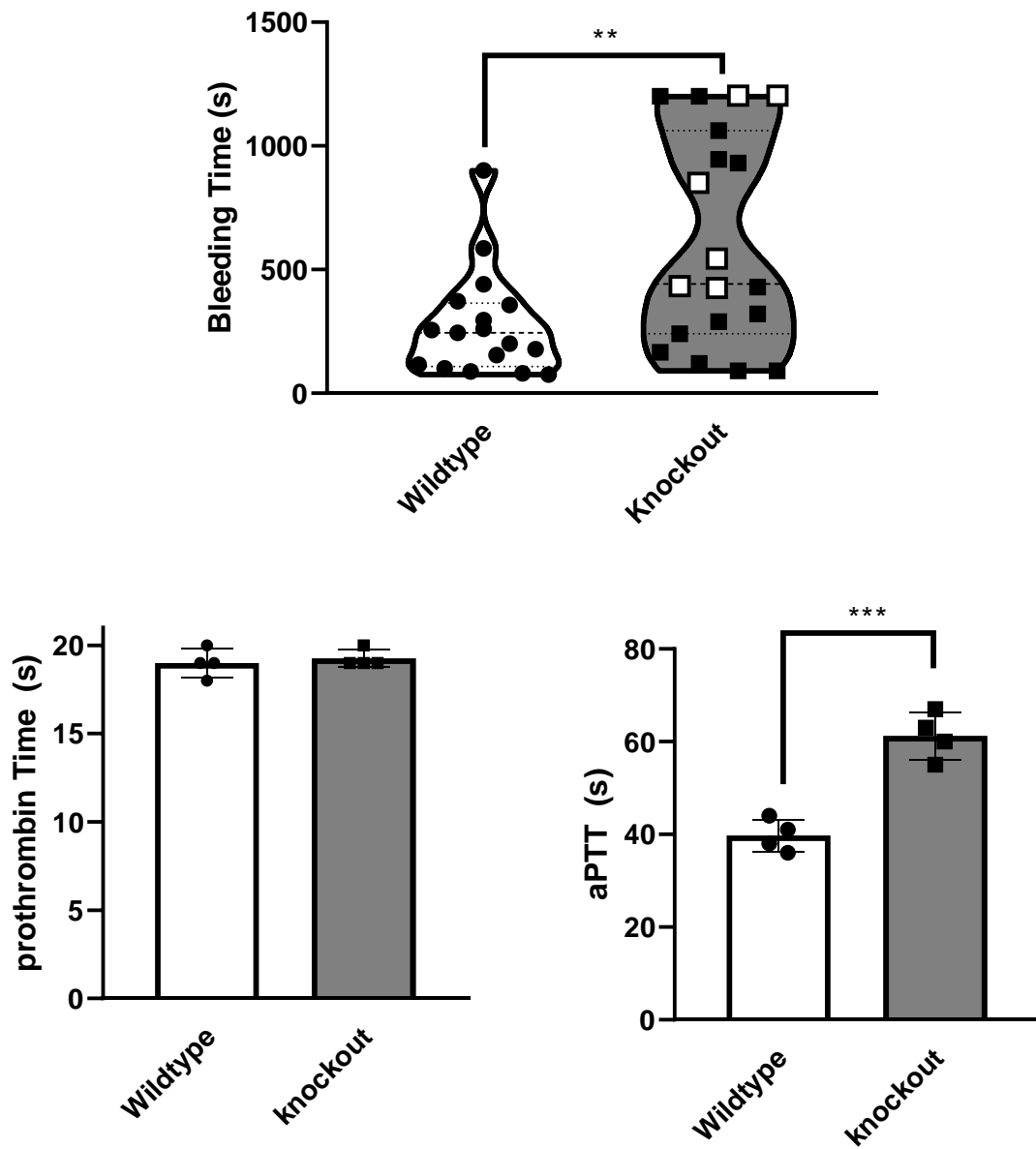


Figure 4-9. Bleeding time assay of wild-type and knockout mice with Prothrombin time and activated partial thromboplastin time. a. The bleed time was recorded for wild-type (circle with white background) and knockout mice (square with grey background), each datapoint is represented with a circle or square, and white-filled datapoints represent a rebleeding event. Data represented as a violin plot with datapoints, $N=18$ ($P=0.0051$). b. The prothrombin time assay was conducted on PRP from wild-type (white) and knockout (grey) mice and timed until a fibrin clot became visible. Data presented as Mean \pm SEM $N=4$ $P=0.999$. c. The activated partial thromboplastin time was completed on PRP from both Wild-type (white) and Knockout (grey) mice. Data presented as Mean \pm SEM $N=4$ $P=0.0004$.

4.4. α -synuclein knockout platelets have an aggregation defect.

Following the observation of a bleeding phenotype in the α -synuclein knockout mice that was not mediated by the extrinsic pathway, further examination of platelet function was conducted in isolation using LTA. To establish whether the bleeding diathesis was a result of a singular compromised activation pathway, platelets were stimulated with either thrombin, collagen or U46619 (Figure 4-10). Stimulation of wild-type platelets with 0.05U/mL thrombin induced $74.8\% \pm 11.76$ aggregation. Following this, when the knockout platelets were stimulated with thrombin 0.05U/mL thrombin, it induced $44.50\% \pm 11.33$ ($P=0.0001$) aggregation. Heterozygous platelets had a significantly lower aggregation compared to wild-type platelets, however, to less of an extent ($53.25\% \pm 10.5$) ($P=0.0489$). When the dosage of thrombin was reduced to 0.025U/mL, the maximal aggregation was reduced to $18.8\% \pm 5.9$ in wild-type platelets. Aggregation in the knockout platelets at this low concentration was almost completely abrogated, with multiple samples showing no aggregation at all $2.75\% \pm 5.9$ ($P=0.0329$).

Furthermore, platelet aggregation in response to the thromboxane A_2 analogue U46619, at 0.05 μ M reached maximal aggregation of $78.29\% \pm 4.497$ in wild-type platelets, whereas knockout platelets aggregated significantly less at $38.83\% \pm 12.2$ ($P=0.0083$). Using a lower concentration of 0.025 μ M, reduced the maximal aggregation of wild-type platelets to $49.6\% \pm 6.33$, and the knockout to $39.4\% \pm 6.9$. However, the difference between the samples was not significant ($P=0.0896$). When the dosage of U46619 was decreased to 0.0125 μ M, platelet aggregation of both wild-type and knockout platelets decreased to $50.80\% \pm 11.386$ and $13.50\% \pm 4.9$, respectively. Additionally, at this low dosage, some platelet samples from the knockout samples failed to aggregate ($P=0.0104$).

The final agonist we tested was collagen, the initial high dosage used at 2.5 μ g/mL in the wild-type mice, resulted in an average maximal aggregation of $69.67\% \pm 4.20$, whereas heterozygous mice had a slightly lower average of $59.0\% \pm 3.53$, and the knockout mice having an average aggregation of $66.33\% \pm 4.33$. Although heterozygous platelets had a lower average aggregation this was not significant ($P=0.407$), and the knockout mice had nearly identical aggregation values ($p=0.94$). Interestingly, when we reduced the dose of collagen to 1 μ g/mL there was only a modest reduction of aggregation in WT platelets to $53.42\% \pm 7.42$, but the aggregation

of both the heterozygous and knockout platelets were significantly reduced. The heterozygous platelets had an average aggregation of $15.6\% \pm 5.2$ ($P=0.0001$) and knockout platelets $6.00\% \pm 1.813$ ($P=0.0001$). These data suggest that the inhibition of platelets aggregation caused by the deletion of α -synuclein can be overcome by high dosages of collagen, but not with thrombin or U46619.

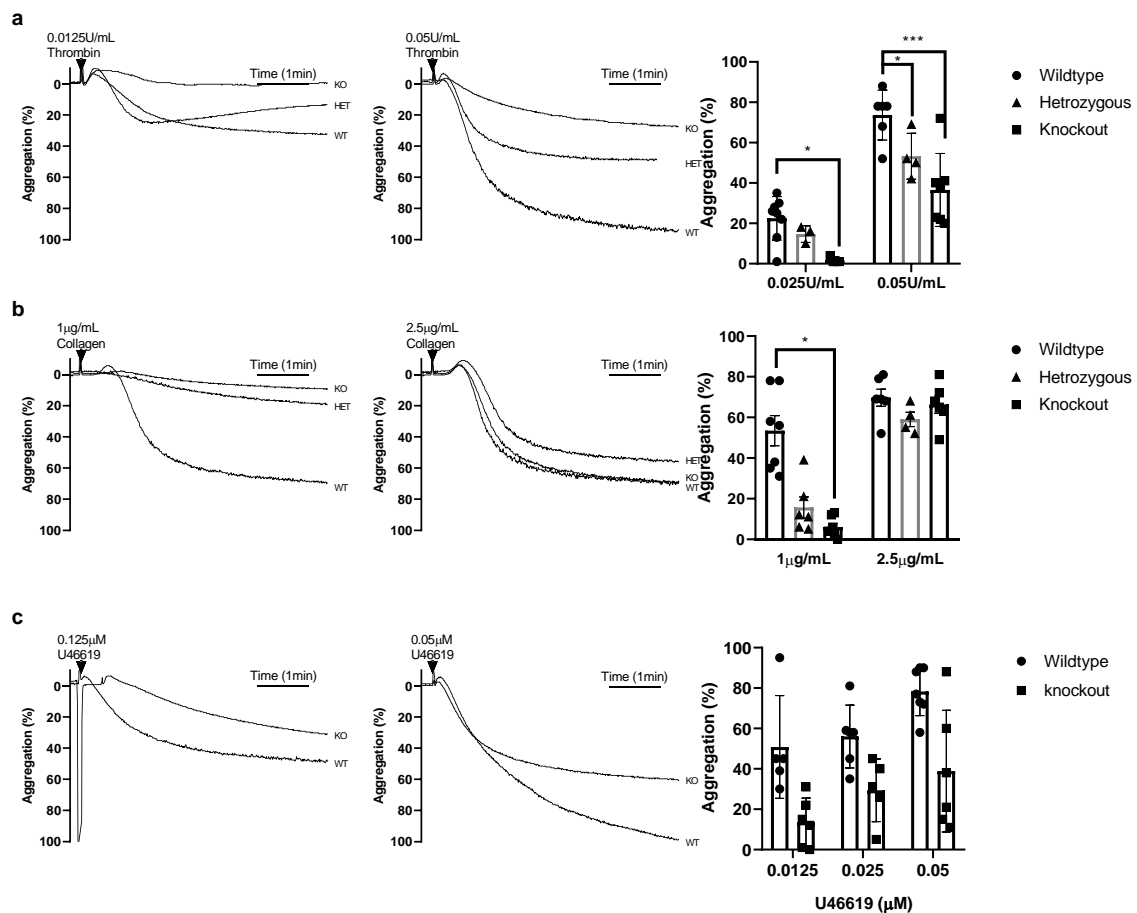


Figure 4-10. Platelet aggregation is reduced in α -synuclein deficient mouse platelets. PRP from mice was centrifuged at 800g in the presence of 0.3M citric acid, before resuspending in wash buffer and centrifuging again, this was then resuspended in Modified Tyrode's buffer for counting, Platelet concentrations were corrected to 3.0×10^8 for all aggregation assays. Platelets from KO or WT mice were stimulated with either (a) collagen, (b) thrombin or (c) U46619 at indicated concentrations and aggregation were recorded for 5 minutes. All aggregations were conducted in stirring conditions (1000 RPM) on a chrono-log 4+4 aggregometer. Representative aggregation traces for dosages of agonist (Left and middle) Graphs (right) of overall data $N=5$. Percentage aggregation is presented by mean \pm standard error of mean (SEM) * $P < 0.05$, ** $P < 0.01$ compared to wild-type.

4.5. Platelet adhesion to extracellular molecules

Platelet adhesion to the extracellular matrix (ECM) is key for platelets to achieve their role in haemostasis. Collagen is the major component within the ECM to which platelets bind, through GPVI and GPIb-V-IX. Additionally, platelets adhere to fibrin which is generated from the cleavage of fibrinogen within the blood plasma by thrombin. Binding to fibrinogen through GPVI and GPIIb IIIa is key in clot formation facilitating thrombus stabilization (Alshehri et al., 2015, Mattheij et al., 2016, Lee et al., 2012).

4.5.1. α -synuclein deletion has no impact on platelet adhesion to fibrinogen.

Previous literature states that murine platelets failed to spread on fibrinogen due to the inability of the immobilised matrix to activate mouse GPVI (Mangin et al., 2018, Watson et al., 2005, Wonerow et al., 2003). Therefore, we examined the static spreading of murine platelets on a fibrinogen matrix in wild-type and knockout platelets both with and without pre-stimulation with 0.02U/mL thrombin (Figure 4-11). The pre-activation of platelets with PAR4 had been shown previously to modulate the initial spreading of murine platelets to spread fully on human fibrinogen (Lee et al., 2012) (Figure 4-11). Platelets were assessed at 4 time points, 15-,30-, 45- and 60 minutes, throughout every time point in the pre-stimulated samples there was no significant change in the area of the platelets spread on the fibrinogen matrix (15 min $P=0.09$, 30 min $P=0.35$, 45min $P=0.067$, 60 min $P=0.68$). We then calculated the number of platelets bound per mm^2 at each time point. This showed that as time increased the number of platelets bound to the surface increased, however, there were no significant differences between the wild-type and the knockout (15 min $P=0.23$, 30 min $P=0.24$, 45min $P=0.26$, 60 min $P=0.30$). We also noted that at all time points, almost all platelets were fully spread on the surfaces, we believed this was due to the pre-activation of platelets before adding them to the coverslips. Therefore, we proceeded to repeat the experiment omitting the pre-stimulation of platelets with 0.02U/mL thrombin.

Under these conditions, platelets were still able to bind fibrinogen without prior stimulation with thrombin. As expected, the area of the platelets at all time points was significantly less in the platelets that had not been pre-stimulated with thrombin (WT 15 min $P=0.001$, 30 min $P=>0.0001$, 45min $P=>0.0001$, 60 min $P=0.1717$, KO 15 min $P=>0.0001$, 30 min $P=>0.0001$, 45min $P=0.0002$, 60 min $P=0.0012$). Interestingly, although there were fewer wild-type platelets bound to the surface, the decrease was not significant (15 min $P=0.99$, 30 min $P=0.97$, 45min $P=0.23$, 60 min $P=0.07$). In knockout samples the reductions in platelets were still observed, however, it was only the final 1-hour timepoint that showed a significant reduction (15 min $P=0.99$, 30 min $P=0.30$, 45min $P=0.11$, 60 min $P=0.0084$). Pre-stimulation with thrombin resulted in platelets being significantly more spread however it did not significantly affect the number of platelets that bind to the matrix, as such, going forward all spreading experiments were conducted with no pre-stimulation.

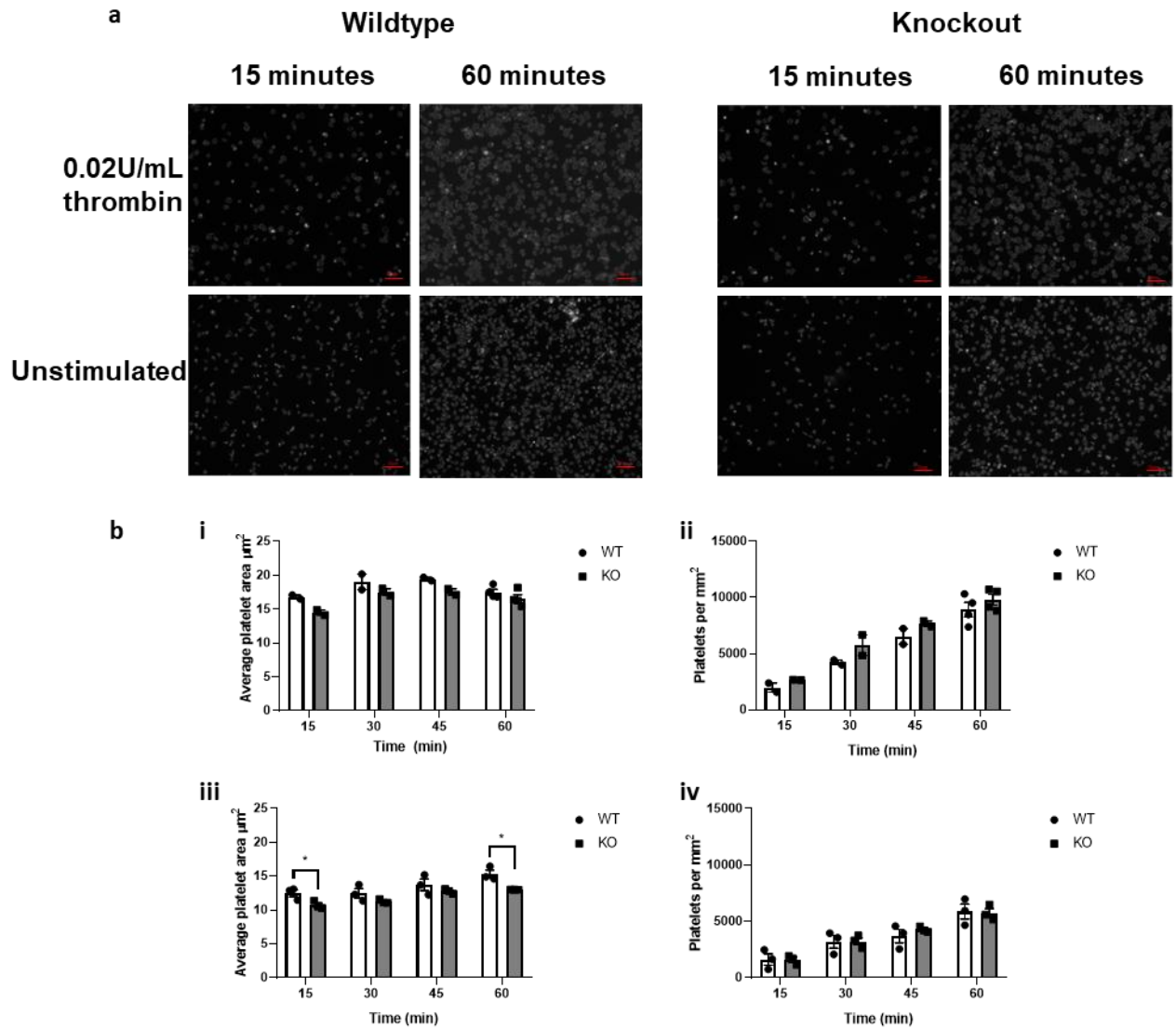


Figure 4-11. Effects on the static spreading of murine platelets to fibrinogen matrices in untreated and pre-stimulated conditions. *a.* representative images of platelets spread on fibrinogen matrix 100 μ l of 1×10^7 washed platelets (WP) from either WT or KO mice were seeded on 12mm coverslips, for thrombin-stimulated samples platelets were activated with 0.02U/mL thrombin immediately before addition to the coverslip. Coverslips were covered with 100 μ g/mL fibrinogen and platelets left to bind to the indicated time points. *b.* images were assessed for; (i,iii) average platelet area, (ii,iv) platelets per mm^2 . presented by mean \pm standard error of mean (SEM) * $P < 0.05$, ** $P < 0.01$ compared to wild-type $N = 3$.

Next, we examined the impact of α -synuclein on platelet adhesion by allowing platelets to spread on a 100 μ g/mL fibrinogen matrix (Figure 4-12). When comparing the average area of the spread platelets, there was a significant decrease in the size of knockout platelets at the 15- and 60-minute time points, and small decreases at 30 and 45 minutes (15 min $P = 0.043$, 30 min $P = 0.15$, 45min $P = 0.33$, 60 min $P = 0.015$). We then examined the number of platelets that adhered to the matrix over time and found no significant difference in the number of platelets binding (15 min $p = 0.949$, 30 min $p = 0.966$, 45 min $p = 0.40$, 60 min $p = 0.88$). These data show that the binding ability

of the α -synuclein-deficient platelet remains intact, however, in response to fibrinogen there is a slight reduction in the ability of platelets to spread; this was, however, not significant. It has been hypothesised that the SNARE complex may also play a differential role in platelet spreading, this was first interrogated following that spreading requires the binding of VAMP7 to the membrane (Ren et al., 2007, Golebiewska and Poole, 2013)

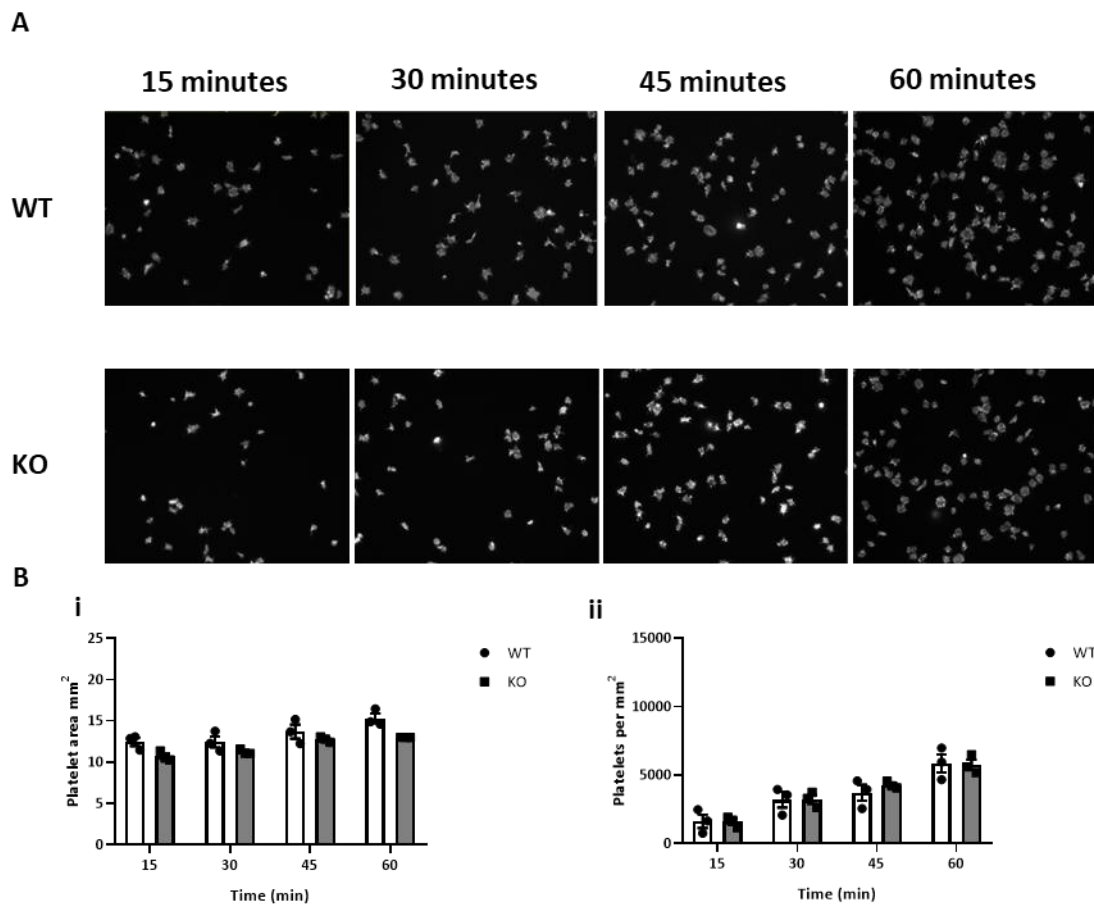


Figure 4-12. Static spreading of unstimulated murine platelets on a matrix. 100 μ l of 1×10^7 washed platelets (WP) from either WT or KO mice were seeded on 12mm coverslips. Coverslips were covered with 100 μ g/mL fibrinogen. Average platelet area in mm² increased significantly over the time course of both KO and WT ($P=0.0009$, $P=0.0001$) respectively. There was a significant difference between the area of knockout and wild-type platelets at 15 and 60 minutes (15 min $P=0.03$, 30 min $P=0.10$ 45 min $P=0.31$ 60 min $P=0.006$). Platelets per mm² are displayed as mean \pm standard error of the mean (SEM). The number of platelets per mm² increases over time ($P=0.003$) but did not differ between wild-type and α -synuclein knockout at any timepoint, (15 min $p=0.949$, 30min $p=0.966$, 45 min $p=0.40$, 60 min $p=0.88$). * $p>0.05$ ** $P>0.01$ *** $P>0.001$.

4.5.2. α -synuclein deletion has no impact on platelet adhesion to collagen.

The binding of platelets to collagen is key for their initial role in haemostasis, therefore we sought to assess the ability of α -synuclein knockout platelets to bind to collagen in comparison to wild-type counterparts (Figure 4-13). First, we analysed the average surface area of the bound platelets and found no significant change in the ability of α -synuclein deficient platelets to spread on collagen (15 min $p=0.74$, 30 min $p=0.29$, 45 min $p=0.30$, 60 min $p=0.52$). Following this, we assessed the number of platelets per mm^2 , similarly to fibrinogen, and found no significant change in the ability of α -synuclein knockout platelets to bind to collagen (15 min $p=0.202$, 30 min $p=0.173$, 45 min $p=0.755$, 60 min $p=0.844$). Interestingly, when analysing the spreading data, although there was no difference in size and count there was an observed difference in the phenotype distributions between the knockout and wild-types changed. The wild-type platelets were observed to have a “spikier” appearance, with multiple filopodial protrusions, whereas the knockout platelets were more often spread but had a smoother appearance. The interaction of α -synuclein and the actin-binding factor Cofilin-1 has been observed, a study also has shown that increased concentrations of α -synuclein in neurons increase the number of lamellipodia and filopodia in hippocampal neurons (Dasgupta and Thiagarajan, 2020, Bellani et al., 2014, Oliveira da Silva and Liz, 2020).

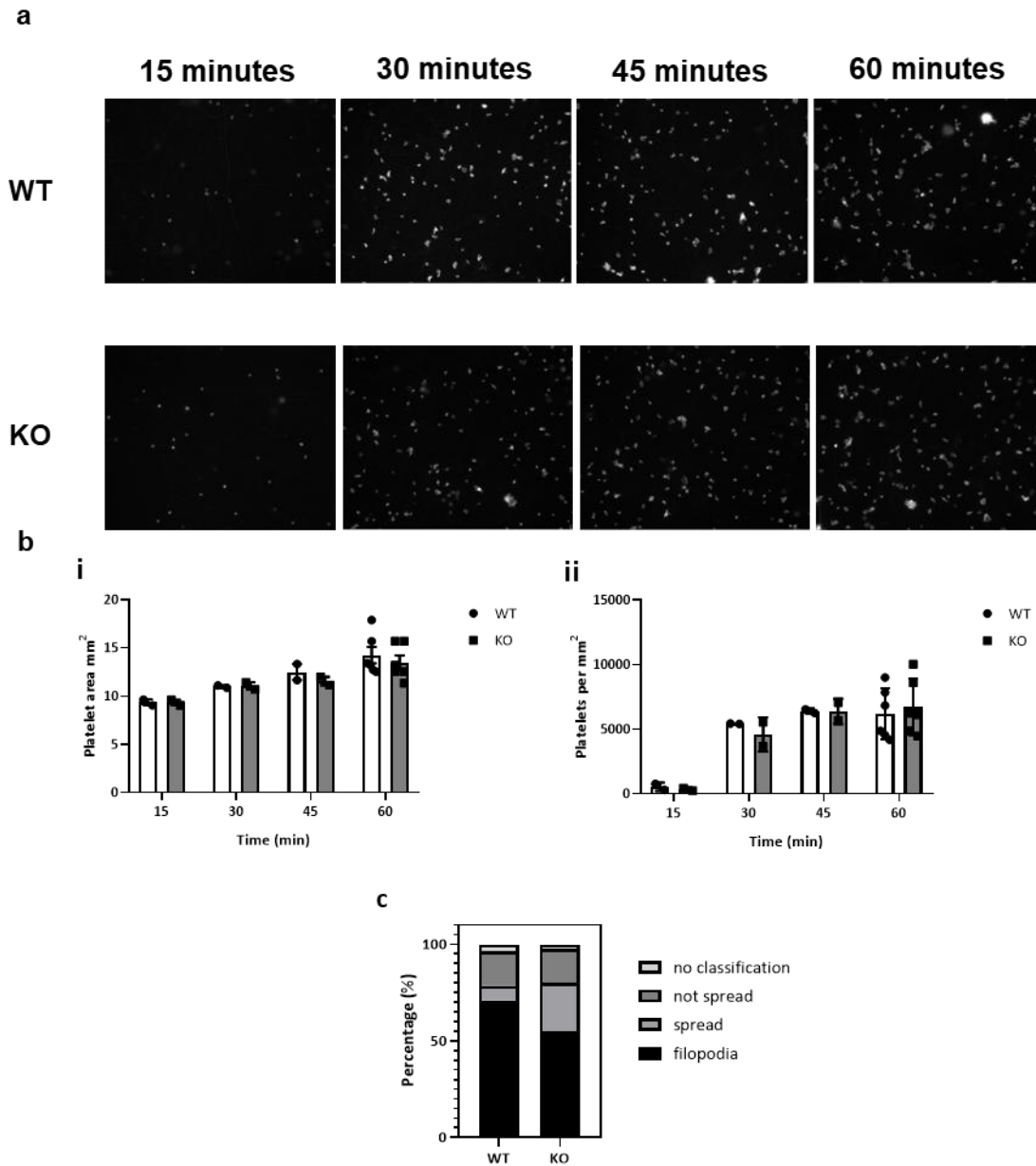


Figure 4-13. Static spreading of unstimulated murine platelets on a collagen matrix. 100 μ l of 1×10^7 washed platelets (WP) from either WT or KO mice were seeded on 12mm coverslips. Coverslips were covered with 100 μ g/mL collagen. Representative images for each timepoint and genotype are displayed. Graphs representing platelet area and platelets per mm² are displayed as mean \pm standard error of the mean (SEM). The number of platelets per mm² increases over time ($P=0.0008$) however is not significantly different between wild-type and α -synuclein knockout except for the 60-minute time point (15 min $P=0.99$, 30 min $P=0.53$, 45 min $P=0.999$, 60 min $P=0.03$). initial data shows that the area of platelet spread does not significantly increase ($P=0.306$). While the Wild-type platelets are more likely to be spikey than fully spread there is no significant difference. * $p>0.05$ ** $P>0.01$ *** $P>0.001$ 30,40 minute $N=2$ 15-60 mimunte $N=5$.

4.5.1. α -synuclein deletion impairs thrombus formation *in vitro*.

Platelets circulate in the body and are subjected to shear stresses. Under physiological conditions, typical shear rates experienced by platelets are 300–800^{s⁻¹} in the large arteries, 15–200^{s⁻¹} in veins and 450–1,600^{s⁻¹} in micro arterioles (Gogia and Neelamegham, 2015). Therefore, we examined platelet adhesion and thrombus formation under these physiologically relevant conditions in response to collagen (Figure 4-14). Whole blood was stained with DIOC6 and flowed at a shear rate of 20dynes/cm² which is equivalent to time-averaged physiological arterial shear rates *in vivo* (Yap et al., 2012). The wild-type platelets were observed to clump together and begin to form distinct thrombi to cover on average 10.44±1.1 % of the slide. In contrast, knockout platelets exhibited sporadic binding and a significantly reduced propensity to form thrombi structures. Further supporting this observation, optical sectioning of the thrombus revealed that wild-type thrombi had an average height of 8.25µm±0.75, whereas knockout samples averaged 2.5µm±0.64 in height. This marked difference indicated a significant decrease in both thrombus coverage (P=0.031) and height (P=0.0011).

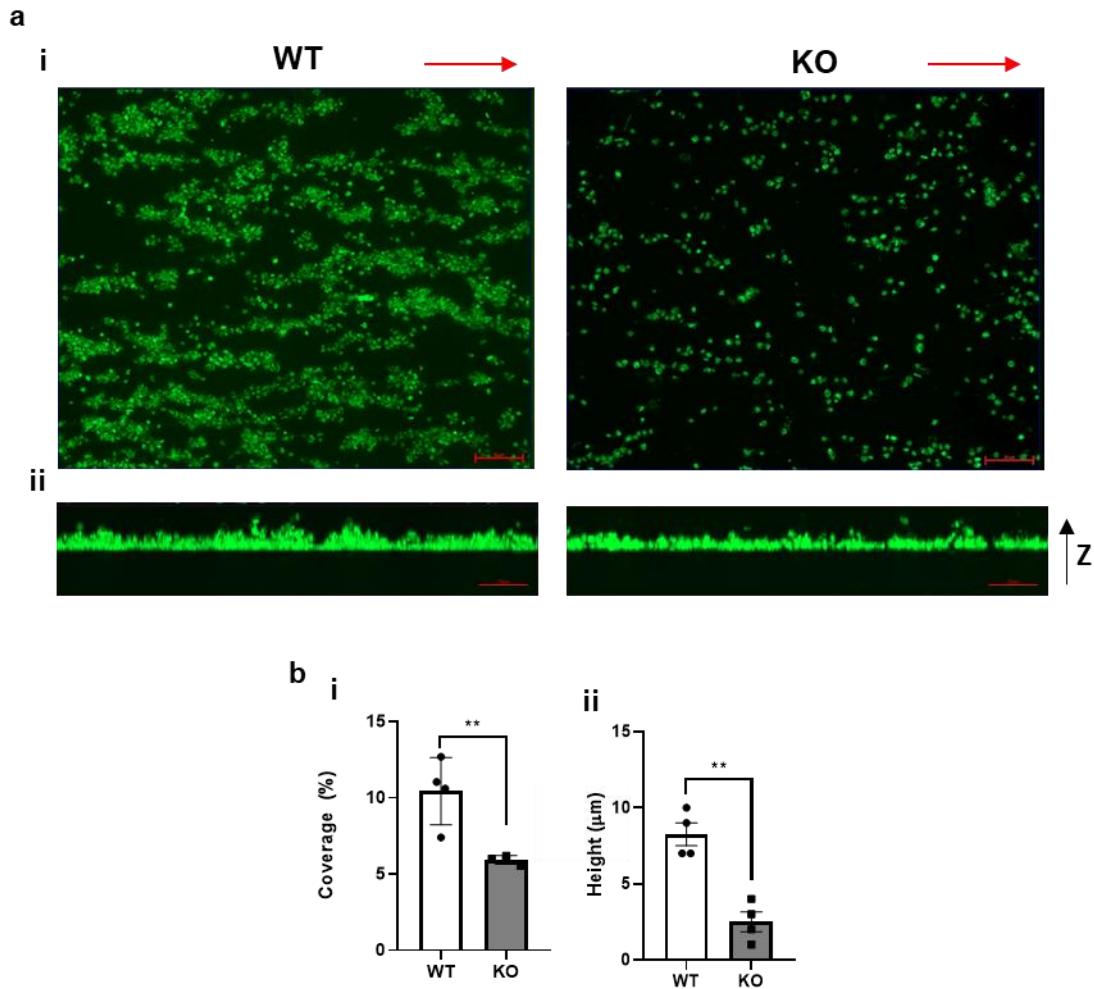


Figure 4-14. Platelet adhesion to collagen matrices under flowing conditions. Whole blood stained with DIOC6 was flowed over 100μg/mL collagen matrix at arterial shear rates (20dynes/cm²) for 2 minutes before washing with PBS and fixing), the chips were then imaged using confocal microscopy and displayed as maximum intensity projections. (ai) Images were then analysed using ImageJ to assess surface coverage, the coverage of KO platelets was significantly less than WT, and the KO platelets also formed much smaller thrombi in comparison. (aii) Z stacks were used to assess the thrombus height, Z-axis shown. (Bi-ii) Coverage and thrombus height results displayed as Mean±SEM N=5 P=0.031).

4.6. Immunofluorescence analysis of α-synuclein with SNARE components

A role of α-synuclein that has been elucidated in neuronal cells is the facilitation of the SNARE complex formation and chaperoning activity, one study in platelets also identified α-synuclein interaction with SNARE components, however, observed only a limited role in platelet function (Smith et al., 2023). We sought to examine the localisation of α-synuclein in platelets following activation, and its proximity to other known SNARE proteins using immunofluorescence microscopy, Additionally to VAMP8, STX11 and SNAP23 we assessed STX4, VAMP2 and VAMP7.

In the first instance, we assessed the specificity of the secondary antibodies binding to platelets with no primary antibodies present, and WGA 350 was used to label platelet membranes (Figure 4-15). Unstimulated and stimulated samples showed clear staining for WGA, there were also some signal from both 568nm and 667nm channels showing a very small amount of nonspecific binding to the platelets in both Wild-type and knockout and in basal and stimulated samples. This shows that any signal that is observed is not due to non-specific binding or background fluorescence.

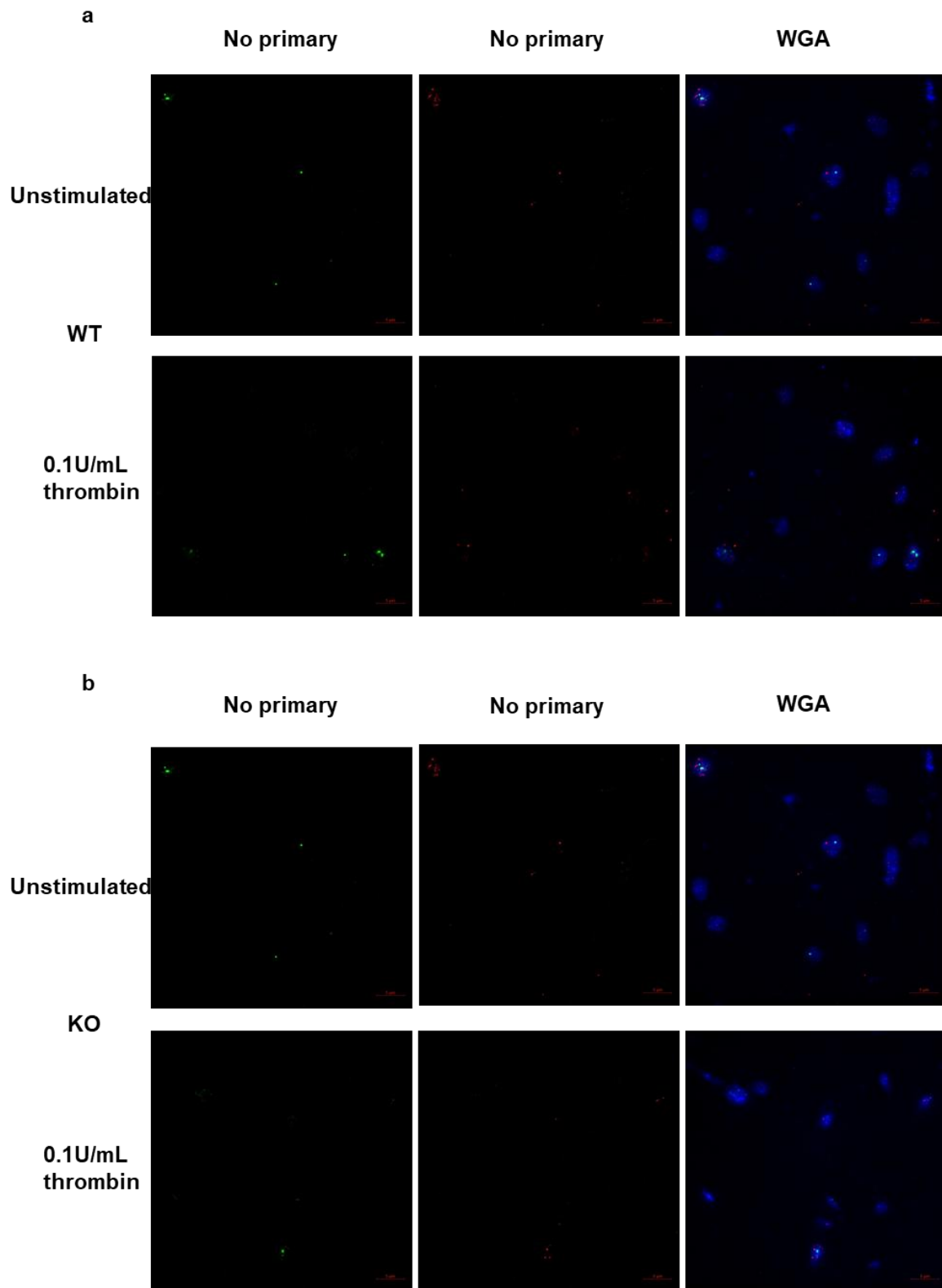


Figure 4-15. Confirmation of specificity of secondary antibodies. Platelets were isolated from wild-type (a) or α -synuclein knockout (b) murine blood through centrifugation. Stimulated platelet samples were activated with 0.1U thrombin immediately before the addition of samples to Poly-L-Lysine coverslips, followed with incubation for 1 hour at 37°C. cover slides were then washed and blocked with 0.5% BSA for 1 hour, before fixing with permeabilisation at room temperature with 4% PFA and 0.3% Triton-x100 respectively. Following washing with PBS the slides were incubated 1:1000 Anti-mouse (568), Anti rabbit (667) and 5.0 μ g/mL WGA, Alexa Fluor® 350 for 1 hour at 37°C away from light. Samples were mounted with gelvitol and imaged. Representative image

of $N=3$. The syntaxins are a family of membrane-bound proteins, syntaxin11 (STX11) has been characterised as the most important member of this family for platelet granule secretion (Golebiewska and Poole, 2013). In the wild-type platelets, STX11 was visible throughout the platelet, as was α -synuclein, however, there was little co-localisation observed (Figure 4-16A). In the wild-type platelets that were stimulated with 0.1U/mL thrombin, there was a similar distribution of STX11 throughout the platelet, yet, the α -synuclein was observed to be much more visible and spread out than in unstimulated samples. Interestingly although STX11 and α -synuclein appeared to be more spread out there were more co-localisation events between STX11 and α -synuclein (yellow), suggesting that they may interact upon platelet activation.

In wild-type α -synuclein knockout platelets in unstimulated conditions, STX11 remained spread throughout the platelet (Figure 4-16). We observed some very weak staining for α -synuclein in the knockout sample mostly localised to the platelets, however, this may be some bleed-through from the other fluorophores. Following stimulation, platelets did not spread to the same extent as the wild-type platelets, this is concordant with previous spreading data in human platelets, although the distribution of STX11 was maintained following activation.

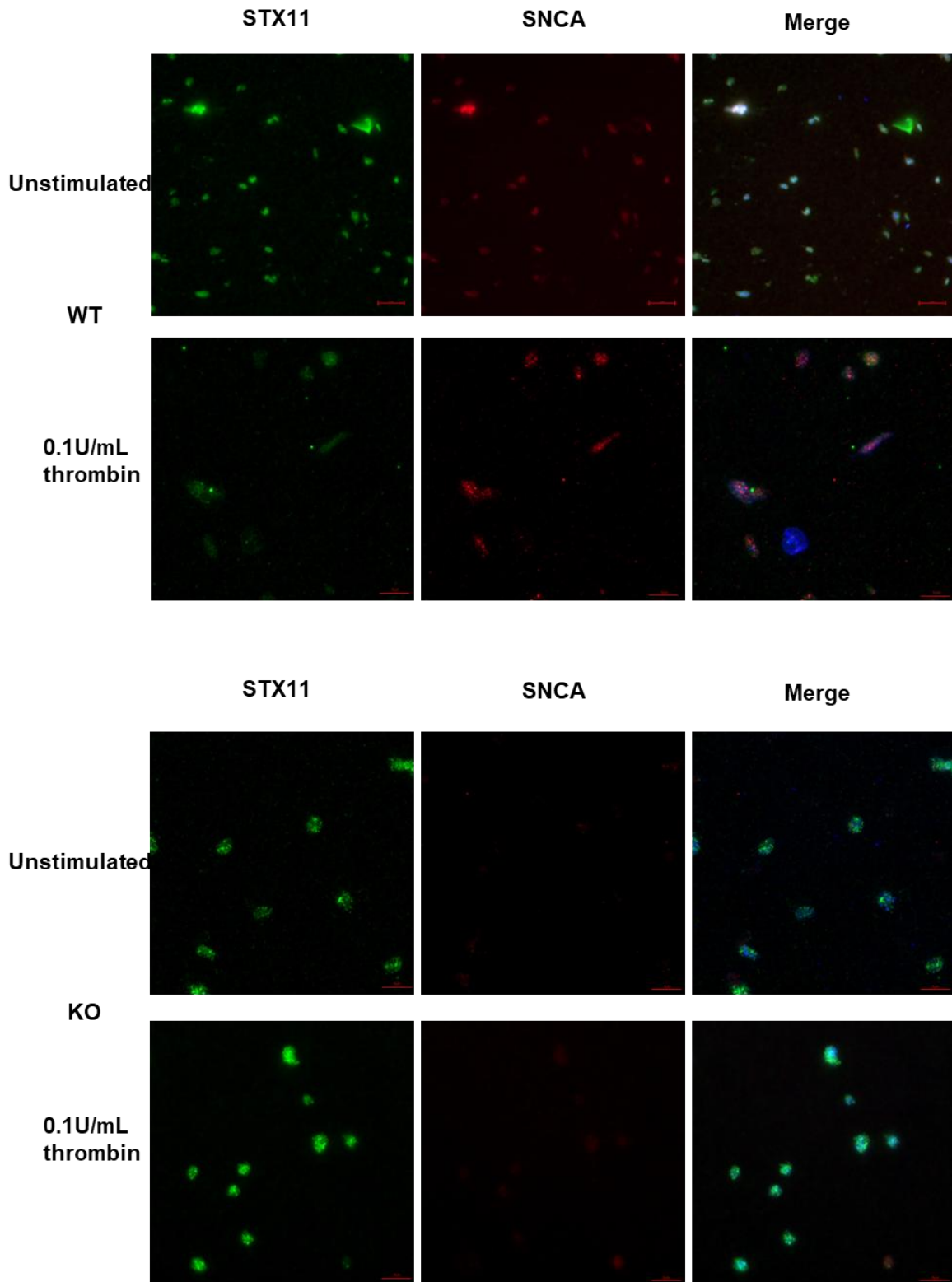


Figure 4-16. Effects of α -synuclein knockout on Syntaxin 11 in platelets. Platelets were isolated from wild-type (a) or α -synuclein knockout (b) murine blood through centrifugation. Stimulated samples were activated with 0.1U thrombin directly before addition to Poly-L-Lysine coverslips followed by incubation for 1 hour at 37°C, cover slides were then washed and blocked with 0.5% BSA for 1 hour, before fixing and permeabilization at room temperature with 4% PFA and 0.3% Triton-x100 respectively. Platelets were then incubated with 1:200 α -synuclein (CST 4179) and 1:100 STX11 (SC- 377121) for 1 hour at 37°C. Following washing with PBS the slides were incubated 1:1000 Anti-mouse (568), Anti rabbit (667) and 5.0 μ g/mL WGA, Alexa Fluor® 350 for 1 hour at 37°C, protected from light. Samples were mounted with gelvitol and imaged. Representative image of N=3. Images were then false-coloured α -synuclein (red) Stx11 (green) membrane (blue).

Following this, we interrogated the effects of α -synuclein knockout on SNAP23 movement and localisation (Figure 4-17). In unstimulated wild-type platelets, SNAP23 was distributed throughout the platelet, whereas the distribution of α -synuclein was comparable to what was observed when interrogating STX11. In samples stimulated with 0.1U/mL thrombin, SNAP23 colocalised towards the periphery of the platelets, forming a ring around the periphery that was very similar to α -synuclein. There were multiple locations around the edge of the platelet where the SNAP23 and α -synuclein were co-localised, however, there were locations for both where there was 1 protein observed without the other. Interestingly, the examination of α -synuclein knockout platelets revealed that SNAP23 also distributed heterogeneously throughout the cell. Similarly to STX11, there was a small amount of α -synuclein positive signal within the platelet. When Knockout platelets were stimulated with 0.1U/mL thrombin, SNAP23 moved towards the periphery slightly. However, this movement was less pronounced compared to wild-type platelets, where SNAP23 was observed to spread throughout many of the platelets.

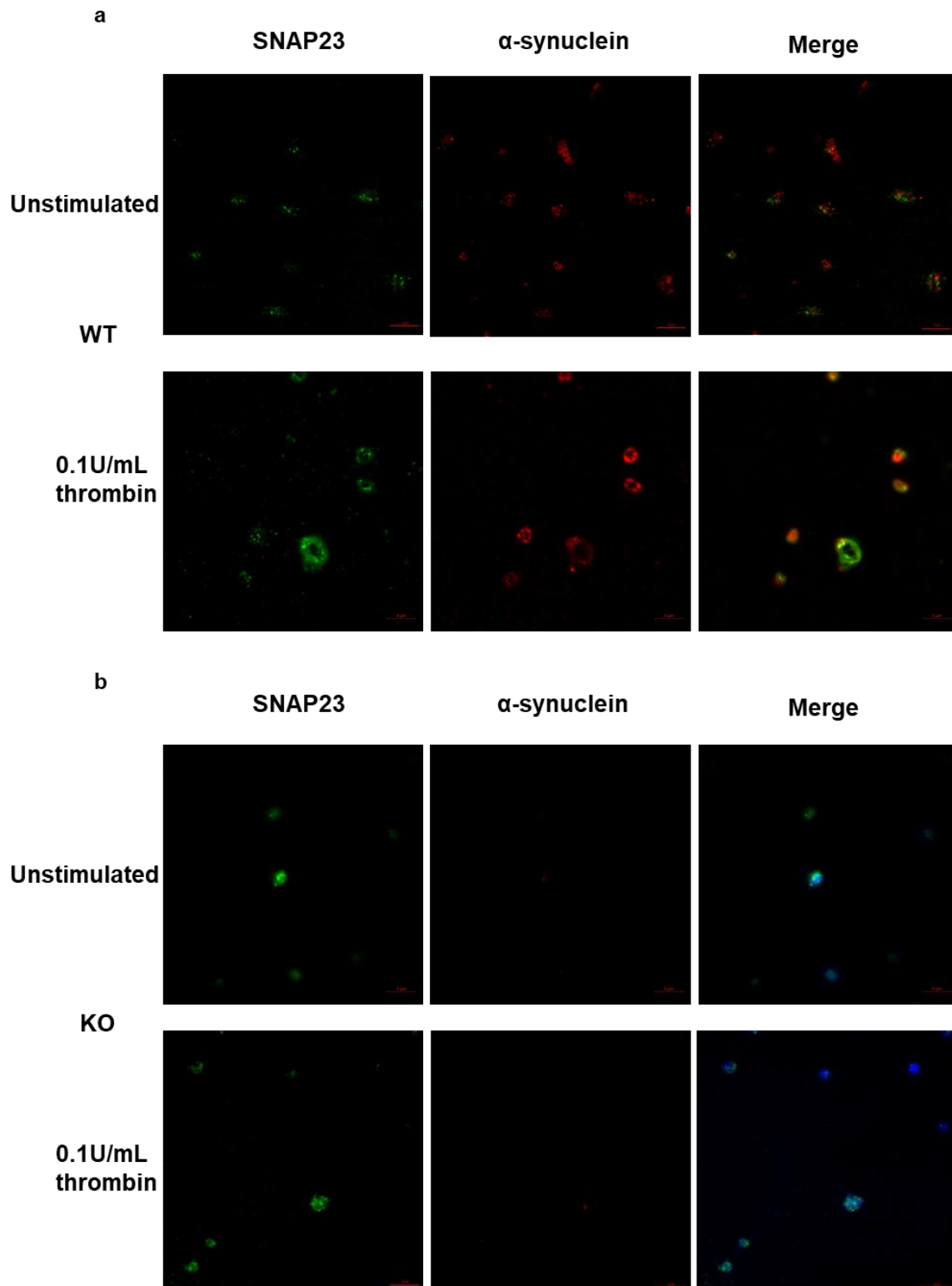


Figure 4-17 Effects of α -synuclein knockout on SNAP23 in platelets. Platelets were isolated from wild-type (a) or α -synuclein knockout (b) murine blood through centrifugation. Stimulated platelet samples were activated with 0.1U/mL thrombin immediately before the addition of samples to Poly-L-Lysine coverslips, followed with incubation for 1 hour at 37°C, cover slides were then washed and blocked with 0.5% BSA for 1 hour, before fixing with permeabilisation at room temperature with 4% PFA and 0.3% Triton-x100 respectively. Platelets were then incubated with 1:100 α -synuclein (CST 4179) and 1:100 SNAP23 (SC-734215) for 1 hour at 37°C. Following washing with PBS the slides were incubated 1:1000 Anti-mouse (568), Anti rabbit (667) and 5.0 μ g/mL WGA, Alexa Fluor® 350 for 1 hour at 37°C away from light. Samples were mounted with gelvitol and imaged. Representative image of N=3 α -synuclein (red) SNAP23 (green) Membrane (blue).

Next, we investigated the effects of α -synuclein knockout on the movement of VAMP8 within platelets (Figure 4-18). VAMP8 is present on the granules which bind to STX11 for the major SNARE complex, therefore if α -synuclein is required for chaperoning we may see a change in the movement of VAMP8 (Thon et al., 2012). In wild-type platelets, VAMP8 was distributed heterogeneously throughout the platelet, upon stimulation, the VAMP8 was moved towards the periphery of the platelet, however, there was still a significant amount of VAMP8 present throughout the platelet. The movement of α -synuclein as expected was like that in STX11 and SNAP23 images where the α -synuclein in unstimulated conditions is spread throughout the platelet and moves towards the periphery of the cell upon stimulation. In unstimulated conditions, both VAMP8 and α -synuclein co-localised at many points throughout the platelet. Following stimulation, co-localisation was still observed, however to a lesser extent, albeit most co-localisation events observed were at the peripheries of the cell as opposed to the centre.

In the α -synuclein knockout samples, we showed that the VAMP8 was spread homogeneously throughout the platelet, however, there was a small amount of signal from α -synuclein. These signals showed very little co-localisation. Following stimulation of platelets, the VAMP8 remained spread homogeneously throughout the cell with a lower propensity for moving towards the periphery. This indicates that the platelet granules are not moving towards the peripheries of the cell as effectively in the α -synuclein knockout mice as in the wild-type.

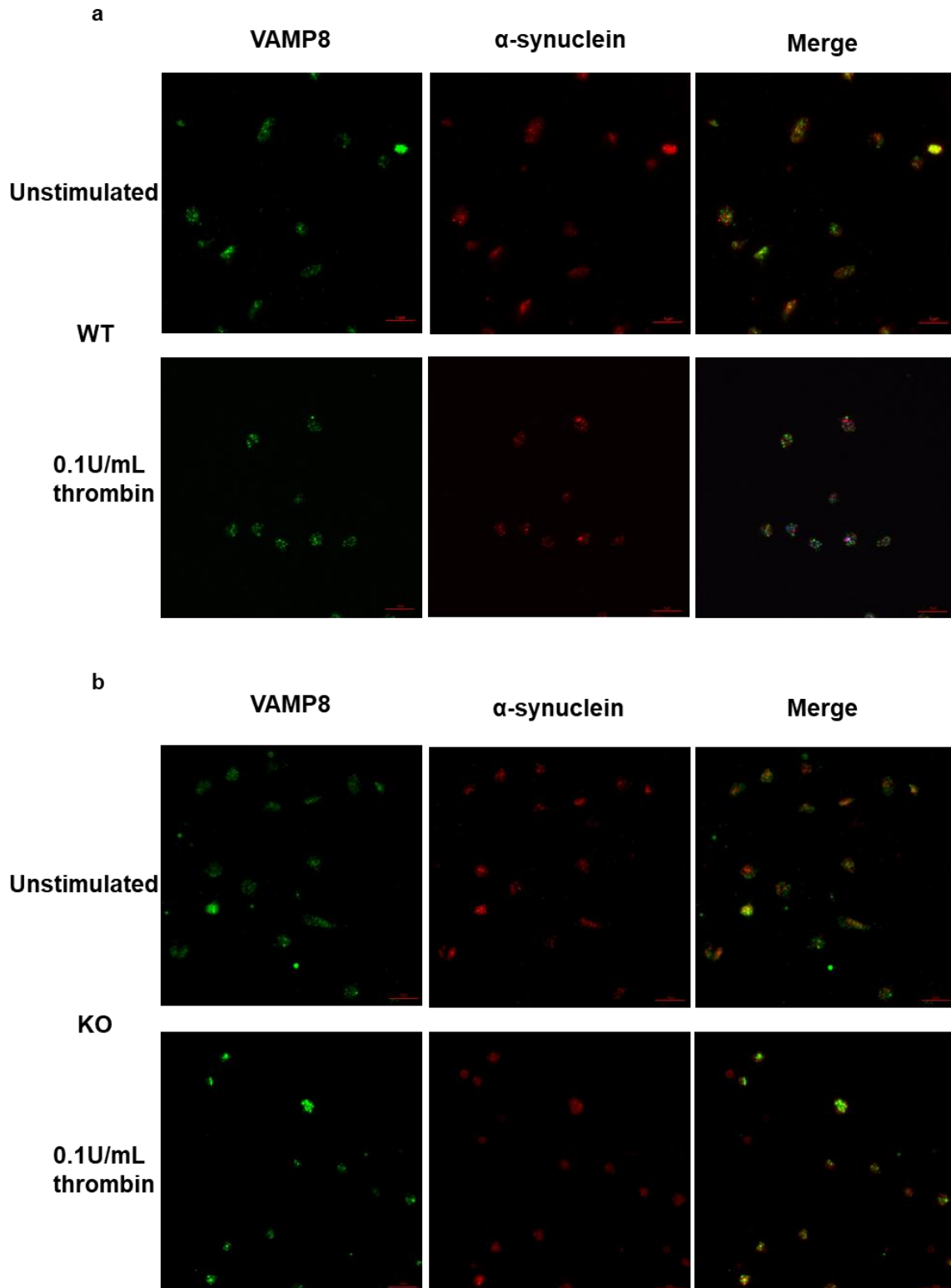


Figure 4-18. Effects of α -synuclein knockout on VAMP8 in platelets. Platelets were isolated from wild-type (a) or α -synuclein knockout (b) murine blood through centrifugation. Stimulated platelet samples were activated with 0.1U/mL thrombin immediately before the addition of samples to Poly-L-Lysine coverslips, followed by incubation for 1 hour at 37°C, cover slides were then washed and blocked with 0.5% BSA for 1 hour, before fixing with permeabilization at room temperature with 4% PFA and 0.3% Triton-x100 respectively. Platelets were then incubated with 1:100 SNCA (sc-515879) and 1:100 VAMP8 (cst -13060s) for 1 hour at 37°C. Following washing with PBS the slides were incubated 1:1000 Anti-mouse (568), Anti rabbit (667) and 5.0 μ g/mL WGA, Alexa Fluor® 350 for 1 hour at 37°C away from light. Samples were mounted with gelvitol and imaged. Representative image of N=3 α -synuclein (red) VAMP8 (green) Membrane (blue).

In addition to the main SNARE complex proteins used for platelet granule release, we investigated the additional SNARE members, STX4, VAMP2 and VAMP7. Syntaxin 4, like syntaxin11, is a membrane-bound protein, this was confirmed in unstimulated samples both wild-type and knockout where the STX4 signal was predominantly observed around the peripheries (Figure 4-19). The distribution pattern of α -synuclein resembled that of other samples. In unstimulated conditions, there are a small amount of α -synuclein and STX4 co-localisation events, which showed minimal increase upon stimulation with 0.1 U/mL thrombin (Figure 4-19). In α -synuclein knockout platelets, the distribution of STX4 within the platelet did not show noticeable differences under basal or stimulated conditions, which is expected given STX4's presence on the platelet membrane (target membrane).

We then investigated the effects of α -synuclein knockout on VAMP2, which like VAMP8, is present on the membranes of granules within the platelet (Figure 4-20). In unstimulated conditions, VAMP2 was spread heterogeneously throughout the platelets, and when stimulated with 0.1U/mL thrombin it moves towards the periphery of the cell, while there was still a signal throughout the whole of the cell. In unstimulated conditions, there were very few co-localisation events observed between α -synuclein and VAMP2. After stimulation with 0.1U/mL thrombin, there were more observed co-localisation events, but as with VAMP8 although co-localised in places there were both proteins located at the periphery that were not observed together.

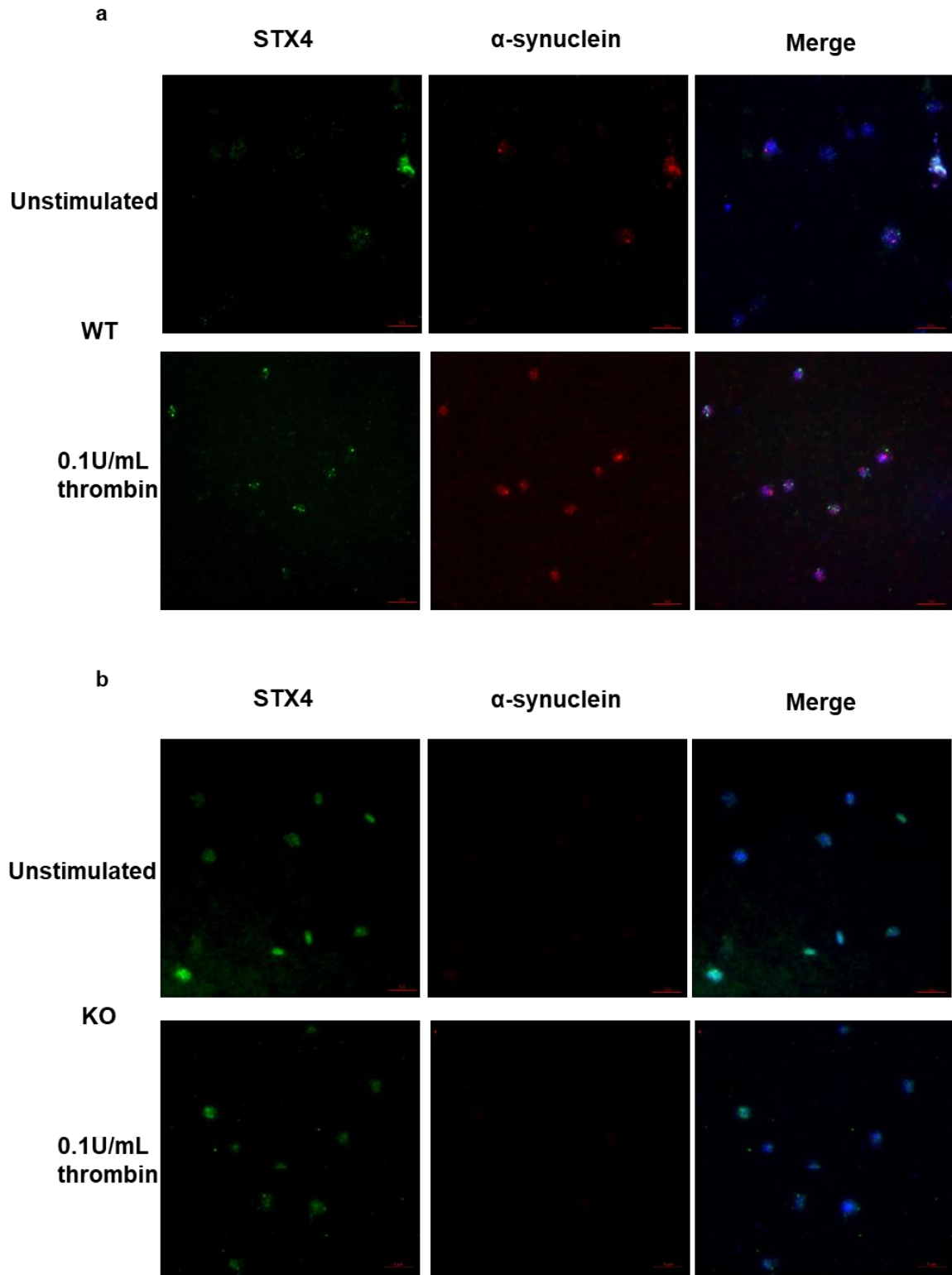


Figure 4-19. Effects of α -synuclein knockout on Syntaxin 4 in platelets. Platelets were isolated from wild-type (a) or α -synuclein knockout (b) murine blood through centrifugation. Stimulated platelet samples were activated with 0.1U thrombin immediately before addition of samples to Poly-L-Lysine coverslips, followed by incubation for 1 hour at 37°C, cover slides were then washed and blocked with 0.5% BSA for 1 hour, before fixing with permeabilization at room temperature with 4% PFA and 0.3% Triton-x100 respectively. Platelets were then incubated with 1:100 α -synuclein (CST 4179) and 1:100 STX4 (SC-101301) for 1 hour at 37°C. Following washing with PBS the slides were incubated 1:1000 Anti-mouse (568), Anti rabbit (667) and 5.0 μ g/mL WGA, Alexa Fluor® 350 for 1 hour at 37°C away from light. Samples were mounted with gelvitol and imaged. Representative image of N=3 α -synuclein (red) STX4 (green) Membrane (blue).

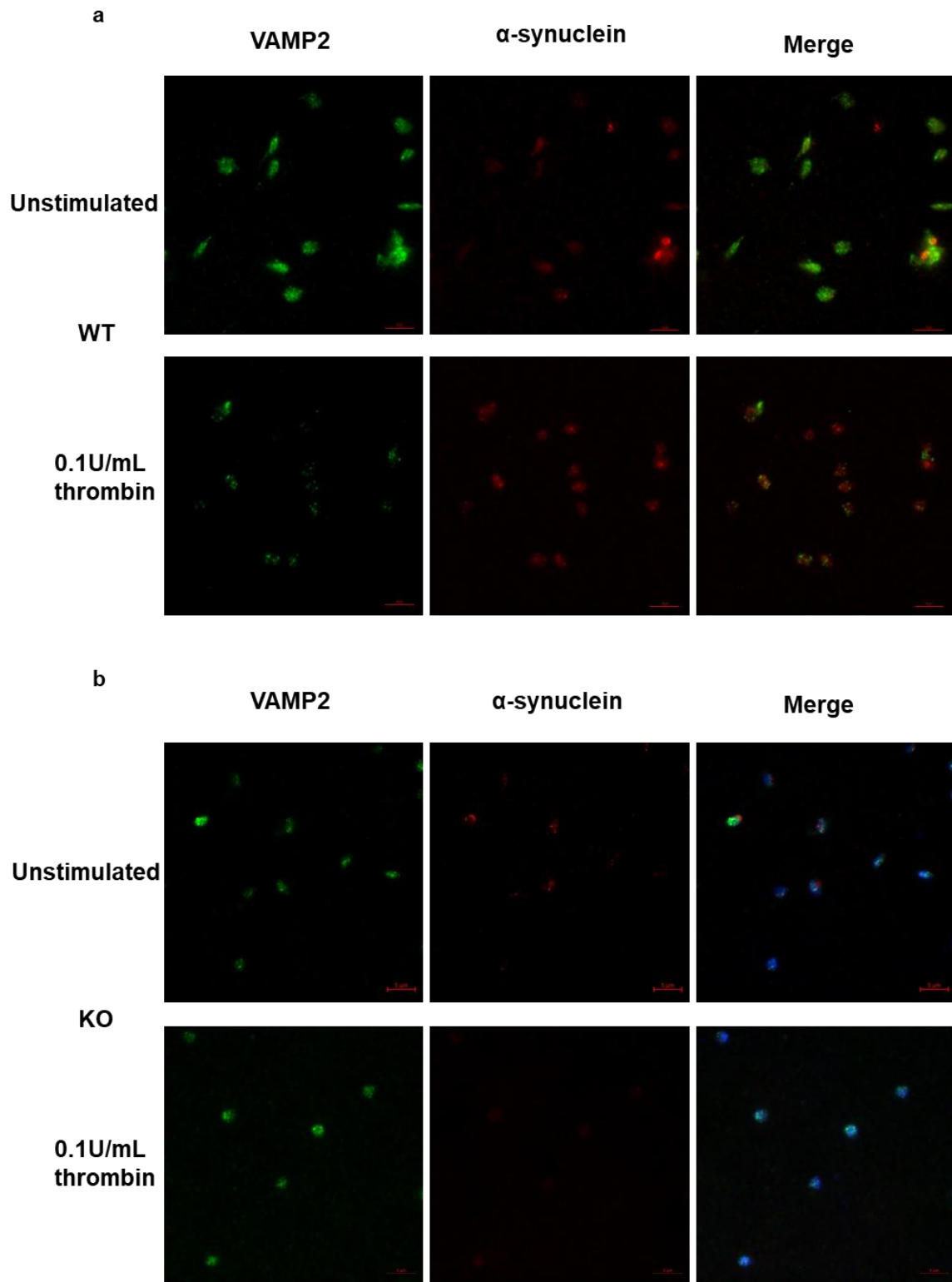


Figure 4-20. Effects of α -synuclein knockout on VAMP2 in platelets. Platelets were isolated from wild-type (a) or α -synuclein knockout (b) murine blood through centrifugation. Stimulated platelet samples were activated with 0.1U thrombin immediately before the addition of samples to Poly-L-Lysine coverslips, followed with incubation for 1 hour at 37°C, cover slides were then washed and blocked with 0.5% BSA for 1 hour, before fixing with permeabilisation at room temperature with 4% PFA and 0.3% Triton-x100 respectively. Platelets were then incubated with 1:100 α -synuclein (CST 4179) and 1:100 Vamp 2 (SC-69706) for 1 hour at 37°C. Following washing with PBS the slides were incubated 1:1000 Anti-mouse (568), Anti rabbit (667) and 5.0 μ g/mL WGA, Alexa Fluor® 350 for 1 hour at 37°C away from light. Samples were mounted with gelvitol and imaged. Representative image of N=3 α -synuclein (red) VAMP2 (green) Membrane (blue).

VAMP7 showed similar distribution and response to thrombin stimulation to other members of the VAMP family in WT platelets, with a heterogenic distribution under unstimulated conditions. Similarly, to the other VAMP proteins, VAMP7 has some co-localisation in basal samples, interestingly, upon stimulation, the amount of co-localisation events did not visibly look to increase (Figure 4-21). When imaged in knockout platelets the VAMP7 exhibited movement highly analogous to within the WT platelets, starting heterogeneous in unstimulated samples, and moving towards the periphery upon stimulation with 0.1U/mL thrombin, albeit to a lesser extent.

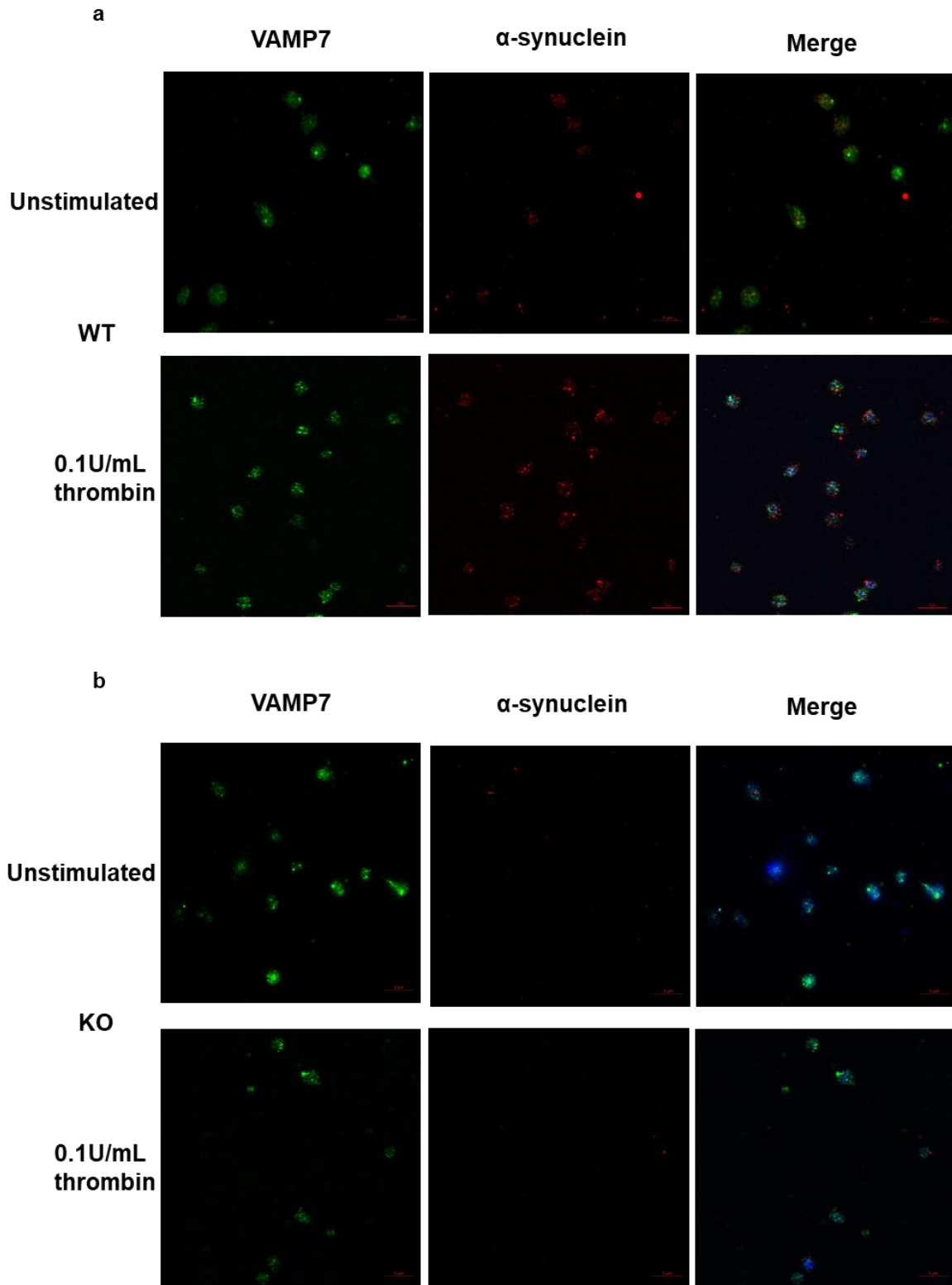


Figure 4-21. Effects of α -synuclein knockout on VAMP7 in platelets. Platelets were isolated from wild-type (a) or α -synuclein knockout (b) murine blood through centrifugation. Stimulated platelet samples were activated with 0.1U thrombin immediately before the addition of samples to Poly-L-Lysine coverslips, followed with incubation for 1 hour at 37°C, cover slides were then washed and blocked with 0.5% BSA for 1 hour, before fixing with permeabilisation at room temperature with 4% PFA and 0.3% Triton-x100 respectively. Platelets were then incubated with 1:100 SNCA (sc-515879) and 1:100 VAMP7 (CST- 14811) for 1 hour at 37°C. Following washing with PBS the slides were incubated 1:1000 Anti-mouse (568), Anti rabbit (667) and 5.0 μ g/mL WGA, Alexa Fluor® 350 for 1 hour at 37°C away from light. Samples were mounted with gelvitol and imaged. Representative image of N=3 α -synuclein (red) VAMP7 (green) Membrane (blue).

Finally, we interrogated the movement of α -synuclein p^{ser129} (Figure 4-22) Both α -synuclein and its phosphorylated form were observed to be present throughout the cell in basal conditions. As expected, there is almost complete co-localisation between the phosphorylated protein and the total α -synuclein, however, there are also significant regions observed where there is α -synuclein that is not phosphorylated. Upon stimulation with 0.1U/mL thrombin, both the phosphorylated and non-phosphorylated α -synuclein were observed to move towards the periphery of the cell. Interestingly, the phosphorylated protein was seen to make a ring around the outside of the non-phosphorylated α -synuclein closer to the edge of the cell. In knockout samples, there were some sporadic signals however no significant signal was observed when compared with the negative control.

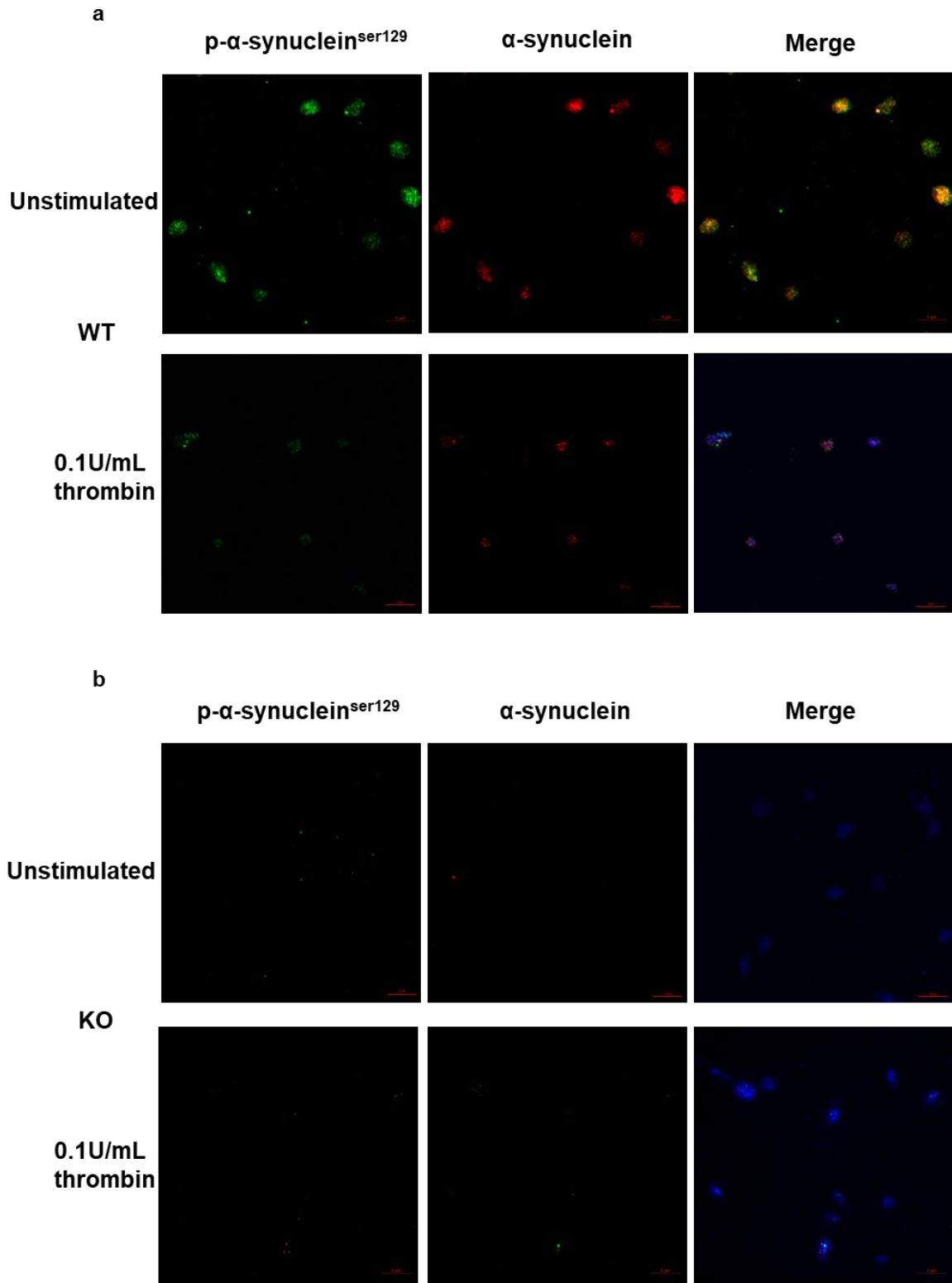


Figure 4-22. Movement of α -synuclein and in α -synuclein pser129 platelets. Platelets were isolated from wild-type (a) or α -synuclein knockout (b) murine blood through centrifugation. Stimulated platelet samples were activated with 0.1U thrombin immediately before the addition of samples to Poly-L-Lysine coverslips, followed by incubation for 1 hour at 37°C, cover slides were then washed and blocked with 0.5% BSA for 1 hour, before fixing with permeabilisation at room temperature with 4% PFA and 0.3% Triton-x100 respectively. Platelets were then incubated with 1:100 SNCA (sc-515879) and 1:100 pSNCA (sc -135638) for 1 hour at 37°C. Following washing with PBS the slides were incubated 1:1000 Anti-mouse (568), Anti rabbit (667) and 5.0 μ g/mL WGA, Alexa Fluor® 350 for 1 hour at 37°C away from light. Samples were mounted with gelvitol and imaged. Representative image of N=3 α -synuclein (red) α -synuclein pser129 (green) Membrane (blue).

4.7. Flow cytometric analysis of platelet activation.

4.7.1. Optimisation of flow cytometry conditions.

Multiple parameters must be optimised and remain consistent throughout experimentation to ensure the data is reliable and accurate. Firstly, to achieve consistent staining, platelet concentration was optimised to 2×10^7 platelets and then diluted to 1:10 for the final staining volume, as per the manufacturer's instructions. Next, the optimal concentrations of antibodies were optimised to achieve greater sensitivity and reduce overall antibody volumes used. Alongside the optimal concentration of antibody, the voltage of the machine was optimised to create the greatest separation between the unstimulated and activated samples. The final laser powers were adjusted to maximise the separation between the basal and positive samples while maintaining the basal MFI being low, the optimal voltages used were: FITC-580, PE-549, PE-CY7 -663 APC-580, Alexa-700 – 565.

Unstimulated samples were incubated with the highest dosage of antibody tested, for the positive samples, stimulated platelets were used and were incubated with the indicated concentration of antibody (Figure 4-23). PD-L1 APC was the first antibody evaluated, at low-5ng/ μ L, medium- 10ng/ μ L and high- 20ng/ μ L, basally an MFI at low and medium doses the signal observed is almost identical to the unstimulated sample, the high dosage however yielded an overall increase in MFI therefore 20ng/ μ L (5 μ L) APC was used.

Next was LAMP1, a marker of lysosome release. LAMP1 was conjugated to Alexa-700, in unstimulated conditions MFI of 3.85 was observed, after stimulation, it was assessed with Low-12.5ng/ μ L, Medium-25ng/ μ L and high-50ng/ μ L, where all MFI were within the same range, 43.6, 50.1 and 48.8, respectively. Therefore, we determined the optimal volume to be 12.5ng/ μ L (1.25 μ L), as it yielded the same MFI has higher doses using less antibody.

The platelet activation marker JON/A PE was used, basally an MFI of 580 was observed; stimulated samples were incubated with Low-1.25 μ L, Medium-2.5 μ L or high-5 μ L, volumes of antibody. The MFI of samples increased with antibody volume, Low volumes of antibody resulted in a lower than basal MFI, Medium of 1358 and High concentrations increased further to 2614. The highest dose tested was determined to be the optimal dose. Alongside this activation marker, p-selectin was used, as an

indicator of platelet activation and α -granule release. The P-selectin used was conjugated to FITC, there was little basal signal present with an MFI of 62.9. When stimulated samples were incubated with Low-1.25 μ L, Medium-2.5 μ L or high-5 μ L, volumes of antibody. The MFI increased in a dose-dependent manner, with low antibody concentration having an MFI of 431, a middle dose of 344, and the highest concentration yielding an MFI of 1340. The highest concentration of antibody used yielded the highest MFI and due to the basal sample treated with the same concentration showing a significantly lower signal it can be concluded this was not increased background.

The final antibody tested was for the dense granule maker CD63, this antibody was conjugated to PE-CY7. Basally an MFI of 65.5 was observed; stimulated samples incubated with low-5ng/ μ L, medium- 10ng/ μ L and high- 20ng/ μ L, volumes of antibody yielded a dose-on-dose increase, of 420, 585, and 630. With the small increase between the medium and high volumes, it was established that the middle dose of 10ng/ μ L (2.5 μ L) was optimal.

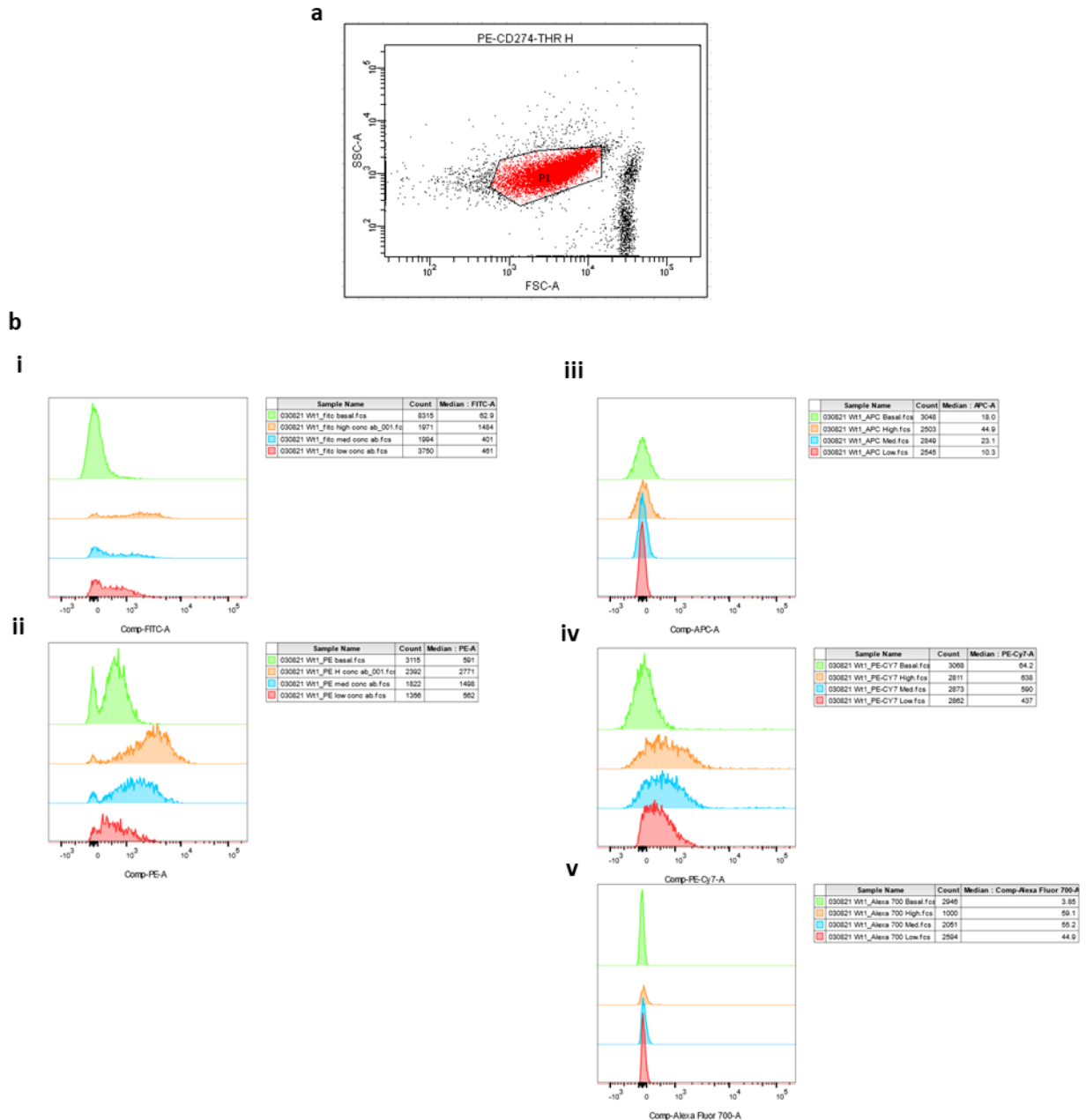


Figure 4-23. Antibody titration of flow cytometry antibodies. To assess the concentration of antibody needed for maximal signal with minimum antibody usage, antibody concentration was titrated and tested on wild-type mouse platelets stimulated with 0.1U/mL thrombin. Basal samples utilised the highest concentration of antibody on unstimulated samples as a baseline. Data is presented as histograms of fluorescent intensity from samples stained with concentrations of antibody.

Additionally, to the standardisation of all flow cytometry parameters, the collection of blood was of great importance (Figure 4-24). To ensure that the anti-coagulants were not a contributing factor it was crucial that all blood was drawn into sodium citrate with a 1:10 dilution. Compounding this, substandard bleeds resulted in a significantly decreased fold increase in both the activation markers (p-selectin, Jon/A) and the

markers for granule secretion (P-selectin, CD63 and LAMP1), this was also evidenced by a large increase of debris in the FSC and SSC.

A good bleed was characterised by a single attempt with little resistance to acquire 540 μ L of blood into 60 μ L sodium citrate. Average bleeds were characterised by either 2 attempts or less to acquire blood, or a resistance in the syringe when drawing the full volume. A bad bleed was characterised by multiple attempts required to puncture the heart, high resistance, or inability to draw the full volume. It was observed that with bleeds of poorer quality both the basal signal was increased, alongside the reduction in stimulated MFI, P-selectin was most sensitive to this with a drop from 33-fold increase to just 1.1x. In all bad bleed samples, the average fold increase for every marker was less than 1.5x. In comparison to average bleeds, P selectin and JON/A were both highly sensitive, however a significant decrease in all parameters was seen. It was observed that only good bleeds yielded acceptable data from which to draw conclusions.

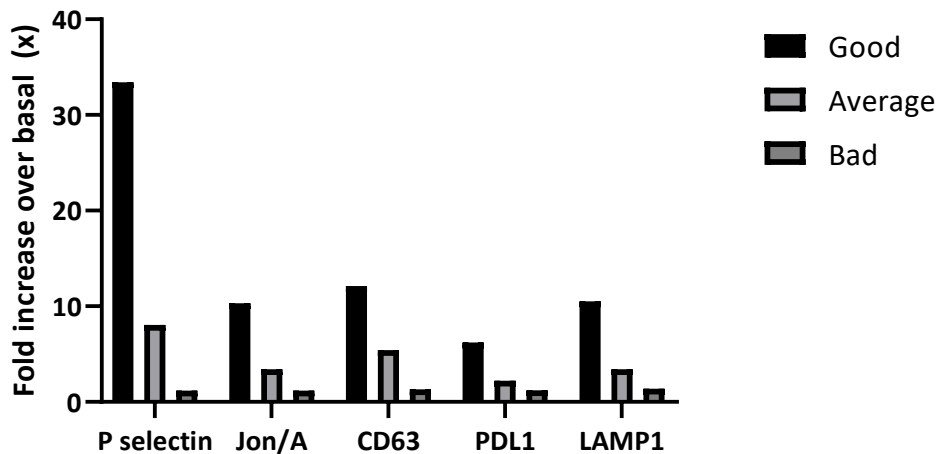


Figure 4-24. Effect of bleed quality on flow cytometry data. Murine blood was collected via Direct cardiac puncture after sacrifice by CO₂. Citric acid 150 μ L was used in collection syringes, initially if a bleed went well the platelets were used. A) early experiments showed the quality of the bleed greatly impacted the result of the flow cytometry, displayed in fold increase over basal. Due to this, it was decided that 600 μ L of blood would be taken. If a bleed did not reach this volume, it was not used and no more than 600 μ L was drawn to keep ratios of Citric acid the same between donors.

The use of a five-colour assay allowed for the comparison of the activation markers concurrently with the secretion markers and PD-L1 expression. However, these fluorophores can have a spillover into neighbouring channels creating an aberrant signal, necessitating the use of compensation for all parameters (Table 17). Single stained samples were run, and additional spillover was removed in the DIVA software which was used for all samples.

Table 17. Compensation matrix of 5 colour flow cytometric analysis

	FITC	PE	PE-CY7	APC	Alexa-700
FITC	0	1.8	0	0	0
PE	1.7	0	1.0	0	0
PE-CY7	0	0	0	12	0
APC	0	0	0	2.0	0.4
Alexa-700	1.5	0	4.5	2.9	0

4.7.2. Whole population flow cytometric analysis of platelet activation and secretion.

4.7.2.1. Assessing platelet activation in response to thrombin

The JON/A antibody only binds to activated $\alpha_2\beta_3$ in mouse platelets, the MFI from JON/A increased in a dose-dependent manner in response to stimulation with thrombin (Figure 4-25). In unstimulated conditions, both the knockout and wild-type platelets expressed similar levels of JON/A, with the knockout platelets even having a slightly higher expression. However, when stimulated with thrombin the JON/A MFI from knockout platelets was consistently lower than that of the wild-type platelets, this was only significant in the highest (0.1U/mL) dose of thrombin (P=0.025).

P-selectin is present within the α -granules in inactivated platelets and translocated to the plasma membrane upon activation. This makes P-selectin a good indicator of both activation and secretion of α -granules. The expression of P-selectin in basal conditions is similar in both Wild-type and knockout samples. When stimulated with thrombin, the P-selectin expression increases significantly in both samples. Comparatively to each other the p-selectin expression is significantly affected by the knockout with an interaction value of P=0.0050, this was most notable with a significant decrease in the top dose of thrombin (P=>0.0001).

Alongside assessing the MFI for JON/A and P-selectin signals, we also interrogated the percentage of positive JON/A and P-selectin in the platelet sample. Interestingly at top doses of thrombin, the percentage of JON/A positive platelets is higher in the knockout- (77.6%) than in wild-type samples (62%). This was mirrored by the amount of P-selectin positive cells, with knockout samples having 76% of positive cells and Wild-type 59%.

CD63 is a constituent of dense granules, similarly to P-selectin it is also expressed on the cell surface after the activation of platelets and resultant dense granule secretion. This also gives the ability to use CD63 as a marker of activation along with its more specific role of elucidating dense granule release. In basal samples there was no significant difference between the expression of CD63, when stimulated with thrombin, at low and medium doses the knockout platelets expressed less CD63, however, this was not a significant reduction. When platelets were subject to the highest dose of thrombin the expression of CD63 on knockout platelets was reduced, however not significantly.

LAMP1 is a constituent of the Lysosome membrane, and upon lysosome secretion, it translocates to the platelet membrane, allowing for the quantification of lysosomal secretion in platelets (Eskelinen, 2006). In basal conditions, the LAMP1 signals for both wild-type and knockout mice were homogeneous. When stimulated with thrombin both wild-type and knockout samples increased LAMP1 expression in a thrombin dose-dependent manner. Although knockout samples were consistently lower in MFI, there was no significant decrease in any dosage, it was also observed that the MFI of LAMP1 was low for all time points suggesting the expression always remains low.

The final marker we observed was PD-L1. PD-L1 is traditionally an immune checkpoint inhibitor but has also been linked with thrombotic events. We sought to assess whether PD-L1 expression in platelets could be affected by the knockout of α -synuclein. Interestingly, we saw a significant increase in PD-L1 with thrombin stimulation, this increase was not significantly affected by the knockout of α -synuclein at any dosage.

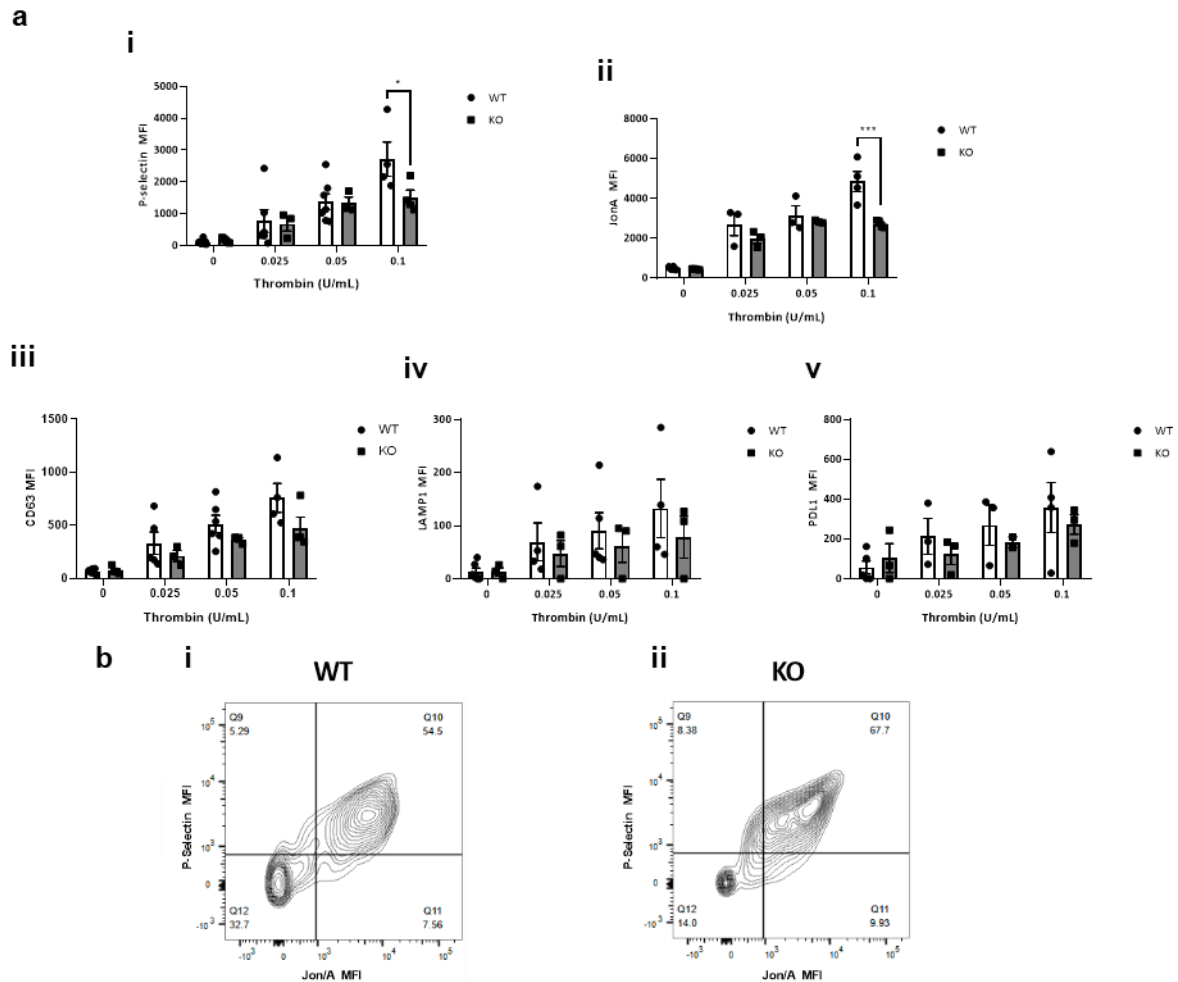


Figure 4-25. Whole population analysis of thrombin-stimulated platelets. Expression of surface markers was conducted on wild-type (white) and α -synuclein knockout (grey) platelets isolated through centrifugation and stained with the antibody cocktail for simultaneous detection per platelet. The Median fluorescent intensity (MFI) was utilised for 10,000 platelets per sample. Platelets were stimulated with indicated concentration of thrombin and expression of P-selectin (ai), JON/A (aii), CD63 (aiii), LAMP1 (aiv), and PD-L1 (av) was recorded. Data is presented as Mean \pm SEM. A quadrant gate was generated on unstimulated samples and added to contour plots for 0.1U/mL thrombin-stimulated platelets showing changes in the percentage of P-selectin positive events on the Y-axis and Jon/A positive events on the X-axis. wild-type (bi) and α -synuclein knockout (bii) Data presented as a contour plot of concatenated datasets N=6.

4.7.2.2. Assessing platelet activation in response to CRP-XL

Due to collagen having a fibrous structure, its use in flow cytometry is not appropriate. Therefore, CRP-XL was used as an analogue simulating platelet reaction to GPVI activation. Utilising the same antibody panel, we elucidated the effects of α -synuclein knockout on the secretion of platelets activated through GPVI signalling (Figure 4-26). The activation of platelets by CRP-XL was assessed through JON/A. The unstimulated samples were highly concordant between wild-type and knockout, which is identical to the thrombin samples. When platelet samples were stimulated with CRP-XL, the MFI

of JON/A increased, however, interestingly there was no significant increase of JON/A MFI between the highest and lowest dosages of CRP-XL. When comparing Wild-type and knockout samples, there was no significant difference between samples at any dosage.

We next assessed the effects of α -synuclein knockout on CRP-XL stimulation through P-selectin, CD63, and LAMP1. P-selectin significantly increased when stimulated with CRP-XL ($P=0.047$), however, there was no significant difference between the doses, and there were also no significant differences observed between the knockout and wild-type samples. CD63, Similarly to P-selectin was observed to have a significant increase when stimulated with CRP-XL ($P=0.049$), but no significant change between dosages; there is also no difference between the knockout and wild-type samples at any concentration. The final secretion marker LAMP1 again showed a significant increase when stimulated with CRP-XL $P=0.0024$, but there was still no significant difference between Knockout and wild-type at any dosage.

a

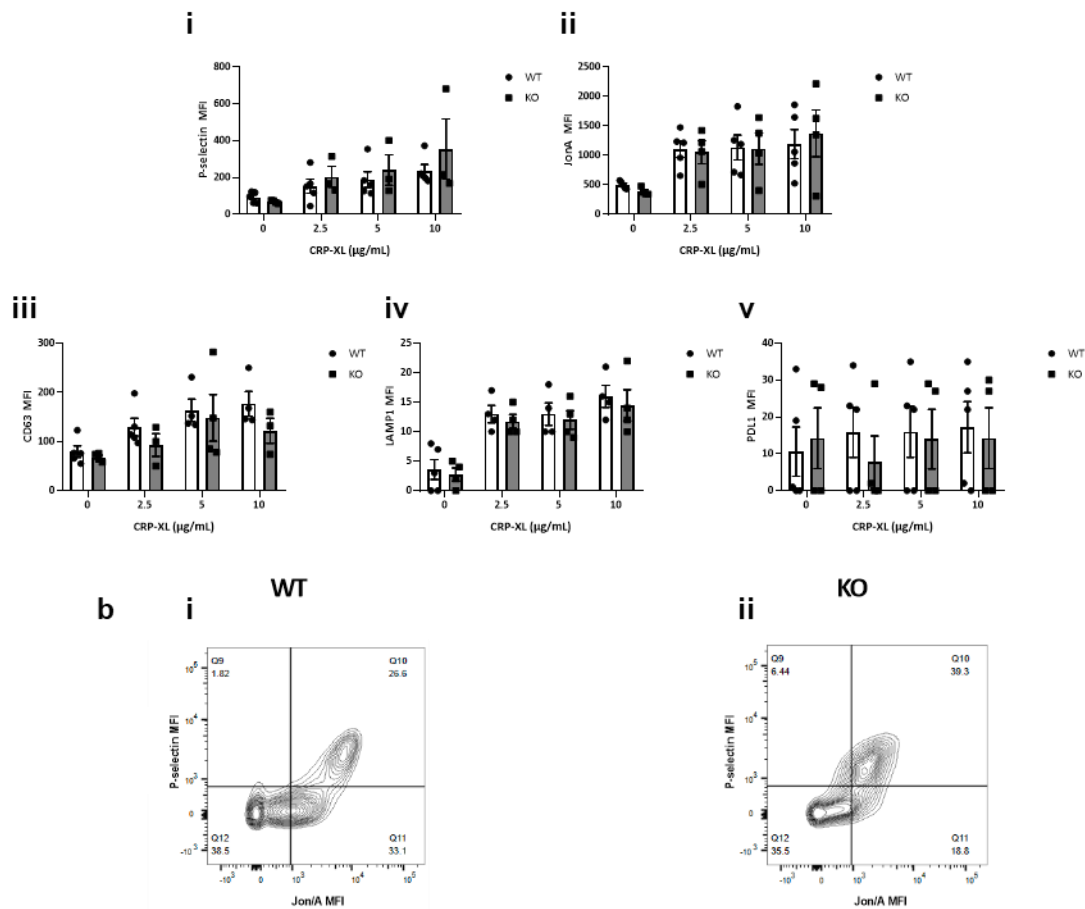


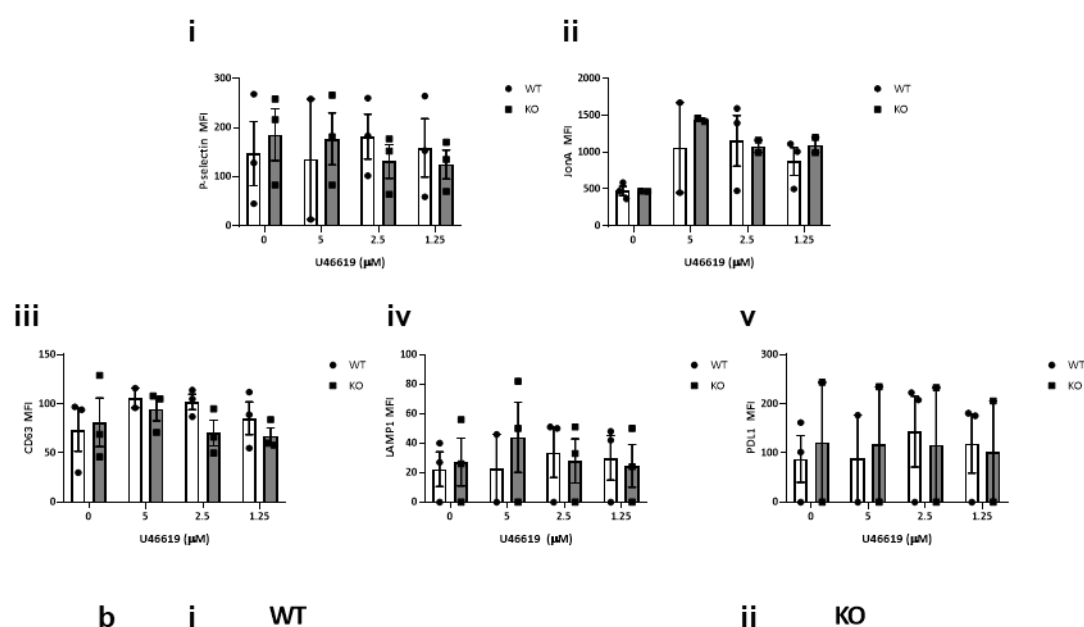
Figure 4-26. Whole population analysis of CRP-XL stimulated platelets. Expression of surface markers was conducted on wild-type (white) and α -synuclein knockout (Grey) platelets isolated through centrifugation and stained with the antibody cocktail for simultaneous detection per platelet. The Median fluorescent intensity (MFI) was used for 10,000 platelets per sample. Platelets were stimulated with indicated amounts of CRP-XL and expression of P-selectin (i), Jon/A (ii), CD63 (iii), LAMP1 (iv), and PD-L1 (v) was observed. Data is presented as Mean \pm SEM. A quadrant gate was generated on basal samples was added to contour plots for 10µg/mL CRP-XL-stimulated platelets showing changes in the percentage of P-selectin positive events on the Y-axis and Jon/A positive events on the x axis. wild-type (left) and α -synuclein knockout (right) Data presented as a contour plot of concatenated datasets.

When platelets were stimulated with CRP-XL it did not appear to have any effect on the surface expression of PD-L1, with the basal and stimulated samples showing an insignificant increase. This was recapitulated when comparing the wild-type and knockout samples at each dose, with no significant up or down-regulation of the PD-L1 marker. Cumulatively this data suggests that CRP-XL does activate platelets and initiate platelet granule release through a process that is independent of α -synuclein. They also suggest that PDL1 presentation on the platelet surface is independent of GPVI activation.

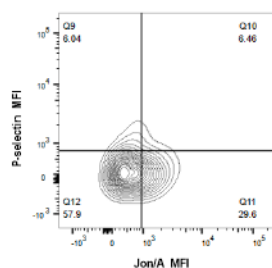
4.7.2.3. Assessing platelet activation in response to U46619

The next agonist we investigated was the thromboxane analogue U46619 (Figure 4-27). It binds to thromboxane receptor, and similarly to thrombin the downstream signalling is mediated by G proteins. Interestingly, when platelets were stimulated with 5 μ M U46619, there was no observed increase in any marker over basal samples suggesting that even at top dosage there was no activation of platelets, or secretion of any granule type. This was at odds with the aggregation data which showed a maximal aggregation at this dosage in wild-type platelets.

a



b i WT



ii KO

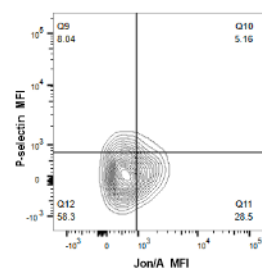
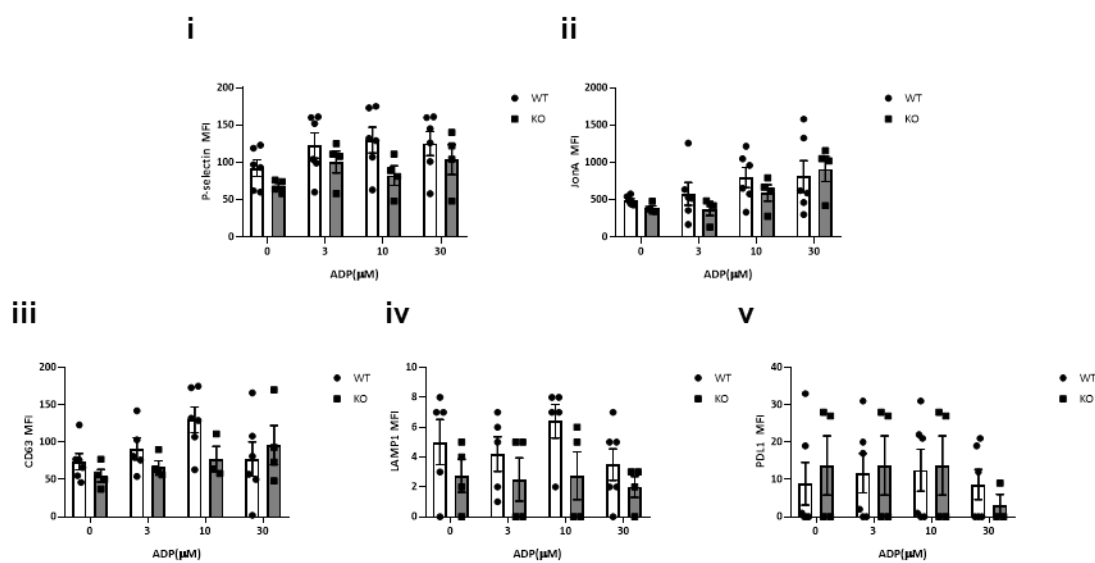


Figure 4-27 Whole population analysis of U46619 stimulated platelets. Expression of surface markers was conducted on wild-type (white) and α -synuclein knockout (Grey) platelets isolated through centrifugation and stained with the antibody cocktail for simultaneous detection per platelet. The Median fluorescent intensity (MFI) was utilised for 10,000 platelets per sample. Platelets were stimulated with indicated amounts of U46619 and expression of P-selectin (ai), Jon/A (a ii), CD63 (a iii), LAMP1 (a iv), and PD-L1 (a v) was observed. Data is presented as Mean \pm SEM. A quadrant gate was generated on basal samples was added to contour plots for 0.05 μ M U46619-stimulated platelets showing changes in the percentage of P-selectin positive events on the Y-axis and Jon/A positive events on the X-axis. wild-type (bi) and α -synuclein knockout (bii). Data is presented as a contour plot of concatenated datasets.

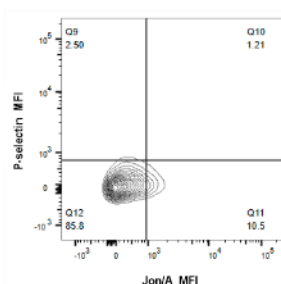
4.7.2.4. Elucidating the activation of platelets in response to ADP

The final agonist we tested was ADP (Figure 4-28). First, we assessed the activation marker JON/A, we saw a significant increase in JON/A signal when stimulated with ADP ($P= 0.017$), which increased with ADP dose, however, the increased doses did not yield a significantly higher signal. When comparing Wild-type and knockout samples there was no significant difference at any dosage.

a



b i WT



ii KO

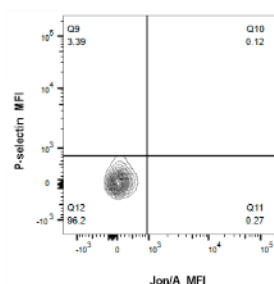


Figure 4-28. Whole population analysis of ADP stimulated platelets. Expression of surface markers was conducted on wild-type (white) and α -synuclein knockout (Grey) platelets isolated through centrifugation and stained with the antibody cocktail for simultaneous detection per platelet. The Median fluorescent intensity (MFI) was utilised for 10,000 platelets per sample. Platelets were stimulated with indicated amounts of ADP and expression of P-selectin (ai), Jon/A (aii), CD63 (aiii), LAMP1 (aiv), and PD-L1 (av) was observed. Data is presented as Mean \pm SEM. A quadrant gate was generated on basal samples was added to contour plots for 30 μ M ADP-stimulated platelets showing changes in the percentage of P-selectin positive events on the Y-axis and Jon/A positive events on the x-axis. wild-type (bi) and α -synuclein knockout (bii). Data is presented as a contour plot of concatenated datasets.

Next, we assessed the effects of ADP on platelet secretion markers in wild-type and knockout platelets. When interrogating P-selectin there was a slight increase observed upon stimulation, however, this was not significant. Also, while the knockout samples were consistently lower than wild-types, there was no significant difference, they yielded an insignificant increase from basal samples. CD63 secretion data showed that the dense granule release was not significantly upregulated in any ADP stimulated platelets, this also showed there was no significant difference between the knockout and wild-type samples. The final secretion marker LAMP1 showed there was no significant lysosome release from the platelets stimulated by ADP, with stimulated samples being insignificantly different from basal samples. While the knockout samples were slightly decreased there was no significant difference.

Stimulation with ADP did not induce the expression of PD-L1 on the platelet surface at any dosage assessed for either the wild-type or knockout samples. When taken together, in this study, ADP was able to activate platelets however it was not able to illicit a secretory response. There was also no significant difference between the knockout or wild-type samples as neither increased nor decreased.

4.7.3. Flow cytometry single-cell analysis of platelet activation

For all single cell analysis t-distributed stochastic neighbour embedding (t-SNE) was utilised. The application of t-SNE analysis allowed for the dimensionality reduction of data to a 2D map clustering similar groups within the dataset. The rationale for using t-SNE analysis was due to its robustness when challenged with outlying datapoints, and that it does not assume linear relationships between features, unlike some other clustering models. Many of the shortfalls of t-SNE analysis such as its speed, inability to manage missing data, and sensitivity to initialisation conditions were not an issue for this application. To begin the t-SNE analysis the conditions to assess must be selected (Figure 4-29).

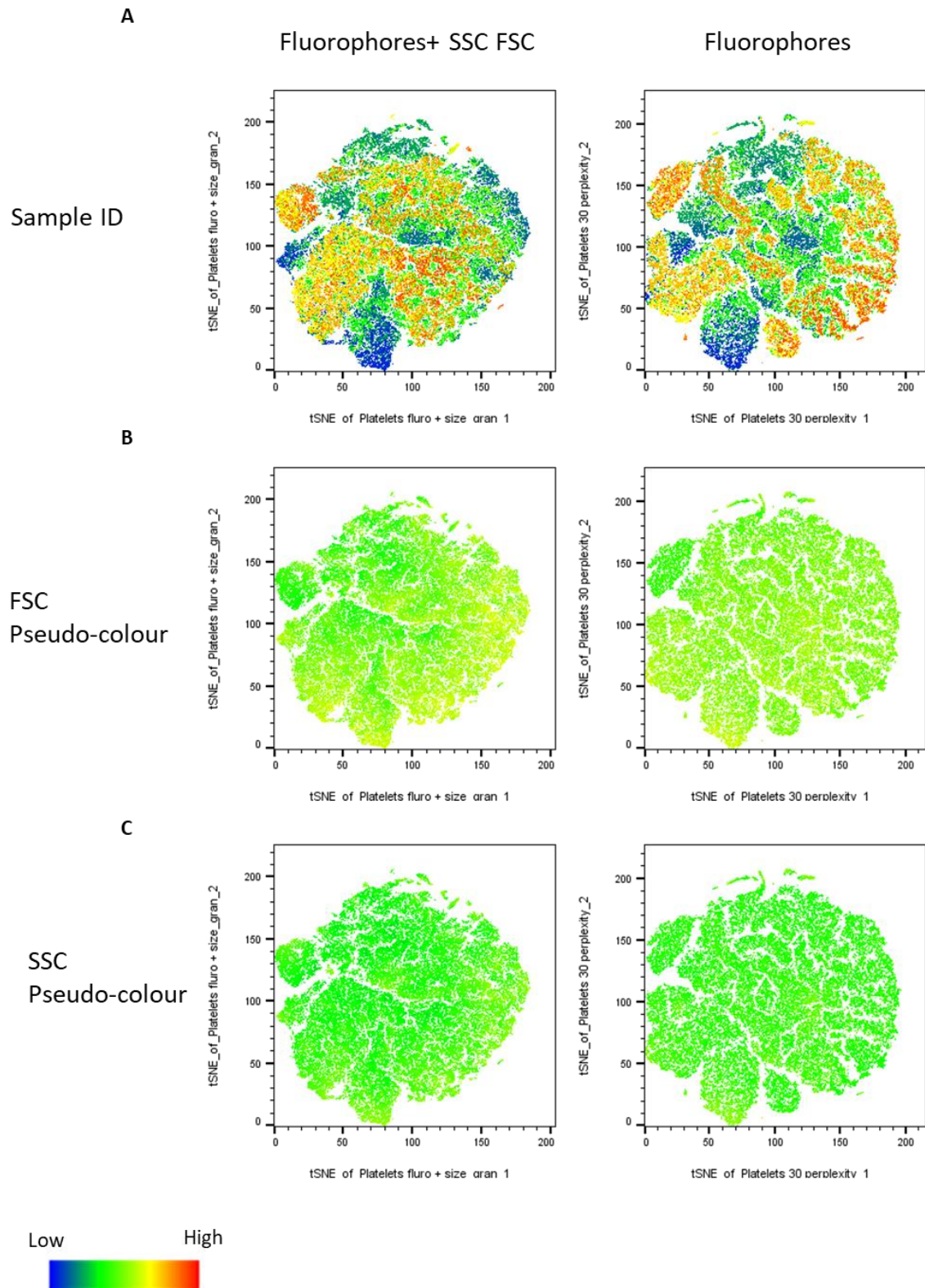


Figure 4-29. *t*-SNE analysis condition selection. Wild-type mouse platelets stimulated with 0.1U thrombin were incubated with an antibody cocktail containing FITC-P-selectin, PE-Jon/A, PE-cy7 CD63, Alexaflour700 LAMP1, and APC PD-L1. Data from 5 samples were then concatenated and *t*-SNE analysis was conducted. Analysis of the fluorophores: FITC, PE, APC, A700, and PE-Cy7 including FSC and SSC was conducted with 30 perplexity and 7% learning rate (left column). Where analysis of the Fluorophores alone was conducted with identical perplexity and learning rates (Right column). The *t*-SNE maps were then pseudo coloured for Sample ID (top) Forward scatter (middle) and side scatter (bottom).

We compared the t-SNE of fluorophores alone and fluorophores accompanied by the SSC and FSC data (Figure 4-29). The distribution of the separate samples was then delineated by the sample IDs, interestingly this results in a more homogeneous distribution of samples on the t-SNE map. To assess whether the inclusion of FSC and SSC influenced the distribution of samples we pseudo-coloured the map. The map generated including SSC and FSC showed a population separated from the main area which had a lower forward scatter, with the rest of the map having the general trend of smaller on the left and larger on the bottom right. This trend did however have patches of larger cells spread throughout the map. Interestingly, the map that was generated without taking FSC and SSC into account also had this singular small population separated from the main mass, there was also a gradient of small to large platelet samples as seen with the analysis including the FSC and SSC.

Next, we assessed the effects of the condition selected on the SSC data. With the t-SNE map pseudo-coloured to show SSC samples, it shows that there is very little change in the SSC across the entire platelet population observed. There was a slightly elevated SSC towards the right-hand side of the t-SNE map, there were also some darker regions scattered throughout the map, but no populations that were separated spatially. In the fluorophore-only map, the same pattern is observed, with a small lighter area at the bottom of the map showing the higher SSC, with the darker low SSC patches dotted throughout the map.

Taken together the inclusion of FSC and SSC does not have a significant effect on the separation of samples, even when not included in the t-SNE criteria a similar pattern emerges, this was expected due to the different scale in which FSC and SSC are measured in. Therefore, we chose to include the FSC and SSC on all t-SNE map generation going forward.

The perplexity is key for the optimal separation of the dataset, it sets the number of nearest neighbours each datapoint is compared to (Figure 4-30). Previous literature states that a perplexity between 2 and 50 is recommended, we started with a perplexity value of 2, this perplexity value resulted in a t-SNE map that was almost completely heterogeneous, showing that the perplexity score was too low (Van der Maaten and Hinton, 2008). When the perplexity is set to 30 neighbours, the t-SNE map spread apart, resulting in the clustering of multiple distinct populations within the t-SNE map

that was previously not visible. We then increased the perplexity to 50, although we saw a lot of similar populations to the perplexity 30 setting some populations that were previously visible such as the top left population had begun to merge back into the main mass. Other populations that stayed separate began to form much tighter clusters which were hard to visualise. The tight clustering and remerging of populations was a result of the perplexity being too high reducing the ability of the algorithm to differentiate the populations.

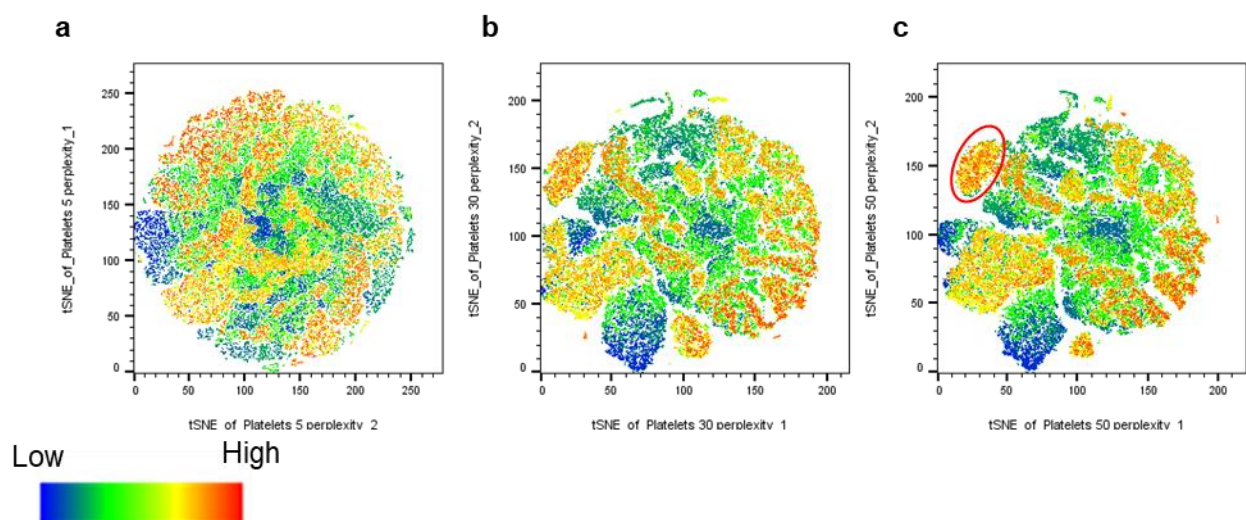


Figure 4-30. t-SNE analysis optimisation, - perplexity tuning. Wild-type mouse platelets stimulated with 0.1U thrombin were incubated with an antibody cocktail containing FITC-p-selectin, PE-Jon/A, PE-cy7 CD63, Alexafluor700 LAMP1, and APC PD-L1 and analysed by flow cytometry. Data from 5 samples were then concatenated and t-SNE analysis conducted. The perplexity of the t-SNE analysis was tested to assess its effects, starting with a perplexity of 5 (a) a medium perplexity of 30 (b) and the highest recommended perplexity of 50 (c). Data is presented as a False coloured t-SNE map consisting of 5 datasets concatenated.

The final optimisation of the t-SNE algorithm is tuning the learning rate (Figure 4-31). This controls the weights of the algorithm with each iteration, allowing for the minimum probability difference to be attained and separate out the populations. First, we tried a learning rate of 3% this resulted in a rounded map with a small amount of spatially separated groups, however within the main bulk of the map there is no separation. The learning rate was then set to 7% of the total of the cells present, this resulted in a t-SNE map that has multiple distinct populations spread throughout the map with subpopulations separated spatially there was also populations within the main bulk of the map with slight spatial separation from the rest of the mass it also resulted in a

less rounded map. Finally, the learning rate was set to 10% of the total amount of datapoints this resulted in a much more rounded map similar to the low learning rate. Comparatively to the 7% graph, the 10% graphs did better cluster some outlying populations, however the separation observed in the more central regions is less defined resulting in difficulty in delineating different populations. Therefore, we chose a 7% learning rate for all experimentation going forward as it produced a map with the greatest spatial distribution of datapoints.

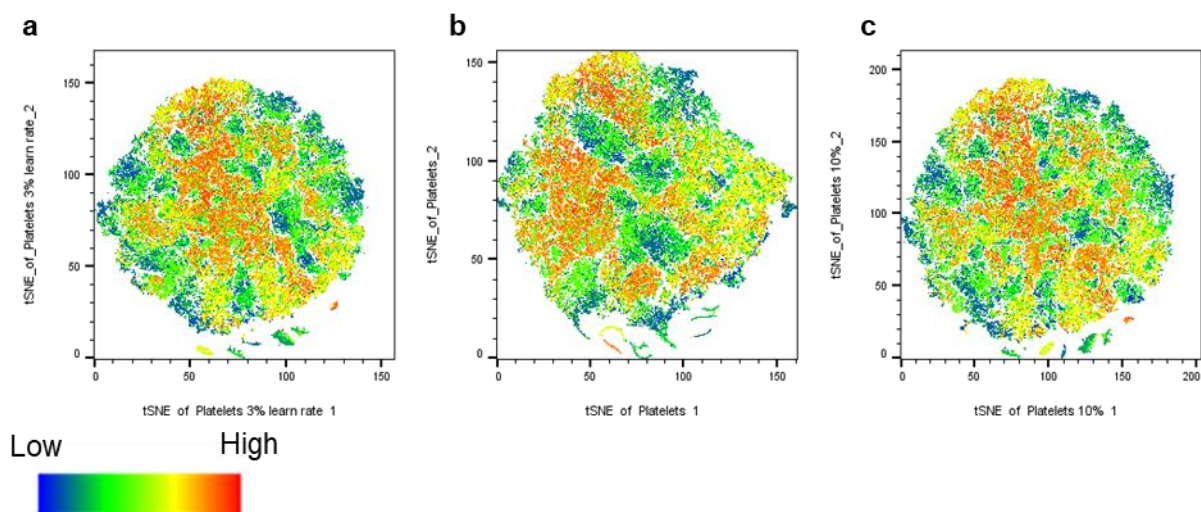


Figure 4-31. t-SNE analysis optimisation - learning rate optimisation. Wild-type mouse platelets stimulated with 0.1U thrombin were incubated with an antibody cocktail containing FITC-p-selectin, PE-Jon/A, PE-cy7 CD63, Alexafluor700 LAMP1, and APC PD-L1 and analysed by flow cytometry. Data from 5 samples were then concatenated and t-SNE analysis conducted the Learning rate of the t-SNE analysis was tested to assess its effects, starting with a rate of 3% (a) a medium perplexity of 7% (b) and the highest recommended perplexity of 10% (c). Data is presented as a False coloured t-SNE map consisting of 5 datasets concatenated.

4.7.4. Classification of activated platelets for t-SNE analysis

Initially, we applied a traditional gate to the dataset delineating P-selectin positive platelet populations and JON/A positive populations. We then overlaid these gates on to the whole population t-SNE maps (Figure 4-32). Using a standard gating strategy, it was observed that 78.2% of the platelet population was positive, this was overlaid to the t-SNE map and false coloured. The P-selectin positive population (blue) consisted of the majority of the t-SNE map, spanning over multiple groups, negative (orange) population included a spatially separated group at the top, however there was an observed spillover to the main mass of the map which was close to P-selectin positive cells.

When this process was repeated utilising the JON/A marker for platelet activation, there was 84.7% positivity, slightly higher than P-selectin. Similarly, to P-selectin, the Jon/A positive (blue) cells consisted of the majority of the map covering 3 main groups. Unlike P-selectin the Jon/A negative populations are spatially separated from the positive cells. Both P-selectin and Jon/A positive groups were observed to be the same groups of cells, however, the Jon/A positive cells also included a population at the top of the main cluster which the P-selectin positive group did not. Taken together we chose to use Jon/A positive gated platelets as they yielded a gating that was more highly congruent with the t-SNE map than the P-selectin gated populations and specifically targets platelet activation markers. Additionally to this, studies by (Acquasaliente et al., 2022) have associated exogenous α -synuclein from other cells to suppress P-selectin expression on platelets, which further reinforced our decision.

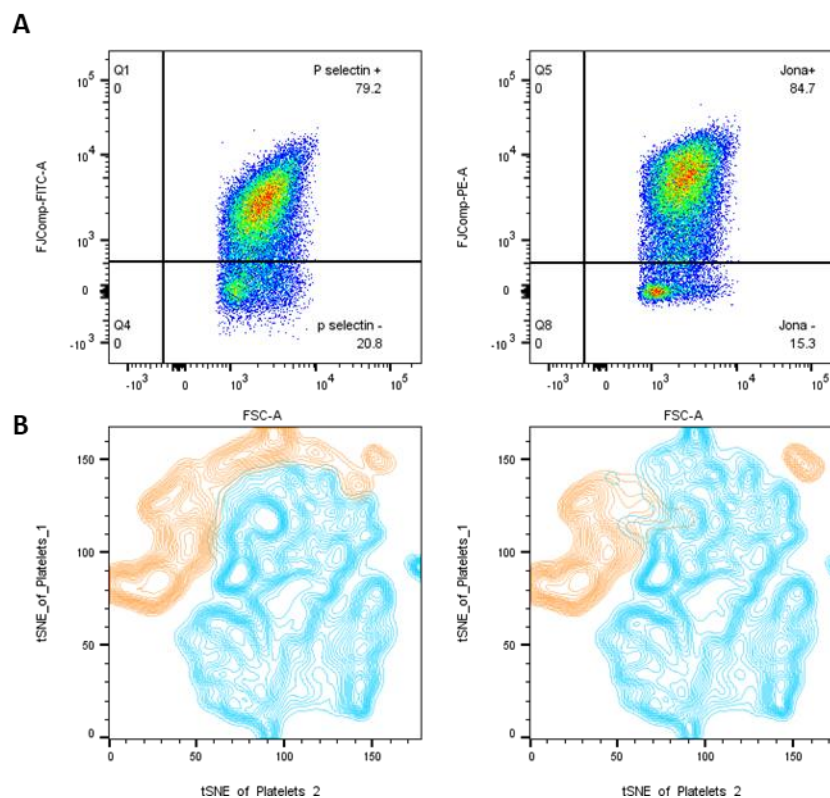


Figure 4-32. Gating strategy for activated platelets plotted on a tSNE map. Gating strategy for activated platelets plotted on a tSNE map. Quadrant gates were created on basal maps and placed on the concatenated heatmap data for platelets stimulated with 0.05U thrombin highlighting P-selectin (left) and Jon/A (right). After running t-SNE analysis the P-selectin positive (blue) and negative gates (orange) were then applied to t-SNE maps (left). The Jon/A positive (blue) and negative (orange) gates were also overlaid on the same t-SNE map.

4.7.5. Flow cytometric single-cell analysis of platelet activation and secretion markers

Following whole population analysis of the platelet activation and secretion markers, we applied multidimensional analysis to our five-colour assay, in the form of Flt-SNE. The application of this Flt-SNE allowed for the mapping of multidimensional data in 2D space, it also separates clusters of cells that have unique receptor expression profiles. The analysis was conducted on data concatenated from all previous whole population data with a minimum of 30,000 platelet events present in each sample from multiple biological repeats. The t-SNE maps were then pseudo coloured for each marker, elucidating the expression of each within the separate populations. The blue areas represent platelets with a low expression, shades of green are middling expression and the yellow to red spectrum shows a high expression.

We started by interrogating Wild-type and knockout basal samples, first, we manually gated JON/A + (blue) and JON/A- (orange) cell populations and overlaid this on the t-SNE map (Figure 4-33). Interestingly, although no agonist was added to the sample 19.95% of platelets expressed enough JON/A binding to be considered active, however, this may be due to trauma caused through direct cardiac puncture. There was one main cluster containing 98% of all events, however, there were also two smaller groups containing 1.24% and 0.69% of events. We observed the clustering of these samples on these maps, although this did not create a spatially separated cluster. We then pseudo-coloured the t-SNE map for the different fluorophores, the P-selectin map shows small clusters of P-selectin-expressing cells spread throughout the map with no specific grouping, interestingly this was not specifically localised to the region of the map associated with activated platelets. The expression of P-selectin was largely homogeneous throughout the entire map and within the three specific spatially distanced groups. Using the same method, we visualised JON/A expression, we observed a gradient of increasing expression from left to right in the major grouping, with the furthest right section being classed as the activated platelets. In groups -2 and -3 there were no changes up or down-regulation of JON/A.

Following this we observed CD63, in group 1 the lowest expression was clustered to the top right, with the more highly expressing events being clustered towards the peripheries at the bottom, left and right. Interestingly these were not solely associated with the higher expression JON/A samples. Alongside this, in Group 2 there are

samples which highly express CD63, and in Group 3 all data points show a high expression. This shows that in basal conditions there is a constituent CD63 expression on the cells with a small subpopulation which are highly CD63 expressing irrelevant of platelet activation. The final secretion marker we observed was LAMP1, which shows that there is very little LAMP1 expression in any platelet at basal samples, Interestingly groups 2 and 3 also exhibited a high expression of LAMP-1 independent of platelet activation. It was also observed that PD-L1 had a highly analogous expression to CD63 in groups 2 and 3, interestingly in group 1 the PD-L1 expression is generally opposite of CD63.

Unstimulated knockout platelets were also interrogated in the same way as wild-type. Knockout platelets also were observed to have a population of activated platelets (blue) 8.64%. There were 4 major clusters separated on the t-SNE map. Group 1 is a small group of 6.8% of the parent comprised of highly expressing JON/A platelets, interestingly upon applying pseudo colour overlays for each fluorophore it was observed that there is only a small subpopulation of platelets within this group that is also highly expressing of p-selectin. Within group 1 there is a middling expression of CD63, PD-L1 and LAMP1 in comparison to the rest of the platelet population. Although there was an observed differential expression of P-selectin within this group, there was no spatial separation and therefore were classed as a single group.

Group 2 was the largest subset of data being 78.8% of the total population, within this population there was a small subpopulation there was platelets with very low JON/A expression with a gradient to activated platelets. Interestingly as with the wild-type the high JON/A expression was not mutually exclusive to high P-selectin expression, with a small region of highly p-selectin expressing events also having a low JON/A expression. LAMP 1 was largely uniform across the entire population, especially through groups 1,2 and 3. CD63 on the other hand had a more varied expression, however its expression did not seem to be significantly affected by any other markers. When interrogating PD-L1 it was also observed that there is a generally low overall expression within group 2, with a small region of more highly expressing platelets, however, these were not co-localised to any other marker, suggesting that PD-L1 expression from these cells was not dependent on secretion events or platelet activation.

A third group of platelets was distally separated from the main mass of the t-SNE map, the P-selectin, JON/A CD63 and LAMP1 expressions are similar to that within group 2, however, the PD-L1 expression is reduced. This shows that in the knockout platelets, there is a significant population of 12.2% of events that have a significantly decreased PD-L1 expression in comparison to the main population. The final population we observed was like in the wild-type, a small group of 1.58% of the total count which was averagely expressing P-selectin and JON/A but had a high expression of PD-L1 CD63 and LAMP1.

Taken together this shows that although there has been no additional stimulation the process of blood collection, platelet separation and staining has resulted in a small subpopulation of activated platelets which was not reduced by the knockout of α -synuclein. Both knockout and wild-type samples had small populations of highly co-expressing CD63, LAMP1 and PD-L1 clusters, which did not express significantly increase P-selectin or JON/A. Interestingly, the knockout samples displayed a smaller percentage of activated platelets and a separate PD-L1-expressing population which was not present in the wild-type samples.

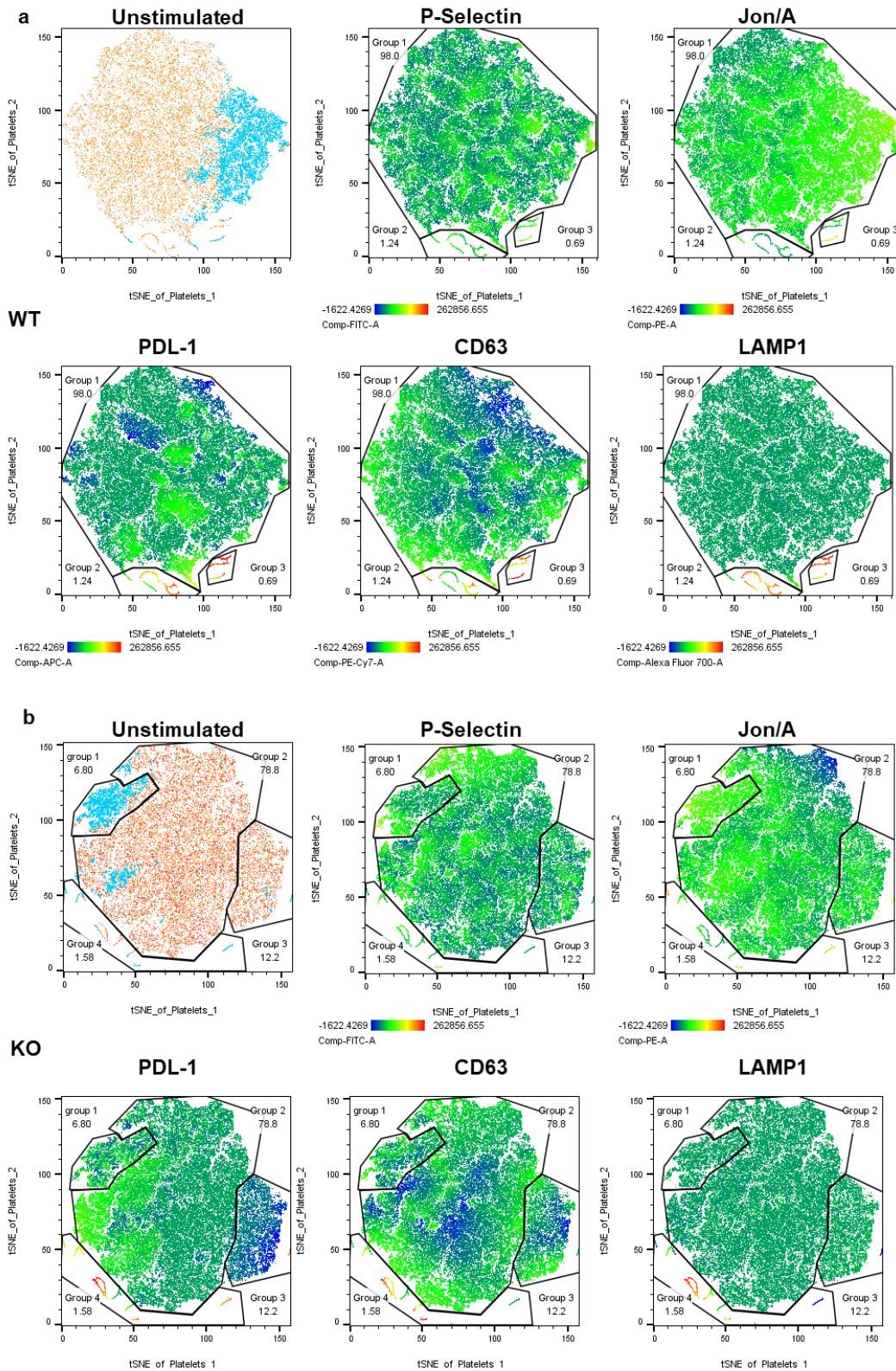


Figure 4-33. *t*-SNE analysis of platelets with no agonist stimulation. Wild-type (A) or α -synuclein knockout (b) mouse platelets with no stimulation were incubated with an antibody cocktail containing FITC-p-selectin, PE-Jon/A, PE-cy7 CD63, Alexafluor700 LAMP1, and APC PD-L1 and analysed by flow cytometry. The data was then concatenated before *t*-SNE analysis, a learning rate of 7% of the total population, a perplexity of 30 was used, and the algorithm was instructed to only take FITC- PE, PE-Cy7, A700 and APC into account when generating the maps. To visualise activated and basal platelets, Jon/a + and – gates from whole population analysis were applied to *t*-SNE maps, basal (orange) and activated (blue) (Ai, Bi). Spatially separated groups were then manually gated.

Following whole population analysis on platelets stimulated with 0.1U/mL thrombin, we concatenated all datasets and subjected them to tSNE analysis (Figure 4-34). This population was first scrutinised for JON/A positivity, these gates were then overlaid onto the t-SNE plots (basal – orange, Activated-blue) the activated platelet group was then investigated further. Interestingly the α -synuclein knockout population had a larger proportion of platelets which presented as JON/A positive (WT=62.06%, KO=77.63).

Stimulated wild-type platelets run through t-SNE analysis resulted in 6 spatially separated groups, this is in contrast to the knockout samples which only separated into 3 groups. Wild-type groups 1 and 2 were the most numerous totalling 48.2% of the overall platelet population, these exhibited very similar expressions for CD63, P-selectin and PD-L1, their main differential feature was that group one had a slightly higher JON/A expression and a lower LAMP1 expression. Group 3 had a high JON/A and P-selectin expression but had lower expression levels of PD-L1, CD63 and LAMP1; this expression pattern only accounted for 2.1% of all platelets but was not observed in the knockout populations. The wild-type Group 4 had similar expression patterns to that of Group 3, however, it lacked a high P-selectin expression, this was only a small population of 2.97% of platelet, but again was not present in the Knockout population. Group 5 consists of 6.3% of the total platelet population, interestingly, it has a similar expression of Jon/A and P-selectin to Group 1 but is on the opposite side of the t-SNE map. Where Group 5 differs from Group 1 is the increased LAMP1, with all other expression levels being similar this group is also not observed in the α -synuclein knockout populations.

The sixth group observed on the wild-type platelets represented 1.05% of the total platelet population, it was shown to be a low expressor of P-selectin and JON/A, while it has a significant expression of PD-L1, CD63 and LAMP1. This population was also observed in the Knockout population however it was less numerous only consisting of 0.62% of the total platelet population.

When taken together there are clear groups in the wild-type population that express LAMP1, CD63, and p-selectin expression markers which are not present in the Knockout population which total 5.11% of the total platelet population. Overall, fewer

populations that exhibit significantly increased secretion markers in the Knockout population than in the wild-type. These small highly expressing populations may result in the increased secretion marker expression observed in the whole population analysis even with the knockout samples having a higher amount of JON/A positive cells.

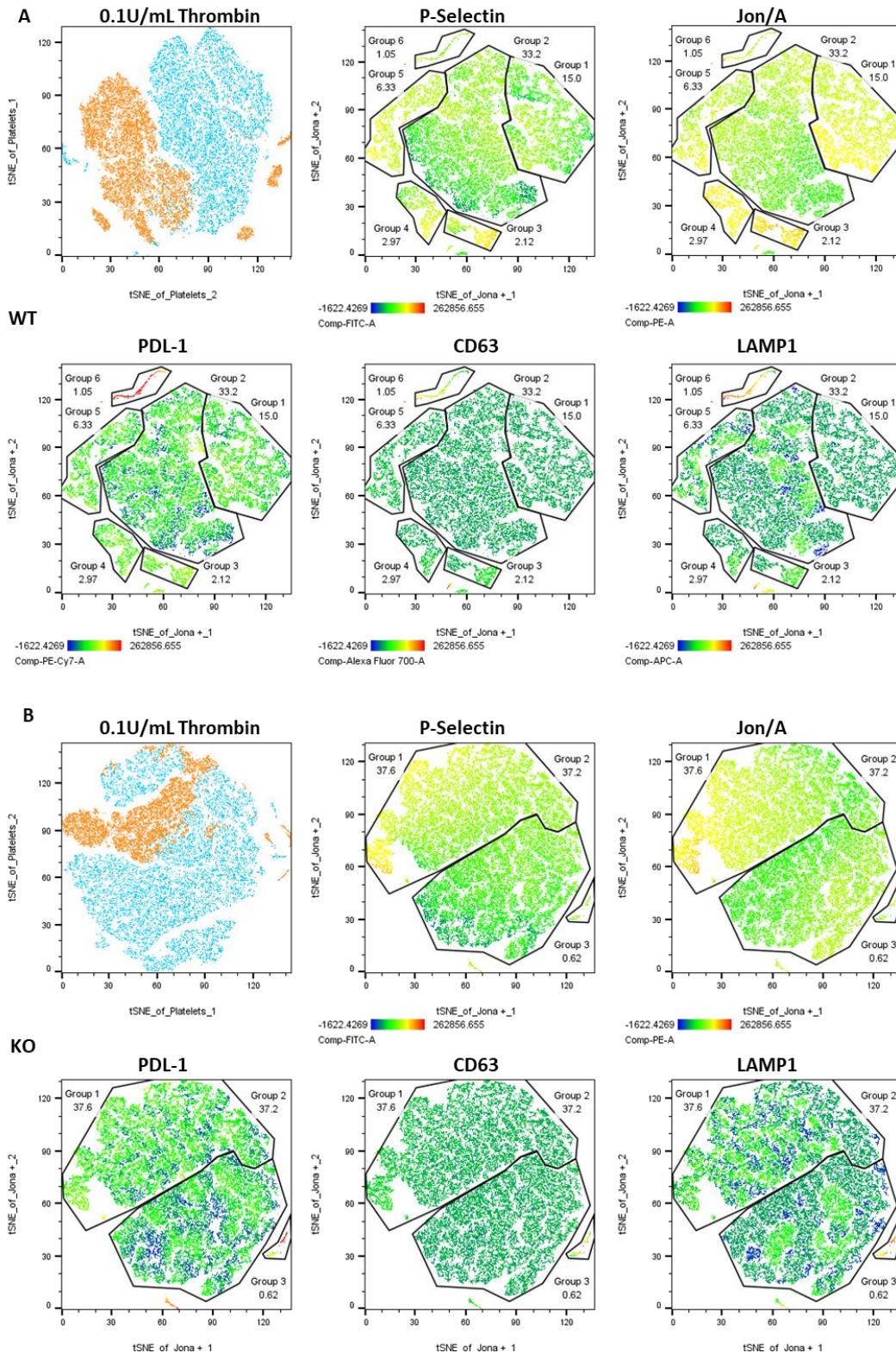


Figure 4-34. *t*-SNE analysis of thrombin stimulated platelets comparing Wild-type and knockout platelets. Wild-type (a) or α -synuclein knockout (b) mouse platelets stimulated with 0.1U thrombin were incubated with an antibody cocktail containing FITC-p-selectin, PE-Jon/A, PE-cy7 CD63, Alexafluor700 LAMP1, and APC PD-L1 and analysed by flow cytometry. The data for was then concatenated before *t*-SNE analysis, a learning rate of 7% of the total population, a perplexity of 30 was used, the algorithm was instructed to only take FITC- PE, PE-Cy7, A700, and APC into account when generating the maps. To establish activated populations on the *t*-SNE plot, a manual gate was used as a pseudo colour Basal (orange) and activated (blue). Activated platelets were gated out of the total population and subject to identical *t*-SNE mapping, The activated platelet maps (aii-vi, bii-bvi) had spatially separated groups that were then manually gated.

Following this we also interrogated the effects of CRP-XL on platelet activation (*Figure 4-35*). The whole platelet population results indicated that there is no significant difference between the knockout and wild-type platelet secretion markers. There was also no difference in the number of Activated platelets between the two populations as measured with JON/A being 59.7% in the wild-type and 58.1% in the knockout.

Following this, we assessed the differential effects of stimulating α -synuclein knockout and wild-type platelets with 10 μ g/mL CRP-XL. *Figure 4-35*. Interestingly, although there was not a significant increase in the whole population analysis, the activated wild-type platelets separated into 3 populations. Group 3 in the middle being the most numerous totalling 39% of the total platelet population. This main group had an average expression of JON/A, CD63 and LAMP1, interestingly there seemed to be a varied expression of P-selectin, towards the top left of the population. Additionally, the PD-L1 expression was highly variable in this population with a loose association with the expression of P-selectin. This expression pattern in group 3 of the wild-type population is highly analogous to that of group 2 in the knockout population, which also consisted mostly of the positive cells, totalling 44.5% of the overall platelet population.

The next two groups in the wild-type samples are smaller in comparison to this main population being 8.21% and 9.73% for groups 1 and 2 respectively. Group 1 had a much higher expression of JON/A in comparison to the other groups, alongside a slightly higher expression of PD-L1. Group 2 had an increased JON/A and P-selectin expression over Group 3, but less than Group 1. The smaller group in the Knockout platelet population (group1) accounts for 10.3% of the overall platelet population has a similar presentation to Group 2 of the wild-type population, with a slightly increased JON/A and P-selectin expression over the main population.

Interestingly in neither the wild-type or knockout populations was there a specific, highly expressing population for CD63 or LAMP1 secretion markers as seen in the thrombin-stimulated populations. Additionally, to this, the expression of CD63 and LAMP1 remained unchanged. This is corroborated by the whole population data; however, this data does not agree with other literature stating that stimulation with CRP-XL should induce dense granule secretion (Babur et al., 2020).

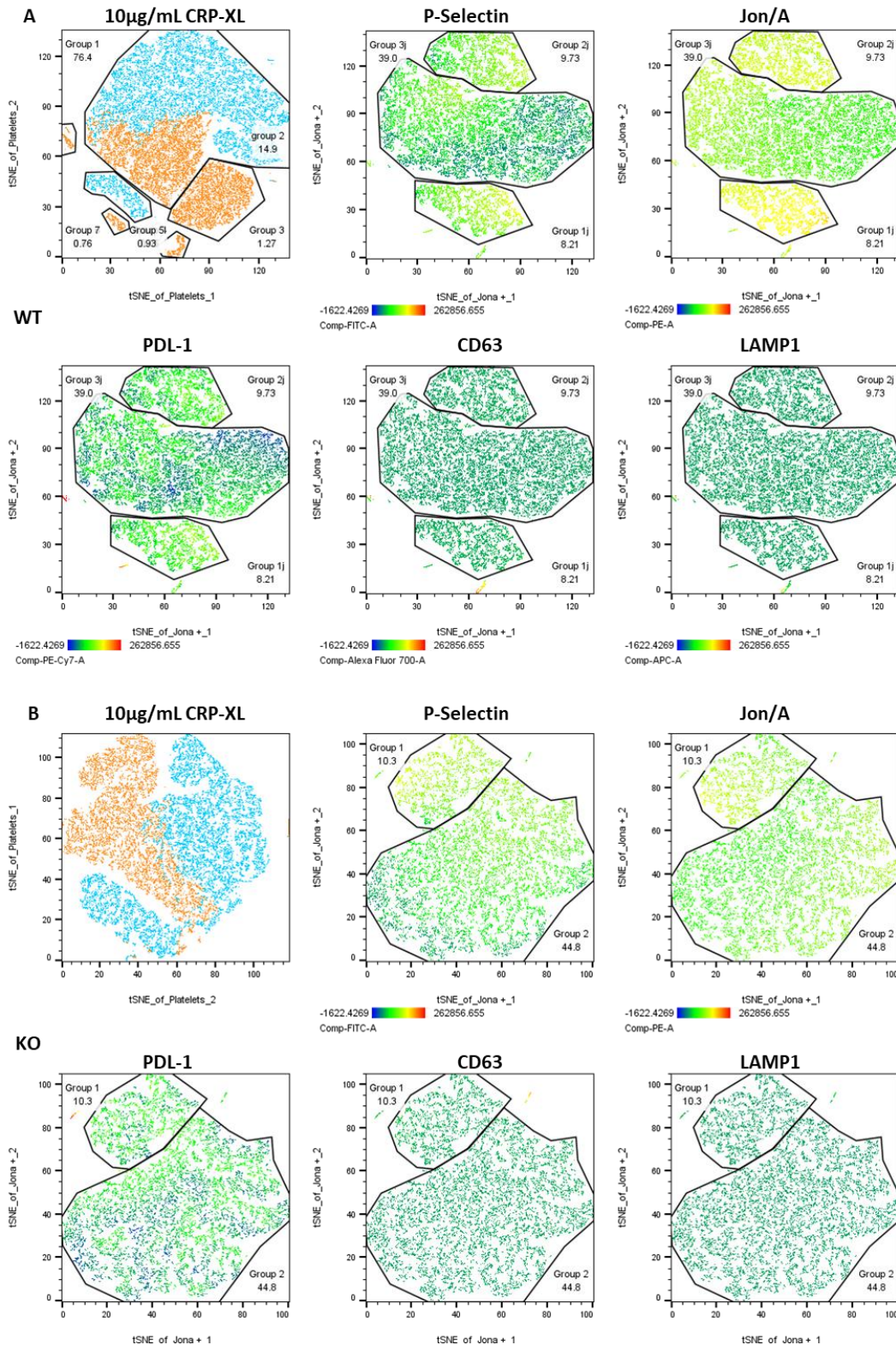


Figure 4-35. *t*-SNE analysis of CRP-XL stimulation comparing Wild-type and knockout platelets. Wild-type (a) or α -synuclein knockout (b) mouse platelets stimulated with 10 μ g/mL CRP-XL were incubated with an antibody cocktail containing FITC-p-selectin, PE-Jon/A, PE-cy7 CD63, Alexafluor700 LAMP1, and APC PD-L1 and analysed by flow cytometry. The data for was then concatenated before *t*-SNE analysis, a learning rate of 7% of the total population, a perplexity of 30 was used, the algorithm was instructed to only take FITC- PE, PE-Cy7, A700, and APC into account when generating the maps. To establish activated populations on the *t*-SNE plot, a manual gate was used as a pseudo colour Basal (orange) and activated (blue). Activated platelets were gated out of the total population and subject to identical *t*-SNE mapping. The activated platelet maps (aii-vi, bii-bvi) had spatially separated groups that were then manually gated.

Next was the assessment of wild-type and α -synuclein knockout platelets in reaction to stimulation with 0.05 μ M U46619 (Figure 4-36). The Wild-type and knockout samples had a similar percentage of activated platelets, 36.06 and 33.6% respectively. There were three distinct clusters of platelets observed in both the activated wild-type and knockout samples.

Group 2 was the most numerous totalling 30.9% of the total platelet population, interestingly this group exhibited a wide range of expression of P-selectin, PD-L1 and LAMP1, with JON/A and CD63 remaining consistent. There was a small island in the middle of the group which may be considered to be spatially separated, which exhibited a slightly higher amount of Jon/A expression, also PD-L1 and LAMP1 in comparison to the surrounding cells. The PD-L1 expression in this group was on a gradient from low on the left to higher on the right, with the slightly increased expressing group in the middle. CD63 remained consistent throughout the group, and LAMP1 was distributed on a gradient from highly expressed at the top of the map to low expressing at the bottom. When compared to p-selectin the distribution of expression was much more sporadic than all other markers observed, with patches of high and low expression neighbouring each other. This expression pattern is identical to that in the Knockout samples; however, the knockout sample does not have the group in the middle of slightly higher expressing cells. Similarly, it is also the biggest group in the knockout samples comprising of 27.8% of the total platelet population.

The next most abundant group in the wild-type sample is group 1, which consists of 1.77% of the total platelet population, this population had a median p-selectin expression, an above average JON/A expression, where the population started to differ from Group 2 is the high expression of PD-L1, CD63 and LAMP1. This group was highly analogous to Group 1 in the knockout platelet group, which exhibited the same expression profile, however it was only 1.03% of the total platelet population.

The final spatially separated population was group 3, this group was the smallest consisting of just 0.45% of the total platelet population, interestingly this group did not visually have a differential population from the main body of the map in group 2. It exhibited a middling expression of all markers, this group was also observed in the knockout platelet population, which contained 1.64% of the total platelet population.

These data indicate that there is a small subset of platelets that express LAMP1 and PD-L1, that is present in both wild-type and knockout platelets. It also shows that there are no differential subpopulations present in the wild-type that are not present in the knockout samples. These data are concordant with our whole population data and show an insignificant difference between populations.

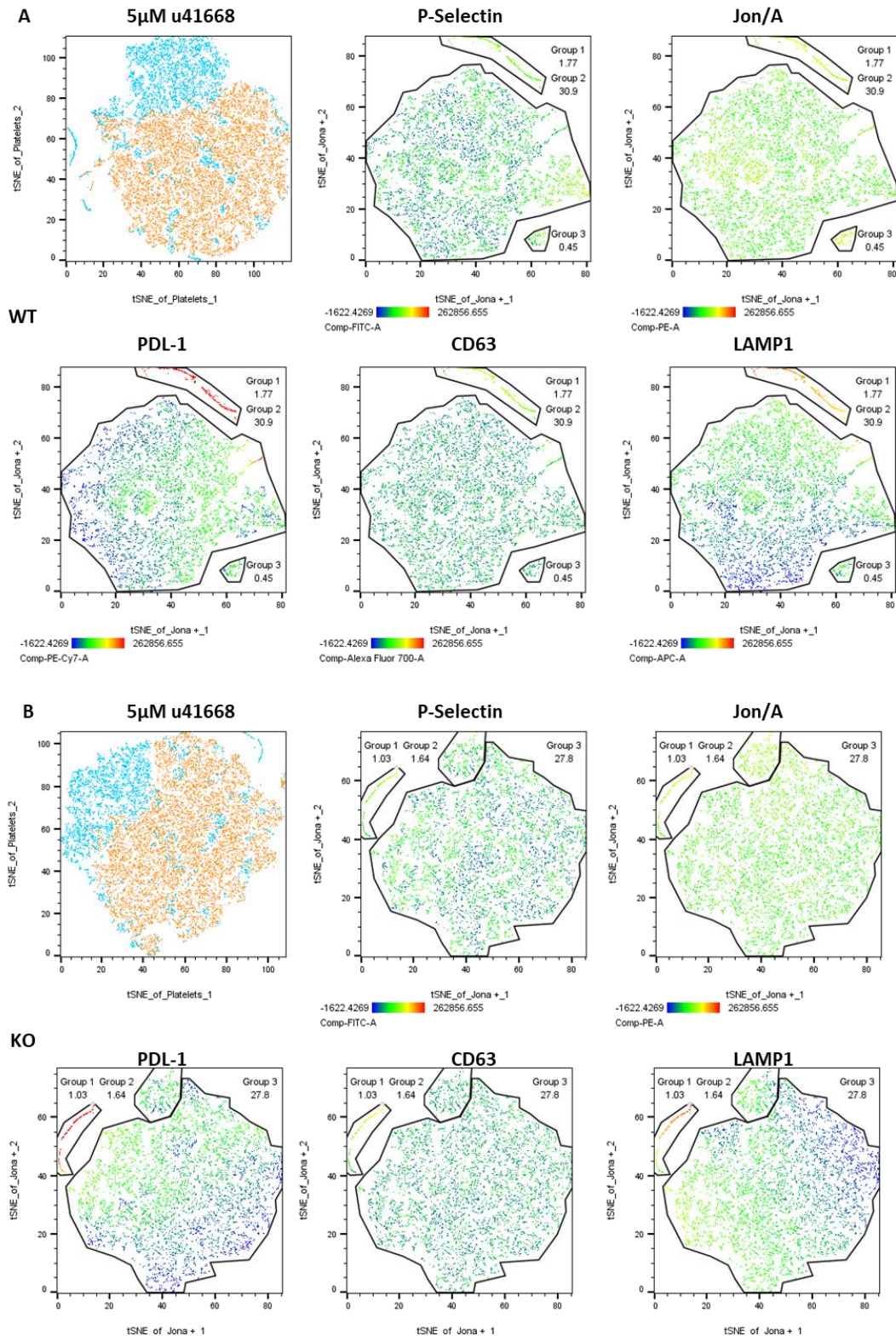


Figure 4-36. *t*-SNE analysis of U46619 stimulation comparing Wild-type and knockout platelets. Wild-type (a) or α -synuclein knockout (b) mouse platelets stimulated with 5 μ M U46619U46619U46619 were incubated with an antibody cocktail containing FITC-p-selectin, PE-Jon/A, PE-cy7 CD63, Alexaflour700 LAMP1, and APC PD-L1 and analysed by flow cytometry. The data was then concatenated before *t*-SNE analysis, a learning rate of 7% of the total population, a perplexity of 30 was used, and the algorithm was instructed to only take FITC- PE, PE-Cy7, A700, and APC into account when generating the maps. To establish activated populations on the *t*-SNE plot, a manual gate was used as a pseudocolour Basal (orange) and activated (blue). Activated platelets were gated out of the total population and subject to identical *t*-SNE mapping. The activated platelet maps were spatially separated groups that were then manually gated.

4.7.6. Single cell flow cytometric analysis of Thrombin stimulated platelets

The use of t-SNE for dimensionality reduction and cluster identification is a powerful tool, however, we noticed in the basal single-cell analysis that within these clusters there was a high heterogeneity within the groups for multiple markers. Observing this we sought to interrogate the dataset further using FlowSom to delineate clusters and visualise these on the t-SNE map.

When analysing the thrombin-simulated platelets with FlowSOM we were able to delineate further populations within the t-SNE map. There were eight separate populations observed in both the wild-type and knockout populations which we then overlaid onto the preexisting t-SNE map (Figure 4-37). Interestingly, as before some subpopulations within the t-SNE clusters spanned between multiple different t-SNE populations. Most of the populations that FlowSOM detected were confined to a single t-SNE population but were scattered throughout the group, similar to what we observed in manual gating.

In the wild-type group when we assessed the amount of platelets present in each population, we saw that the majority of the platelets (77.7%) were in population 0, with no other population making up more than 10%, and populations 2,-4 and -5 comprising of less than 0.5% of the activated platelet population (Figure 4-37). In the knockout group, we saw a much more varied spread between the groups, again population 0 being the most numerous with 38.1% of the activated platelet population. Interestingly similarly to the wild-type analysis, there were three populations with less than 0.5% of the platelet population in each being population-2, -3 and -4.

When comparing the wild-type and knockout populations to each other, there are some similarly expressing populations represented. Population 3 in the wild-type is highly similar to population 4 in the knockout having very highly expressing CD63 and PD-L1, although in the wild-type group this population is threefold higher in abundance than in the knockout.

The Use of FlowSOM analysis allowed for a more granular and specific analysis of the platelet population, however with some of the separation representing such a small subpopulation of the platelets, the robustness of these populations remains questionable. Therefore, we chose not to pursue this analysis further for this study.

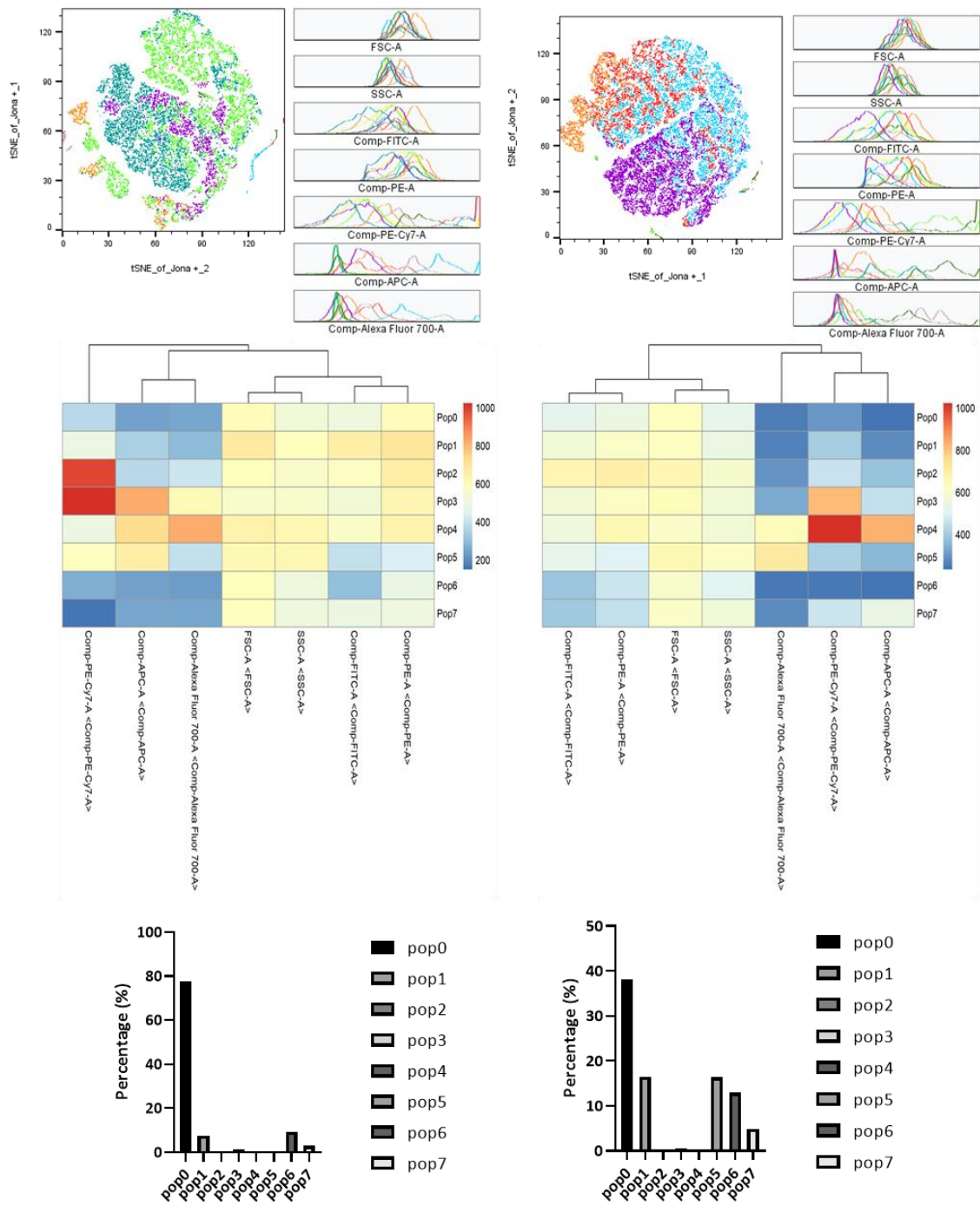


Figure 4-37. Flowsom analysis of t-SNE maps generated from thrombin stimulated Wild-type and knockout murine platelets. FlowSOM analysis was conducted on Jon/A positive cells from the concatenated stimulated populations, and groups overlaid on the corresponding t-SNE map with adjunct histogram receptor expression intensity (a). Data presented as a heatmap for each population and fluorescent marker, including FSC and SSC (b). percentage of events within each population false coloured to match the population colour on the t-SNE map (c).

4.8. Effects of endotoxemia on α -synuclein knockout platelets

Platelet granules store hundreds of factors which mediate the response of many different cell types additionally to the platelets themselves, with growing evidence demonstrating that platelets contribute to local and systemic inflammatory processes. Additionally, GPIb/IX/V, p-selectin, and α IIb β 3 have all been linked with sepsis (Jenne et al., 2013, Manne et al., 2017). Following the observation of reduced surface expression of PD-L1 and granule secretion in α -synuclein knockout platelets upon activation we sought to assess these effects in a setting of endotoxemia. Wild-type and knockout mice were subject to subcutaneous inoculation with 10mg/g Lipopolysaccharide (LPS), following this the mice were observed for 24 hours (Figure 4-38).

There was no significant difference in clinical scores between α -synuclein deficient mice and their wild-type littermates, although an increase was observed (WT= 3.66 \pm 1.6, KO= 7.33 \pm 1.08, P=0.092). The clinical score was assessed by animal house staff who were blinded to the treatment of the mice with LPS or PBS. The clinical score was determined through observational scoring of; the gait, piloerection (and visual appearance of the fur), mucus in the eyes, breathing (laboured/fast shallow) and apatite. If any single score reached the maximal of 3 within the first 4 hours or for 2 consecutive timepoint checks the experiment was ceased, additionally, if the clinical score reached a sum of 10 the experiment was halted.

In the first instance, we assessed platelet activation using JON/A and found no significant difference between the knockout and wild-type mice, however, this was due to the large spread of data in the knockout samples (WT= 61.6 \pm 7.1, KO= 168.4 \pm 79.1 MFI P=0.95). After stimulation with 0.1U/mL thrombin as before there was no significant difference between the knockout and wild-type samples, however, the knockout platelets had a lower MFI than their wild-type counterparts (WT=853 \pm 100.24, KO= 517.00 \pm 302.8 MFI P=0.45). Interestingly, when observed in respect to fold increase, the Wild-type platelets had a much higher fold increase over basal of 13.9 in comparison to the knockout platelets with a fold increase of 3.07.

Following this, the surface expression of P-selectin was observed to assess α -granule secretion, initially in basal samples, where there was no significant difference in expression levels, (WT=33.3 \pm 2.5, KO= 42.4 \pm 10.3 P=0.99). There was also no significant difference in P-selectin expression following stimulation with 0.1U/mL thrombin (WT= 226.3 \pm 37, KO= 152 \pm 80, P=0.82). Interestingly, when observed as a fold increase over basal, the wild-type mice resulted in a fold increase of 6.78 whereas knockout mice only exhibit a 3.6-fold increase for p-selectin expression after stimulation.

Finally, we assessed the dense granule secretion. Comparing basal samples there was no significant difference between the knockout and wild-type samples, however, conversely to P-selectin and JON/A, wild-type platelets had a slightly higher expression (WT= 530.75 \pm 62.35, KO= 280.00 \pm 15.52 P=0.97). Interestingly, after stimulation with 0.1U/mL thrombin although there is no significant difference the knockout samples have a higher expression of CD63 on their surface, although both had a wide variance (WT= 1101.75 \pm 460.69, KO= 1501 \pm 882.01 P=0.92). When observed in the context of fold increase the wild-type had an increase of 2.07 whereas the Knockout samples yielded an increase of 5.37.

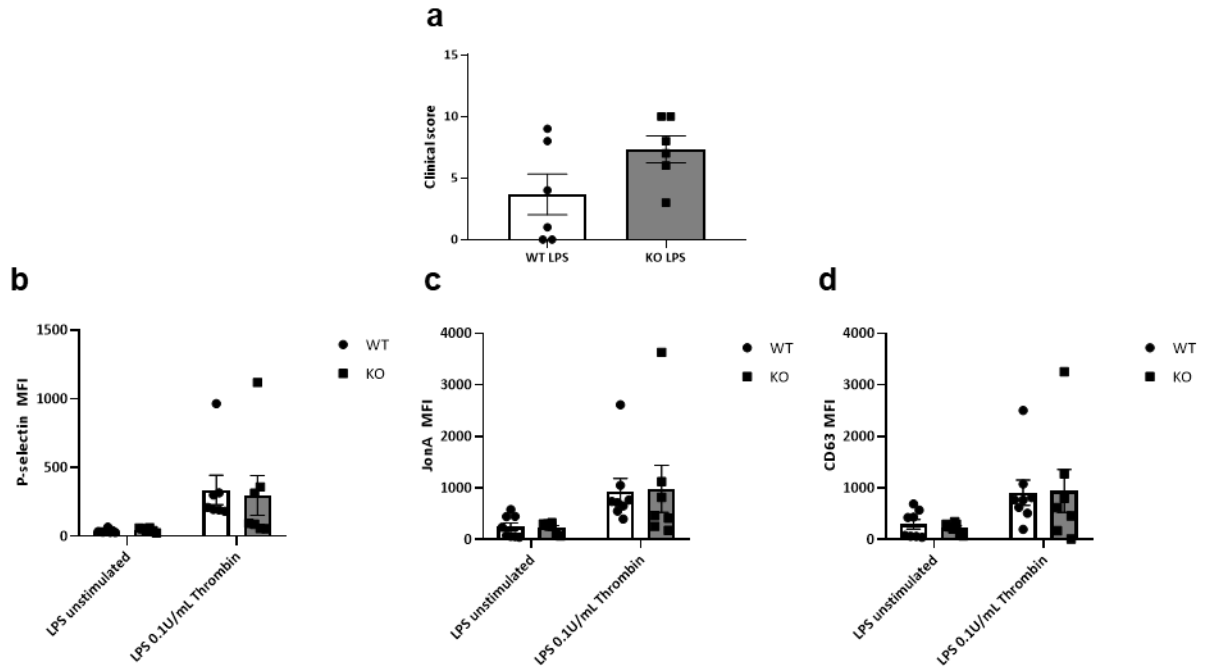


Figure 4-38. Effects of endotoxemia on α -synuclein knockout mice. Mice were subject to subcutaneous inoculation with 10mg/g LPS and observed for 24 hours. Mice were observed for changes in behaviour such as reduced reaction to noise or touch alongside physical changes such as piloerection each category was marked on a scale of 1:3, and the totals were summed. The expression of P-selectin, JON/A and CD63 was then assessed through flow cytometry in basal and 0.1U/mL thrombin stimulated conditions. (Data displayed as Median \pm SEM (* p >0.05 ** P >0.01 *** P >0.001).

In whole population analysis, it was clear that the knockout samples were spread into 2 clusters in P-selectin and JON/A when stimulated with thrombin, a high expression group and low expression group where the wild-type creating large variances in the samples. Therefore, we assessed the effects of clinical score on the basal expression of the secretion and activation markers (Figure 4-39). We started by assessing the amount of unstimulated JON/A positive platelets in comparison to clinical score, there was no significant effect on basal JON/A percent positive cells in the wild-type samples, however there was a slight decrease in percent positive as the clinical score increased ($P=0.14$). Comparatively, in the knockout samples, there was no observable difference in the JON/A MFI and the clinical score, with the line appearing nearly flat ($P=0.85$). This was mirrored when we observed the Raw MFI against the clinical scores with wild-type having an almost flat line with a slight downward slope ($P=0.96$) and knockout samples having an insignificant upward slope ($P=0.64$).

Subsequently, we observed the effects of the clinical score on the percentage of P-selectin-positive cells. In wild-type samples, we observed a significant increase in the number of P-selectin-positive cells in comparison to the clinical score. Interestingly, in the knockout samples although the amount of P-selectin positive cells dramatically increases the increase was not deemed to be significant due to the small sample size ($P=0.28$). interestingly when we observed the effects of the clinical score on the P-selectin MFI we saw a significant interaction between clinical score in both the Wild-type ($P=0.018$) and the knockout samples ($P=0.0025$).

We then interrogated the effects of clinical score on the basal expression of CD63 we noted that as the clinical score increased in the wild-type mice there was no significant effect on the expression of CD63 however with a slight positive slope ($P=0.54$). When observing the effects in knockout samples we saw a slightly reduced expression of CD63, as the clinical score of the mice increased however, this was not significant ($P=0.198$).

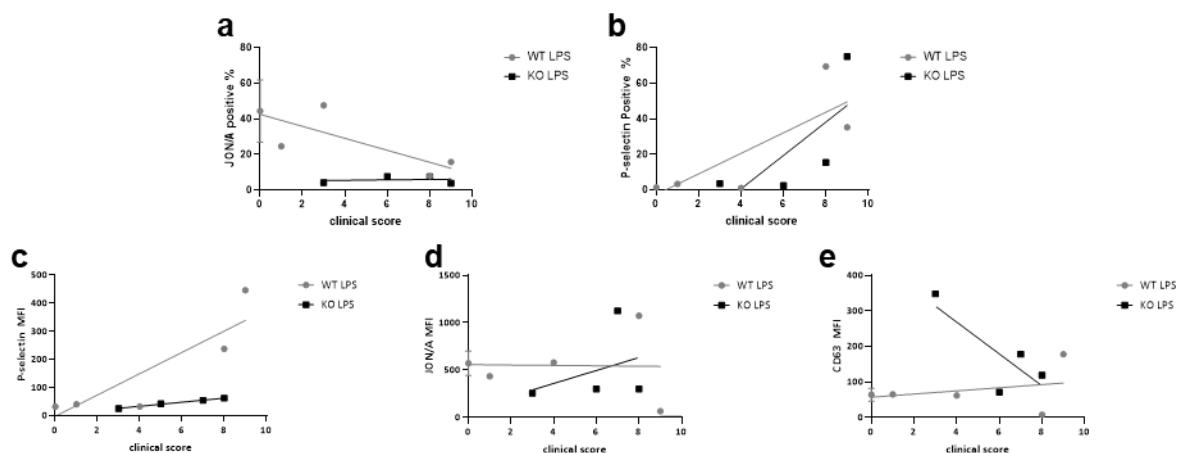


Figure 4-39. Effects of Clinical score on basal expression of platelet activation and secretion markers. Mice were subject to subcutaneous inoculation with 10mg/g LPS and observed for 24 hours. Mice were observed for changes in behaviour such as reduced reaction to noise or touch alongside physical changes such as piloerection each category was marked on a scale of 1:3, and the totals were summed for the total clinical score at the 24-hour time point. The expression of P-selectin, JON/A, and CD63 was then assessed through flow cytometry in basal. This was then plotted against the clinical score and linear regression was conducted. * $P>0.05$ ** $P>0.01$ *** $P>0.001$.

When platelets are subject to endotoxemia there was no significant difference between the expression of P-selectin, JON/A or CD63 either basal or stimulated conditions. Interestingly, the knockout mice were more susceptible to endotoxemia than wild-type mice under the same conditions. Interestingly we noted that the percentage of JON/A positive cells was not affected by the clinical scores in either wild-type or knockout, but the amount of P-selectin positive cells significantly increased. This was mirrored when observing the clinical scores against the expression of P-selectin and JON/A, conversely to this, the secretion of dense granules was not significantly altered either between wild-type and knockout or by clinical score. These data suggest that the platelets are beginning to secrete α - granules alone without inside-out signalling.

4.9. Discussion

The deletion of α -synuclein in a mouse model provided a robust platform for assessing the effects of the protein on platelet function without inducing off-target effects from chemical agents. In this chapter, we demonstrated that α -synuclein deficient mice had a significant bleeding phenotype comparatively to their wild-type littermates. We also demonstrated a significant thrombus formation defect *in vitro*. We were then able to link these observations with significant reductions in secretion markers in knockout platelets in response to thrombin as observed with five-colour flow cytometry.

When assessing the expression of four of the major platelets activating receptors between the knockout and wild-type mice we saw no change, due to the small volume of literature of α -synuclein knockout in mice we were only able to validate this against a single study, which was in agreement with our findings that knockout of α -synuclein does not alter the expression of Syntaxin11 or 4 (Smith et al., 2023). Following this we assessed the size and granularity of the platelets through flow cytometry, analysing the average FSC and SSC. We noted a slight decrease in platelet size; however, this was not significant. This observation agrees with the findings by Tashkandi et al. (2018), which utilised an automated cell blood count on whole blood smears, although these mice were a similar age, the knockout was generated through a different method.

We assessed the expression of STX-11, STX-4, SNAP23, VAMP2 and VAMP8 at the age of 8 weeks. At this time point, we saw no significant change in any of the samples

examined, this was concordant with a study by Greten-Harrison et al. (2010), which used the α -synuclein mice as a foundation to generate a triple synuclein knockout. This paper did, however, expand on this to assess the effects of this triple synuclein knockout in 12-month-aged mice and saw significant changes in multiple SNARE complex proteins. Although not directly comparable due to additional protein knockouts it is highly analogous.

Interestingly, Tashkandi et al. (2018) reported hypercoagulability in platelets contrary to our findings. However, their study did not provide details on methodology or results regarding aggregation studies, and blood collection was performed in heparinized capillary tubes. It has been shown that heparin can interact with PF4, it has also been shown to potentiate α IIb β 3-mediated outside-in signalling which may give a different result in the different results found (Nguyen et al., 2020, Gao et al., 2011).

This study represents the second of its kind to evaluate the haemostatic capabilities of an α -synuclein knockout mouse model, however, the Smith study did not include assessments of PT or aPTT, leaving us without a baseline for these assays. Although this has not been investigated, the relationship between bleeding time and PT/aPTT is well-established. A prolonged aPTT can be indicative of a bleeding phenotype (Capoor et al., 2015). The interplay between platelets and the coagulation system has been extensively studied and is recognised to be important for both the mechanical activation of the cascade and the release of multiple proteins from the α and dense granules that propagate the cascade (Sang et al., 2021). The prolonged aPTT may also be indicative of reduced levels of vWF present or lower activity, (Munsanje et al., 2021, Tomokiyo et al., 2005). The reduction of thrombus formation can also be a result in decreased vWF activity, which we did observe, research states that it is due to a reduced collagen binding, which was observed in flow thrombus formation, but not in static spreading and adhesion assays. To resolve this a Factor 8 assay would provide key insight into whether these observations are due to vWF.

Research into the interaction of α -synuclein with the SNARE complex in the context of platelets has not been characterised well in literature, with a single paper dedicated to investigating this. There are reports of interaction between α -synuclein with VAMP2, Syntaxin4, SNAP23 (Lou et al., 2017, Zhao et al., 2022) in different cell types; with further studies associating VAMP3, -7, and -8 with α -synuclein secretion from neural

cells. There have been no experiments published utilising immunoprecipitation to quantify any of these interactions, most of which rely on α -synuclein overexpression models which makes direct comparisons unreliable. A study by (Ren et al., 2007) found that VAMP8, is the primary mechanism for granule secretion with VAMP2, -3 and -7 performing a small role in secretion in comparison. Taken with the previous findings that α -synuclein has only been observed to interact directly with VAMP2, show that there are interactions between α -synuclein and other SNARE or SNARE regulatory proteins due to the extent of the observed phenotypic effects.

At the time of research, this study was the first instance of the interrogation of the effects of α -synuclein knockout on platelet aggregation. However, there have been prior studies which can be observed; a study by Sharma et al. (1991) assessed the platelet aggregation in patients with PD, where platelets often contain mutant α -synuclein. A significant decrease in the capability of PD patients' platelets to aggregate in response to ADP compared to healthy donors. This study also observed that there was no change in aggregation capability when stimulated with collagen. Interestingly a study by Acquasaliente et al. (2022) has noted that increases in exogenous α -synuclein reduce the aggregation of platelets in PRP when interrogated through multiple electrode aggregometry (MEA). Taken together this suggests that both, the location, and concentration of α -synuclein influences the aggregation of platelets.

The effects of α -synuclein knockout on platelet spreading previously have not been characterised; however, the spreading of platelets on fibrinogen, and collagen has, allowing for the comparison of wild-types. A study by Alshehri et al. (2015) assessed GPVI knockout on mouse platelets, their wild-type platelets were seen to spread to a similar size to the platelets in this study. This study also compared the spreading of platelets on fibrinogen and fibrin, this was analogous to our spreading with Pre-stimulation with thrombin, they also saw that the platelets spread on fibrin spread further and had a higher propensity to form actin stress fibres and lamellipodia. They also noted that the platelets spread on fibrinogen exhibited actin nodules and filopodia, which are indicative of partial spreading. A study by Mangin et al. (2018) expands upon this using a mouse model expressing human GPVI, which rectifies the spreading deficiency otherwise observed. When interrogating the size of platelets spread on Collagen, although there was no significant size decrease between the WT and KO

mice, they were smaller in comparison to the fibrinogen spread platelets. This observation is comparable with a study by Lee et al. (2012), however, their maximal time for observation was 7 minutes; shorter than our minimum time point for platelet spreading, making it impossible for a direct comparison.

Immunofluorescence was used to assess the movement and co-localisation of SNARE complex proteins with α -synuclein, alongside whether the removal of α -synuclein altered SNARE complex movement. There was no current data interrogating the movement of α -synuclein in platelets, however, there are published data regarding the movement and localisation of different SNARE complex members. STX-11 is a t-SNARE that has been consistently observed at the target membrane for exosome trafficking at the plasma membrane, in multiple different cell types (Dieckmann et al., 2015a, Dabrazhynetskaya et al., 2012, Halimani et al., 2014). It has also been confirmed that STX11 is co-localised with STXBP5 which was observed to be present on the platelet membrane all of which is congruent with our findings (Ye et al., 2012). We also then investigated STX4 movement and co-localisation events with α -synuclein, noting that it was predominantly located at the peripheries of the platelets as expected from previous literature. There were a small number of co-localisation events which did not increase upon platelet stimulation, interestingly a study by (Ye et al., 2014) state that STX4 is not required for platelet secretion. The interaction events between STX4 have been characterised in Neural cells where Zhao et al. (2022) have shown that STX4 mediate α -synuclein secretion.

The location of SNAP23, has been investigated previously in a study by (Polgár et al., 2003), which found that it is found exclusively on the plasma membrane of the platelets which has been corroborated in subsequent studies (Hatsuzawa and Sakurai, 2020). Due to our testing methodology, we were unable to distinguish whether the SNAP23 we observed in basal samples were cytosolic, or on the top/bottom of the platelet, remaining on the membrane. Under stimulated conditions due to the platelet spreading out it was much clearer that the SNAP23 was located on the periphery, in agreement with this study. SNAP23 has been seen to interact with α -synuclein in neural cells facilitating secretion. This interaction has not been observed in platelets until this study, but due to the absence of α -synuclein release from platelets must be attributed to a separate function.

Alongside STX and SNAP proteins we investigated the localisation and interactions with VAMP2, -7 and -8. All VAMP proteins are present on granules within the cell (Koseoglu et al., 2015) which is concordant with our observations of the VAMP proteins being spread throughout the cell and moving to the periphery upon stimulation (Ren et al., 2007). In previous studies, the C-terminus of α -synuclein has been observed to bind with VAMP2 (Burré et al., 2010, Pei and Maitta, 2019, Lou et al., 2017). We also observed interactions between these proteins; when platelets were stimulated with 0.1U/mL thrombin the interaction events increased. There have been no studies elucidating the interaction of α -synuclein with VAMP7 or -8, however we saw co-localisation and interaction in α -synuclein IP blotted against VAMP8 and VAMP2.

We then sought to assess platelet secretion using flow cytometry, assessing P-selectin, CD63 and LAMP-1. Interestingly, a study by (Acquasaliente et al., 2022) state, that in their α -synuclein knockout mice they observed an increased expression of P-selectin, this finding is in contrast to this study where we saw no change in p-selectin at basal levels and a decreased expression comparatively to wild-type littermates to some agonists.

Throughout this chapter we demonstrate a bleeding phenotype in α -synuclein knockout mice which is recapitulated in washed platelet aggregation experiments. Platelets retained their capacity to bind to collagen and fibrinogen in static experiments, however, was significantly reduced when challenged with a flowing conditions. The reduction of platelet functionality was closely linked to a significant reduction in platelet secretion of granules in response to agonists, when probed further we observed the amelioration of highly secretory populations of platelets present in the wildtypes. We also demonstrated that α -synuclein co-localised with STX11, VAMP2 and VAMP8, recapitulating data seen in human IP data.

4.9.1. Limitations

The use of a whole body α -synuclein is a powerful technique to elucidate the systemic effects of the protein within the subject, however, the use of a whole-body knockout may either conceal or enhance the phenotype. To ameliorate these systemic effects, we conducted multiple platelet functional studies in washed platelets. A more precise methodology for testing this would have been the use of a platelet specific α -synuclein, however due to time and budget constraints this was not possible. The use of a platelet specific α -synuclein knockout is compounded by findings of (Acquasaliente et al., 2022) which states a role of α -synuclein in the inhibition of PAR-1 functionality and reduction in p-selectin expression.

Due to time and equipment constraints, we were unable to obtain TEM imaging of platelets from the mice, meaning we were unable to visualize any perturbation of the platelet ultrastructure. Which was important due to a study by Grodzielski and Cidlowski, (2023) who observed a significant upregulation of α -synuclein in the Megakaryocyte transcriptome when stimulated with glucocorticoids.

We also assessed both the size and granularity of the platelets using a flow cytometer, which, although giving accurate measurements in size and granularity, does not allow for the delineation of the granular content. The use of a specific blood cell analyser such as the one used in the (Tashkandi et al., 2018) study, gives more parameters which may highlight differences between the α -synuclein knockout and wild-type platelets.

Thrombus formation studies were conducted *in vitro* utilising a Cellix microfluidic device. Although these devices provide a much more controllable setting in regard to the shear stress and the ECM proteins expressed on the surface, these devices lack the ability to recapitulate the *in vivo* environment completely (Lane et al., 2012). There are two standard *in vivo* thrombus formation methodologies: Ferric chloride injury, and laser injury; with the latter being more accurate due to the method of injury creation. Unfortunately, due to both animal and equipment constraints, we were not able to conduct this experiment. Aside from the stated limitations, using the biochip enabled the observation of decreased thrombus stability in the absence of α -synuclein expression in platelets specifically.

We used immunofluorescence to assess the interaction, movement, and co-localisation of α -synuclein with SNARE proteins. Although immunofluorescence analysis enabled us to visualise the distribution and movement of the different proteins it has significant drawbacks. The first and largest drawback to this is the imaging itself, this was completed on a Zeiss Apotome. Light microscopy does not provide sufficient resolving power to effectively deduce whether proteins are interacting or just within the same vicinity. This was compounded by the small amount of protein present and the reduction of signal resulting from apotome sectioning resultant images had a large amount of noise. This also resulted in difficulty in Z stack images which would enable us to better elucidate the protein location in 3-dimensional space (Dunn et al., 2011b).

Additionally, when we observed what we classified as co-localisation events we were unable to fully state this due to our inability to assess whether they were in the same plane or had a high enough resolution to fully distinguish if they were close or within 40nm of each other. To overcome this the use of a proximity ligation assay (PLA) would provide the most robust data, it would also then allow us to further quantify these findings as co-localisation by colour can be subjective. Another option would be to use TEM, which would also allow us to assess morphological changes within the platelet upon activation.

We used an indirect method of assessing platelet secretion in this study, by multi-colour flow cytometry; this gives us a wide image of what is being expressed on the platelet, however, to fully quantify the secretion capability Lumi-aggregometry should have been conducted also.

Further interrogation of the platelet ultrastructure using TEM would allow for the observation of granule abundance and localisation within the platelets for wild-type and knockout platelets. Additionally, to the assessment of basal conditions, utilising this methodology for platelets stimulated with different agonists, can also illuminate differential granule secretion between the knockout and wild-type platelets.

When assessing the effect of CRP-XL on platelet secretion, we saw a minimal amount of secretion markers, however, we also did not observe the expected large increase in JON/A expression. This is indicative that the CRP-XL is not activating the platelets effectively, in comparison to other literature, the relative fluorescence or percentage of positive cells is used, however, when comparing the JON/A positive cells we

observe similar percentages of positive cells, at around 60% (Aburima et al., 2021, De Simone et al., 2022).

Further work to elucidate the function of α -synuclein more completely would begin with the use of a platelet-specific α -synuclein knockout. This would allow for the examination of the phenotypic effect of α -synuclein on haemostatic capability specifically from platelets, due to the expression of α -synuclein in other cells within the blood. Conducting an *in vivo* thrombus formation assay on this knockout may also provide a more complete image of α -synuclein knockout on thrombus stability. Alongside this, it would better allow for the elucidation of α -synuclein's effect on the ability of the platelets to interact with the immune system.

Additional testing within the *in vitro* thrombus formation assays would elucidate the protein expression of different thrombus stabilising components within the thrombi. Proteins such as Fibronectin, vWF and Fibrin all have roles within thrombus stability and may yield a further explanation of the reduced thrombus stability observed in the knockout mouse models (Fuchs et al., 2010).

In this study, we assessed the interactions of α -synuclein with the main SNARE complex members associated with platelet granule secretion, STX11, VAMP7 and 8, as well as SNAP23. Although we briefly observed expression levels of syntaxin4, and VAMP2 further interrogation may illuminate further roles of α -synuclein. Alongside the interaction partners of α -synuclein, we only focused on a singular PTM, that of phosphorylation at serine129, which has been characterised in neuronal cells. Proteomic analysis can be utilised to assess the interaction partners of α -synuclein in response to different agonists, alongside changes in the PTMs that are observed on the protein.

Chapter 5. Assessment of PD-L1 function in platelets using a knockout model and MPN patient blood.

5.1. Introduction

In addition to their primary haemostatic role, platelets are known for their complex interaction with the immune system (Ali et al., 2015). Platelets have been shown to participate in innate immunity due to the variety of inflammatory and bioactive molecules stored within the granules which are released upon activation (Sonmez and Sonmez, 2017). The impact of platelets on cancer immune evasion and the dynamics of the tumour microenvironment has been addressed in several studies, including both in cancer patients and animal models (Han et al., 2020b, Latchman et al., 2004, Schmied et al., 2021, Maouia et al., 2020).

Platelets secrete multiple immunomodulatory molecules (Table 18) with varying functions (Maouia et al., 2020). A key regulator in immune cell function released by platelets is PD-L1, also known as CD274. PD-L1 binds to the immune checkpoint protein Programmed cell death protein 1 (PD-1) on the surface of activated T cells (Han et al., 2020b). This axis acts as a co-inhibitory factor that can limit the development of T-cell response through the downregulation of T-cell activation, proliferation, T-cell secretion and survival (Han et al., 2020b, Sanmamed and Chen, 2014). It has also been found that the expression of PD-L1 from platelets is correlated with the activation status of the platelet (Hinterleitner et al., 2021). Interestingly, it has also been observed that PD-L1 has a regulatory role on platelet activation and thrombosis (Hinterleitner et al., 2021).

Table 18. Proteins secreted from platelets affecting the immune response.

Protein	Effect	Reference
CCR1	Drives monocyte migration	(Clemetson et al., 2000)
CCR3	cell migration, allergic response, and parasitic infection	(Clemetson et al., 2000)
CCR4	T helper type (Th)2 cell accumulation	(Clemetson et al., 2000)
CXCR4	cell migration and hematopoiesis	(Clemetson et al., 2000)
CD148	Increase cell growth and motility	(Senis et al., 2009)
CXCL4	CCR1 agonist, suppress hematopoiesis, platelet aggregation and regulates immune and inflammatory responses	(Fox, J.M et al., 2018)

Programmed death ligand 1 (PD-L1) is a Type 1 transmembrane glycoprotein that adopts an immunoglobulin structure with an Ig variable (v), and Ig constant (c) region. The IgV region presents as a standard Ig-like domain to the complementary regions in the binding domains on programmed cell death protein 1 (PD-1) akin to antigen recognition by antibodies (Brahmer et al., 2012). PD-L1 is considered to be a co-inhibitory receptor and an immune checkpoint protein that has the ability to suppress cytotoxic T lymphocytes (Guo et al., 2022, Mazel et al., 2015, Han et al., 2020b). PD-L1 is ubiquitously expressed on haematopoietic and non-haematopoietic cells. Its widespread presence allows it to play a key role in modulating immune responses, maintaining immune tolerance, and protecting tissues from auto-immune reactions. This broad expression also implicates PD-L1 in various physiological and pathological processes, including cancer, where it can help tumour cells evade immune detection (Wu et al., 2019).

Under standard physiological conditions, PD-L1 binds PD-1 on activated lymphocytes, dendritic cells, and monocytes (Agata et al., 1996, Freeman et al., 2000). This binding triggers PD-1 signalling, resulting in various effects depending on the cell type it interacts with. PD-L1 ligation to PD-1 on effector T-cells suppresses TCR and induces apoptosis, anergy, and exhaustion, whereas binding to regulator T-cells results in sustained FOXP3 expression and proliferation (Tsushima et al., 2007, Patsoukis, 2015 #751, Patsoukis et al., 2015, Latchman et al., 2001).

Previous studies have shown that PD-L1 expression is increased in both inflamed tissues, and the tumour microenvironment (TMS), where it plays a vital role in inhibiting immune response through modulating the activity of T-cells (Zhang et al., 2020, Han et al., 2020b, Dieterich et al., 2017). These studies have also shown that PD-L1 is upregulated in various malignancies, where it can attenuate the host immune response to tumour cells, and is associated with a poorer prognosis (Yi et al., 2021). Studies have shown that the use of therapeutic plasma exchange (TPE) replacing the patient plasma with colloid solution can effectively remove PD-L1 in its varying forms from the plasma which can reduce the effects of PD-L1 linked resistance displayed by some cancers (Ando et al., 2019, Jacob et al., 2020).

Whole blood transcriptional profiling on patients with myeloproliferative neoplasms (MPNs) showed that PD-L1 expression is significantly increased compared to healthy controls (Veletic et al., 2018, Holmström et al., 2017). These patients often present with bleeding and bruising diathesis, however, there has been no verified link between PD-L1 expression and platelet function in these patients. Additionally, a characteristic feature of MPNs is the presence of Janus Kinase 2 (JAK2) point mutations at JAK2^{V617F}. The JAK2^{V617F} mutation is present in nearly 100% of patients with polycythaemia vera (PV), and over half of those with essential thrombocytosis (ET), and primary myelofibrosis (PMF) (Nielsen et al., 2011, Prestipino et al., 2018). JAK2^{V617F} activity results in signal transducer and activator of transcription 3 (STAT3) and STAT5 phosphorylation, which enhances PD-L1 promotor activity, therefore increasing PD-L1 expression (Zerdes et al., 2019). This has been observed to occur in multiple cell types; including megakaryocytes, monocytes, and platelets (Holmström et al., 2017, Mullally et al., 2010, Prestipino et al., 2018). Furthermore, it has been shown that both PD-L1 and JAK2 share the same locus on chromosome 9p24, with studies showing that oncogenic JAK2 activity enhances PD-L1 promotor activity, particularly in megakaryocytes (Prestipino et al., 2018, Lee et al., 2022).

The expression of PD-L1 on platelets was first reported in 2018 and was thought to be primarily located on the platelet membrane (Rolfes et al., 2018). Subsequently, several studies have corroborated these findings (Hinterleitner et al., 2021). More recently, Hinterleitner and colleagues suggested that PD-L1 is also located within the platelet α -granules, further enhancing their ability to induce immunosuppression following platelet activation resulting in the release of PD-L1 from the platelet alongside

increased surface expression (Hinterleitner et al., 2021, Li et al., 2022). The expression of PD-L1 on platelets has also been shown to be significantly upregulated in JAK2^{V617F} knock-in mice, presenting with primary myelofibrosis (PMF) (Prestipino et al., 2018).

Currently, there is a single study which has assessed the effects of PD-L1 on platelets, to evaluate the impact of platelet-derived PD-L1 on their haemostatic function (Li et al., 2022). The study by Li et al. (2022) demonstrates an inhibition of thrombosis, and decrease in platelet activation to agonists in PRP; however, there are many facets of platelet function that this study did not explore.

The aims of this chapter are to:

- Examine whether PD-L1 upregulation in MPN patients is JAK2^{V617F} mediated.
- Characterise the platelet function in PD-L1 knockout mice.
- Establish a platelet-specific knockout mouse colony to assess platelet PD-L1 *in vivo*.

5.2. Results

First, we established a whole-body knockout mouse model based on the work originally conducted by Latchman et al. (2004). We aimed to use this model to investigate the impact of PD-L1 deletion on platelet function and the effect of PD-L1 inhibitors, assessing both potential off-target effects and any residual PD-L1 activity. This knockout was created by electroporating a NEO cassette in place of the signal exon and IgV region of the PD-L1 gene of C57BL/6 ES cells. Upon receiving the PD-L1 knockout mice from Professor Arlene Sharpe (Harvard University), they were crossbred with C57BL/6 wild-type mice to establish PD-L1 heterozygous offspring (Figure 5-1). These heterozygotes were then mated to produce the experimental animals.

To genotype these mice, we used specific primers that detect the IgV region in the PD-L1 gene. Due to the insertion of the Neo cassette into the gene, the knockout mice were expected to produce a PCR product at 474bp, whereas the wild-type mice would yield a product at 305bp. To accommodate the proximity of these product lengths, we conducted two separate PCR reactions: one targeting PD-L1 detection and the other targeting Neo cassette detection. Knockout samples showed a band only in the Neo reaction, indicating the absence of the PD-L1 gene. In contrast, the wild-type samples showed a positive band only in the PD-L1 reaction. Samples showing bands in both reactions were deemed as heterozygous.

Following the genotyping, we assessed the protein expression of PD-L1 in the platelet population, using western blot analysis. In the wild-type washed platelet samples, a distinct band was detected at 50kDa, corresponding to PD-L1 protein. Heterozygous knockout samples showed significantly reduced PD-L1 expression compared to wild-type, and knockout samples did not show any signal at the PD-L1 band, confirming the successful elimination of PD-L1 protein expression.

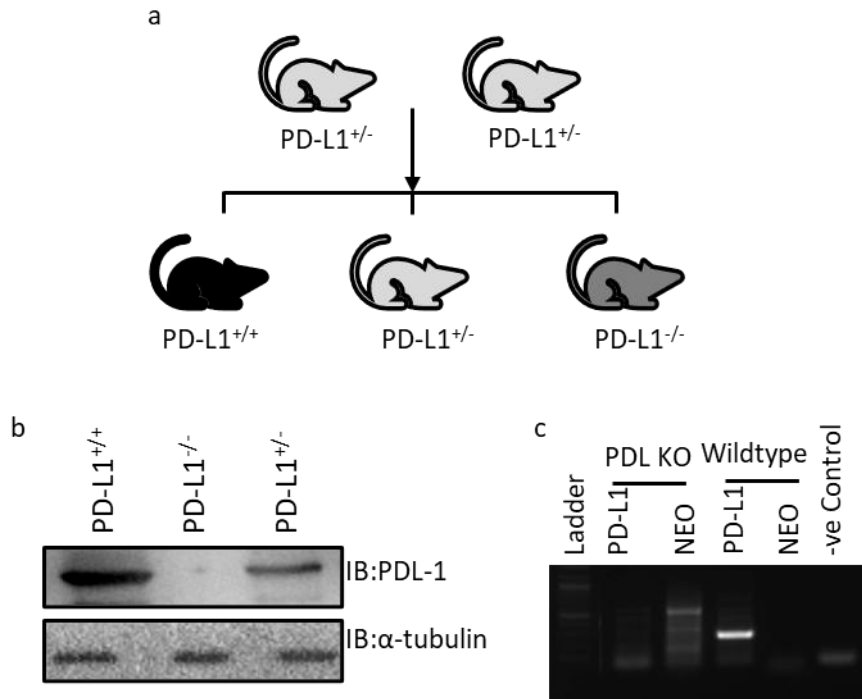


Figure 5-1. Breeding strategy, and quantification of whole-body PD-L1 knockout mice. (a) PD-L1^{-/-} mice were crossbred with C57/BL-6 Wild-type mice to generate PD-L1^{+/-} breeding pairs; these breeding pairs were then mated to produce experimental animals. (b) Representative image of PD-L1 expression in knockout platelets. Platelet lysates were collected and separated through SDS PAGE before transfer to PVDF membranes, these were then blocked with 5% BSA and probed for PD-L1 (sc-293425). (c) Representative image of DNA gel for PD-L1^{-/-} and Wild-type mouse DNA. DNA was extracted from ear biopsies and subject to PCR reaction for the presence of PD-L1 and the NEO cassette in separate reactions.

Next, we proceeded by generating a mouse model with platelet-specific PD-L1 knockout. This mouse was generated not to only investigate the role of platelet specific PD-L1 in the body, but also to explore its implications in various disease states, such as endotoxemia. The PD-L1^{fllox} mice were kindly provided by Professor Arlene Sharpe from Harvard Medical School and the Gplb^{Cre} mice were obtained from Professor Yotis Senis at Université de Strasbourg. The Gplb^{Cre} mice were generated, by inserting T2A-improved-Cre (iCre) between the last amino acid, and the translation codon of the Gplb gene (Nagy et al., 2019) (Figure 5-2). The PD-L1^{Fllox} mice were generated by Sage et al. (2018) by introducing LoxP sites around exons 2 and 3 of the CD274 gene using electroporation of linearised DNA into embryonic stem cells, which were then microinjected into mouse blastocysts. Both the Gplb^{Cre} and PDL-1^{fllox} mice were bred on a C57BL/6 genetic background.

In mice that express the GPIba-T2A-iCre, the T2A sequence induces ribosome skipping upon translation of the mRNA, resulting in the expression of both the GPIb and the Cre protein; therefore, only a single copy of the Cre allele is required to induce the desired phenotype (Song and Palmiter, 2018). The Cre-Lox recombination is a site-specific reaction where in cells that have both LoxP and Cre expression, a recombination event can occur between the LoxP sites. The Cre recombinase proteins bind to the first and last 13 base pairs of the Lox site forming a dimer, this then binds to another dimer to form a tetramer where a double-stranded cut is made by the Cre protein. These strands are then bound together by DNA ligase, which results in the region between the Lox sites forming a looped structure causing a deletion event.

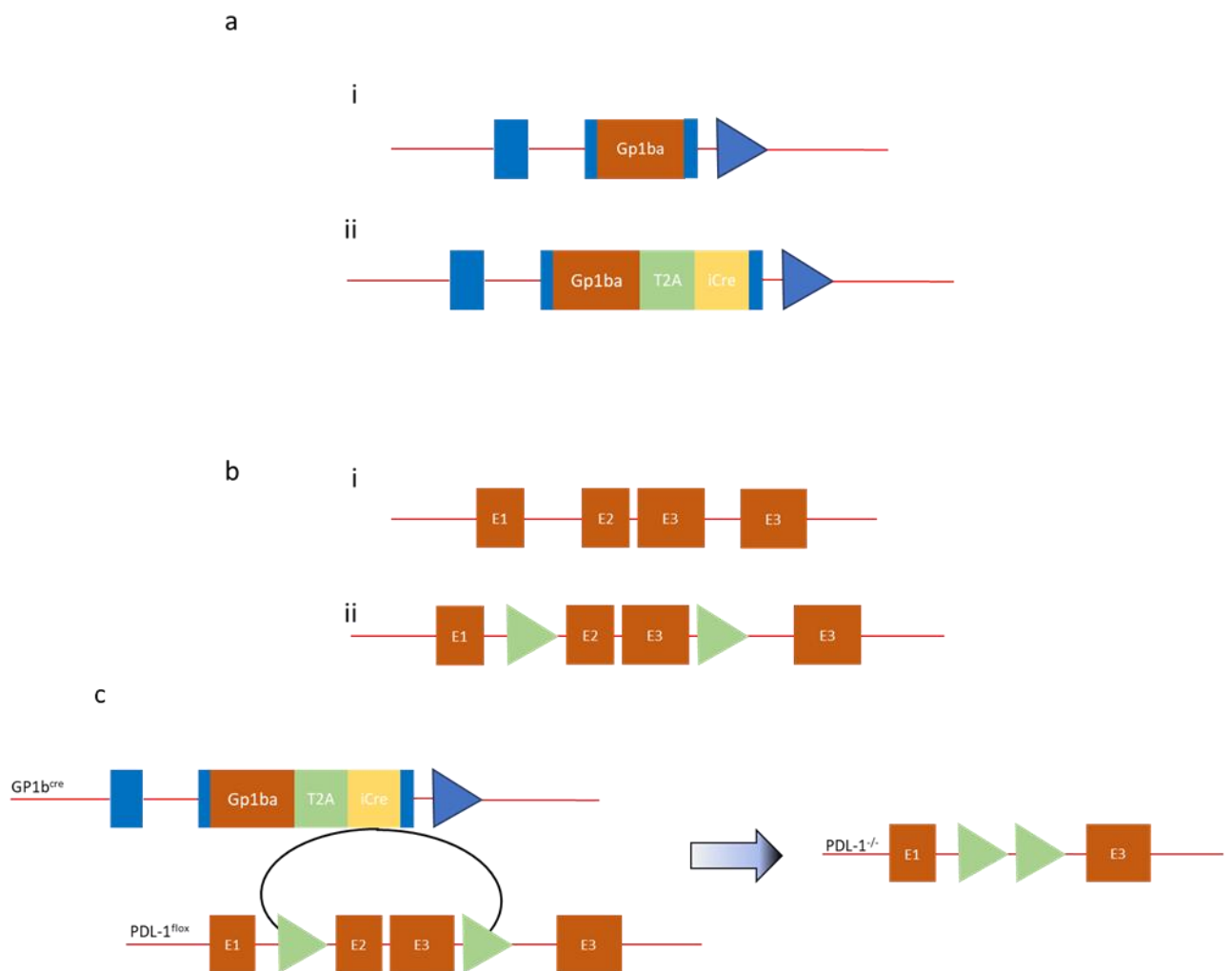


Figure 5-2. Targeting strategy to generate the platelet-specific PD-L1 Knockout Mouse. (a) the mouse *Gp1ba* gene consisting of an untranslated exon, followed by an intron and the translated *Gp1ba*. (ii) The T2A-iCre system was targeted and incorporated into the open reading frame of the GPIBa locus. (b) *Cd274* gene exons 1 to 4 are shown as orange boxes and (ii) loxP sites flanking exons 2 and 3 are depicted as red triangles. (c) Schematic of the iCRE/Flox system to be used to remove the open reading frame of PD-L1 in cells also expressing GPBb.

To acquire the platelet-specific knockout, we implemented a breeding strategy resulting in the final breeding pairs for experimental animals which would generate 75% platelet-specific knockouts, 25% with no cre which we used as a “wild-type” (Figure 5-3). The first generation consisted of PD-L1^{flox/flox} mice and Gplb^{Cre/Cre} which were bred together resulting in progeny with Gplb^{cre} and PD-L1^{flox} heterogeneity (Gplb^{Cre/+} PD-L1^{Flox/+}). These mice were crossbred with PD-L1^{flox/flox} mice, resulting in homozygous flox mice, the Gplb^{Cre/+} mice were then used for generating experimental animals.

The mating of Gplb^{Cre/+} PD-L1^{Flox/Flox} mice resulted in the generation of 3 genotypes: Gplb^{-/-} PD-L1^{Flox/Flox}, which was used as a wild-type control, and the knockout mice, with the genotype Gplb^{Cre/+} PD-L1^{Flox/Flox} or Gplb^{Cre/Cre} PD-L1^{Flox/Flox}. The knockout functions with a single allele of Cre therefore 75% of progeny were experimental knockouts and 25% were wild-type littermates.

We used PCR to determine the genotype of the mice. To verify whether the PCR was working, we tested a wild-type mouse sample that did not carry the Gplb^{Cre} or PD-L1^{flox} alleles. Using primers that would bind just before and after the LoxP sites on the PD-L1 gene, we detected a PCR product at 2.9kb. With the insertion of the LoxP sites on the PD-L1^{Flox} mice, we expected a length of around 3.0Kb which we also detected. When analysing the presence of the Cre gene due to its ability to cut out this section, we expected much shorter PCR products of 540bp, which we detected in mice carrying the Cre allele.

Following on from genotyping we analysed whether the PD-L1 protein expression was specifically deleted in platelets, or if the knockout resulted in differential expression in other tissues. To achieve this, we conducted western blot analysis of platelet lysates alongside spleen tissue lysates. We found that between the wild-type mice and the Floxed PD-L1 mice, there was a slight decrease in PD-L1 expression in the PD-L1^{Flox} mice, however, this was not significant, concordant with previous literature (Sage et al., 2018). Although this was not significant, we chose to use PD-L1^{Flox} mice as our control as they were littermates with the knockout mice, allowing for a more reliable comparison. When the platelet-specific knockout mice were examined, PD-L1 protein expression was undetectable. We then assessed the expression of PD-L1 in spleen

tissue lysates from the same mice and found no change in PD-L1 expression in wild-type, PD-L1 flox or platelet-specific knockout mice (Figure 5-3).

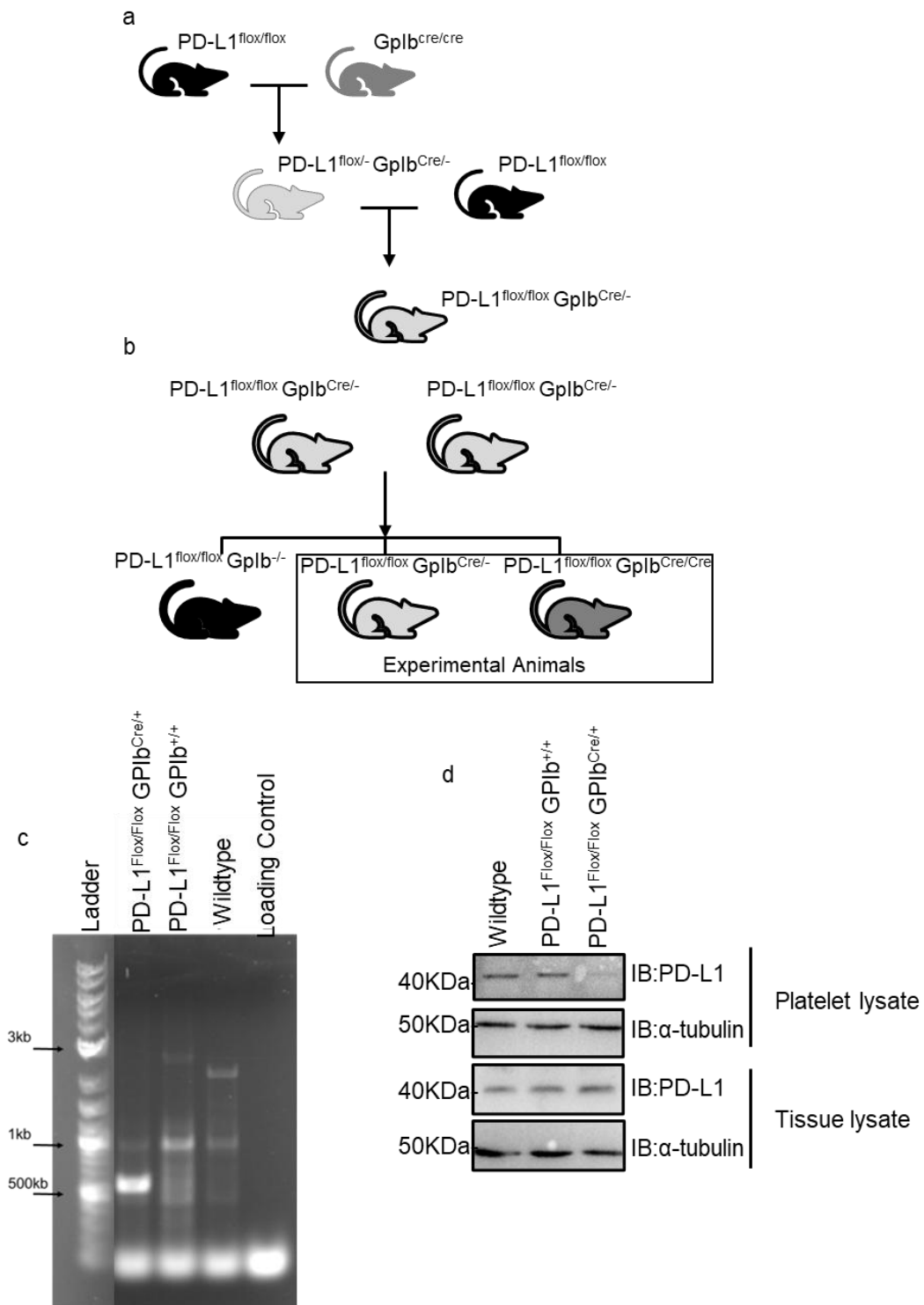


Figure 5-3. Breeding strategy to generate the platelet-specific knockout mice with genetic and proteomic confirmation. (a) breeding schematic to generate animals to be mated to produce experimental animals. (b) breeding schematic for the generation of experimental animals. (c) Representative image of DNA gel for mouse DNA. DNA was extracted from ear biopsies and subject to PCR reaction for the presence of PD-L1. (d) Representative image of PD-L1 expression in knockout platelets and tissue (spleen). Lysates were collected and separated through SDS PAGE before transfer to PVDF membranes, these were then blocked with 5% BSA and probed for PD-L1 (sc-293425).

Following the confirmation of PD-L1 deletion, we assessed the impact of PD-L1 on platelet activation by measuring aggregation and comparing the differences in platelet response between wild-type, whole-body and platelet-specific- knockout mice (Figure 5-4). This enabled us to assess whether the effect caused by PD-L1 expression is platelet-specific or systemic. Wild-type platelets stimulated with either 0.1U/mL and 0.05U/mL thrombin reached aggregation levels of $59.3\% \pm 4.3$ and $58.8\% \pm 3.37$, respectively. There was a significant decrease in platelet aggregation in the whole-body knockout mouse model in response to 0.1U/mL thrombin ($P=0.018$). However, the reduction in platelet aggregation in the platelet-specific knockout was not significant ($P=0.25$).

At a lower thrombin concentration of 0.025U/mL, the maximal aggregation of wild-type platelets was $14.67\% \pm 6.0$, the whole-body knockout showed no change ($10.33\% \pm 5.8$), and the platelet-specific knockout (PLT-PDL1^{-/-}) had a maximal aggregation of $15.5\% \pm 4.5$. As such, there were no significant changes between the Wild-type and the whole-body knockout

When the platelets were stimulated with 3 μ g/mL collagen, the maximal aggregation of wild-type platelets at 5 minutes was $57.8\% \pm 5.6$, the whole-body knockout saw a downward trend to $36.0\% \pm 7.7$, however, this was not significant ($P=0.148$ WT n=9, KO n=3). When the dose of collagen was reduced to 1 μ g/mL the maximal aggregation for wild-type platelets was $38.4\% \pm 6.7$, in comparison to the whole-body knockout which was $17.7\% \pm 6.9$, although a lower average aggregation was observed this also was not a significant reduction ($P=0.31$ WT n=9, KO n=3).

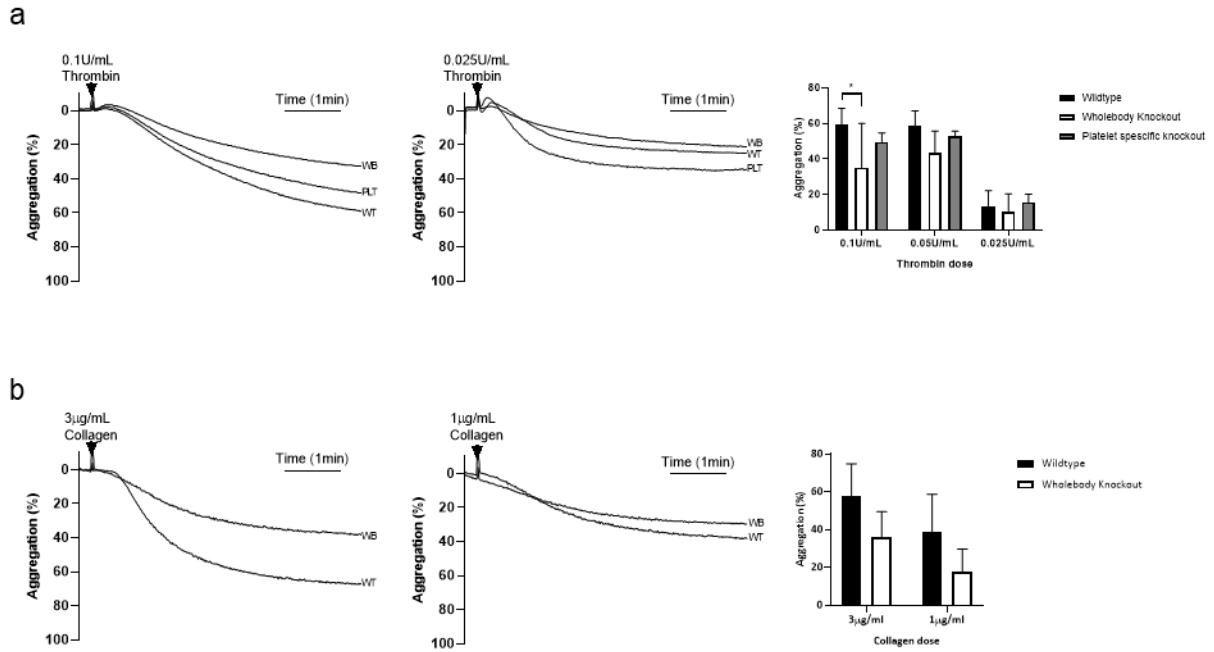


Figure 5-4. Effects of PD-L1 knockout on platelet aggregation to Thrombin and collagen. Washed platelets were diluted to a concentration of 2.5×10^8 with Modified Tyrode's buffer, these were stimulated with indicated agonists and doses and then measured on a chronology 4+4 aggregometer. Representative aggregation traces of platelets stimulated with thrombin (a) and collagen (b). Aggregation data from Wild-type (black), whole-body knockout (light grey), and platelet-specific knockout in response to (a) thrombin and (b) collagen. Data Thrombin $N=5$ collagen $N=3$. Percentage aggregation is presented by mean \pm standard error of the mean (SEM) * $P < 0.05$, ** $P < 0.01$ (WT vs PD-L1^{-/-} $n=3$ WT vs PLT-PD-L1^{-/-}, $n=2$).

Platelet aggregation is driven by the release of granule contents, we next examined platelet secretion following thrombin stimulation (Figure 5-5). We examined P-selectin, CD63 and LAMP1, alongside this we assessed activation through the marker, JON/A. This allowed us to assess whether the aggregation defect observed was influenced by impaired platelet secretion of granules. Interestingly we found a significant decrease in platelet activation as measured by JON/A at 0.1U/mL thrombin, but not at 0.025U/mL ($P=0.0006$, $P=0.999$ respectively). Additionally, to the observed decrease in JON/A, we noted significantly lower expression of the secretion markers P-selectin and CD63 at 0.1U/mL thrombin ($P=0.0011$, $P=>0.0001$), but not at 0.025U/mL thrombin ($P=>0.999$, $P=0.983$). Furthermore, we observed a light decrease in LAMP-1 expression post-stimulation with both 0.1U/mL and 0.025U/mL thrombin; however, this decrease did not reach statistical significance at either dosage.

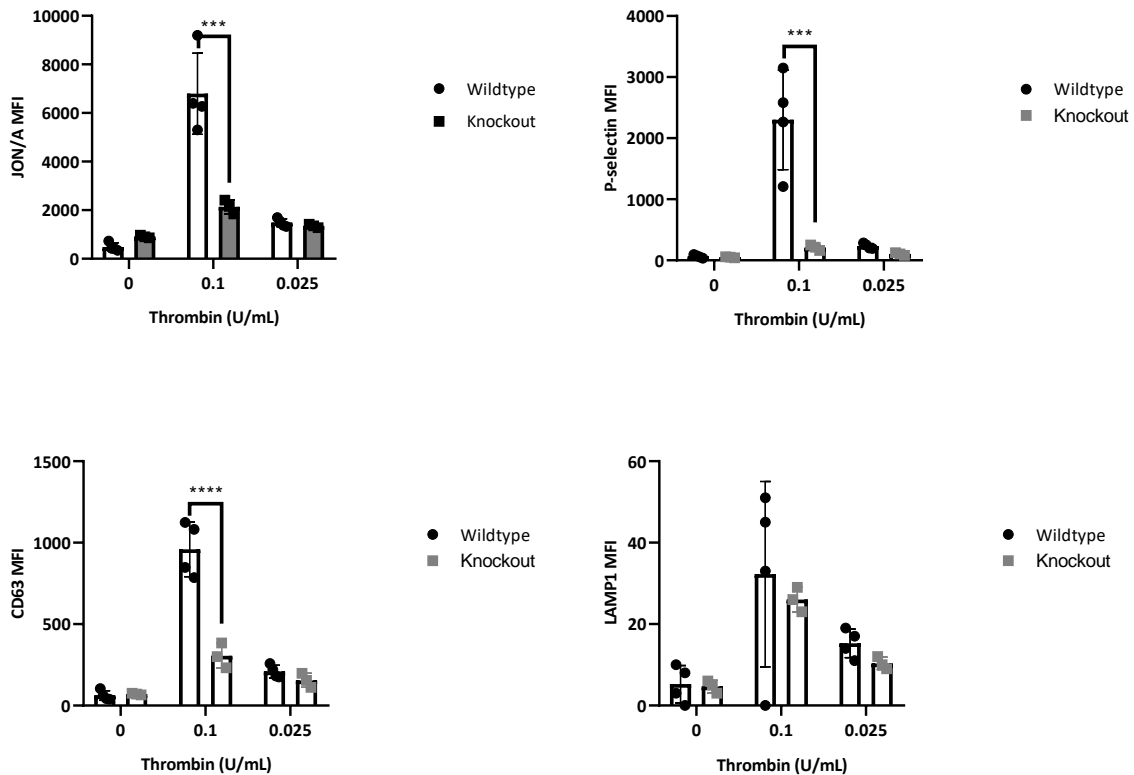


Figure 5-5. PDL-1 knockout significantly reduces granule secretion markers in response to thrombin stimulation. Whole blood collected in Sodium citrate 109mM via direct cardiac puncture was centrifuged at 90g for 6 minutes to separate PRP which was then centrifuged to pellet off platelets. The concentration was then corrected to 2.5×10^7 . Platelets were added to the antibody cocktail, Stimulated samples of thrombin were added at a dose of 0.1U/mL and incubated for 20 minutes at 37°C shielded from light. Following incubation samples were fixed in 0.2% formyl saline for 30 minutes at 4°C before centrifuging and resuspension of the pellet in 200µL formyl saline ready for acquisition. All compensation was conducted on BD DIVA and exported for further analysis using Flowjo where platelet populations were gated, and Median fluorescent intensity (mfi) was recorded. (a) The expression of Jon/A is similar between whole-body knockout and wild-type platelets, however, upon stimulation with 0.1U/mL thrombin there is a significant decrease in expression. This expression pattern is repeated for (b) P-selectin, and (c) CD63, (d) Lamp-1 exhibits a similar expression profile however the decrease in expression is not significant. graphs presented as MFI \pm standard error of mean (SEM) *P<0.05, **P<0.01 *p>0.05 **P>0.01 ***P>0.001. wt N=4 WbKO N=3

After demonstrating that whole-body and platelet-specific PD-L1 knockout have different effects on platelet aggregation and secretion, we interrogated the impact of PD-L1 blockade on platelet aggregation in humans using clinically available anti-PD-L1 blocking antibodies (Figure 5-6). To assess PD-L1 inhibition in human platelets, we treated platelets with either, Atezolizumab or Durvalumab, both of which are anti-PD-L1 monoclonal antibodies (mAbs) that are certified for treating non-small cell lung cancer and urothelial carcinoma (Krishnamurthy and Jimeno, 2017, Syed, 2017). The interaction of these antibodies with PD-L1 inhibits its binding to both PD-1 and CD80,

reducing the immunosuppressive nature of the tumour microenvironment. Unlike small molecule inhibitors which are often associated with off-target effects within cells, mAbs are much more selective and are associated with lower toxicity (Shepard et al., 2017). Atezolizumab and Durvalumab are engineered as IgG1 antibodies lacking glycosylation, achieved by a mutation at N297A. This modification to the antibody, attenuates the unwanted Fc-mediated antibody-dependent cytotoxicity. Durvalumab also incorporates modifications at L234F/L235E and P331S to achieve the same effect (Li et al., 2021, Liu et al., 2020).

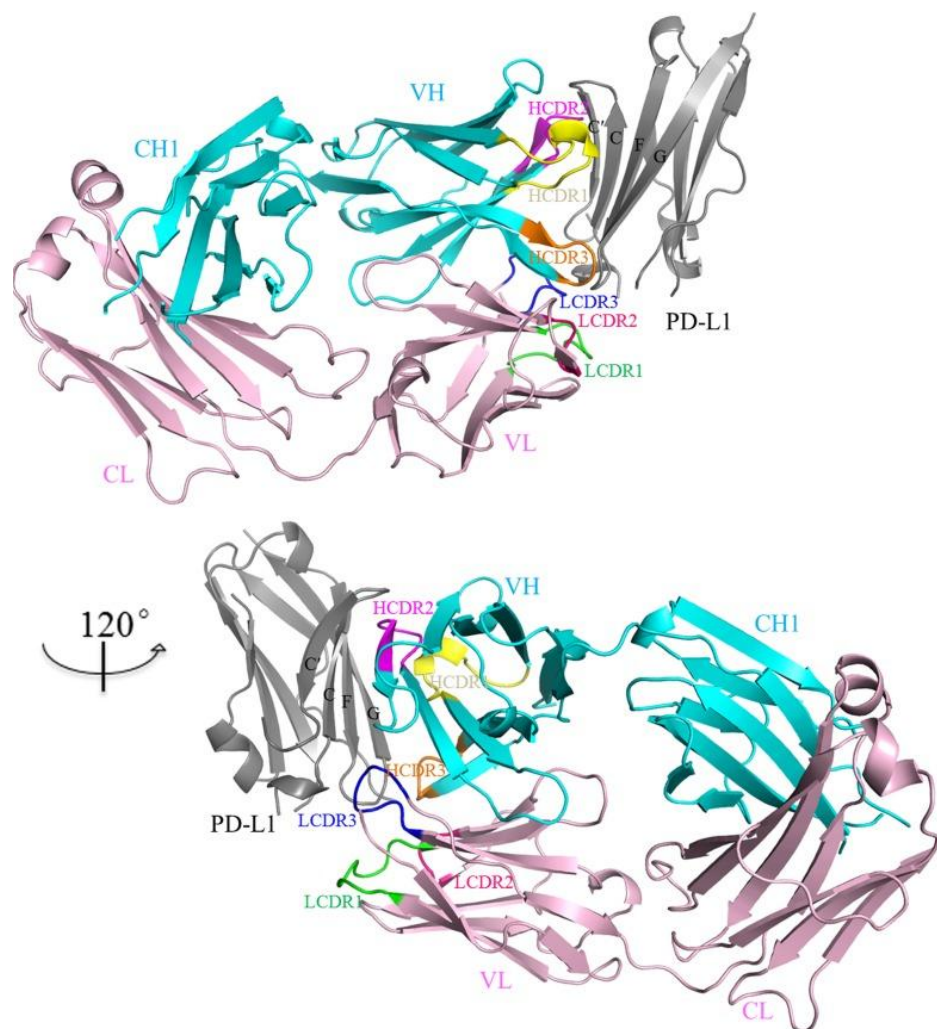


Figure 5-6. Overall structure of PD-L1/Atezolizumab complex. The IgV domain of PD-L1 is shown in grey and the heavy chain and light chain of Atezolizumab are shown in cyan and pink respectively. The Complementarity-determining region (CDR) loops from the heavy chain are coloured in yellow (HCDR1), magenta (HCDR2) and orange (HCDR3) respectively. The CDR loops from the light chain are coloured in green (LCDR1), hot pink (LCDR2) and blue (LCDR3) respectively. Atezolizumab binds the front β -sheet of PD-L1-IgV domain (grey) through three CDR loops from the heavy chain and CDR3 loop (LCDR3) from the light chain.

Initially, we tested the effects of Durvalumab and Atezolizumab on platelet aggregation in PRP (Figure 5-7). Both Durvalumab and Atezolizumab are used clinically at a dosage of 200 µg/mL in plasma, therefore we used dosages around this relevant concentration (Wu et al., 2022). Platelets were stimulated with 3µg/mL collagen following an initial incubation for 20 minutes with indicated inhibitor dosages under stirring conditions at 37°C. At the lowest dose, 100µg/mL Durvalumab and Atezolizumab reduced platelet aggregation from 76.0%±9.66 to 59.5%±16.5 and 59.0%±19.0 respectively, however, this was not a significant decrease due to the large variation in the dataset (Atezolizumab P=0.97, Durvalumab P=0.97). Interestingly, when the dose was doubled to 200µg/mL this reduction was no longer seen in comparison to the control samples Atezolizumab 73.66%±6.33 P= 0.999, Durvalumab 79.0%±6.24 P=0.999). When this dose was increased to 400 µg/mL, aggregation was almost completely abolished in the Durvalumab-treated platelets to 10.5%±0.5 (P=0.023), there was also a significant decrease in the sample incubated with Atezolizumab 28.0%±2.0 P=0.45.

Following inhibition of collagen-induced platelet aggregation activation at high dosages, we sought to assess whether the inhibitory effect is shared with other agonists. Therefore, we stimulated platelets with 0.05µM U41669. At the lowest dose of both inhibitors, there was no change in platelet aggregation: control = 84.00%±8.67 Atezolizumab 83.67%±0.88 P=0.99, Durvalumab 80.33%±1.20 P=0.99. Increasing the concentration of the PD-L1 inhibitors resulted in a downward trend in the aggregation, however, this was not significant (400µg/mL P=0.07). Additionally, we stimulated platelets with ADP to assess whether platelet activation through the P2Y1 and -12 pathways is compromised. Interestingly there was very little effect of PD-L1 inhibition following ADP stimulation, showing no significant decrease at any dosage, and the highest dose of inhibitor yielded no change in maximal aggregation (P=0.99).

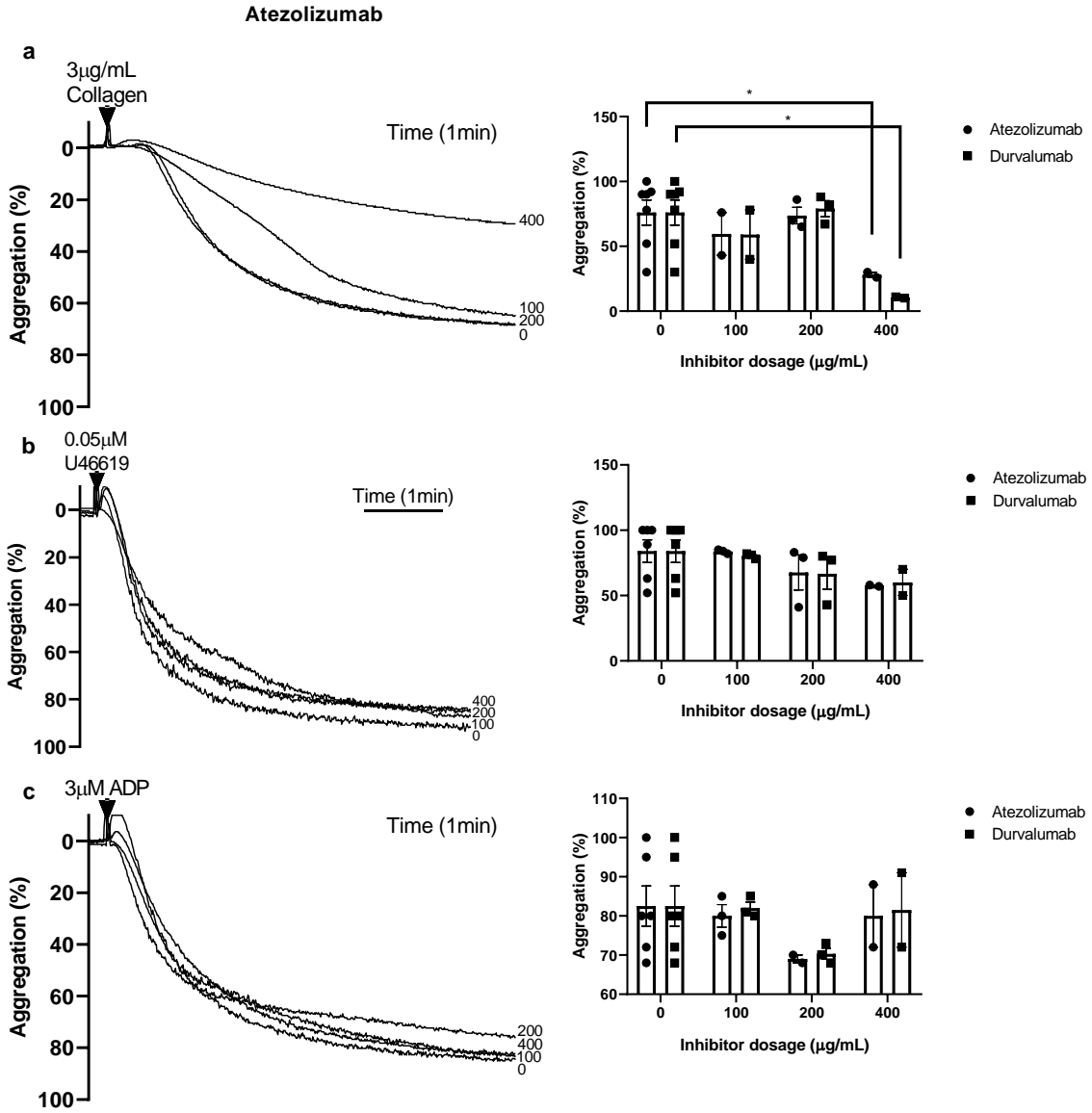


Figure 5-7. Platelet aggregation to agonists is differentially affected by PD-L1 blocking agents. PRP was isolated from healthy donor blood collected into 0.109M ACD by centrifugation at 190g for 15 minutes. Aggregation was measured on a chrono-log 4+4 aggregometer under stirring conditions (1000rpm). Platelets were stimulated with (a) 3.0 μg/mL collagen, (b) 0.05 μM U46619 or (c) 3 μM ADP. representative aggregation traces, the maximal aggregation at 5 minutes was recorded for indicated dosages of inhibitor, Presented as Percentage aggregation Mean ± standard error of mean (SEM) *P<0.05, **P<0.01. (N=5).

There is a basal expression of soluble PD-L1 in the plasma, therefore, using washed platelets, will allow us to assess the effects of platelet activation and secretion PD-L1 inhibition more accurately, and assess the effects of soluble PD-L1 in the plasma on platelet function. Platelets stimulated with 3µg/mL collagen had an average maximal aggregation of 70.25%±4.02, interestingly, following incubation with either 200 µg/mL Atezolizumab or Durvalumab for 15 minutes we saw no change in the ability of the platelets to aggregate (Atezolizumab 73.00%±3.0 P=0.99, Durvalumab 75.5%±7.5 P=0.99) (Figure 5-8). When dosages of inhibitor were increased to 400µg/mL, we observed a slight reduction in platelet aggregation in Atezolizumab -treated samples: 64.0%±2.0 (P=0.91), but a significant decrease to those incubated with Durvalumab: 41.5%±0.5 (P=0.008).

When washed platelets were stimulated with 0.05µM U46619 there was no change in the aggregation capacity of the platelets following incubation with Atezolizumab at any dosage (0 µg/mL 81.2%±5.8, 100 µg/mL 87%±1.00, 200 µg/mL 81.25%±4.46, 400µg/mL 81.33%±4.8). This was recapitulated when platelets were incubated with Durvalumab prior to stimulation with U46619 (0 µg/mL 81.2%±5.8, 100 µg/mL 88.5%±1.50, 200 µg/mL 75.5%±6.8, 400µg/mL 74.33%±7.1).

Additionally, when washed platelets were stimulated with 0.05U/mL, thrombin there was no significant change in platelet aggregation in samples treated with Druvalumab in comparison to, untreated samples. Interestingly, when platelets were incubated with Atezolizumab, there was a slight downward trend in platelet aggregation observed the highest dosages (400µg/mL P=0.274).

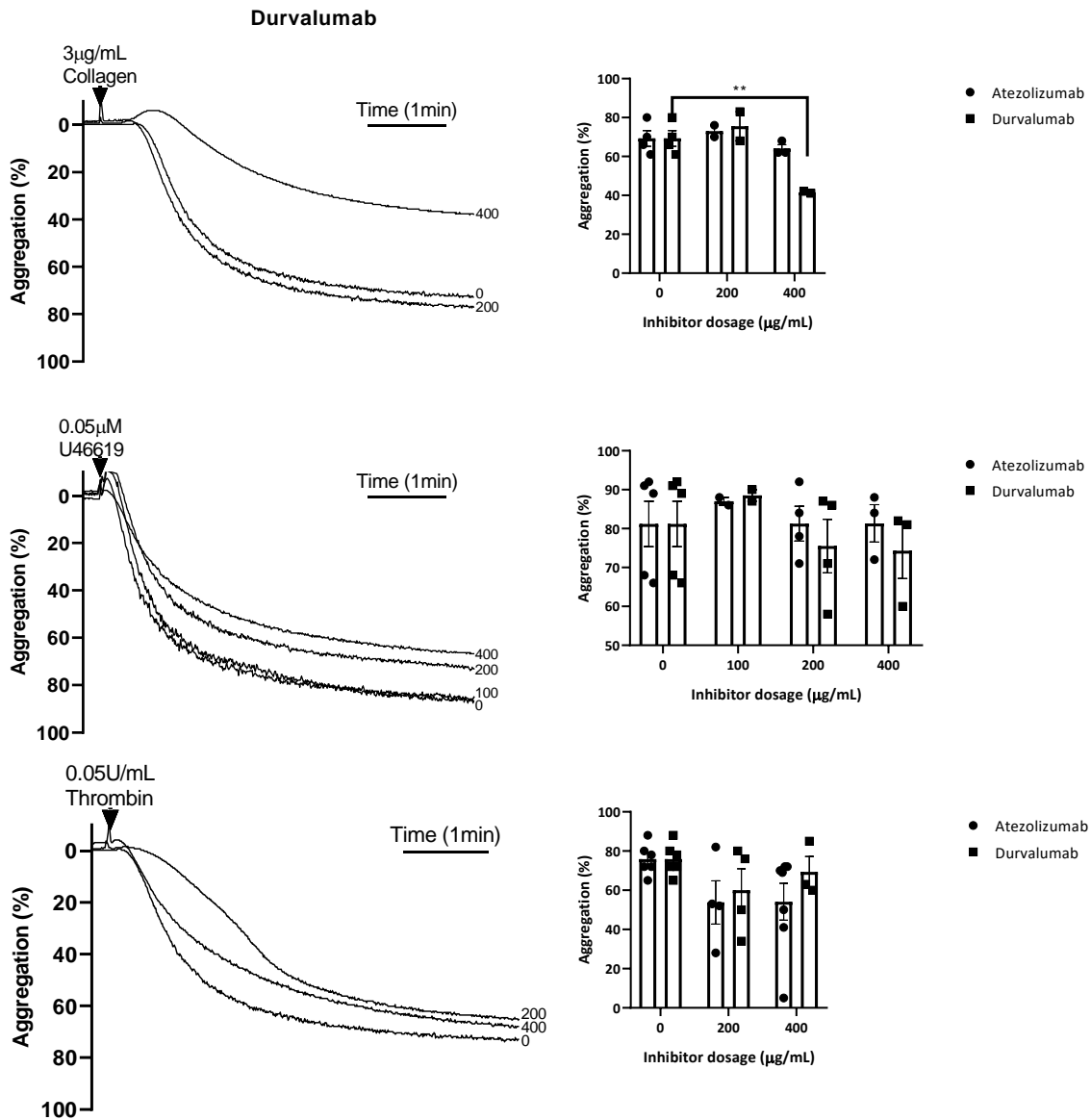


Figure 5-8. Commercial PD-L1 inhibitors Effect platelet aggregation to U41669 and thrombin but not collagen. Washed platelets were obtained by centrifuging PRP at 800g for 15 minutes, and resuspending platelets in Wash buffer before centrifuging a second time at 800g for 12 minutes and resuspending in modified Tyrode's buffer at a concentration of 3.0×10^8 platelets/ml. Aggregation was measured on a chrono-log 4+4 aggregometer under stirring conditions (1000rpm). Platelets were stimulated with (a) 3.0 µg/mL collagen, (b) 0.05 µM U46619 or (c) 0.05 U/mL thrombin. representative aggregation traces are presented alongside the maximal aggregation at 5 minutes was recorded for indicated dosages of inhibitor, Presented as Percentage aggregation Mean \pm standard error of mean (SEM) * $P < 0.05$, ** $P < 0.01$. (N=4).

5.2.1. Investigation platelet PD-L1 expression in MPN Patients

PD-L1 inhibitors have been used to treat multiple forms of cancer, such as non-small cell lung cancer (NSCLC), and renal cancers amongst others (Han et al., 2020b). Interestingly there have been studies that have shown that the increased levels of PD-L1 present on platelets in NSCLC patients in comparison to healthy donors, this has been postulated contribute to the efficacy of Atezolizumab (Colarusso et al., 2023). MPN patients often exhibit PD-1/PD-L1 mediated immune exhaustion, additionally, Essential Thrombocythemia (ET) that is characterised by an increased platelet count (Lee et al., 2022 {Prestipino, 2018 #730, Prestipino et al., 2018}).

Next, we aimed to assess the effects of PD-L1 inhibitors on platelet functionality in patients with MPN. In the first instance, we investigated whether incubation of patient platelets with PD=L1 inhibitors effected the aggregation capabilities of platelets from MPN patients. The patient cohort included all forms of MPN, and an age range of 35 to 88, with an average age of 65.5 years (Figure 5-9). The most frequent MPN observed was ET, making 41% of the dataset, whereas Polycythemia vera (PV) were (18.5%), RT (14.8%) and Myelofibrosis (MF) (11%). Additionally, 15% of patients did not have a known diagnosis. Following this, we compared the disease types to the age of the patients, interestingly, we observed PV patients tended to be younger than average. Myelofibrosis was characterised to be patients in the higher age range with RT patients clustering around the median age. ET on the other hand was heterogeneous and was diagnosed at all age ranges consisting of both the oldest and youngest participants of the study.

One of the main characteristic features of the different MPNs is the aberrant production of specific cell populations; PV is associated with the overproduction of RBCs, ET is characterised by the overproduction of platelets, MF results in scarring of the bone marrow, this can in turn cause either excessive RBC and platelet production or a reduction in these cell populations. We first compared the platelet counts from patients diagnosed within different patient groups. The ET group had the highest count with 745×10^6 platelets/ mL, this was significantly higher than the PV group with 323×10^6 platelets/ mL ($P=0.027$). Interestingly there was no significant difference between ET and Myelofibrosis, however, both samples were categorised as Myelofibrosis/ET ($P=0.94$).

Platelet aggregation was assessed following incubation with PD-L1 inhibitor followed by platelet stimulation with 0.025U/mL of thrombin. The overall data was highly variable due to the interpatient variability, and variations of therapies each participant was undertaking. In untreated platelets, the average aggregation at 5 minutes was $66.3\% \pm 9.84$ with a range of 62%. The interpatient range was consistently high throughout all treatment concentrations. Due to this high variability, there was no significant change in platelet aggregation at any dosage of Atezolizumab. However, when each patient dataset is assessed individually is a significant downward trend in platelet aggregation in response to increasing dosage of Atezolizumab ($P=0.0054$).

When overall platelet aggregation was assessed following incubation with Durvalumab, the data showed a similar pattern, with wide ranges at all treatment dosages. Although there was a general downward trend when assessed for the individual patient, this trend was not significant ($P=0.16$).

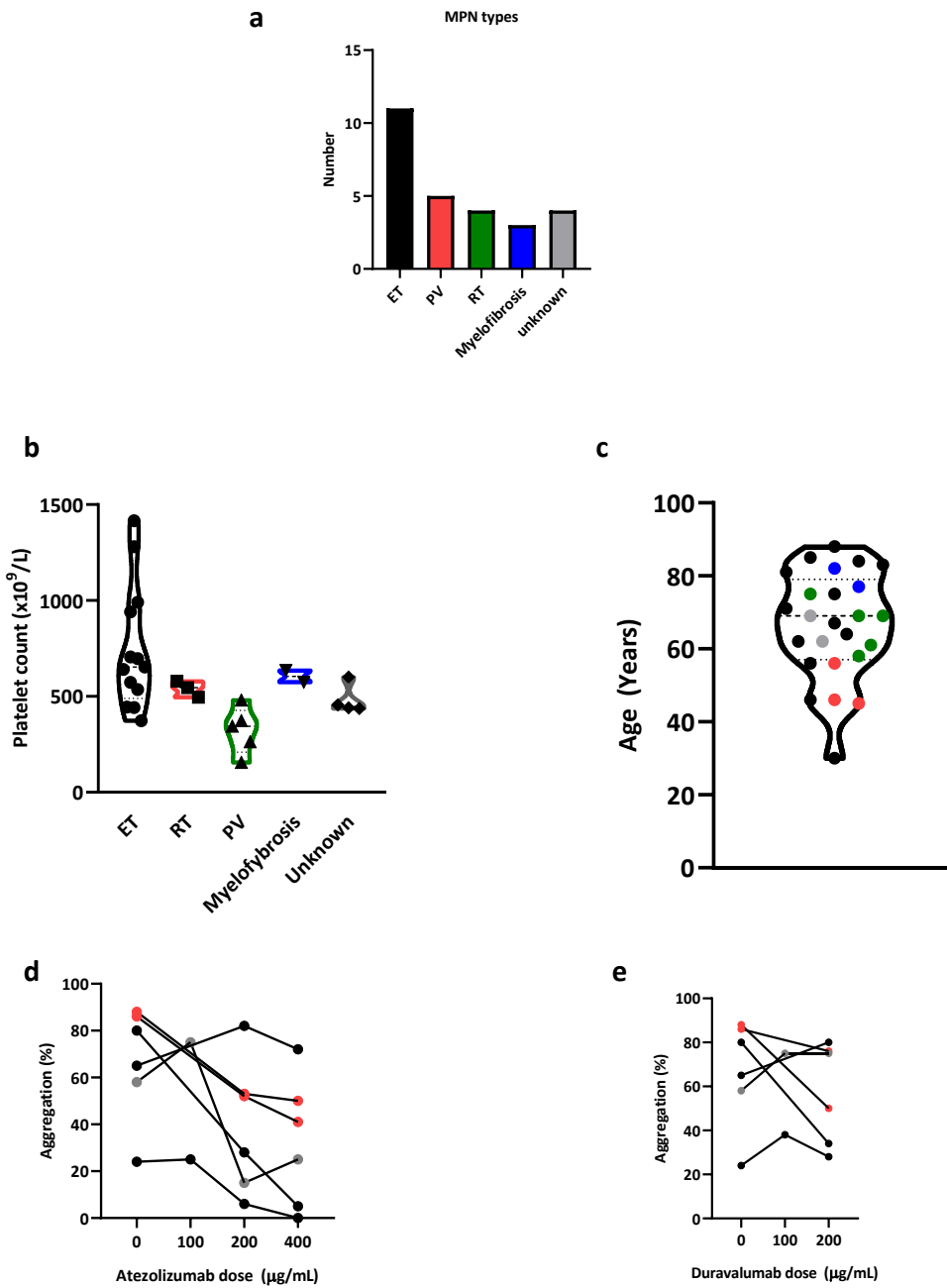


Figure 5-9. Platelets from MPN patients are significantly inhibited following incubation with PD-L1 inhibitors. (a) Subcategories of MPN patients. (b) the platelet counts of MPN patients were collected through full blood count (FBC) and plotted for their subtype of MPN. (c) the average age of MPN patients. Whole blood was collected in ACD vacutainers, Platelets were then prepared through centrifugation then washed for aggregation studies and then incubated for 15 minutes with either (d) Atezolizumab or (e) Durvalumab at indicated dosages.

In addition to platelet aggregation, we assessed the baseline expression of PD-L1 in the unstimulated platelet populations isolated from both healthy donors and patients with MPN (Figure 5-10). The median expression of PD-L1 on platelets was not significantly different between the healthy and MPN patients ($P=0.41$). However, when comparing the percentage of PD-L1 expressing platelets between healthy and MPN samples, significantly more MPN platelets expressed PD-L1 under unstimulated conditions ($P=0.0001$).

To elucidate this change, we compared the histograms of both the healthy control and MPN patient samples. This comparison showed that the similar PD-L1 MFI, was due to a bi-modal, non-Gaussian distribution of the cell populations. Both healthy donor and MPN patients had PD-L1 positive and PD-L1 negative populations, but with significantly different stoichiometry. Since MFI analysis is not applicable for bi-modal datasets, we focused on the percentage of PD-L1 positive cells alone. Interestingly, when comparing the disease types, we found that patients with RT had fewer PD-L1 positive platelets compared to other MPN patients. MPN patients with ET exhibited the greatest spread of PD-L1 expression on their platelets, with a large amount of PD-L1 positive cells and a consistently high percentage of positive cells. Patients with PV had a slightly lower percentage of PD-L1 positive platelet in comparison to the ET population, although this was not significant. However, there was a significant increase in the PD-L1 positive platelets across all MPN subtypes compared to healthy donors.

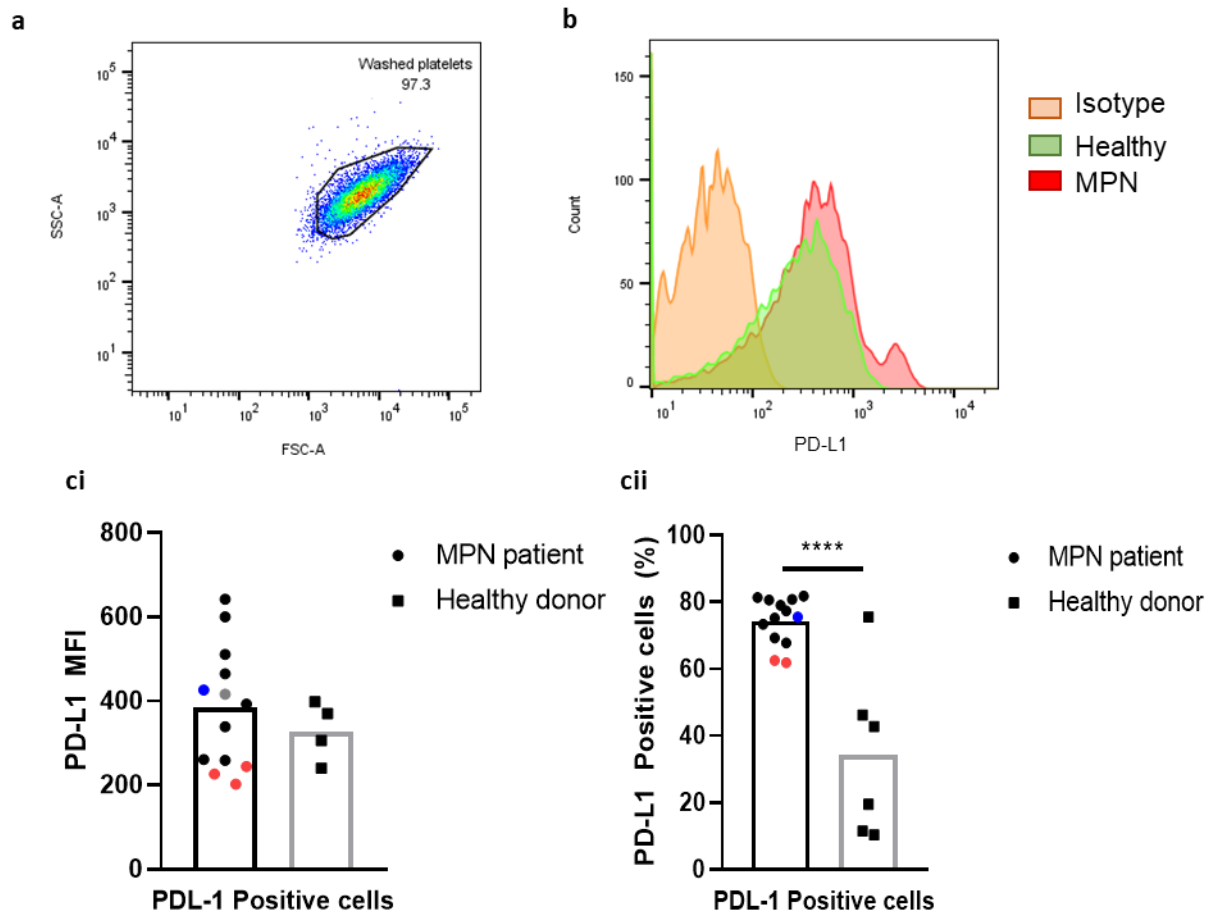


Figure 5-10. Patients with MPNs express similar levels of PD-L1 to healthy donors but by significantly fewer platelets. Whole blood was collected from patients with diagnosed MPNs into 109mM ACD. PRP was separated by centrifugation at 190g for 15 minutes. PRP was incubated in the presence of anti-PD-L1 for 15 minutes at 37°C. Following incubation samples were fixed in 0.2% formyl saline for 30 minutes at 4°C before centrifuging γ Representative histogram of PD-L1 expression for Isotype control (orange), healthy donor (green) and MPN Patient (Red). (ci) The median fluorescent intensity (MFI) was calculated on 10,000 events within the platelet gate. (cii), percentage PD-L1 positive cells, a Positive signal was established through gating against negative control populations and applying this gate to donor populations. Data presented as MFI \pm standard error of mean (SEM) * $P < 0.05$, ** $P < 0.01$ * $p > 0.05$ ** $P > 0.01$ *** $P > 0.001$. MPN N=13 Healthy control N=6.

Interferon-gamma (IFN- γ) is a cytokine that plays a key modulating role in immune responses, particularly in upregulating PD-L1 expression on T-cells (Saunders and Jetten, 1994). In this study, we investigated the effect of IFN- γ on PD-L1 expression in platelets by incubating them with varying doses and durations of IFN- γ exposure (Figure 5-11). In the first instance, we incubated platelets with 1000ng/mL of IFN- γ for up to 24 hours. We observed a basal level of PD-L1 expression on unstimulated platelets, which increased in a time-dependent manner up to 8 hours of incubation, reaching statistical significance ($P = 0.030$). Interestingly, by the 24-hour timepoint, PD-L1 expression decreased to levels similar to those observed after 2-hours of incubation with IFN- γ .

Next, we assessed whether PD-L1 expression was dose-dependent after 5 hours of incubation with IFN- γ . Platelets exposed to 100ng/mL of IFN- γ did not show a significant increase in PD-L1 expression, although there was a trend towards significance ($P=0.061$). However, incubation with 500ng/mL of IFN- γ significantly increased PD-L1 expression compared to unstimulated samples ($P=0.014$). The highest dose tested, 1000 ng/mL, resulted in the largest increase in PD-L1 expression ($P=0.003$). Taken together, these findings indicate that platelets increase PD-L1 expression in response to IFN- γ exposure in a time- and dose-dependent manner up to 8 hours of incubation.

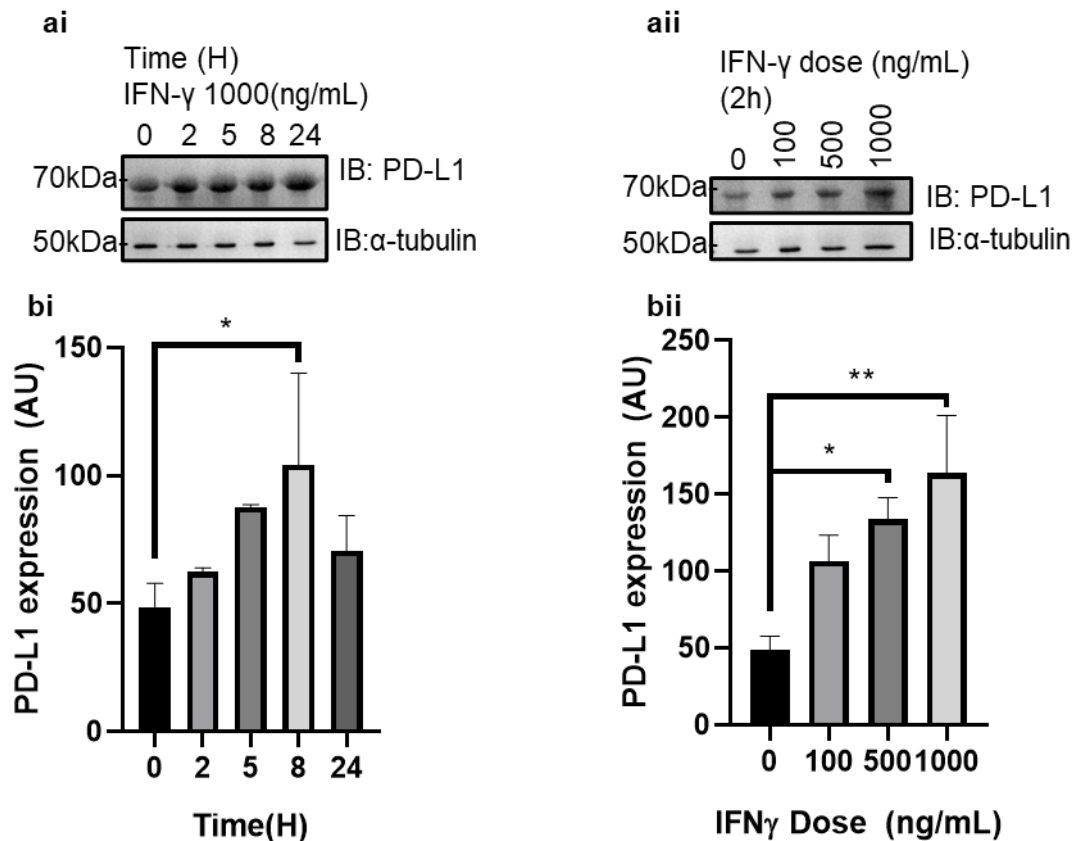


Figure 5-11. Incubation of platelets with IFN- γ increases PD-L1 expression in a time-dependent manner. (ai) Platelets were incubated with 1000ng IFN- γ for the indicated time points and incubated at 37°C. (a ii) IFN- γ was added at indicated doses to platelets and incubated at 37°C for 5 hours. (bi-ii) Densitometry of PD-L1 signal against α -tubulin was conducted and represented as AU, Mean \pm standard error of mean (SEM) * $P < 0.05$, ** $P < 0.01$ * $p > 0.05$ ** $P > 0.01$ *** $P > 0.001$. N=3.

Finally, we assessed whether the increased PD-L1 expression observed in MPN patients was caused by a primary platelet defect in the plasma environment (Figure 5-12). To explore this, we conducted a plasma swap experiment where healthy donor platelets were incubated in the plasma of MPN patients. Both healthy donor and patient platelets underwent standard isolation protocol, after which healthy donor platelets were resuspended in MPN patient plasma for 5 hours. Healthy donor platelets had a low basal expression of PD-L1. By contrast, MPN patient platelets showed a significantly higher PD-L1 expression. Following incubation in MPN plasma, healthy donor platelets displayed a marked increase in PD-L1 expression compared to their basal level. Interestingly, PD-L1 expression was not significantly different between the MPN and plasma-swapped healthy platelets. These results suggest that the elevated PD-L1 expression observed in MPN patients may be influenced by factors present in the plasma environment rather than solely by a primary defect within the platelets themselves.

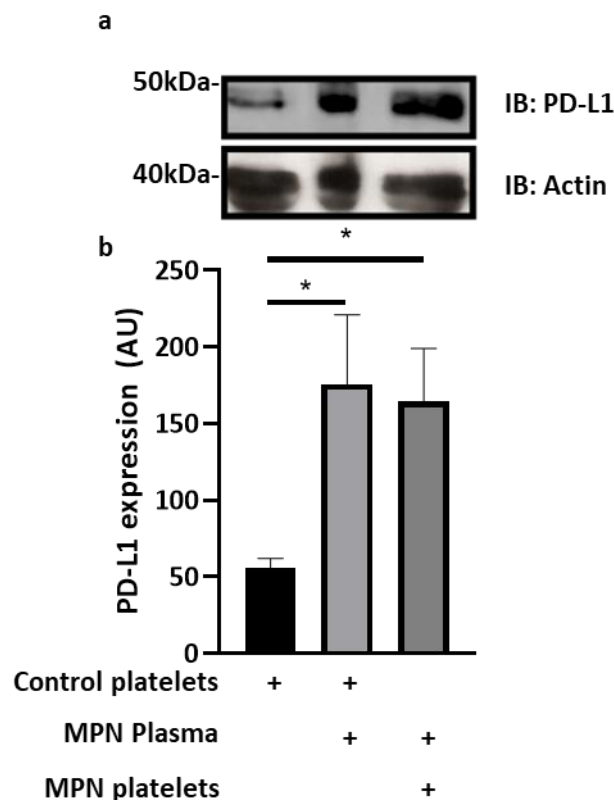


Figure 5-12. Incubation of healthy donor platelets in MPN plasma increases PD-L1 expression. Washed platelets were prepared as in prior experiments, after washing healthy donor platelets were resuspended in equal volumes of PPP acquired from the MPN platelet preparation. Platelets were then incubated for 5 hours at 37°C before lysis and the addition of lamelli buffer. Samples were then run on SDS PAGE and transferred to PVDF membranes, which were blocked with 5% BSA before probing with anti-PD-L1 antibody. Densitometry was then conducted on the western blots and presented as Mean \pm standard error of the mean (SEM) * $P < 0.05$. $N = 4$.

5.3. Discussion

The initial work in this chapter began with the generation and quantification of PD-L1 knockout mice. We confirmed the total deletion of PD-L1 in PD-L1^{-/-} mice using western blotting, this was comparable with the quantification in the original knockout generation study. When quantifying the knockout of PD-L1 in the platelet-specific mice we observed some presented with a very faint band for PD-L1, whereas others were completely clear in the western blot in the platelet sample, showing there was still a small amount of PD-L1 expression in some platelet samples.

The Flox model that we used as a basis for the generation of the platelet-specific PD-L1 knockout had been developed by Sage et al. (2018) where they show a small decrease in PD-L1 expression before the addition of cre. The GPIb^{cre} model was chosen over the PF4^{cre} due to the function of PF4 in lymphoid- and myeloid-derived cells, resulting in off-target knockdown in subpopulations of leukocytes and macrophages (Beckers et al., 2017). The use of the Gplb^{cre} knockout may not ablate the expression of targeted genes as effectively as PF4 due to the expression of GPIb later in megakaryopoiesis, this may result in a small amount of the target protein being expressed in the platelet, albeit unquantified to date (Gollomp and Poncz, 2019). However, the expression of PD-L1 seen may be a result of the uptake of PD-L1 from other cell types and not solely from the incomplete knockout of PD-L1 (Hinterleitner et al., 2021). The heterozygous expression of GPIb Cre yielded identical knockout levels to homozygous Gplb^{Cre} mice.

Initial platelet examination showed a modest decrease in platelet aggregation in response to thrombin, in the whole-body knockout, in comparison, a study by (Li et al., 2022) demonstrated a more significant impact on platelet aggregation. However, the data shown in this project represent a small dataset, the data show a downward trend a larger dataset is needed to assess whether this is significant. Interestingly the study by (Li et al., 2022) shows a significant decrease in platelet aggregation in response to stimulation by collagen, ADP or U46619. We also found a modest decrease in the aggregation of whole-body PD-L1 KO platelets in response to collagen, however, this decrease was not as pronounced. Both our study and the research by Li, (2022) suggest that the aggregation defects can be ameliorated by increased dosages of agonist. When we assessed platelet activation and secretion, we observed a disproportionately large decrease in JON/A, P-selectin, CD63 and LAMP1 expression

on stimulated PD-L1 knockout platelets compared to the decrease in platelet aggregation. P-selectin and JON/A expression decreases were comparable to those reported by Li (2022) in response to thrombin.

We also used anti-PD-L1 inhibitors to examine whether inhibition of PD-L1 in platelets reduces platelet aggregation, we calculated the dosage used clinically and tested relevant dosages. For both antibodies, this was approximately 200µg/mL (Morrissey et al., 2019 {Denault, 2022 #724, Denault et al., 2022}). Durvalumab is a human IgG1k anti-PD-L1 antibody which was engineered with three amino acid substitutions, (L238F, L239E and P335S) which are reported to reduce Fc-Mediated effector functions, to prevent depletion of PD-L1+ T-Cells. Atezolizumab is a humanised IgG1 monoclonal antibody originating from Chinese hamster ovary cells. Similarly to Durvalumab, the Fc region has been engineered to reduce Fc effector function to minimise antibody-dependent cell-mediated toxicity (Deng et al., 2016).

There are no public data for the effects of either Atezolizumab or Durvalumab on platelet functionality, however, there are reports for both resulting in immune-mediated thrombocytopenia following administration (Dougherty et al., 2021, Qiu et al., 2022). Although, these effects could be due to platelets specifically, our data that the milieu has a not insignificant effect on the ability of the platelets to function (Jackson, 2007).

When assessing the platelet counts between the subcategories of MPN; as expected, the ET patients exhibited a significantly higher platelet count than those with PV, interestingly the myelofibrosis cohort also has a high platelet count, which contrasts with previous research stating that myelofibrosis patients have a normal or low platelet count (Masarova et al., 2018). The average age for MPN patients at 66, this was significantly higher than that of the healthy donor cohort. It has been demonstrated that age has a significant effect, reducing platelet count and increasing procoagulant activity (Le Blanc and Lordkipanidzé, 2019, Cowman et al., 2015).

When assessing the amount of PD-L1 present on the cell surface in both the healthy control and MPN platelets we saw a similar median PD-L1 expression on platelets between groups. However, the MPN patients had significantly more platelets that expressed PD-L1, taken together these show that although per platelet the expression is unchanged, the total amount of PD-L1 expressed is significantly higher in the patient cohort.

When patient platelets were stimulated with thrombin and incubated with either Atezolizumab or Durvalumab the general trend was unclear due to the large variance between patients, this was compounded by the anti-platelet therapies that were being administered clinically. This resulted in multiple samples failing to aggregate with a high dose of thrombin with no addition of PD-L1 inhibitor, these data points were deemed unusable for aggregation studies.

IFN- γ has been shown in multiple studies to upregulate the expression of PD-L1 on T-cells (Crouse et al., 2015, Garcia-Diaz et al., 2017, Imai et al., 2020). In our research, we showed that IFN- γ also upregulates PD-L1 expression in platelets. This study presents the first documented instance of the effects of IFN- γ on platelet PD-L1 expression. Our findings demonstrate that PD-L1 expression increases in a time-dependent manner, reaching its peak at 8 hours. This granular assessment of IFN- γ stimulated PD-L1 expression has not been previously explored in the context of platelets; this is an important factor in cancer due to the upregulation of IFN- γ that is frequently observed in many cancer types (Jorgovanovic et al., 2020).

The use of plasma exchange from healthy donors to patients with metastatic melanoma has been demonstrated to efficiently reduce the total PD-L1 expression levels *in vivo* (Davidson et al., 2022) (Jacob et al., 2020). Here we showed that adding plasma from MPN patients to healthy donor platelets, dramatically increased the expression of PD-L1 on platelets, showing that the assumed mechanism of JAK2 mutations upregulating PD-L1 expression may only be a co-factor in the overall levels of PD-L1 expression on cells. This is the first assessment of this interaction and therefore we are unable to compare this to previous research. However, it is a known function of the platelet to present antigens and other molecules to immune cells (Garraud et al., 2019).

In summary, we have generated a unique platelet-specific knockout for PD-L1, which will allow us to examine the impact of platelet PD-L1 in isolation *in vivo*. We demonstrated that PD-L1 deletion reduces the aggregation capability of platelets, which is more substantial on a whole-body knockout, showing that expression of PD-L1 has a role in platelet aggregation, and is likely dependent on PD-L1 uptake from other cell types. We also found that the reduction of platelet aggregation may be due to reduced platelet activation and secretion of granular contents. Furthermore, we

show that MPN patients have a significantly increased amount of PD-L1 positive platelets and, in turn, show an increased sensitivity to PD-L1 inhibitors. We also demonstrated that the upregulation of PD-L1 expression, specifically on platelets in patients with MPN is not determined by the JAK2 mutation, but by soluble components within the plasma.

5.3.1. Limitations

The platelet-specific knockout model while being one of a kind and allowing for further insight into the effects of PD-L1 specifically on platelets was very time-consuming and costly to develop and breed. Once breeding pairs were finalised the number of experimental animals and volumes of blood that were possible to acquire were very low which limits the amount of data that was possible to be attained in this thesis.

The generation of the platelet-specific knockout mice took much longer than expected. This was due to multiple extraneous factors. Firstly, due to logistical issues, there was an 8-month period following the arrival of the first mouse strain where there was no viable mate for breeding. Following this we received news that some of the mice we were sent may have had an additional CD11b Cre knock in. This set us back twofold, at the time we were on the F2 generation of breeding, when we tested for CD11b deletion we saw that the mice were indeed bearing an additional knockout of the CD11b gene. Therefore, we had to reestablish the PD-L1^{Flox/Flox} colony to a point where they only contained the single modification, to the PD-L1 gene. Following this we could then begin breeding again and generation of the platelet-specific knockout, in total, to establish the genotype and restart breeding it set us back a further 8 months.

The Gplb^{cre}-derived platelet-specific knockout of PD-L1 is more specific to platelets, where it does not result in the knockout of target protein in subpopulations of leukocytes and macrophages (Beckers et al., 2017). With the cre knock into the Gplb gene, there is only 1 intact copy, its effect has not been quantified, however has been postulated that it may affect both MK and platelet biology (Nagy et al., 2019).

The acquisition of MPN blood was also limited, which was compounded by the heterogeneity of samples due to multiple factors, such as drug administration, MPN subtype, age and further co-morbidities. With multiple donors being on many anti-platelet therapies such as aspirin and clopidogrel alongside additional drugs which has

also been reported to effect either platelet count or function, such as Hydroxycarbamide and Busulphan, thus the data for each cohort was highly variable. Furthermore, the patients in the PV cohort often had such thrombocytopenia to such a degree, that the number of platelets in the volume given resulted in insufficient platelet counts for comparable aggregometry experiments. This study did also not assess other forms of PD-L1 such as released and soluble forms of PD-L1 or that released in exosomes which may have been released from the platelets and play a significant role. Additionally, we did not assess the expression of IFN- γ , or other cytokines such as IL-27 which has also been observed to induce PD-L1 expression, due to budget and time constraints (Shuming et al., 2019).

5.4. Future work

Further characterisation of the platelet-specific knockout is needed to fully assess the effects of PD-L1 knockout specifically on platelets. Initial characterisation of aggregation to a broader range of agonists and dosages both in washed and PRP conditions will give a more rounded picture of the effects PD-L1 on the milieu. Alongside this, thrombus formation and clot retraction assays will be important to assess the capability of platelets to form a stable thrombus. There are also signalling studies that need to be addressed to elucidate whether there are additional pathways in which PD-L1 acts upon the platelet besides the reported Caspase 3/GDSME pathway reported by Li (2022).

Upon stimulation through IFN- γ , PD-L1 is upregulated on the cell membrane, however, alternate expression also occurs in many cell types. Alongside standard membrane presentation, the exosomes containing PD-L1 can also be released from the cell. Alternate splicing events can produce soluble variants of PD-L1 which can then be measured in the plasma (Imai et al., 2020). Given this, the amount of exosome-bound PD-L1 and soluble PD-L1 can be measured to assess the full extent of expression, and whether the form of expression changes over time. With a larger patient dataset, it will be possible to delineate trends within the different MPNs for both platelet function and PD-L1 expression. We will also be able to use this to assess the effects of PD-L1 overexpression on the interaction between platelets and immune cells.

Utilising both the MPN samples and the knockout mouse models we plan to assess the function of PD-L1 in platelet-immune cell interactions. The knockout will also give the ability to assess these interactions in further disease states, such as diabetes and atherosclerosis.

Chapter 6. Discussion

Platelets are crucial components of haemostasis and play pivotal roles in thrombosis, inflammation, and immune responses. Recent studies have implicated α -synuclein, a protein traditionally associated with neurodegenerative diseases like Parkinson's Disease, in platelet function. In this thesis, we use pharmacological inhibitors and genetic knockout models to investigate α -synuclein's role in platelet biology. Furthermore, the study aims to elucidate the impact of PD-L1 deletion on platelet function, and interaction with immune cells, through the generation of a platelet-specific PD-L1 knockout mouse model.

6.1. Summary of Results

This study began by assessing the haemostatic function of platelets using pharmacological inhibitors targeting α -synuclein in human platelets *in vitro*, and a whole-body α -synuclein knockout mouse model. Our experiments demonstrated a dose-dependent inhibition of platelet aggregation following treatment with the α -synuclein inhibitor ELN484228. Subsequent investigations focused on α -synuclein's localisation and dynamics within platelets, particularly its translocation upon thrombin stimulation and interaction with key SNARE proteins such as VAMP8.

We demonstrated a dose-dependent inhibition of platelet aggregation following treatment with the ELN484228. Upon thrombin stimulation, α -synuclein translocates from a homogeneous distribution to peripheral localisation on the platelet surface, rather than secretion. The distribution of α -synuclein was also shown to be highly analogous to that of VAMP8, with increased co-localisation events following stimulation. Interestingly, although we observed a significant decrease in aggregation when stimulated with collagen or thrombin, this was not recapitulated in U46619, although this could be due to the weak inhibitory effect of the inhibitor, at lower dosages over a longer period this may have a greater effect. Furthermore, we found α -synuclein to be in a complex with syntaxin11, -4 and VAMP8 under unstimulated conditions, with increased interactions following thrombin-stimulation. We also showed that α -synuclein is phosphorylated at serine129 following stimulation with thrombin, collagen and U46619, but not CRP-XL, the increase of phosphorylation in response to agonists has not been reported in any other study. The phosphorylation of serine129 was reduced through the inhibition of RhoA/ROCK by Y-27632 and the

chelation of intracellular calcium with BAPTA-AM, previous studies have shown other inhibitors such as polo-like kinases (PLKs) to inhibit α -synuclein^{ser129} formation, however, this is the first demonstration of RhoA/ROCK inhibition (Teil et al., 2020).

In α -synuclein knockout mice, we showed a distinct bleeding phenotype which, upon further interrogation, was at least in part attributed to a significant reduction in the capability of platelets to release their granular cargo - quantified using flow cytometry. We further interrogated secretion through single-cell flow cytometric analysis which showed the ablation of a “hyper-secretory” population in the standard platelet population when stimulated with thrombin and U46619. This phenotype was corroborated *in vitro* by reduced aggregation and the formation of unstable thrombus formation under flow conditions.

Following this we sought to observe the effects of α -synuclein knockout in endotoxemia, due to the resulting in platelet activation and P-selectin expression over time (Schrottmaier et al., 2016, Violi et al., 2024). Interestingly, we did not observe a significant difference in secretory markers between knockout and wild-type mice with endotoxemia, however, we showed a higher level of P-selectin expressing platelets in unstimulated conditions this is concordant with previous studies (Schrottmaier et al., 2016). Alongside this, we did note that the α -synuclein deficient mice showed a higher clinical score and were more susceptible to endotoxemia than their wild-type littermates.

In addition to our finding that platelet secretion deficiencies worsen outcomes in endotoxemia, it has been demonstrated that platelets can interact with the immune system through multiple pathways (Ali et al., 2015, Arman and Krauel, 2015, Manne et al., 2017). We successfully generated a platelet-specific PD-L1 knockout mouse model (PLT-PD-L1^{-/-}) to investigate the effect of platelets in the immune response with a focus on the PD1/PD-L1 axis. We showed that PD-L1 deletion in platelets or the whole body led to a reduced aggregation in response to thrombin, although PLT-PD-L1^{-/-} showed a milder effect. Interestingly, we saw a significant decrease in platelet integrin activation and markers associated with α - and dense granule release, while lysosome markers were unaffected.

We then assessed the efficacy of PD-L1 inhibitors in healthy human donors. We did not observe a significant change in response to thrombin when we assessed the

aggregation of washed platelets treated with the PD-L1 inhibitors; Atezolizumab and Durvalumab. However, we did see a significant decrease in high dosages of inhibitors when stimulated with collagen, when assessing the aggregation in PRP this inhibition to collagen stimulation was increased. This trend was recapitulated when stimulated with U46619, however, the decrease in aggregation was slight.

We then sought to assess alterations in platelet function in MPN patients, who commonly overexpress PD-L1, and whether these were reversible following inhibition with PD-L1 inhibitors. We characterised PD-L1 expression on the platelets in MPN patients, where we observed a significant increase in the amount of PD-L1 positive platelets. When MPN platelets were treated with Atezolizumab and Durvalumab we showed that there is a downward trend in their ability to aggregate. Alongside this, we assessed the effect of IFN- γ on washed platelets and demonstrated a significant time and dose-dependent increase of PD-L1 in response. When we incubated healthy donor platelets with plasma from MPN patients, we observed a significant increase in the expression of PD-L1.

6.1.1. Interpretation of the overall findings

First, we established the presence of α -synuclein in washed platelets, which is concordant with previous proteomic studies (Senzel et al., 2009). Furthermore, we have characterised, for the first time, the distribution of α -synuclein in resting platelets and its movement following stimulation. Previously the movement of α -synuclein has only been assessed in neural cells (Holmqvist et al., 2014, Ulusoy et al., 2017). Interestingly, in aggregation studies, we saw a large range of results following inhibition with ELN484228 in human platelets. This observation may be due to varying levels of α -synuclein between donors, with participants with high levels of platelet α -synuclein exhibiting a larger inhibition than those with a lower level.

We showed that α -synuclein is homogeneously clustered throughout the platelet in unstimulated conditions, co-localising with VAMP8; following stimulation the α -synuclein was translocated to the peripheries of the cell. This finding has not been reported previously in platelets. However, a similar mechanism has been reported in neurons; with its interaction with VAMP2 exhibiting a chaperoning effect before being recycled back into the neuron (Maroteaux et al., 1988). By contrast, we demonstrate

that, in platelets, α -synuclein remains at the outer membrane following translocation. Alongside interaction with VAMP8, we also show an increase in interaction with STX11 following stimulation with thrombin; neither of which has been observed in the neural cells. Although α -synuclein is known to exhibit promiscuous binding, these data show that α -synuclein binding partners can vary depending on cell type and function (Longhena et al., 2019).

The interaction of α -synuclein with various SNARE proteins following platelet activation indicates that α -synuclein is an integral part of the SNARE complex and remains in the membrane of the platelet following membrane mixing of the granule to the target; this highlights another difference in the mechanism due to α -synuclein being secreted by exosomes from neural cells (Emmanouilidou et al., 2010). We also showed that the activation of platelets induced phosphorylation of α -synuclein, this is concordant with prior research which has linked serine129 phosphorylation with facilitating protein-protein interactions in neurons (Parra-Rivas et al., 2023). The phosphorylation of α -synuclein for physiological function may provide new insights into the extent of α -synuclein functionality.

We also show that calcium chelation significantly decreased α -synuclein phosphorylation. Whilst it is known that calcium is required for modulating synaptic vesicle interaction, as is phosphorylation at serine129, these functions have not been linked (Lautenschläger et al., 2018, Lu et al., 2011). We also show that phosphorylation of α -synuclein increases in both a time- and dose-dependent manner; interestingly, at all-time points observed the phosphorylation does not decrease, showing that unlike in other cell types, its phosphorylation does not appear to be reversed.

We propose that both calcium and the Rho/ROCK pathways are required for serine129 phosphorylation within platelets, as blocking either pathway results in complete ablation of serine129 phosphorylation following platelet activation. This pathway is yet to be elucidated, however, previous studies have also observed the Rho/ROCK pathway affecting α -synuclein function, it is released from neurons and in an extracellular milieu (Zhou et al., 2011).

The bleeding time assay showed that the α -synuclein knockout bled for significantly longer than the wild-type. Additionally, we showed that the mice were significantly more susceptible to rebleeding events. This was recapitulated in *in vitro* flow studies, where thrombi were formed then washed with PBS, and were significantly smaller in volume to the wild-types. Whilst this study focused primarily on platelet α -synuclein, previous studies have shown that exogenous α -synuclein can inhibit thrombin-induced platelet activation (Acquasaliente et al., 2022). If this is accurate, the expected inhibitory effect induced by the presence of α -synuclein in the plasma would increase thrombus formation and size, however, we observed the opposite. Comparing exogenous recombinant protein and knockout models is not possible, although the study by Acquasaliente et al. (2022) may highlight an additional role of α -synuclein on platelets.

When we subjected mice to endotoxemia, the α -synuclein knockout mice were more susceptible, having significantly higher clinical scores. Interestingly, this heightened susceptibility did not correspond with changes in platelet secretion markers, suggesting additional roles for α -synuclein during endotoxemia. This finding aligns with previous studies demonstrating that α -synuclein is involved in various aspects of the immune system, including B cell Lymphopoiesis to ROS generation (Grozdanov and Danzer, 2020, Pei and Maitta, 2019, Allen Reish and Standaert, 2015). Additionally, it has been shown that NK cells scavenge α -synuclein aggregates, this could be an additional mechanism for the removal of platelets following activation (Earls et al., 2020).

6.1.2. Smith 2023 paper

In 2023, a study by Smith et al., reported that an α -synuclein knockout mice displayed no significant bleeding diathesis when tested, which is in contrast to our findings (Smith et al., 2023). However, similar to our results, the Smith study reported a modest defect in activation-dependent platelet secretion and a co-localisation of α -synuclein with α -granules. They also did not observe any compensatory changes in the expression of SNARE complex proteins.

The Smith study utilised a knockout generated by a different group, which has a different construction to the one used in this study (Abeliovich et al., 2000). The

method of euthanasia used is comparable to ours, blood collection procedures varied significantly. The Smith study exposed the thoracic region and collected blood into sodium citrate, apyrase, and prostaglandin, whereas we collected into sodium citrate alone via direct cardiac puncture without inducing injury and potential pre-activation of platelets. The Smith study also added 1mM CaCl₂ back into the washed platelets before experimentation. Studies have shown that the addition of CaCl₂ induces morphological changes, microparticle release and fibrin formation, alongside the increase of P-Selectin expression (Toyoda et al., 2018). Because we demonstrated that the phosphorylation of α -synuclein is calcium-dependent, the addition of the CaCl₂ may have affected this platelet activation.

Although multiple findings express a similar trend in *in vitro* experiments, the overall phenotype observed in the Smith paper is significantly different. This highlights an inherent weakness of knockout murine models, although the same gene may be removed/inhibited, due to different methods of removal, there can still be a somewhat differential expression on a protein level. Additionally, genetic drift occurs in isolated populations of mice with insufficient backcrossing.

Taken together, we show that α -synuclein is an important member of the secretory machinery, which interacts with the SNARE complex, although with sufficient stimulation the *in vitro* deficiencies can be overcome. α -synuclein is also phosphorylated downstream the RhoA/ROCK pathway and in a calcium-dependent manner. α -synuclein associates with the granules and VAMP8 within platelets but is not part of the granular contents and is not released upon granular secretion but does move and is presented on the platelet membrane (Figure 6-1).

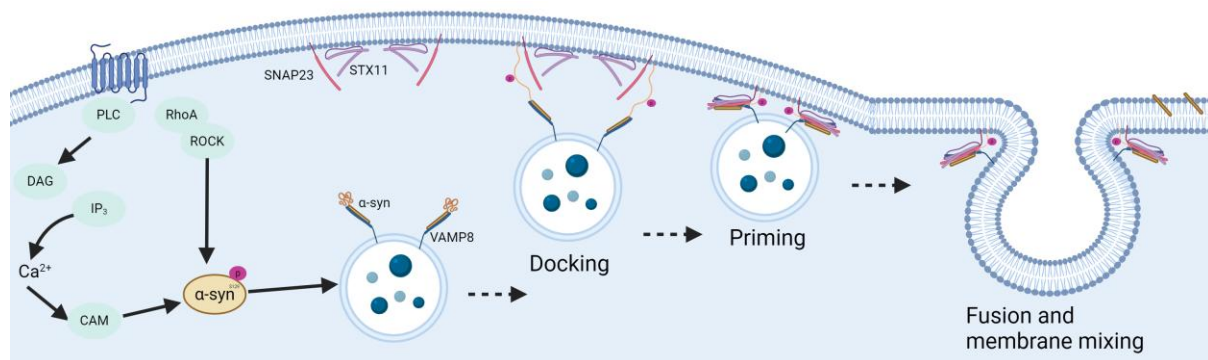


Figure 6-1. Proposed mechanism of action for α -synuclein in platelet granule secretion.

To further elucidate the role of α -synuclein, the use of a platelet-specific knockout should be utilised, especially for any involvement with the immune system. Further quantification of the interaction partners of α -synuclein, utilising a top-down proteomic approach in both unstimulated and stimulated conditions would allow for a broader picture of the role of α -synuclein within the platelet environment. Quantifying the amount of α -synuclein in platelets from healthy donors versus that in PD patients, alongside platelet function studies, may also highlight whether under- or over-expression of α -synuclein affects platelets in humans. To ensure there are no off-target effects of ELN484228, further testing in the platelet milieu must be completed, in the form of a microarray or proteomic analysis to aid in further human platelet testing.

At the time of research, the role of α -synuclein was untested in the platelet milieu, following the study by (Smith et al., 2023), we can compare aspects of both studies to draw distinct parallels and similarities in the data. This thesis, however, goes more in-depth into the mechanisms and effects that α -synuclein has on platelets, both in murine knockout models and in healthy donor platelets. Although many experiments yielded concordant data, the juxtaposition in *in vivo* findings between the studies needs to be further assessed. This thesis also supports the role of α -synuclein that has been observed in neurons and lymphocytes previously.

6.2. PD-L1

We generated and characterised the first murine platelet-specific knockout of PD-L1. Our results demonstrate a slight decrease in platelet aggregation, which was less pronounced compared to the whole-body PD-L1 knockout. We also show that, in the whole-body knockout, there is a significant decrease in JON/A, P-selectin, and CD63 expression on platelets stimulated with thrombin, but no change in LAMP1 secretion markers. We also show a dose-dependent inhibition of platelet aggregation in response to PD-L1 inhibition in human platelets.

In patients with MPNs, we observed a negative correlation between PD-L1 inhibitor dose and platelet aggregation at 5 minutes in response to thrombin. We also demonstrate that, although the PD-L1 expression is not significantly increased in MPN patients, the number of platelets that are PD-L1 positive is significantly higher. When platelets are incubated with IFN- γ , the expression of PD-L1 increases in both a time-

and dose-dependent manner, peaking at 8 hours. We also showed that incubating healthy donor platelets in the plasma of MPN patients resulted in a significant increase in PD-L1 expression on the surface of platelets.

When platelet-specific PD-L1 knockout mice were generated, The GPIb^{cre} was chosen over the traditional PF4^{cre} knock-in, due to the GPIb^{cre} knock-in having a higher specificity to platelets, whereas PF4 knock-in can affect immune cells (Pertuy et al., 2015). Whilst the GPIb^{cre} knock-in is more specific to platelets due to the later expression in megakaryocytes, there can still be small counts of target protein made. Upon examination of platelet lysates for PD-L1 in the specific knockout, we indeed saw a very faint band, suggesting that a minimal amount of PD-L1 might be present (Gollomp and Poncz, 2019). One hypothesis for the presence of PD-L1 on platelets may be due to the incomplete knockout caused by PD-L1 expression before the GPIb was transcribed, another hypothesis is that the platelets interacted with and displayed PD-L1 present in the plasma generated from other cells (Masood et al., 2023, Hinterleitner et al., 2021).

When assessing platelet function in washed platelets from the whole-body platelet-specific knockout and the wild-type, we showed that the whole-body knockout was affected to a greater extent than the platelet-specific knockout. The residual PD-L1 still present in the platelet-specific knockout may be a contributory factor to this increased aggregation. It has previously been shown that the aggregation of platelets in whole-body knockout mice is inhibited, in response to thrombin, collagen, ADP or U46619. Although mostly concordant, we find the aggregation defect to be weaker (Li et al., 2022). The mice we used in this study have the same C57BL/6 background as those used in the Li study, however, the Li study uses untreated wild-type mice as their controls, in this study, we used heterozygous breeding pairs to generate wild-type littermates. The Li study also used pentobarbital narcosis before blood collection, the use of barbiturates has been previously shown to affect platelet aggregation *in vitro* (Sato et al., 2003).

When we assessed activation and secretion markers on platelets in whole-body PD-L1^{-/-} mice, we found a significant decrease in platelet activation alongside the secretion of dense- and α -granules. PD-L1 is a co-inhibitory factor in the immune response, therefore, we were not expecting a decrease in platelet activity upon its

deletion. However, this finding is in agreement with a previous study of PD-L1 knockouts in platelets (Li et al., 2022). It has been shown that PD-L1 knockout inhibits platelet outside-in-signalling through the Caspase-3/GSDME pathway, however, inhibiting Caspase-3 has been shown not to affect the secretion of α -granules, indicating an additional impairment in platelet function (Shcherbina and Remold-O'Donnell, 1999, Cohen et al., 2007, Li et al., 2022). The study by (Li et al., 2022) also investigated the effects of PD-L1 deletion on the thrombus formation. Interestingly, they showed that the PD-L1^{-/-} had a significant effect on both clot formation and retraction. They propose that this is due to a regulatory function acting upon GSDME; assessing this pathway in the platelet-specific knockout may provide valuable insight as to whether this effect is recapitulated when PD-L1 is added.

We showed that at high doses, both Atezolizumab and Durvalumab inhibit platelet aggregation *in vitro* in response to collagen or thrombin. Additionally, we found that PD-L1 inhibition yields a larger effect when in PRP. The exact effects of PD-L1 inhibitors have not been assessed prior to this study, however, studies have shown that administration of these drugs can result in thrombocytopenia and bleeding diathesis (Delanoy et al., 2019, Kroll et al., 2022). Due to the greater inhibition of aggregation in PRP, we hypothesise that PD-L1 in the plasma also plays a role in platelet aggregation.

Patients with MPNs had a significantly higher number of platelets expressing PD-L1 compared to healthy donors. This increased PD-L1 expression resulted in a more pronounced effect of PD-L1 inhibitors on reducing platelet aggregation. The overexpression of PD-L1 in MPNs is well-documented and has been linked to the JAK2 mutation, Interestingly, we observe a significant increase in platelet PD-L1 expression in JAK2^{v617F} negative samples, although, no study has linked the increased expression of PD-L1 with platelets specifically (Prestipino et al., 2018, Milosevic Feenstra et al., 2022). The expression of PD-L1 in T cells has been shown to increase in response to IFN- γ (Imai et al., 2020), and we provided evidence that this mechanism is recapitulated in platelets. Interestingly, we found that PD-L1 expression decreases between the 8- and 24-hour timepoint, suggesting that there may be regulatory mechanisms that modulate PD-L1 levels after initial upregulation. This decline could indicate feedback inhibition or receptor internalisation and degradation processes that limit the duration of PD-L1 expression on platelets. Further research is needed to

elucidate the specific mechanisms underlying this time-dependent decrease in PD-L1 expression.

Effective reduction in PD-L1 expression in patients with metastatic melanoma has been achieved through removal of the host plasma and replacement from healthy donors (Davidson et al., 2022). Our data suggests that this mechanism may be due to a plasma constituent. When healthy platelets were incubated in plasma from MPN patients, we found a significant increase in PD-L1 expression. This increase may be due to the influence of soluble PD-L1, or, PD-L1 present in extracellular vesicles which have been shown to affect the platelet population (Chmielewska et al., 2023, Oya et al., 2022). Furthermore, IFN- γ present in MPN plasma could also contribute to the upregulation of PD-L1 on platelets. As such, the elevated PD-L1 expression observed in MPN patients' platelets may be multifactorial, involving both soluble factors and cytokine-mediated mechanisms.

In this thesis, we have shown that not only are platelets capable of presenting PD-L1 on their surface, but they can be actively upregulated through exposure to IFN- γ . The upregulation of PD-L1 is also correlated with a poorer prognosis which we hypothesise is due, at least in part, to the immunoregulatory role of platelets. We also show that PD-L1 knockout reduces the capability of the platelet to aggregate and secrete *in vitro*. The higher levels of platelet PD-L1 in cancers such as melanoma, breast, gastric, liver, kidney, MPN, and pancreatic may also contribute to the hypercoagulable state that is often present in these cancer types (Han et al., 2020b, Yamaguchi et al., 2022, Hudson et al., 2020).

The results of this thesis show that α -synuclein plays an important role in the function of the SNARE complex, and the removal of α -synuclein ameliorates the highly active secretory populations observed in wild-types. We also recapitulate that granule secretion is a key factor in the immune response to endotoxemia and reducing this secretion by α -synuclein knockout results in a poorer prognosis. Furthermore, we demonstrate that PD-L1 can facilitate platelet activation and granule secretion, in addition to its immunomodulatory role, in addition to the previously known GSDME/Caspasae-3 pathway.

6.2.1. Future work

The work carried out in this thesis illuminated many interesting paths to investigate further.

- The pathological function of α -synuclein has been linked with phosphorylation at serine129. We highlighted potential physiological functions of α -synuclein serine129 in concordance with (Ramalingam et al., 2023). Further investigation of phosphorylation at different sites on α -synuclein may yield hitherto unknown functionality of the protein in different cells (Manzanza et al., 2021). Further interrogation of the function of α -synuclein serine129 should be explored as to how it differs from its non-phosphorylated counterpart.
- Platelets are known to activate immune cells through multiple cellular processes, however, in this thesis we demonstrate that the removal of α -synuclein may have a role in downregulating the immune response (Allen Reish and Standaert, 2015). The extent of the immune cell interaction through an α -synuclein axis should be explored more thoroughly with a platelet-specific knockout.
- In this thesis we demonstrated the effective deletion of PD-L1 in platelets using the GPIb^{Cre} model. Future research could investigate whether PD-L1 derived from platelets influences disease states such as atherosclerosis, potentially offering new avenues for therapeutic intervention.
- We show that PD-L1 expression can be induced by the presence of IFN- γ , which has been demonstrated previously on T-cells (Garcia-Diaz et al., 2017, Qian et al., 2018). Additional studies have shown that PD-L1 expression may also be induced by the presence of tumour necrosis factor α (TNF α), and Interleukin-6 (IL6) on T cells (Chan et al., 2019, Lim et al., 2016). It would be interesting to determine whether these factors would upregulate PD-L1 expression in platelets, and whether the knockout of PD-L1 within platelets results in a protective phenotype against certain cancers.

References

- ABBACCHIO, M. P., BURNSTOCK, G., BOEYNAEMS, J.-M., BARNARD, E. A., BOYER, J. L., KENNEDY, C., KNIGHT, G. E., FUMAGALLI, M., GACHET, C. & JACOBSON, K. A. 2006. International Union of Pharmacology LVIII: update on the P2Y G protein-coupled nucleotide receptors: from molecular mechanisms and pathophysiology to therapy. *Pharmacological reviews*, 58, 281-341.
- ABELIOVICH, A. & GITLER, A. D. 2016. Defects in trafficking bridge Parkinson's disease pathology and genetics. *Nature*, 539, 207-216.
- ABELIOVICH, A., SCHMITZ, Y., FARIÑAS, I., CHOI-LUNDBERG, D., HO, W. H., CASTILLO, P. E., SHINSKY, N., VERDUGO, J. M., ARMANINI, M., RYAN, A., HYNES, M., PHILLIPS, H., SULZER, D. & ROSENTHAL, A. 2000. Mice lacking alpha-synuclein display functional deficits in the nigrostriatal dopamine system. *Neuron*, 25, 239-52.
- ABURIMA, A., BERGER, M., SPURGEON, B. E. J., WEBB, B. A., WRAITH, K. S., FEBBRAIO, M., POOLE, A. W. & NASEEM, K. M. 2021. Thrombospondin-1 promotes hemostasis through modulation of cAMP signaling in blood platelets. *Blood*, 137, 678-689.
- ACQUASALIENTE, L., PONTAROLLO, G., RADU, C. M., PETERLE, D., ARTUSI, I., PAGOTTO, A., ULIANA, F., NEGRO, A., SIMIONI, P. & DE FILIPPIS, V. 2022. Exogenous human α -Synuclein acts in vitro as a mild platelet antiaggregant inhibiting α -thrombin-induced platelet activation. *Scientific Reports*, 12, 9880.
- AGATA, Y., KAWASAKI, A., NISHIMURA, H., ISHIDA, Y., TSUBATA, T., YAGITA, H. & HONJO, T. 1996. Expression of the PD-1 antigen on the surface of stimulated mouse T and B lymphocytes. *Int Immunol*, 8, 765-72.
- AGBANI, E. O., WILLIAMS, C. M., LI, Y., VAN DEN BOSCH, M. T., MOORE, S. F., MAUROUX, A., HODGSON, L., VERKMAN, A. S., HERS, I. & POOLE, A. W. 2018. Aquaporin-1 regulates platelet procoagulant membrane dynamics and in vivo thrombosis. *JCI insight*, 3.
- AHMED, M. U., KANEVA, V., LOYAU, S., NECHIPURENKO, D., RECEVEUR, N., BRIS, M. L., JANUS-BELL, E., DIDELOT, M., RAUCH, A., SUSEN, S., CHAKFÉ, N., LANZA, F., GARDINER, E. E., ANDREWS, R. K., PANTELEEV, M., GACHET, C., JANDROT-PERRUS, M. & MANGIN, P. H. 2020. Pharmacological Blockade of Glycoprotein VI Promotes Thrombus Disaggregation in the Absence of Thrombin. *Arteriosclerosis, Thrombosis, and Vascular Biology*, 40, 2127-2142.
- AHN, B.-H., RHIM, H., KIM, S. Y., SUNG, Y.-M., LEE, M.-Y., CHOI, J.-Y., WOLOZIN, B., CHANG, J.-S., LEE, Y. H., KWON, T. K., CHUNG, K. C., YOON, S.-H., HAHN, S. J., KIM, M.-S., JO, Y.-H. & MIN, D. S. 2002. α -Synuclein Interacts with Phospholipase D Isozymes and Inhibits Pervanadate-induced Phospholipase D Activation in Human Embryonic Kidney-293 Cells. 277, 12334-12342.
- ALFARO, J. F., GONG, C. X., MONROE, M. E., ALDRICH, J. T., CLAUSS, T. R., PURVINE, S. O., WANG, Z., CAMP, D. G., 2ND, SHABANOWITZ, J., STANLEY, P., HART, G. W., HUNT, D. F., YANG, F. & SMITH, R. D. 2012. Tandem mass spectrometry identifies many mouse brain O-GlcNAcylated proteins including EGF domain-specific O-GlcNAc transferase targets. *Proc Natl Acad Sci U S A*, 109, 7280-5.
- ALI, R. A., WUESCHER, L. M. & WORTH, R. G. 2015. Platelets: essential components of the immune system. *Current trends in immunology*, 16, 65-78.
- ALLEN REISH, H. E. & STANDAERT, D. G. 2015. Role of α -synuclein in inducing innate and adaptive immunity in Parkinson disease. *J Parkinsons Dis*, 5, 1-19.
- ALSHEHRI, O. M., HUGHES, C. E., MONTAGUE, S., WATSON, S. K., FRAMPTON, J., BENDER, M. & WATSON, S. P. 2015. Fibrin activates GPVI in human and mouse platelets. *Blood*, 126, 1601-1608.
- AMBROSIO, A. L. & DI PIETRO, S. M. 2017. Storage pool diseases illuminate platelet dense granule biogenesis. *Platelets*, 28, 138-146.
- AN, S., YANG, J., SO, S. W., ZENG, L. & GOETZL, E. J. 1994. Isoforms of the EP3 subtype of human prostaglandin E2 receptor transduce both intracellular calcium and cAMP signals. *Biochemistry*, 33, 14496-14502.
- ANDERSON, J. P., WALKER, D. E., GOLDSTEIN, J. M., DE LAAT, R., BANDUCCI, K., CACCAVELLO, R. J., BARBOUR, R., HUANG, J., KLING, K. & LEE, M. 2006. Phosphorylation of Ser-129 is the dominant pathological modification of α -synuclein in familial and sporadic Lewy body disease. *Journal of Biological Chemistry*, 281, 29739-29752.

- ANDO, K., HAMADA, K., WATANABE, M., OHKUMA, R., SHIDA, M., ONOUE, R., KUBOTA, Y., MATSUI, H., ISHIGURO, T. & HIRASAWA, Y. 2019. Plasma levels of soluble PD-L1 correlate with tumor regression in patients with lung and gastric cancer treated with immune checkpoint inhibitors. *Anticancer research*, 39, 5195-5201.
- ANTONIN, W., HOLROYD, C., FASSHAUER, D., PABST, S., VON MOLLARD, G. F. & JAHN, R. 2000a. A SNARE complex mediating fusion of late endosomes defines conserved properties of SNARE structure and function. *The EMBO journal*, 19, 6453-6464.
- ANTONIN, W., HOLROYD, C., TIKKANEN, R., HONING, S. & JAHN, R. 2000b. The R-SNARE endobrevin/VAMP-8 mediates homotypic fusion of early endosomes and late endosomes. *Molecular biology of the cell*, 11, 3289-3298.
- ARMAN, M. & KRAUEL, K. 2015. Human platelet IgG Fc receptor FcγRIIA in immunity and thrombosis. *Journal of Thrombosis and Haemostasis*, 13, 893-908.
- ASLAN, J. E., ITAKURA, A., GERTZ, J. M. & MCCARTY, O. J. 2012. Platelet shape change and spreading. *Methods Mol Biol*, 788, 91-100.
- ASQUITH, N. L., CARMINITA, E., CAMACHO, V., RODRIGUEZ-ROMERA, A., STEGNER, D., FREIRE, D., BECKER, I. C., MACHLUS, K. R., KHAN, A. O. & ITALIANO, J. E. 2024. The bone marrow is the primary site of thrombopoiesis. *Blood*, 143, 272-278.
- AUNIS, D. & BADER, M.-F. 1988. The cytoskeleton as a barrier to exocytosis in secretory cells. *Journal of Experimental Biology*, 139, 253-266.
- AUSTIN, L. A. & HEATH III, H. 1981. Calcitonin: physiology and pathophysiology. *New England Journal of Medicine*, 304, 269-278.
- BABUR, Ö., MELROSE, A. R., CUNLIFFE, J. M., KLIMEK, J., PANG, J., SEPP, A.-L. I., ZILBERMAN-RUDENKO, J., TASSI YUNGA, S., ZHENG, T., PARRA-IZQUIERDO, I., MINNIER, J., MCCARTY, O. J. T., DEMIR, E., REDDY, A. P., WILMARTH, P. A., DAVID, L. L. & ASLAN, J. E. 2020. Phosphoproteomic quantitation and causal analysis reveal pathways in GPVI/ITAM-mediated platelet activation programs. *Blood*, 136, 2346-2358.
- BAKER, R. W. & HUGHSON, F. M. 2016. Chaperoning SNARE assembly and disassembly. *Nature reviews Molecular cell biology*, 17, 465-479.
- BALANA, A. T., MAHUL-MELLIER, A.-L., NGUYEN, B. A., HORVATH, M., JAVED, A., HARD, E. R., JASIQUI, Y., SINGH, P., AFRIN, S. & PEDRETTI, R. 2023. O-GlcNAc modification forces the formation of an α -Synuclein amyloid-strain with notably diminished seeding activity and pathology. *bioRxiv*, 2023.03.07.531573.
- BANERJEE, M., HUANG, Y., JOSHI, S., POPA, G. J., MENDENHALL, M. D., WANG, Q. J., GARVY, B. A., MYINT, T. & WHITEHEART, S. W. 2020. Platelets Endocytose Viral Particles and Are Activated via TLR (Toll-Like Receptor) Signaling. *Arteriosclerosis, Thrombosis, and Vascular Biology*, 40, 1635-1650.
- BARBOUR, R., KLING, K., ANDERSON, J. P., BANDUCCI, K., COLE, T., DIEP, L., FOX, M., GOLDSTEIN, J. M., SORIANO, F., SEUBERT, P. & CHILCOTE, T. J. 2008. Red Blood Cells Are the Major Source of Alpha-Synuclein in Blood. *Neurodegenerative Diseases*, 5, 55-59.
- BAUER, M., RETZER, M., WILDE, J. I., MASCHBERGER, P., ESSLER, M., AEPFELBACHER, M., WATSON, S. P. & SIESS, W. 1999. Dichotomous regulation of myosin phosphorylation and shape change by Rho-kinase and calcium in intact human platelets. *Blood*, 94, 1665-72.
- BEARER, E. L., PRAKASH, J. M. & LI, Z. 2002. Actin dynamics in platelets. *International Review of Cytology*. Academic Press.
- BECKERS, C. M., SIMPSON, K. R., GRIFFIN, K. J., BROWN, J. M., CHEAH, L. T., SMITH, K. A., VACHER, J., CORDELL, P. A., KEARNEY, M. T. & GRANT, P. J. 2017. Cre/lox studies identify resident macrophages as the major source of circulating coagulation factor XIII-A. *Arteriosclerosis, thrombosis, and vascular biology*, 37, 1494-1502.
- BELLANI, S., MESCOLA, A., RONZITTI, G., TSUSHIMA, H., TILVE, S., CANALE, C., VALTORTA, F. & CHIAREGATTI, E. 2014. GRP78 clustering at the cell surface of neurons transduces the action of exogenous alpha-synuclein. *Cell Death & Differentiation*, 21, 1971-1983.
- BENNETT, J. S. 2001. Novel platelet inhibitors. *Annual Review of Medicine*, 52, 161-184.
- BENNETT, J. S., BERGER, B. W. & BILLINGS, P. C. 2009. The structure and function of platelet integrins. *J Thromb Haemost*, 7 Suppl 1, 200-5.
- BERNSTEIN, A. M. & WHITEHEART, S. W. 1999. Identification of a cellubrevin/vesicle associated membrane protein 3 homologue in human platelets. *Blood, The Journal of the American Society of Hematology*, 93, 571-579.
- BERTONCINI, C. W., JUNG, Y.-S., FERNANDEZ, C. O., HOYER, W., GRIESINGER, C., JOVIN, T. M. & ZWECKSTETTER, M. 2005. Release of long-range tertiary interactions potentiates

- aggregation of natively unstructured α -synuclein. *Proceedings of the National Academy of Sciences*, 102, 1430-1435.
- BLAIR, P. & FLAUMENHAFT, R. 2009. Platelet alpha-granules: basic biology and clinical correlates. *Blood Rev*, 23, 177-89.
- BODNER, C. R., DOBSON, C. M. & BAX, A. 2009a. Multiple tight phospholipid-binding modes of alpha-synuclein revealed by solution NMR spectroscopy. *J Mol Biol*, 390, 775-90.
- BODNER, C. R., DOBSON, C. M. & BAX, A. 2009b. Multiple Tight Phospholipid-Binding Modes of α -Synuclein Revealed by Solution NMR Spectroscopy. *Journal of Molecular Biology*, 390, 775-790.
- BONIFACINO, J. S., GERSHLICK, D. C. & DELL'ANGELICA, E. C. 2016. Immunoprecipitation. *Current Protocols in Cell Biology*, 71.
- BONIFACINO, J. S. & GLICK, B. S. 2004. The Mechanisms of Vesicle Budding and Fusion. *Cell*, 116, 153-166.
- BOSWELL, K. L., JAMES, D. J., ESQUIBEL, J. M., BRUINSMA, S., SHIRAKAWA, R., HORIUCHI, H. & MARTIN, T. F. 2012. Munc13-4 reconstitutes calcium-dependent SNARE-mediated membrane fusion. *J Cell Biol*, 197, 301-12.
- BOULAFTALI, Y., HESS, P. R., KAHN, M. L. & BERGMEIER, W. 2014. Platelet immunoreceptor tyrosine-based activation motif (ITAM) signaling and vascular integrity. *Circulation research*, 114, 1174-1184.
- BOYLAN, B., GAO, C., RATHORE, V., GILL, J. C., NEWMAN, D. K. & NEWMAN, P. J. 2008. Identification of Fc γ RIIIa as the ITAM-bearing receptor mediating α IIb β 3 outside-in integrin signaling in human platelets. *Blood*, 112, 2780-6.
- BRAHMER, J. R., TYKODI, S. S., CHOW, L. Q., HWU, W.-J., TOPALIAN, S. L., HWU, P., DRAKE, C. G., CAMACHO, L. H., KAUF, J. & ODUNSI, K. 2012. Safety and activity of anti-PD-L1 antibody in patients with advanced cancer. *New England Journal of Medicine*, 366, 2455-2465.
- BUNEEVA, O. & MEDVEDEV, A. 2022. Atypical Ubiquitination and Parkinson's Disease. *Int J Mol Sci*, 23.
- BURAI, R., AIT-BOUZIAD, N., CHIKI, A. & LASHUEL, H. A. 2015. Elucidating the Role of Site-Specific Nitration of α -Synuclein in the Pathogenesis of Parkinson's Disease via Protein Semisynthesis and Mutagenesis. *Journal of the American Chemical Society*, 137, 5041-5052.
- BURKHART, J. M., VAUDEL, M., GAMBARYAN, S., RADAU, S., WALTER, U., MARTENS, L., GEIGER, J., SICKMANN, A. & ZAHEDI, R. P. 2012. The first comprehensive and quantitative analysis of human platelet protein composition allows the comparative analysis of structural and functional pathways. *Blood*, 120, e73-82.
- BURRÉ, J. 2015. The Synaptic Function of α -Synuclein. *Journal of Parkinson's Disease*, 5, 699-713.
- BURRÉ, J., SHARMA, M., TSETSENIS, T., BUCHMAN, V., ETHERTON, M. R. & SÜDHOF, T. C. 2010. α -Synuclein Promotes SNARE-Complex Assembly in Vivo and in Vitro. *Science*, 329, 1663-1667.
- BUSSELL, R. & ELIEZER, D. 2001. Residual structure and dynamics in Parkinson's disease-associated mutants of α -synuclein. *Journal of biological chemistry*, 276, 45996-46003.
- CABIN, D. E., SHIMAZU, K., MURPHY, D., COLE, N. B., GOTTSCHALK, W., MCILWAIN, K. L., ORRISON, B., CHEN, A., ELLIS, C. E. & PAYLOR, R. 2002. Synaptic vesicle depletion correlates with attenuated synaptic responses to prolonged repetitive stimulation in mice lacking α -synuclein. *Journal of Neuroscience*, 22, 8797-8807.
- CAPOOR, M. N., STONEMETZ, J. L., BAIRD, J. C., AHMED, F. S., AWAN, A., BIRKENMAIER, C., INCHIOSA JR, M. A., MAGID, S. K., MCGOLDRICK, K. & MOLMENTI, E. 2015. Prothrombin time and activated partial thromboplastin time testing: a comparative effectiveness study in a million-patient sample. *PloS one*, 10, e0133317.
- CARDENAS, R. A., GONZALEZ, R., SANCHEZ, E., RAMOS, M. A., CARDENAS, E. I., RODARTE, A. I., ALCAZAR-FELIX, R. J., ISAZA, A., BURNS, A. R., HEIDELBERGER, R. & ADACHI, R. 2021. SNAP23 is essential for platelet and mast cell development and required in connective tissue mast cells for anaphylaxis. *Journal of Biological Chemistry*, 296, 100268.
- CERLETTI, C., TAMBURRELLI, C., IZZI, B., GIANFAGNA, F. & DE GAETANO, G. 2012. Platelet-leukocyte interactions in thrombosis. *Thrombosis research*, 129, 263-266.
- CHAI, Y. J., SIERECKI, E., TOMATIS, V. M., GORMAL, R. S., GILES, N., MORROW, I. C., XIA, D., GÖTZ, J., PARTON, R. G. & COLLINS, B. M. 2016. Munc18-1 is a molecular chaperone for α -synuclein, controlling its self-replicating aggregation. *Journal of Cell Biology*, 214, 705-718.
- CHAN, L.-C., LI, C.-W., XIA, W., HSU, J.-M., LEE, H.-H., CHA, J.-H., WANG, H.-L., YANG, W.-H., YEN, E.-Y., CHANG, W.-C., ZHA, Z., LIM, S.-O., LAI, Y.-J., LIU, C., LIU, J., DONG, Q.,

- YANG, Y., SUN, L., WEI, Y., NIE, L., HSU, J. L., LI, H., YE, Q., HASSAN, M. M., AMIN, H. M., KASEB, A. O., LIN, X., WANG, S.-C. & HUNG, M.-C. 2019. IL-6/JAK1 pathway drives PD-L1 Y112 phosphorylation to promote cancer immune evasion. *The Journal of Clinical Investigation*, 129, 3324-3338.
- CHANG, C.-W., YANG, S.-Y., YANG, C.-C., CHANG, C.-W. & WU, Y.-R. 2020. Plasma and serum alpha-synuclein as a biomarker of diagnosis in patients with Parkinson's disease. *Frontiers in neurology*, 10, 1388.
- CHAPMAN, E. R. 2002. Synaptotagmin: A Ca²⁺ sensor that triggers exocytosis? *Nature Reviews Molecular Cell Biology*, 3, 498-508.
- CHAPMAN, E. R., AN, S., BARTON, N. & JAHN, R. 1994. SNAP-25, a t-SNARE which binds to both syntaxin and synaptobrevin via domains that may form coiled coils. *J Biol Chem*, 269, 27427-32.
- CHEN, H., HERNDON, M. E. & LAWLER, J. 2000. The cell biology of thrombospondin-1. *Matrix Biology*, 19, 597-614.
- CHEN, Y., YUAN, Y. & LI, W. 2018. Sorting machineries: how platelet-dense granules differ from α -granules. *Bioscience Reports*, 38.
- CHENG, Y., AUSTIN, S. C., ROCCA, B., KOLLER, B. H., COFFMAN, T. M., GROSSER, T., LAWSON, J. A. & FITZGERALD, G. A. 2002. Role of prostacyclin in the cardiovascular response to thromboxane A₂. *Science*, 296, 539-41.
- CHMIELEWSKA, I., GREUDA, A., KRAWCZYK, P., FRAK, M., KUŹNAR KAMIŃSKA, B., MITURA, W. & MILANOWSKI, J. 2023. The influence of plasma sPD-L1 concentration on the effectiveness of immunotherapy in advanced NSCLC patients. *Cancer Immunol Immunother*, 72, 4169-4177.
- CHO, J., FURIE, B. C., COUGHLIN, S. R. & FURIE, B. 2008. A critical role for extracellular protein disulfide isomerase during thrombus formation in mice. *The Journal of clinical investigation*, 118, 1123-1131.
- CHOI, B.-K., CHOI, M.-G., KIM, J.-Y., YANG, Y., LAI, Y., KWEON, D.-H., LEE, N. K. & SHIN, Y.-K. 2013. Large α -synuclein oligomers inhibit neuronal SNARE-mediated vesicle docking. *Proceedings of the National Academy of Sciences*, 110, 4087-4092.
- CHOU, S.-C., TAI, C.-H. & TSENG, S.-H. 2022. Platelet abnormalities in patients with Parkinson's disease undergoing preoperative evaluation for deep brain stimulation. *Scientific Reports*, 12, 14625.
- CHUNG, J., JEONG, D., KIM, G.-H., GO, S., SONG, J., MOON, E., HUH, Y. H. & KIM, D. 2021. Super-resolution imaging of platelet-activation process and its quantitative analysis. *Scientific Reports*, 11, 10511.
- CLEMETSON, K. J., CLEMETSON, J. M., PROUDFOOT, A. E., POWER, C. A., BAGGIOLINI, M. & WELLS, T. N. 2000. Functional expression of CCR1, CCR3, CCR4, and CXCR4 chemokine receptors on human platelets. *Blood, The Journal of the American Society of Hematology*, 96, 4046-4054.
- COGNASSE, F., LARADI, S., BERTHELOT, P., BOURLET, T., MAROTTE, H., MISMETTI, P., GARRAUD, O. & HAMZEH-COGNASSE, H. 2019. Platelet Inflammatory Response to Stress. *Frontiers in Immunology*, 10.
- COHEN, Z., DAVIDSON, L. & RITTER, L. 2007. Platelet aggregation requires caspases, but is not apoptosis. *The FASEB Journal*, 21, A1126-A1126.
- COLARUSSO, C., FALANGA, A., TERLIZZI, M., DE ROSA, I., SOMMA, P., SOMMELLA, E. M., CAPONIGRO, V., PANICO, L., SALVIATI, E., CAMPIGLIA, P., SALATIELLO, G., TRAMONTANO, T., MAIOLINO, P., PINTO, A. & SORRENTINO, R. 2023. High levels of PD-L1 on platelets of NSCLC patients contributes to the pharmacological activity of Atezolizumab. *Biomedicine & Pharmacotherapy*, 168, 115709.
- COSEMANS, J. M., ANGELILLO-SCHERRER, A., MATTHEIJ, N. J. & HEEMSKERK, J. W. 2013. The effects of arterial flow on platelet activation, thrombus growth, and stabilization. *Cardiovascular research*, 99, 342-352.
- COSSARIZZA, A., CHANG, H. D., RADBRUCH, A., ACS, A., ADAM, D., ADAM-KLAGES, S., AGACE, W. W., AGHAEPOUR, N., AKDIS, M., ALLEZ, M., ALMEIDA, L. N., ALVISI, G., ANDERSON, G., ANDRÄ, I., ANNUNZIATO, F., ANSELMO, A., BACHER, P., BALDARI, C. T., BARI, S., BARNABA, V., BARROS-MARTINS, J., BATTISTINI, L., BAUER, W., BAUMGART, S., BAUMGARTH, N., BAUMJOHANN, D., BAYING, B., BEBAWY, M., BECHER, B., BEISKER, W., BENES, V., BEYAERT, R., BLANCO, A., BOARDMAN, D. A., BOGDAN, C., BORGER, J. G., BORSELLINO, G., BOULAIS, P. E., BRADFORD, J. A., BRENNER, D., BRINKMAN, R. R., BROOKS, A. E. S., BUSCH, D. H., BÜSCHER, M.,

- BUSHNELL, T. P., CALZETTI, F., CAMERON, G., CAMMARATA, I., CAO, X., CARDELL, S. L., CASOLA, S., CASSATELLA, M. A., CAVANI, A., CELADA, A., CHATENOU, L., CHATTOPADHYAY, P. K., CHOW, S., CHRISTAKOU, E., ČIČIN-ŠAIN, L., CLERICI, M., COLOMBO, F. S., COOK, L., COOKE, A., COOPER, A. M., CORBETT, A. J., COSMA, A., COSMI, L., COULIE, P. G., CUMANO, A., CVETKOVIC, L., DANG, V. D., DANG-HEINE, C., DAVEY, M. S., DAVIES, D., DE BIASI, S., DEL ZOTTO, G., DELA CRUZ, G. V., DELACHER, M., DELLA BELLA, S., DELLABONA, P., DENIZ, G., DESSING, M., DI SANTO, J. P., DIEFENBACH, A., DIELI, F., DOLF, A., DÖRNER, T., DRESS, R. J., DUDZIAK, D., DUSTIN, M., DUTERTRE, C. A., EBNER, F., ECKLE, S. B. G., EDINGER, M., EEDE, P., EHRHARDT, G. R. A., EICH, M., ENGEL, P., ENGELHARDT, B., ERDEI, A., et al. 2019. Guidelines for the use of flow cytometry and cell sorting in immunological studies (second edition). *Eur J Immunol*, 49, 1457-1973.
- COVIC, L., GRESSER, A. L. & KULIOPULOS, A. 2000. Biphasic Kinetics of Activation and Signaling for PAR1 and PAR4 Thrombin Receptors in Platelets. *Biochemistry*, 39, 5458-5467.
- COWMAN, J., DUNNE, E., OGLESBY, I., BYRNE, B., RALPH, A., VOISIN, B., MÜLLERS, S., RICCO, A. J. & KENNY, D. 2015. Age-related changes in platelet function are more profound in women than in men. *Scientific Reports*, 5, 12235.
- CROUSE, J., KALINKE, U. & OXENIUS, A. 2015. Regulation of antiviral T cell responses by type I interferons. *Nature Reviews Immunology*, 15, 231-242.
- CROZAT, K., HOEBE, K., UGOLINI, S., HONG, N. A., JANSSEN, E., RUTSCHMANN, S., MUDD, S., SOVATH, S., VIVIER, E. & BEUTLER, B. 2007. Jinx, an MCMV susceptibility phenotype caused by disruption of Unc13d: a mouse model of type 3 familial hemophagocytic lymphohistiocytosis. *The Journal of experimental medicine*, 204, 853-863.
- DABRAZHNETSKAYA, A., MA, J., GUERREIRO-CACAIS, A. O., ARANY, Z., RUDD, E., HENTER, J. I., KARRE, K., LEVITSKAYA, J. & LEVITSKY, V. 2012. Syntaxin 11 marks a distinct intracellular compartment recruited to the immunological synapse of NK cells to colocalize with cytotoxic granules. *J Cell Mol Med*, 16, 129-41.
- DANIEL, J. L., DANGELMAIER, C., JIN, J., ASHBY, B., SMITH, J. B. & KUNAPULI, S. P. 1998. Molecular basis for ADP-induced platelet activation: I. Evidence for three distinct ADP receptors on human platelets. *Journal of Biological Chemistry*, 273, 2024-2029.
- DANIELE, S., FROSINI, D., PIETROBONO, D., PETROZZI, L., LO GERFO, A., BALDACCI, F., FUSI, J., GIACOMELLI, C., SICILIANO, G., TRINCAVELLI, M. L., FRANZONI, F., CERAVOLO, R., MARTINI, C. & BONUCCELLI, U. 2018. α -Synuclein Heterocomplexes with β -Amyloid Are Increased in Red Blood Cells of Parkinson's Disease Patients and Correlate with Disease Severity. *Frontiers in molecular neuroscience*, 11, 53-53.
- DANIELSON, S. R., HELD, J. M., SCHILLING, B., OO, M., GIBSON, B. W. & ANDERSEN, J. K. 2009. Preferentially increased nitration of α -synuclein at tyrosine-39 in a cellular oxidative model of Parkinson's disease. *Analytical chemistry*, 81, 7823-7828.
- DASGUPTA, S. K. & THIAGARAJAN, P. 2020. Cofilin-1-induced actin reorganization in stored platelets. *Transfusion*, 60, 806-814.
- DAVIDSON, T. M., FOSTER, N., LUCIEN, F., MARKOVIC, S., DONG, H., WINTERS, J. L., PARK, S. S. & ORME, J. J. 2022. Rescuing Cancer Immunity by Plasma Exchange in Metastatic Melanoma (ReCIPE-M1): protocol for a single-institution, open-label safety trial of plasma exchange to clear sPD-L1 for immunotherapy. *BMJ Open*, 12, e050112.
- DE CANDIA, E., HALL, S. W., RUTELLA, S., LANDOLFI, R., ANDREWS, R. K. & DE CRISTOFARO, R. 2001. Binding of thrombin to glycoprotein Ib accelerates the hydrolysis of Par-1 on intact platelets. *Journal of Biological Chemistry*, 276, 4692-4698.
- DE SIMONE, I., BAATEN, C., JANDROT-PERRUS, M., GIBBINS, J. M., TEN CATE, H., HEEMSKERK, J. W. M., JONES, C. I. & VAN DER MEIJDEN, P. E. J. 2022. Coagulation Factor XIIIa and Activated Protein C Activate Platelets via GPVI and PAR1. *Int J Mol Sci*, 23.
- DELANOY, N., MICHOT, J.-M., COMONT, T., KRAMKIMEL, N., LAZAROVIC, J., DUPONT, R., CHAMPIAT, S., CHAHINE, C., ROBERT, C. & HERBAUX, C. 2019. Haematological immune-related adverse events induced by anti-PD-1 or anti-PD-L1 immunotherapy: a descriptive observational study. *The Lancet Haematology*, 6, e48-e57.
- DELGADO-MARTÍNEZ, I., NEHRING, R. B. & SØRENSEN, J. B. 2007. Differential Abilities of SNAP-25 Homologs to Support Neuronal Function. *The Journal of Neuroscience*, 27, 9380-9391.
- DENAULT, M. H., KUANG, S., SHOKOOHI, A., LEUNG, B., LIU, M., BERTHELET, E., LASKIN, J., SUN, S., ZHANG, T., MELOSKEY, B. & HO, C. 2022. Comparison of 2-Weekly Versus 4-Weekly Durvalumab Consolidation for Locally Advanced NSCLC Treated With Chemoradiotherapy: A Brief Report. *JTO Clin Res Rep*, 3, 100316.

- DENG, R., BUMBACA, D., PASTUSKOVAS, C. V., BOSWELL, C. A., WEST, D., COWAN, K. J., CHIU, H., MCBRIDE, J., JOHNSON, C., XIN, Y., KOEPPEN, H., LEABMAN, M. & IYER, S. 2016. Preclinical pharmacokinetics, pharmacodynamics, tissue distribution, and tumor penetration of anti-PD-L1 monoclonal antibody, an immune checkpoint inhibitor. *MAbs*, 8, 593-603.
- DESHPANDE, M. & RODAL, A. A. 2016. Beyond the SNARE: Munc18-1 chaperones α -synuclein. *The Journal of cell biology*, 214, 641-643.
- DESPLATS, P., LEE, H.-J., BAE, E.-J., PATRICK, C., ROCKENSTEIN, E., CREWS, L., SPENCER, B., MASLIAH, E. & LEE, S.-J. 2009. Inclusion formation and neuronal cell death through neuron-to-neuron transmission of α -synuclein. *Proceedings of the National Academy of Sciences*, 106, 13010-13015.
- DETTMER, U., NEWMAN, A. J., VON SAUCKEN, V. E., BARTELS, T. & SELKOE, D. 2015. KTKEGV repeat motifs are key mediators of normal α -synuclein tetramerization: Their mutation causes excess monomers and neurotoxicity. *Proceedings of the National Academy of Sciences*, 112, 9596-9601.
- DIAO, J., BURRÉ, J., VIVONA, S., CIPRIANO, D. J., SHARMA, M., KYOUNG, M., SÜDHOF, T. C. & BRUNGER, A. T. 2013. Native α -synuclein induces clustering of synaptic-vesicle mimics via binding to phospholipids and synaptobrevin-2/VAMP2. *elife*, 2, e00592.
- DIAO, J., LIU, R., RONG, Y., ZHAO, M., ZHANG, J., LAI, Y., ZHOU, Q., WILZ, L. M., LI, J. & VIVONA, S. 2015. ATG14 promotes membrane tethering and fusion of autophagosomes to endolysosomes. *Nature*, 520, 563-566.
- DIECKMANN, N. M., HACKMANN, Y., ARICÒ, M. & GRIFFITHS, G. M. 2015a. Munc18-2 is required for Syntaxin 11 Localization on the Plasma Membrane in Cytotoxic T-Lymphocytes. *Traffic*, 16, 1330-41.
- DIECKMANN, N. M. G., HACKMANN, Y., ARICÒ, M. & GRIFFITHS, G. M. 2015b. Munc18-2 is required for Syntaxin 11 Localization on the Plasma Membrane in Cytotoxic T-Lymphocytes. *Traffic*, 16, 1330-1341.
- DIETERICH, L. C., IKENBERG, K., CETINTAS, T., KAPAKLIKAYA, K., HUTMACHER, C. & DETMAR, M. 2017. Tumor-Associated Lymphatic Vessels Upregulate PDL1 to Inhibit T-Cell Activation. *Frontiers in Immunology*, 8.
- DOEBBER, T. W., WU, M. S., ROBBINS, J. C., CHOY, B. M., CHANG, M. N. & SHEN, T. 1985. Platelet activating factor (PAF) involvement in endotoxin-induced hypotension in rats. Studies with PAF-receptor antagonist kadsurenone. *Biochemical and biophysical research communications*, 127, 799-808.
- DOUGHERTY, S. C., LYNCH, A. C. & HALL, R. D. 2021. Drug-induced immune-mediated thrombocytopenia secondary to durvalumab use. *Clin Case Rep*, 9, e04227.
- DU, X., PLOW, E. F., FRELINGER III, A. L., O'TOOLE, T. E., LOFTUS, J. C. & GINSBERG, M. H. 1991. Ligands "activate" integrin α IIb β 3 (platelet GPIIb-IIIa). *Cell*, 65, 409-416.
- DUERSCHMIED, D. & BODE, C. 2009. The role of serotonin in haemostasis. *Hämostaseologie*, 29, 356-359.
- DULUBOVA, I., SUGITA, S., HILL, S., HOSAKA, M., FERNANDEZ, I., SÜDHOF, T. C. & RIZO, J. 1999. A conformational switch in syntaxin during exocytosis: role of munc18. *The EMBO journal*, 18, 4372-4382.
- DUNN, K. W., KAMOCCA, M. M. & MCDONALD, J. H. 2011a. A practical guide to evaluating colocalization in biological microscopy. *Am J Physiol Cell Physiol*, 300, C723-42.
- DUNN, K. W., KAMOCCA, M. M. & MCDONALD, J. H. 2011b. A practical guide to evaluating colocalization in biological microscopy. *American Journal of Physiology-Cell Physiology*, 300, C723-C742.
- DURRANT, T. N., VAN DEN BOSCH, M. T. & HERS, I. 2017. Integrin α (IIb) β (3) outside-in signaling. *Blood*, 130, 1607-1619.
- EARLS, R. H., MENEES, K. B., CHUNG, J., GUTEKUNST, C.-A., LEE, H. J., HAZIM, M. G., RADA, B., WOOD, L. B. & LEE, J.-K. 2020. NK cells clear α -synuclein and the depletion of NK cells exacerbates synuclein pathology in a mouse model of α -synucleinopathy. *Proceedings of the National Academy of Sciences*, 117, 1762-1771.
- ECKLY, A., RINCKEL, J. Y., PROAMER, F., ULAS, N., JOSHI, S., WHITEHEART, S. W. & GACHET, C. 2016. Respective contributions of single and compound granule fusion to secretion by activated platelets. *Blood*, 128, 2538-2549.
- EL-BROLOS, M. A. & STAINIER, D. Y. R. 2017. Genetic compensation: A phenomenon in search of mechanisms. *PLoS Genet*, 13, e1006780.

- ELSTAK, E. D., NEEFT, M., NEHME, N. T., VOORTMAN, J., CHEUNG, M., GOODARZIFARD, M., GERRITSEN, H. C., VAN BERGEN EN HENEGOUWEN, P. M. P., CALLEBAUT, I., DE SAINT BASILE, G. & VAN DER SLUIJS, P. 2011. The munc13-4–rab27 complex is specifically required for tethering secretory lysosomes at the plasma membrane. *Blood*, 118, 1570-1578.
- EMMANOUILIDOU, E., MELACHROINOY, K., ROUMELIOTIS, T., GARBIS, S. D., NTZOUNI, M., MARGARITIS, L. H., STEFANIS, L. & VEKRELLIS, K. 2010. Cell-produced alpha-synuclein is secreted in a calcium-dependent manner by exosomes and impacts neuronal survival. *J Neurosci*, 30, 6838-51.
- ERBE, D. V., WATSON, S. R., PRESTA, L. G., WOLITZKY, B. A., FOXALL, C., BRANDLEY, B. K. & LASKY, L. A. 1993. P- and E-selectin use common sites for carbohydrate ligand recognition and cell adhesion. *The Journal of cell biology*, 120, 1227-1235.
- ERENT, M., MELI, A., MOISOI, N., BABICH, V., HANNAH, M., SKEHEL, P., KNIFE, L., ZUPANČIČ, G., OGDEN, D. & CARTER, T. 2007. Rate, extent and concentration dependence of histamine-evoked Weibel–Palade body exocytosis determined from individual fusion events in human endothelial cells. *The Journal of Physiology*, 583, 195-212.
- ESKELINEN, E.-L. 2006. Roles of LAMP-1 and LAMP-2 in lysosome biogenesis and autophagy. *Molecular Aspects of Medicine*, 27, 495-502.
- ESSEX, D. W., CHEN, K. & SWIATKOWSKA, M. 1995. Localization of protein disulfide isomerase to the external surface of the platelet plasma membrane. *Blood*, 86, 2168-2173.
- ESTEVEZ, B., DELANEY, M. K., STOJANOVIC-TERPO, A. & DU, X. 2014. A Signaling Mechanism By Which Platelet Glycoprotein Ib-IX Promotes Thrombin-Induced Platelet Activation. *Blood*, 124, 2759-2759.
- FACTOR, S. A., ORTOF, E., DENTINGER, M. P., MANKES, R. & BARRON, K. D. 1994. Platelet morphology in Parkinson's disease: an electron microscopic study. *J Neurol Sci*, 122, 84-9.
- FALCON, C., PFLIEGLER, G., DECKMYN, H. & VERMYLEN, J. 1988. The platelet insulin receptor: detection, partial characterization, and search for a function. *Biochemical and Biophysical Research Communications*, 157, 1190-1196.
- FASSHAUER, D., SUTTON, R. B., BRUNGER, A. T. & JAHN, R. 1998. Conserved structural features of the synaptic fusion complex: SNARE proteins reclassified as Q- and R-SNAREs. *Proceedings of the National Academy of Sciences*, 95, 15781-15786.
- FEANY, M. B. & BENDER, W. W. 2000. A Drosophila model of Parkinson's disease. *Nature*, 404, 394-398.
- FENG, D., CRANE, K., ROZENVAYN, N., DVORAK, A. M. & FLAUMENHAFT, R. 2002. Subcellular distribution of 3 functional platelet SNARE proteins: human cellubrevin, SNAP-23, and syntaxin 2. *Blood, The Journal of the American Society of Hematology*, 99, 4006-4014.
- FENG, W., CHANG, C., LUO, D., SU, H., YU, S., HUA, W., CHEN, Z., HU, H. & LIU, W. 2014. Dissection of autophagy in human platelets. *Autophagy*, 10, 642-651.
- FISCH, A. S., PERRY, C. G., STEPHENS, S. H., HORENSTEIN, R. B. & SHULDINER, A. R. 2013. Pharmacogenomics of anti-platelet and anti-coagulation therapy. *Current cardiology reports*, 15, 381-381.
- FLAUMENHAFT, R. 2011. Platelets get the message. *Blood*, 118, 1712-1713.
- FLAUMENHAFT, R., DILKS, J. R., ROZENVAYN, N., MONAHAN-EARLEY, R. A., FENG, D. & DVORAK, A. M. 2005. The actin cytoskeleton differentially regulates platelet α -granule and dense-granule secretion. *Blood*, 105, 3879-3887.
- FORTIN, D. L., NEMANI, V. M., NAKAMURA, K. & EDWARDS, R. H. 2010. The behavior of α -synuclein in neurons. *Movement Disorders*, 25, S21-S26.
- FREEDMAN, J. E. & LOSCALZO, J. 2002. Platelet–monocyte aggregates: bridging thrombosis and inflammation. *Am Heart Assoc*.
- FREEMAN, G. J., LONG, A. J., IWAI, Y., BOURQUE, K., CHERNOVA, T., NISHIMURA, H., FITZ, L. J., MALENKOVICH, N., OKAZAKI, T., BYRNE, M. C., HORTON, H. F., FOUSSER, L., CARTER, L., LING, V., BOWMAN, M. R., CARRENO, B. M., COLLINS, M., WOOD, C. R. & HONJO, T. 2000. Engagement of the PD-1 immunoinhibitory receptor by a novel B7 family member leads to negative regulation of lymphocyte activation. *J Exp Med*, 192, 1027-34.
- FROJMOVIC, M. M. 1998. Platelet aggregation in flow: Differential roles for adhesive receptors and ligands. *American Heart Journal*, 135, S119-S131.
- FROJMOVIC, M. M. & MILTON, J. G. 1982. Human platelet size, shape, and related functions in health and disease. *Physiological Reviews*, 62, 185-261.
- FUCHS, T. A., BRILL, A., DUERSCHMIED, D., SCHATZBERG, D., MONESTIER, M., MYERS JR, D. D., WROBLESKI, S. K., WAKEFIELD, T. W., HARTWIG, J. H. & WAGNER, D. D. 2010.

- Extracellular DNA traps promote thrombosis. *Proceedings of the National Academy of Sciences*, 107, 15880-15885.
- FUJIWARA, I., ZWEIFEL, M. E., COURTEMANCHE, N. & POLLARD, T. D. 2018. Latrunculin A Accelerates Actin Filament Depolymerization in Addition to Sequestering Actin Monomers. *Curr Biol*, 28, 3183-3192.e2.
- FUKUDA, M. 2006. Rab27 and its effectors in secretory granule exocytosis: a novel docking machinery composed of a Rab27- effector complex. Portland Press Ltd.
- FURIE, B. & FURIE, B. C. 2008. Mechanisms of thrombus formation. *New England Journal of Medicine*, 359, 938-949.
- GAO, C., BOYLAN, B., FANG, J., WILCOX, D. A., NEWMAN, D. K. & NEWMAN, P. J. 2011. Heparin promotes platelet responsiveness by potentiating $\alpha\text{IIb}\beta\text{3}$ -mediated outside-in signaling. *Blood*, 117, 4946-4952.
- GAO, Y., ZORMAN, S., GUNDERSEN, G., XI, Z., MA, L., SIRINAKIS, G., ROTHMAN, J. E. & ZHANG, Y. 2012. Single reconstituted neuronal SNARE complexes zipper in three distinct stages. *Science*, 337, 1340-3.
- GARCIA-DIAZ, A., SHIN, D. S., MORENO, B. H., SACO, J., ESCUIN-ORDINAS, H., RODRIGUEZ, G. A., ZARETSKY, J. M., SUN, L., HUGO, W., WANG, X., PARISI, G., SAUS, C. P., TORREJON, D. Y., GRAEBER, T. G., COMIN-ANDUIX, B., HU-LIESKOVAN, S., DAMOISEAUX, R., LO, R. S. & RIBAS, A. 2017. Interferon Receptor Signaling Pathways Regulating PD-L1 and PD-L2 Expression. *Cell Rep*, 19, 1189-1201.
- GARRAUD, O., COGNASSE, F. & MONCHARMONT, P. 2019. Immunological Features in the Process of Blood Platelet-Induced Alloimmunisation, with a Focus on Platelet Component Transfusion. *Diseases*, 7.
- GAWAZ, M., NEUMANN, F.-J., DICKFELD, T., REININGER, A., ADELSBERGER, H., GEBHARDT, A. & SCHÖMIG, A. 1997. Vitronectin receptor ($\alpha\text{v}\beta\text{3}$) mediates platelet adhesion to the luminal aspect of endothelial cells: implications for reperfusion in acute myocardial infarction. *Circulation*, 96, 1809-1818.
- GEORGE, J. M., JIN, H., WOODS, W. S. & CLAYTON, D. F. 1995. Characterization of a novel protein regulated during the critical period for song learning in the zebra finch. *Neuron*, 15, 361-372.
- GERBER, S. H., RAH, J.-C., MIN, S.-W., LIU, X., DE WIT, H., DULUBOVA, I., MEYER, A. C., RIZO, J., ARANCILLO, M. & HAMMER, R. E. 2008. Conformational switch of syntaxin-1 controls synaptic vesicle fusion. *Science*, 321, 1507-1510.
- GHASEMZADEH, M. & HOSSEINI, E. 2013. Platelet-leukocyte crosstalk: Linking proinflammatory responses to procoagulant state. *Thrombosis Research*, 131, 191-197.
- GHOSHAL, K. & BHATTACHARYYA, M. 2014. Overview of platelet physiology: its hemostatic and nonhemostatic role in disease pathogenesis. *ScientificWorldJournal*, 2014, 781857.
- GIASSON, B. I., DUDA, J. E., MURRAY, I. V., CHEN, Q., SOUZA, J. M., HURTIG, H. I., ISCHIROPOULOS, H., TROJANOWSKI, J. Q. & -Y. LEE, V. M. 2000. Oxidative damage linked to neurodegeneration by selective α -synuclein nitration in synucleinopathy lesions. *Science*, 290, 985-989.
- GITZ, E. 2013. *Glycoprotein Iba clustering in platelet storage and function*.
- GOGIA, S. & NEELAMEGHAM, S. 2015. Role of fluid shear stress in regulating VWF structure, function and related blood disorders. *Biorheology*, 52, 319-335.
- GOLEBIEWSKA, E. M., HARPER, M. T., WILLIAMS, C. M., SAVAGE, J. S., GOGGS, R., FISCHER VON MOLLARD, G. & POOLE, A. W. 2015. Syntaxin 8 regulates platelet dense granule secretion, aggregation, and thrombus stability. *The Journal of biological chemistry*, 290, 1536-1545.
- GOLEBIEWSKA, E. M. & POOLE, A. W. 2013. Secrets of platelet exocytosis - what do we really know about platelet secretion mechanisms? *Br J Haematol*, 165, 204-16.
- GOLEBIEWSKA, E. M. & POOLE, A. W. 2015. Platelet secretion: From haemostasis to wound healing and beyond. *Blood reviews*, 29, 153-162.
- GOLINO, P. 2013. Characteristics of new P2Y₁₂ inhibitors: selection of P2Y₁₂ inhibitors in clinical practice. *J Cardiovasc Med (Hagerstown)*, 14 Suppl 1, S22-30.
- GOLLA, K., PAUL, M., LENGYELL, T. C., SIMPSON, E. M., FALET, H. & KIM, H. 2022. A novel association between filamin A and SNARE proteins regulates platelet granule secretion. *Research and Practice in Thrombosis and Haemostasis*, 100019.
- GOLLOMP, K. & PONCZ, M. 2019. Gp1ba-Cre or Pf4-Cre: pick your poison. *Blood*, 133, 287-288.
- GREENBAUM, E. A., GRAVES, C. L., MISHIZEN-EBERZ, A. J., LUPOLI, M. A., LYNCH, D. R., ENGLANDER, S. W., AXELSEN, P. H. & GIASSON, B. I. 2005. The E46K mutation in α -synuclein increases amyloid fibril formation. *Journal of Biological Chemistry*, 280, 7800-7807.

- GRESELE, P., HARRISON, P., GACHET, C., HAYWARD, C., KENNY, D., MEZZANO, D., MUMFORD, A., NUGENT, D., NURDEN, A. & CATTANEO, M. 2015. Diagnosis of inherited platelet function disorders: guidance from the SSC of the ISTH. *Journal of Thrombosis and Haemostasis*, 13, 314-322.
- GREWAL, P. K. 2010. Chapter Thirteen - The Ashwell–Morell Receptor. *In*: FUKUDA, M. (ed.) *Methods in Enzymology*. Academic Press.
- GROZDANOV, V. & DANZER, K. M. 2020. Intracellular Alpha-Synuclein and Immune Cell Function. *Frontiers in Cell and Developmental Biology*, 8.
- GROZOVSKY, R., BEGONJA, A. J., LIU, K., VISNER, G., HARTWIG, J. H., FALET, H. & HOFFMEISTER, K. M. 2015. The Ashwell-Morell receptor regulates hepatic thrombopoietin production via JAK2-STAT3 signaling. *Nat Med*, 21, 47-54.
- GUEGUEN, G., GAIGÉ, B., GRÉVY, J.-M., ROGALLE, P., BELLAN, J., WILSON, M., KLAÉBÉ, A., PONT, F., SIMON, M.-F. & CHAP, H. 1999. Structure–Activity Analysis of the Effects of Lysophosphatidic Acid on Platelet Aggregation. *Biochemistry*, 38, 8440-8450.
- GUO, Q., MALLOY, M. W., ROWETH, H. G., MCALLISTER, S. S., ITALIANO, J. E. & BATTINELLI, E. M. 2022. Platelets upregulate tumor cell programmed death ligand 1 in an epidermal growth factor receptor-dependent manner in vitro. *Blood Advances*, 6, 5668-5675.
- GURNEY, A. L., CARVER-MOORE, K., DE SAUVAGE, F. J. & MOORE, M. W. 1994. Thrombocytopenia in c-mpl-deficient mice. *Science*, 265, 1445-1447.
- GYULKHANDANYAN, A. V., MUTLU, A., FREEDMAN, J. & LEYTIN, V. 2013. Selective triggering of platelet apoptosis, platelet activation or both. *British Journal of Haematology*, 161, 245-254.
- HALIMANI, M., PATTU, V., MARSHALL, M., CHANG, H., MATTI, U., JUNG, M., BECHERER, U., KRAUSE, E., HOTH, M., EVA C, S. & RETTIG, J. 2014. Syntaxin11 serves as a t-SNARE for the fusion of lytic granules in human cytotoxic T lymphocytes. *European journal of immunology*, 44, 573-584.
- HAN, P., HANLON, D., ARSHAD, N., LEE, J. S., TATSUNO, K., YURTER, A., ROBINSON, E., FILLER, R., SOBOLEV, O. & COTE, C. 2020a. Platelet P-selectin initiates cross-presentation and dendritic cell differentiation in blood monocytes. *Science advances*, 6, eaaz1580.
- HAN, X., LI, P., YANG, Z., HUANG, X., WEI, G., SUN, Y., KANG, X., HU, X., DENG, Q. & CHEN, L. 2017. Zyxin regulates endothelial von Willebrand factor secretion by reorganizing actin filaments around exocytic granules. *Nature communications*, 8, 14639.
- HAN, Y., LIU, D. & LI, L. 2020b. PD-1/PD-L1 pathway: current researches in cancer. *Am J Cancer Res*, 10, 727-742.
- HARDY, J., LEWIS, P., REVESZ, T., LEES, A. & PAISAN-RUIZ, C. 2009. The genetics of Parkinson's syndromes: a critical review. *Current Opinion in Genetics & Development*, 19, 254-265.
- HART, C. E., BAILEY, M., CURTIS, D. A., OSBORN, S., RAINES, E., ROSS, R. & FORSTROM, J. W. 1990. Purification of PDGF-AB and PDGF-BB from human platelet extracts and identification of all three PDGF dimers in human platelets. *Biochemistry*, 29, 166-172.
- HARTWIG, J. H. & DESISTO, M. 1991. The cytoskeleton of the resting human blood platelet: structure of the membrane skeleton and its attachment to actin filaments. *J Cell Biol*, 112, 407-25.
- HASHIMOTO, M., YOSHIMOTO, M., SISK, A., HSU, L. J., SUNDSMO, M., KITTEL, A., SAITOH, T., MILLER, A. & MASLIAH, E. 1997. NACP, a synaptic protein involved in Alzheimer's disease, is differentially regulated during megakaryocyte differentiation. *Biochemical and biophysical research communications*, 237, 611-616.
- HATSUZAWA, K. & SAKURAI, C. 2020. Regulatory Mechanism of SNAP23 in Phagosome Formation and Maturation. *Yonago Acta Med*, 63, 135-145.
- HAWK, B. J. D., KHOUNLO, R. & SHIN, Y.-K. 2019. Alpha-Synuclein Continues to Enhance SNARE-Dependent Vesicle Docking at Exorbitant Concentrations. *Frontiers in Neuroscience*, 13.
- HECHLER, B., NONNE, C., ECKLY, A., MAGNENAT, S., RINCKEL, J. Y., DENIS, C., FREUND, M., CAZENAVE, J. P., LANZA, F. & GACHET, C. 2010. Arterial thrombosis: relevance of a model with two levels of severity assessed by histologic, ultrastructural and functional characterization. *Journal of thrombosis and haemostasis*, 8, 173-184.
- HEEMSKERK, J. W., BEVERS, E. M. & LINDHOUT, T. 2002. Platelet activation and blood coagulation. *Thrombosis and haemostasis*, 88, 186-193.
- HEIJNEN, H. & VAN DER SLUIJS, P. 2015. Platelet secretory behaviour: as diverse as the granules ... or not? *Journal of Thrombosis and Haemostasis*, 13, 2141-2151.
- HINTERLEITNER, C., STRÄHLE, J., MALENKE, E., HINTERLEITNER, M., HENNING, M., SEEHAWER, M., BILICH, T., HEITMANN, J., LUTZ, M. & MATTERN, S. 2021. Platelet PD-L1

- reflects collective intratumoral PD-L1 expression and predicts immunotherapy response in non-small cell lung cancer. *Nature Communications*, 12, 7005.
- HOLINSTAT, M. 2017. Normal platelet function. *Cancer metastasis reviews*, 36, 195-198.
- HOLMQVIST, S., CHUTNA, O., BOUSSET, L., ALDRIN-KIRK, P., LI, W., BJÖRKLUND, T., WANG, Z.-Y., ROYBON, L., MELKI, R. & LI, J.-Y. 2014. Direct evidence of Parkinson pathology spread from the gastrointestinal tract to the brain in rats. *Acta Neuropathologica*, 128, 805-820.
- HOLMSTRÖM, M., HJORTSØ, M., AHMAD, S., MET, Ö., MARTINENAITE, E., RILEY, C., STRATEN, P., SVANE, I., HASSELBALCH, H. & ANDERSEN, M. 2017. The JAK2V617F mutation is a target for specific T cells in the JAK2V617F-positive myeloproliferative neoplasms. *Leukemia*, 31, 495-498.
- HONG, N. H., QI, A. & WEAVER, A. M. 2015. PI(3,5)P2 controls endosomal branched actin dynamics by regulating cortactin–actin interactions. *Journal of Cell Biology*, 210, 753-769.
- HONG, W. 2005. SNAREs and traffic. *Biochimica et Biophysica Acta (BBA) - Molecular Cell Research*, 1744, 120-144.
- HORNE, R. I., ANDRZEJEWSKA, E. A., ALAM, P., BROTZAKIS, Z. F., SRIVASTAVA, A., AUBERT, A., NOWINSKA, M., GREGORY, R. C., STAATS, R., POSSENTI, A., CHIA, S., SORMANNI, P., GHETTI, B., CAUGHEY, B., KNOWLES, T. P. J. & VENDRUSCOLO, M. 2024. Discovery of potent inhibitors of α -synuclein aggregation using structure-based iterative learning. *Nature Chemical Biology*, 20, 634-645.
- HOUNG, A., POLGAR, J. & REED, G. L. 2003. Munc18-syntaxin complexes and exocytosis in human platelets. *Journal of Biological Chemistry*, 278, 19627-19633.
- HUDSON, K., CROSS, N., JORDAN-MAHY, N. & LEYLAND, R. 2020. The Extrinsic and Intrinsic Roles of PD-L1 and Its Receptor PD-1: Implications for Immunotherapy Treatment. *Frontiers in Immunology*, 11.
- HUTAGALUNG, A. H. & NOVICK, P. J. 2011. Role of Rab GTPases in membrane traffic and cell physiology. *Physiological reviews*, 91, 119-149.
- IMAI, Y., CHIBA, T., KONDO, T., KANZAKI, H., KANAYAMA, K., AO, J., KOJIMA, R., KUSAKABE, Y., NAKAMURA, M., SAITO, T., NAKAGAWA, R., SUZUKI, E., NAKAMOTO, S., MUROYAMA, R., TAWADA, A., MATSUMURA, T., NAKAGAWA, T., KATO, J., KOTANI, A., MATSUBARA, H. & KATO, N. 2020. Interferon- γ induced PD-L1 expression and soluble PD-L1 production in gastric cancer. *Oncol Lett*, 20, 2161-2168.
- ISRAELS, S. J. & MCMILLAN-WARD, E. M. 2005. CD63 modulates spreading and tyrosine phosphorylation of platelets on immobilized fibrinogen. *Thromb Haemost*, 93, 311-8.
- ITALIANO, J. E., JR., RICHARDSON, J. L., PATEL-HETT, S., BATTINELLI, E., ZASLAVSKY, A., SHORT, S., RYEOM, S., FOLKMAN, J. & KLEMENT, G. L. 2008a. Angiogenesis is regulated by a novel mechanism: pro- and antiangiogenic proteins are organized into separate platelet alpha granules and differentially released. *Blood*, 111, 1227-1233.
- ITALIANO, J. E., JR., RICHARDSON, J. L., PATEL-HETT, S., BATTINELLI, E., ZASLAVSKY, A., SHORT, S., RYEOM, S., FOLKMAN, J. & KLEMENT, G. L. 2008b. Angiogenesis is regulated by a novel mechanism: pro- and antiangiogenic proteins are organized into separate platelet alpha granules and differentially released. *Blood*, 111, 1227-33.
- IYER, A., ROETERS, S. J., KOGAN, V., WOUTERSEN, S., CLAESSENS, M. M. A. E. & SUBRAMANIAM, V. 2017. C-Terminal Truncated α -Synuclein Fibrils Contain Strongly Twisted β -Sheets. *Journal of the American Chemical Society*, 139, 15392-15400.
- JACKSON, S. P. 2007. The growing complexity of platelet aggregation. *Blood*, 109, 5087-5095.
- JACOB, J. O., ELIZABETH ANN, L. E., FABRICE, L.-M., HEATHER, D., EDWIN, B., SUSAN, M. H., MATTHEW, K. B., AARON, S. M., SEAN, S. P., MATHEW, S. B., SVETOMIR, N. M., YIYI, Y., HAIDONG, D., ROXANA, S. D. & JEFFREY, L. W. 2020. Therapeutic plasma exchange clears circulating soluble PD-L1 and PD-L1-positive extracellular vesicles. *Journal for ImmunoTherapy of Cancer*, 8, e001113.
- JAHN, R. & FASSHAUER, D. 2012. Molecular machines governing exocytosis of synaptic vesicles. *Nature*, 490, 201-207.
- JAHN, R., LANG, T. & SÜDHOF, T. C. 2003. Membrane Fusion. *Cell*, 112, 519-533.
- JAHN, R. & SCHELLER, R. H. 2006. SNAREs—engines for membrane fusion. *Nature reviews Molecular cell biology*, 7, 631-643.
- JAO, C. C., HEGDE, B. G., CHEN, J., HAWORTH, I. S. & LANGEN, R. 2008. Structure of membrane-bound α -synuclein from site-directed spin labeling and computational refinement. *Proceedings of the National Academy of Sciences*, 105, 19666-19671.

- JENKINS, C. S. P., PACKHAM, M. A., KINLOUGH-RATHBONE, R. L. & MUSTARD, J. F. 1971. Interactions of Polylysine With Platelets. *Blood*, 37, 395-412.
- JENNE, C., URRUTIA, R. & KUBES, P. 2013. Platelets: bridging hemostasis, inflammation, and immunity. *International journal of laboratory hematology*, 35, 254-261.
- JENNINGS, L. K. 2009a. Mechanisms of platelet activation: need for new strategies to protect against platelet-mediated atherothrombosis. *Thrombosis and Haemostasis*, 102, 248-257.
- JENNINGS, L. K. 2009b. Role of Platelets in Atherothrombosis. *The American Journal of Cardiology*, 103, 4A-10A.
- JESSICA, M.-O., FIORELLA, R., OCATAVIO, S., LINNETTE, R., NAHOMY, L., KANTH, M. B., BISMARCK, M., RONDINA, M. T. & VALANCE, W. A. 2018. TLT-1-CONTROLS EARLY THROMBUS FORMATION AND STABILITY BY FACILITATING AIIBB3 OUTSIDE-IN SIGNALING IN MICE. *International journal of advanced research*, 6, 1143.
- JO, E., MCLAURIN, J., YIP, C. M., ST. GEORGE-HYSLOP, P. & FRASER, P. E. 2000. α -Synuclein Membrane Interactions and Lipid Specificity *. *Journal of Biological Chemistry*, 275, 34328-34334.
- JONES, LYN H. 2012. Chemistry and Biology of Biomolecule Nitration. *Chemistry & Biology*, 19, 1086-1092.
- JONNALAGADDA, D., IZU, L. T. & WHITEHEART, S. W. 2012. Platelet secretion is kinetically heterogeneous in an agonist-responsive manner. *Blood*, 120, 5209-16.
- JORGOVANOVIC, D., SONG, M., WANG, L. & ZHANG, Y. 2020. Roles of IFN- γ in tumor progression and regression: a review. *Biomarker Research*, 8, 49.
- JOSHI, S., BANERJEE, M., ZHANG, J., KESARAJU, A., POKROVSKAYA, I. D., STORRIE, B. & WHITEHEART, S. W. 2018. Alterations in platelet secretion differentially affect thrombosis and hemostasis. *Blood advances*, 2, 2187-2198.
- JUNG, S. M. & MOROI, M. 2008. Platelet glycoprotein VI. *Adv Exp Med Biol*, 640, 53-63.
- KÁDKOVÁ, A., RADECKE, J. & SØRENSEN, J. B. 2019. The SNAP-25 Protein Family. *Neuroscience*, 420, 50-71.
- KARINA, WAHYUNINGSIH, K. A., SOBARIAH, S., ROSLIANA, I., ROSADI, I., WIDYASTUTI, T., AFINI, I., WANANDI, S. I., SOEWONDO, P., WIBOWO, H. & PAWITAN, J. A. 2019. Evaluation of platelet-rich plasma from diabetic donors shows increased platelet vascular endothelial growth factor release. *Stem cell investigation*, 6, 43-43.
- KAROLCZAK, K., PIENIAZEK, A. & WATALA, C. 2017. Inhibition of glutamate receptors reduces the homocysteine-induced whole blood platelet aggregation but does not affect superoxide anion generation or platelet membrane fluidization. *Platelets*, 28, 90-98.
- KAUSHANSKY, K. 2005. The molecular mechanisms that control thrombopoiesis. *The Journal of clinical investigation*, 115, 3339-3347.
- KAUSHANSKY, K. 2006. Lineage-Specific Hematopoietic Growth Factors. *New England Journal of Medicine*, 354, 2034-2045.
- KAWAHATA, I., FINKELSTEIN, D. I. & FUKUNAGA, K. 2022. Pathogenic Impact of α -Synuclein Phosphorylation and Its Kinases in α -Synucleinopathies. *Int J Mol Sci*, 23.
- KAYLOR, J., BODNER, N., EDRIDGE, S., YAMIN, G., HONG, D. P. & FINK, A. L. 2005. Characterization of oligomeric intermediates in alpha-synuclein fibrillation: FRET studies of Y125W/Y133F/Y136F alpha-synuclein. *J Mol Biol*, 353, 357-72.
- KELM, R., SWORDS, N. A., ORFEO, T. & MANN, K. G. 1994. Osteonectin in matrix remodeling. A plasminogen-osteonectin-collagen complex. *Journal of Biological Chemistry*, 269, 30147-30153.
- KHAN, S., ANDREWS, K. L. & CHIN-DUSTING, J. P. F. 2019. Cyclo-Oxygenase (COX) Inhibitors and Cardiovascular Risk: Are Non-Steroidal Anti-Inflammatory Drugs Really Anti-Inflammatory? *Int J Mol Sci*, 20.
- KILBOURNE, E. J. & WINNEKER, R. C. 2001. Serotonin 5-HT₁ receptors potentiate histamine and thrombin stimulated prostaglandin synthesis in endothelial cells. *Thrombosis and haemostasis*, 85, 924-928.
- KIM, K. S., PARK, J.-Y., JOU, I. & PARK, S. M. 2010. Regulation of Weibel-Palade body exocytosis by α -synuclein in endothelial cells. *Journal of Biological Chemistry*, 285, 21416-21425.
- KIM, S., JEON, B. S., HEO, C., IM, P. S., AHN, T. B., SEO, J. H., KIM, H. S., PARK, C. H., CHOI, S. H., CHO, S. H., LEE, W. J. & SUH, Y. H. 2004. Alpha-synuclein induces apoptosis by altered expression in human peripheral lymphocyte in Parkinson's disease. *Faseb j*, 18, 1615-7.
- KNIGHT, C. G., MORTON, L. F., ONLEY, D. J., PEACHEY, A. R., ICHINOHE, T., OKUMA, M., FARNDAL, R. W. & BARNES, M. J. 1999. Collagen-platelet interaction: Gly-Pro-Hyp is

- uniquely specific for platelet Gp VI and mediates platelet activation by collagen. *Cardiovasc Res*, 41, 450-7.
- KNIGHT, C. G., MORTON, L. F., PEACHEY, A. R., TUCKWELL, D. S., FARNDALE, R. W. & BARNES, M. J. 2000. The collagen-binding A-domains of integrins alpha(1)beta(1) and alpha(2)beta(1) recognize the same specific amino acid sequence, GFOGER, in native (triple-helical) collagens. *J Biol Chem*, 275, 35-40.
- KOBILKA, B., MATSUI, H., KOBILKA, T., YANG-FENG, T., FRANCKE, U., CARON, M., LEFKOWITZ, R. & REGAN, J. 1987. Cloning, sequencing, and expression of the gene coding for the human platelet α 2-adrenergic receptor. *Science*, 238, 650-656.
- KOÇER, A., YAMAN, A., NIFTALIYEV, E., DÜRÜYEN, H., ERYILMAZ, M. & KOÇER, E. 2013. Assessment of Platelet Indices in Patients with Neurodegenerative Diseases: Mean Platelet Volume Was Increased in Patients with Parkinson's Disease. *Current Gerontology and Geriatrics Research*, 2013, 986254.
- KOEDAM, J. A., CRAMER, E. M., BRIEND, E., FURIE, B., FURIE, B. C. & WAGNER, D. D. 1992. P-selectin, a granule membrane protein of platelets and endothelial cells, follows the regulated secretory pathway in AtT-20 cells. *The Journal of cell biology*, 116, 617-625.
- KOIKE, S. & JAHN, R. 2019. SNAREs define targeting specificity of trafficking vesicles by combinatorial interaction with tethering factors. *Nature Communications*, 10, 1608.
- KONOPATSKAYA, O., MATTHEWS, S. A., HARPER, M. T., GILIO, K., COSEMANS, J. M. E. M., WILLIAMS, C. M., NAVARRO, M. N., CARTER, D. A., HEEMSKERK, J. W. M., LEITGES, M., CANTRELL, D. & POOLE, A. W. 2011. Protein kinase C mediates platelet secretion and thrombus formation through protein kinase D2. *Blood*, 118, 416-424.
- KONSTANTINIDES, S., WARE, J., MARCHESI, P., ALMUS-JACOBS, F., LOSKUTOFF, D. J. & RUGGERI, Z. M. 2006. Distinct antithrombotic consequences of platelet glycoprotein Iba and VI deficiency in a mouse model of arterial thrombosis. *Journal of Thrombosis and Haemostasis*, 4, 2014-2021.
- KOSEOGLU, S., PETERS, C. G., FITCH-TEWFIK, J. L., AISIKU, O., DANGLLOT, L., GALLI, T. & FLAUMENHAFT, R. 2015. VAMP-7 links granule exocytosis to actin reorganization during platelet activation. *Blood*, 126, 651-60.
- KRISHNAMURTHY, A. & JIMENO, A. 2017. Atezolizumab: A novel PD-L1 inhibitor in cancer therapy with a focus in bladder and non-small cell lung cancers. *Drugs Today (Barc)*, 53, 217-237.
- KROLL, M. H., ROJAS-HERNANDEZ, C. & YEE, C. 2022. Hematologic complications of immune checkpoint inhibitors. *Blood*, 139, 3594-3604.
- KUIJPERS, M. J. E., WITT, S. D., NERGIZ-UNAL, R., KRUCHTEN, R. V., KORPORAAL, S. J. A., VERHAMME, P., FEBBRAIO, M., TJWA, M., VOSHOL, P. J., HOYLAERTS, M. F., COSEMANS, J. M. E. M. & HEEMSKERK, J. W. M. 2014. Supporting Roles of Platelet Thrombospondin-1 and CD36 in Thrombus Formation on Collagen. *Arteriosclerosis, Thrombosis, and Vascular Biology*, 34, 1187-1192.
- KUNAPULI, S. P., DING, Z., DORSAM, R. T., KIM, S., MURUGAPPAN, S. & QUINTON, T. M. 2003a. ADP receptors--targets for developing antithrombotic agents. *Curr Pharm Des*, 9, 2303-16.
- KUNAPULI, S. P., DING, Z., DORSAM, R. T., KIM, S., MURUGAPPAN, S. & QUINTON, T. M. 2003b. ADP receptors--targets for developing antithrombotic agents. *Current pharmaceutical design*, 9, 2303-2316.
- LAEMMLI, U. K. 1970. Cleavage of Structural Proteins during the Assembly of the Head of Bacteriophage T4. *Nature*, 227, 680-685.
- LAI, Y., KIM, S., VARKEY, J., LOU, X., SONG, J.-K., DIAO, J., LANGEN, R. & SHIN, Y.-K. 2014. Nonaggregated α -synuclein influences SNARE-dependent vesicle docking via membrane binding. *Biochemistry*, 53, 3889-3896.
- LANE, W. O., JANTZEN, A. E., CARLON, T. A., JAMIOLKOWSKI, R. M., GRENET, J. E., LEY, M. M., HASELTINE, J. M., GALINAT, L. J., LIN, F.-H. & ALLEN, J. D. 2012. Parallel-plate flow chamber and continuous flow circuit to evaluate endothelial progenitor cells under laminar flow shear stress. *JoVE (Journal of Visualized Experiments)*, e3349.
- LASHUEL, H. A., OVERK, C. R., OUESLATI, A. & MASLIAH, E. 2013. The many faces of α -synuclein: from structure and toxicity to therapeutic target. *Nature reviews. Neuroscience*, 14, 38-48.
- LATCHMAN, Y., WOOD, C. R., CHERNOVA, T., CHAUDHARY, D., BORDE, M., CHERNOVA, I., IWAI, Y., LONG, A. J., BROWN, J. A. & NUNES, R. 2001. PD-L2 is a second ligand for PD-1 and inhibits T cell activation. *Nature immunology*, 2, 261-268.
- LATCHMAN, Y. E., LIANG, S. C., WU, Y., CHERNOVA, T., SOBEL, R. A., KLEMM, M., KUCHROO, V. K., FREEMAN, G. J. & SHARPE, A. H. 2004. PD-L1-deficient mice show that PD-L1 on T

- cells, antigen-presenting cells, and host tissues negatively regulates T cells. *Proc Natl Acad Sci U S A*, 101, 10691-6.
- LAUNAY, J., VITTET, D., VIDAUD, M., RONDOT, A., MATHIEU, M., LALAU-KERALY, C., CANTAU, B. & CHEVILLARD, C. 1987. V1a-vasopressin specific receptors on human platelets: potentiation by ADP and epinephrine and evidence for homologous down-regulation. *Thrombosis research*, 45, 323-331.
- LAUTENSCHLÄGER, J., STEPHENS, A. D., FUSCO, G., STRÖHL, F., CURRY, N., ZACHAROPOULOU, M., MICHEL, C. H., LAINE, R., NESPOVITAYA, N., FANTHAM, M., PINOTSI, D., ZAGO, W., FRASER, P., TANDON, A., ST GEORGE-HYSLOP, P., REES, E., PHILLIPS, J. J., DE SIMONE, A., KAMINSKI, C. F. & SCHIERLE, G. S. K. 2018. C-terminal calcium binding of α -synuclein modulates synaptic vesicle interaction. *Nat Commun*, 9, 712.
- LE BLANC, J. & LORDKIPANIDZÉ, M. 2019. Platelet Function in Aging. *Front Cardiovasc Med*, 6, 109.
- LEE, D., FONG, K. P., KING, M. R., BRASS, L. F. & HAMMER, D. A. 2012. Differential dynamics of platelet contact and spreading. *Biophys J*, 102, 472-82.
- LEE, J. C., LAI, B. T., KOZAK, J. J., GRAY, H. B. & WINKLER, J. R. 2007. α -Synuclein tertiary contact dynamics. *The Journal of Physical Chemistry B*, 111, 2107-2112.
- LEE, J. T., WHEELER, T. C., LI, L. & CHIN, L.-S. 2008. Ubiquitination of α -synuclein by Siah-1 promotes α -synuclein aggregation and apoptotic cell death. *Human molecular genetics*, 17, 906-917.
- LEE, S.-H., LIN, C.-C., WEI, C.-H., CHANG, K.-P., YUAN, C.-T., TSAI, C.-H., LIU, J.-H., HOU, H.-A., TANG, J.-L., CHOU, W.-C. & TIEN, H.-F. 2022. PD-L1 expression in megakaryocytes and its clinicopathological features in primary myelofibrosis patients. *The Journal of Pathology: Clinical Research*, 8, 78-87.
- LEFRANÇAIS, E., ORTIZ-MUÑOZ, G., CAUDRILLIER, A., MALLAVIA, B., LIU, F., SAYAH, D. M., THORNTON, E. E., HEADLEY, M. B., DAVID, T., COUGHLIN, S. R., KRUMMEL, M. F., LEAVITT, A. D., PASSEGUÉ, E. & LOONEY, M. R. 2017. The lung is a site of platelet biogenesis and a reservoir for haematopoietic progenitors. *Nature*, 544, 105-109.
- LEVINE, P. M., GALESIC, A., BALANA, A. T., MAHUL-MELLIER, A.-L., NAVARRO, M. X., DE LEON, C. A., LASHUEL, H. A. & PRATT, M. R. 2019. α -Synuclein O-GlcNAcylation alters aggregation and toxicity, revealing certain residues as potential inhibitors of Parkinson's disease. *Proceedings of the National Academy of Sciences*, 116, 1511-1519.
- LI, J.-Y., JENSEN, P. H. & DAHLSTRÖM, A. 2002a. Differential localization of α -, β - and γ -synucleins in the rat CNS. *Neuroscience*, 113, 463-478.
- LI, J., UVERSKY, V. N. & FINK, A. L. 2002b. Conformational behavior of human α -synuclein is modulated by familial Parkinson's disease point mutations A30P and A53T. *Neurotoxicology*, 23, 553-567.
- LI, M., ZHAO, R., CHEN, J., TIAN, W., XIA, C., LIU, X., LI, Y., LI, S., SUN, H., SHEN, T., REN, W. & SUN, L. 2021. Next generation of anti-PD-L1 Atezolizumab with enhanced anti-tumor efficacy in vivo. *Scientific Reports*, 11, 5774.
- LI, Y., XIN, G., LI, S., DONG, Y., ZHU, Y., YU, X., WAN, C., LI, F., WEI, Z., WANG, Y., ZHANG, K., CHEN, Q., NIU, H. & HUANG, W. 2022. PD-L1 Regulates Platelet Activation and Thrombosis via Caspase-3/GSDME Pathway. *Frontiers in Pharmacology*, 13, 921414.
- LIGEON, L.-A., MOREAU, K., BAROIS, N., BONGIOVANNI, A., LACORRE, D.-A., WERKMEISTER, E., PROUX-GILLARDEAUX, V., GALLI, T. & LAFONT, F. 2014. Role of VAMP3 and VAMP7 in the commitment of *Yersinia pseudotuberculosis* to LC3-associated pathways involving single-or double-membrane vacuoles. *Autophagy*, 10, 1588-1602.
- LIM, S.-O., LI, C.-W., XIA, W., CHA, J.-H., CHAN, L.-C., WU, Y., CHANG, S.-S., LIN, W.-C., HSU, J.-M., HSU, Y.-H., KIM, T., CHANG, W.-C., HSU, J. L., YAMAGUCHI, H., DING, Q., WANG, Y., YANG, Y., CHEN, C.-H., SAHIN, A. A., YU, D., HORTOBAGYI, G. N. & HUNG, M.-C. 2016. Deubiquitination and Stabilization of PD-L1 by CSN5. *Cancer Cell*, 30, 925-939.
- LING, L., WANG, F. & YU, D. 2022. Beyond neurodegenerative diseases: α -synuclein in erythropoiesis. *Hematology*, 27, 629-635.
- LIU, R., OLDHAM, R. J., TEAL, E., BEERS, S. A. & CRAGG, M. S. 2020. Fc-Engineering for Modulated Effector Functions-Improving Antibodies for Cancer Treatment. *Antibodies (Basel)*, 9.
- LIU, Y., QIANG, M., WEI, Y. & HE, R. 2011a. A novel molecular mechanism for nitrated α -synuclein-induced cell death. *Journal of molecular cell biology*, 3, 239-249.

- LIU, Y., SUGIURA, Y. & LIN, W. 2011b. The role of synaptobrevin1/VAMP1 in Ca²⁺-triggered neurotransmitter release at the mouse neuromuscular junction. *The Journal of physiology*, 589, 1603-1618.
- LIU, Z., CHAN, R. B., CAI, Z., LIU, X., WU, Y., YU, Z., FENG, T., YANG, Y. & ZHANG, J. 2022. α -Synuclein-containing erythrocytic extracellular vesicles: essential contributors to hyperactivation of monocytes in Parkinson's disease. *J Neuroinflammation*, 19, 53.
- LO, B., LI, L., GISSEN, P., CHRISTENSEN, H., MCKIERNAN, P. J., YE, C., ABDELHALEEM, M., HAYES, J. A., WILLIAMS, M. D., CHITAYAT, D. & KAHR, W. H. A. 2005. Requirement of VPS33B, a member of the Sec1/Munc18 protein family, in megakaryocyte and platelet α -granule biogenesis. *Blood*, 106, 4159-4166.
- LONGHENA, F., FAUSTINI, G., SPILLANTINI, M. G. & BELLUCCI, A. 2019. Living in Promiscuity: The Multiple Partners of Alpha-Synuclein at the Synapse in Physiology and Pathology. *Int J Mol Sci*, 20.
- LÓPEZ-BERGES, M., ARST, H., PINAR, M. & PEÑALVA, M. 2017. Genetic studies on the physiological role of CORVET in *Aspergillus nidulans*. *FEMS microbiology letters*, 364.
- LOU, X., KIM, J., HAWK, B. J. & SHIN, Y.-K. 2017. α -Synuclein may cross-bridge v-SNARE and acidic phospholipids to facilitate SNARE-dependent vesicle docking. *Biochemical Journal*, 474, 2039-2049.
- LOWRY, O. H., ROSEBROUGH, N. J., FARR, A. L. & RANDALL, R. J. 1951. Protein measurement with the Folin phenol reagent. *J Biol Chem*, 193, 265-75.
- LU, Y., PRUDENT, M., FAUVET, B., LASHUEL, H. A. & GIRAULT, H. H. 2011. Phosphorylation of α -synuclein at Y125 and S129 alters its metal binding properties: implications for understanding the role of α -synuclein in the pathogenesis of Parkinson's disease and related disorders. *ACS chemical neuroscience*, 2, 667-675.
- MA, C., LI, W., XU, Y. & RIZO, J. 2011. Munc13 mediates the transition from the closed syntaxin–Munc18 complex to the SNARE complex. *Nature structural & molecular biology*, 18, 542-549.
- MACFARLANE, S. R., SEATTER, M. J., KANKE, T., HUNTER, G. D. & PLEVIN, R. 2001. Proteinase-activated receptors. *Pharmacological reviews*, 53, 245-282.
- MAHAUT-SMITH, M. P., TOLHURST, G. & EVANS, R. J. 2004. Emerging roles for P2X1 receptors in platelet activation. *Platelets*, 15, 131-144.
- MAKHOUL, S., DORSCHER, S., GAMBARYAN, S., WALTER, U. & JURK, K. 2020. Feedback Regulation of Syk by Protein Kinase C in Human Platelets. *International Journal of Molecular Sciences*, 21, 176.
- MALSAM, J., PARISOTTO, D., BHARAT, T. A., SCHEUTZOW, A., KRAUSE, J. M., BRIGGS, J. A. & SÖLLNER, T. H. 2012. Complexin arrests a pool of docked vesicles for fast Ca²⁺-dependent release. *The EMBO journal*, 31, 3270-3281.
- MANGIN, P. H., ONSELAER, M. B., RECEVEUR, N., LE LAY, N., HARDY, A. T., WILSON, C., SANCHEZ, X., LOYAU, S., DUPUIS, A., BABAR, A. K., MILLER, J. L., PHILIPPOU, H., HUGHES, C. E., HERR, A. B., ARIÈNS, R. A., MEZZANO, D., JANDROT-PERRUS, M., GACHET, C. & WATSON, S. P. 2018. Immobilized fibrinogen activates human platelets through glycoprotein VI. *Haematologica*, 103, 898-907.
- MANNE, B. K., XIANG, S. C. & RONDINA, M. T. 2017. Platelet secretion in inflammatory and infectious diseases. *Platelets*, 28, 155-164.
- MANZANZA, N. O., SEDLACKOVA, L. & KALARIA, R. N. 2021. Alpha-Synuclein Post-translational Modifications: Implications for Pathogenesis of Lewy Body Disorders. *Front Aging Neurosci*, 13, 690293.
- MAOUIA, A., REBETZ, J., KAPUR, R. & SEMPLE, J. W. 2020. The Immune Nature of Platelets Revisited. *Transfus Med Rev*, 34, 209-220.
- MARGITTAI, M., FASSHAUER, D., JAHN, R. & LANGEN, R. 2003. The Habc Domain and the SNARE Core Complex Are Connected by a Highly Flexible Linker. *Biochemistry*, 42, 4009-4014.
- MARGRAF, A., NUSSBAUM, C. & SPERANDIO, M. 2019. Ontogeny of platelet function. *Blood advances*, 3, 692-703.
- MAROTEAUX, L., CAMPANELLI, J. T. & SCHELLER, R. H. 1988. Synuclein: a neuron-specific protein localized to the nucleus and presynaptic nerve terminal. *J Neurosci*, 8, 2804-15.
- MARTINEZ-ARCA, S., ALBERTS, P., ZAHRAOUI, A., LOUVARD, D. & GALLI, T. 2000. Role of tetanus neurotoxin insensitive vesicle-associated membrane protein (TI-VAMP) in vesicular transport mediating neurite outgrowth. *The Journal of cell biology*, 149, 889-900.
- MASAROVA, L., ALHURAIJI, A., BOSE, P., DAVER, N., PEMMARAJU, N., CORTES, J., PIERCE, S., KANTARJIAN, H. & VERSTOVSEK, S. 2018. Significance of thrombocytopenia in patients

- with primary and postessential thrombocythemia/polycythemia vera myelofibrosis. *Eur J Haematol*, 100, 257-263.
- MASLIAH, E., ROCKENSTEIN, E., VEINBERGS, I., MALLORY, M., HASHIMOTO, M., TAKEDA, A., SAGARA, Y., SISK, A. & MUCKE, L. 2000. Dopaminergic loss and inclusion body formation in α -synuclein mice: implications for neurodegenerative disorders. *Science*, 287, 1265-1269.
- MASOOD, A. B., BATOOL, S., BHATTI, S. N., ALI, A., VALKO, M., JOMOVA, K. & KUČA, K. 2023. Plasma PD-L1 as a biomarker in the clinical management of glioblastoma multiforme—a retrospective cohort study. *Front Immunol*, 14, 1202098.
- MATTHEIJ, N. J., SWIERINGA, F., MASTENBROEK, T. G., BERNY-LANG, M. A., MAY, F., BAATEN, C. C., VAN DER MEIJDEN, P. E., HENSKENS, Y. M., BECKERS, E. A. & SUYLEN, D. P. 2016. Coated platelets function in platelet-dependent fibrin formation via integrin α IIb β 3 and transglutaminase factor XIII. *Haematologica*, 101, 427.
- MAY, F., HAGEDORN, I., PLEINES, I., BENDER, M., VÖGTLE, T., EBLE, J., ELVERS, M. & NIESWANDT, B. 2009. CLEC-2 is an essential platelet-activating receptor in hemostasis and thrombosis. *Blood*, 114, 3464-3472.
- MAZEL, M., JACOT, W., PANTEL, K., BARTKOWIAK, K., TOPART, D., CAYREFOURCQ, L., ROSSILLE, D., MAUDELONDE, T., FEST, T. & ALIX-PANABIÈRES, C. 2015. Frequent expression of PD-L1 on circulating breast cancer cells. *Molecular oncology*, 9, 1773-1782.
- MCCARTY, O. J. T., ZHAO, Y., ANDREW, N., MACHESKY, L. M., STAUNTON, D., FRAMPTON, J. & WATSON, S. P. 2004. Evaluation of the role of platelet integrins in fibronectin-dependent spreading and adhesion. *Journal of Thrombosis and Haemostasis*, 2, 1823-1833.
- MCGRATH, R. T., MCRAE, E., SMITH, O. P. & O'DONNELL, J. S. 2010. Platelet von Willebrand factor—structure, function and biological importance. *Br J Haematol*, 148, 834-43.
- MEETHS, M., CHIANG, S. C. C., WOOD, S. M., ENTESARIAN, M., SCHLUMS, H., BANG, B., NORDENSKJÖLD, E., BJÖRKLUND, C., JAKOVLJEVIC, G., JAZBEC, J., HASLE, H., HOLMQVIST, B.-M., RAJIĆ, L., PFEIFER, S., ROSTHØJ, S., SABEL, M., SALMI, T. T., STOKLAND, T., WINIARSKI, J., LJUNGGREN, H.-G., FADEEL, B., NORDENSKJÖLD, M., HENTER, J.-I. & BRYCESON, Y. T. 2011. Familial hemophagocytic lymphohistiocytosis type 3 (FHL3) caused by deep intronic mutation and inversion in UNC13D. *Blood*, 118, 5783-5793.
- MENTER, D. G., TUCKER, S. C., KOPETZ, S., SOOD, A. K., CRISSMAN, J. D. & HONN, K. V. 2014. Platelets and cancer: a casual or causal relationship: revisited. *Cancer metastasis reviews*, 33, 231-269.
- MERCADO, C. P. & KILIC, F. 2010. Molecular mechanisms of SERT in platelets: regulation of plasma serotonin levels. *Molecular interventions*, 10, 231.
- MERTEN, M. & THIAGARAJAN, P. 2000. P-selectin expression on platelets determines size and stability of platelet aggregates. *Circulation*, 102, 1931-1936.
- MIKHAILIDIS, D. & GANOTAKIS, E. 1996. Plasma albumin and platelet function: relevance to atherogenesis and thrombosis. *Platelets*, 7, 125-137.
- MILOSEVIC FEENSTRA, J. D., JÄGER, R., SCHISCHLIK, F., IVANOV, D., EISENWORT, G., RUMI, E., SCHUSTER, M., GISSLINGER, B., MACHHERNDL-SPANDL, S., BETTELHEIM, P., KRAUTH, M.-T., KEIL, F., BOCK, C., CAZZOLA, M., GISSLINGER, H., KRALOVICS, R. & VALENT, P. 2022. PD-L1 overexpression correlates with JAK2-V617F mutational burden and is associated with 9p uniparental disomy in myeloproliferative neoplasms. *American Journal of Hematology*, 97, 390-400.
- MISURA, K. M., SCHELLER, R. H. & WEIS, W. I. 2000. Three-dimensional structure of the neuronal-Sec1–syntaxin 1a complex. *Nature*, 404, 355-362.
- MOON, S. P., BALANA, A. T., GALESIC, A., RAKSHIT, A. & PRATT, M. R. 2020. Ubiquitination Can Change the Structure of the α -Synuclein Amyloid Fiber in a Site Selective Fashion. *J Org Chem*, 85, 1548-1555.
- MORALES, M., COLICOS, M. A. & GODA, Y. 2000. Actin-dependent regulation of neurotransmitter release at central synapses. *Neuron*, 27, 539-550.
- MORRELL, C. N., MATSUSHITA, K., CHILES, K., SCHARPF, R. B., YAMAKUCHI, M., MASON, R. J., BERGMEIER, W., MANKOWSKI, J. L., BALDWIN III, W. M. & FARADAY, N. 2005. Regulation of platelet granule exocytosis by S-nitrosylation. *Proceedings of the National Academy of Sciences*, 102, 3782-3787.
- MORRISSEY, K. M., MARCHAND, M., PATEL, H., ZHANG, R., WU, B., PHYLLIS CHAN, H., MECKE, A., GIRISH, S., JIN, J. Y., WINTER, H. R. & BRUNO, R. 2019. Alternative dosing regimens for atezolizumab: an example of model-informed drug development in the postmarketing setting. *Cancer Chemother Pharmacol*, 84, 1257-1267.

- MORTON, L. F., HARGREAVES, P. G., FARNDAL, R. W., YOUNG, R. D. & BARNES, M. J. 1995. Integrin alpha 2 beta 1-independent activation of platelets by simple collagen-like peptides: collagen tertiary (triple-helical) and quaternary (polymeric) structures are sufficient alone for alpha 2 beta 1-independent platelet reactivity. *Biochem J*, 306 (Pt 2), 337-44.
- MULLALLY, A., LANE, S. W., BALL, B., MEGERDICHIAN, C., OKABE, R., AL-SHAHROUR, F., PAKTINAT, M., HAYDU, J. E., HOUSMAN, E. & LORD, A. M. 2010. Physiological Jak2V617F expression causes a lethal myeloproliferative neoplasm with differential effects on hematopoietic stem and progenitor cells. *Cancer cell*, 17, 584-596.
- MUMFORD, A. D., FRELINGER III, A. L., GACHET, C., GRESELE, P., NORIS, P., HARRISON, P. & MEZZANO, D. 2015. A review of platelet secretion assays for the diagnosis of inherited platelet secretion disorders. *Thrombosis and haemostasis*, 114, 14-25.
- MUNSANJE, M. M., KAILE, T., KOWA, S., SINKALA, M., SIMAKANDO, M., NDHLOVU, J. & CHILUBA, B. C. 2021. von Willebrand factor activity and activated partial thromboplastin time as proxy biomarkers for coagulopathies in women with menorrhagia in Zambia: a case-control study. *Pan Afr Med J*, 39, 13.
- MYLLYHARJU, J. & KIVIRIKKO, K. I. 2001. Collagens and collagen-related diseases. *Annals of medicine*, 33, 7-21.
- NAGY, Z., VÖGTLE, T., GEER, M. J., MORI, J., HEISING, S., DI NUNZIO, G., GAREUS, R., TARAKHOVSKY, A., WEISS, A., NEEL, B. G., DESANTI, G. E., MAZHARIAN, A. & SENIS, Y. A. 2019. The Gp1ba-Cre transgenic mouse: a new model to delineate platelet and leukocyte functions. *Blood*, 133, 331-343.
- NAKAHATA, N. 2008. Thromboxane A2: physiology/pathophysiology, cellular signal transduction and pharmacology. *Pharmacol Ther*, 118, 18-35.
- NAKANISHI-MATSUI, M., ZHENG, Y. W., SULCINER, D. J., WEISS, E. J., LUDEMAN, M. J. & COUGHLIN, S. R. 2000. PAR3 is a cofactor for PAR4 activation by thrombin. *Nature*, 404, 609-13.
- NAKATA, M., YADA, T., SOEJIMA, N. & MARUYAMA, I. 1999. Leptin promotes aggregation of human platelets via the long form of its receptor. *Diabetes*, 48, 426-429.
- NALLS, M. A., PLAGNOL, V., HERNANDEZ, D. G., SHARMA, M., SHEERIN, U. M., SAAD, M., SIMÓN-SÁNCHEZ, J., SCHULTE, C., LESAGE, S., SVEINBJÖRNSDÓTTIR, S., STEFÁNSSON, K., MARTINEZ, M., HARDY, J., HEUTINK, P., BRICE, A., GASSER, T., SINGLETON, A. B. & WOOD, N. W. 2011. Imputation of sequence variants for identification of genetic risks for Parkinson's disease: a meta-analysis of genome-wide association studies. *Lancet*, 377, 641-9.
- NEMANI, V. M., LU, W., BERGE, V., NAKAMURA, K., ONOA, B., LEE, M. K., CHAUDHRY, F. A., NICOLL, R. A. & EDWARDS, R. H. 2010. Increased expression of α -synuclein reduces neurotransmitter release by inhibiting synaptic vesicle recluster after endocytosis. *Neuron*, 65, 66-79.
- NGUYEN, T. H., XU, Y., BRANDT, S., MANDELKOW, M., RASCHKE, R., STROBEL, U., DELCEA, M., ZHOU, W., LIU, J. & GREINACHER, A. 2020. Characterization of the interaction between platelet factor 4 and homogeneous synthetic low molecular weight heparins. *J Thromb Haemost*, 18, 390-398.
- NIELSEN, C., BIRGENS, H. S., NORDESTGAARD, B. G., KJAER, L. & BOJESEN, S. E. 2011. The JAK2 V617F somatic mutation, mortality and cancer risk in the general population. *Haematologica*, 96, 450-3.
- NIESWANDT, B., BRAKEBUSCH, C., BERGMIEIER, W., SCHULTE, V., BOUVARD, D., MOKHTARI-NEJAD, R., LINDHOUT, T., HEEMSKERK, J. W., ZIRNGIBL, H. & FÄSSLER, R. 2001. Glycoprotein VI but not alpha2beta1 integrin is essential for platelet interaction with collagen. *Embo j*, 20, 2120-30.
- NIESWANDT, B. & WATSON, S. P. 2003. Platelet-collagen interaction: is GPVI the central receptor? *Blood*, 102, 449-461.
- NINKINA, N., CONNOR-ROBSON, N., USTYUGOV, A. A., TARASOVA, T. V., SHELKOVNIKOVA, T. A. & BUCHMAN, V. L. 2015. A novel resource for studying function and dysfunction of α -synuclein: mouse lines for modulation of endogenous Snca gene expression. *Sci Rep*, 5, 16615.
- NISHIZAWA, E. E., MILLER, W. L., GORMAN, R. R., BUNDY, G. L., SVENSSON, J. & HAMBERG, M. 1975. Prostaglandin D2 as a potential antithrombotic agent. *Prostaglandins*, 9, 109-121.
- NOÉ, L., PEETERS, K., IZZI, B., VAN GEET, C. & FRESON, K. 2010. Regulators of platelet cAMP levels: clinical and therapeutic implications. *Curr Med Chem*, 17, 2897-905.

- NONAKA, T., IWATSUBO, T. & HASEGAWA, M. 2005. Ubiquitination of α -synuclein. *Biochemistry*, 44, 361-368.
- NURDEN, A. T. 2011. Platelets, inflammation and tissue regeneration. *Thromb Haemost*, 105 Suppl 1, S13-33.
- NURDEN, A. T. & CAEN, J. P. 1975. Specific roles for platelet surface glycoproteins in platelet function. *Nature*, 255, 720-722.
- NURDEN, A. T. & NURDEN, P. 2007. The gray platelet syndrome: clinical spectrum of the disease. *Blood reviews*, 21, 21-36.
- OFFENHÄUSER, C., LEI, N., ROY, S., COLLINS, B. M., STOW, J. L. & MURRAY, R. Z. 2011. Syntaxin 11 Binds Vti1b and Regulates Late Endosome to Lysosome Fusion in Macrophages. *Traffic*, 12, 762-773.
- OKOCHI, M., WALTER, J., KOYAMA, A., NAKAJO, S., BABA, M., IWATSUBO, T., MEIJER, L., KAHLE, P. J. & HAASS, C. 2000. Constitutive phosphorylation of the Parkinson's disease associated alpha-synuclein. *J Biol Chem*, 275, 390-7.
- OLIVEIRA DA SILVA, M. I. & LIZ, M. A. 2020. Linking Alpha-Synuclein to the Actin Cytoskeleton: Consequences to Neuronal Function. *Front Cell Dev Biol*, 8, 787.
- OLMSTED, J., 3RD & KEARNS, D. R. 1977. Mechanism of ethidium bromide fluorescence enhancement on binding to nucleic acids. *Biochemistry*, 16, 3647-54.
- OSTROWSKI, M., CARMO, N. B., KRUMEICH, S., FANGET, I., RAPOSO, G., SAVINA, A., MOITA, C. F., SCHAUER, K., HUME, A. N., FREITAS, R. P., GOUD, B., BENARROCH, P., HACOEN, N., FUKUDA, M., DESNOS, C., SEABRA, M. C., DARCHEN, F., AMIGORENA, S., MOITA, L. F. & THERY, C. 2010. Rab27a and Rab27b control different steps of the exosome secretion pathway. *Nat Cell Biol*, 12, 19-30; sup pp 1-13.
- OYA, K., SHEN, L. T.-W., MARUO, K. & MATSUSAKA, S. 2022. Plasma Exchange May Enhance Antitumor Effects by Removal of Soluble Programmed Death-Ligand 1 and Extracellular Vesicles: Preliminary Study. *Biomedicines*, 10, 2483.
- PARK, S. M., JUNG, H. Y., KIM, H. O., RHIM, H., PAIK, S. R., CHUNG, K. C., PARK, J. H. & KIM, J. 2002. Evidence that α -synuclein functions as a negative regulator of Ca^{++} -dependent α -granule release from human platelets. *Blood*, 100, 2506-2514.
- PARRA-RIVAS, L. A., MADHIVANAN, K., AULSTON, B. D., WANG, L., PRAKASHCHAND, D. D., BOYER, N. P., SAIA-CEREDA, V. M., BRANES-GUERRERO, K., PIZZO, D. P., BAGCHI, P., SUNDAR, V. S., TANG, Y., DAS, U., SCOTT, D. A., RANGAMANI, P., OGAWA, Y. & SUBHOJIT, R. 2023. Serine-129 phosphorylation of α -synuclein is an activity-dependent trigger for physiologic protein-protein interactions and synaptic function. *Neuron*, 111, 4006-4023.e10.
- PATEL-HETT, S., RICHARDSON, J. L., SCHULZE, H., DRABEK, K., ISAAC, N. A., HOFFMEISTER, K., SHIVDASANI, R. A., BULINSKI, J. C., GALJART, N., HARTWIG, J. H. & ITALIANO, J. E., JR. 2008. Visualization of microtubule growth in living platelets reveals a dynamic marginal band with multiple microtubules. *Blood*, 111, 4605-16.
- PATSOUKIS, N., BARDHAN, K., CHATTERJEE, P., SARI, D., LIU, B., BELL, L. N., KAROLY, E. D., FREEMAN, G. J., PETKOVA, V. & SETH, P. 2015. PD-1 alters T-cell metabolic reprogramming by inhibiting glycolysis and promoting lipolysis and fatty acid oxidation. *Nature communications*, 6, 6692.
- PAUL, B. Z., JIN, J. & KUNAPULI, S. P. 1999. Molecular Mechanism of Thromboxane A2-induced Platelet Aggregation: ESSENTIAL ROLE FOR P2TAC and α 2ARECEPTORS. *Journal of Biological Chemistry*, 274, 29108-29114.
- PAUMET, F., RAHIMIAN, V. & ROTHMAN, J. E. 2004. The specificity of SNARE-dependent fusion is encoded in the SNARE motif. *Proceedings of the National Academy of Sciences*, 101, 3376-3380.
- PEI, Y. & MAITTA, R. W. 2019. Alpha synuclein in hematopoiesis and immunity. *Heliyon*, 5, e02590.
- PERRIN, R. J., WOODS, W. S., CLAYTON, D. F. & GEORGE, J. M. 2000. Interaction of human α -synuclein and Parkinson's disease variants with phospholipids: structural analysis using site-directed mutagenesis. *Journal of Biological Chemistry*, 275, 34393-34398.
- PERTUY, F., AGUILAR, A., STRASSEL, C., ECKLY, A., FREUND, J. N., DULUC, I., GACHET, C., LANZA, F. & LEON, C. 2015. Broader expression of the mouse platelet factor 4-cre transgene beyond the megakaryocyte lineage. *Journal of Thrombosis and Haemostasis*, 13, 115-125.
- PFEFFERKORN, C. M., JIANG, Z. & LEE, J. C. 2012. Biophysics of α -synuclein membrane interactions. *Biochim Biophys Acta*, 1818, 162-71.
- PIENIMAELKI-ROEMER, A., KUHLMANN, K., BÖTTCHER, A., KONOVALOVA, T., BLACK, A., ORSÓ, E., LIEBISCH, G., AHRENS, M., EISENACHER, M., MEYER, H. E. & SCHMITZ, G.

2015. Lipidomic and proteomic characterization of platelet extracellular vesicle subfractions from senescent platelets. *Transfusion*, 55, 507-521.
- PIERRE, H. M., MARIE-BLANCHE, O., NICOLAS, R., NICOLAS LE, L., ALEXANDER, T. H., CLARE, W., XIMENA, S., STÉPHANE, L., ARNAUD, D., AMIR, K. B., JEANETTE, L. C. M., HELEN, P., CRAIG, E. H., ANDREW, B. H., ROBERT, A. S. A., DIEGO, M., MARTINE, J.-P., CHRISTIAN, G. & STEVE, P. W. 2018. Immobilized fibrinogen activates human platelets through glycoprotein VI. *Haematologica*, 103, 898-907.
- PLUTHERO, F. G. & KAHR, W. H. A. 2016. Platelet production: new players in the field. *Blood*, 127, 797-799.
- POKROVSKAYA, I. D., JOSHI, S., TOBIN, M., DESAI, R., ARONOVA, M. A., KAMYKOWSKI, J. A., ZHANG, G., WHITEHEART, S. W., LEAPMAN, R. D. & STORRIE, B. 2018. SNARE-dependent membrane fusion initiates α -granule matrix decondensation in mouse platelets. *Blood advances*, 2, 2947-2958.
- POKROVSKAYA, I. D., YADAV, S., RAO, A., MCBRIDE, E., KAMYKOWSKI, J. A., ZHANG, G., ARONOVA, M. A., LEAPMAN, R. D. & STORRIE, B. 2020. 3D ultrastructural analysis of α -granule, dense granule, mitochondria, and canalicular system arrangement in resting human platelets. *Res Pract Thromb Haemost*, 4, 72-85.
- POLGÁR, J., LANE, W. S., CHUNG, S.-H., HOUNG, A. K. & REED, G. L. 2003. Phosphorylation of SNAP-23 in Activated Human Platelets *. *Journal of Biological Chemistry*, 278, 44369-44376.
- POLYMEROPOULOS, M. H., LAVEDAN, C., LEROY, E., IDE, S. E., DEHEJIA, A., DUTRA, A., PIKE, B., ROOT, H., RUBENSTEIN, J., BOYER, R., STENROOS, E. S., CHANDRASEKHARAPPA, S., ATHANASSIADOU, A., PAPAPETROPOULOS, T., JOHNSON, W. G., LAZZARINI, A. M., DUVOISIN, R. C., DI IORIO, G., GOLBE, L. I. & NUSSBAUM, R. L. 1997. Mutation in the α -Synuclein Gene Identified in Families with Parkinson's Disease. *Science*, 276, 2045-2047.
- POOLE, A., GIBBINS, J. M., TURNER, M., VAN VUGT, M. J., VAN DE WINKEL, J. G. J., SAITO, T., TYBULEWICZ, V. L. J. & WATSON, S. P. 1997. The Fc receptor γ -chain and the tyrosine kinase Syk are essential for activation of mouse platelets by collagen. *The EMBO Journal*, 16, 2333-2341.
- PORTIER, I. & CAMPBELL, R. A. 2021. Role of Platelets in Detection and Regulation of Infection. *Arterioscler Thromb Vasc Biol*, 41, 70-78.
- POULTER, N. S., POLLITT, A. Y., DAVIES, A., MALINOVA, D., NASH, G. B., HANNON, M. J., PIKRAMENOU, Z., RAPPOPORT, J. Z., HARTWIG, J. H. & OWEN, D. M. 2015. Platelet actin nodules are podosome-like structures dependent on Wiskott–Aldrich syndrome protein and ARP2/3 complex. *Nature communications*, 6, 7254.
- PRESTIPINO, A., EMHARDT, A. J., AUMANN, K., O'SULLIVAN, D., GORANTLA, S. P., DUQUESNE, S., MELCHINGER, W., BRAUN, L., VUCKOVIC, S., BOERRIES, M., BUSCH, H., HALBACH, S., PENNISI, S., POGGIO, T., APOSTOLOVA, P., VERATTI, P., HETTICH, M., NIEDERMANN, G., BARTHOLOMÄ, M., SHOUMARIYEH, K., JUTZI, J. S., WEHRLE, J., DIERKS, C., BECKER, H., SCHMITT-GRAEFF, A., FOLLO, M., PFEIFER, D., ROHR, J., FUCHS, S., EHL, S., HARTL, F. A., MINGUET, S., MIETHING, C., HEIDEL, F. H., KRÖGER, N., TRIVIAI, I., BRUMMER, T., FINKE, J., ILLERT, A. L., RUGGIERO, E., BONINI, C., DUYSSTER, J., PAHL, H. L., LANE, S. W., HILL, G. R., BLAZAR, B. R., VON BUBNOFF, N., PEARCE, E. L. & ZEISER, R. 2018. Oncogenic JAK2(V617F) causes PD-L1 expression, mediating immune escape in myeloproliferative neoplasms. *Sci Transl Med*, 10.
- QIAN, J., WANG, C., WANG, B., YANG, J., WANG, Y., LUO, F., XU, J., ZHAO, C., LIU, R. & CHU, Y. 2018. The IFN- γ /PD-L1 axis between T cells and tumor microenvironment: hints for glioma anti-PD-1/PD-L1 therapy. *Journal of Neuroinflammation*, 15, 290.
- QIU, G., LI, S., LI, B., YANG, Q., DENG, H., YANG, Y., XIE, X., LIN, X., SEKI, N., MIURA, S., SHUKUYA, T., ZHOU, C. & LIU, M. 2022. Immune thrombocytopenia in a small cell lung cancer patient treated with atezolizumab: a case report. *Transl Lung Cancer Res*, 11, 2346-2355.
- RAJAGOPALAN, S. & ANDERSEN, J. K. 2001. Alpha synuclein aggregation: is it the toxic gain of function responsible for neurodegeneration in Parkinson's disease? *Mechanisms of Ageing and Development*, 122, 1499-1510.
- RAMAKRISHNAN, N. A., DRESCHER, M. J. & DRESCHER, D. G. 2012. The SNARE complex in neuronal and sensory cells. *Mol Cell Neurosci*, 50, 58-69.
- RAMALINGAM, N., JIN, S.-X., MOORS, T. E., FONSECA-ORNELAS, L., SHIMANAKA, K., LEI, S., CAM, H. P., WATSON, A. H., BRONTESI, L., DING, L., HACIBALOGU, D. Y., JIANG, H., CHOI, S. J., KANTER, E., LIU, L., BARTELS, T., NUBER, S., SULZER, D., MOSHAROV, E.

- V., CHEN, W. V., LI, S., SELKOE, D. J. & DETTMER, U. 2023. Dynamic physiological α -synuclein S129 phosphorylation is driven by neuronal activity. *npj Parkinson's Disease*, 9, 4.
- RANA, A., WESTEIN, E., NIEGO, B. E. & HAGEMeyer, C. E. 2019. Shear-Dependent Platelet Aggregation: Mechanisms and Therapeutic Opportunities. *Frontiers in Cardiovascular Medicine*, 6.
- RASCHE, H. 2001. Haemostasis and thrombosis: an overview. *European heart journal supplements*, 3, Q3-Q7.
- RAVN, H. B., VISSINGER, H., KRISTENSEN, S. D., WENNMALM, A., THYGESEN, K. & HUSTED, S. E. 1996. Magnesium inhibits platelet activity-an infusion study in healthy volunteers. *Thrombosis and haemostasis*, 75, 939-944.
- REALES, E., SHARMA, N., LOW, S. H., FÖLSCH, H. & WEIMBS, T. 2011. Basolateral sorting of syntaxin 4 is dependent on its N-terminal domain and the AP1B clathrin adaptor, and required for the epithelial cell polarity. *PLoS One*, 6, e21181.
- REED, G. L., HOUNG, A. K. & FITZGERALD, M. L. 1999. Human platelets contain SNARE proteins and a Sec1p homologue that interacts with syntaxin 4 and is phosphorylated after thrombin activation: implications for platelet secretion. *Blood*, 93, 2617-26.
- REMIJN, J. A., WU, Y.-P., JENINGA, E. H., IJSSELDIJK, M. J. W., WILLIGEN, G. V., GROOT, P. G. D., SIXMA, J. J., NURDEN, A. T. & NURDEN, P. 2002. Role of ADP Receptor P2Y₁₂ in Platelet Adhesion and Thrombus Formation in Flowing Blood. *Arteriosclerosis, Thrombosis, and Vascular Biology*, 22, 686-691.
- REN, Q., BARBER, H. K., CRAWFORD, G. L., KARIM, Z. A., ZHAO, C., CHOI, W., WANG, C.-C., HONG, W. & WHITEHEART, S. W. 2007. Endobrevin/VAMP-8 is the primary v-SNARE for the platelet release reaction. *Molecular biology of the cell*, 18, 24-33.
- RENDU, F. & BROHARD-BOHN, B. 2001. The platelet release reaction: granules' constituents, secretion and functions. *Platelets*, 12, 261-273.
- RIBATTI, D. & CRIVELLATO, E. 2007. Giulio Bizzozzero and the discovery of platelets. *Leukemia research*, 31, 1339-1341.
- RICARD-BLUM, S. 2011. The collagen family. *Cold Spring Harbor perspectives in biology*, 3, a004978-a004978.
- RICCI, A., BRONZETTI, E., MANNINO, F., MIGNINI, F., MOROSETTI, C., TAYEBATI, S. K. & AMENTA, F. 2001. Dopamine receptors in human platelets. *Naunyn-Schmiedeberg's archives of pharmacology*, 363, 376-382.
- RIVERA, J., LOZANO, M. L., NAVARRO-NUNEZ, L. & VICENTE, V. 2009. Platelet receptors and signaling in the dynamics of thrombus formation. *Haematologica*, 94, 700-711.
- ROBERTS, W., MAGWENZI, S., ABURIMA, A. & NASEEM, K. M. 2010. Thrombospondin-1 induces platelet activation through CD36-dependent inhibition of the cAMP/protein kinase A signaling cascade. *Blood*, 116, 4297-4306.
- RODRIGUEZ-ARAUJO, G., NAKAGAMI, H., TAKAMI, Y., KATSUYA, T., AKASAKA, H., SAITOH, S., SHIMAMOTO, K., MORISHITA, R., RAKUGI, H. & KANEDA, Y. 2015. Low alpha-synuclein levels in the blood are associated with insulin resistance. *Scientific reports*, 5, 12081-12081.
- ROLFES, V., IDEL, C., PRIES, R., PLÖTZE-MARTIN, K., HABERMANN, J., GEMOLL, T., BOHNET, S., LATZ, E., RIBBAT-IDEL, J. & FRANKLIN, B. S. 2018. PD-L1 is expressed on human platelets and is affected by immune checkpoint therapy. *Oncotarget*, 9, 27460.
- ROODVELDT, C., CHRISTODOULOU, J. & DOBSON, C. M. 2008. Immunological features of α -synuclein in Parkinson's disease. *Journal of Cellular and Molecular Medicine*, 12, 1820-1829.
- ROSADO, J. A., JENNER, S. & SAGE, S. O. 2000. A role for the actin cytoskeleton in the initiation and maintenance of store-mediated calcium entry in human platelets: evidence for conformational coupling. *Journal of Biological Chemistry*, 275, 7527-7533.
- ROTHMAN, J. E. 1994. Mechanisms of intracellular protein transport. *Nature*, 372, 55-63.
- RUGGERI, Z. M., ORJE, J. N., HABERMANN, R., FEDERICI, A. B. & REININGER, A. J. 2006. Activation-independent platelet adhesion and aggregation under elevated shear stress. *Blood*, 108, 1903-1910.
- RUSSO, A., SOH, U. J. & TREJO, J. 2009. Proteases display biased agonism at protease-activated receptors: location matters! *Mol Interv*, 9, 87-96.
- SACHS, U. J. & NIESWANDT, B. 2007. In vivo thrombus formation in murine models. *Circ Res*, 100, 979-91.
- SAGE, P. T., SCHILDBERG, F. A., SOBEL, R. A., KUCHROO, V. K., FREEMAN, G. J. & SHARPE, A. H. 2018. Dendritic Cell PD-L1 Limits Autoimmunity and Follicular T Cell Differentiation and Function. *J Immunol*, 200, 2592-2602.

- SAMUEL, F., FLAVIN, W. P., IQBAL, S., PACELLI, C., RENGANATHAN, S. D. S., TRUDEAU, L.-E., CAMPBELL, E. M., FRASER, P. E. & TANDON, A. 2016. Effects of serine 129 phosphorylation on α -synuclein aggregation, membrane association, and internalization. *Journal of Biological Chemistry*, 291, 4374-4385.
- SANG, Y., ROEST, M., DE LAAT, B., DE GROOT, P. G. & HUSKENS, D. 2021. Interplay between platelets and coagulation. *Blood reviews*, 46, 100733.
- SANMAMED, M. F. & CHEN, L. 2014. Inducible expression of B7-H1 (PD-L1) and its selective role in tumor site immune modulation. *Cancer J*, 20, 256-61.
- SASAKI, A., ARAWAKA, S., SATO, H. & KATO, T. 2015. Sensitive western blotting for detection of endogenous Ser129-phosphorylated α -synuclein in intracellular and extracellular spaces. *Scientific Reports*, 5, 14211.
- SATO, M., HIRAKATA, H., NAKAGAWA, T., ARAI, K. & FUKUDA, K. 2003. Thiamylal and pentobarbital have opposite effects on human platelet aggregation in vitro. *Anesth Analg*, 97, 1353-1359.
- SAUNDERS, N. A. & JETTEN, A. M. 1994. Control of growth regulatory and differentiation-specific genes in human epidermal keratinocytes by interferon gamma. Antagonism by retinoic acid and transforming growth factor beta 1. *Journal of Biological Chemistry*, 269, 2016-2022.
- SAVCHENKO, A., MARTINOD, K., SEIDMAN, M., WONG, S., BORISSOFF, J., PIAZZA, G., LIBBY, P., GOLDHABER, S., MITCHELL, R. & WAGNER, D. 2014. Neutrophil extracellular traps form predominantly during the organizing stage of human venous thromboembolism development. *Journal of Thrombosis and Haemostasis*, 12, 860-870.
- SCHAFF, M., TANG, C., MAURER, E., BOURDON, C., RECEVEUR, N., ECKLY, A., HECHLER, B., ARNOLD, C., DE ARCANGELIS, A. & NIESWANDT, B. 2013. Integrin α 6 β 1 is the main receptor for vascular laminins and plays a role in platelet adhesion, activation, and arterial thrombosis. *Circulation*, 128, 541-552.
- SCHMIED, L., HÖGLUND, P. & MEINKE, S. 2021. Platelet-Mediated Protection of Cancer Cells From Immune Surveillance - Possible Implications for Cancer Immunotherapy. *Front Immunol*, 12, 640578.
- SCHROTTMAIER, W., KRAL, J., ZEITLINGER, M., SALZMANN, M., JILMA, B. & ASSINGER, A. 2016. Platelet activation at the onset of human endotoxemia is undetectable in vivo. *Platelets*, 27, 1-5.
- SCHUEPBACH, R. A., MADON, J., ENDER, M., GALLI, P. & RIEWALD, M. 2012. Protease-activated receptor-1 cleaved at R46 mediates cytoprotective effects. *J Thromb Haemost*, 10, 1675-84.
- SEABRA, M. C. & COUDRIER, E. 2004. Rab GTPases and myosin motors in organelle motility. *Traffic*, 5, 393-399.
- SEET, R. C., LEE, C.-Y. J., LIM, E. C., TAN, J. J., QUEK, A. M., CHONG, W.-L., LOOI, W.-F., HUANG, S.-H., WANG, H. & CHAN, Y.-H. 2010. Oxidative damage in Parkinson disease: Measurement using accurate biomarkers. *Free Radical Biology and Medicine*, 48, 560-566.
- SELVADURAI, M. V. & HAMILTON, J. R. 2018. Structure and function of the open canalicular system – the platelet's specialized internal membrane network. *Platelets*, 29, 319-325.
- SEMPLE, J. W., ITALIANO, J. E., JR. & FREEDMAN, J. 2011. Platelets and the immune continuum. *Nat Rev Immunol*, 11, 264-74.
- SENIS, Y. A., TOMLINSON, M. G., ELLISON, S., MAZHARIAN, A., LIM, J., ZHAO, Y., KORNERUP, K. N., AUGER, J. M., THOMAS, S. G., DHANJAL, T., KALIA, N., ZHU, J. W., WEISS, A. & WATSON, S. P. 2009. The tyrosine phosphatase CD148 is an essential positive regulator of platelet activation and thrombosis. *Blood*, 113, 4942-54.
- SENZEL, L., GNATENKO, D. V. & BAHOU, W. F. 2009. The platelet proteome. *Curr Opin Hematol*, 16, 329-333.
- SEPULVEDA, F. E., DEBEURME, F., MÉNASCHÉ, G., KUROWSKA, M., CÔTE, M., PACHLOPNIK SCHMID, J., FISCHER, A. & DE SAINT BASILE, G. 2013. Distinct severity of HLH in both human and murine mutants with complete loss of cytotoxic effector PRF1, RAB27A, and STX11. *Blood*, 121, 595-603.
- SHAMELI, A., XIAO, W., ZHENG, Y., SHYU, S., SUMODI, J., MEYERSON, H. J., HARDING, C. V. & MAITTA, R. W. 2016. A critical role for alpha-synuclein in development and function of T lymphocytes. *Immunobiology*, 221, 333-340.
- SHANKAR, H., GARCIA, A., PRABHAKAR, J., KIM, S. & KUNAPULI, S. P. 2006. P2Y12 receptor-mediated potentiation of thrombin-induced thromboxane A2 generation in platelets occurs through regulation of Erk1/2 activation. *J Thromb Haemost*, 4, 638-47.

- SHAPIRO, A. L., VIÑUELA, E. & MAIZEL, J. V., JR. 1967. Molecular weight estimation of polypeptide chains by electrophoresis in SDS-polyacrylamide gels. *Biochem Biophys Res Commun*, 28, 815-20.
- SHARDA, A. & FLAUMENHAFT, R. 2018. The life cycle of platelet granules. *F1000Res*, 7, 236.
- SHARMA, M., BURRÉ, J. & SÜDHOF, T. C. 2011. CSP α promotes SNARE-complex assembly by chaperoning SNAP-25 during synaptic activity. *Nature cell biology*, 13, 30-39.
- SHARMA, P., NAG, D., ATAM, V., SETH, P. & KHANNA, V. 1991. Platelet aggregation in patients with Parkinson's disease. *Stroke*, 22, 1607-1608.
- SHARP, P. A., SUGDEN, B. & SAMBROOK, J. 1973. Detection of two restriction endonuclease activities in *Haemophilus parainfluenzae* using analytical agarose-ethidium bromide electrophoresis. *Biochemistry*, 12, 3055-3063.
- SHCHERBINA, A. & REMOLD-O'DONNELL, E. 1999. Role of Caspase in a Subset of Human Platelet Activation Responses. *Blood*, 93, 4222-4231.
- SHEPARD, H. M., PHILLIPS, G. L., C, D. T. & FELDMANN, M. 2017. Developments in therapy with monoclonal antibodies and related proteins. *Clin Med (Lond)*, 17, 220-232.
- SHIBASAKI, Y., BAILLIE, D., CLAIR, D. S. & BROOKES, A. 1995. High-resolution mapping of SNCA encoding α -synuclein, the non-A β component of Alzheimer's disease amyloid precursor, to human chromosome 4q21. 3 \rightarrow q22 by fluorescence in situ hybridization. *Cytogenetic and Genome Research*, 71, 54-55.
- SHIDA, Y., RYDZ, N., STEGNER, D., BROWN, C., MEWBURN, J., SPONAGLE, K., DANISMENT, O., CRAWFORD, B., VIDAL, B., HEGADORN, C. A., PRUSS, C. M., NIESWANDT, B. & LILLICRAP, D. 2014. Analysis of the role of von Willebrand factor, platelet glycoprotein VI, and α 2 β 1-mediated collagen binding in thrombus formation. *Blood*, 124, 1799-1807.
- SHIDA, Y., SWYSTUN, L. L., BROWN, C., MEWBURN, J., NESBITT, K., DANISMENT, O., RICHES, J. J., HOUGH, C. & LILLICRAP, D. 2019. Shear stress and platelet-induced tensile forces regulate ADAMTS13-localization within the platelet thrombus. *Research and Practice in Thrombosis and Haemostasis*, 3, 254-260.
- SHIN, E.-K., PARK, H., NOH, J.-Y., LIM, K.-M. & CHUNG, J.-H. 2017. Platelet Shape Changes and Cytoskeleton Dynamics as Novel Therapeutic Targets for Anti-Thrombotic Drugs. *Biomolecules & therapeutics*, 25, 223-230.
- SHIN, E. C., CHO, S. E., LEE, D. K., HUR, M. W., PAIK, S. R., PARK, J. H. & KIM, J. 2000. Expression patterns of alpha-synuclein in human hematopoietic cells and in *Drosophila* at different developmental stages. *Mol Cells*, 10, 65-70.
- SHOULDERS, M. D. & RAINES, R. T. 2009. Collagen structure and stability. *Annual review of biochemistry*, 78, 929-958.
- SHUMING, C., GEORGE, A. C., THERESA, S. P., TRACEE, L. M., PING, W., DREW, M. P., FAN, P. & SUZANNE, L. T. 2019. Mechanisms regulating PD-L1 expression on tumor and immune cells. *Journal for ImmunoTherapy of Cancer*, 7, 305.
- SIDDIQUI, I. J., PERVAIZ, N. & ABBASI, A. A. 2016. The Parkinson Disease gene SNCA: Evolutionary and structural insights with pathological implication. *Scientific reports*, 6, 24475-24475.
- SMETHURST, P. A., ONLEY, D. J., JARVIS, G. E., O'CONNOR, M. N., KNIGHT, C. G., HERR, A. B., OUWEHAND, W. H. & FARNDAL, R. W. 2007. Structural basis for the platelet-collagen interaction: the smallest motif within collagen that recognizes and activates platelet Glycoprotein VI contains two glycine-proline-hydroxyproline triplets. *J Biol Chem*, 282, 1296-304.
- SMITH, A. N., JOSHI, S., CHANZU, H., ALFAR, H. R., SHRAVANI PRAKHYA, K. & WHITEHEART, S. W. 2023. α -Synuclein is the major platelet isoform but is dispensable for activation, secretion, and thrombosis. *Platelets*, 34, 2267147.
- SMITH, A. N., JOSHI, S. & WHITEHEART, S. W. 2020. α -Synuclein's Role in Platelet Exocytosis. *The FASEB Journal*, 34, 1-1.
- SMITH, N. L., RICE, K. M., BOVILL, E. G., CUSHMAN, M., BIS, J. C., MCKNIGHT, B., LUMLEY, T., GLAZER, N. L., VAN HYLCKAMA Vlieg, A. & TANG, W. 2011. Genetic variation associated with plasma von Willebrand factor levels and the risk of incident venous thrombosis. *Blood, The Journal of the American Society of Hematology*, 117, 6007-6011.
- SMYTH, E. M. 2010. Thromboxane and the thromboxane receptor in cardiovascular disease. *Clin Lipidol*, 5, 209-219.
- SODE, K. 2007. Effect of Reparation of Repeat Sequences in the Human α -Synuclein on Fibrillation Ability. 1-7.

- SÖLLNER, T., BENNETT, M. K., WHITEHEART, S. W., SCHELLER, R. H. & ROTHMAN, J. E. 1993. A protein assembly-disassembly pathway in vitro that may correspond to sequential steps of synaptic vesicle docking, activation, and fusion. *Cell*, 75, 409-418.
- SONG, A. J. & PALMITER, R. D. 2018. Detecting and Avoiding Problems When Using the Cre-lox System. *Trends Genet*, 34, 333-340.
- SONMEZ, O. & SONMEZ, M. 2017. Role of platelets in immune system and inflammation. *Porto Biomed J*, 2, 311-314.
- SORRENTINO, Z. A. & GIASSON, B. I. 2020. The emerging role of α -synuclein truncation in aggregation and disease. *J Biol Chem*, 295, 10224-10244.
- STALKER, T. J. 2020. Mouse laser injury models: variations on a theme. *Platelets*, 31, 423-431.
- STALKER, T. J., TRAXLER, E. A., WU, J., WANNEMACHER, K. M., CERMIGNANO, S. L., VORONOV, R., DIAMOND, S. L. & BRASS, L. F. 2013. Hierarchical organization in the hemostatic response and its relationship to the platelet-signaling network. *Blood, The Journal of the American Society of Hematology*, 121, 1875-1885.
- STEFANIUK, C. M., HONG, H., HARDING, C. V. & MAITTA, R. W. 2018. α -Synuclein concentration increases over time in plasma supernatant of single donor platelets. *European journal of haematology*, 101, 630-634.
- STEFANIUK, C. M., SCHLEGELMILCH, J., MEYERSON, H. J., HARDING, C. V. & MAITTA, R. W. 2022. Initial assessment of α -synuclein structure in platelets. *J Thromb Thrombolysis*, 53, 950-953.
- STEINHOFF, M., BUDDENKOTTE, J., SHPACOVITCH, V., RATTENHOLL, A., MOORMANN, C., VERGNOLLE, N., LUGER, T. & HOLLENBERG, M. 2005. Proteinase-Activated Receptors: Transducers of Proteinase-Mediated Signaling in Inflammation and Immune Response. *Endocrine reviews*, 26, 1-43.
- STOJKOVSKA, I. & MAZZULLI, J. R. 2021. Detection of pathological alpha-synuclein aggregates in human iPSC-derived neurons and tissue. *STAR Protoc*, 2, 100372.
- SUGENO, N., TAKEDA, A., HASEGAWA, T., KOBAYASHI, M., KIKUCHI, A., MORI, F., WAKABAYASHI, K. & ITOYAMA, Y. 2008. Serine 129 phosphorylation of alpha-synuclein induces unfolded protein response-mediated cell death. *J Biol Chem*, 283, 23179-88.
- SUN, J., WANG, L., BAO, H., PREMI, S., DAS, U., CHAPMAN, E. R. & ROY, S. 2019. Functional cooperation of α -synuclein and VAMP2 in synaptic vesicle recycling. *Proc Natl Acad Sci U S A*, 116, 11113-11115.
- SUNG, Y.-H. & ELIEZER, D. 2007. Residual structure, backbone dynamics, and interactions within the synuclein family. *Journal of molecular biology*, 372, 689-707.
- SURIN, W. R., BARTH WAL, M. K. & DIKSHIT, M. 2008. Platelet collagen receptors, signaling and antagonism: Emerging approaches for the prevention of intravascular thrombosis. *Thrombosis Research*, 122, 786-803.
- SUZUKI-INOUE, K., TULASNE, D., SHEN, Y., BORI-SANZ, T., INOUE, O., JUNG, S. M., MOROI, M., ANDREWS, R. K., BERNDT, M. C. & WATSON, S. P. 2002. Association of Fyn and Lyn with the proline-rich domain of glycoprotein VI regulates intracellular signaling. *J Biol Chem*, 277, 21561-6.
- SWIERINGA, F., BAATEN, C. C. F. M. J., VERDOOLD, R., MASTENBROEK, T. G., RIJNVELD, N., LAAN, K. O. V. D., BREEL, E. J., COLLINS, P. W., LANCÉ, M. D., HENSKENS, Y. M. C., COSEMANS, J. M. E. M., HEEMSKERK, J. W. M. & MEIJDEN, P. E. J. V. D. 2016. Platelet Control of Fibrin Distribution and Microelasticity in Thrombus Formation Under Flow. *Arteriosclerosis, Thrombosis, and Vascular Biology*, 36, 692-699.
- SYED, Y. Y. 2017. Durvalumab: First Global Approval. *Drugs*, 77, 1369-1376.
- TANG, B. L. 2015. A unique SNARE machinery for exocytosis of cytotoxic granules and platelets granules. *Molecular Membrane Biology*, 32, 120-126.
- TASHKANDI, H., SHAMELI, A., HARDING, C. V. & MAITTA, R. W. 2018. Ultrastructural changes in peripheral blood leukocytes in α -synuclein knockout mice. *Blood Cells, Molecules, and Diseases*, 73, 33-37.
- TASHKANDI, H., SHAMELI, A. & MAITTA, R. Dysregulation of platelet function and morphology in the setting of alpha-synuclein deficiency. *Transfusion*, 2016. WILEY-BLACKWELL 111 RIVER ST, HOBOKEN 07030-5774, NJ USA, 117A-117A.
- TEIL, M., AROT CARENA, M. L., FAGGIANI, E., LAFERRIERE, F., BEZARD, E. & DEHAY, B. 2020. Targeting α -synuclein for PD Therapeutics: A Pursuit on All Fronts. *Biomolecules*, 10.
- THON, J. N., PETERS, C. G., MACHLUS, K. R., ASLAM, R., ROWLEY, J., MACLEOD, H., DEVINE, M. T., FUCHS, T. A., WEYRICH, A. S., SEMPLE, J. W., FLAUMENHAFT, R. & ITALIANO, J.

- E., JR 2012. T granules in human platelets function in TLR9 organization and signaling. *Journal of Cell Biology*, 198, 561-574.
- TOLMACHOVA, T., ÅBRINK, M., FUTTER, C. E., AUTHI, K. S. & SEABRA, M. C. 2007. Rab27b regulates number and secretion of platelet dense granules. *Proceedings of the National Academy of Sciences*, 104, 5872-5877.
- TOMOKIYO, K., KAMIKUBO, Y., HANADA, T., ARAKI, T., NAKATOMI, Y., OGATA, Y., JUNG, S. M., NAKAGAKI, T. & MOROI, M. 2005. Von Willebrand factor accelerates platelet adhesion and thrombus formation on a collagen surface in platelet-reduced blood under flow conditions. *Blood*, 105, 1078-1084.
- TOTH, G., GARDAI, S. J., ZAGO, W., BERTONCINI, C. W., CREMADES, N., ROY, S. L., TAMBE, M. A., ROCHET, J.-C., GALVAGNION, C. & SKIBINSKI, G. 2014. Targeting the intrinsically disordered structural ensemble of α -synuclein by small molecules as a potential therapeutic strategy for Parkinson's disease. *PloS one*, 9.
- TOUCHBERRY, C. D., SILSWAL, N., TCHIKRIZOV, V., ELMORE, C. J., SRINIVAS, S., AKTHAR, A. S., SWAN, H. K., WETMORE, L. A. & WACKER, M. J. 2014. Cardiac thromboxane A2 receptor activation does not directly induce cardiomyocyte hypertrophy but does cause cell death that is prevented with gentamicin and 2-APB. *BMC Pharmacology and Toxicology*, 15, 73.
- TOUCHMAN, J. W., DEHEJIA, A., CHIBA-FALEK, O., CABIN, D. E., SCHWARTZ, J. R., ORRISON, B. M., POLYMERPOULOS, M. H. & NUSSBAUM, R. L. 2001. Human and mouse alpha-synuclein genes: comparative genomic sequence analysis and identification of a novel gene regulatory element. *Genome Res*, 11, 78-86.
- TOYODA, T., ISOBE, K., TSUJINO, T., KOYATA, Y., OHYAGI, F., WATANABE, T., NAKAMURA, M., KITAMURA, Y., OKUDERA, H., NAKATA, K. & KAWASE, T. 2018. Direct activation of platelets by addition of CaCl₂ leads coagulation of platelet-rich plasma. *International Journal of Implant Dentistry*, 4, 23.
- TRAN, T. H. T., ZENG, Q. & HONG, W. 2007. VAMP4 cycles from the cell surface to the trans-Golgi network via sorting and recycling endosomes. *Journal of cell science*, 120, 1028-1041.
- TRIMBUCH, T. & ROSENMUND, C. 2016. Should I stop or should I go? The role of complexin in neurotransmitter release. *Nature Reviews Neuroscience*, 17, 118-125.
- TSUKUBA, T., OKAMOTO, K., YASUDA, Y., MORIKAWA, W., NAKANISHI, H. & YAMAMOTO, K. 2000. New functional aspects of cathepsin D and cathepsin E. *Molecules and cells*, 10, 601-611.
- TSUSHIMA, F., YAO, S., SHIN, T., FLIES, A., FLIES, S., XU, H., TAMADA, K., PARDOLL, D. M. & CHEN, L. 2007. Interaction between B7-H1 and PD-1 determines initiation and reversal of T-cell anergy. *Blood, The Journal of the American Society of Hematology*, 110, 180-185.
- TURNER, M., SCHWEIGHOFFER, E., COLUCCI, F., DI SANTO, J. P. & TYBULEWICZ, V. L. 2000. Tyrosine kinase SYK: essential functions for immunoreceptor signalling. *Immunol Today*, 21, 148-54.
- ULMER, T. S., BAX, A., COLE, N. B. & NUSSBAUM, R. L. 2005. Structure and dynamics of micelle-bound human alpha-synuclein. *J Biol Chem*, 280, 9595-603.
- ULUSOY, A., PHILLIPS, R. J., HELWIG, M., KLINKENBERG, M., POWLEY, T. L. & DI MONTE, D. A. 2017. Brain-to-stomach transfer of α -synuclein via vagal preganglionic projections. *Acta Neuropathologica*, 133, 381-393.
- VAN DER MAATEN, L. & HINTON, G. 2008. Visualizing data using t-SNE. *Journal of machine learning research*, 9.
- VAN DER MEIJDEN, P. E., FEIJGE, M. A., GIESEN, P. L., HUIJBERTS, M., VAN RAAK, L. P. & HEEMSKERK, J. W. 2005. Platelet P2Y₁₂ receptors enhance signalling towards procoagulant activity and thrombin generation. *Thrombosis and haemostasis*, 93, 1128-1136.
- VAN DER WATEREN, I. M., KNOWLES, T. P. J., BUELL, A. K., DOBSON, C. M. & GALVAGNION, C. 2018. C-terminal truncation of α -synuclein promotes amyloid fibril amplification at physiological pH. *Chemical Science*, 9, 5506-5516.
- VAN HOLTEN, T. C., BLEIJERVELD, O. B., WIJTEN, P., DE GROOT, P. G., HECK, A. J., BARENDRECHT, A. D., MERKX, T. H., SCHOLTEN, A. & ROEST, M. 2014. Quantitative proteomics analysis reveals similar release profiles following specific PAR-1 or PAR-4 stimulation of platelets. *Cardiovasc Res*, 103, 140-6.
- VAN NISPEN TOT PANNERDEN, H., DE HAAS, F., GEERTS, W., POSTHUMA, G., VAN DIJK, S. & HEIJNEN, H. F. 2010. The platelet interior revisited: Electron tomography reveals tubular α -granule subtypes. *Blood, The Journal of the American Society of Hematology*, 116, 1147-1156.

- VAN NISPEN TOT PANNERDEN, H. E., VAN DIJK, S. M., DU, V. & HEIJNEN, H. F. 2009. Platelet protein disulfide isomerase is localized in the dense tubular system and does not become surface expressed after activation. *Blood, The Journal of the American Society of Hematology*, 114, 4738-4740.
- VAN OOST, B. 1986. Acid hydrolase secretion. *Platelet responses and metabolism*, 163-191.
- VARANI, K., PORTALUPPI, F., MERIGHI, S., ONGINI, E., BELARDINELLI, L. & BOREA, P. A. 1999. Caffeine alters A_{2A} adenosine receptors and their function in human platelets. *Circulation*, 99, 2499-2502.
- VELETIC, I., MANSHOURI, T., NOGUERAS GONZÁLEZ, G. M., PRIJIC, S., BOVE, J. E., IV, ZHANG, Y., VERSTOVSEK, S. & ESTROV, Z. E. 2018. PD-1-Mediated T Cell Exhaustion Is Prevalent Among Patients with MPN-Associated Myelofibrosis Independent of JAK1/2 Inhibition. *Blood*, 132, 5487-5487.
- VENDA, L. L., CRAGG, S. J., BUCHMAN, V. L. & WADE-MARTINS, R. 2010. α -Synuclein and dopamine at the crossroads of Parkinson's disease. *Trends in Neurosciences*, 33, 559-568.
- VIOLI, F., PASTORI, D., PIGNATELLI, P. & CAMMISOTTO, V. 2024. Endotoxemia and Platelets. *JACC: Basic to Translational Science*, 9, 404-413.
- VIVACQUA, G., CASINI, A., VACCARO, R., FORNAI, F., YU, S. & D'ESTE, L. 2011. Different sub-cellular localization of alpha-synuclein in the C57BL/6J mouse's central nervous system by two novel monoclonal antibodies. *Journal of Chemical Neuroanatomy*, 41, 97-110.
- VIVONA, S., LIU, C. W., STROP, P., ROSSI, V., FILIPPINI, F. & BRUNGER, A. T. 2010. The longin SNARE VAMP7/TI-VAMP adopts a closed conformation. *J Biol Chem*, 285, 17965-73.
- WANG, B. & ZHENG, J. 2016. Platelet generation in vivo and in vitro. *Springerplus*, 5, 787.
- WANG, F., GAO, Y., ZHOU, L., CHEN, J., XIE, Z., YE, Z. & WANG, Y. 2022. USP30: Structure, Emerging Physiological Role, and Target Inhibition. *Front Pharmacol*, 13, 851654.
- WANG, G. F., LI, C. & PIELAK, G. J. 2010a. 19F NMR studies of α -synuclein-membrane interactions. *Protein Sci*, 19, 1686-91.
- WANG, Q., YAO, S., YANG, Z.-X., ZHOU, C., ZHANG, Y., ZHANG, Y., ZHANG, L., LI, J.-T., XU, Z.-J., ZHU, W.-L., ZHANG, N.-X., YE, Y. & FENG, L.-Y. 2023. Pharmacological characterization of the small molecule 03A10 as an inhibitor of α -synuclein aggregation for Parkinson's disease treatment. *Acta Pharmacologica Sinica*, 44, 1122-1134.
- WANG, Z., UDESHI, N. D., O'MALLEY, M., SHABANOWITZ, J., HUNT, D. F. & HART, G. W. 2010b. Enrichment and site mapping of O-linked N-acetylglucosamine by a combination of chemical/enzymatic tagging, photochemical cleavage, and electron transfer dissociation mass spectrometry. *Mol Cell Proteomics*, 9, 153-60.
- WARREN, B. A. 1971. The platelet pseudopodium and its involvement in aggregation and adhesion to vessel walls. *British journal of experimental pathology*, 52, 378-387.
- WATSON, S., AUGER, J., MCCARTY, O. & PEARCE, A. 2005. GPVI and integrin α IIb β 3 signaling in platelets. *Journal of Thrombosis and Haemostasis*, 3, 1752-1762.
- WEBER, T., ZEMELMAN, B. V., MCNEW, J. A., WESTERMANN, B., GMACHL, M., PARLATI, F., SÖLLNER, T. H. & ROTHMAN, J. E. 1998. SNAREpins: Minimal Machinery for Membrane Fusion. *Cell*, 92, 759-772.
- WEI, A. H. & LI, W. 2013. Hermansky-Pudlak syndrome: pigmentary and non-pigmentary defects and their pathogenesis. *Pigment cell & melanoma research*, 26, 176-192.
- WELSH, J. D., STALKER, T. J., VORONOV, R., MUTHARD, R. W., TOMAIUOLO, M., DIAMOND, S. L. & BRASS, L. F. 2014. A systems approach to hemostasis: 1. The interdependence of thrombus architecture and agonist movements in the gaps between platelets. *Blood*, 124, 1808-1815.
- WENCEL-DRAKE, J. D., PAINTER, R. G., ZIMMERMAN, T. S. & GINSBERG, M. H. 1985. Ultrastructural localization of human platelet thrombospondin, fibrinogen, fibronectin, and von Willebrand factor in frozen thin section.
- WEYAND, A. C., LOMBEL, R. M., PIPE, S. W. & SHAVIT, J. A. 2016. The Role of Platelets and ϵ -Aminocaproic Acid in Arthrogyposis, Renal Dysfunction, and Cholestasis (ARC) Syndrome Associated Hemorrhage. *Pediatric Blood & Cancer*, 63, 561-563.
- WHITE, J. G. 1998. Use of the electron microscope for diagnosis of platelet disorders. *Semin Thromb Hemost*, 24, 163-8.
- WONEROW, P., PEARCE, A. C., VAUX, D. J. & WATSON, S. P. 2003. A critical role for phospholipase C γ 2 in α IIb β 3-mediated platelet spreading. *Journal of Biological Chemistry*, 278, 37520-37529.

- WORONOWICZ, K., DILKS, J. R., ROZENVAYN, N., DOWAL, L., BLAIR, P. S., PETERS, C. G., WORONOWICZ, L. & FLAUMENHAFT, R. 2010. The platelet actin cytoskeleton associates with SNAREs and participates in α -granule secretion. *Biochemistry*, 49, 4533-4542.
- WU, B., STERNHEIM, N., AGARWAL, P., SUCHOMEL, J., VADHAVKAR, S., BRUNO, R., BALLINGER, M., BERNAARDS, C. A., CHAN, P., RUPPEL, J., JIN, J., GIRISH, S., JOSHI, A. & QUARMBY, V. 2022. Evaluation of atezolizumab immunogenicity: Clinical pharmacology (part 1). *Clinical and Translational Science*, 15, 130-140.
- WU, K., LI, D., XIU, P., JI, B. & DIAO, J. 2020. O-GlcNAcylation inhibits the oligomerization of alpha-synuclein by declining intermolecular hydrogen bonds through a steric effect. *Physical Biology*, 18, 016002.
- WU, Y., CHEN, W., XU, Z. P. & GU, W. 2019. PD-L1 Distribution and Perspective for Cancer Immunotherapy-Blockade, Knockdown, or Inhibition. *Front Immunol*, 10, 2022.
- XIAO, W., SHAMELI, A., HARDING, C. V., MEYERSON, H. J. & MAITTA, R. W. 2014. Late stages of hematopoiesis and B cell lymphopoiesis are regulated by α -synuclein, a key player in Parkinson's Disease. *Immunobiology*, 219, 836-844.
- XU, J. & SHI, G.-P. 2014. Vascular wall extracellular matrix proteins and vascular diseases. *Biochimica et biophysica acta*, 1842, 2106-2119.
- YAMAGUCHI, H., HSU, J.-M., YANG, W.-H. & HUNG, M.-C. 2022. Mechanisms regulating PD-L1 expression in cancers and associated opportunities for novel small-molecule therapeutics. *Nature Reviews Clinical Oncology*, 19, 287-305.
- YAMASHITA, A. & ASADA, Y. 2008. Atherothrombosis and thrombus propagation. *Recent Advances in Thrombosis and Hemostasis 2008*, 614-624.
- YAN, C., JIANG, J., YANG, Y., GENG, X. & DONG, W. 2022. The function of VAMP2 in mediating membrane fusion: An overview. *Frontiers in Molecular Neuroscience*, 15, 948160.
- YAP, C. H., SAIKRISHNAN, N. & YOGANATHAN, A. P. 2012. Experimental measurement of dynamic fluid shear stress on the ventricular surface of the aortic valve leaflet. *Biomechanics and modeling in mechanobiology*, 11, 231-244.
- YAROVOI, H. V., KUFRIN, D., ESLIN, D. E., THORNTON, M. A., HABERICHTER, S. L., SHI, Q., ZHU, H., CAMIRE, R., FAKHARZADEH, S. S., KOWALSKA, M. A., WILCOX, D. A., SACHAIS, B. S., MONTGOMERY, R. R. & PONCZ, M. 2003. Factor VIII ectopically expressed in platelets: efficacy in hemophilia A treatment. *Blood*, 102, 4006-13.
- YE, S., HUANG, Y., JOSHI, S., ZHANG, J., YANG, F., ZHANG, G., SMYTH, S. S., LI, Z., TAKAI, Y. & WHITEHEART, S. W. 2014. Platelet secretion and hemostasis require syntaxin-binding protein STXBP5. *The Journal of Clinical Investigation*, 124, 4517-4528.
- YE, S., KARIM, Z. A., AL HAWAS, R., PESSIN, J. E., FILIPOVICH, A. H. & WHITEHEART, S. W. 2012. Syntaxin-11, but not syntaxin-2 or syntaxin-4, is required for platelet secretion. *Blood*, 120, 2484-92.
- YEAMAN, M. R. 2010. Platelets in defense against bacterial pathogens. *Cellular and molecular life sciences : CMLS*, 67, 525-544.
- YI, M., NIU, M., XU, L., LUO, S. & WU, K. 2021. Regulation of PD-L1 expression in the tumor microenvironment. *Journal of Hematology & Oncology*, 14, 10.
- YOO, G., SHIN, Y.-K. & LEE, N. K. 2023. The Role of α -Synuclein in SNARE-mediated Synaptic Vesicle Fusion. *Journal of Molecular Biology*, 435, 167775.
- YOON, T.-Y. & MUNSON, M. 2018. SNARE complex assembly and disassembly. *Current Biology*, 28, R397-R401.
- YU, H., RATHORE, S. S., LOPEZ, J. A., DAVIS, E. M., JAMES, D. E., MARTIN, J. L. & SHEN, J. 2013. Comparative studies of Munc18c and Munc18-1 reveal conserved and divergent mechanisms of Sec1/Munc18 proteins. *Proceedings of the National Academy of Sciences*, 110, E3271-E3280.
- YU, S., LI, X., LIU, G., HAN, J., ZHANG, C., LI, Y., XU, S., LIU, C., GAO, Y. & YANG, H. 2007. Extensive nuclear localization of α -synuclein in normal rat brain neurons revealed by a novel monoclonal antibody. *Neuroscience*, 145, 539-555.
- YUI, Y., AOYAMA, T., MORISHITA, H., TAKAHASHI, M., TAKATSU, Y. & KAWAI, C. 1988. Serum prostacyclin stabilizing factor is identical to apolipoprotein AI (Apo AI). A novel function of Apo AI. *The Journal of clinical investigation*, 82, 803-807.
- YUN, S.-H., SIM, E.-H., GOH, R.-Y., PARK, J.-I. & HAN, J.-Y. 2016. Platelet Activation: The Mechanisms and Potential Biomarkers. *BioMed Research International*, 2016, 1-5.
- ZEILER, M., MOSER, M. & MANN, M. 2014. Copy number analysis of the murine platelet proteome spanning the complete abundance range. *Mol Cell Proteomics*, 13, 3435-45.

- ZENG, Q., TRAN, T. T. H., TAN, H.-X. & HONG, W. 2003. The cytoplasmic domain of Vamp4 and Vamp5 is responsible for their correct subcellular targeting: the N-terminal extension of VAMP4 contains a dominant autonomous targeting signal for the trans-Golgi network. *Journal of Biological Chemistry*, 278, 23046-23054.
- ZERDES, I., WALLERIUS, M., SIFAKIS, E. G., WALLMANN, T., BETTS, S., BARTISH, M., TSEMETZIS, N., TOBIN, N. P., COUCORAVAS, C., BERGH, J., RASSIDAKIS, G. Z., ROLNY, C. & FOUKAKIS, T. 2019. STAT3 Activity Promotes Programmed-Death Ligand 1 Expression and Suppresses Immune Responses in Breast Cancer. *Cancers (Basel)*, 11.
- ZHANG, C., PEI, Y., ZHANG, Z., XU, L., LIU, X., JIANG, L., PIELAK, G. J., ZHOU, X., LIU, M. & LI, C. 2022. C-terminal truncation modulates α -Synuclein's cytotoxicity and aggregation by promoting the interactions with membrane and chaperone. *Communications Biology*, 5, 798.
- ZHANG, J., HUANG, Y., CHEN, J., ZHU, H. & WHITEHEART, S. W. 2018. Dynamic cycling of t-SNARE acylation regulates platelet exocytosis. *J Biol Chem*, 293, 3593-3606.
- ZHANG, J., LI, X. & LI, J.-D. 2019. The Roles of Post-translational Modifications on α -Synuclein in the Pathogenesis of Parkinson's Diseases. *Frontiers in Neuroscience*, 13.
- ZHANG, X., ZHANG, P., AN, L., SUN, N., PENG, L., TANG, W., MA, D. & CHEN, J. 2020. Miltirone induces cell death in hepatocellular carcinoma cell through GSDME-dependent pyroptosis. *Acta Pharmaceutica Sinica B*, 10, 1397-1413.
- ZHANG, Y. & HUGHSON, F. M. 2021. Chaperoning SNARE folding and assembly. *Annual review of biochemistry*, 90, 581-603.
- ZHAO, X., GUAN, Y., LIU, F., YAN, S., WANG, Y., HU, M., LI, Y., LI, R. & ZHANG, C. X. 2022. SNARE Proteins Mediate α -Synuclein Secretion via Multiple Vesicular Pathways. *Mol Neurobiol*, 59, 405-419.
- ZHOU, Z., KIM, J., INSOLERA, R., PENG, X., FINK, D. J. & MATA, M. 2011. Rho GTPase regulation of α -synuclein and VMAT2: Implications for pathogenesis of Parkinson's disease. *Molecular and Cellular Neuroscience*, 48, 29-37.
- ZHU, Q., YAMAKUCHI, M., TURE, S., DE LA LUZ GARCIA-HERNANDEZ, M., KO, K. A., MODJESKI, K. L., LOMONACO, M. B., JOHNSON, A. D., O'DONNELL, C. J., TAKAI, Y., MORRELL, C. N. & LOWENSTEIN, C. J. 2014a. Syntaxin-binding protein STXBP5 inhibits endothelial exocytosis and promotes platelet secretion. *The Journal of clinical investigation*, 124, 4503-4516.
- ZHU, Q., YAMAKUCHI, M., TURE, S., DE LA LUZ GARCIA-HERNANDEZ, M., KO, K. A., MODJESKI, K. L., LOMONACO, M. B., JOHNSON, A. D., O'DONNELL, C. J. & TAKAI, Y. 2014b. Syntaxin-binding protein STXBP5 inhibits endothelial exocytosis and promotes platelet secretion. *The Journal of clinical investigation*, 124, 4503-4516.

Supplementary

6.3. Reagents

Table 19. General reagents

Component	Company	Code
Tri-sodium citrate	VWR	W302600
Citric Acid monohydrate	sigma	C7129
ADP	Sigma	A2754
CRP-XL	CAMBCOL laboratories	XL-CRP
EDTA	Sigma	E6758-500G
Sodium Chloride (NaCl)	Sigma	S3014-5KG
EGTA	Sigma	4100-50GM
Tris Base	Sigma	11814273001
Glycerol	Sigma	G5516
SDS	Sigma	75746
Bromophenol blue	Sigma	B5525
2-mercapto-ethanol	Sigma	M6250
N-(2-Hydroxyethyl) piperazine-N'-(2- ethanesulfonic acid), 4-(2- Hydroxyethyl) piperazine- 1-ethanesulfonic acid (HEPES)	Sigma	H4034-1KG
Potassium Chloride (KCl)	Sigma	P5405-1KG
Sodium phosphate dibasic (Na ₂ HPO ₄ .12H ₂ O)	Sigma	S5136-1KG
Sodium bicarbonate (NaHCO ₃)	Sigma	S5761-1KG
Magnesium Chloride (MgCl ₂)	sigma	M8266-1KG

Table 20. Primary Antibodies for western blotting

Antibody	Catalogue number/ supplier	Dilution factor
Phospho α -synuclein serine129	Santa Cruz (sc-135638)	1:1000
α -synuclein total	Santa Cruz (Sc-515879)	1:1000
α -synuclein total	CST (4179)	1:1000
VAMP7	CST (14811)	1:1000
VAMP2	Santa Cruz (sc-69706)	1:1000
Syntaxin 4	Santa Cruz (sc-101301)	1:1000
Syntaxin 11	Santa Cruz (sc-377121)	1:1000
Vamp8	CST (13060s)	1:1000
4g10	Millipore (#05-321X)	1:1000
α -tubulin	Santa Cruz (sc-5286)	1:1000
SNAP23	Santa Cruz sc-734215	1:1000
GAPDH	Santa Cruz (sc-32233)	1:1000
TSP-1	Neomarkers MS-1066-10	1:1500
PD-L1(E1L3N)	CST 13684t	1:1000

Table 21. Secondary antibodies for Western blot

Antibody	Catalogue number/ supplier	Dilution factor
IR Dye 680CW anti-rabbit igGR	Li-Cor (827-08365)	1:10000
IR Dye 680CW anti-Mouse igG	Li-Cor (827-08363)	1:10000
IR Dye 800CW anti-Rabbit igG	Li-Cor (926-68171)	1:10000
IR Dye 800CW anti-Mouse igG	Li-Cor (926-32210)	1:10000
HRP- conjugated anti-Rabbit igG	Dakko	1:5000
HRP- conjugated anti-Mouse igG	Dakko	1:5000

Table 22. Antibodies used in Flow cytometry.

Antibody	Catalogue number/ supplier	Dilution factor
PE/Cyanine7 anti-mouse CD107a	Biolegend- 121620	1:200
APC anti-mouse CD274	Biolegend - 124334	1:100
FITC-labeled Wug.E9	Emfret M130-1	1:100
PE- labeled Anti-CD41 (jon/A)	Emfret MO23-2	1:100
Alexaflour700 labeled LAMP1	Biolegend	1:400

Table 23. Primary antibodies used in Immunofluorescence.

Antibody	Catalogue number/ supplier	Dilution factor
FITC- Phalloidin	Sigma	1:500
TRITC- Phalloidin	sigma	1:500
α -synuclein (rabbit)	CST 4179	1:200
α -synuclein (mouse)	sc-515879	1:100
STX4	SC-101301	1:50
STX11	SC - 377121	1:100
SNAP23	SC-734215	1:50
Vamp 2	SC-69706	1:50
VAMP7	CST- 14811	1:100
VAMP8	cst -13060s	1:100
p- α -synuclein ^{ser129}	sc -135638	1:100

Table 24. secondary antibodies used in Immunofluorescence.

Antibody	Catalogue number/ supplier	Dilution factor
Anti- mouse- 568	Sigma (SAB4600313)	1:1000
Anti-rabbit -667	sigma	1:1000
WGA - 350	CST 4179	1:200

Table 25. Platelet inhibitors used in inhibition experiments.

Inhibitor	Target	Catalogue number/ supplier	Final concentration
Tirofiban	glycoprotein IIb/IIIa	Sigma	1 $\mu\text{g}/\text{mL}^{-1}$
Indomethacin	COX inhibition	Sigma	
Apyrase	ATP/ADP hydrolysis	Sigma	2U/mL
BAPTA/AM (1,2-bis(o-aminophenoxy)ethane-N,N,N',N'-tetraacetic acid)	Ca ²⁺ Chelation	Sigma	50 μM
prostacyclin	prostacyclin receptor inhibition	Sigma	1-100nM
Y27632	p160ROCK inhibition	Sigma	
Citric acid		Sigma	3-6mM

Table 26. Platelet agonists used in experiments.

Platelet Agonist	Target	Catalogue number/ supplier	Final concentration
Crosslinked Collagen related peptide (CRP-XL)	GPVI	CambCol laboratories (XLCRP)	1-10 $\mu\text{g}/\text{ml}$
TRAP6 (Thrombin Receptor Activator Peptide 6)	PAR1	Cambridge Bioscience (H-2936-0005)	1-10 μM
ADP	$\alpha_2\text{b}\beta_3$	Sigma (A2754)	1-30 μM
Collagen	GPVI, $\alpha_2\text{b}\beta_3$	Nycomed	0.5-3 $\mu\text{g}/\text{ml}$
Thrombin	PAR1, PAR2, GPIb-ix-v	Sigma (T8885)	0.0175-0.1U/mL
U46619	Thromboxane a ²	Sigma (D8174)	0.25-1.0 μM

6.4. Buffers and solutions

All Buffers were prepared with Purified water from a Suez select fusion (Thame, UK), and pH adjusted by the addition of HCL and NaOH measured with a FiveEasy Plus pH meter (Columbus, USA).

6.4.1. Modified Tyrode's

Modified Tyrode's was made, pH adjusted to 7.3 at room temperature then stored at 4°C. Glucose was added to aliquots which were used within 14 days of creation.

Table 27. Modified tyrodes buffer components

Component	g/1000ml	molarity
HEPES	4.766	20mM
Sodium Chlorite	7.83	134mM
Potassium Chloride	0.149	2mM
Sodium hydrogen phosphate (Na ₂ HPO ₄ .12H ₂ O)	0.1215	0.34mM
Sodium Hydrogen carbonate	1.008	12mM
Magnesium Chloride	0.095	1mM
D-Glucose anh.	1.01	5.6mM

6.4.2. Acid-citrate dextrose buffer (ACD)

ACD was created and pH adjusted to 6.5, This was then stored at 4°C and aliquots passed through a 0.22µm filter and warmed to room temperature before use.

Table 28. Acid Citrate Dextrose components

Component	g/1000ml	molarity
D-glucose anhydrous	20.5	113.8mM
trisodium citrate dihydrate	8.79	29.9mM
NaCl	4.24	72.6mM
citric acid monohydrate	0.59	2.9mM

6.4.3. Sodium citrate

Sodium citrate was dissolved, and pH adjusted to 7.4, this was stored at 4°C and aliquots warmed to room temperature for use.

Table 29. Sodium citrate components

Component	g/1000ml	molarity
sodium citrate	32.08	124mM

6.4.4. Wash buffer

Wash buffer was made, and pH adjusted to pH 6.5, this was stored at 4°C and aliquots warmed to room temperature before use.

Table 30. Platelet wash buffer components

Component	g/1000ml	molarity
citric acid monohydrate	7.57	36mM
EDTA	3.80	10mM
D-glucose anhydrous	0.9	5mM
KCl	0.37	5mM
NaCl	5.26	90mM

6.4.5. Laemmli buffer pH 6.8

Table 31. Laemmli buffer components

Component	g/1000ml	molarity
Tris Base	6.05	0.0625M
SDS	40	0.07M
Glycerol	10%	
2-mercapto-ethanol	5%	
Bromophenol blue	trace	

6.4.6. SDS sample buffer

Sample buffer was made in 80ml volumes with pH adjusted to 7.5 and 2ml of NP-40 added before volume was increased to final 100ml volume by adding H₂O.

Table 32. SDS sample buffer components

Component	g/1000ml	molarity
DisodiumEDTA	0.745	2mM
Sodium Chloride	17.5	300mM
EGTA	0.77	2mM
Tris base	2.4	20mM

6.4.7. TAE

A 50x TAE buffer was made and pH Adjusted to 8.3, this solution was then diluted 1:50 in dH₂O for use with all experiments.

Table 33. Tris-Acetate-EDTA buffer components

Component	g/1000ml	molarity
Tris Base	242	20mM
0.5M EDTA	100 mL	0.5M
Glacial Acetic Acid	57.2 mL	

6.4.8. 4% paraformaldehyde

100mL of 37% formaldehyde was added to 900mL dH₂O and stored at room temperature.

Table 34. 4% Paraformaldehyde components

Component	g/1000ml	molarity
37% formaldehyde	100mL	4%

6.4.9. 0.2% Formyl Saline

0.9% saline was made and 5.4mL saline replaced with 37% formaldehyde, this was then stored at room temperature.

Table 35. 0.2% formyl saline components

Component	g/1000ml	molarity
NaCl	8.28	150mM
37% formaldehyde	5.40mL	0.2%

6.4.10. Subcellular fractionation buffer

Sucrose and HEPES were dissolved in dH₂O and the pH adjusted to 7.4, This was then stored at 4°C and aliquots were filtered through a 0.22um filter when required. Na₃VO₄ and protease inhibitor cocktail were added within 1 week before use.

Table 36. Subcellular fractionation components

Component	g/1000ml	molarity
Sucrose	109.5	320mM
HEPES	1.04	4mM
Na ₃ VO ₄	2.5ml/200mM	0.5mM
Protease inhibitor cocktail	1 tablet per 10 ml	

6.4.11. Gel buffer I

This buffer was made in dH₂O and the pH adjusted to 8.8.

Table 37. Resolving gel buffer components

Component	g/1000ml	molarity
Tris base	181.5	1.5M
0.4% (w/v) Laryl Sulphate	4	

6.4.12. Gel buffer II

This buffer was made in dH₂O and the pH adjusted to 6.8.

Table 38. Stacking gel buffer components

Component	g/1000ml	molarity
Tris base	60.5	1.5M
0.4% (w/v) Laryl Sulphate	4	

6.4.13. Running buffer

A 10x solution of running buffer was made and then diluted 1:10 in dH₂O for use.

Table 39. SDS page run buffer components

Component	g/1000ml	molarity
Glycine	144	1.92M
Tris base	30.3	0.25M
0.1% (w/v) SDS	20	1%

6.4.14. Citric Acid

Citric acid was prepared in dH₂O and stored at room temperature for no longer than 2 months.

Table 40. Citric acid components

Component	g/1000ml	molarity
Citric acid	63	0.3M

6.4.15. ECL Reagents

ECL reagents were made and used within 1 month, stored in UV protected containers at 4°C

Table 41. ECL reagent components

Component	ECL I	ECL II
dH ₂ O	88.56mL	89.9mL
Tris-HCl 1M pH8.5	10mL	10mL
Luminol	1 mL	0
Coumaric acid	0.44 mL	0
Hydrogen peroxide (H ₂ O ₂)	0	64µL

6.5. α -Synuclein Deletion Impairs Platelet Function: A Role for SNARE Complex Assembly



Article

α -Synuclein Deletion Impairs Platelet Function: A Role for SNARE Complex Assembly

Christopher Sennett ¹, Wanzhu Jia ¹, Jawad S. Khalil ², Matthew S. Hindle ³, Charlie Coupland ¹, Simon D. J. Calaminus ¹, Julian D. Langer ⁴, Sean Frost ⁵, Khalid M. Naseem ², Francisco Rivero ⁵, Natalia Ninkina ⁶, Vladimir Buchman ⁶ and Ahmed Aburima ^{1,*}

- ¹ Biomedical Institute for Multimorbidity, Hull York Medical School, University of Hull, Hull HU6 7RX, UK; hywj2@hyms.ac.uk (W.J.)
 - ² Discovery and Translational Science Department, Leeds Institute of Cardiovascular & Metabolic Medicine, University of Leeds, Leeds LS2 9JT, UK; j.s.khalil@leeds.ac.uk (J.S.K.)
 - ³ Centre for Biomedical Science Research, School of Health, Leeds Beckett University, Leeds LS1 3HE, UK; m.hindle@leedsbeckett.ac.uk
 - ⁴ Department of Molecular Membrane Biology, Max Planck Institute of Biophysics, 60438 Frankfurt am Main, Germany; julian.langer@biophys.mpg.de
 - ⁵ Centre for Biomedicine, Hull York Medical School, University of Hull, Hull HU6 7RX, UK; sean.frost@hyms.ac.uk (S.F.); francisco.rivero@hyms.ac.uk (F.R.)
 - ⁶ School of Biosciences, Cardiff University, Museum Avenue, Cardiff CF10 3AX, UK; ninkinan@cf.ac.uk (N.N.)
- * Correspondence: ahmed.aburima@hyms.ac.uk; Tel.: +44-(0)-1482466678

Abstract: Granule secretion is an essential platelet function that contributes not only to haemostasis but also to wound healing, inflammation, and atherosclerosis. Granule secretion from platelets is facilitated, at least in part, by Soluble N-ethylmaleimide-Sensitive Factor (NSF) Attachment Protein Receptor (SNARE) complex-mediated granule fusion. Although α -synuclein is a protein known to modulate the assembly of the SNARE complex in other cells, its role in platelet function remains poorly understood. In this study, we provide evidence that α -synuclein is critical for haemostasis using α -synuclein-deficient ($^{-/-}$) mice. The genetic deletion of α -synuclein resulted in impaired platelet aggregation, secretion, and adhesion in vitro. In vivo haemostasis models showed that α -synuclein $^{-/-}$ mice had prolonged bleeding times and activated partial thromboplastin times (aPTTs). Mechanistically, platelet activation induced α -synuclein serine (ser) 129 phosphorylation and re-localisation to the platelet membrane, accompanied by an increased association with VAMP 8, syntaxin 4, and syntaxin 11. This phosphorylation was calcium (Ca^{2+})- and RhoA/ROCK-dependent and was inhibited by prostacyclin (PGI_2). Our data suggest that α -synuclein regulates platelet secretion by facilitating SNARE complex formation.

Keywords: α -synuclein; platelets; SNARE; secretion



Citation: Sennett, C.; Jia, W.; Khalil, J.S.; Hindle, M.S.; Coupland, C.; Calaminus, S.D.J.; Langer, J.D.; Frost, S.; Naseem, K.M.; Rivero, F.; et al. α -Synuclein Deletion Impairs Platelet Function: A Role for SNARE Complex Assembly. *Cells* **2024**, *13*, 2089. <https://doi.org/10.3390/cells13242089>

Academic Editor: Stepan Gambaryan

Received: 18 November 2024

Revised: 4 December 2024

Accepted: 12 December 2024

Published: 17 December 2024



Copyright: © 2024 by the authors. Licensee MDPI, Basel, Switzerland. This article is an open access article distributed under the terms and conditions of the Creative Commons Attribution (CC BY) license (<https://creativecommons.org/licenses/by/4.0/>).

1. Introduction

At sites of vascular damage, platelets adhere to the exposed extracellular matrix to form a primary haemostatic plug. A critical element of this response is the release of over 300 proteins from α -granules, dense granules, and lysosomes [1]. Platelet secretion involves granule fusion with the plasma membrane to release their cargo into the extracellular space. In mammalian cells, secretion is regulated by SNAREs, comprising v-SNAREs present on vesicles/granules (also termed VAMPs), t-SNAREs located on the target plasma membrane (syntaxins), and soluble components consisting of NSF and soluble NSF attachment proteins (SNAPs). Fusion between membranes requires the formation of ternary core complexes between t-SNAREs and a v-SNARE [2].

Despite the significance of platelet secretion, the underlying molecular mechanisms remain complex and poorly understood. Platelet secretion occurs when ligands (e.g., collagen) bind to receptors on the plasma membrane, activating phospholipase C. This leads

to the production of IP3 and DAG, raising cytosolic Ca²⁺ levels, which, along with protein kinase C activation, triggers granule fusion with the plasma membrane and secretion [3]. Despite recent proteomic advances, the precise mechanisms that facilitate SNARE complex formation in platelets and thus granule release remain unclear. Syntaxin 11, SNAP 23, VAMP 3, VAMP 7, and VAMP 8 have all been recently established as core proteins regulating platelet secretion [4,5], but redundancy and compensation mechanisms exist, as evidenced by incomplete secretion defects in SNARE-deficient models [6–8].

α -synuclein, initially characterised for its role in neuronal function and implicated in neurodegenerative disorders like Parkinson's disease, is a small, soluble protein predominantly found in presynaptic terminals [9]. In nerve cells, α -synuclein acts to promote SNARE complex assembly through a non-enzymatic mechanism involving simultaneous α -synuclein binding to VAMP 2 via its C terminus [10,11]. In platelets, α -synuclein is co-localised with α -granules, indicating a role in secretion [12]. Recombinant α -synuclein reduces platelet α -granule secretion but not dense or lysosomal secretion, although the mechanism(s) is currently unknown [13]. Consistent with this observation, C57BL/6 mice carrying a spontaneous large chromosomal deletion that includes both the multimerin-1 and α -synuclein loci display aggregation defects to thrombin in vitro and both delayed and unstable thrombus formation in vivo [14]. Whether multimerin-1, α -synuclein, or both are responsible for platelet dysfunction remains to be established. In a recent study by Whiteheart's group [15], α -synuclein deletion in B6; 129X1-Snca^{tm1Rosl}/J mice had no significant impact on platelet aggregation, secretion, bleeding, or in vivo thrombus formation, suggesting that α -synuclein may be redundant for platelet function.

Given the crucial role of SNAREs in platelet function and the established role of α -synuclein in neurons, we used an α -synuclein^{-/-} mouse model on a pure C57Bl6J genetic background [16,17] to reassess the importance of α -synuclein in platelet function. Our data indicate that α -synuclein^{-/-} mice display longer bleeding times with a tendency to rebleed. In vitro analysis revealed that α -synuclein^{-/-} platelets exhibit more defects in aggregation, secretion, and adhesion compared to wildtype (WT) littermates, suggesting that α -synuclein plays a vital role in platelet activation.

2. Materials and Methods

2.1. Reagents

Dade™ Innovin™ was purchased from Siemens (Forchheim, Germany). PPACK (Phe-Pro-Arg-Chloromethylketone) was from ENZO (New York, NY, USA). Collagen reagent Horm was from Nycomed (Munich, Germany). α -synuclein (51510), P-VASP (3111), VAMP 7 (14811), and VAMP 8 (13060) antibodies were from Cell Signalling Technology (Delft, The Netherlands). DIO6C (D273) was purchased from ThermoFisher Scientific (Waltham, MA, USA). HRP-conjugated anti-rabbit antibody was purchased from DAKO (Santa Clara, CA, USA). Vena8 FLUORO+ Biochips were from Cellix (Dublin, Ireland). FITC-labelled CD49b (M070-1), FITC-labelled CD42B (M040-1), FITC-labelled GPVI (M011-1), PE-labelled Jon/A, and FITC-Wug.E9 (D200) antibodies were from Emfret analytics (Eibelstadt, Germany). PE/Cyanine7-labelled anti-mouse CD63 (143910) and Alexa Fluor 700-labelled anti-mouse LAMP-1 (121627) antibodies were purchased from Biolegend (San Diego, CA, USA). FITC-labelled CD41 antibody (553848) was purchased from BD Pharmingen (Franklin Lakes, NJ, USA). α -synuclein (sc-515879), P- α -synuclein (ser129, sc-135638), syntaxin 11 (sc-377121), syntaxin 4 (sc-101301), and SNAP-23 (sc-373743) antibodies were purchased from Santa Cruz Biotechnology (Santa Cruz, CA, USA). All other reagents were purchased from Merck (Poole, UK).

2.2. Mouse Strains

The α -synuclein^{-/-} mouse strain targeting the *Snca* gene on the C57Bl6J genetic background was described previously and was bred using heterozygous crosses [18]. Experiments with murine samples were approved by the Hull York Medical School Ethics

to the production of IP3 and DAG, raising cytosolic Ca²⁺ levels, which, along with protein kinase C activation, triggers granule fusion with the plasma membrane and secretion [3]. Despite recent proteomic advances, the precise mechanisms that facilitate SNARE complex formation in platelets and thus granule release remain unclear. Syntaxin 11, SNAP 23, VAMP 3, VAMP 7, and VAMP 8 have all been recently established as core proteins regulating platelet secretion [4,5], but redundancy and compensation mechanisms exist, as evidenced by incomplete secretion defects in SNARE-deficient models [6–8].

α -synuclein, initially characterised for its role in neuronal function and implicated in neurodegenerative disorders like Parkinson's disease, is a small, soluble protein predominantly found in presynaptic terminals [9]. In nerve cells, α -synuclein acts to promote SNARE complex assembly through a non-enzymatic mechanism involving simultaneous α -synuclein binding to VAMP 2 via its C terminus [10,11]. In platelets, α -synuclein is co-localised with α -granules, indicating a role in secretion [12]. Recombinant α -synuclein reduces platelet α -granule secretion but not dense or lysosomal secretion, although the mechanism(s) is currently unknown [13]. Consistent with this observation, C57BL/6 mice carrying a spontaneous large chromosomal deletion that includes both the multimerin-1 and α -synuclein loci display aggregation defects to thrombin in vitro and both delayed and unstable thrombus formation in vivo [14]. Whether multimerin-1, α -synuclein, or both are responsible for platelet dysfunction remains to be established. In a recent study by Whiteheart's group [15], α -synuclein deletion in B6; 129X1-Snca^{tm1Rosl}/J mice had no significant impact on platelet aggregation, secretion, bleeding, or in vivo thrombus formation, suggesting that α -synuclein may be redundant for platelet function.

Given the crucial role of SNAREs in platelet function and the established role of α -synuclein in neurons, we used an α -synuclein^{-/-} mouse model on a pure C57Bl6J genetic background [16,17] to reassess the importance of α -synuclein in platelet function. Our data indicate that α -synuclein^{-/-} mice display longer bleeding times with a tendency to rebleed. In vitro analysis revealed that α -synuclein^{-/-} platelets exhibit more defects in aggregation, secretion, and adhesion compared to wildtype (WT) littermates, suggesting that α -synuclein plays a vital role in platelet activation.

2. Materials and Methods

2.1. Reagents

Dade™ Innovin™ was purchased from Siemens (Forchheim, Germany). PPACK (Phe-Pro-Arg-Chloromethylketone) was from ENZO (New York, NY, USA). Collagen reagent Horm was from Nycomed (Munich, Germany). α -synuclein (51510), P-VASP (3111), VAMP 7 (14811), and VAMP 8 (13060) antibodies were from Cell Signalling Technology (Dellaertweg, The Netherlands). DIO6C (D273) was purchased from ThermoFisher Scientific (Waltham, MA, USA). HRP-conjugated anti-rabbit antibody was purchased from DAKO (Santa Clara, CA, USA). Vena8 FLUORO+ Biochips were from Cellix (Dublin, Ireland). FITC-labelled CD49b (M070-1), FITC-labelled CD42B (M040-1), FITC-labelled GPVI (M011-1), PE-labelled Jon/A, and FITC-Wug.E9 (D200) antibodies were from Emfret analytics (Eibelstadt, Germany). PE/Cyanine7-labelled anti-mouse CD63 (143910) and Alexa Fluor 700-labelled anti-mouse LAMP-1 (121627) antibodies were purchased from Biolegend (San Diego, CA, USA). FITC-labelled CD41 antibody (553848) was purchased from BD Pharmingen (Franklin Lakes, NJ, USA). α -synuclein (sc-515879), P- α -synuclein (ser129, sc-135638), syntaxin 11 (sc-377121), syntaxin 4 (sc-101301), and SNAP-23 (sc-373743) antibodies were purchased from Santa Cruz Biotechnology (Santa Cruz, CA, USA). All other reagents were purchased from Merck (Poole, UK).

2.2. Mouse Strains

The α -synuclein^{-/-} mouse strain targeting the *Snca* gene on the C57Bl6J genetic background was described previously and was bred using heterozygous crosses [18]. Experiments with murine samples were approved by the Hull York Medical School Ethics

with Zeiss Plan-Apochromat 63× and 100× NA 1.4 objectives and an AxioCam 506 (Carl Zeiss Meditec AG, Jena, Germany).

2.10. Flow Cytometry

PRP was incubated with fluorophore-conjugated antibodies in the presence of Gly-Pro-Arg-Pro amide peptide (5 μM) before stimulation with thrombin for 20 min at 37 °C, then fixed with 0.2% paraformaldehyde solution before analysis. Samples were acquired on a BD Biosciences LSRFortessa and analysed using FlowJo™ software version 10.

2.11. Immunoblotting

WPs (5×10^8 platelets/mL) were treated with indomethacin (10 μM), apyrase (2 U/mL), and tirofiban (0.5 μg/mL) prior to stimulation with agonists at 37 °C with stirring for the indicated times. Reactions were stopped by the addition of an equal volume of ice-cold Laemmli buffer. Lysates were separated by SDS-PAGE then analysed by immunoblotting as previously described [21]. To enhance the detection of P-α-synuclein (ser129, sc-135638), membranes were fixed with 0.4% PFA in TBS for 20 min before blocking. After fixation, membranes were blocked in 5% non-fat milk in TBS-T (0.1% Tween-20) for 1 h.

2.12. Statistical Analysis

All results are presented as the mean ± standard error of the mean (SEM) unless otherwise stated. All statistical analyses were performed on GraphPad Prism 8.0 (GraphPad software, La Jolla, CA, USA). Data normality was determined by Shapiro–Wilk tests. For a comparison of the two groups, an unpaired *t*-test or Mann–Whitney U test was, respectively, used for parametric and non-parametric data. Statistical significance was determined when the *p* value was equal to or less than 0.05. All flow cytometric analyses were completed using FlowJo (v10, BD, Ashlan, OR, USA).

3. Results

3.1. α-Synuclein-Deficient Mice Display a Haemostatic Defect

In this study, we examined the role of α-synuclein in haemostasis using α-synuclein^{-/-} mice (Figure 1a). In tail bleeding/rebleeding experiments, an indicator of haemostatic capacity, bleeding times for α-synuclein^{-/-} mice were significantly increased compared with WT littermates (216 ± 51.4 s vs. 618 ± 97.7 s; $p = 0.0051$) (Figure 1b). Interestingly, α-synuclein^{-/-} mice had an increased propensity for rebleeding, indicating that clot stability was reduced. To determine whether this phenotype was linked to defects in secondary haemostasis, we measured prothrombin time (PT) and activated partial thromboplastin time (aPTT). PT measurements showed no difference between α-synuclein^{-/-} and WT littermates ($p = 0.977$) (Figure 1c), indicating an intact extrinsic coagulation pathway. However, aPTT was significantly prolonged in α-synuclein^{-/-} mice compared with WT littermates (61.25 ± 2.5 s vs. 39.75 ± 1.75 s; $p = 0.0002$), suggesting a defect in the intrinsic pathway.

3.2. Platelet Granule Secretion Is Reduced in α-Synuclein^{-/-} Mice

Disorders such as Gray Platelet Syndrome or Hermansky–Pudlak Syndrome, characterised by impaired platelet secretion, also present with prolonged aPTT due to impaired factor VIII release, a key component of the intrinsic pathway [22–24]. Therefore, to investigate the contribution of platelets to the haemostatic defect in α-synuclein^{-/-} mice in isolation, we assessed platelet secretion. We examined α-granule, dense granule, and lysosome secretion using P-selectin (CD62p), CD63, and LAMP1 as markers, respectively. The stimulation of platelets with thrombin caused a significant increase in α-granule (CD62p) and dense granule (CD63) secretion in WT compared with α-synuclein^{-/-} platelets but no difference in lysosome (LAMP1) secretion (Figure 2a–c). This suggests a selective role for α-synuclein in granule secretion, with reduced secretion from α-granules (factor VIII source) likely contributing to the haemostatic defects.

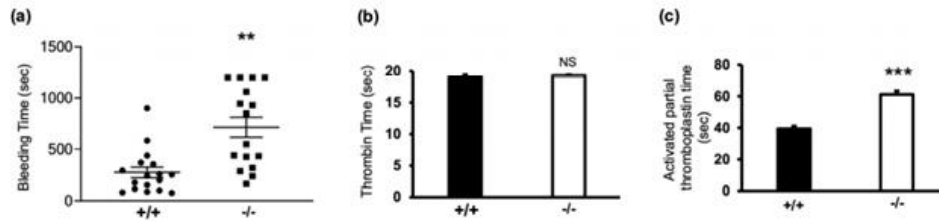


Figure 1. α -synuclein deficiency prolongs bleeding time. (a) Animals were scored after cessation of tail bleeding for 1 min. Experiment was stopped after 30 min if no cessation of blood flow occurred. Data are presented in scatter plot; each dot represents individual animal, and lines indicate mean and SEM. +/+ denotes WT, and -/- denotes α -synuclein^{-/-} mice. Prothrombin time (b) and activated partial thromboplastin time (c) were measured in PPP. Data are presented as mean \pm SEM. NS, not significant; ** $p < 0.01$, *** $p < 0.001$ compared with WT, Mann–Whitney U test.

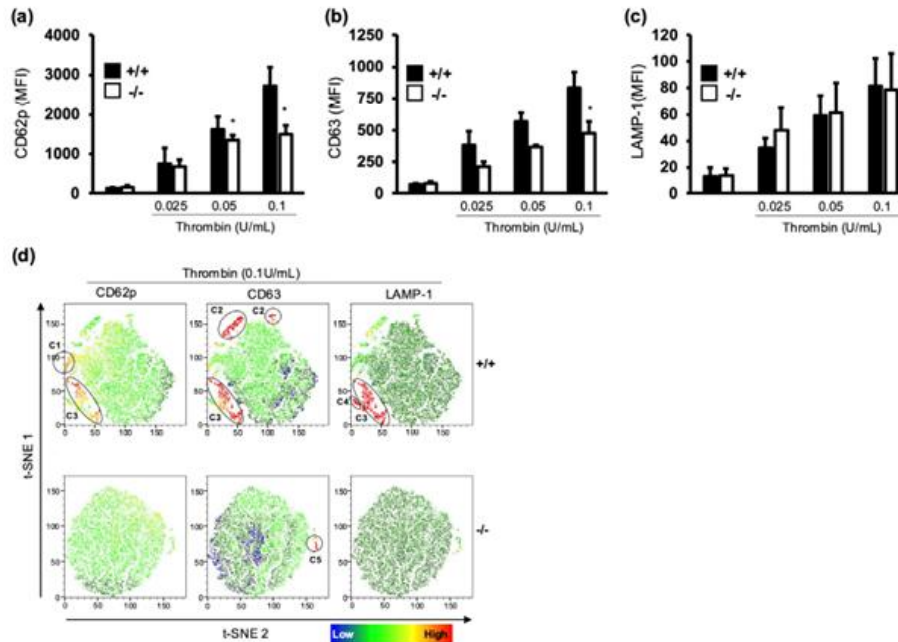


Figure 2. α -synuclein deficiency inhibits platelet granule secretion. Platelet-rich plasma (PRP) from WT (+/+) and α -synuclein^{-/-} (-/-) mice were stimulated with thrombin (0.025–0.1 U/mL) for 20 min, and platelet alpha-granule (a), dense granule (b), and lysosome (c) secretion was assessed by using flow cytometry. Median fluorescence intensity (MFI) is presented as mean \pm SEM. (d) t-Distributed Stochastic Neighbourhood Embedding (t-SNE) analysis was performed on flow cytometry data to visualise subpopulations of platelets based on granule secretion markers in WT (+/+) and α -synuclein^{-/-} (-/-) platelets after stimulation with thrombin (0.1 U/mL). Heatmaps represent median fluorescence intensity (MFI) for CD62p (left column), CD63 (middle column), and LAMP-1 (right column). * $p < 0.05$, Mann–Whitney U test.

To gain further insights into the impact of α -synuclein deletion on platelet function, we next opted for a t-Distributed Stochastic Neighbourhood Embedding (t-SNE) analysis of

the flow cytometry data. T-SNE analysis allows for the visualisation of multi-dimensional data in two dimensions by the formation of clusters of related cells/events [25]. Under unstimulated conditions, both WT and α -synuclein^{-/-} platelets displayed homogeneous populations. However, thrombin stimulation caused subpopulations to emerge in WT platelets only (Figure 2d). This emergence of distinct subpopulations in WT but not α -synuclein^{-/-} platelets further underscores the role of α -synuclein in platelet activation and secretion. The false colouring of CD62p, CD63, and LAMP1 over the t-SNE map shows that WT platelets, but not α -synuclein^{-/-} platelets, display a distinct clustering of CD62p, CD63, and LAMP1 populations. WT platelets clustered into several populations that were CD62p^{hi}CD63^{lo}LAMP1^{lo} (Cluster C1), CD62p^{lo}CD63^{hi}LAMP1^{lo} (C2) CD62p^{hi}CD63^{hi}LAMP1^{lo} (C3), and CD62p^{lo}CD63^{lo}LAMP1^{hi} (C4). α -synuclein^{-/-} platelets only grouped into a small CD62p^{lo}CD63^{hi}LAMP1^{lo} cluster (C5), with no distinct double or triple stain. These data suggest that the deletion of α -synuclein diminishes platelet secretion and affects the complexity of platelet activation states.

3.3. α -Synuclein Deficiency Results in a Platelet Function Defect

Several studies established the importance of platelet secretion in driving platelet aggregation and the proper functioning of haemostasis. To investigate whether secretion defects impact platelet function in α -synuclein^{-/-} mice, we examined platelet aggregation in vitro. WT and α -synuclein^{-/-} platelets were stimulated with either collagen, thrombin, or a thromboxane A2 analogue, U46619 (Figure 3a–c). Our findings show that α -synuclein^{-/-} platelets displayed an aggregation defect in response to all agonists when compared with WT littermates, suggesting that the defect is shared between different signalling pathways. Interestingly, α -synuclein^{-/-} platelets achieved aggregation levels equivalent to those of WT platelets when stimulated with higher concentrations of collagen ($67.50 \pm 6.25\%$, $67.86 \pm 6.25\%$; $p = 0.93$) (Figure 3bii), suggesting a dose dependency. An analysis of α -synuclein^{-/-} platelets revealed that the receptor expression levels of major platelet receptors, CD49b, CD42b, GPVI, and CD41, were comparable to those of WT platelets (Supplemental Figure S1a–d). Therefore, the presence of platelet aggregation defects was not due to receptor expression alterations.

The capacity for platelets to adhere to and spread at the site of injury is key for thrombus formation and stability [26]. To examine the impact of α -synuclein deletion on platelet adhesion, platelets were allowed to adhere on fibrinogen-coated (Supplemental Figure S2) or collagen-coated surfaces for up to 60 min. Interestingly, we found no difference in adhesion ($p = 0.844$) or spreading ($p = 0.52$) on collagen between WT and α -synuclein^{-/-} platelets (Figure 4ai–aiii). However, fewer α -synuclein^{-/-} platelets formed filopodia (Figure 4aiv). Importantly, platelet size and granularity in WT and α -synuclein^{-/-} platelets were comparable (Supplemental Figure S3), suggesting that differences are specific to functional morphology rather than general platelet development or structure.

Several lines of evidence support the role of filopodia in stable platelet adhesion under flow conditions [11], important for thrombus stability and growth. Therefore, we examined the role of α -synuclein in thrombus formation using a microfluid flow-controlled in vitro system (Cellix). Whole blood from α -synuclein^{-/-} or WT mice was perfused over a collagen-coated surface in a flow chamber at a 1000 s^{-1} shear rate (Figure 4bi). α -synuclein^{-/-} samples exhibited lower surface coverage ($10.43 \pm 1.1\%$ vs. 5.9 ± 0.1 ; $p = 0.003$) (Figure 4bii) and thrombus height ($8.25 \pm 0.75 \mu\text{m}$ vs. $2.5 \pm 0.64 \mu\text{m}$; $p = 0.0005$) (Figure 4biii) compared to WT samples, suggesting that α -synuclein plays a significant role in stabilising platelet adhesion and in thrombus formation and stability at high shear rates.

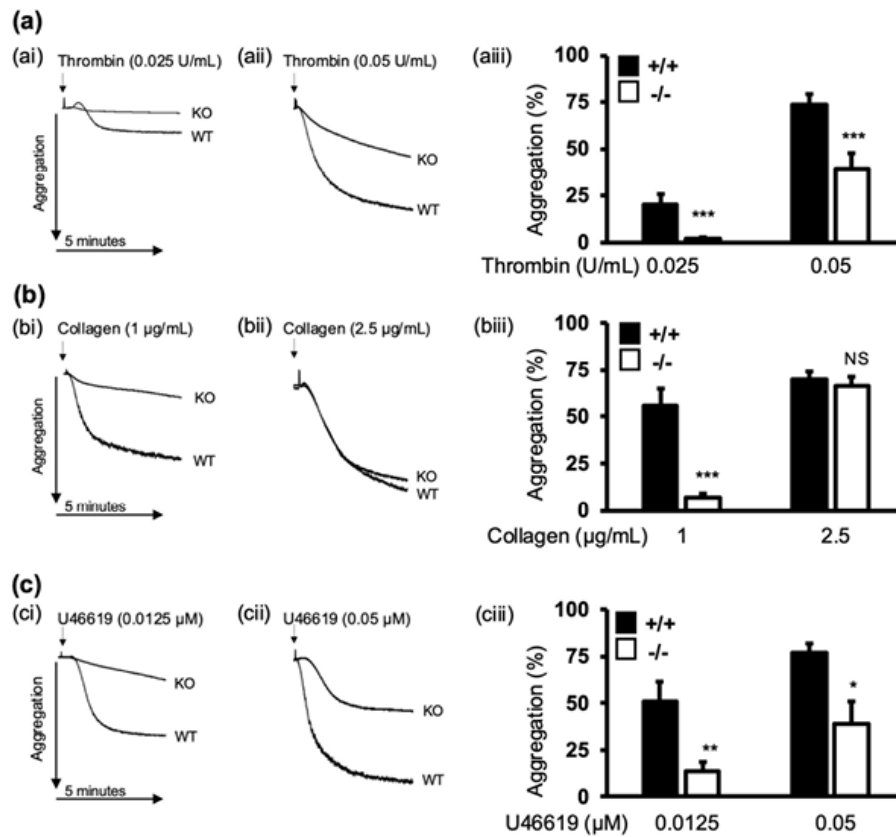


Figure 3. α -synuclein deficiency impairs platelet aggregation. WPs (3×10^8 platelets/mL) from WT and α -synuclein $^{-/-}$ mice were stimulated with thrombin (a), collagen (b), or U46619 (c) at indicated concentrations, and platelet aggregation was measured under constant stirring (1000 rpm) at 37 °C for 5 min by Born aggregometry. Representative traces (i,ii) and percent aggregation (iii). Percent aggregation is presented as mean \pm SEM of $n = 5$. NS, not significant; * $p < 0.05$, ** $p < 0.01$, *** $p < 0.001$ compared with WT platelets, Mann–Whitney U test.

3.4. Platelet Activation Causes Membrane Compartmentalisation of α -Synuclein

To evaluate the spatiotemporal regulation of α -synuclein, we used human platelets as a model system. Using immunofluorescence, we showed that in resting conditions, α -synuclein was predominantly localised in clusters within the platelet. However, following stimulation with thrombin, α -synuclein re-localised to the cell periphery (Figure 5a). To investigate whether α -synuclein is secreted during activation, platelet releasates were analysed for the presence of α -synuclein, with thrombospondin-1 (TSP-1) as a positive marker. While TSP-1 was detected in both the pellet and releasates, α -synuclein was absent in the releasates (Figure 5b), indicating that α -synuclein undergoes intracellular redistribution upon activation without being released into the extracellular milieu.

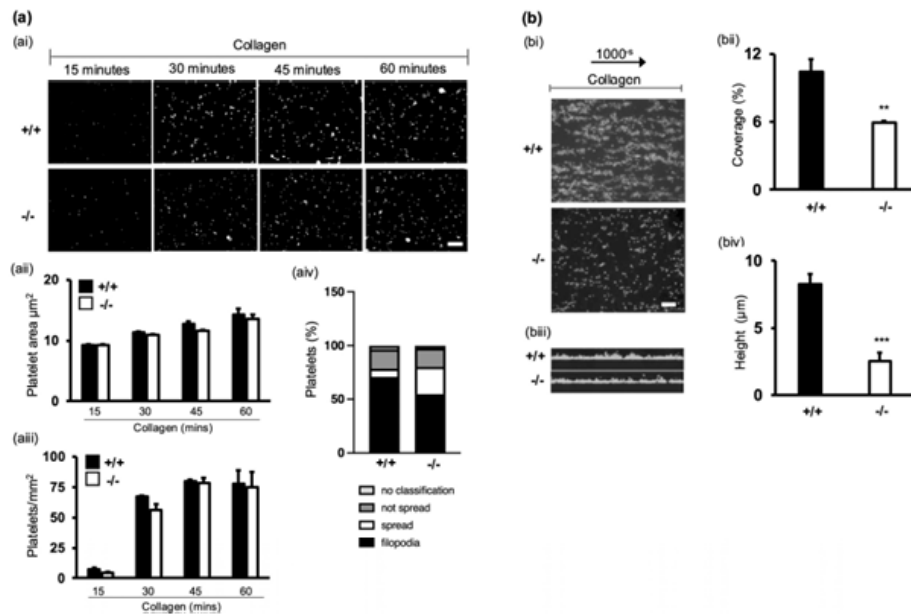


Figure 4. α -synuclein deficiency impairs thrombus formation in vitro. **(ai)** Adhesion of washed platelets to glass coverslips coated with collagen (100 $\mu\text{g}/\text{mL}$). Adherent platelets were fixed, permeabilised, and stained with TRITC-phalloidin. Images were acquired with fluorescence microscope equipped with structured illumination attachment and deconvolved. Scale bar represents 25 μm . **(a(ii))** Surface coverage per platelet calculated by thresholding using ImageJ 1.54e. **(a(iii))** Number of platelets per mm^2 . Five fields each 12,500 μm^2 in size from five independent experiments were scored per condition. Data represent mean \pm SEM. No significant differences were found between WT and α -synuclein $^{-/-}$ platelets for any condition (Mann–Whitney U-test). **(a(iv))** Quantification of different spreading phases of platelets. **(bi)** Whole blood from WT and α -synuclein $^{-/-}$ mice was perfused at arterial shear 1000 s^{-1} for 2 min over collagen matrix (100 $\mu\text{g}/\text{mL}$). Images of adherent platelets were taken using fluorescence microscopy. Scale bar represents 25 μm . **(b(ii))** Data are expressed as percentage surface coverage. **(b(iii))** Z stacks were acquired to assess thrombus height (μm) **(b(iv))**. Data are presented as mean \pm SEM of $n = 5$. ** $p < 0.01$, *** $p < 0.001$, Mann–Whitney U test.

Given the results of previous studies on the essential roles of VAMP 8 and syntaxin 11 in platelet secretion [6], it is likely that α -synuclein interacts with these proteins as part of the platelet secretory machinery. To explore this, coimmunoprecipitation experiments were performed using anti- α -synuclein antibodies. Figure 5c shows that in resting conditions, α -synuclein formed a complex with syntaxin 4 and syntaxin 11. However, platelet stimulation caused an increase in α -synuclein association with syntaxin 4 and syntaxin 11, while it resulted in the recruitment of VAMP 8. These findings suggest a dynamic role for α -synuclein as a SNARE protein involved in forming complexes with other platelet SNARE proteins during the secretory process. Importantly, the assessment of major SNARE proteins in WT and α -synuclein $^{-/-}$ platelets revealed no changes in protein expression, indicating that the absence of α -synuclein does not lead to compensatory increases in other SNARE proteins. This lack of redundancy underscores the specific and non-redundant role of α -synuclein in platelet secretion (Supplemental Figure S4a).

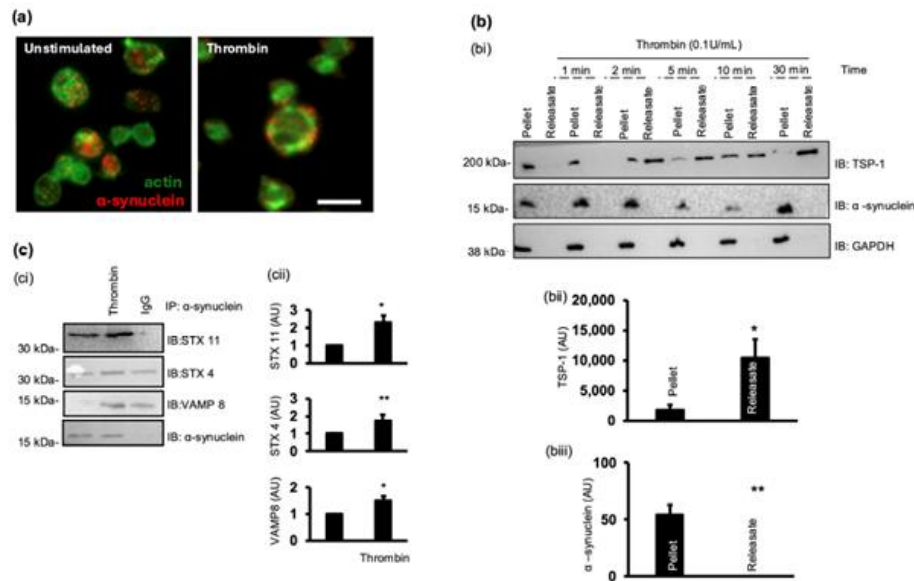


Figure 5. Platelet activation causes α -synuclein re-localisation and assembly with SNARE complex. (a) Human WPs (1×10^7 platelets/mL) were stimulated with thrombin (0.05 U/mL) for 5 min and left to adhere to cover slides coated in poly-L-lysine for 15 min before fixing with 4% PFA. Cover slides were incubated for 1 h with α -synuclein primary antibody before incubation with FITC phalloidin (1:200) and anti-mouse PE antibody in dark for 1 h. Images were acquired with fluorescence microscope equipped with structured illumination attachment and deconvolved. Scale bar represents 5 μ m. (b) Human WPs (5×10^8 platelets/mL) were stimulated with thrombin (0.1 U/mL) for up to 30 min. Pellet and releasates were collected and analysed by Western blotting for presence of α -synuclein and TSP-1. (bii,biii) Densitometric analysis of amount of α -synuclein and TSP-1 after 5 min of stimulation. (c) WPs (8×10^8 platelets/mL) were stimulated with thrombin (0.1 U/mL) for up to 5 min; reaction was stopped with lysis buffer, and α -synuclein was immunoprecipitated. Immunoprecipitates were then immunoblotted for presence of STX 11, STX 4, VAMP 8, and α -synuclein. Representative immunoblots of 4 independent experiments. (cii) Densitometric analysis of amount of SNARE proteins present in immunoprecipitates. * $p < 0.05$, ** $p < 0.01$ compared with basal.

3.5. Platelet Activation Induces α -Synuclein Phosphorylation

The phosphorylation of α -synuclein on ser129 has been linked with increased membrane binding capabilities in neurons [27]. The stimulation of platelets with thrombin or treatment with the phosphatase inhibitor calyculin A induced a robust increase in α -synuclein ser129 phosphorylation, whereas the basal levels of ser129 phosphorylation were diminished in PGI_2 -treated platelets, suggesting that α -synuclein ser129 is phosphorylated downstream an “activatory” signal (Supplemental Figure S4b). This was interrogated further, and platelets were stimulated with thrombin (Figure 6a), which caused an increase in α -synuclein ser129 phosphorylation in a dose- and time-dependent manner.

4. Discussion

Our study investigating the impact of α -synuclein deletion on platelet function reveals significant implications for haemostasis. α -synuclein^{-/-} mice exhibited prolonged bleeding times and increased rebleeding tendency compared to WT littermates, indicating a critical role for α -synuclein in maintaining haemostatic balance. Platelet aggregation experiments revealed a pronounced defect in α -synuclein^{-/-} platelets across various agonists. Microfluidic flow chamber experiments demonstrated reduced thrombus formation and stability in α -synuclein^{-/-} mice under physiological shear rates. These findings highlight α -synuclein's critical role in promoting stable platelet aggregates, essential for effective haemostasis in dynamic vascular environments.

These findings, however, contrast with a recent study led by Smith et al. (2023) that found no significant haemostatic defects or aggregation impairment in an α -synuclein-deficient model [15]. The discrepancy may be attributed to differences in knockout mouse models and experimental methodologies. Although *Snc*a^{-/-} mice originally produced by Abeliovich et al. [30] were used in both studies, they were maintained on different genetic backgrounds: mixed 129/C57Bl6J in the Smith et al. study vs. pure C57Bl6J in our study. This difference in genetic background could contribute to the observed variations. Additionally, their blood collection method involved exposing the thoracic region and using sodium citrate, apyrase, and prostaglandin, whereas we used sodium citrate alone via direct cardiac puncture without inducing injury and the potential pre-activation of platelets. They also reintroduced 1 mM CaCl₂ into the washed platelets before experimentation, which has been shown to induce morphological changes, microparticle release, fibrin formation, and increased P-selectin expression [31]. Of note, human studies linking α -synuclein mutations with bleeding diatheses further underscore the translational relevance of our findings [32,33].

An analysis of platelet granule secretion patterns in α -synuclein^{-/-} mice revealed diminished α -granule and dense granule secretion upon activation, indicating a selective role for α -synuclein in regulating specific granule types. Our t-SNE analysis indicated that α -synuclein deletion leads to a reduction in the diversity of platelet secretion patterns. WT platelets demonstrate a broader range of secretory responses characterised by distinct clusters, indicating varying degrees of α -granule (CD62p), dense granule (CD63), and lysosome (LAMP1) secretion. In contrast, α -synuclein^{-/-} platelets exhibit a more limited secretion profile, suggesting a diminished ability to release their cargo in response to stimulation. These findings further emphasise the crucial role of α -synuclein in regulating platelet secretion dynamics, which are essential for effective haemostasis. This contrasts with broader impacts reported in the Smith study, suggesting that α -synuclein plays a minor role in granule secretion [15].

Investigations into α -synuclein's spatiotemporal dynamics and phosphorylation status upon platelet activation demonstrate a rapid re-localisation of α -synuclein to the cell periphery and enhanced ser129 phosphorylation, crucial for membrane binding and activation responses [27]. These observations underscore α -synuclein's conserved role in modulating platelet membrane dynamics and secretion processes across diverse cell types. Furthermore, our results demonstrate that α -synuclein Ser129 phosphorylation is Ca²⁺-dependent, as it is abolished by intracellular Ca²⁺ chelation with BAPTA-AM. However, as PKA activation by PGI₂ also inhibits α -synuclein phosphorylation, the precise mechanism—whether mediated directly by PKA or indirectly via the suppression of Ca²⁺ mobilisation—remains unclear and warrants further investigation.

The phosphorylation of α -synuclein at Ser129 is a critical post-translational modification that modulates its aggregation propensity and cellular interactions. In neuronal systems, several kinases—including G-protein-coupled receptor kinases (GRK2 and GRK5), casein kinases (CK1 and CK2), polo-like kinase 2 (PLK2), and leucine-rich repeat kinase 2 (LRRK2)—have been identified as mediators of this phosphorylation event [34–36]. However, the specific kinase responsible for Ser129 phosphorylation in platelets remains unidentified. Our findings indicate that this phosphorylation is calcium-dependent and modulated

by the cAMP/PKA pathway, suggesting the potential involvement of calcium-sensitive kinases. Further research is necessary to elucidate the exact kinase involved in platelets, which could provide deeper insights into the regulatory mechanisms of α -synuclein in platelet function.

A recent study found that the addition of exogenous α -synuclein inhibits platelet aggregation by interfering with the signalling pathway of the α -thrombin/protease-activated receptor 1 (PAR1) axis [37]. Interestingly, α -synuclein levels were found to increase in the plasma supernatant of platelets from a single donor over time, suggesting a time-dependent release of α -synuclein from platelets into the plasma [38]. Our Western blot data indicate that α -synuclein is not released during platelet activation, suggesting that any α -synuclein detected in plasma is unlikely to originate from platelets. This discrepancy underscores the potential presence of alternative cell sources within single-donor platelets [39], despite differences in detection techniques.

5. Conclusions

Our study provides strong evidence that α -synuclein plays a crucial role in platelet function and haemostasis. The absence of α -synuclein leads to significant impairments in platelet aggregation, granule secretion, and thrombus stability, highlighting its non-redundant role in these processes. These findings offer new insights into the molecular mechanisms of platelet regulation and suggest that targeting α -synuclein pathways could be a novel therapeutic approach to managing thrombotic disorders. Further research is warranted to explore the potential clinical implications of these findings.

Supplementary Materials: The following supporting information can be downloaded at <https://www.mdpi.com/article/10.3390/cells13242089/s1>, Figure S1. α -synuclein deficiency has no impact on cell surface receptor expression; Figure S2. α -synuclein deficiency does not impact platelet adhesion; Figure S3. α -synuclein deficiency has no impact on platelet size or granularity; Figure S4. α -synuclein deficiency has no impact on SNARE protein expression.

Author Contributions: C.S. designed and performed experiments and analysed data; W.J., J.S.K., M.S.H. and C.C. performed experiments; S.D.J.C., S.F., J.D.L., N.N. and V.B. provided essential materials; K.M.N. and F.R. designed this research; A.A. designed this research, analysed data, and wrote the manuscript. All authors have read and agreed to the published version of the manuscript.

Funding: This research was funded by the BRITISH HEART FOUNDATION, grant numbers FS/19/38/34441, FS/19/10/34128 and FS/PhD/22/29208.

Institutional Review Board Statement: This study was conducted in accordance with the Declaration of Helsinki and approved by the Research Ethics Committee of the NHS Health Research Authority (IRAS 283854, approved on 2 August 2021).

Informed Consent Statement: Informed consent was obtained from all subjects involved in this study.

Data Availability Statement: The original contributions presented in this study are included in the article/Supplementary Material; further inquiries can be directed to the corresponding author.

Conflicts of Interest: The authors declare no conflicts of interest.

References

1. Golebiewska, E.M.; Poole, A.W. Platelet secretion: From haemostasis to wound healing and beyond. *Blood Rev.* **2015**, *29*, 153–162. [[CrossRef](#)] [[PubMed](#)]
2. Edwardson, J.M. Membrane fusion: All done with SNAREpins? *Curr. Biol.* **1998**, *8*, R390–R393. [[CrossRef](#)]
3. Ware, J.A.; Chang, J.D. Protein Kinase C and Its Interactions with Other Serine-Threonine Kinases. In *Platelets and Their Factors*; Springer: Berlin/Heidelberg, Germany, 1997; pp. 247–262. [[CrossRef](#)]
4. Golebiewska, E.M.; Harper, M.T.; Williams, C.M.; Savage, J.S.; Goggs, R.; Fischer von Mollard, G.; Poole, A.W. Syntaxin 8 regulates platelet dense granule secretion, aggregation, and thrombus stability. *J. Biol. Chem.* **2015**, *290*, 1536–1545. [[CrossRef](#)] [[PubMed](#)]
5. Koseoglu, S.; Peters, C.G.; Fitch-Tewfik, J.L.; Aisiku, O.; Danglot, L.; Galli, T.; Flaumenhaft, R. VAMP-7 links granule exocytosis to actin reorganization during platelet activation. *Blood* **2015**, *126*, 651–660. [[CrossRef](#)] [[PubMed](#)]

6. Ye, S.; Karim, Z.A.; Al Hawas, R.; Pessin, J.E.; Filipovich, A.H.; Whiteheart, S.W. Syntaxin-11, but not syntaxin-2 or syntaxin-4, is required for platelet secretion. *Blood* **2012**, *120*, 2484–2492. [[CrossRef](#)]
7. Ren, Q.; Barber, H.K.; Crawford, G.L.; Karim, Z.A.; Zhao, C.; Choi, W.; Wang, C.-C.; Hong, W.; Whiteheart, S.W.; Woo, S.S.; et al. Endobrevin/VAMP-8 is the primary v-SNARE for the platelet release reaction. *Mol. Biol. Cell* **2007**, *18*, 24–33. [[CrossRef](#)] [[PubMed](#)]
8. Schraw, T.D.; Rutledge, T.W.; Crawford, G.L.; Bernstein, A.M.; Kalen, A.L.; Pessin, J.E.; Whiteheart, S.W. Granule stores from cellubrevin/VAMP-3 null mouse platelets exhibit normal stimulus-induced release. *Blood* **2003**, *102*, 1716–1722. [[CrossRef](#)]
9. Maroteaux, L.; Campanelli, J.T.; Scheller, R.H. Synuclein: A neuron-specific protein localized to the nucleus and presynaptic nerve terminal. *J. Neurosci.* **1988**, *8*, 2804–2815. [[CrossRef](#)]
10. Bonini, N.M.; Giasson, B.I. Snaring the Function of alpha-Synuclein. *Cell* **2005**, *123*, 359–361. [[CrossRef](#)]
11. Burré, J.; Sharma, M.; Tsetsenis, T.; Buchman, V.; Etherton, M.R.; Südhof, T.C. Alpha-synuclein promotes SNARE-complex assembly in vivo and in vitro. *Science* **2010**, *329*, 1663–1667. [[CrossRef](#)]
12. Hashimoto, M.; Yoshimoto, M.; Sisk, A.; Hsu, L.J.; Sundsmo, M.; Kittel, A.; Saitoh, T.; Miller, A.; Masliah, E. NACP, a synaptic protein involved in Alzheimer's disease, is differentially regulated during megakaryocyte differentiation. *Biochem. Biophys. Res. Commun.* **1997**, *237*, 611–616. [[CrossRef](#)] [[PubMed](#)]
13. Park, S.M.; Jung, H.Y.; Kim, H.O.; Rhim, H.; Paik, S.R.; Chung, K.C.; Park, J.H.; Kim, J. Evidence that alpha-synuclein functions as a negative regulator of Ca(++)-dependent alpha-granule release from human platelets. *Blood* **2002**, *100*, 2506–2514. [[CrossRef](#)]
14. Reheman, A.; Tasneem, S.; Ni, H.; Hayward, C.P.M. Mice with deleted multimerin 1 and alpha-synuclein genes have impaired platelet adhesion and impaired thrombus formation that is corrected by multimerin 1. *Thromb. Res.* **2010**, *125*, e177–e183. [[CrossRef](#)] [[PubMed](#)]
15. Smith, A.N.; Joshi, S.; Chanzu, H.; Alfar, H.R.; Shrivani Prakhya, K.; Whiteheart, S.W. alpha-Synuclein is the major platelet isoform but is dispensable for activation, secretion, and thrombosis. *Platelets* **2023**, *34*, 2267147. [[CrossRef](#)]
16. Goloborsheva, V.V.; Chaprov, K.D.; Teterina, E.V.; Ovchinnikov, R.; Buchman, V.L. Reduced complement of dopaminergic neurons in the substantia nigra pars compacta of mice with a constitutive “low footprint” genetic knockout of alpha-synuclein. *Mol. Brain* **2020**, *13*, 75. [[CrossRef](#)]
17. Ninkina, N.; Connor-Robson, N.; Ustyugov, A.A.; Tarasova, T.V.; Shelkovnikova, T.A.; Buchman, V.L. A novel resource for studying function and dysfunction of alpha-synuclein: Mouse lines for modulation of endogenous Snca gene expression. *Sci. Rep.* **2015**, *5*, 16615. [[CrossRef](#)] [[PubMed](#)]
18. Connor-Robson, N.; Peters, O.M.; Millership, S.; Ninkina, N.; Buchman, V.L. Combinational losses of synucleins reveal their differential requirements for compensating age-dependent alterations in motor behavior and dopamine metabolism. *Neurobiol. Aging* **2016**, *46*, 107–112. [[CrossRef](#)] [[PubMed](#)]
19. Aburima, A.; Berger, M.; Spurgeon, B.E.J.; Webb, B.A.; Wraith, K.S.; Febbraio, M.; Poole, A.W.; Naseem, K.M. Thrombospondin-1 promotes haemostasis through modulation of cAMP signalling in blood platelets. *Blood* **2021**, *137*, 678–689. [[CrossRef](#)] [[PubMed](#)]
20. Magwenzi, S.; Woodward, C.; Wraith, K.S.; Aburima, A.; Raslan, Z.; Jones, H.; McNeil, C.; Wheatcroft, S.; Yuldasheva, N.; Febbraio, M.; et al. Oxidized LDL activates blood platelets through CD36/NOX2-mediated inhibition of the cGMP/protein kinase G signaling cascade. *Blood* **2015**, *125*, 2693–2703. [[CrossRef](#)]
21. Aburima, A.; Wraith, K.S.; Raslan, Z.; Law, R.; Magwenzi, S.; Naseem, K.M. cAMP signaling regulates platelet myosin light chain (MLC) phosphorylation and shape change through targeting the RhoA-Rho kinase-MLC phosphatase signaling pathway. *Blood* **2013**, *122*, 3533–3545. [[CrossRef](#)]
22. McFadyen, J.; Butler, J.; Malan, E.; Tran, H. Causes and clinical significance of prolonged activated partial thromboplastin times in thalassaemia major. *Ann. Hematol.* **2014**, *93*, 867–868. [[CrossRef](#)]
23. Brass, L. Understanding and evaluating platelet function. *Hematol./Educ. Program Am. Soc. Hematol. Am. Soc. Hematol. Educ. Program* **2010**, *2010*, 387–396. [[CrossRef](#)] [[PubMed](#)]
24. Capoor, M.N.; Stonemetz, J.L.; Baird, J.C.; Ahmed, F.S.; Awan, A.; Birkenmaier, C.; Inchiosa, M.A.; Magid, S.K.; McGoldrick, K.; Molmenti, E.; et al. Prothrombin time and activated Partial Thromboplastin Time testing: A comparative effectiveness study in a million-patient sample. *PLoS ONE* **2015**, *10*, e0133317. [[CrossRef](#)] [[PubMed](#)]
25. Hindle, M.S.; Spurgeon, B.E.; Cheah, L.T.; Webb, B.A.; Naseem, K.M. Multidimensional flow cytometry reveals novel platelet subpopulations in response to prostacyclin. *J. Thromb. Haemost.* **2021**, *19*, 1800–1812. [[CrossRef](#)] [[PubMed](#)]
26. Gorog, D.A.; Fayad, Z.A.; Fuster, V. Arterial Thrombus Stability: Does It Matter and Can We Detect It? *J. Am. Coll. Cardiol.* **2017**, *70*, 2036–2047. [[CrossRef](#)]
27. Sneed, D.; Eliezer, D. Alpha-Synuclein Function and Dysfunction on Cellular Membranes. *Exp. Neurobiol.* **2014**, *23*, 292–313. [[CrossRef](#)]
28. Tadokoro, S.; Nakazawa, T.; Kamae, T.; Kiyomizu, K.; Kashiwagi, H.; Honda, S.; Kanakura, Y.; Tomiyama, Y. A potential role for alpha-actinin in inside-out IIb3 signaling. *Blood* **2011**, *117*, 250–258. [[CrossRef](#)]
29. Atkinson, B.T.; Stafford, M.J.; Pears, C.J.; Watson, S.P. Signalling events underlying platelet aggregation induced by the glycoprotein VI agonist convulxin. *Eur. J. Biochem.* **2001**, *268*, 5242–5248. [[CrossRef](#)] [[PubMed](#)]
30. Abeliovich, A.; Schmitz, Y.; Fariñas, L.; Choi-Lundberg, D.; Ho, W.H.; Castillo, P.E.; Shinsky, N.; García-Verdugo, J.M.; Armanini, M.; Ryan, A.; et al. Mice lacking alpha-synuclein display functional deficits in the nigrostriatal dopamine system. *Neuron* **2000**, *25*, 239–252. [[CrossRef](#)] [[PubMed](#)]

31. Toyoda, T.; Isobe, K.; Tsujino, T.; Koyata, Y.; Ohyagi, F.; Watanabe, T.; Nakamura, M.; Kitamura, Y.; Okudera, H.; Nakata, K.; et al. Direct activation of platelets by addition of CaCl₂ leads coagulation of platelet-rich plasma. *Int. J. Implant. Dent.* **2018**, *4*, 23. [[CrossRef](#)]
32. Tana, C.; Lauretani, F.; Ticinesi, A.; Prati, B.; Nouvenne, A.; Meschi, T. Molecular and clinical issues about the risk of venous thromboembolism in older patients: A focus on parkinson's disease and parkinsonism. *Int. J. Mol. Sci.* **2018**, *19*, 1299. [[CrossRef](#)]
33. Daida, K.; Tanaka, R.; Yamashiro, K.; Ogawa, T.; Oyama, G.; Nishioka, K.; Shimo, Y.; Umemura, A.; Hattori, N. The presence of cerebral microbleeds is associated with cognitive impairment in Parkinson's disease. *J. Neurol. Sci.* **2018**, *393*, 39–44. [[CrossRef](#)] [[PubMed](#)]
34. Ramalingam, N.; Dettmer, U. α -Synuclein serine129 phosphorylation—the physiology of pathology. *Mol. Neurodegener.* **2023**, *18*, 84. [[CrossRef](#)] [[PubMed](#)]
35. Parra-Rivas, L.A.; Madhivanan, K.; Aulston, B.D.; Wang, L.; Prakashchand, D.D.; Boyer, N.P.; Saia-Cereda, V.M.; Branes-Guerrero, K.; Pizzo, D.P.; Bagchi, P.; et al. Serine-129 phosphorylation of α -synuclein is an activity-dependent trigger for physiologic protein-protein interactions and synaptic function. *Neuron* **2023**, *111*, 4006–4023.e10. [[CrossRef](#)]
36. Arawaka, S.; Sato, H.; Sasaki, A.; Koyama, S.; Kato, T. Mechanisms underlying extensive Ser129-phosphorylation in α -synuclein aggregates. *Acta Neuropathol. Commun.* **2017**, *5*, 48. [[CrossRef](#)]
37. Acquasaliente, L.; Pontarollo, G.; Radu, C.M.; Peterle, D.; Artusi, I.; Pagotto, A.; Uliana, F.; Negro, A.; Simioni, P.; De Filippis, V. Exogenous human α -Synuclein acts in vitro as a mild platelet antiaggregant inhibiting α -thrombin-induced platelet activation. *Sci. Rep.* **2022**, *12*, 9880. [[CrossRef](#)]
38. Stefaniuk, C.M.; Hong, H.; Harding, C.V.; Maitta, R.W. α -Synuclein concentration increases over time in plasma supernatant of single donor platelets. *Eur. J. Haematol.* **2018**, *101*, 630–634. [[CrossRef](#)] [[PubMed](#)]
39. Barbour, R.; Kling, K.; Anderson, J.P.; Banducci, K.; Cole, T.; Diep, L.; Fox, M.; Goldstein, J.M.; Soriano, F.; Seubert, P.; et al. Red blood cells are the major source of alpha-synuclein in blood. *Neurodegener. Dis.* **2008**, *5*, 55–59. [[CrossRef](#)] [[PubMed](#)]

Disclaimer/Publisher's Note: The statements, opinions and data contained in all publications are solely those of the individual author(s) and contributor(s) and not of MDPI and/or the editor(s). MDPI and/or the editor(s) disclaim responsibility for any injury to people or property resulting from any ideas, methods, instructions or products referred to in the content.